ISSN 1018-5593

Commission of the European Communities

SUMMARY REPORTS OF THE R&D PROGRAMME

Primary raw materials (1986-89)

VOLUME 3

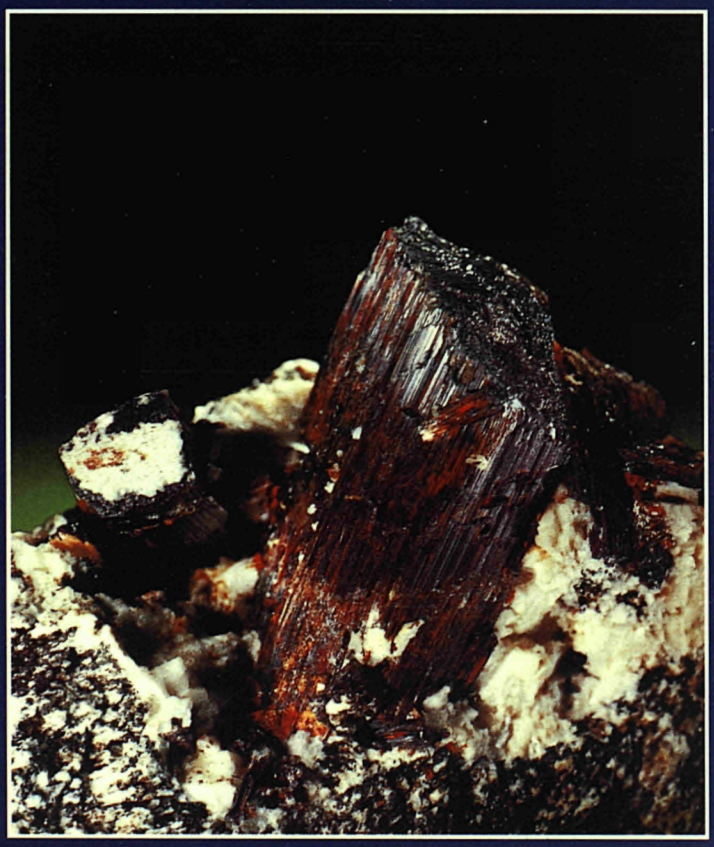

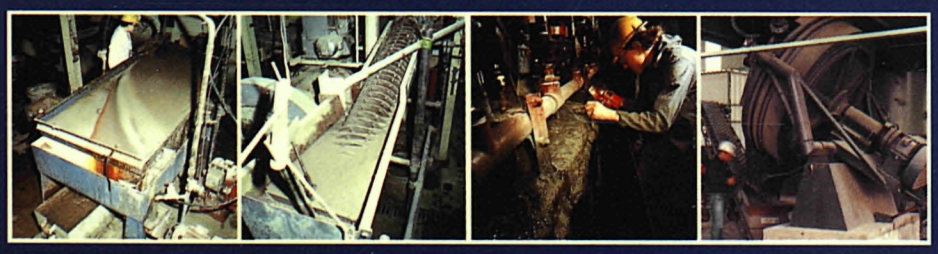

Report
EUR 13647/III EN

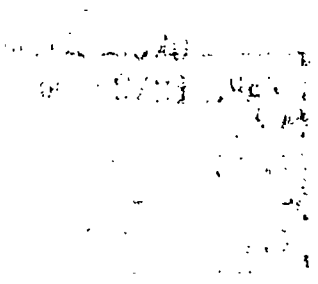

Commission of the European Communities

Summary reports of the R&D programme: Primary raw materials (1986-89) Volume III

Edited by :
M. Donato

Commission of the European Communities
200 rue de la Loi
B-1049 Brussels

Summary reports

Directorate-General
Science, Research and Development

1992

Published by the
COMMISSION OF THE EUROPEAN COMMUNITIES
Directorate-General
Telecommunications, Information Industries and Innovation
L-2920 Luxembourg

ISBN 92-826-3793-X (volumes 1-3)

Cataloguing data can be found at the end of this publication

Luxembourg: Office for Official Publications of the European Communities, 1992

ISBN 92-826-3796-4

Printed in Belgium

SUMMARY REPORTS OF THE R & D PROGRAMME:

PRIMARY RAW MATERIALS (1986-1989)

VOLUME 3. MINERAL PROCESSING

TABLE OF CONTENTS

3. MINERAL PROCESSING

RESEARCH AREA 3.1

PHYSICAL SEPARATION TECHNIQUES

THE APPLICATION OF HIGH INTENSITY MAGNETIC SEPARATION TO THE BENEFICIATION OF COMPLEX ORES

Project Leader: C.W. NOTEBAART,
F.P. VAN DER MEER
Billiton Research, Arnhem, Netherlands

J.H.P. WATSON, Z. LI
University of Southampton, United Kingdom

P. TUCKER, S. NEWTON
Warren Spring Laboratory, Stevenage, United Kingdom

Contract MA1M-0041

1. OBJECTIVES

The objectives of this research programme were:

1. To improve selectivity in high intensity high gradient magnetic separation.

2. To develop a mathematical model of high intensity magnetic separation for the prediction of separation performance.

2. INTRODUCTION

High intensity, high gradient magnetic separation (HGMS) is an established technique in the purification of clay minerals for the paper industry. Wet high intensity magnetic separation (WHIMS, usually referring to devices with lower field gradients than those in HGMS) is widely used in the processing of iron ores. Other applications of HGMS/WHIMS in mineral processing include the separation of wolframite from associated ore and gangue minerals, removal of copper minerals from lead sulphide concentrate, and beneficiation of fine-grained chromite.

The advent of very powerful magnet systems allowed the recovery of weakly magnetic minerals down to micron sizes. Yet the application of HGMS to mineral processing is still rather limited. One of the reasons could be a selectivity problem in the conventional HGMS technique. Therefore the study of selectivity was undertaken in this project with a view to finding methods to increase the separation performance and to broaden the field of application of HGMS to more complex ores.

Mathematical modelling has been applied to HGMS to study the capture process in particular of monomineralic feed materials.

Modelling of separations between different minerals has so far been based on ideal deposition conditions and therefore has been of limited applicability to actual mineral processing. In view of this it was decided to develop a practical model in conjunction with the selectivity studies to predict separation performance and to be included in a general purpose simulation package for mineral processing.

The experimental work aimed at improving selectivity was done jointly by Billiton Research and the University of Southampton. The modelling work was carried out by Warren Spring laboratory.

3. THE SELECTIVITY PROBLEM

Testwork showed that two mechanisms affected the overall selectivity of separation:

1. Mechanical entrainment

   Incorporation of very weakly magnetic gangue minerals by mechanical entrainment in irregularities of the magnetics deposit formed on the matrix elements.

2. Simultaneous magnetic capture of gangue minerals

   Even when the differences in magnetic susceptibilities between the mineral to be recovered and the associated gangue minerals are relatively large, it is expected from basic modelling studies of the capture process, that large particles with low magnetic susceptibility can have capture probabilities similar to those of small particles with higher susceptibility. The separation conditions should be set such that the latter type of particles are captured to ensure acceptable recoveries. This then causes magnetic capture of the former particles, and consequent lowering of the product grade.

4. CAPTURE PROCESSES OF GANGUE MINERALS

Experiments were carried out by Billiton Research in a Sala 10-15-20 canister-type HGMS unit with a maximum field strength of 1670 kA/m (2.1 Tesla). Stainless steel expanded metal was used as the matrix in most experiments.

Separation tests were done using a mixture of the relatively strong paramagnetic mineral wolframite (volume magnetic susceptibility K_V= 3490x10^{-6} SI) in mixtures with quartz (diamagnetic with K_V= -1.8x10^{-6} SI) and arsenopyrite (paramagnetic with K_V=25x10^{-6} SI).

Parallel testwork was conducted by the University of Southampton using a single matrix wire cell fitted with a microscope system to observe the capture processes.

The testwork with the wolframite-quartz mixture demonstrated the importance of mechanical entrainment, the wolframite magnetics deposit contained typically 5-10 % quartz (feed content: 70 % quartz). Remarkable was the relatively high level of quartz contamination in the +50 μm fraction, which may be due to local settling in the canister and/or screening by the deposit itself (partially closing off interstitial spaces). Apart from these two effects the normal inclusion of quartz is thought to occur in pore spaces and in larger irregularities in the deposit.

Testwork on the magnetic capture of weakly magnetic gangue mineral arsenopyrite indicated that along the assumed mechanical entrainment also magnetic capture occurred as the As content of the magnetics increased with increasing field strength.

5. REDUCTION OF CONTAMINATION BY GANGUE MINERALS

5.1 REPROCESSING OF MAGNETICS

Mechanical entrainment can be reduced by re-processing of the magnetics until the required product grade is obtained.

5.2 PARAMAGNETIC LIQUIDS

To reduce the competitive magnetic capture of a weakly magnetic gangue component a magnetic liquid with the same susceptibility could be used. The magnetic force on the particle, which is proportional to the difference in magnetic susceptibilities of the particle and surrounding medium, would therefore be eliminated. Such a particle would then behave as a "non-magnetic" mineral[1].

The properties of various paramagnetic liquids (solutions of $FeCl_2$, $FeSO_4$, $MnSO_4$, $MnCl_2$, $Mn(NO_3)_2$) were determined. Most tests were carried out using a mixture of wolframite and arsenopyrite.

Tests in the Sala separator with the wolframite-arsenopyrite mixture showed a strong reduction in arsenic of the wolframite deposit with increasing susceptibility of the medium ($MnCl_2$). The As content of the magnetics using water as the medium the As content was 8.1 % and decreased to 1.9 % when increasing the medium susceptibility to 200x10^{-6} (SI).

6. MODELLING

6.1 EXPERIMENTAL TECHNIQUES

A laboratory scale separator was developed based on the Boxmag-Rapid Laboratory High Intensity Magnetic Separator LHW. This consists of a conventional iron-yoked electromagnet in which the matrix container is inserted. A special feed system ensured constant and controllable feed conditions during the experiments.

In the laboratory testwork artificial mixtures of garnet-quartz and wolframite-siderite-quartz were used as feed material to evaluate the effects of various operating conditions on separation performance. The magnetic properties of these feed components were determined with a vibrating sample magnetometer. From these data and measurements of the bulk magnetic properties of the separation products their mineral compositions and thus the mass balance of the separation could be calculated.

The initial testwork using the binary mixture was aimed at determining the sensitivities of the various operational parameters, i.e. those related to the material being separated and those concerned with the machine settings. This information was then used to study the effects of the more sensitive parameters, for which a factorial experiment design was employed.

Work continued on the three component feed to quantify the effect of material properties of the feed material on separation performance. This was followed by testwork on real ores, i.e. a hematite iron ore and a wolframite-siderite ore (Berait).

Finally it was verified that the performance of the laboratory separator matched that in a production plant. For this purpose feed material from Wheal Jane, Cornwall was obtained. Plant sampling exercises were conducted to evaluate performance of the full-scale separator.

6.2 TESTWORK RESULTS

6.2.1 Field intensity and matrix type

The dominant factor controlling the performance of the WHIMS is the field intensity.

The performance differences between the matrix types were quite small once comparison was made on the basis of field strength instead of magnet current. Typical test results are shown in Figure 1. In view of this the inclined wedge wire matrix was used in most of the other testwork.

The results obtained on artificial mixtures and the Beralt plant sample linked up quite well when recovery for each size susceptibility fraction was plotted against field intensity (Figure 2).

It was found that the presence of a mineral with higher susceptibility tended to depress the recovery of the mineral with lower recovery (i.e. siderite and wolframite respectively), indicating competition for the available capture sites on the matrix.

6.2.2 Feed rate, feed time, pulp density and feed grade

The results of this work indicated that the performance of the process was insensitive to changes in feed grade, feed rate, pulp density and feed time.

The relative insensitivity of the performance to changes in feed rate and time were explained by the fact that the volume of matrix through which the pulp flowed increased in proportion to these changes.

The insensitivity to changes in feed grade was explained by the fact that the loading was well below the maximum loading capacity of the matrix. Operation at high pulp density was expected to result in more mechanical entrainment, but this appeared not to be the case, possibly due to the changes being small compared to the overall level of entrainment.

6.2.3 Tests on real ores

Tests on the hematite ore gave results corresponding closely to those reported from operating plants using WHIMS.

The tests on the Beralt ore showed the expected grade recovery relationship.

6.3 MATHEMATICAL MODEL DEVELOPMENT

The modelling strategy adopted for WHIMS modelling was based on proven methodology developed at Warren Spring Laboratory for gravity concentration devices. Separation performance is represented as a set of transfer coefficients (T_{IJK}) which describe the probability of transfer of material of size I, S(I), magnetic susceptibility, Sus(J) to the K_{th} output stream and include subsets of operating and model parameters, the latter given by an auxilliary model.

The recovery to the magnetics was modelled by two functions, the main function covering field intensities, for which the transfer to the magnetics was > 25 %. This defined a threshold field intensity (H_o).

The two functions are:

for $H>H_o$ $\quad T(I,J) = \tanh (f\ (S(I),\ Sus(J),\ H,\ H_o))$

with three model parameters P_{1-3} included in f.

for $H<H_o$ $\quad T(I,J) = \tanh (\ f\ (Sus(J),\ H,\ H_o,\ G))$

being dependent also on the matrix type G.

The full model equation based on these transfer functions is as follows:

$$m(I,J) = T(I,J)*M(I,J) + a*(1-T(I,J))*M(I,J)$$

where M(I,J) and m(I,J) are the mass flows of size I and susceptibility fraction J of the feed and magnetics respectively; a is an entrainment parameter.

This empirical model, developed from the results of the above laboratory testwork, gave good agreement with the data collected from the plant survey. However, it should be realised that the model relationships do not necessarily hold outside the range of the variables tested.

7. CONCLUSIONS

1. Mechanical entrainment and magnetic capture of gangue minerals have been shown to act in conjunction in conventional HGMS.

2. Paramagnetic liquids can effectively reduce competitive magnetic capture of impurity minerals.

3. The modelling studies have given an insight into the mechanisms that control the performance of a WHIMS type magnetic separator. A model has been formulated on an empirical basis and will be incorprorated in a general purpose simulator for mineral processing.

8. REFERENCES

1. WATSON, J.H.P.: Wet HGMS applied to the removal of tungsten from tin ores from tin ores. IEEE Trans., MAG-16, 1980, p. 937-939.

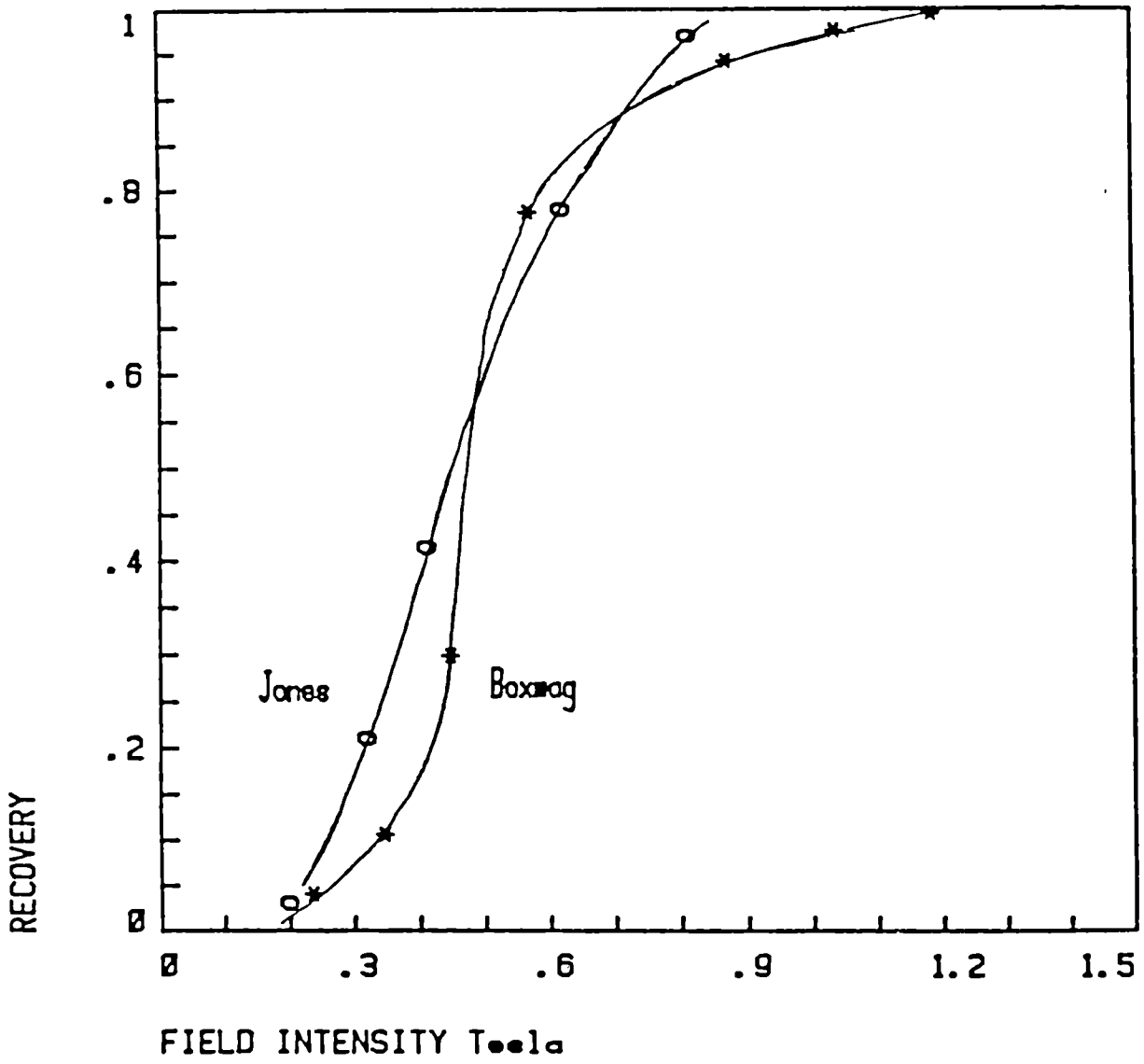

FIGURE 1

Recovery of garnet as a function of field intensity for different matrix types

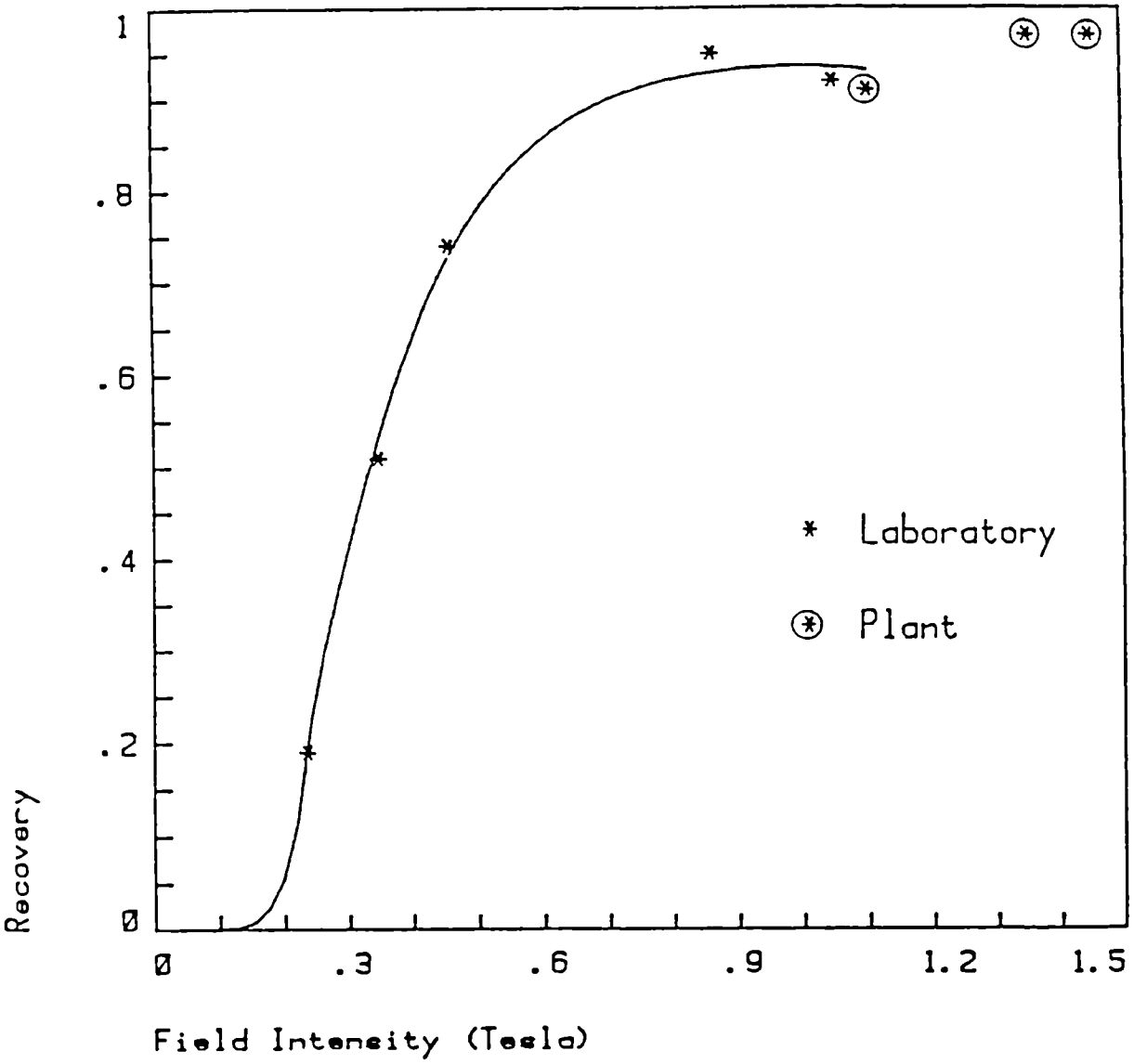

FIGURE 2

Recovery of siderite (-90 +63 μm) as a function of field intensity

THE SEPARATION OF MATERIALS USING SELECTIVE MAGNETIC COATING

Project Leader: P.PARSONAGE
Warren Spring Laboratory, Stevenage, Herts., United Kingdom

G. BAUDET, J.L. CECILE
Bureau de Recherches Géologiques et Minières, Orléans, France

Contract MA1M-0046-C

1. OBJECTIVES

To develop the Selective Magnetic Coating Process to a stage where it could be implemented industrially. The aim was to achieve this through an understanding of the fundamental processes which lead to the selective adsorption of fine magnetite onto mineral surfaces in mixed pulps and to apply the findings at pilot scale.

2. INTRODUCTION

In the period 1982-1986 the selective magnetic coating process was developed at Warren Spring Laboratory (WSL) as a method of mineral separation for difficult to treat ores. [1-4]. The principle of the process is to deposit a coating of fine ferromagnetic particles onto the surface of selected mineral phases so that they can be subsequently recovered by conventional magnetic separation. The control of the coating is primarily achieved through manipulation of the surface chemical properties of the particles in the system.

The process is of particular interest in its potential application to the difficult separation of carbonate minerals such as calcite and dolomite from phosphate minerals in the processing of sedimentary phosphate rock.

Alternative methods of treatment such as froth flotation have serious drawbacks in terms of selectivity of separation and inability to treat particles coarser than a few hundred microns.

The collaborative research project between WSL and BRGM (Bureau de Recherches Geologiques et Minieres) which was developed to investigate the process further had the following components:

WSL would study

i) the surface chemical properties of the mineral particles and the magnetite and how these affect the formation of selective magnetic coatings

ii) the development of a methodology of reagent selection to optimize the selectivity of the coatings

iii) the effect of mixing and turbulence on the formation and disruption of the coatings

iv) magnetic coating materials to allow the most economic material to be used in commercial application

v) control parameters in the low and high intensity magnetic separation stage

vi) scale-up parameters and pilot-scale studies

BRGM would study

i) implementation of the process for specific ores for which there is at present no satisfactory method of treatment including phosphate/carbonate ores.

ii) effects of operating variables on continuous operation

iii) relevant surface properties of sulphide minerals using techniques such as spectroscopy and microcalorimetry.

3. EXPERIMENTAL WORK

The following techniques and equipment were used in the project:

Size analysis/fractionation

Sieving
Warman cyclosizer
Malvern 2600c Size Analyser
Cilas 715
Sedigraph 5000D
Ladal centrifuge

Surface area analysis

Quantasorb (BET)

Electrokinetic measurements

Malvern Zetasizer II
Rank Bros. Mark II

Microscopy

SEM (Cambridge Instruments)
Reflected & transmitted
Optical
Microprobe

Magnetite coating level

Vibrating Sample Magnetometer
Magnetic balance

Amine adsorption

Bromocresol green method

Mixing

Servodyne power controller
Turbine mixer
Rotating drum

Interfacial Tension

Analite surface tension meter

Flux density

Hirch gaussmeter (Hall probe)

Magnetic Separation: lab

Cook lab. separator
Boxmag-Rapid High Int. LHW
Davis Tube

Magnetic Separation: dry

Permroll
Boxmag-Rapid OG disc
Belt separator

Magnetic Separation: WHIMS

Eriez CF 5-MM
Boxmag-Rapid SHW2

Magnetic Separation: drum

Eriez L-8 wet drum
Sala
Eriez Rare Earth Drum

Pilot plant

Attrition scrubber (Denver)
Lamella thickener (Sala)
Pumps

Details of the procedures used for the coating tests are given in the appropriate reports [6-10].

4. RESULTS

4.1. FORMATION OF COATINGS

The deposition and adhesion of magnetite onto spherical soda glass particles in a stirred aqueous suspension was studied. Variables investigated were the particle size of magnetite, the quantity of magnetite, the particle size of the glass target particles, the zeta potentials and hydrophobicity of the surfaces. The cationic surfactant hexadecyltrimethyl-ammonium bromide, (CTAB), was used to alter the surface properties of the components. The results showed that for magnetite to be effective in coating under these conditions it should have a particle diameter of below about 2 microns. The surface density of the coating on different sized target particles does not vary a great deal over the range 19 microns to 1180 microns; this results in the finer particles having a relatively higher volume fraction of magnetite because of their higher surface to mass ratio. Coating densities increase in proportion to the magnetite addition at least up to levels of 5 gm-2 magnetite. Highest coating levels occur where the electrical repulsions between the magnetite and glass are low. Use of oil allows coatings to form on hydrophobic surfaces by capillary forces; selectivity is then limited to hydrophobic/hydrophilic mixtures ie the same as for froth flotation. The influence of interparticle forces on coating formation has been extensively discussed elsewhere. [5, 11-12]

4.2. REAGENT SELECTION

Dense coatings form when repulsion is low and conversley coating can be prevented by use of dispersants which increase repulsion between the minerals and magnetite. With dissolved metals present the effects of complex formation need to be taken into account. Detailed discussion of complexing and dispersing action has been reported elsewhere [13,14].

Hydrophobizing the surface increases the adhesion of the coating particle. Selective hydrophobization may be accomplished using surfactants and collectors as in froth flotation. Surfactant concentrations in excess of the critical micelle concentration lead to a reduction in coating level. Mineral oil used in conjunction with surfactant allows coarser coating particles to adhere.

Polymeric flocculants can be used for fine particle treatment. Selective co-flocculation of one component with magnetite results in the formation of magnetic flocs which can then be separated: this was the method for separating clay and salt tested at pilot scale (see section 4.7.)

4.3. EFFECTS OF MIXING

The influence of stirring on the magnetic coating process has been investigated. Increase in stirring intensity usually results in a reduction of coating level; this is a critical factor in coating coarse particles where gentle contacting is essential to prevent abrasion of the coating. The opposite effect, the shear-flocculation phenomenon, manifesting itself by an increase of coating level with increasing shear rate, has also been observed.

In the magnetic co-flocculation process, as used in the pilot plant work mixing is an important factor. Too low a shear rate causes entrainment of salt minerals in the flocs, wheras too long a period of high shear results in floc break-up and a reduced recovery of the clays in the magnetic separation stage.

4.4. COARSE PARTICLE SEPARATION

Treatment of coarse particles by magnetic coating methods was investigated using synthetic mixtures of quartz and fluorite. Particles of up to 26.5 mm diameter have been successfully separated; the coarsest ever reported using such a process. Contacting of the feed with heavy-media grade magnetite/diesel oil mixture was carried out in a container on a roller bed. After drying, permanent roll, disc and belt magnetic separators were used for fractionation. The coating was relatively easily removed during separation; this may be advantageous because it facilitates recovery of the magnetite for recycling. Treatment of coarse phosphate rock is described in section 4.7

4.5. COATING MATERIALS

Fine grained magnetite from Norway was used in most of the testwork. It is commercially available at below 20 microns and development samples of nominally minus 2 micron and

minus 1 micron were tested. A number of other magnetic materials have been investigated for their applicability as magnetic coating materals. The materials comprise natural magnetite which has been ground to various sizes, and some magnetic waste products. The results have shown that the effectiveness is dependent mainly on the particle size and surface properties of the magnetic phase. Particles coarser than a few microns do not develop sufficiently strong adhesion to remain attached to the mineral surface under the influence of the competing liquid drag forces during agitation. When oil is used in addition to surfactant, an additional force due to capillary effects is present which enables coarser particles to adhere to the mineral surface. The coarser materials are of use for coating under such conditions but the type of materials amenable to separation is more restricted.

Methods of preparing artificial magnetite were investigated. Preparations by precipitation both from mixed ferrous/ferric solutions and also from ferrous solutions in the presence of an oxidising agent were successful. The surface areas of the precipitates formed were in the range 15 to 113 m^2/g.

4.6. MAGNETIC SEPARATION STAGE

To model the behaviour of magnetite coated particles, closely sized spherical glass spheres in the size range 18-530 microns were coated with magnetite, then passed through a wet high intensity magnetic separator under different operating conditions. For particles in the size range studied there was adequate time for migration of the particles to the collecting plates under the influence of the magnetic force. The major reason for non-collection of particles is the opposing forces of gravity and fluid drag acting on the particles at the pole plate surface.It was shown that the ratio of the calculated magnetic force to the combined gravitational and drag forces acting on particles held onto the pole plate surface can be used to predict the recoveries of particles of various sizes and magnetite levels. For a range of operating conditions and particle sizes it was shown that the required level of coating for high magnetics recovery was 0.1-1% magnetite.

A theoretical model of a wet drum magnetic separator was developed and tested using a rare earth magnet drum with synthetic particles to simulate magnetic flocs.

4.7. PILOT PLANT DEMONSTRATION

A pilot plant demonstration of magnetic coating was operated during the course of the project at Boulby potash mine in Northern England. The specific process used was co-flocculation with magnetite. In this process, finely divided

magnetite is introduced, then a polymeric flocculant is used to selectively flocculate the insolubles (clay and gypsum) with the gypsum so producing magnetic flocs; the salt minerals (halite and sylvite) remain unflocculated. Tailings (-30 micron) were used as feed to the pilot circuit. Separation was by high intensity magnetic separation. Throughputs of 100 kg/hr were achieved. With a low KCl feed, reductions of insolubles from 50% to 20% were achieved. Reagent additions of 75 kg/t magnetite and 400 g/t flocculant were used. Magnetite can be recycled - up to 97.5% was recovered by high intensity separation after deflocculation. It was shown that BOS slimes, a waste product from steelmaking could be substituted for magnetite but that a greater weight was required. The flowsheet is shown in Fig.1. [15,16]

Although the process was not adopted, due mainly to the low value of the stream being treated, it was technically successful. The pilot plant was notable in that it is believed to be the first ever pilot scale demonstration of such a magnetic co-flocculation process.

4.8. APPLICATION TO PHOSPHATE SEPARATION

Phosphates from deposits currently under exploitation in North and West Africa were treated. Separation after coating the phosphate (direct) and after coating the gangue (reverse) were both demonstrated. Feed materials were conditioned with reagents such as those used in flotation - including anionic and cationic surfactants, diesel oil, emulsifiers and depressants. Results were better when magnetite and phosphate were conditioned separately.

In one series of experiments the feed was screened and dried before treatment on a belt type magnetic separator. Using the direct process a -1.2+0.315 mm fraction of phosphate feed of 29.7% P_2O_5 was upgraded to 36.2% P_2O_5 at a phosphate recovery of 94.8% using a tall oil + diesel oil addition of 8.3 kg/t. 50 kg/t magnetite (av. diam 8.5 micron) was added - most (>90%) did not adhere and could be recovered easily by screening. Using the reverse process, with a phosphate depressant, 36.2% P_2O_5 was achieved at a 97.5% recovery.

In the second type of experiment the conditioned material was processed wet. It was shown that wet high intensity magnetic separation was not as efficient as dry separation at recovering coarse particles. Using the reverse process the best separation produced a concentrate of 34.4% P_2O_5 at 83.5%. A matrix of stainless steel screens proved superior to a horizontal wedge wire matrix. In the direct process, a 34.7% P_2O_5 concentrate was produced at 95.6% recovery.

Substantial desorption of magnetite from the coated particles' surfaces could be achieved by attriting the coated product at high pulp density under acidic conditions.

5. CONCLUSIONS

i) the surface adsorption density of magnetic coating formed is strongly dependent on the particle size of the coating material. Under mixing conditions typical of industrial mixers or conditioners particle adhesion on smooth surfaces was only significant when the coating particles were below about 2 microns. Use of oil allows coarser coating materials to be used although the type of mixtures which are amenable to separation are more restricted.

Size of the target particle over the range of 20-1000 microns does not have a big influence on the density of the coating (weight of magnetite per unit surface area). But, because of the greater surface to mass ratio of the smaller particles the percentage magnetite content is greater.

ii) high coating levels occur when the forces of interaction between the target particle and coating particle are attractive (or when there is only a low energy barrier to overcome) and when the forces of disruption are low. Hydrophobic surfaces, low zeta potentials, high ionic strength, surface hydrocarbon chains and bridging flocculation tend to favour adhesive coating formation. When oil is used capillary forces become operative.

iii) a model for the recovery of magnetite coated particles by wet high intensity magnetic separation has been developed. Experimental testwork has shown that in the size range studied (18-30 microns) magnetite levels of 0.1-1% wt are required, the precise level depending mainly on fluid velocity through the separator.

A model for magnetic wet drum separation for the recovery of magnetic flocs has been developed.

iv) the magnetic coating process is applicable to coarse particle separation - treated particles up to 26.5 mm have been separated on permanent magnetic roll separators.

v) the performance of selective magnetic coating as applied to phosphate processing appears promising. This is especially true for coarse particle separation for which magnetic coating separation could be considered as an alternative to flotation.

vi) various commercially produced magnetites and also waste products have potential for use in the coating process. BOS slime from steel production is of particular interest because of the large quantities in which it is produced and also because of its fine particle size.

vii) magnetic coating processes can be run successfully at pilot scale using conventional mineral processing equipment.

6. REFERENCES

1. PARSONAGE P. 1984. "Selective magnetic coating for mineral separation" Trans. Inst. Min. Metall., Sect. C, Min. Process. Extr. Metall., **93**: C37-44.

2. PARSONAGE P. 1985. "The recovery of phosphate from carbonaceous gangue by selective magnetic coating - a novel method of mineral separation by control of surface properties" In: Fifteenth International Mineral Processing Congress, Cannes, 1985, (St. Etienne, edition GEDIM, 1985), Vol. 3, pp. 345-356.

3. PARSONAGE P. 1986. "Treatment of carbonate-phosphate rock by selective magnetic coating" Trans. Inst. Min. Metall., Sect. A, Min. Industry, **95**: A154-A158.

4. PARSONAGE P. 1987. "Method of Separation of Material from Material Mixtures" U.S. Patent **4,643,822**.

5. PARSONAGE P. 1988. "Principles of mineral separation by selective magnetic coating" Int. J. Miner. Process., **24**: 269-293.

6a PARSONAGE P. "The separation of materials using selective magnetic coating: First progress report: Adsorption of magnetite onto the surface of spherical glass particles" WSL Report CR 3106 (MM). 1988.

6b PARSONAGE P. and FRU C. 1991. "The adsorption of magnetite for magnetic coating processes" Submitted to Minerals Engineering.

7. PARSONAGE P. "The separation of materials using selective magnetic coating: Second progress report: Pilot plant scale operation of magnetite co-flocculation process at Boulby potash mine" WSL Report CR 3180 (MM). 1989.

8. PARSONAGE P. "The separation of materials using selective magnetic coating: Third progress report: Inmvestigation of potential coating materials" WSL Report CR 3261 (MM). 1990.

9. PARSONAGE P. "The separation of materials using selective magnetic coating: Fourth progress report: Coarse particle treatment and shear flocculation" WSL Report CR 3333 (BT). 1990.

10. PARSONAGE P. "The separation of materials using selective magnetic coating: Fifth progress report: Magnetic separation of magnetite bearing particles" WSL Report CR 3334 (BT). 1991.

11. PARSONAGE P. 1987. "Particle interactions in colloidal suspensions" Rep. Warren Spring Lab. No. LR 600(MM), 46pp.

12. PARSONAGE P. 1991. "Coating and carrier methods for enhancing magnetic and flotation separations" In: Colloid Chemistry in Mineral Processing (J. S. Laskowski and J. Ralston, Eds.), Elsevier. In press.

13. PARSONAGE P. and MARSDEN A. 1987. "The influence of the structure of reagents on their effectiveness as dispersants for cassiterite suspensions" Int. J. Miner. Process., 20, 161-192.

14. PARSONAGE P. and MARSDEN A. 1988. "The role of complexing and dispersing properties of reagents on the stability of suspensions in the presence of divalent metal ions: Quartz and cassiterite in the presence of Cu(II) and Fe(II)" XVI International Mineral processing Congress, (E. Forssberg, Ed.) Elsevier: Amsterdam, 739-749.

15. PARSONAGE P., PASSANT N. and FRU C. 1988. "The recovery of soluble salt minerals from potash tailings by co-flocculation of insoluble impurities with magnetite" In: A.J. Plumpton (Editor), Production and Processing of Fine Particles. Canadian Institute of Mining and Metallurgy, pp 465-474.

16. PARSONAGE P., PASSANT N., PEARL M. and HOLYFIELD G. 1991. "Laboratory and pilot plant scale operation of magnetite co-flocculation process at Boulby potash mine" To be presented at XVII International Mineral Processing Congress, Dresden, 1991.

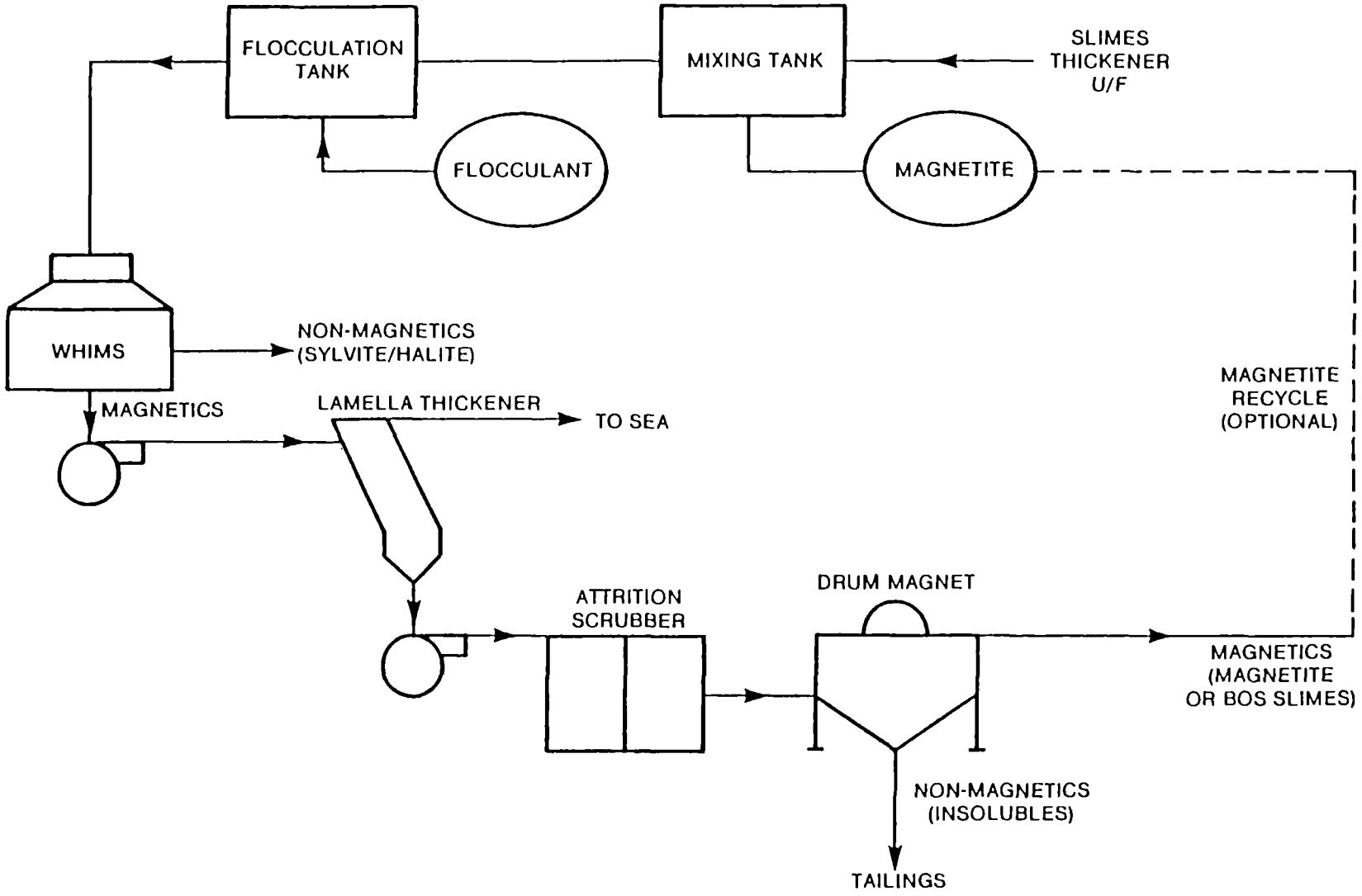

Fig. 1 FLOWSHEET AS USED AT BOULBY MINE

Materials and main operating conditions	P_2O_5 content %	P_2O_5 recovery %	Fe_2O_3 content %	MgO content %
Phosphate 1				
head - 1.6 + 0.315 mm	29.4	100	1.70	
head - 1.6 + 0.4 mm	28.1	100	1.65	
- Direct separation technique				
• Dry mode - 1.6 + 0.4 mm induced roll separator 30 kg/h/cm	36,5	93.3	2.83	
after removal of magnetite	36.9	90.7	1.91	
• Wet mode - 1.6 + 0.4 mm screen matrix low attrition in conditioning,solids concentration 20 %, pulp velocity: 6.5 cm/s	36.2	88.3	2.79	
after removal of magnetite	36.5	86.2	1.88	
• Wet mode - 1.6 + 0.315 mm screen matrix, normal attrition in conditioning, solids concentration: 20 %, pulp velocity: 16.4 cm/s	35.3	79.6	4.95	
• Wet mode - 1.6 + 0.315 mm grooved plates matrix, normal attrition in conditioning solids concentration: 20 %, pulp velocity: 9.4 cm/s	34.4	93.3	2.73	
- Reverse separation technique				
• Dry mode - 1.6 + 0.315 mm induced roll separator 20 kg/h/cm	36.0	90.1	1.33	
• Wet mode - 1.6 + 0.315 mm screen matrix, normal attrition in conditioning solids concentration 20 %, pulp velocity: 6.5 cm/s	35.5	81.5	1.65	
Phosphate 2				
- Direct separation technique				
• Dry mode				
head: - 2.5 + 2 mm	26.3	100	1.62	
Permroll separator 30 kg/h/cm	34.3	91.5	2.42	
after removal of magnetite	34.5	90.1	1.78	
head - 2 + 1 mm	29.5	100	1.67	
Permroll separator: 30 kg/h/cm	35.3	93.2	2.59	
after removal of magnetite	35.6	90.7	1.80	
Phosphate 3				
- Reverse separation technique				
. Dry mode				
head: - 0.6 + 0.2 mm	29.8	100	0.38	1.31
induced roll separator 25 kg/h/cm	31.4	88.3	0.45	0.57
head: - 0.2 + 0.05 mm	27.80	100	0.27	2.29
induced roll separator:15 kg/h/cm	30.7	83.5	0.40	0.68

Table 1: Summary table. Separation performance of the selective magnetic coating process applied to sedimentary phosphate rock samples.

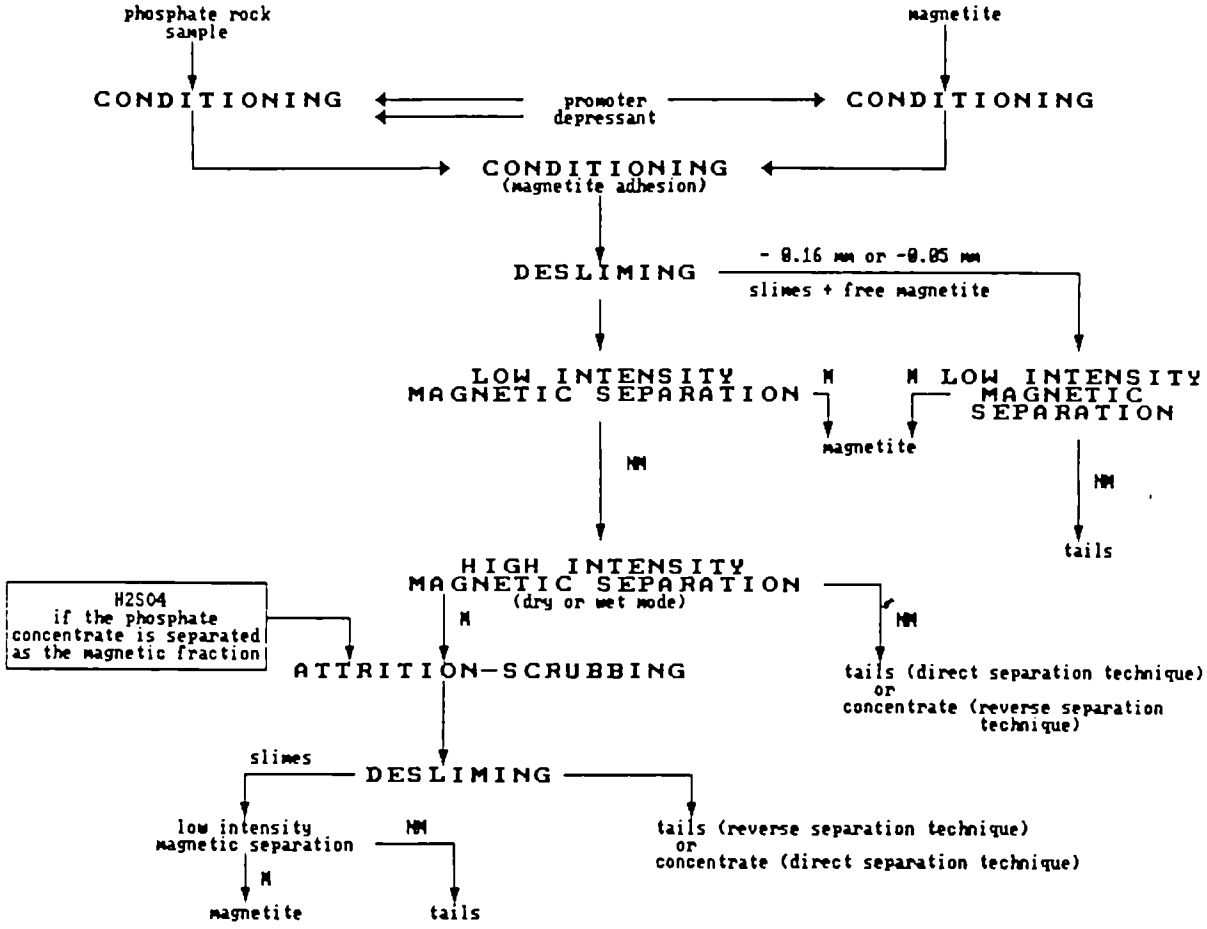

FIGURE N° 2 : BASIC FLOWSHEET FOR BENEFICIATION OF PHOSPHATE ROCK BY SELECTIVE MAGNETIC COATING

FIGURE N 3 :PHOSPHATE CONTENT AND RECOVERY BY SIZE.PHOSPHATE 1.

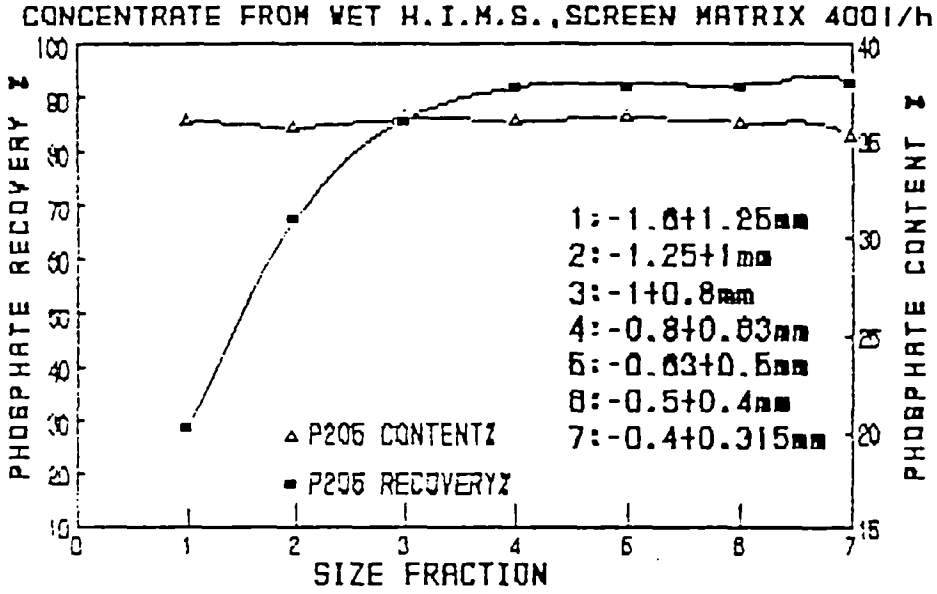

FIGURE N 4 :PHOSPHATE CONTENT AND RECOVERY BY SIZE.PHOSPHATE 1.

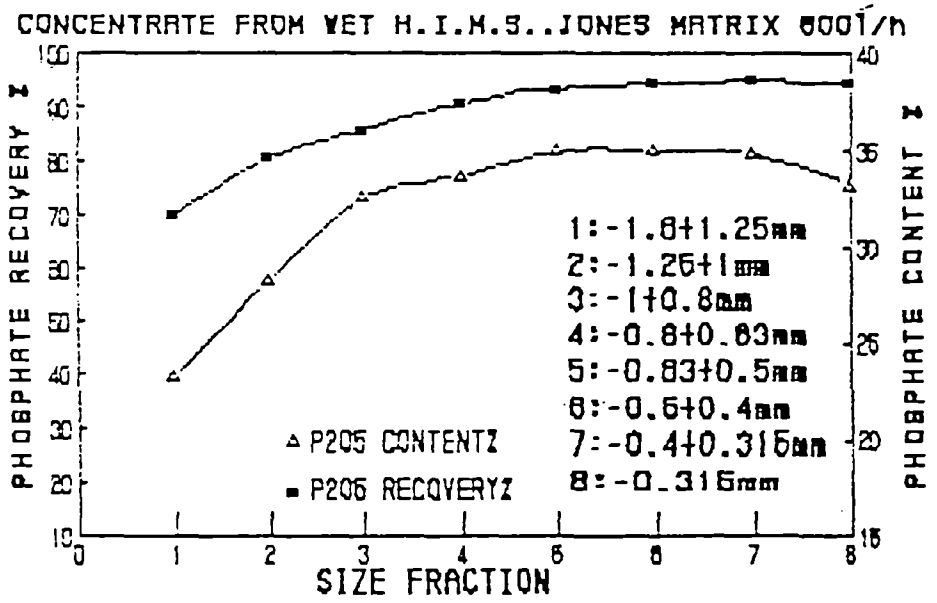

FIGURE N 5 :PHOSPHATE CONTENT
AND RECOVERY BY SIZE.PHOSPHATE 1.
CONCENTRATE FROM DRY H.I.M.S.

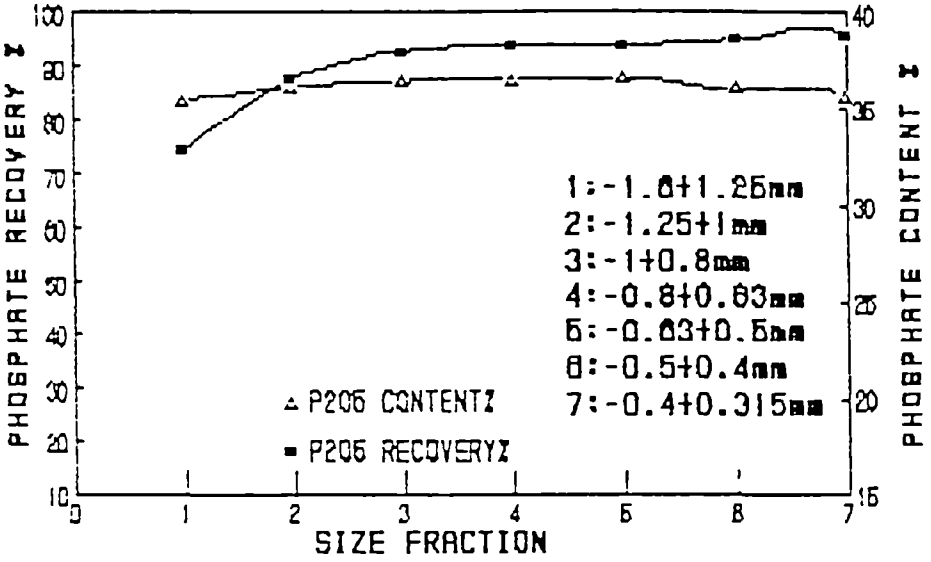

FIGURE N 6 :PHOSPHATE CONTENT
AND RECOVERY BY SIZE.PHOSPHATE 1.
CONCENTRATE FROM WET H.I.M.S..SCREEN MATRIX 10001/h

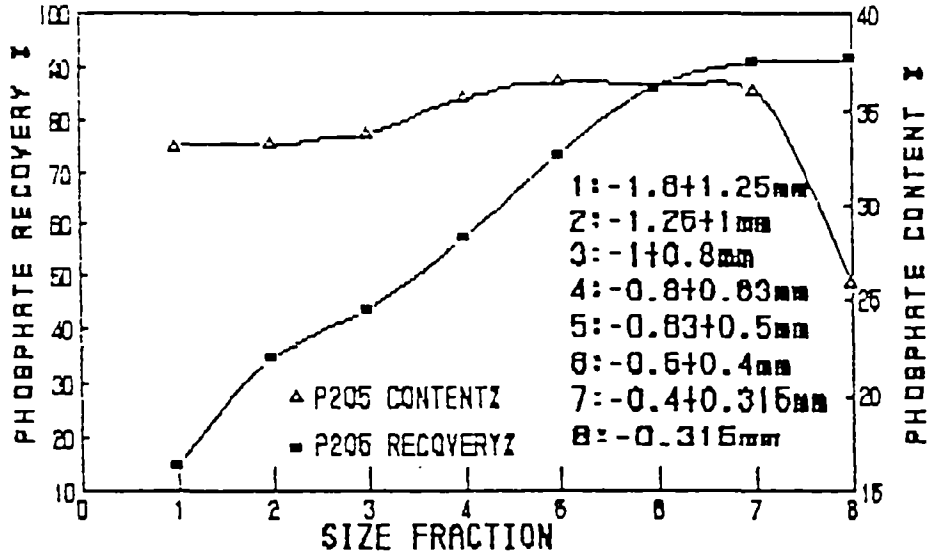

A PROCESS DESIGN STUDY FOR A FINELY DISSEMINATED, PARTIALLY OXIDIZED COMPLEX SULFIDE ORE FROM THE MOLAI AREA, SOUTHERN GREECE

Project Leader : M. GROUSSOU-VALTA
M. Patronis
Institute of Geology and Mineral Exploration, Athens, Greece

A. MARABINI
P.C. Huang, V. Alesse
Istituto per il Trattamento dei Minerali, Rome, Italy

J.M. PREVOSTEAU
F. El Kaliobi, C. Gateau
Bureau de Recherches Geologiques et Minieres (BRGM), Orléans, France

Contract MA1M-0051-C (AM)

1. OBJECTIVES

The aim of this project was to develop a beneficiation process for the treatment of the Molai polymetallic sulfide ore deposit.

Within the scope of the project, the main problems that have to be faced were : (a) the intergrowth texture and the close association of the metallic minerals, (b) the oxidation of sphalerite and galena, (c) the silver recovery.

The aforementioned problems result in low recoveries, high reagent consumption, losses of metal values in the slimes and losses of contained Ag values in zinc concentrate. All these lead to a relatively high operating cost, which affects the overall cost of the investment.

Therefore, a systematic study of the characteristics of the ore was of great importance for the future of the Molai mine-mill venture.

The project deals with the development of new beneficiation techniques, the use of modern mineralogical and analytical methods and the use of new flotation reagents.

2. INTRODUCTION

The Molai polymetallic sulfide ore deposit is situated in the Lakonia county, S.E. Peloponnese. It was located by a systematic exploration programme which commenced in 1980 and was carried out by IGME.

The mineralization was explored to a maximum distance of 1300 m along strike and 200 m across dip and was found to be developed along rather well defined zones and sub-zones. Geostatistical evaluation of the drilling campaign results from the surface (+165 m) down to a -50 m level indicated mineable reserves of 2.3 million tons with an average estimated grade of 9.0 % Zn, 1.8 % Pb and 50 g/t Ag. The above data will be re-evaluated after the completion of ongoing research activities in the Molai area.

Presently an exploratory drift is being excavated by METBA S.A., aiming at the investigation of the optimal mining method and estimation of the corresponding capital and operating costs. During the trial mining exploration, bulk ore was produced for subsequent beneficiation tests in laboratory and pilot plant scale. Technical and economical data thus obtained will be employed in the final feasibility study for the potential exploitation of the Molai sulfide ore deposit.

3. EXPERIMENTAL WORK - RESULTS

3.1 MINERALOGY

Detailed mineralogical study was conducted on drill core samples and bulk samples from the exploratory drift, as well as on the different products of the various test procedures.

Microscopic studies indicated that the major sulfide minerals are sphalerite (6-25 wt %), pyrite (3-7 wt %) and galena (1-3 wt %).

The minor and rare metallic minerals observed, as well as the supergene and gangue minerals identified are listed in Table I.

Zinc is mainly associated with sphalerite; however, an amount of approximately 5-15 % is distributed within the supergene minerals, smithsonite-monheimite. Galena is reported as the major lead bearing mineral, while small quantities of anglesite and cerussite were also observed especially in the oxidized samples.

The ore minerals mainly occur as polycrystallic aggregates and rarely as unmixed concentrations or independent crystals.

Sphalerite occurs in two types. The fist one is iron free and consist of grains and aggregates ranging from 30 to 300 microns in size. The second one, less frequently observed, contains up to 3 % iron and consist of finer grains ranging from 20 to 200 microns in size. Sphalerite grains contain numerous and various inclusions - exsolutions covering their surface, such as pyrite crystals from a few microns to 100 microns in size, pyrrhotite, arsenopyrite, hematite, chalcopyrite, galena, anglesite, tetrahedrite - freibergite - tennantite. In some cases these inclusions exhibit a linear-banded form into sphalerite. Also, in some sphalerite crystals the rare phenomenon of Fe exsolutions in the form of hematite can be observed. It is anticipated that inclusions of iron bearing minerals within sphalerite grains would adversely affect the kinetics of zinc separation by flotation.

Furthermore, on the boundaries of sphalerite grains galena was observed in a form that was difficult to liberate and would potentially result in the early activation of zinc in the lead circuit.

Galena crystals are smaller in size ranging from 5 to 100 microns. They contain very fine inclusions (less than 5 microns) of anglesite, tetrahedrite - tennantite, boulangerite and silver minerals. When galena is forming aggregates, pyrite is often included in a fine grained intergrowth texture.

Pyrite occurs as grains, aggregates and inclusions of a few microns within sphalerite and galena.

The supergene minerals such as smithsonite, monheimite and anglesite are often observed in close association with the base metal sulfides. Zinc carbonates also occur as fine inclusions (4-5 microns) within quartz and silicates.

Silver was located within the following mineralogical phases: in tetrahedrite - tennantite series, mainly in freibergite and in the three Ag-Sb bearing minerals, diaphorite, pyrargirite and stephanite. Freibergite occurs in the form of inclusions or intergrowths mainly associated with sphalerite, while the other three Ag-Sb minerals are exclusively found as microinclusions within galena.

The main characteristics of the Molai ore are fine grained texture, the intergrowths often observed between sphalerite - galena, galena - pyrite and the numerous inclusions present, particularly in sphalerite grains. The above mineralogical features, illustrated in Fig. 1 (a-f), adversely affect the flotability of lead and zinc minerals during conventional flotation.

3.2 LIBERATION

A detailed liberation study was conducted on bulk samples from the Molai mine, in order to determine the optimum grinding size for the flotation of lead and zinc minerals.

From analytical results in Table II, it is deducted that the Molai ore belongs to the fine grained minerals group. To liberate the majority of sphalerite and galena as monomineral grains, the required grinding size is 26 and 12 microns respectively.

On the other hand, for bulk flotation the liberation size of sphalerite estimated to 70 microns is significantly coarser than the corresponding to zinc carbonates, galena and anglesite.

The majority of zinc carbonates are liberated at 20 microns; however, at this mesh of grind an amount is still bound in the form of inclusions within silicates. Galena and anglesite were the most difficult to liberate, the reason being their fine dissemination not only within zinc bearing minerals but also within pyrite, quartz and other silicates.

Thus, if bulk flotation is to be applied for the treatment of the Molai ore, a grinding size of 60 microns would be adequate in order to liberate both sphalerite and a considerable amount of lead minerals from pyrite and gangue material. In that case, a percentage of valuable minerals is not anticipated to report in the tails.

The above liberation study has also shown that due to the fine intergrowths between lead and zinc minerals and the numerous inclusions observed within sphalerite, finer grinding of approximately 10 microns is required for the separation of the lead minerals.

3.3 GRINDABILITY

Wet batch grinding tests in a laboratory rod mill were used for determining the grindability G_d of material (ore) with particle size $\leq$ d, for the various sizes d which are of interest for flotation tests.

By means of the computer, the slope K_d of the straight part of each curve on Fig. 2 is calculated. These slopes represent the initial rates of formation of net material (ore) with particle size $\leq$ d, for the various sizes d. From these slopes, grindabilities are calculated (Table III).

The main conclusions from grinding and grindability test are: (a) Grinding times between 15 and 20 min are considered appropriate in order not to overgrind the ore and to achieve a sufficient liberation degree of the valuable minerals from the gangue, (b) Grindability of material with particle size $\leq$ 0.038 mm (slimes) is relatively high for the Molai ore because it abrades easily. This increased grindability had caused problems during flotation tests (reagents consumption, conditioning times, etc.).

3.4. FLOTATION

The conclusions already mentioned have shown that from both technical and economical point of view, bulk flotation is considered the most appropriate beneficiation method for the treatment of the Molai ore. In spite of this fact, for the completion of research work both differential and bulk flotation were applied.

Flotation tests were run on two different bulk samples : (a) one representing the oxidized part of the ore body and (b) the composite one, representing the main ore reserves. Head assays of those two samples are given in Table IV.

The use of conventional and new reagents has been studied in the flotation tests, together with the study of other parameters. The results obtained are summarized below.

3.4.1 Differential flotation tests

Differential flotation

Many systematic tests were performed on the oxidized bulk sample of the Molai ore for examining the influence of the following factors :

- Type of collectors used individually (new synthetic* and conventional** collectors).
- Collector system and pH value.
- Grinding size.
- Regrinding and process structure.
- Confirming test (Test 41/42***).

* MMBT : Metyl-Mercapto-Benzothiazole MT : Methyl-Ethyl-Mercaptothiazole
DN 68 : 6N-Propyl-Mercapto-Benzothiazole DN 65 : 5n Hexyloxy-2 Amino Thiophenole

** NaEx: Sodium ethyl xantahte NaBx: Sodium butyl xanthate Amine: Dodecyl-Amine-Acetate

*** Test numbers refer to those used in ITMI's "Final Report".

The best results obtained from the flow sheet without cleaning and with cleaning are given in Table V. The most representative flow sheet in this stage is reported in Fig. 3. From the above results, the following conclusions are drawn :

a. Most of the sulfide minerals can be recovered by flotation, but it is very difficult to separate Pb minerals from Zn minerals.

b. Most of the Zn-Fe minerals cannot be recovered by flotation.

c. The efficiency of new and of conventional collectors is almost the same, although selectivity is a little higher and operation simpler (sulfidization is not necessary) with new collectors.

d. Feed grinding at 80 % -54 microns and regrinding of the tailings before scavenger stage in the Zn circuit are almost ineffective.

e. The proper pH is between 8 and 9.

Magnetic separation and flotation

To examine the possibility of recovering Zn-Fe oxidized minerals and upgrading the final Zn concentrate, systematic magnetic separation tests were performed on the tailings of the previous flotation tests and on the raw oxidized bulk sample. The parameter studied was magnetic intensity, its value ranging from 7000 to 20000 Gauss.

The above study had resulted in the development of a new magnetic separation / flotation process. This process consists of magnetic separation followed by flotation to upgrade the magnetic and the non-magnetic product individually.

The major results and the most representative flow sheet obtained at this stage are reported in Table VI and Fig. 4 respectively. From the above results, the following conclusions are drawn :

a. Magnetic separation is very effective for recovering Zn oxidized minerals associated with iron. Almost 77 % of Zn oxidized minerals, which could not be recovered by flotation, can be recovered by magnetic separation. Total recovery of Zn has been increased from 70 to 90 %, without any decrease in the grade of concentrate.

b. It is possible to upgrade the magnetic product by 5 to 7 %, through flotation with sodium oleate [$C_{17}H_{33}COONa$] and citric acid [$HOC_3H_4(COOH)_3$].

3.4.2 Bulk flotation tests

For the determination of the optimum bulk flotation conditions of the Molai ore, a number of relevant tests were conducted on the composite sample.

The above tests were carried out in batches. Each batch of tests has been designed for the study of one of the factors affecting flotation performance. This study is achieved by changing the certain factor's quantity from one test to the other, while keeping other factors constant, and monitoring the relevant effect on flotation (One Factor At A Time Method).

Then the best tests on the batch -with respect to high recovery bulk concentrate, low grade bulk tailings and cleaner concentrate with grade appropriate for metallurgical treatment- are selected and embodied in the next batch for the study of another factor, etc., until the optimum attainable bulk flotation conditions are reached.

In the case of test B5* (Fig. 5, Table VII), Zn recovery reaches 80 % in the cleaner concentrate. Although Pb and Ag recoveries are a little low (i.e. ±53 % and ±62 % respectively), this concentrate, assaying 45.20 % Zn, 4.70 % Pb and 167 ppm Ag, is appropriate for conventional metallurgical treatment. Furthermore, bulk tailings of test B5* assay 1.30 % Zn and 0.45 % Pb. Comparing these values with oxidized Zn and Pb head assay of the feed (i.e. Zn_{ox} = 1.15 % and Pb_{ox} = 0.79 %), we conclude that almost all non-oxidized Zn and all non-oxidized Pb contained in the feed have been recovered.

The results of test B16* (Fig. 6, Table VII) show recoveries greater than 80 % for Zn, Pb and Ag in the total bulk concentrate and greater than 70 % in the cleaner concentrate, assaying 27.10 % Zn, 4.10 % Pb and 116 ppm Ag. Those grades are rather low for conventional metallurgical treatment of the concentrate (Imperial Smelting, etc.) and some special method suitable rather for the treatment of high grade Zn-Pb bearing tailings or metallurgical slags produced during the processing of rich Zn-Pb concentrates must be employed.

A final evaluation shows that the procedure of test B5* is both cheaper and simpler than that of test B16*. Taking into account the low grading of the Molai ore in Pb and Ag (i.e. 1.10% Pb and 28 ppm Ag), it could be proven preferable to use a cheap, simple and Zn recovery orientated method of processing, such as that of test B5*. On the other hand, if priority is to be given in recovering together with Zn as much Pb and Ag as possible, then the procedure of test B16* might be followed. In any case, the final decision making will be the result of the appropriate feasibility study.

3.5 PILOT PLANT TESTS

After completion of the laboratory work, bulk flotation tests were performed in a 50 kgr/hr DENVER flotation pilot plant, installed at IGME's Laboratories and consisting of the following items : (a) Silo, (b) Vibrating Feeder, (c) 12" x 24" DENVER Rod Mill, (d) 6" DENVER Spiral Rake Classifier, (e) 3/4" DENVER Vertical Sand Pump, (f) 24" x 36" DENVER Conditioner and (g) 6-Cell #5 DENVER Flotation Machine.

In all the above tests the composite sample has been used and conventional reagents were employed. The objective of those tests was to study and stabilize the various parameters affecting pilot plant performance, e.g. feed rate, water flow, reagent feeding, etc., in order to adjust the pilot plant for the final test.

This final test has been carried out according to the conditions of laboratory bulk flotation test B5*. The relevant flow sheet and results are given in Fig. 7 and Table IX respectively.

Comparing the results of the final pilot plant test to those of laboratory test B5* (Fig. 5, Table VII), it can be seen that they match very well. The minor discrepancies observed may be attributed to the slightly different size distribution of the flotation cells feed and to some unavoidable increase in the oxidation degree of the several composite samples used for the pilot tests, during the time the sample has been kept stored at the laboratory.

Detailed assays for the feed, the bulk cleaner concentrate and the bulk tailings of the final pilot plant test are given in Table X. From the assay of the bulk cleaner concentrate we can conclude that -as was the case with the laboratory test B5*- this product is appropriate for conventional metallurgical treatment.

The final decision making whether the scaling up of the proposed pilot plant flow sheet is feasible will be the result of the study of the various relevant economical factors.

* Test numbers refer to those used in IGME's "Final Report".

4. GENERAL CONCLUSIONS

a. There is a finely disseminated, partially oxidized Zn-Pb-Ag sulfide ore deposit in the Molai area (Southern Greece) with an average grade of 6.80 % Zn, 1.10 % Pb and 28 ppm Ag. Ore reserves have been estimated at 2.3 million tons.

b. Zn is found mainly in sphalerite and smithsonite (monheimite), Pb in galena, cerussite and anglesite and Ag in tetrahedrite - tennantite and freibergite.

c. The fine grained texture, the intergrowths (often between sphalerite - galena and galena - pyrite) and the numerous inclusions, particularly in sphalerite, are the main reasons for the inconvenience in establishing the optimum grain size for liberating each one of the valuable minerals from the others and from the gangue.

d. For liberating the majority of sphalerite and galena, the required grinding size is 26 and 12 microns respectively, while for the oxidized Zn and Pb minerals the above sizes become 20 and less than 10 microns. On the other hand, for liberating the majority of sphalerite and Pb minerals from pyrite and gangue material, a grinding size of 60 microns would be sufficient. Hence, for the beneficiation of the Molai ore bulk flotation is considered more suitable than differential.

e. Zn carbonate (oxidized) minerals are very difficult to recover due to their close association with iron minerals. A new process, consisting of magnetic separation followed by flotation to upgrade the magnetic and the non-magnetic product individually, has been developed for recovering these Zn minerals.

f. Laboratory grinding tests and kinetics study on the composite sample of the Molai ore have shown that it abrades easily, thus producing a relatively high quantity of slimes. For keeping this quantity as low as possible and for achieving the sufficient liberation degree of the valuable minerals from the gangue in order to apply bulk flotation, a grinding time close to 20 min is considered appropriate.

g. A cleaner concentrate suitable for conventional metallurgical treatment -assaying 45.20 % Zn, 4.70 % Pb and 167 ppm Ag with recoveries 79.47 %, 53.23 % and 61.87 % respectively- has been obtained from the best laboratory bulk flotation test on the composite sample of the Molai ore. The low grading of the ore in Pb and Ag (i.e. 1.10 % Pb and 28 ppm Ag) justifies the somewhat low Pb and Ag recoveries in the above concentrate.

h. The above results were very well matched in the final bulk flotation pilot plant test, where the cleaner 2800 ppm Cd with recoveries 79.46 %, 52.54 %, 62.95 % and 80.97 % respectively.

i. The relatively low Zn recovery (±80 %) in the cleaner concentrates of both the laboratory and the pilot plant flotation tests, as well as the special characteristics of the Molai ore, suggest that further research work may be undertaken for examining the applicability of column flotation with conventional and new reagents at very fine grinding size or of hydrometallurgical methods for its beneficiation.

5. GENERAL REFERENCES

1. ADAM, K., PREVOSTEAU, JM., KONTOPOULOS, A., STEPHANAKIS, M., ERRINGTON, M. : "Applications of process mineralogy on the treatment of Olympias pyrite concentrate", Gold 90, 32, 1990, pp. 341-351.

2. AMOV, G.B. : "Evolution of uranogenic and thorogenic lead. A dynamic model of continuous isotopic evolution", Earth and Planet Sci. Letters 65, Elsevier, 1983.

3. ANGELOPOULOS, C. and CONSTANTINIDES, D. : "The Molai Zn-Ag-Pb deposit, Laconia, Greece", Inter. South European Symposium on Exploration Geochemistry, Athens, 1986.

4. ANGELOPOULOS, C. and CONSTANTINIDES, D. : "The Molai Zn-Pb-Ag deposit, Laconia, S.E. Peloponnese", Bulletin of the Geological Society, Athens, Greece, Vol. XX/2, 1988.

5. ARROWSMITH, P. : "Laser ablation of solids for elemental analysis by inductively coupled plasma mass spectrometry", Anal. Chem. 59, 1987, pp. 1437-1444.

6. ASTIER, J.E. : "The future of mineral processing", Trans. Inst. Min. Metall., C112, 1988.

7. BAIXI, J. : "Information for mineral processing of lead-zinc" (in Chinese).

8. BAIXI, J. : "Reagent of flotation" (in Chinese).

9. BILL, M. : "Developments and results obtained in the treatment of zinc oxide ores at AMMI mines", Mineral Processing - Proceedings of the 6th International Congress, 1963.

10. BULATOVIC, S.M. : "Process development for complex Cu-Pb-Zn ores laboratory pilot plant studies", XIV IMPC, IV-3.12.

11. BULATOVIC, S.M., WYSLOUZIL, D.M. : "Selection of reagent scheme to treat massive sulphide ores", Complex Sulphides, (D. Zunkel et al., Editors), TMS, 1985.

12 CASES, J.M. : "Finely disseminated complex sulphide ores", Complex Sulphide Ores, (M.J. Jones, Editor), IMM Conference Proceedings, 1980.

13. CYANAMID : "Mining Chemicals Handbook", 1989.

14. DANA, J.D., DANA, E.S. : "The system of Mineralogy", Vols. I, II.

15. EL KALIOBI, F., PREVOSTEAU, JM., REMOND, G. : "Study of the Olympias ore", Rapport BRGM R30280, Departement Analyse, EC Contract No. MAIM 0069, 1989.

16. EL KALIOBI, F., GATEAU, C., JACQUIN, JP. : "Bilans métaux dans les minérais complexes", à publier.

17. FIEDLER, K.J. : "Commissioning and operation of 800 t/h heavy medium cyclone plant at Mount Isa Ltd", Trans. Inst. Min. Metall., C41, 1986.

18. FINKELSTEIN, N.P. and ALLISON, S.A. : "The chemistry of activation, deactivation and depression in the flotation of zinc sulphide. A review", Flotation, Vol.1, (M.G. Fuerstenau, Editor), New York, 1976.

19. GATEAU, C., EL KALIOBI, F., PREVOSTEAU, JM. : "Contribution de la microscopie électronique à balayage à la minéralogie quantitative", Industrie Minérale, 1986, pp.115-118.

20. GROSSOU-VALTA, M. et al. : "Discussion on the possible treatment of the Molai mixed sulphide ore after experimental investigation of typical samples", Metallurgical Research Reports, No 37, IGME, Athens, 1984.

21. IGME : "Concise report on the prefeasibility study of the Molai massive sulphide deposit in Laconia", IGME, Athens, 1985.

22. IGME, BRGM, ITMI : "A process design study for a finely disseminated, partially oxidized complex sulphide ore from the Molai area, Southern Greece", EC Contract No. MA1M-0051-C(AM).
1st Progress Report, November 1988.
2nd " " May 1989.
3rd " " November 1989.
4th " " July 1990.

23. INGERTTILA, K., KAUKKANEN, J., HINTIKKA, V. : "On mineralogy and flotation tests of Molai ore", Technical Research Center of Finland, 1986.

24. JACQUIN, JP., GATEAU, C. : "Développements de la minéralogie appliquée au traitement des minérais", Industrie Minérale, Vol. 66, No. 1, 1984, pp. 172-188.

25. JOWETT, A. : "Investigation of lead recovery problems in the lead-zinc concentrator at Mount Isa, Queensland, Australia", Trans. Inst. Min. Metall., C74, 1981.

26. LABORATORIO GEOTECNICO : "Integrazione del lavoro in microsonda relativo alla mineralizzazione di Molai", 1989.

27. MARABINI, A., ALESSE, V., BARBARO, M. : "New synthetic collectors for selective flotation of zinc and lead oxidized minerals", XVI IMPC, 1988.

28. MaCAVANNA, M. : "Bulk flotation as an alternative to the benification of very finely disseminated complex sulphide ores in a massive pyrite matrix", XIV IMPC, IV-19.

29. MARABINI, A., HUANG, P.C. : "Fourth progress report of mineral processing -A process design study for a finely disseminated, partially oxidized complex sulphide lead/zinc ore from the Molai area, South Greece", Inner Report, 1990.

30. METBA : "Optimization of the exploitation of thin vein polymetallic sulphide deposits through mathematical modelling and rock mechanics. An application to the Molai mine", EC Contract No. MAIM-0025-C(TT), 2nd Progress Report, December 1989.

31. METBA : "Molai base metal massive sulphides", EC Project GRE 02/09/002, 2nd Progress Report, April 1990.

32. MUNRO, P.D. : "The design, construction and commissioning of heavy medium plant for silver-lead-zinc ore treatment (Mount Isa Mines Ltd)", XIV IMPC, VI-6 P.1, 1982.

33. NORRGRAN, D.A. and ARMSTRONG, R.O. : "Developing a selective flotation concentration technique for polymetallic ores", Complex Sulphides, (A.D. Zunkel et al., Editors), TMS, 1985.

34. PATRONIS, M.E. : "Dry batch grinding kinetics of homogeneous ores and industrial minerals", PhD Thesis, N.T.U. Athens, 1985 (in Greek).

35. RAUSCH, D.O., MARIACHER, B.C. : "Lead and Zinc", Vol.1, 1970.

36. REMOND, G., CESBRON, F., TRAXELL, JL., CABRI, LJ. : "Electron microprobe analysis and proton induced X-ray spectrometry applied to trace element analysis in sulfides; problems and prospects", Scanning Microscopy, Vol. 3, 1987, pp. 1017-1037.

37. REY, M. : "Some factors affecting selectivity in the differential flotation of lead-zinc minerals", IMPC, 1960.

38. REY, M. : "The flotation of the oxidized zinc ores", Recent Development in Mineral Processing, 1953.

39. SUTTIL, K.R. : "Why are we content with ninety percent?", Engineering and Mining Journal, Vol. 191, No.11 (November 1990), pp. 26-29.

40. THE SOGERSA STAFF : "The mines of the SOGERSA Co. with special regard to mineralogical plants", 1975.

41. WILLS, B.A. : "Mineral processing technology".

42. ZHANG HUI-WEI : "New flotation flowsheet for treatment of Fankou complex lead-zinc ore", Min. Pro. Extr. Metal. Congr., 1984.

TABLE I
Minerals of the Molai ore body

		Main	Minor	Rare
A. Hypogene sulfides-sulfosalts-oxides				
Sphalerite	ZnS	*		
Pyrite	FeS_2	*		
Galena	PbS	*		
Tetrahedrite-Tennantite	$Cu_{12}(As,Sb)_4S_{13}$		*	
Magnetite	Fe_3O_4		*	
Hematite	Fe_2O_3		*	
Geocronite	$Pb_5(Sb,As)S_8$		*	
Freibergite	$(CuAgFe)_{12}Sb_4S_{13}$		*	
Chalcopyrite	$CuFeS_2$		*	
Marcasite	FeS_2		*	
Pyrrhotite	FeS		*	
Bornite	Cu_5FeS_4		*	
Enargite	Cu_3AsS_4			*
Famatinite	Cu_3SbS_4			*
Arsenopyrite	$FeAsS$			*
Boulangerite	$Pb_5Sb_4S_{11}$			*
Seligmannite(?)	$CuPbAsS_3(+Sb)$			*
Diaphorite	$Ag_3Pb_2Sb_3S_8$			*
Stephanite	Ag_5SbS_4			*
Pyrargyrite	Ag_3SbS_3			*
Lazarevicite	$Cu_3(As,V)S_4$			*
B. Supergene minerals				
Cerussite	$PbCO_3$		*	
Anglesite	$PbSO_4$		*	
Smithsonite (Monheimite)	$ZnCO_3 \cdot (Fe,Zn,Mn,Ca)CO_3$		*	
Goethite	$a\text{-}Fe_2O_3 \cdot H_2O(FeHO_2)$		*	
Chalcosite	Cu_2S		*	
Covellite	CuS		*	
C. Gangue minerals				
Quartz	SiO_2	*		
Calcite	$CaCO_3$	*		
Dolomite	$Ca(Mg,Fe)(CO_3)_2$		*	
Siderite	$FeCO_3$		*	
Kaolinite	$Al_2O_3 \cdot 2SiO_2 \cdot 2H_2O$		*	
Illite	$KAl_2(OH)_2AlSi_3(O \cdot OH)_{10}$		*	
Chlorite	$Mg_5(Al,Fe)(OH)_8(Al,Si)_4O_{14}$		*	
Barite	$BaSO_4$		*	

TABLE II
Liberation size of major Pb-Zn minerals

	LIBERATION SIZE (microns)			
	Pb-minerals/ Sphalerite	Sphalerite	Oxidized Zn-minerals	Galena/ Anglesite
Differential flotation	-	26*	-	12/2
Bulk flotation	55	70**	20	7

* monomineral
** with metallic inclusions

TABLE III
Grindability tests results.

d mm	K_d % units/min	Correlation coefficient, r^2	Grindability, G_d gr/min
0.500	5.168	0.9953	49.93
0.250	3.823	0.9994	36.93
0.125	2.444	0.9993	23.61
0.075	1.716	0.9984	16.58
0.038	1.093	0.9979	10.56

TABLE IV

Head assays of the composite bulk sample and the oxidized bulk sample of the Molai ore.

	COMPOSITE BULK SAMPLE	OXIDIZED BULK SAMPLE
Zn_{total}	6.80 %	5.20 %
Zn_{ox}	1.15 %	2.44 %
Pb_{total}	1.10 %	0.48 %
Pb_{ox}	0.70 %	0.44 %
Ag	28 ppm	10 ppm
Cd	400 ppm	
Fe	5.03 %	4.86 %
Cu	0.03 %	
Ba	0.08 %	
Bi	0.10 %	
Sb	0.02 %	
As	0.05 %	
S		4.07 %
C		1.60 %
CaO	3.60 %	1.40 %
MgO	1.90 %	1.36 %
Na_2O	0.80 %	
K_2O	3.50 %	
Al_2O_3	11.90 %	12.58 %
SiO_2	50.80 %	50.59 %
L.O.I.	9.00 %	

TABLE V

Major testing results of oxidized sample

Differential flotation

Method used	Test No.*	Collectors	Product	Weight %	Grade % Zn	Grade % Pb	Distribution % Zn	Distribution % Pb
Differential flotation without cleaning	33	New collectors (MT,DN65,DN68)	Pb concentrate	20.80	7.32	1.36	29.18	66.56
			Zn concentrate	21.64	10.45	0.39	43.35	19.81
			Final Tailings	57.56	2.49	0.10	27.47	13.63
	29	Conventional collectors (NaBX)	Pb concentrate	9.70	8.24	2.64	14.72	56.78
			Zn concentrate	32.21	9.23	0.46	54.76	32.62
			Final Tailings	58.09	2.85	0.08	30.52	10.60
Differential flotation with cleaning	41	New collectors (MT,DN65,DN68)	Pb concentrate	3.64	11.12	5.04	7.81	41.69
			Zn concentrate	3.71	48.16	1.16	34.49	9.78
			Final Tailings	60.14	2.40	0.14	27.90	19.36
	42	Conventional collectors (NaBX,Amine)	Pb concentrate	2.40	10.80	7.80	4.83	42.40
			Zn concentrate	4.20	40.16	0.80	31.10	9.24
			Final Tailings	69.40	3.00	0.14	30.63	24.44

* Test numbers refer to those used in IIMI's "Final Report"

TABLE VI

Major testing results of oxidized sample

Magnetic separation and flotation

Method used	Test No.*	Collectors	Product	Weight %	Grade % Zn	Grade % Pb	Distribution % Zn	Distribution % Pb
Magnetic separation on flotation tailings	44	1st stage: 10222 Gauss 2nd stage: 15222 Gauss	Magnetic	19.48	11.38	0.26	77.47	15.97
			Non-magnetic	80.68	0.88	0.33	22.53	84.03
			Feed**	100.00	2.85	0.32	100.00	100.00
Flotation followed by magnetic separation	41 + 44	New collectors (MI,DN85,DN85)	Magnetic	11.67	11.38		24.37	
			Pb concentrate	3.64	11.12	5.84	7.81	41.69
			Zn concentrate	3.71	48.16	1.16	34.49	9.78
			Final Tailings	60.14	2.48	0.14	27.98	19.36
Magnetic separation followed by differntial flotation	46	New collectors (MI,DN85, $C_{17}H_{33}COONa$)	Magnetic	23.35	10.55	0.47	42.26	24.45
			ZnO M.1***	5.87	22.60	0.79	22.76	10.35
			ZnS concentrate	4.33	41.58	1.85	30.82	10.15
			Pb concentrate	2.79	25.65	4.49	12.27	27.96
			Final Tailings	61.89	0.94	0.18	9.87	24.63
	45	Conventional collectors (NaEX,NaBX)	ZnO M.1	2.40	14.55	1.79	5.85	8.17
			ZnS concentrate	4.88	40.95	1.88	27.99	8.38
			Pb concentrate	4.41	22.90	4.47	16.92	37.40
			Final Tailings	68.45	0.82	0.16	8.37	18.39

* Test numbers refer to those used in IIMI's "Final Report"

** Feed is the final tailings of flotation test 41

*** ZnO M.1 is a part of magnetic product

TABLE VII
Results of Bulk Flotation Test No. B5

PRODUCT	WEIGHT %	ASSAYS Zn %	Pb %	Ag ppm	DISTRIBUTION Zn %	Pb %	Ag %
Bulk Cleaner Concentrate	10.8	45.20	4.70	167.0	79.47	53.23	61.87
Bulk Cleaner Tailings	4.6	3.60	1.45	40.0	2.71	7.04	6.36
Bulk Concentrate	15.5	32.71	3.72	128.9	82.18	60.27	68.23
Bulk Tailings	84.5	1.30	0.45	11.0	17.82	39.73	31.77
Feed	100.0	6.17	0.96	29.3	100.00	100.00	100.00
Head Assay		6.00	1.10	28.0			

TABLE VIII
Results of Bulk Flotation Test No. B16

PRODUCT	WEIGHT %	ASSAYS Zn %	Pb %	Ag ppm	DISTRIBUTION Zn %	Pb %	Ag %
Bulk Cleaner Concentrate	17.6	27.10	4.10	116.0	78.38	71.57	76.66
Bulk Cleaner Tailings	8.5	2.45	1.20	21.0	3.42	10.12	6.70
Total Bulk Concentrate	26.1	19.07	3.16	85.1	81.80	81.69	83.37
Bulk Tailings	73.9	1.50	0.25	6.0	18.20	18.31	16.63
Feed	100.0	6.09	1.01	26.6	100.00	100.00	100.00
Head Assay		6.00	1.10	28.0			

Test numbers refer to those used in IGME's "Final Report"

TABLE IX
Results of Final Pilot Plant Test

PRODUCT	WEIGHT	ASSAYS				DISTRIBUTION			
		Zn	Pb	Ag	Cd	Zn	Pb	Ag	Cd
	%	%	%	ppm	ppm	%	%	%	%
Bulk Cleaner Concentrate	11.9	46.92	4.96	152.0	2000.0	79.46	52.54	62.95	80.97
Bulk Cleaner Tailings	18.1	2.42	1.01	20.0	162.0	3.50	9.15	7.00	4.01
Bulk Concentrate	22.0	26.41	3.14	91.0	1584.0	82.96	61.68	70.04	84.98
Bulk Tailings	78.0	1.53	0.55	11.0	79.0	17.04	38.32	29.96	15.02
Feed	100.0	7.00	1.12	29.0	410.0	100.00	100.00	100.00	100.00
Head Assay		6.00	1.10	28.0	400.0				

TABLE X

Feed, bulk cleaner concentrate and bulk tailings assay for the final pilot plant test.

	FEED	BULK CLEANER CONCENTRATE	BULK TAILINGS
Zn_{total}	6.80 %	46.92 %	1.53 %
Zn_{ox}	1.15 %	0.98 %	1.33 %
Pb_{total}	1.10 %	4.96 %	0.55 %
Pb_{ox}	0.70 %	1.10 %	0.55 %
Ag	28 ppm	152 ppm	11 ppm
Cd	400 ppm	2800 ppm	79 ppm
Fe	5.03 %	4.69 %	4.55 %
Cu	0.03 %	0.12 %	0.11 %
Ba	0.08 %	0.35 %	3.25 %
Bi	0.10 %	0.10 %	0.10 %
Sb	0.02 %	0.03 %	0.08 %
As	0.05 %	0.05 %	0.05 %
CaO	3.60 %	1.60 %	3.80 %
MgO	1.90 %	0.30 %	1.65 %
Na_2O	0.80 %	0.18 %	0.85 %
K_2O	3.50 %	0.15 %	4.25 %
Al_2O_3	11.90 %	1.30 %	12.95 %
SiO_2	50.80 %	13.10 %	51.00 %
L.O.I.	9.00 %	15.45 %	6.85 %

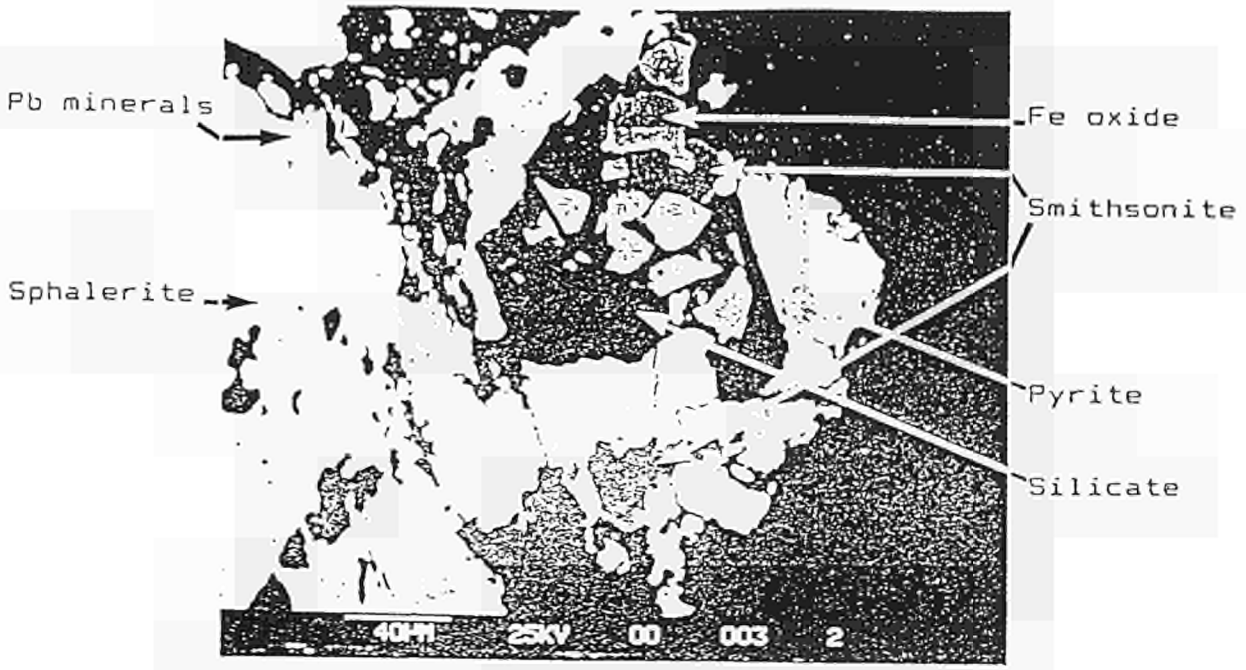

Fig.1(a). View in backscaterred electron mode, showing the close association between the minerals and the difficulty in individual detection of Pb- and Zn-bearing ones (galena, sphalerite, smithsonite)

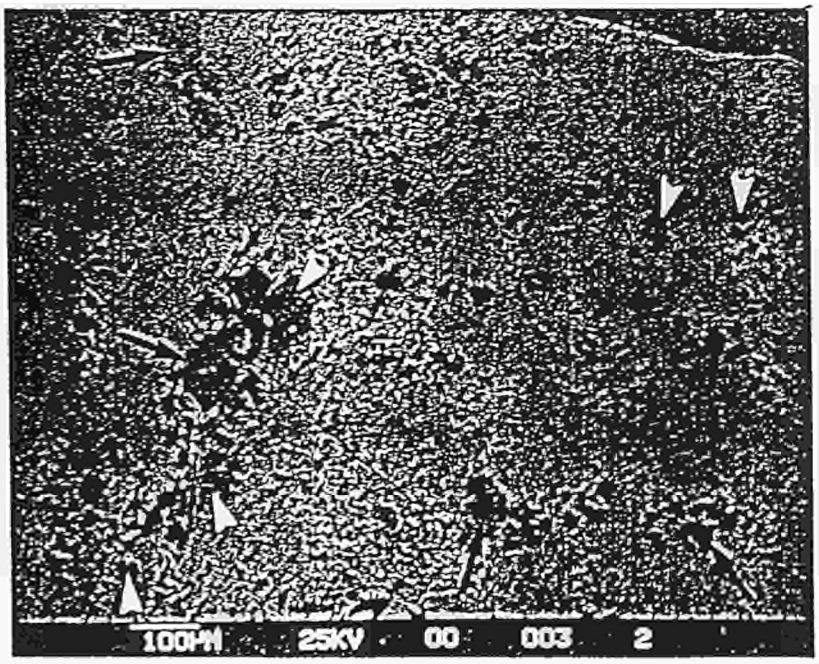

Fig.1(b). View in backscaterred electron mode of another area, showing the fine dissemination of pyrite (black arrowed zones) and hematite - magnetite (white arrowed zones) in sphalerite

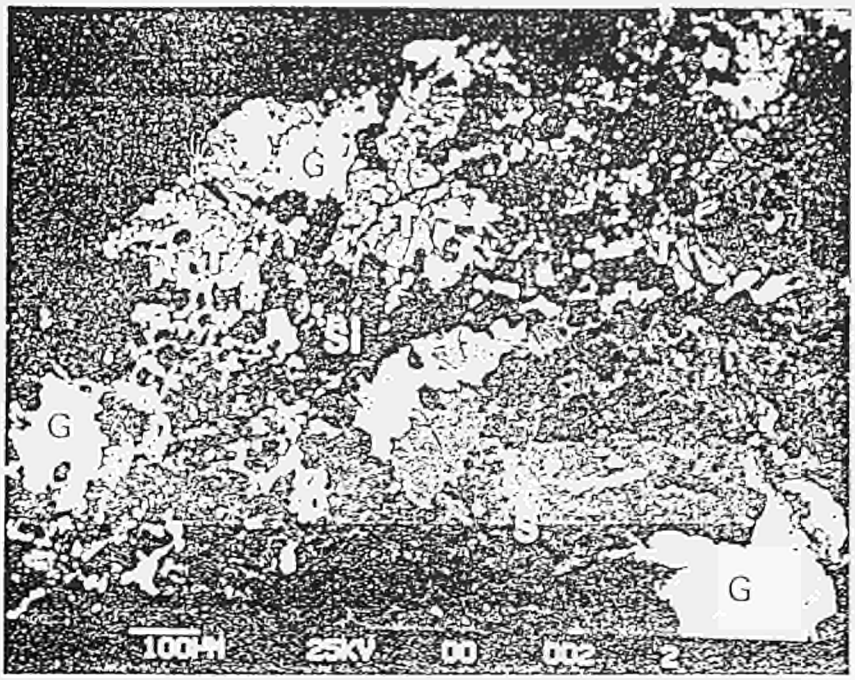

Fig.1(c). Area in backscaterred electron mode, showing the close association between galena (G), sphalerite (S), tetrahedrite (T) and silicates (Si)

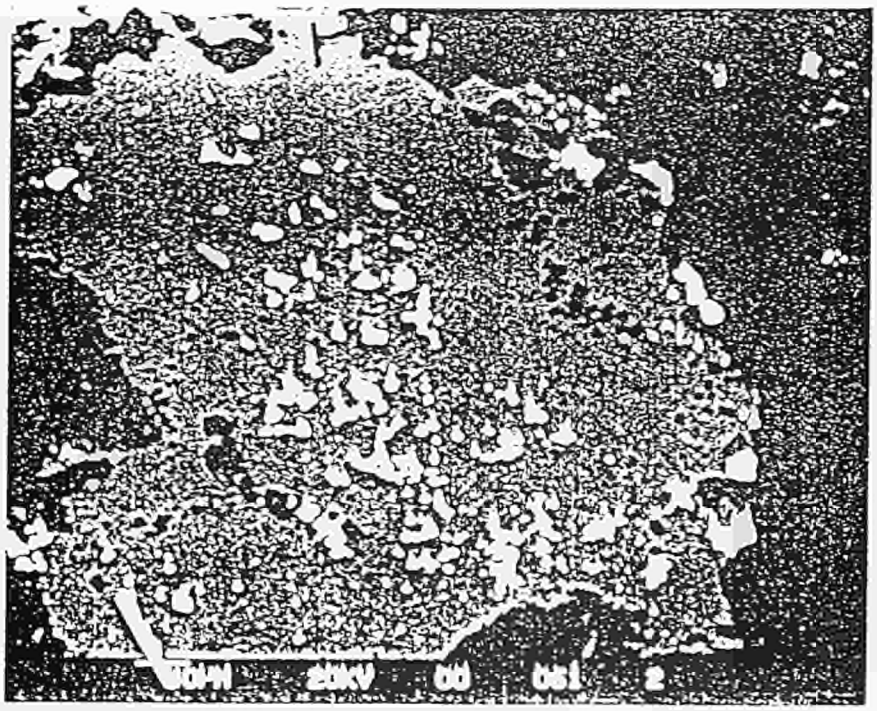

Fig. 1 (d). View in backscaterred electron mode, where galena (appears in white) is finely disseminated in sphalerite (appears in grey)

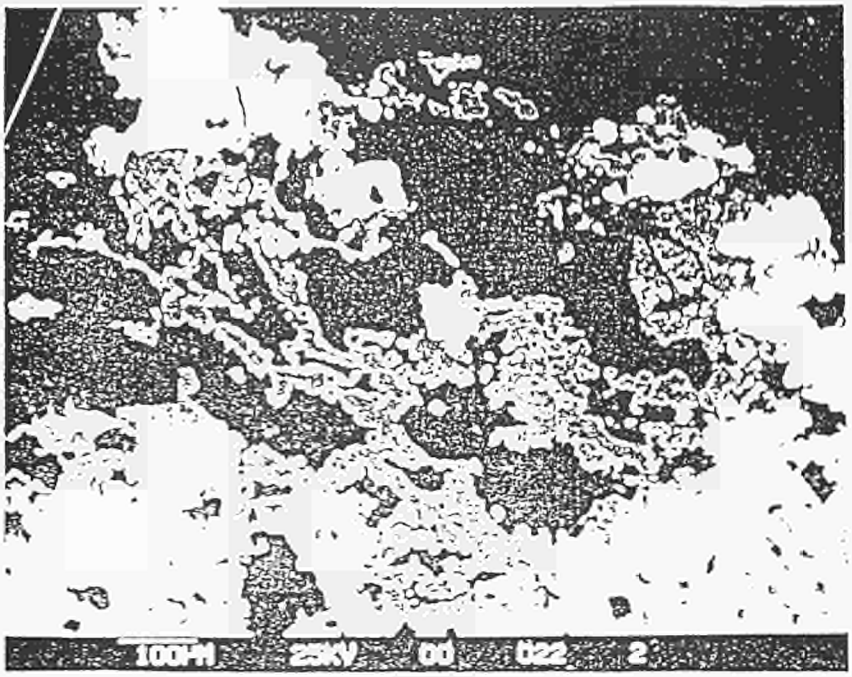

Fig.1(e). View in backscaterred electron mode, showing the zoning in smithsonite (appears in grey). Sphalerite + Pb-bearing minerals appear in white and silicates in black

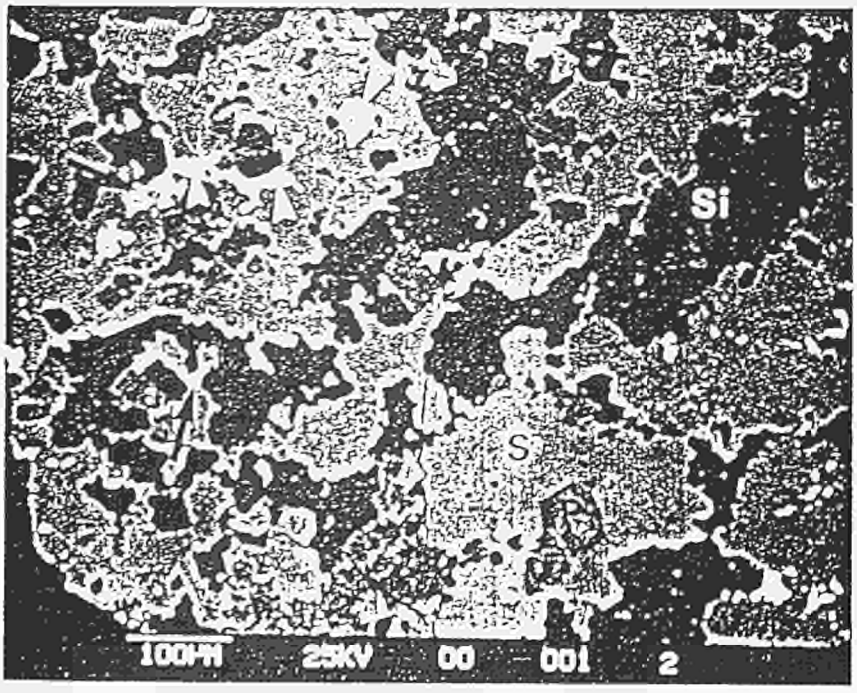

Fig. 1 (f). Another area showing the close association and fine dissemination of the minerals ; sphalerite (S), pyrite (P), tetrahedrite (arrowed in white), galena (arrowed in black). Quartz and silicates (Si) appear in black

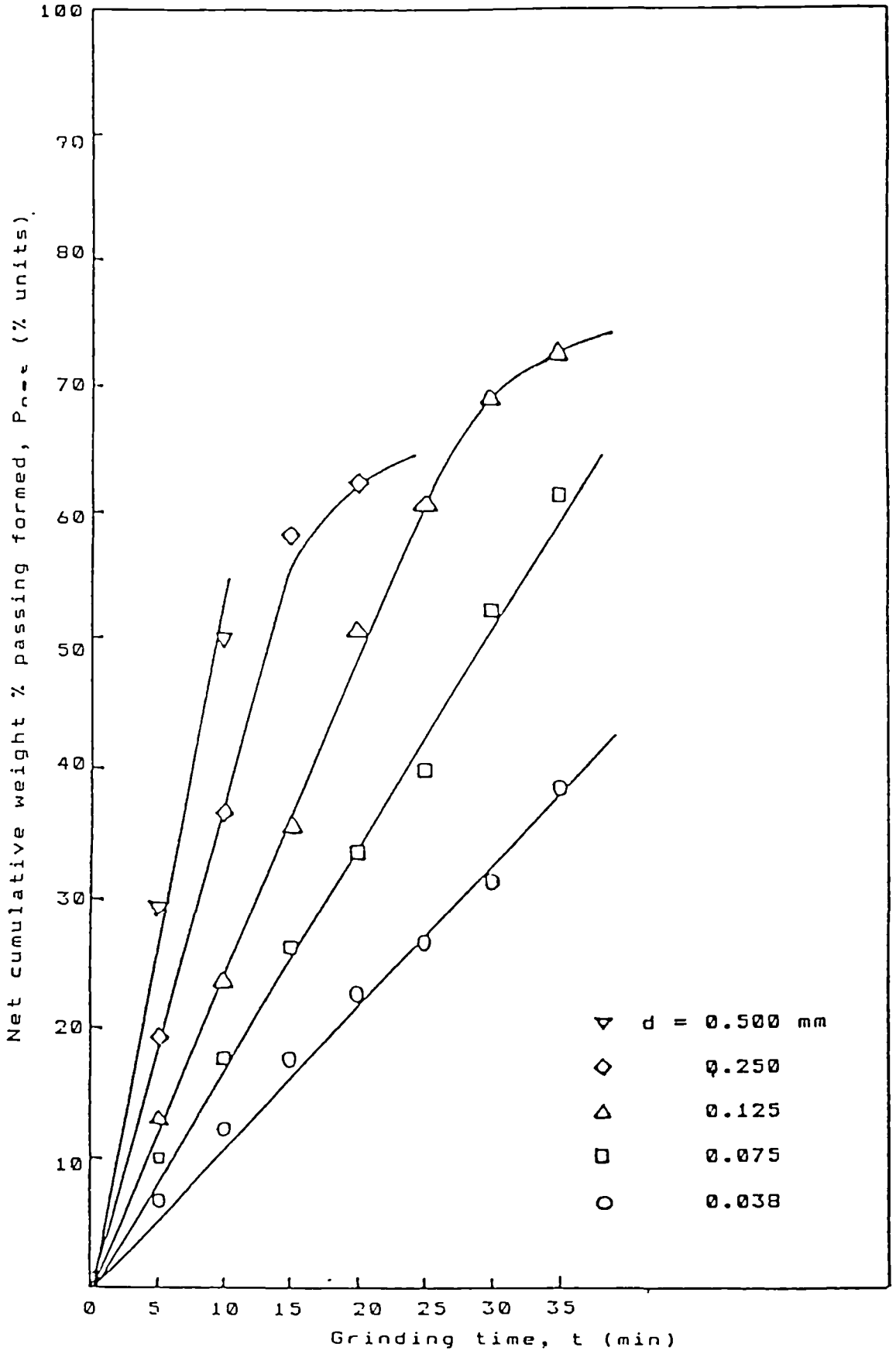

Fig. 2. Initial rate of formation of net material with particle size ≤ d, for various sizes d

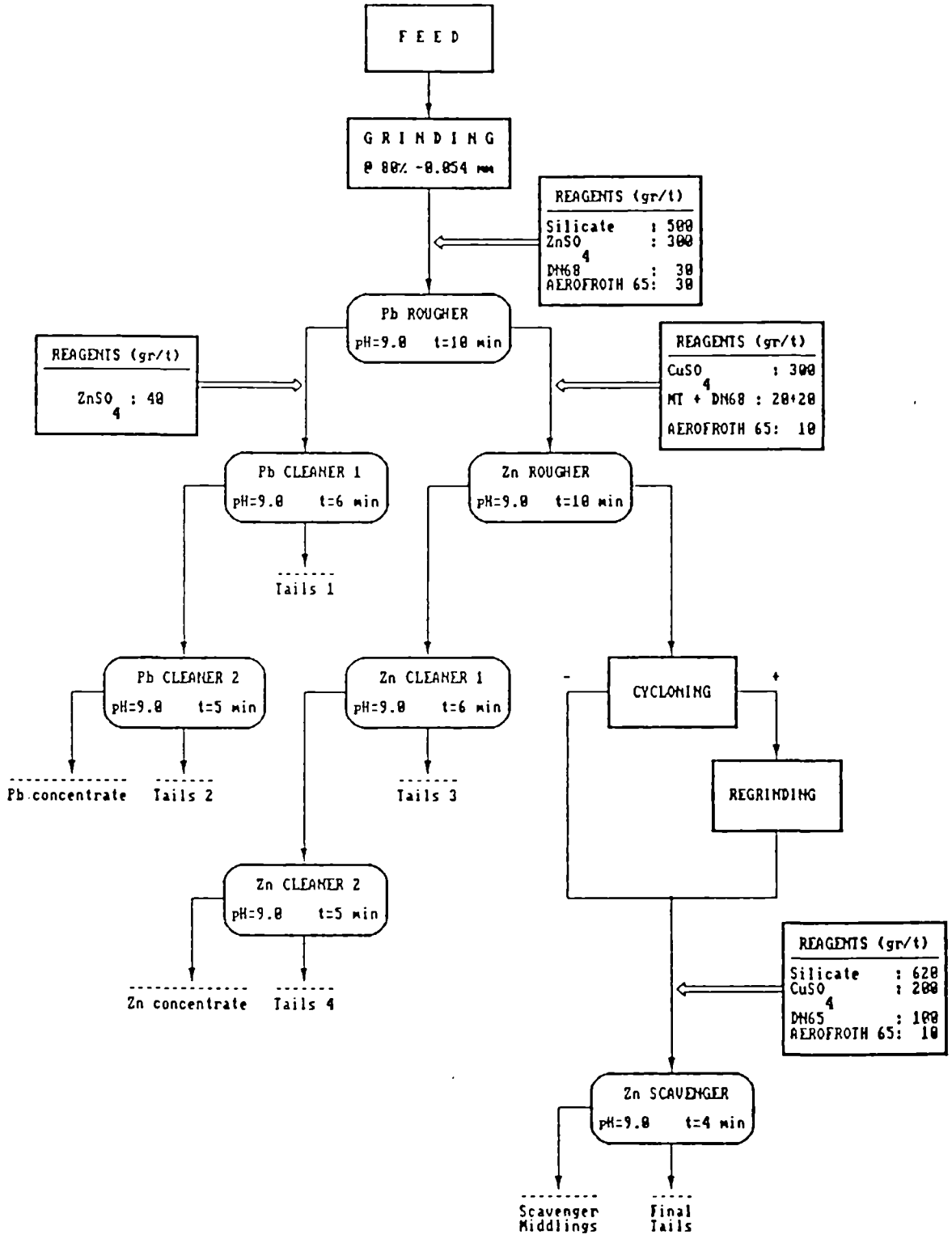

Fig. 3. Representative flow sheet for differential flotation of confirming test (test 41) with new collectors for the oxidized sample

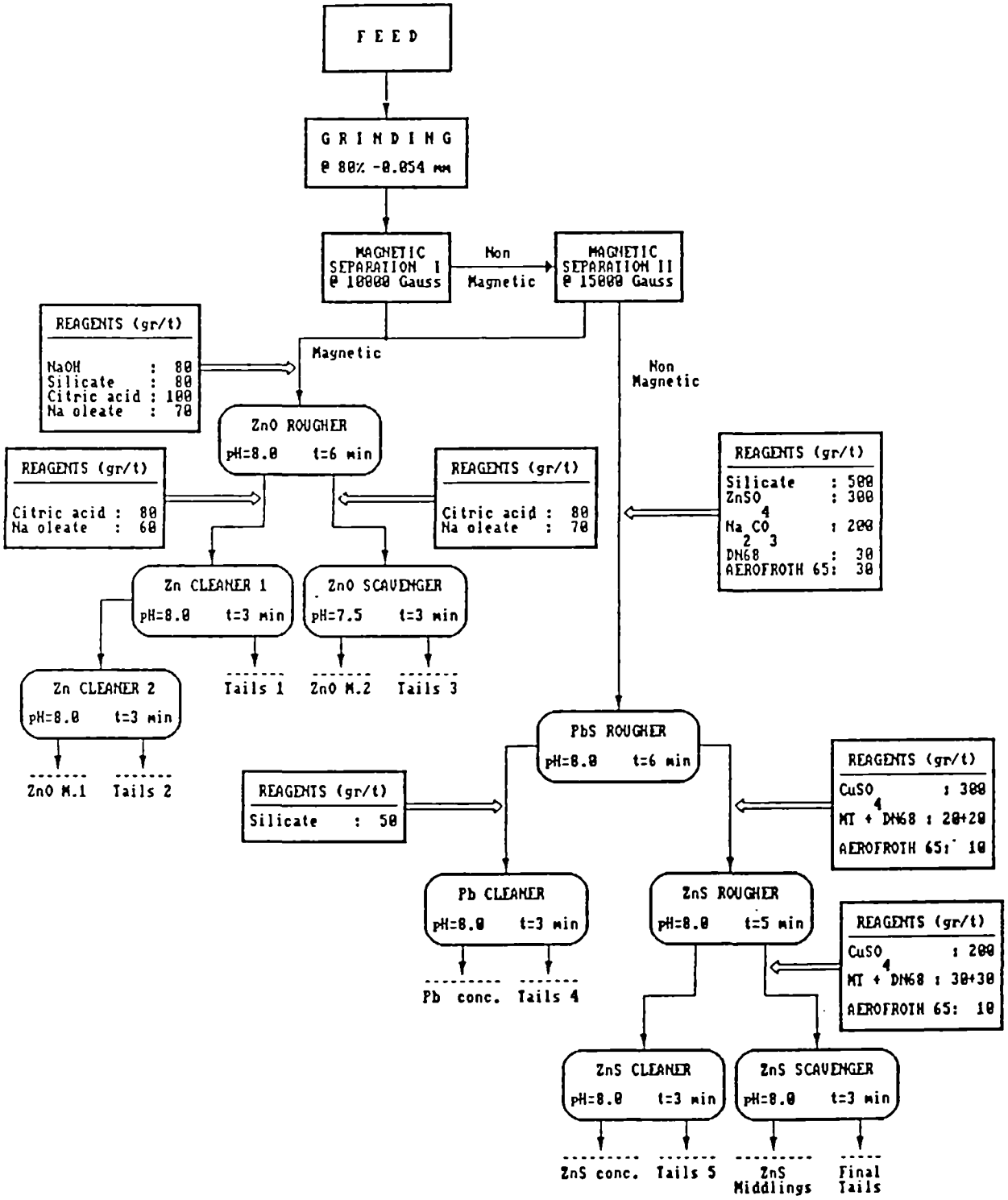

Fig. 4. Representative flow sheet for magnetic separation and flotation (test 46) with new collectors for the oxidized sample (raw sample)

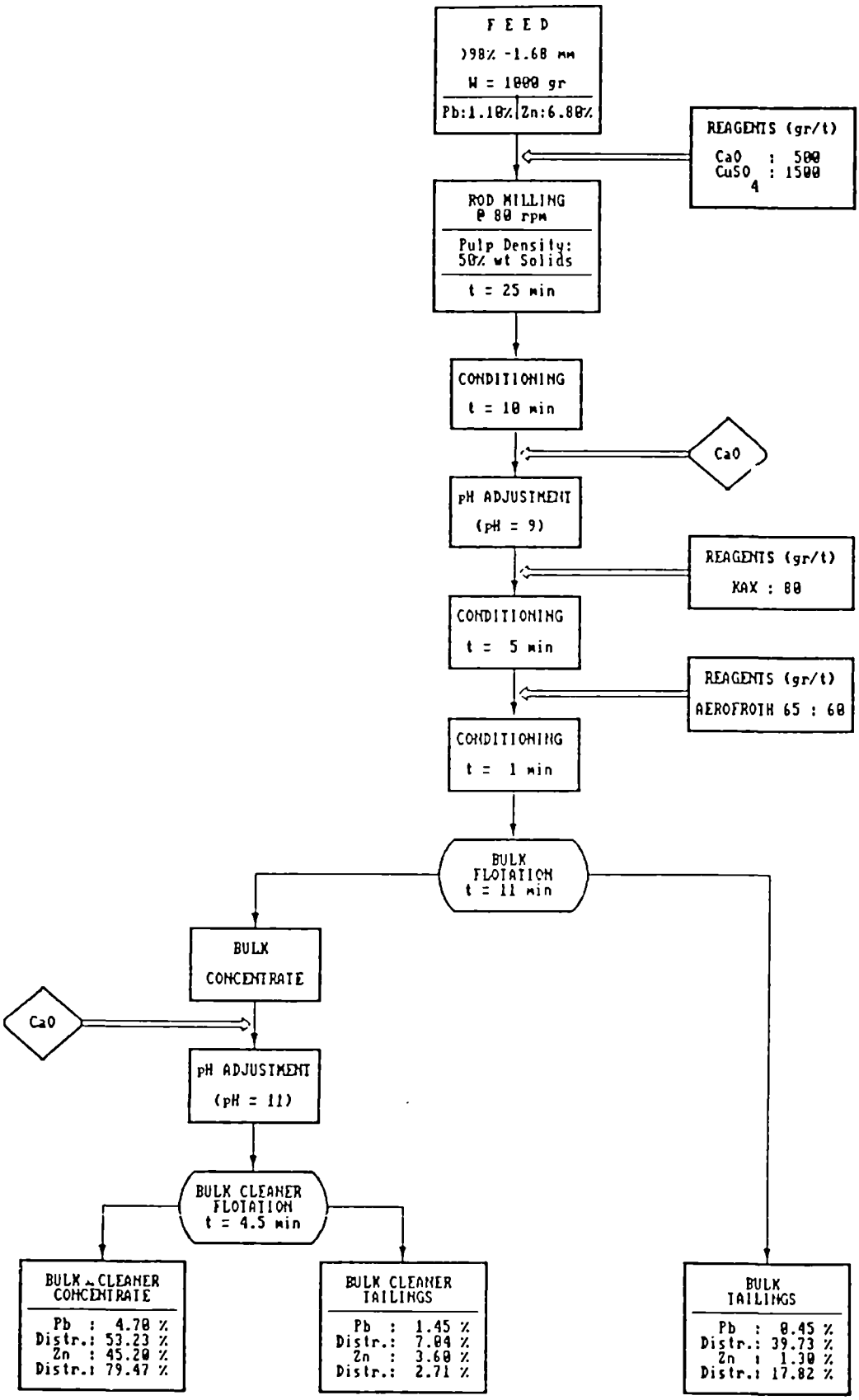

Fig. 5. Flow sheet and conditions for Bulk Flotation Test No. B5

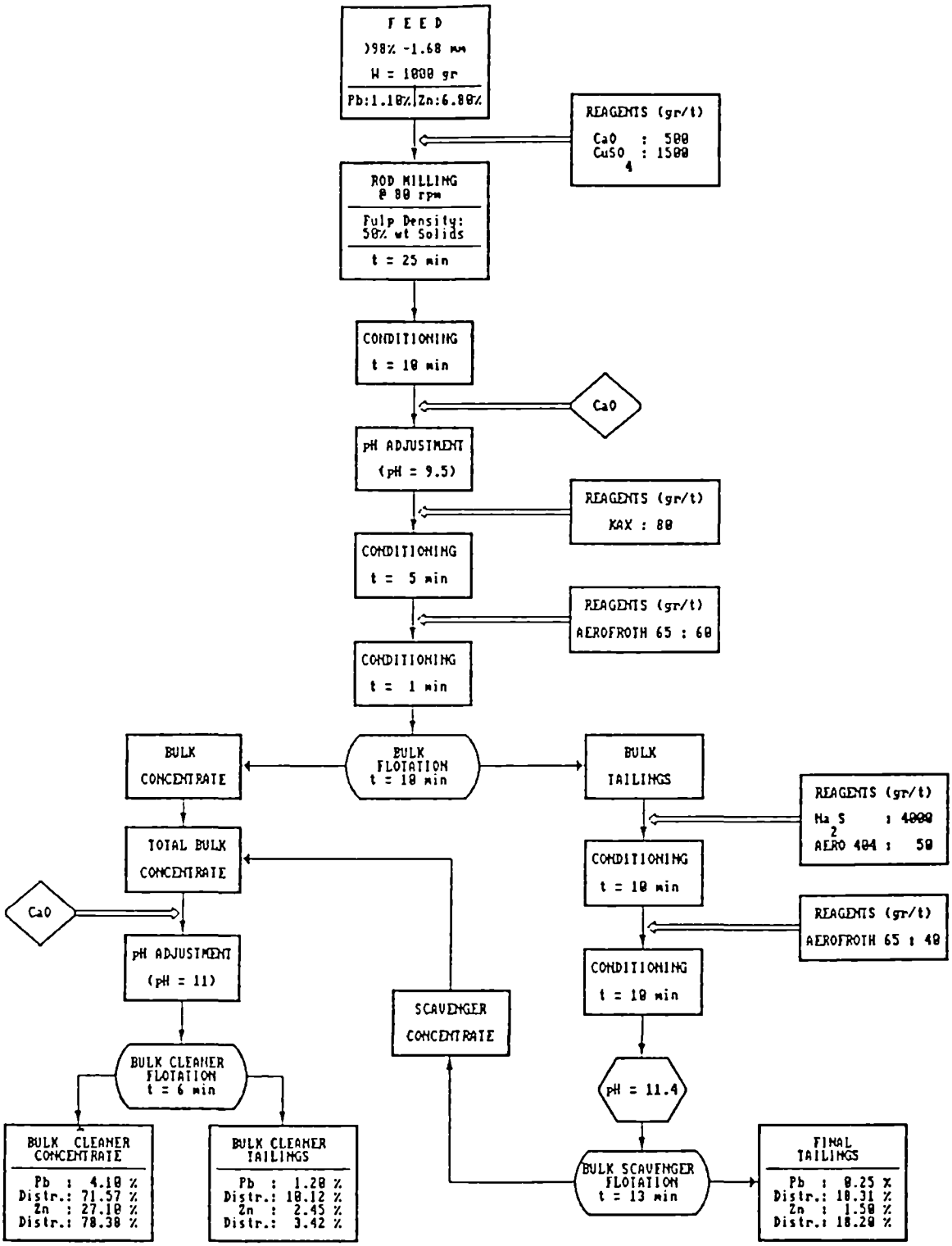

Fig. 6. Flow sheet and conditions for Bulk Flotation Test No. B16

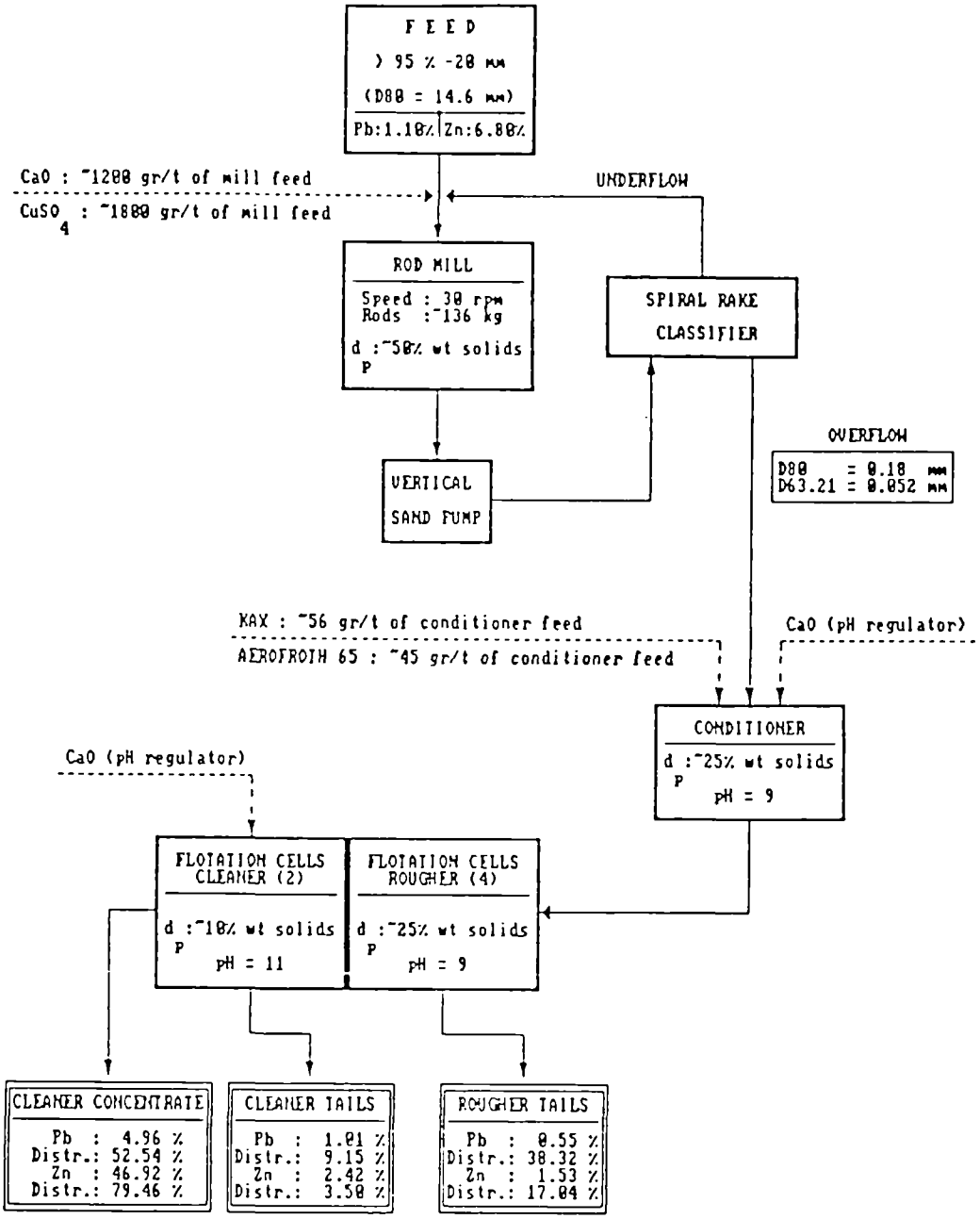

Fig. 7 : Flow sheet for the Final Pilot Plant Test

APPLICATION OF PHOSPHORIC ESTERS TO THE FLOTATION OF FINELY DIVIDED OXIDIZED ORES:

Project Leader: G. BAUDET
Bureau de Recherches Géologiques et Minières (BRGM), Orléans, France

G. MORTEANI
Technische Universität München, Lehrstuhl Für Angewandte Mineralogie and Geochemie, Munich, Germany

M.P. STRUB
C.E.C.A. – S.H.P.C. Laboratoire Recherche Application S.H.P.C., Corbehem, France

Contract MA1M-0059-C

1. OBJECTIVES

The objectives of the Research program were:

- to develop new phosphoric ester (P.E.) for flotation collectors with optimum performance for concentrating finely divided oxidized Rare Earth Elements bearing ores (R.E.E.)
- to define R.E.E. bearing minerals occurring in typical ores
- to develop flotation processes using P.E. derivatives, alone or in conjunction with other promoters, as collectors applicable to difficult to beneficiate R.E.E. ores. This could promote the development of new deposits which would constitute new potential R.E.E. sources for European producers.

2. INTRODUCTION

Preliminary laboratory studies have shown that particular types of phosphoric esters, jointly developed by GERLAND (at present C.E.C.A. - S.H.P.C.) and B.R.G.M. [2] [3], for separating carbonates from phosphate by flotation of sedimentary high carbonate phosphate rock, exhibit good selectivity and strong collecting properties for certain finely oxidized divided minerals. This specially applies to rare earth oxides (R.E.O.), as an example a high R.E.O. concentration ratio value of 11 was achieved using a P.E. as a collector, on a - 20 μm stabilized slimes sample containing less than 1 % total R.E.O. as monazite [1], associated with clays, silica, feldspar and iron minerals.

Despite a R.E.O. world production well below the mining capacity, it appears that R.E.O. supply to Europe and production of refined derivatives are sensitive to the following factors:

- increased semi-refining and refining capacities in R.E.O. concentrates producing countries,

- fluctuating demand in certain rare earth derivatives depending upon end uses and new developing applications. This is related to the relative amounts of rare earth elements contained in bastnaesite, monazite and xenotime concentrates,

- occurrence of radio active Th in high amount in most of the monazite concentrates, which are widely used in Europe, along with a significantly lower total R.E.O. content with respect to bastnaesite concentrates dominantly used by the refining plants in the U.S.A.,

- insufficiently diversified sources of concentrates and low acceptable grade ore reserves,

- emergence of China as a major producer of both R.E.O. concentrates, with high Eu content, and refined oxides.

With a view to increase diversification and quality of European sources of R.E.O. concentrates it would be desirable to evaluate new potentially interesting deposits the development of which closely depends upon performance of beneficiation. This applies to flotation which appears as the most flexible and promising process for recovering R.E.O. values from difficult to beneficiate ores containing finely divided R.E.O.

The collaborative research project between B.R.G.M., the Technical University of Munich, C.E.C.A. - S.H.P.C. laboratories was developed to investigate the response to flotation of R.E.E. minerals with P.E. as collectors.

The research program covers the following:

B.R.G.M. and the Technical University of MUNICH	- selection and characterization of R.E.E. ore samples, with special attention given to determinations of R.E.E. contents in R.E.E. bearing minerals
B.R.G.M.	- preparation of R.E.E. ores to liberate minerals to be separated
	- laboratory flotation tests to correlate compositions of phosphoric esters to their performance for R.E.E. concentration

C.E.C.A.-S.H.P.C. and B.R.G.M.	- synthesis and characterization of new phosphoric ester collectors
	- analysis of flotation data in order to select the more selective P.E. and optimize their composition

3. EXPERIMENTAL WORK

3.1. MATERIALS

Three samples taken from deposits under the exploration-evaluation phase, containing different major R.E.E. bearing minerals have been selected:

- ore 1: containing R.E.E. and Y rich apatite, from NORTH AMERICA
- ore 2: containing low Th monazite, from AFRICA
- ore 3: containing bastnaesite, from TURKEY.

Ores 1 and 2 have been collected and characterized by the B.R.G.M., ore 3 by the Technical University of Munich (T.U.M.).

3.2. METHODS

3.2.1. Characterization of materials

3.2.1.1 *Microscopy - Ore mineralogy*

- Optical microscopy. Observations by both reflected and transmitted light on polished sections and polished thin sections

- Scanning electron microscopy, for qualitative or semi-quantitative chemical determinations of minerals. An EDAX analysis system coupled with the S.E.M. was used by the T.U.M.

- Analysis by the electron microprobe. Quantitative chemical determinations of minerals were made by B.R.G.M. laboratories, using a CAMECA microprobe and data processing specially designed for R.E.E. analysis. P, Ca, Si, Fe, Ce, Pr, Nd, La, Sm, Gd, Y (or Dy, Yb and Er substituted for Ce, Pr and La) were determined on R.E.E. bearing minerals ; S, Ba, Sr, Cu, Tl, Mn, Mg, La, Fe, Ce, Si, P, on gangue minerals.

- X ray diffraction analysis

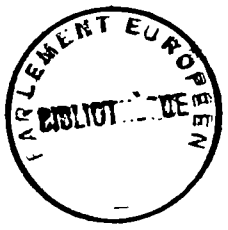

3.2.1.2 *Chemical analysis on ores and products from the treatment*

A number of techniques were used including:

- Induced coupled plasma associated to mass spectrometry (I.C.P./M.S.) for determinations of R.E.E. and other trace elements (T.U.M. and B.R.G.M.) X Ray Fluorescence for R.E.E. (T.U.M.)

- XRF on glass beads for determinations of major elements (B.R.G.M. and T.U.M.)

- Wet chemical analysis (B.R.G.M. and T.U.M.)

- FADCP, DCP, DCPA, FAA and GFAA methods (T.U.M.)

- Part of the flotation products were analyzed for Fe, Sr, Ba, La, Ce by a portable XRF analyzer (SYRANO) using a radio-active source.

3.2.1.3 *Size analysis and fractionations*

Laser light diffractometry and sieving.

3.2.2. Characterization of phosphoric esters (C.E.C.A. - S.H.P.C.)

A number of analytical and separation techniques were used to determine mono and di orthophosphoric esters, pyrophosphoric esters, free orthophosphoric acid, free pyrophosphoric acid, residual non phosphated substances, non ionic products, total P_2O_5:

- separations by ion exchange resins and by organic solvents ($CHCl_3$ + BuOH/H2O),

- potentiometry, liquid and gas phases chromatography, colorimetry, high pressure liquid chromatography.

Procedures are referenced as CFD 110 - A - 157, and CFD 110 - A - 163 methods.

3.2.3. Synthesis of phosphoric esters

Synthesis of phosphoric ester collectors involves phosphatation of alcohol, ether or phenol, including o to n oxialkylene groups, with $POCl_3$, PCl_5, PCl_3, P_2O_5, H_3PO_4 or condensed phosphoric acids. Phosphoric ester promoters are complex mixtures of mono and diesters:

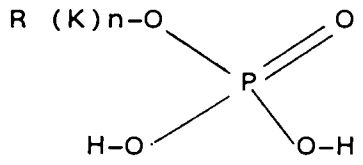

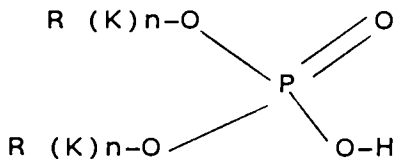

where:

- R is an hydrophobic radical: alkyl, aryl or alkyl - aryl

- (K)n are oxialkylene groups (alkyloxi)

associated with residual acids or non ionic products which affect frothing properties and collecting power: residue of phosphatation agents (pyrophosphoric and phosphoric acids, as examples), residues of alcohol or alkylphenol, esters of pyro or meta phosphoric acids ...

Frothing and collection properties, hydrophobicity of the collector coating, as well as selectivity of adsorption, are affected by numerous parameters, such as the nature of the R chain: linear chain, chains including aromatic rings, branched chains, distribution of molecular weights (or lengths) of initial alcohols subjected to phosphatation (fatty and synthetic alcohols), the nature and number of the oxialkylene groups, the nature and proportions of the residual products, the relative proportions of mono and diesters. Most of these parameters strongly depend on the operating conditions followed in the phosphatation of the initial raw material (alcohol, alkyl-phenol ...) as well as conditions used for purifying the reaction products.

Samples of phosphoric esters submitted for flotation tests were produced by C.E.C.A.-S.H.P.C. at laboratory scale, using proprietary procedures which led to control the basic parameters such as the ratio monoester/diester, the proportions of residual non phosphated substances and free acids.

Ten phosphoric ester collectors were tested and evaluated:

B 110 D 4 - 92, B 110 69032, B 110 D 4 - 70 E PE 88094, P 301, P 312, T 4 - 55 E, D 2 - 45 E, D 7 - 61 E, IM 7 - 58 (PE 89124), EA 14 - 89 (PE 89122).

3.2.4. Preparation of ore samples for flotation tests

Batch preparation was accomplished at laboratory scale using a combination of:

stage - crushing, attrition - scrubbing, wet sizing and desliming, stage rod milling down to about 200 or 160 μm (ores no 1 and 2) and 125 μm (ore no 3).

Rod milled materials were deslimed at 10 μm prior to be used as feeds to flotation.

Gravity preconcentrates - 80 + 10 μm separated by tabling from the R.E.E. ore sample 2 were also subjected to flotation.

3.2.5. Laboratory flotation tests

Tests were made using conventional laboratory mechanical flotation cells: AGITAIR or 1.5 and 5 l capacity, MINEMET of 0.8 and 2.5 l capacity.

4. RESULTS

4.1. CHARACTERIZATION OF R.E.E. ORE SAMPLES

4.1.1. Ore 1

Most of the R.E.E. mineralization occurs as apatite with small contents in heavy R.E.O., assaying 9.04% R.E.O., and 1.74% Y_2O_3. Other minor R.E.O. bearing minerals were found to be :

	Total REO content %	Y_2O_3 content %
a Cerium-britholite	50.39	4.55
a Yttrium-britholite	11.13	27.12
allanite	22.93	0
a Cerium-apatite	41.71	0.49
other REO bearing minerals (bastnaesite, parisite)	61.74	1.18
a secondary apatite with a low REO content	n.d.	n.d.

Gangue minerals consist of clinopyroxene, magnetite, biotite, albite, amphibola, ilmenite, zircon, iron carbonate, pyrite and clay minerals: kaolinite, smectite, chlorite, sepiolite and talc.

4.1.2. Ore 2

R.E.O. bearing minerals occur as:

	total REO content %
monazite (major R.E.O. bearing mineral)	69.65
apatite	4.51
trace amounts of bastnaesite and parisite	n.d.

Gangue minerals or potentially valuable minerals occur as:

- carbonates:
  - . Mn and Fe containing dolomite
  - . stontianite
  - . siderite containing Mn, Ca, Mg
  - . calcite
- sulfate : baryte
- oxides : - manganese oxides (psilomelane) containing varying amounts of Fe, Ba, Ce, Sr
  - magnetite;
- quartz

4.1.3. Ore 3

Is a mixture of two types of ores:

TU1: fluorite-baryte-REE minerals
TU2: high carbonate ore

- The first type consists of:

fluorite: 15-60%, baryte: 10-50%, bastnaesite: up to 20%, Fe-Mn oxides: up to 10%, white mica and phlogopite: up to 15%, calcite and dolomite: up to 20%, chlorite, quartz, chalcedony and other R.E.E.-minerals: up to 3%.

Most of the bastnaesite occurs in extremely fine grained felty aggregates which will generate slimes on grinding and will cause problems for its concentration and recovery by flotation.

- The second type consists of:

calcite and dolomite: 40-50%, fluorite: 15-25%, baryte: 15-20%, bastnaesite: up to 15%, white micas and phlogopite, Fe-

Mn oxides and other R.E.E.-minerals (R.E.O. containing phosphates): up to 3%.

Similarly to the first type, most of the basnaesite grains exhibit a felty texture characterizing associations of fine sized crystals as aggregates.

Chemical compositions of R.E.E. ore samples are shown in table 1.

4.2. ORE PREPARATION

- 160 + 10 μm fractions, separated from the ground ores no 1 and 2, had the following compositions:

	- 160 + 10 µm fractions	
	Ore n° 1	Ore n° 2
Weight recovery %	95.36	88.81
P_2O_5 recovery %	97.17	90.19
Total R.E.O. recovery %	95.94	93.10
Y recovery %	95.30	90.34
P_2O_5 assay %	3.19	3.62
Ca O assay %	7.41	16.95
Si O_2 assay %	57.30	4.51
Fe_2O_3 assay %	13.22	6.40
Al_2O_3 assay %	7.91	0.76
Mg O assay %	1.49	13.29
Sr O assay %		10.39
Ba O assay %		1.27
CO_2 assay %		31.29
TOTAL R.E.O. assay ppm	6528	46929
Y assay ppm	970	62

Preparation of ore 3 gave rise to production of a high proportion of - 10 μm slimes, highly enriched in R.E.E.:

	Total - 125 + 10 µm	Total - 10 µm slimes
Weight recovery %	74.57	25.43
F recovery %	79.86	20.14
Ba recovery %	94.13	5.87
Total R.E.E. recovery %	36.85	63.15
Y recovery %	57.36	42.64
F assay %	31.03	22.94
Ba assay %	14.34	2.62
Total R.E.E. assay ppm	36899	185442
Y assay ppm	306	668

Concentration of R.E.E. was even higher in the primary - 10 μm (1) slimes generated by attrition - scrubbing, total R.E.E. content was 241369 ppm, accounting for 52.85 % of the total R.E.E. contained in the initial material, recoveries of light R.E.E. (from La to Sm) in - 10 μm (1) slimes was higher: 50.3 to 53.5 %, than those of heavy R.E.E. ranging from 30 to 47.6 %. Since most of the R.E.E. bearing minerals report to the - 10 μm attrition and grinding slimes, further concentration by flotation or other physical separation process appeared to be extremely difficult.

4.3. FLOTATION TESTS - EVALUATION OF PHOSPHORIC ESTER COLLECTORS

4.3.1. Ore 1

Prior to flotation, most of the magnetite was removed from the - 160 + 10 fm fraction by a low intensity magnetic drum separator, preliminary tests conducted on the - 160 + 10 μm NM fraction have shown that:

- selectivity of separation of the Y containing apatite by flotation, using certain types of phosphoric ester promoters, was superior to that obtained through conventional apatite flotation using direct anionic flotation of apatite with an aqueous emulsion of tall oil, diesel oil and an emulsifier reagent, sodium silicate as depressant and dispersant of the silíceous gangue and corn starch as a depressant of iron bearing minerals.

- addition of specific depressants for both silicates and iron containing minerals was necessary to produce low R_2O_3 and MgO apatite concentrates, using phosphoric esters as collectors for apatite at pulp pH of about 9. The best depressant was a solution of sodium silicate and citrate (with 5/1 concentration ratio) in combination with dextrine or waxi starch.

Preliminary testwork has led to the definition of a standard flotation flowsheet for separating R.E.E. and Y containing apatite from silicates and iron bearing minerals.

Basic flowsheet shown in figure 1 was applied to the - 0.2 + 0.01 mm ore, using 8 types of phosphoric ester collectors, collector dosage was 225 g/ton of flotation feed.

Results of tests are shown, in a synthetic manner, as grade-recovery curves for P_2O_5 in diagrams of the figure no 2.

Positions of grade-recovery curves reflect performances of phosphoric ester collectors in terms of selectivity and apatite recovery, it can be seen that the B 110 - 88094 provides the best response of the ore to flotation.

Performances of phosphoric esters are in the following decreasing order: 88094 - 69032 - T455E - B110 - D245E - D761E - P301 - P312.

The collecting power increases with n, while selectivity appears to be detrimentally affected at high n values.

Linear chains in the hydrophobic radicals R provide better selectivity than branched chains, optimum performances are obtained for n = 4, 70 % monoester and low amount (about 5 %) of residual non phosphated products, influence of free phosphoric acids is not clearly understood.

Chemical compositions of apatite concentrates separeted using the phosphoric ester reagent 88094 as a promoter are given below:

	Apatite concentres		Feed to flotation
	F 3 + F 4	F 3	
P_2O_5 %	31.82	33.10	3.42
CaO %	45.72	46.35	7.74
SaO_2 %	6.92	5.75	62.56
Fe_2O_3 %	1.20	0.95	5.92
Al_2O_3 %	0.55	0.42	8.69
Mg O %	0.53	0.50	1.64
L.O.I. %	3.10	2.31	1.09
La ppm	7650	7610	1679
Ce ppm	14800	14220	3009
Nd ppm	7030	6830	1124
Sm ppm	1525	1485	217.5
Eu ppm	149.9	155	20.2
Gd ppm	1640	1650	209.2
Dy ppm	1420	1480	185.1
Er ppm	853	870	102.5
Yb ppm	783	792	89.7
Y ppm	8015	8080	1006.2
Total R.E.E. ppm	43865.9	43172	7642.4
CaO/P_2O_5	1.437	1.400	2.263
R_2O_3/P_2O_5	0.055	0.041	4.272
T.C.P. %	69.53	72.32	7.47
P_2O_5 recovery	81.93	64.54	100

Separation of apatite with phosphoric ester leads to marketable grade phosphate concentrates with low contents in contaminants such as R_2O_3 and MgO. Conversion of P_2O_5 values to marketable wet process phosphoric acid appears to be possible besides recovery of rare earth elements and yttrium.

The enrichment ratio for P_2O_5 ranges between 9.3 and 9.7, the enrichment ratio is 5.74 - 5.65 for R.E.E. + Y, 7.96 - 8.93 for Y.

Phosphate concentrates assaying 31.8 - 33.1 % P_2O_5, 4.39 - 4.32 % R.E.E. + Y, 0.8 - 0.81 % Y can be produced at satisfactory recoveries on flotation feed basis: 81.93 - 64.54 % for P_2O_5, 50.4 - 37.5 % for R.E.E. + Y and 69.9 - 53.2 % for Y.

Differences between R.E.E. - Y and P recoveries account for R.E.E. and Y losses in flotation tails as R.E.E. and Y containing silicates: britholite and allanite which were identified by the mineralogical study. R.E.E. and Y bearing silicates are not amenable to flotation using phosphoric esters as collectors.

4.3.2. Ore 2

Extensive laboratory testwork was effectuated on:

- the - 0.05 + 0.01 mm size fraction separated from the ore ground down to 0.16 mm

- gravity preconcentrates separated by tabling from the - 0.08 + 0.01 mm fraction of the ore ground down to 0.16 mm.

Flotation involves separation of monazite from: Mn - Fe containing dolomite, strontianite, calcite and baryte.

Results have shown that:

. separation of baryte as a non float product is possible, using H_2SO_4 as a baryte depressant and pH regulator, phosphoric ester P301 as a collector for monazite and strontianite

. strontianite could be floated with pretroleum sulfonate as a collector

. conditioning with CO_2 can depress Fe - Mn dolomite, calcite and strontianite when monazite is floated with phosphoric ester in a weak acidic pulp. Separation of monazite from strontianite requires a high number of cleaning stages.

- Performance of flotation on the - 0.05 + 0.01 mm fraction of the ore with a monazite content of 13 %, was poor in terms of R.E.E. recovery: the best concentrate assays 11.61 % La_2O_3 and 19.77 % CeO_2 at 32.3 and 31.8 % La and Ce recoveries. This corresponds to a 40.9 % content in total R.E.O. or a monazite content of 58.7 %. Further enrichment of this preconcentrate appears to be possible using multiple cleaning stages in an attempt to remove residual iron bearing dolomite.

- Response to flotation of the gravity preconcentrate with a monazite content of 68.5 %, is promising since the flotation concentrate assays 19.3 % La_2O_3 and 32.38 % CeO_2 at 68.0 and 68 % La and Ce recoveries, for a phosphoric ester consumption of 70 g/t.

The flotation concentrate assays 67.4 % total R.E.O., corresponding to a monazite content of 96.7 %.

Retreatment of middling products could probably lead to improved monazite recoveries in concentrates.

It should be pointed out that magnetic separation applied to this gravity preconcentrate does not lead to a satisfactory monazite concentrate due to the fact that Fe - Mn dolomite and monazite have similar magnetic susceptibilities.

Phosphoric ester collectors were evaluated for their capability to float monazite from the - 80 + 10 μm gravity preconcentrate, using the basic flowsheet shown in figure no. 3.

Flotation performance is shown as grade - recovery curves in figure no. 4, phosphoric ester dosages were 70 g/t for long chain reagents and 120 g/t for short chain esters.

Data of figure 4 indicate that the best performances were obtained using EA 14-89 and D9PS2 reagents at low dosages of 70 g/t, concentrates assaying 93.3-94.3 % monazite at 79.3-80 % recovery were separated in batch operation, excluding retreatment of middling products.

High number of oxialkylene group appears to promote both high selectivity and collecting power, proportions of residual non phosphated products as well as the monoester/diester ratio have no clear influence on selectivity. Collectors with branched chains show higher collecting power with respect to linear chains reagents for similar numbers of oxialkylene groups.

The behaviour of phosphoric esters in monazite flotation is found to be different to that observed in flotation of Y containing apatite, this could be attributed to the different compositions of the gangue minerals.

4.3.3. Ore 3

Flotation of the - 125 + 10 μm fraction with phosphoric esters led to moderate concentration of fluorite and R.E.E. minerals in float fractions, however, selectivity for R.E.E. was poor, probably due to the fact that the R.E.E. minerals are insufficiently liberated as shown by results of heavy liquid separations.

Results of flotation tests on - 10 μm primary slimes also showed no significant concentration of R.E.E., this could be related to the extremely fine size distribution of the flotation feed material : 89.1% by weight minus 6 μm, 55.5% minus 3 μm, 33.5% minus 2 μm.

5. CONCLUSIONS

Laboratory investigations conducted on three R.E.E. ore samples differing by the nature of the main R.E.E. bearing minerals clearly show that certain types of phosphoric esters exhibit high affinity for Y and R.E.E. containing apatite as well as for monazite, and could be used as collectors for concentrating these minerals by flotation provided that the composition of the gangue allows selectivity to be achieved. Results of flotation tests on the monazite ore indicate that monazite could be efficiently separated from strontianite, baryte, iron and manganese oxides, whereas concentration performance sharply drops in the presence of high proportions of Mn and Fe containing dolomite which responds quite well to flotation with phosphoric esters. Removing most of this contaminant by tabling leads to a gravity preconcentrate which is refined by flotation to produce concentrates assaying 94 to 97 % monazite. Results of flotation tests on the bastnaesite ore suggest that phosphoric esters have low affinity for bastnaesite.

Separation of Y and R.E.E. containing apatite from silicates and iron minerals by flotation with a phosphoric ester collector has led to marketable grade apatite concentrates with acceptable contents of residual MgO and R_2O_3.

This makes possible conversion of P_2O_5 values into marketable wet process phosphoric acid besides recovery of rare earth elements and yttrium.

The best separation performance for R.E.E. containing apatite has been obtained with a P.E. collector including 70 % monoester, 4 ethylene oxide groups per molecule, a linear hydrophobic chain and a low amount of residual non phosphated products. As a rule flotation tests indicate that the collecting power of P.E. increases with the number of oxiakylene groups, within a range of variation of 2 to 14, collectors with branched chains also show higher collecting power in comparison with linear chains.

Clear conclusions cannot be drawn regarding the influence of the composition of P.E. on the selectivity of separation, results obtained on the apatite and monazite ores suggest that the composition of the collector should be adapted to the minerals to be separated.

6. REFERENCES

[1] G. BAUDET, J.L. CECILE, P. OLLIVIER (1983):
Traitement des grès armoricains à titane, zirconium et terres rares : production d'un concentré global.
Rapport BRGM 83 SGN 480 MIN
CEC contract no MPP-131-F (RS) July 1983.

[2] G. BAUDET, J.L. CECILE, A. HENCHIRI, M. SAVE (1984)
Enrichissement des minerais sédimentaires à gangue carbonatée par flottation inverse et double flottation, utilisant un ester phosphorique comme collecteur.
L'Industrie Minérale - Les Techniques, Février 1984, pp. 123 - 149.

[3] G. BAUDET, M. LAROUCI, P. MONDI, M. SAVE (1989)
Performance des procédés de flottation par les esters phosphoriques dans le traitement des minerais de phosphate sédimentaire à gangue carbonatée.
L'Industrie Minérale - Mines et Carrières - Les Techniques
Janvier - Février 1989, pp. 48 - 63.

[4] G. BAUDET (1989 - 1990)
Application of phosphoric esters to flotation of finely divided oxidized ores.
Progress report no 1 - April 1989
Progress report no 2 - March 1990.

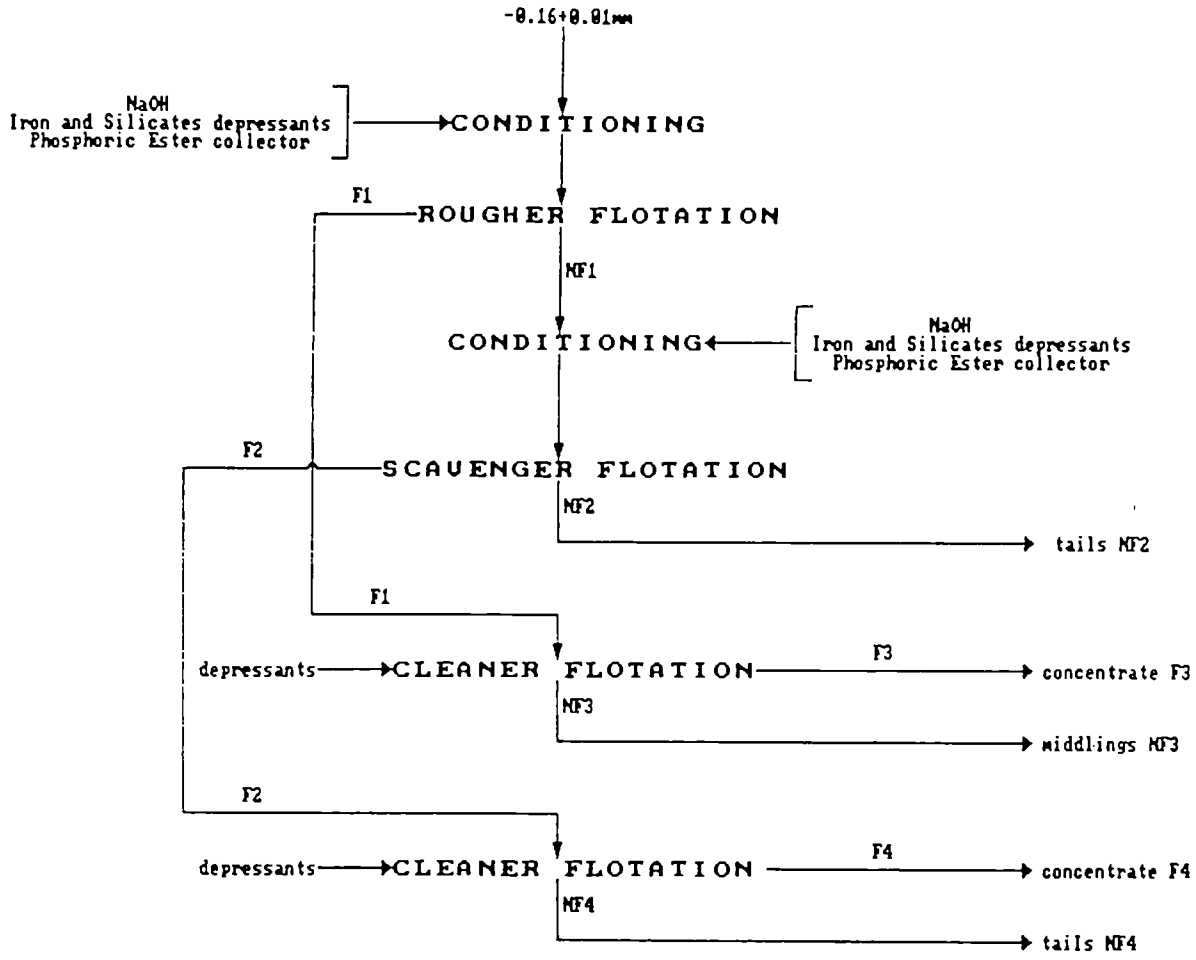

FIGURE n° 1 : basic flowsheet for flotation of the REO ore sample n°1.

FIGURE N 2.

R.E.O. ORE SAMPLE 1.FLOTATION TESTS

PERFORMANCE OF PHOSPHORIC ESTERS

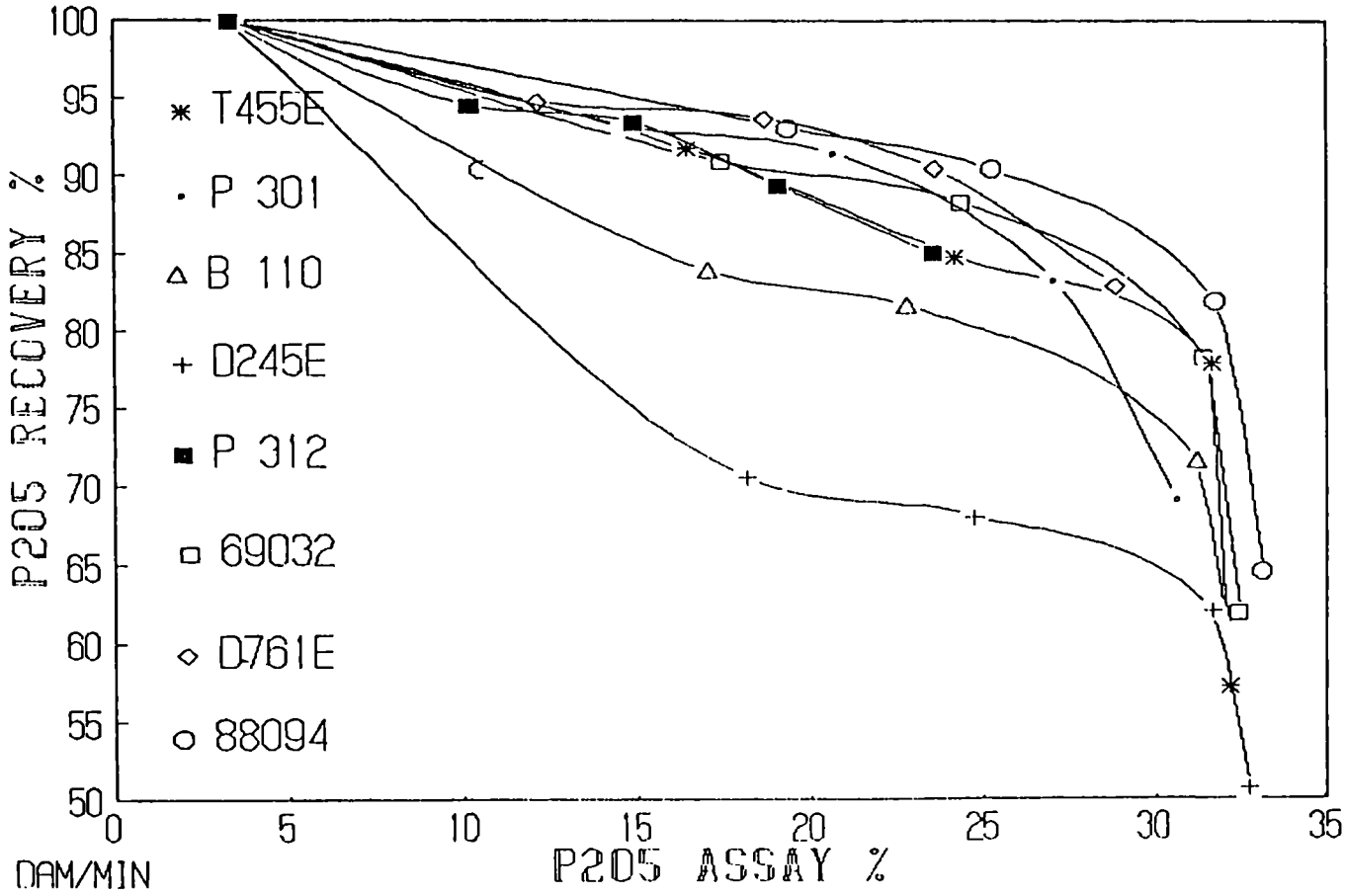

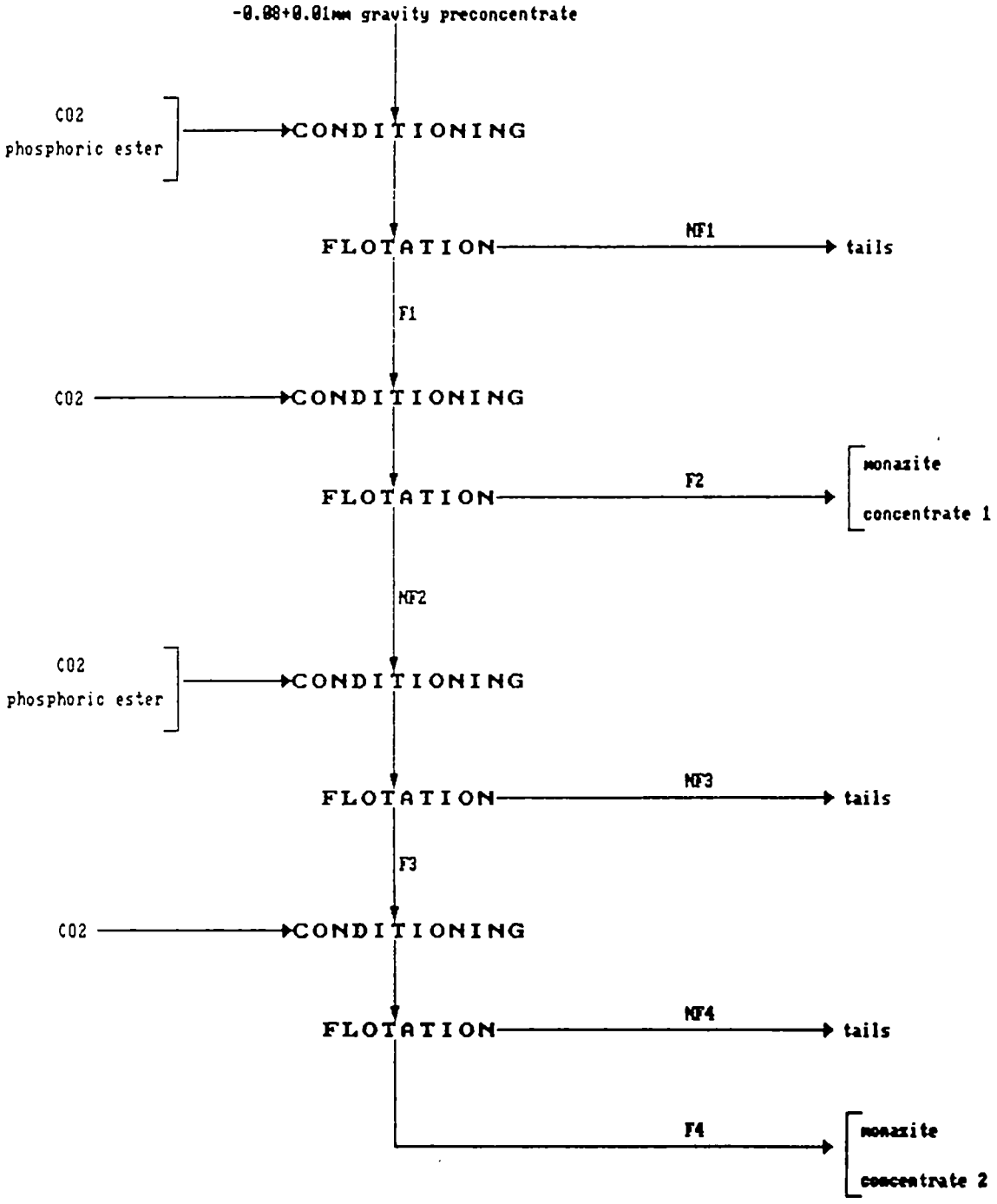

FIGURE n° 3 :basic flowsheet for flotation of -0.08+0.01mm gravity preconcentrates separated from the R.I.O. ore sample n°2 ground down to -0.16mm.

FIGURE N 4

R.E.O. ORE SAMPLE 2.FLOTATION TESTS

PERFORMANCE OF PHOSPHORIC ESTERS

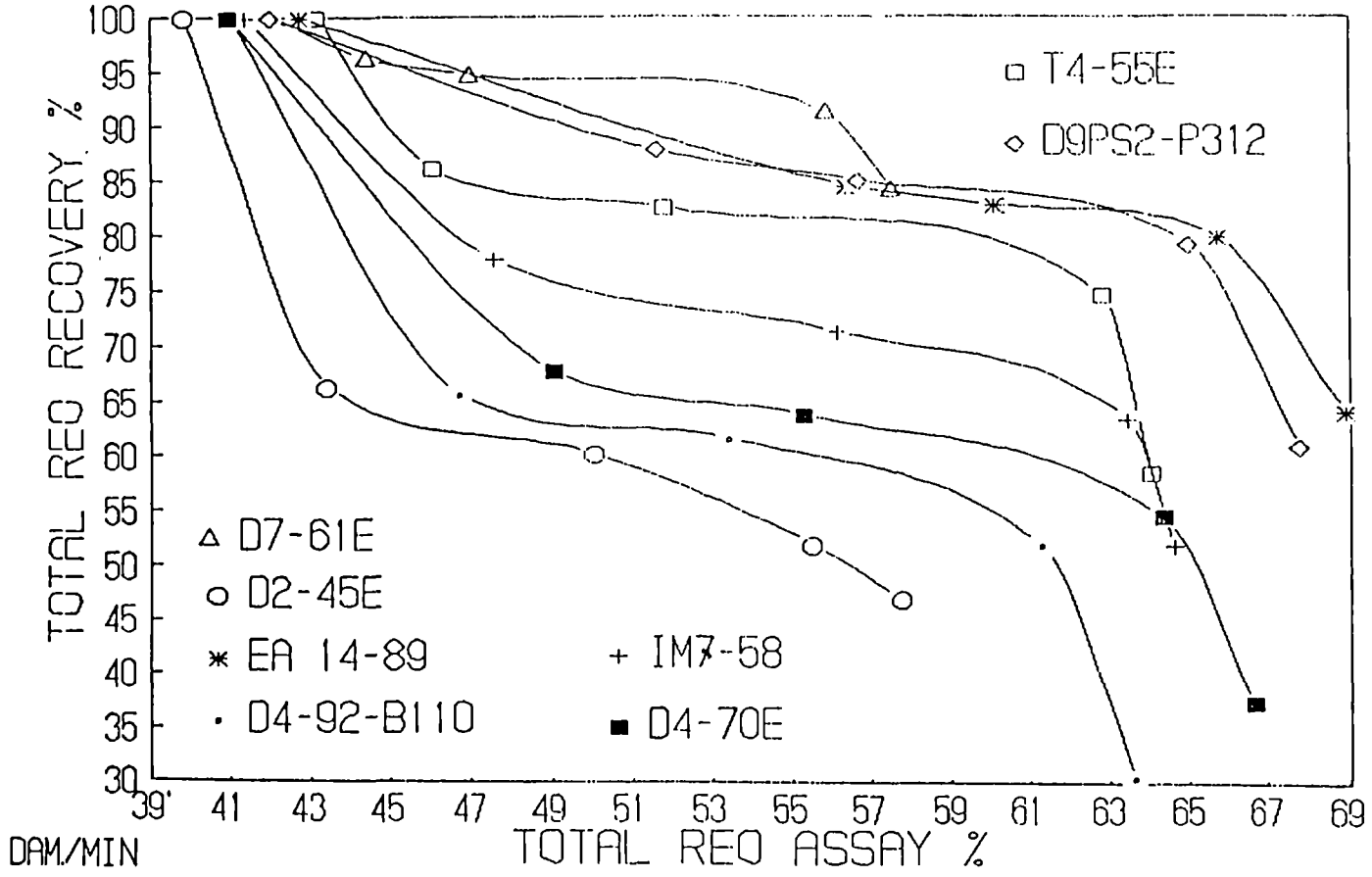

IMPROVEMENT OF COMPLEX SULPHIDE FLOTATION USING NEW REAGENT CHEMISTRY

Project Leader: M. ACOSTA FERNANDEZ
Minas de Almagrera S.A., Spain

S.A. LAMBERT
Cyanamid U.K. Ltd, United Kingdom

K.P. WILLIAMS & R.J. EDWARDS
University of Wales College of Cardiff, United Kingdom

Contract MA1M-0064-C

1. OBJECTIVE

The primary objective of this project was to determine whether flotation reagents other than those in current use at Minas de Almagrera would be capable of providing the improvements in metallurgical performance given in the table 1.

Secondary objectives involved gaining improved understanding of the process mineralogy and surface chemical effects contributing to reagent adsorption.

2. INTRODUCTION

This project involved a tripartite collaboration between Minas de Almagrera S.A., Cyanamid G.B. Ltd. and University of Wales College of Cardiff, U.K.

Cyanamid G.B. Ltd. were responsible for providing well characterised flotation chemicals, limited development of new reagents, and for providing technical input on all chemical matters.

The majority of the experimental work was carried out in the laboratories of the Mining and Minerals Engineering Division of the School of Engineering at the University of Wales College of Cardiff, where the project coordination was performed by Dr. K. P. Williams. A Research Associate was employed at Cardiff for the duration of the project, and a member of the technical staff at Almagrera was seconded to Cardiff for a period of three months during the first year.

Since commencement of operations, the processing plant at Almagrera has seen continuous modifications aimed at improvement of grades and recoveries for the three metal concentrates and pyrite for acid manufacture. Such modifications have involved reconfiguration of process routes, reduction of milling capacity, and more recently the replacement of cleaner cells in the lead and zinc circuits by column flotation. Limited work has been performed with different reagent suites.

At an early stage in the project it was agreed between the collaborators that attention should be focused on the copper circuit, with the constraint that minimal departure from the existing flotation circuit should be considered in the first instance. It was considered that use of strong pyrite depressants might be harmful to the subsequent performance of the zinc circuit, an area which has received much attention by the plant personnel. For this reason a significant effort has been aimed at improving copper flotation performance, principally by means of alternative collectors and modifications to the chemical conditions in the pulp, but also by variation in comminution.

This report summarises the information given in the interim and final reports submitted periodically during the investigation, 1-4.

3. RESULTS AND DISCUSSION

3.1. BASE-LINE PLANT STUDY

From historical data collected at the mine and from the results of a plant investigation conducted at an early stage in this project, the flotation behaviour of each of the three metals, Cu, Pb and Zn were studied as functions of particle size. Figures 1, 2 and 3 show typical size/recovery data generated at Almagrera for each of the base metals in the copper, lead and zinc concentrates respectively. Clearly the copper recoveries increase as the particle size decreases, whilst as expected the galena float deteriorates below about 10 μm. Size has less effect on zinc recovery. There is some evidence to suggest that Cu recoveries will also decrease in the very finest fractions.

The distributions of metals between size fractions in certain streams is interesting. For example, in the primary cyclone overflow, over 53% of the Pb is found in the -8μm fraction, whilst less than 45% of the C is found in this size range. In the concentrates the metal values exist predominantly in the finer fractions. For this reason it is not surprising to find that comparatively little size reduction is achieved in either of the regrind mills. Plant trials without using the copper circuit regrind mill have so far proved inconclusive, and work is continuing at Almagrera in this area.

This initial plant study demonstrated high losses of Cu and Pb in both the +15μm and -8μm size fractions.

3.2. MINERALOGY OF THE ALMAGRERA ORE

Prior to commencement of current operations at Almagrera, a detailed mineralogical study of drill cores taken from the orebody was performed by Empresa National Adaro de Investigaciones Mineras (ENAIM) S.A. in 1973. The Spanish report was translated into English as part of this present study, and in addition further mineralogical examinations of polished sections of run-of-mine ore have been performed.

The mineralogy is basically simple in that the only important minerals are pyrite, sphalerite galena and chalcopyrite, with only the fineness of associations allowing this ore to be termed "complex".

The Almagrera orebody consists of pyrite layers within which the following occur:

a) A deposit enriched in copper (chalcopyrite), which is generally located on the outside of the central mass.
b) A nucleus enriched in zinc (sphalerite) and lead (galena).
c) The remaining pyrite mass.

3.2.1. Size Distributions and Individual Liberation of the Main Ores

Sphalerite

The granulometry of sphalerite is identical and log normal for both the enriched nucleus and the pyrite, with 50% occurring with a diameter greater than 50μm and only 10% less than μ7m. Within the copper pyrite, where the bands of Pb-Zn are less abundant, the sphalerite is more finely sized; 50% with a diameter greater than 15μm and 10% less than 3μm.

Galena

The size distribution is again log normal and similar in both the enriched nucleus and pyrite, with 50% of the galena found with diameter greater than 60μm and 10% less than 13μm.

Chalcopyrite

The granulometry of the chalcopyrite was found to be more disperse. For the copper pyrites 50% was found to have a diameter greater than 17μm and 10% with less than 2.2μm. With the copper shales, 50% had a diameter greater than 20μm and 10% less than 2μm.

3.3. PROCESS MINERALOGY

3.3.1. Qualitative Investigation of Process Streams

Selected sized samples from key points around the processing plant were prepared and examined. The specimens were produced by combining some of the powder sample with a mixture of acrylic beads dissolved in 1-2 dichloroethane (approximately 1:10) and allowing to dry on the bottom ram of a standard metallurgical hot mounting press. The specimen was then mounted using transoptic powder and ground and polished using standard techniques.

The mineralogical study established the following:

a) The important minerals are predominantly liberated below a size of 10 to 12μm. Furthermore, it would appear that within the slimes fraction (nominally -8m) there is little or no problem with liberation.

b) There are significantly numbers of locked particles in the +15μm fraction, in particular locked particles of galena with sphalerite and all the important minerals locked with pyrite.

c) Misplaced minerals in the copper and lead concentrates are predominantly liberated and confined largely to the slimes fractions.

3.3.2. Quantitative Mineralogy of the Almagrera Flotation Feed

The underflow from the thickener feeding the copper flotation circuit at Almagrera was the stream studied. A sample of the solids from this stream was split into six sizes using the Warman cyclosizer, and each fraction prepared for optical microscopy.

For each polished section, particle counting was performed manually to assess the proportions of the mineral of interest which occurred in the volume percent bands 0-10, 10-20, 20-30 etc. up to 90-100%. This assessment was made with reference to classical intergrowth patterns, although most of the mineral associations in this ore were simple binary except for the coarsest size fraction. The procedure was performed for sphalerite, galena and chalcopyrite, counting at least 2000 particles per mineral.

Figure 4 shows the results of this study. It is seen clearly that for all three minerals, liberation is complete below about 15μm. Sphalerite exhibits more than 70% liberation at all sizes, galena at sizes less than 30μm, but chalcopyrite requires grinding to below 23μm to achieve the 70% liberation.

3.4. LABORATORY FLOTATION TESTWORK

Extensive testwork was performed initially to establish a standard flotation procedure (see Table 2) and to assess the effects of storage on the behaviour. It was established that the best sample storage involved freezing at -18°C and discarding all material if stored for more than about six months. A steady deterioration of performance was noted during this time period and was accommodated by performing a standard test with potassium amyl xanthate on each day that flotation testwork occurred.

Approximately 300 laboratory flotation tests have been performed in Cardiff as part of this project. All tests involve an element of kinetic study since two concentrates are generally collected, the first up to 5 minutes and the second during the next 10 minutes of flotation.

3.4.1. Effect of Xanthate Hydrophobicity on Copper Rougher Performance

Potassium amyl xanthate (PAX) is used as a selective copper collector in the rougher cells operating at pH 10 at Almagrera. The first series of tests in the present laboratory study was designed to examine the effects of alkyl chain length on the performance of xanthate as a copper collector for this ore.

Figure 5 shows that the recoveries all increase with increasing chain length, but perhaps surprisingly the selectivity for Cu is maintained even with five carbon atoms in the alkyl chain. Results for the six-carbon chain were very similar to those for a standard test with PAX, with only a slight decrease in selectivity, especially for Pb. The low copper recovery with ethyl xanthate indicates how difficult it is to float this particular metal in the Almagrera ore.

3.4.2. Effects of Replacement Collectors for PAX at Standard Operating Conditions

Experience at the mine and preliminary tests at Cardiff indicated that with suitable activation by $CuSO_4$ and pH modification by lime, good Zn recoveries could be achieved with PAX. Effort was therefore concentrated on investigating

whether alternative collectors or collector combinations existed for Cu and Pb flotation. Initially this work was restricted to operation at standard conditions as described above, and over twenty separate collectors were tried at dosages from 10 to 40 g/t. These collectors spanned a wide range of chemistries, and were chosen because of their historical effectiveness in copper flotation, particularly in the presence of pyrite gangue. On the basis of their performance on this particular ore, collectors were grouped as being (a) selective for Cu only, (b) selective for Cu and Pb, and (c) ineffective for Cu or Pb. Figures 6, 7 and 8 are examples of Grade/Recovery plots for collectors of each type respectively, and the summary of results is given in Table 3. In all cases the recoveries with the more selective Cu collectors were lower than those achieved with PAX at comparable concentrate grade. Similarly no improvement over the performance of PAX could be achieved by partial replacement with any of the above reagents.

3.4.3. Effects of Varying Copper Rougher Flotation Conditions Other than Grind Size

In an attempt to improve the performance of the alternative collectors, several changes were made to the flotation conditions, but retaining a d_{80} of approximately 50μm. Summaries of the more important findings are given below.

Additions of NaSH

Dosages from 100 to 300 g/t at a fixed aeration time of 5 minutes were used with no improvement over the performance of PAX. Grades of Cu were reduced as a result of greater recoveries of other metals, in particular Zn, as NaSH dose was increased.

Varying Aeration Time Prior to Flotation at Neutral and High pH

Results of extensive aeration testwork showed that there is no beneficial effect on Cu recovery or grade. It is interesting to note that the selectivity against Pb deteriorates as aeration time is increased for all three reagents tested, being very marked for PAX at pH 10 and for 3418A at pH 6-7. The recoveries of Zn and Fe are not greatly influenced by aeration.

Addition of Low Odour Petroleum Solvent (LOPS)

In order to investigate whether small quantities of easily floatable organic contaminants might be responsible in part for the poor Cu recoveries, one test was conducted with the addition of 20 g/t of LOPS to float-off this material prior

to subsequent flotation with PAX at neutral pH. No significant improvement was obtained by adopting this approach.

Addition of SO_2 (as sulphurous acid)

In all tests conducted with SO_2 added to the rougher cell, Cu recovery was decreased significantly along with that of all other metals.

Semi Bulk Flotation

Variation of collector dosages and use of combinations of collectors (e.g. 3894 + 3418A) with staged additions showed that semi bulk flotation of Cu and Pb offered no advantages over selective flotation in this system.

pH Variation

Operation at pH's down to 2.5 using H_2SO_4 and a range of collectors did not result in any improvement in metallurgical performance, and in general only served to activate pyrite. Use of pH modifiers other than lime (e.g. sodium carbonate and hydroxide) did not result in any improved performance at high pH. Operation at a very high pH of 12.5 using lime and PAX depressed both copper and iron minerals whilst recoveries of Pb and Zn increased over those obtained in the standard test at pH 10.

Grinding in Stainless Steel Rod Mill

By grinding in an all-stainless steel rod mill it was possible to avoid large negative redox potential in the flotation pulp. Indeed it was found that the potential (relative to calomel) was approximately +200 mV at the end of grinding. It is well known that Cu recoveries will be increased under such conditions, and this proved to be the case in this present study but at the expense of lower grades due to the activation of all other minerals.

Addition of Dispersants

Again this resulted in no significant improvement, a slight disadvantage being the extra Pb floated.

3.4.4. Copper Cleaning Testwork

In the laboratory it was found that operation at neutral pH with PAX gives the best performance despite a greater initial pyrite float in the rougher. Three stages of cleaning resulted in a copper concentrate with a grade of

approximately 23% at the highest recovery achieved during this programme of laboratory flotation. There is evidence to suggest that staged addition of collector to the cleaner cells will result in greater recoveries at acceptable grades.

On the basis of this encouraging laboratory result, a plant trial with the Cu rougher cells operated without lime addition was conducted. However, because of build-up in recirculating loads the trial was abandoned.

3.4.5. Examination of the Causes for Poor Cu/Pb Recoveries

Concurrent with the flotation testwork, investigations into the causes of the poor Cu recoveries and grades in the rougher were performed. These involved more detailed quantitative mineralogical studies on laboratory generated samples (reported in Section 3.5) and numerous miscellaneous studies.

An investigation into the oxidation of galena revealed that approximately 10% wt. of the Pb in the ore became soluble in dilute acetic acid after the ore had been agitated in the flotation cell for less than two hours without aeration. This indicates that galena oxidises quite rapidly in this ore and might explain the poor recovery of Pb in the slimes fractions. Negligible amounts of Cu or Zn became soluble in this time period suggesting that oxidation is probably not entirely responsible for the poor Cu performance, although the presence of thin surface coatings cannot be ruled out.

In order to assess whether any of the reagents tested gave rise to real improvements in metallurgical performances, correlations of grade versus recovery and recoveries of Cu versus those of other metals were performed regularly. Figures 9 and 10 are two examples of the relationship between Cu recovery and the recoveries of the other metals to the copper concentrate. The former contains data from all the tests using PAX and 3894 on the third ore sample, whilst the latter uses data from the kinetic test, No. 054, where concentrate samples were collected every minute during the early stages. Both figures show that a sharp increase in Fe recovery (which correlates with pyrite recovery for this ore since the concentrations of other iron-containing minerals are low) occurs at a Cu recovery of approximately 70%.

The explanations for this trend involve considerations of both poor liberation and unfavourable flotation kinetics for any liberated particle in the slimes. A simple material balance over the laboratory copper rougher cell using manually generated liberation and size analysis data shows that the copper losses are roughly equally distributed between coarse locked particles and essentially liberated particles in the slimes fraction. It appears that any

efforts to recover more of either size fraction with the chemical tested will result in poorer concentrates. For this reason it was decided that alteration of process chemistry alone would not be effective at the grind size currently being used at Almagrera, and attention was focused on improving copper flotation by means of different comminution practice.

3.4.6. Variation in Comminution

Guided by past experience on the plant and by the rather disappointing laboratory flotation results of the present study, it was decided to explore the potential for extra copper recovery from the coarser fractions of the current feed. Clearly this requires extra grinding, but this can be achieved in various ways, and the alternative methods explored are discussed in turn below.

Prolonged Milling

The flotation tests reported above, designed to investigate the effects of alternative flotation chemistry, were performed on a pulp produced by grinding for 16 minutes in a laboratory mild steel rod mill. In order to examine the effect of prolonged milling, a series of tests was performed where standard flotation was conducted on pulps generated by milling for 16, 23 and 30 minutes. The results demonstrated that copper recoveries decrease markedly from 67% to less than 48% as grind time is increased. Grades of concentrates did, however, increase correspondingly from 3.13 to 3.99% Cu, whilst d_{80} was decreased from approximately 50μm to 20μm. Redox potential of the pulp at the end of milling became increasingly negative as milling time increased (-186 at 16 minutes, -310 at 30 minutes) whilst pH varied only slightly, with a mean of approximately 7.5.

Staged Milling

It has been established that the copper rougher concentrate contains relatively little coarse material and regrinding would not be very effective. The tailings, however, do contain material where copper locking is severe, and work has been performed to examine the effect of regrinding this material.

The exact conditions for the staged grinding tests are given elsewhere[4]. In order to summarise the effects of the various comminution steps, the grades and recoveries of all tests conducted on the third ore sample are plotted on Figure 11. The results for the stage grinding tests consistently appear towards the top right hand side of this diagram despite being performed on a comparatively old ore sample, which showed significant reduction in recovery and grade in the standard flotation test. It would appear that

the Cu recovery could be improved by approximately 10% at comparable grade to the standard by adopting staged grinding.

3.5. QUANTITATIVE MINERALOGICAL INVESTIGATIONS OF LABORATORY FLOTATION SAMPLES

During the periods of flotation testwork it became apparent that copper rougher recoveries above about 70% would be difficult to achieve without serious deterioration in grade. Therefore, alongside the continuation of the main theme of this project, i.e. the search for improved metallurgical performance by variation in process chemistry, further and more detailed mineralogical studies were initiated. These studies were performed by classical manual techniques in Cardiff and by automated electron microscopic techniques in CANMET and Imperial College of Science and Technology, London. The object of the studies was to determine whether the poor flotation response for copper was due to poor liberation or to the presence of oxidised or unexpected copper minerals.

There exist differences between the results of these three investigations, reflecting the different techniques involved. However, all three studies agree that liberation is poor in the coarser fractions (+20μm) where approximately 60% of the copper in the tails exists. The greatest potential for extra copper recovery must therefore exist in regrinding this material. However, only limited success was obtained in the laboratory by following this route, which probably reflects the extremely fine dissemination of chalcopyrite grains in the coarser fractions of the tailings.

4. SUMMARY AND CONCLUSIONS

Initial studies of plant operation and mineralogy established that potential existed for further metal recoveries from liberated minerals in the fine size fractions. However, extensive laboratory flotation studies of Cu and Pb flotation with an extremely wide range of alternative collectors and various process chemistry changes failed to improve on the performance obtained with the collector currently in use, potassium amyl xanthate. Promising laboratory results, operating the copper rougher at neutral pH, could not be sustained when transferred to plant operation.

The poor flotation performance (in the Cu and Pb circuits) was attributed to non-selective flotation in the slime fractions and poor liberation in the coarser material. Quantitative mineralogical examinations of the tailings confirmed the latter and some success was obtained with improving comminution practice. It has been demonstrated

that approximately 10% improvement in copper recovery should be possible with finer grinding but at the expense of lower lead recoveries. Translation of this finding to plant operation would require significant process alterations and was beyond the scope of the project.

It is concluded that no commercial benefit is currently possible by alteration of collector or other reagents. Some attention should, however, be focused on improving the performance of the copper cleaning circuit. The greatest potential for extra recovery of copper involves finer grinding but this must be carefully controlled.

5. ACKNOWLEDGEMENTS

The three collaborating organisations wish to express their appreciation of the many helpful discussions with Drs. Bill Petruk of CANMET and Meurig Jones of Imperial College, concerning the mineralogy of the Almagrera ore. The assistance with experimental investigations by these two laboratories is gratefully acknowledged.

6. REFERENCES

1. WILLIAMS K.P., ACOSTA FERNANDEZ M., EDWARDS R.J., and LAMBERT S.A.
"Improvement of complex sulphide flotation using new reagent chemistry"
First six-monthly report, Contract MA1M-0064-C, September 1988.

2. WILLIAMS K.P., et al.
"Improvement of complex sulphide flotation using new reagent chemistry"
Second six-monthly report, Contract MA1M-0064-C, March 1989.

3. WILLIAMS K.P., et al.
"Improvement of complex sulphide flotation using new reagent chemistry"
Third six-monthly report, Contract MA1M-0064-C, September 1989.

4. WILLIAMS K.P., et al.
"Improvement of complex sulphide flotation using new reagent chemistry"
Final Report, Contract MA1M-0064-C, June 1990.

TABLE 1

Statement of Primary Project Targets

Metal	Typical Current Performance		Target Performance	
	Grade	Recovery	Grade	Recovery
Cu	21	50	23	60
Pb	42	40	50	50
Zn	48	76	50	83

TABLE 2

Standard Laboratory Flotation Procedure for Copper Rougher Studies.

1. Rod mill grinding for 16 minutes with 1 kg of -5mm ore and 500 ml of water.

   Typical final pH = 7.0, Eh = -170 mV

2. Transfer to 2.5 litre Denver flotation cell and stir (without aeration) for 10 minutes.

   Typical equilibrium pH = 7.2, Eh = -240 mV

3. Aeration at 2 litres/min air until Eh = 0

   Time taken = 2 to 3 minutes. Typical pH = 6.0

4. Adjust pH to 10.0 with lime

   Time taken = 2 minutes. Typical Eh = -180 mV

5. Add frother (25 g/T) and condition for 1 minute

6. Add collector and condition for 3 minutes

7. Float at 5 litres air/minute for 15 minutes collecting samples during first 5 and second 10 minutes.

   Typical final pH = 8.7, Eh = +90 mV

Notes: Compressed air is supplied at a fixed rate from a cylinder.

Impellar speed is constant at 1100 rpm.

TABLE 3 : PERFORMANCE OF COPPER AND LEAD COLLECTORS AT STANDARD CONDITIONS

Selective for Cu only	Selective for Cu and Pb	Ineffective as Cu or Pb collectors
5415	3418 A	5688
3894	241	3302
S 5816	242	400
3477	70-1	80-5
4530	88-2	
407		
4037		
S 6526		
90-1		
93-4		

Others gave good recoveries but were non-selective.

FIGURE 1

RECOVERIES FOR SIZE FRACTIONS

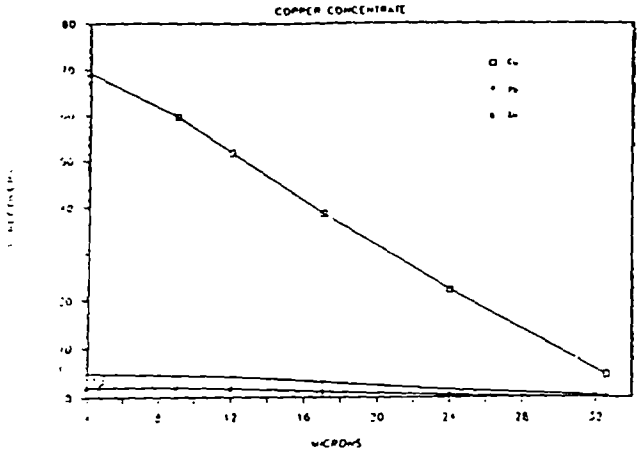

FIGURE 2

RECOVERIES FOR SIZE FRACTIONS

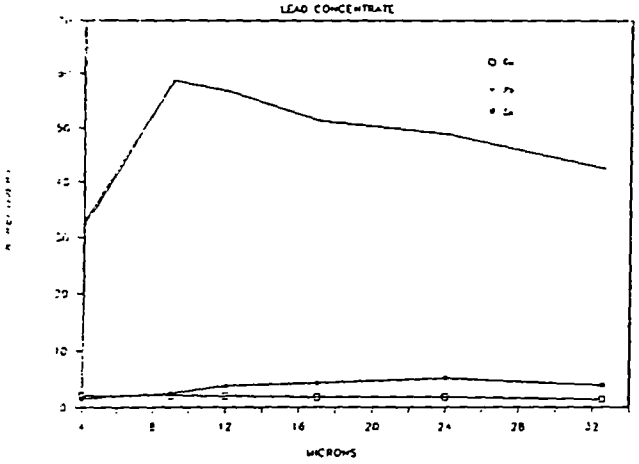

FIGURE 3

RECOVERIES FOR SIZE FRACTIONS

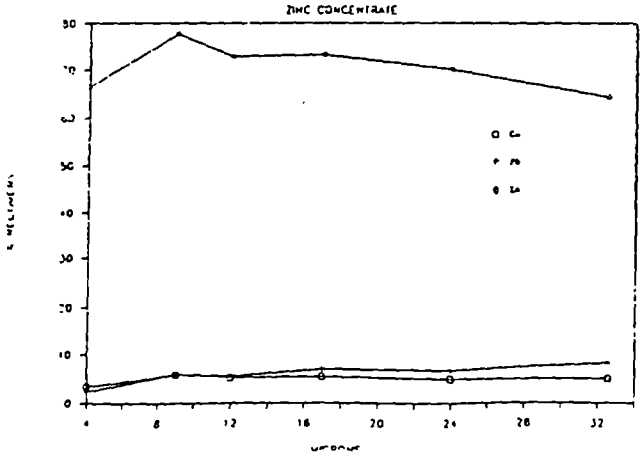

FIGURE 4

Mineral Liberation Data for the Milled Product at Almagrera, April 1988

Data for -56μm fraction only (representing 83% of the sample)

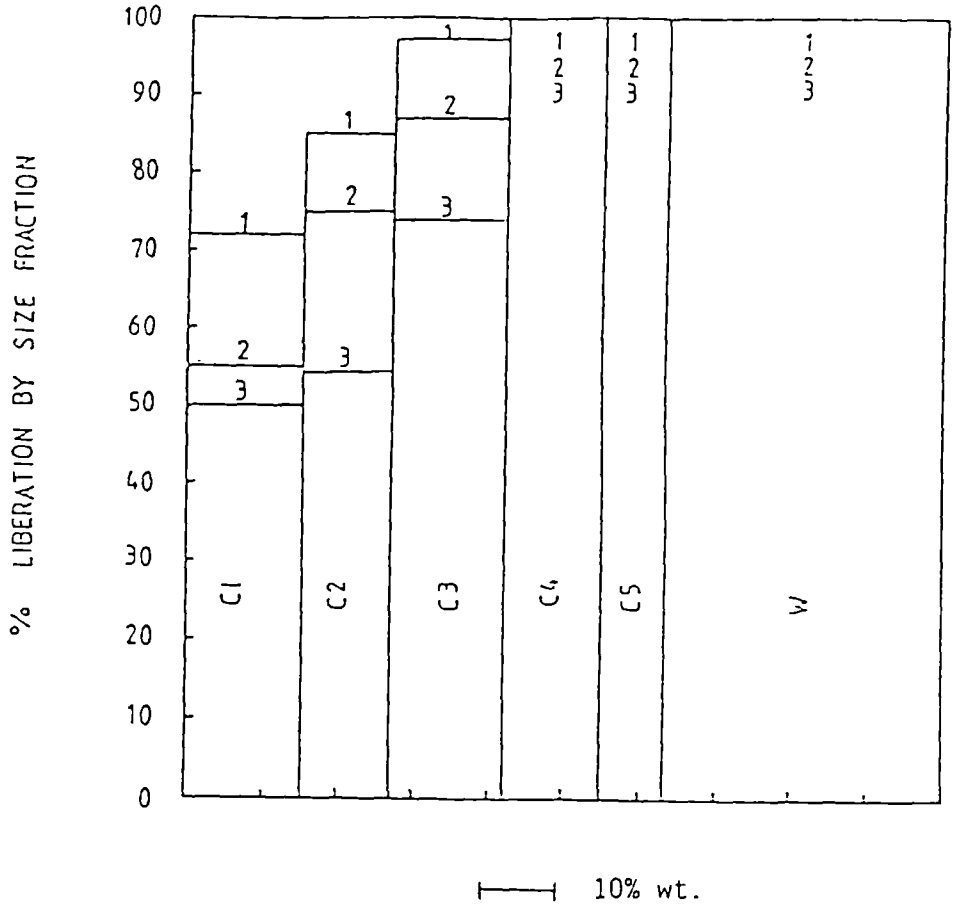

1 – Sph
2 – Gn
3 – Cpy

Cyclosizer Fraction	Nominal Size μm
C1	-56 +30
C2	-30 +23
C3	-23 +15
C4	-15 +12
C5	-12 + 8
W	-8

FIGURE 5

EFFECT OF XANTHATE ON Cu ROUGHER FLOTATION
pH 10

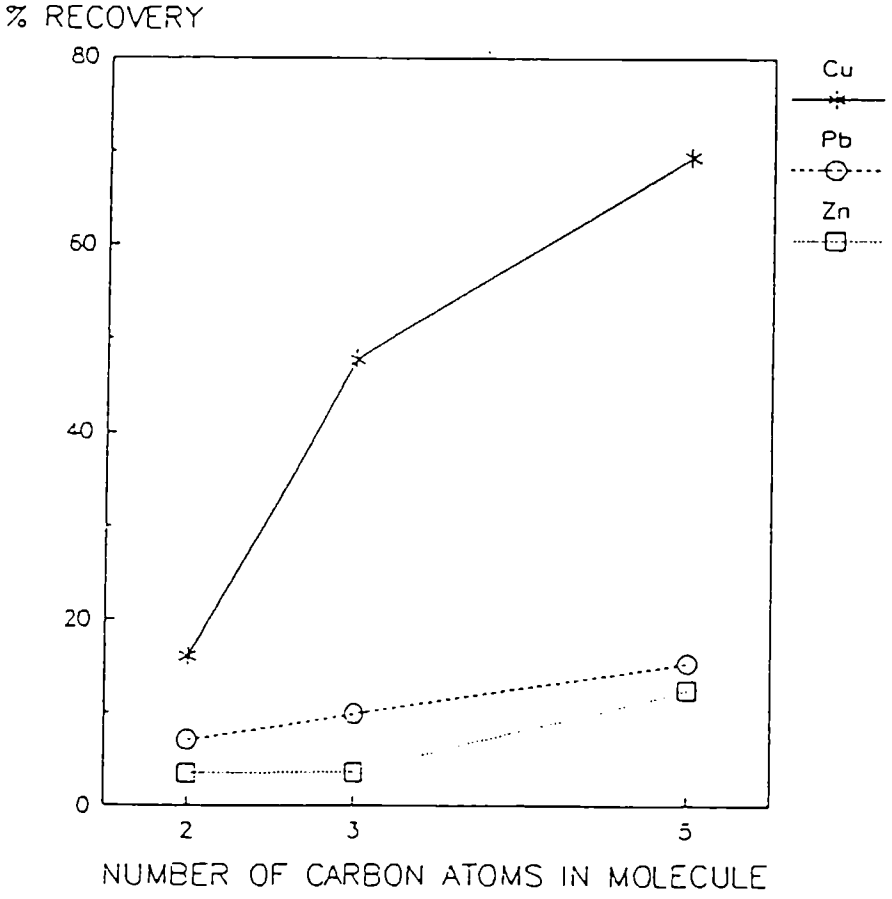

FIGURE 6

FLOTATION REAGENT ASSESSMENT - Cu ROUGHER
REAGENT DESCRIPTION - S5816

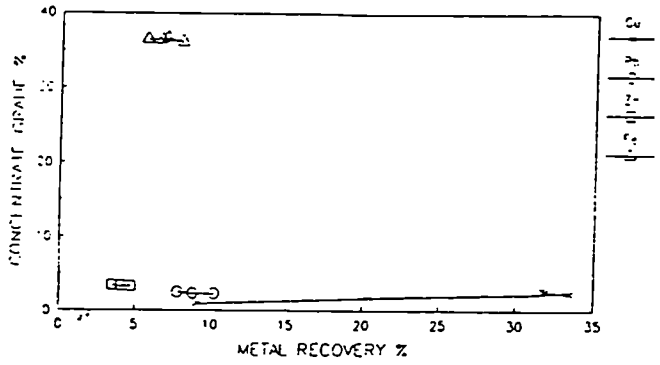

REAGENT DOSE RANGE - 10 to 40 g/tonne

FIGURE 7

FLOTATION REAGENT ASSESSMENT - Cu ROUGHER
REAGENT DESCRIPTION - 3418A

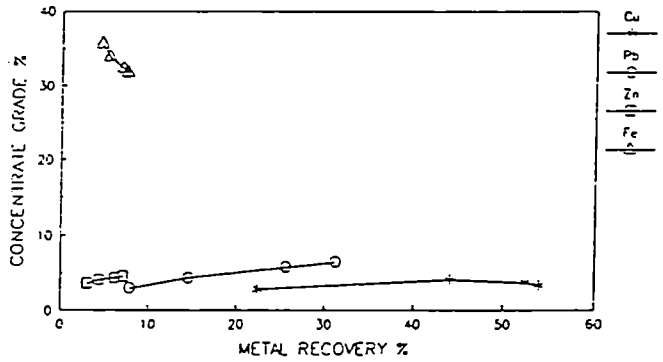

REAGENT DOSE RANGE - 10 to 40 g/tonne

FIGURE 8

FLOTATION REAGENT ASSESSMENT - Cu ROUGHER
REAGENT DESCRIPTION - 3302

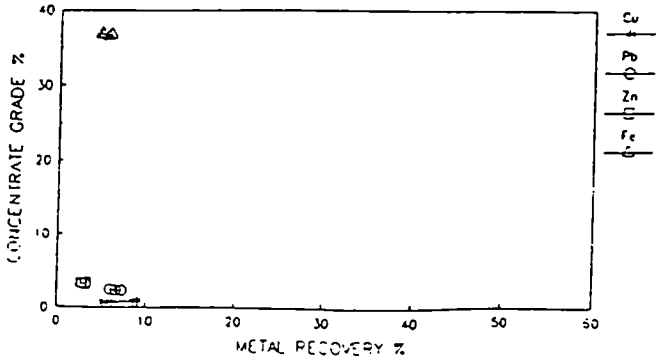

FIGURE 9

Cu/Fe Recovery Plots

for PAX and 3894

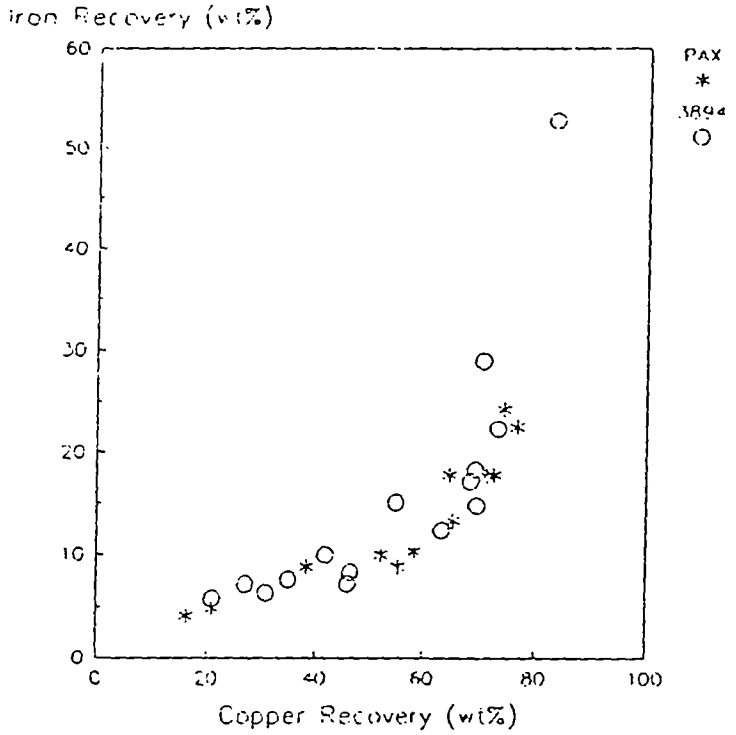

FIGURE 10

Cu Recovery V Pb,Zn,Fe

for Test 054

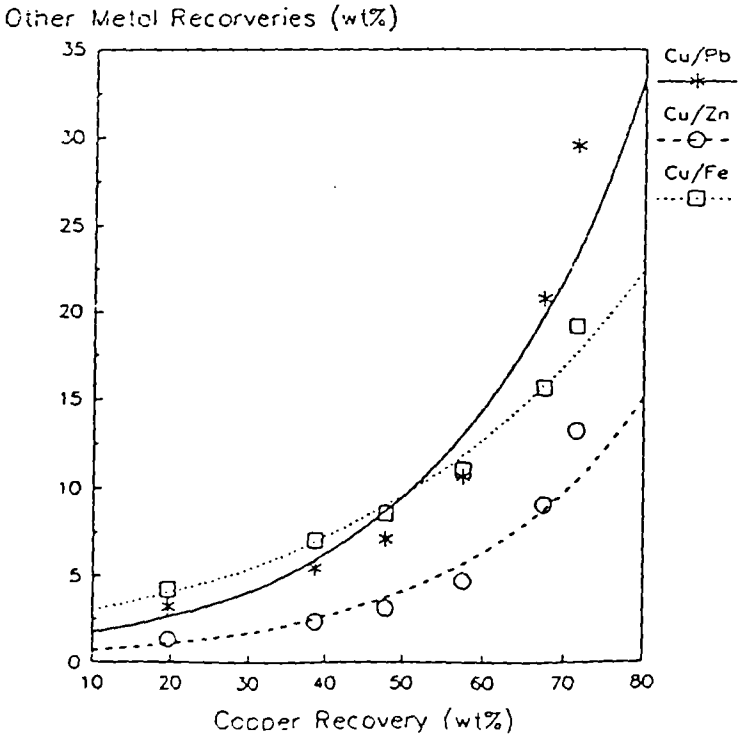

FIGURE 11

COPPER GRADE VERSUS RECOVERY
0XX SERIES - ALL TESTS

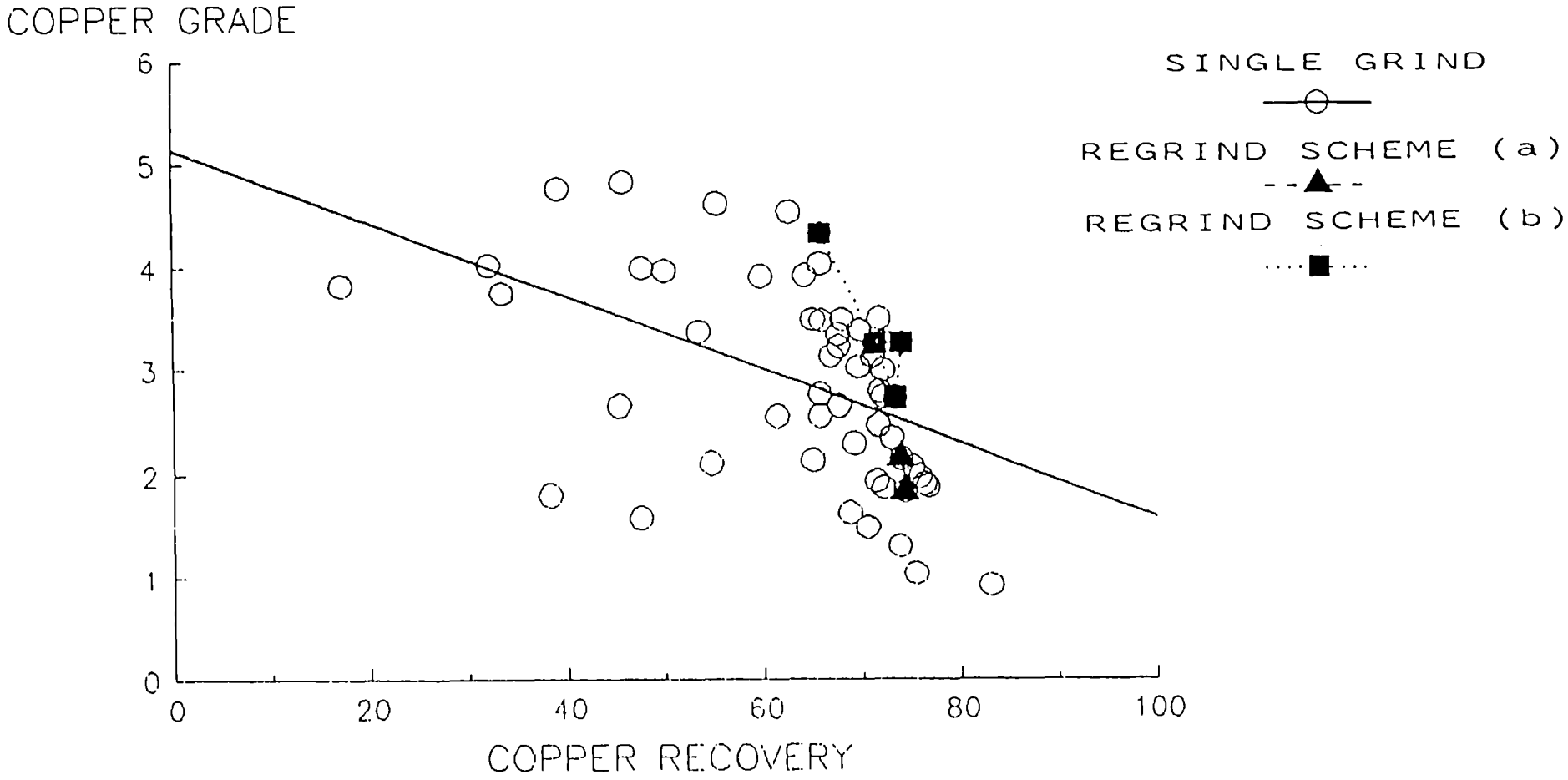

RECOVERY OF Ta AND Nb FROM CONCENTRATES AND BY-PRODUCTS OF EUROPEAN ORES TYPE ECHASSIERES (FRANCE) AND GOLPEJAS AND PENOUTA (SPAIN)

Project Leader: I. GABALLAH
Centre de Recherche sur la Valorisation des Minerais, France

J.C. RUIZ-SIERRA
Centro Nacional de Investigationes Metalúrgicas, Spain

Contract MA1M-0071-C(CD)

1. OBJECTIVE

I. Physicochemical characterization of primary concentrates, ores and tailing.

II. Mineral processing of ores such as kaolinized granite ECHASSIERES (FRANCE), or alterated pegmatite such as GOLPEJAS and/or PENOUTA (SPAIN).

III. Recovery of tantalum and niobium chlorinated compounds by selective chlorination and/or carbochlorination of concentrates produced in step II.

IV. Exploration of the possibilities of treating the concentrates from step I by high temperature carburation or treatment in plasma furnace in order to separate the tantalum and niobium from their bearing minerals.

2. INTRODUCTION

Besides the importance of tantalum and niobium in the research and development in the present and future high technologies, they are classified as strategic and critical materials (1, 2) which are defense related because of their use in aerospace, electronics, energy production and transportation industries, etc.

For these reasons, the European communities and governments support several projects about the geological survey and the mineral processing of the European tantalum and niobium bearing ores.

It is well known that most of tin ores contain tantalum and niobium bearing minerals. Figure 1 (3) shows the tin belt which passes from Cornwall into United Kingdom through the western part of Massif Central of France. The tin deposits are related to Hercynian granites, the continuation of this belt towards Italy is characterized by Tertiary tin deposits at Elbe, Tuscany and probably Sicily. A second tin belt passes through Spain and Northern Portugal. This belt is also related to the Hercynian granites.
Most of these tin deposits have been exploited and are considered actually as economically marginal. However, some of these sites are exploited for other minerals where tin, tantalum and niobium ores are considered, for the time being, as by products.

For instance, Echassières, exploited for its kaolin, had an estimated reserve of 55 million tons of leucogranite containing 0.023% and 0.022% of Ta_2O_5 and Nb_2O_5 respectively (4). This corresponds to about 25 000 tons of tantalum and niobium pentaoxides. The estimated reserve of the Penouta, which is mainly leucogranite, is 13.25 to about 28 million tons containing some 2 500 tons of Ta_2O_5 and Nb_2O_5 respectively (5). Reserves of tantalum and niobium bearing minerals of the tin belts in Europe, based on geological documentation from France, Portugal and Spain, is estimated to some 40 000 to 80 000 tons.

The classical ore processing methods (flotation, magnetic and gravity separation) leads to a low grade concentrate of Ta and Nb oxides with a modest rate of recovery.s

This research is aimed to the use of advanced technology in the areas of high intensity magnetic separation, plasma, means of calculation and thermodynamic data banks, the advanced hydrometallurgy and pyrometallurgy processes and their complementarity, in order to explore a possible new process for the mineral processing and the extraction of Ta_2O_5 and Nb_2O_5. This research will be focused on the kaolinized granite (Echassières, France) and the alterated pegmatite (Golpejas and Penouta, Spain).

3. EXPERIMENTAL WORK

I. Characterization of minerals, concentrates, tailings, by-products, processed products, etc by classical chemical analysis, size analysis, ThermoGravimetric Analysis "TGA", X Rays Diffraction "XRD", XRays Florescence "XRF", Scanning Electron Microscope "SEM", Microprobe, etc.

II. Mineral Processing:

Classical equipments for size reduction, classification, flotation, gravity separation, magnetic & electrostatic separation, High Intensity Magnetic Separator "HIMS" using a superconducting magnet.

III. Chlorination and carbochlorination:

Two set of experimental apparatus are used:

The first consist of a purification and metering units for the preparation of the gas mixture introduced in a horizontal quartz reactor which includes the sample's nacelle followed by a cooled finger so as to condensate the volatile metal chlorinated compounds and finally a purification system before the gas mixture realize to the atmosphere. The second set is a thermogravimetric analysis apparatus which is exactly the same as the first with the exception that the reactor is vertical.

IV. High temperature treatment:

Classical furnace to agglomerate the sample at temperatures of about 1300 °C, oven for sample treatment at temperatures $\leq$ 1800 °C and arc transfered plasma furnace for the tantalum and niobium oxide bearing minerals treatments.

4. RESULTS

4.1 PHYSICOCHEMICAL CHARACTERIZATION

The Echassières primary concentrate chemical analysis is summarized in table I.

This table shows the average chemical and mineralogical composition of a typical primary concentrate of Echassières. The minerals present in this concentrate are heavy minerals obtained from the washing of the kaolin of Echassières. The tantalum and niobium bearing minerals are essentially microlite and tantalo-columbite. Cassiterite, topaz, micas, rutile, ilmenite and oxy/hydroxide of iron are present in variable amounts. The latter cements the different minerals mentioned above. Only the important minerals are described below.

Figure 2 is a Rosin-Rammler curve of the primary concentrate of Echassières. It indicates a sharp change of slope around 150 μm. Using the above mentioned tecniques, it seems that the majority of the tantalo-columbite is concentrated in the size fraction $\geq$ 150 μm.

4.1.1. Microlite

Microlite represents the tantalum pole of the pyrochlore-microlite series and has the general formula:

$$A_{2-m}B_2O_6(O,OH,F)_{1-n}\cdot pH_2O$$

where A = Ca, Na, U, R.E.E., Ba, Pb, K, Sn, Bi
& B = Nb, Ta, Ti

For the Echassières samples, analyzed by the microprobe, the cations of group B are essentially Ta and Nb (the titanium content is negligible). Elements of group A are U, Ca, Na, Pb, Ba (see table II).

Group A cation contents are extremely variable from one grain to the other and within the same grain. The most important cation is uranium because of its subsequent dangerous concentration in the reactor during halogenation. The average value is 6.6% UO_2. The other cations of group A (Ca, Na, Pb, Ba) have a low average content which, in some cases, can exceed 10%. These results make it difficult to define a precise formula for the Echassières microlite. However, if H_2O, OH^- & F^- are neglected the following formula could be considered:

$$(Ta_{1,279}\ Nb_{0,571}\ W_{0,125}\ \square_{0,025})\ (Na_{0,108}\ Ca_{0,214}\ Ba_{0,156}\ Pb_{0,064}\ U_{0,256}\ \square_{0,202})\ O_6$$

It may be important to mention that the microlite contains very fine fluid inclusion, small fissures and porous zones. This leads to an important variation of the specific gravity of this mineral and causes a lot of trouble for its mineral processing.

4.1.2. Tantalo-columbite

The tantalo-columbite group forms an isomorphic series between tantalite $(Fe, Mn)Ta_2O_6$ and columbite $(Fe, Mn)Nb_2O_6$.

The general formula is: AB_2O_6

where $A = Fe^{2+}, Mn^{2+}$ and $B = Nb^{5+}, Ta^{5+}$

The chemical composition of the tantalo-columbite is simple and almost stoichiometric. For the naturally formed minerals, the substitution of the B cations is negligible. However, that of Ti^{4+} is common and those of Sn^{4+} and W^{6+} have been observed.

Table III, summarizes the chemical composition of the columbo-tantalite of the three deposits (Echassières, Penouta and Golpejas) as obtained from the microprobe analysis.

The average formula of Echassières mineral is:

$$(Ta_{0,413}\ Nb_{1,513}\ W_{0,061}\ Ti_{0,013})\ (Fe_{0,22}\ Mn_{0,78})O_6$$

Based on the nomenclature of M.V. KUZ'MENKO (6), table III shows that the concentrate of Echassières is tantalo-columbite while that of Golpejas and Penouta could be considered as columbo-tantalite. However, all will be considered as columbo-tantalite.

4.1.3. Cassiterite

The cassiterite of the primary concentrates contains Ta_2O_5 and Nb_2O_5. Their contents can range from 1.7% to 2.2 and from 0.1 to 1.1% respectively (see table III). The tantalum and niobium compounds are present in the SnO_2 structure, probably as microinclusions, which aren't perceptible by the microprobe (<1μm).

The tantalum and niobium microinclusions of cassiterite present some 5 to 15% of the total Ta and Nb pentaoxide content in the primary concentrate. They are not recovered during the mineral processing and will be concentrated in the tin slag during the elaboration of tin.

4.2. MINERAL PROCESSING

The classical flow sheets for the mineral processing of leucogranite (more or less greisenied) of Echassières, Penouta and Golpejas are similar. That of Echassières is summarized in figure 3. They are based on crushing, size classification, gravity, magnetic and electrostatic separation.

The proposed mineral processing of the primary concentrate of Echassières is based on the above mentioned physical methods associated to a hydro and pyrobeneficiation process before their halogenation. The steps of this process are summarized in figure 4 and are based on properties such as magnetic susceptibility, density, dielectric constants, etc...

The primary concentrate is treated by HCl (3N, 60 °C, 4h) so as to eliminate the iron oxy/hydroxides and by consequence to liberate the Ta and Nb bearing minerals, to minimize the mixed particles and to increase the recovery rate. Another advantage of the elimination of the iron oxy/hydroxides, for the subsequent halogenation phase, is the saving of the halogenating agent and the simplification of chemical reactions during this operation. The particle size classification is applied in order to increase the efficiency of the magnetic, electrostatic and gravity separation. Dry magnetic separation at intensity $\leq$ 2 Testla permits the recovery of tantalo-columbite with a recovery rate of about 100 %. The concentration of this mineral in the magnetic fraction is about 80 to 100 % and depends on the particle size of the mineral.

The non magnetic fraction is subjected to a gravity separation so as to eliminate the topaz in the light part. Microlite is supposed to be in the heavy part and theoretically could be separated from the cassiterite thanks to the electrostatic separation.

However, these techniques give a concentrate containing 30 to 50 % of microlite with a modest recovery rate which is a funtion of the particles size.

The electrostatic separation is not efficient for the fine particles $\leq$ 65 μm where most of the microlite is concentrated; the difference between the specific gravity of microlite and that of topaz is small and subject to change due to the variations of the former; the microlite content, in the primary concentrate, is low.

Tests on the separation of microlite, by high intensity magnetic field (superconducting bobbin of =5.5 T) show little amelioration with respect to the proposed flow-sheet.

The non magnetic non-conductive fraction contains essentially microlite, cassiterite and topaz. The cassiterite is reduced by hydrogen at 700 °C and the tin is dissolved by hydrochloric acid. The filtration residue is dried and classified by means of sieve analysis. After this treatment, the size of the microlite decreases while that of topaz remains constant.

A particle size classification permits the concentration of the microlite in the fines. The intermediate sizes are recycled. The content of microlite in this concentrate is about 65 % and the recovery rate is higher than 80 %.

4.3. SELECTIVE CHLORINATION

Chlorination or carbochlorination of tantalum and niobium bearing minerals or concentrate is a well known operation applied on industrial (7-10), pilot and laboratory scale (11-38). Actualized bibliography of this subject may be consulted from the references 35 and 36. Only a summary of this bibliography is given below. Most of these researches were focused on the recovery of volatile chlorides or oxychlorides of tantalum and niobium, their purification from impurities and the separation of tantalum compounds from those of niobium.

The solids used in these studies had been pure pentaoxides of Nb_2O_5 (9,18, 21-23, 25, 32) & Ta_2O_5 (18, 21, 24-25) or minerals such as pyrochlore (10, 12, 22, 27-28, 30, 32-33, 36), euxinite (11, 17, 20, 22), laporite (22), columbite (9, 13, 26), tantalo-columbite (36) or industrial wastes such as tin slag (9, 31-33, 35, 37-38), ferroniobium (14-16, 34).

The different chlorinating agents are Cl_2 (14-16,27,36), Cl_2+C (9-13, 17-18, 20, 22-24, 26-27, 31-33, 35), Cl_2+CO (25, 27, 36), CCl_4 (21), $COCL_2^+$ (22), Cl_2+N_2 (9, 37), Cl_2+He (29-30), Cl_2+A (34), Cl_2+SO_2 (27), HCl (27, 28).

Depending on the reactivity of the Ta & Nb bearing solids, the investigated temperature range was <500°C (17-18, 21-22, 26, 34, 37-38),> 500 °C (25, 28), > 1000 °C (29-30) or in the temperature range of 300 < T < 1000 °C (9-13, 18, 20, 22-25, 327, 31-33, 35-38).

Experimental methods used for the characterization of the reaction products are essentially x ray fluorescence (27, 29, 32, 33, 37-38), x ray diffraction (27, 32-33, 37-38), atomic absorption (29, 37-38), scanning electron microscope (32-33, 36-38), microprobe (36-38), etc...

Most of the above mentioned studies confirm the formation of the tantalum and niobium chlorides or oxychlorides, depending on the experimental conditions. However due to the intrinsic character of $NbCl_5$, it decomposes partially or completely to $NbCl_5$ + $NbOCl_3$ (23) or $NbCl_5$ + NbO_2Cl + $NbOCl_3$ (9, 18, 36-38) or NbO_2Cl + $NbOCl_3$ (29-30) or $NbOCl_3$ (10, 26-27, 32-33, 35). The chlorination of tantalum pentaoxide leads to the formation of oxychloride of this element. However, the tantalum oxychlorides are much less stable than those of niobium and their dismutation give $TaCl_5$ + Ta_2O_5 (31). High temperature chlorination of tantalum and niobium bearing materials, such as columbite (13), tin slags (32-33, 38), ferroniobium (14, 16) etc..., gives condensates which are mixtures of Ta and Nb compounds mainly chlorides, oxychlorides and oxides. On the other hand, low temperature chlorination of tantalo-columbite, microlite and tin slag leads to a condensate rich in Nb and a residue rich in Ta (36-38). This tends to prove the existence of a limited selective chlorination of niobium compounds with respect to those of tantalum. Separation of tantalum compounds from those of niobium may be done by fractional distillation (16), solvent extraction (11, 20), or by the famous Marignac process (39).

Impurities such as Fe, Mn, U, Ca, Mg, Na, etc... are also chlorinated and could be found in the condensate (Fe, Mn, U, etc) or in the residue (Ca, Mg, etc...).

Research on the separation of impurities from tantalum and niobium compounds had been conducted by different methods (11-12, 14-15, 17, 26, 28).

One may mention that no studies on the chlorination of tantalo-columbite, microlite and specially those of Echassières or Penouta are reported. On the other hand, microlite and tantalo-columbite contain some ten and six elements respectively. The complexity of the chlorination reaction of these elements and the interaction of the reaction products between themselves and with air, H_2O, CO_2, etc necessitate the use of different techniques of investigation and characterization, described in paragraph 3, in order to define the qualitative and quantitative nature of condensates and residues.

Figure 5 shows the chlorination apparatus used in this study. Measured quantities of industrial gases such as Cl_2, CO, N_2 are purified from water vapor by phosphorus pentaoxide and from oxygen by a carbon furnace and sulfuric acid.

Minerals are chlorinated in a quartz reactor and the volatile chlorides or oxychlorides are condensed on the cold finger. Gases are purified from Cl_2, by passage on solid and liquid sodium hydroxide. The temperature of the furnaces is regulated within $\pm$ 2 °C. Air is used for cooling the condensation finger. The material balance is defined by the determination of the weight changes of the treated sample. The reaction products are recovered at the end of the experiment and the qualitative and quantitative characterization of these products was possible by the use of the above mentioned techniques.

4.3.1. Chlorination of columbo-tantalite concentrates

The chemical composition of the minerals used in this study are summarized in table V. One may mention that these samples contain other elements due to the presence of impurities, such as topaz, lepidolite, ilmenite, etc...

Figure 6 compares the evolution of the samples percent weight loss in function of the temperature for the three concentrates. The percent weight loss (% W.L.) of the Echassières concentrates exceeds the LL* limits. This means that tantalum pentaoxide had reacted with chlorine and the tantalum chlorinated compounds are volatilized. In the case of Penouta and Golpejas concentrates, chlorination is selective in the sense that only the oxides of Fe, Mn and Nb are chlorinated and that the solid residues contains mainly tantalum compounds.

Tables VI and VII summarize the evolution of the chemical composition of the residues and the condensates of chlorination for the Echassières and Golpejas concentrates. Table VI shows that the four elements of Echassières columbo-tantalite are chlorinated and found in the condensates even at 500 °C. The final residue is free of all the elements of columbo-tantalite. In the case of Golpejas columbo-tantalite, the tantalum compounds are concentrated in the residues of chlorination until 800°C. At higher temperatures, traces of Ta compounds are detected in the condensates. It seems that the presence of aluminium compounds in the Echassières concentrates promotes the chlorination reaction, while in the case of Golpejas the absence of this element leads to a selective reaction.

Figure 7 schematizes the thermogravimetric analysis of the three samples at 950 °C. It is clear that the order of the reactivity of the columbo-tantalite with respect to chlorine gas increases from Penouta, Golpejas to Echassières. It

seems that the iron and manganese oxides of the Penouta concentrates are chlorinated selectively. Figure 8 confirms this result. It is clear that at 900 °C and for a reaction time of 600 to 1200 minutes, only oxides of iron and manganese have been chlorinated. This leads to the concentration of the Ta and Nb pentaoxides in the residues of chlorination. The same effect is also observed at 950 °C.

4.3.2. Carbochlorination of tantalo-columbite concentrates

Figure 9 groups the curves of the evolution of the percent weight loss in function of the temperature for the three concentrates using the experimental apparatus reported by figure 5. The curves of Penouta and Echassières decrease or stabilized at 650 °C due to the formation of a $MnCl_2$ (M.Pt. = 650 & B.Pt. = 1190 °C) liquid layer which decreases the gas - solid reaction rate. These differences are due to the MnO content which is 6 % for Golpejas concentrates compared to 14.5 and 15.4 % for the Echassières and Penouta concentrates respectively (see table III). The carbochlorination of the Spanish concentrates starts at temperatures of about 300 °C and is complete at 500 °C. While that of Echassières is much less reactive.

Tables VIII and IX indicate the semi quantitative analysis of the carbochlorination residues and condensates for the Echassières and Golpejas columbo-tantalite concentrates respectively. At temperature less than 1000 °C and during the carbochlorination of Echassières, the tantalum oxide is concentrated in the residues while traces of tantalum compounds are found in the condensates.

Table IX shows that the Golpejas columbo-tantalite carbochlorination leads to the formation of volatile tantalum chlorinated compounds at temperatures higher than 300 °C. Only $MnCl_2$ and SiO_2 are detected in the 650 °C carbochlorination residue.

This leads to the conclusions that full carbochlorination of Golpejas columbo-tantalite is reached while selective carbochlorination of Echassières columbo-tantalite concentrates, with respect to Ta_2O_5, is possible.

4.3.3. Chlorination of microlite concentrates

Figure 10 shows the evolution of the percent weight loss in function of the temperature for the chlorination of microlite (see table II). For temperatures less than 400 °C, tantalum compounds are concentrated in the residues (see table X). While at temperature higher than 450 °C, the condensates main composition is tantalum and niobium chlorianted compounds. XRD indicates that the microlite decomposes partially to tantalum pentaoxide at temperature of about 400 °C. Microprobe analysis, of the chlorination residues, shows that the ratio of (Ta_2O_5/Nb_2O_5) incresases from 3.7 to 9.8 as the temperature augment from 200 to 700 °C.

The apparent chlorination selectivity, with respect to tantalum compounds, at < 450 °C seems to be purely kinetics. One may underline that, in the temperature range of 450 $\leq$ T $\leq$ 700 °C, the U, Ca and Ba compounds are concentrated in the resisue of chlorination.

4.3.4. Carbochlorination of microlite concentrates

The carbochlorination of microlite is possible between 250 and 350 °C as shown by figure 10. The tantalum and niobium chlorinated compounds are the main constituents of the condensates (see table XI).

The presence of chlorides in the condensates at temperatures lower than their melting points for elements such as potassium, uranium, etc could be explained by the synthesis of compounds such as $KCl.UCl_4$ (40) (M.Pt. = 350 °C) or again by the formation of gaseous complex metal chlorides as summarized in table XII (41-53). One may underline that in spite of the presence of uranium compounds in the condensates, the major part of this element is concentrated in the residues of carbochlorination.

The rate of microlite carbochlorination is higher than that of its chlorination and its reaction temperature is lower. It seems that the carbochlorination of the microlite is less selective than its chlorination.

4.4. HIGH TEMPERATURE TREATMENT

The samples have been agglomerated in a classical furnace at about 1300 °C. Tests on this materials indicates that softening and the fusion temperature of columbo-tantalite are 1431 and 1465 °C. Carburation of the Penouta columbo-tantalite at 1550 °C with carbon and under argon shows the formation of tantalum and niobium carbides in a matrix composed of tantalum and manganese compounds. As the reaction progress, the matrix manganese content decreases and a needles rich Ta - Mn carbides are formed. Thermogravimetric analysis, XRD, SEM and microprobe analysis indicate that the most probable reaction are the following equations [54-58].

Ta_2O_5	+	7	C	--->	2	TaC	+	5	CO	I
Nb_2O_5	+	7	C	--->	2	NbC	+	5	CO	II
MnO	+		C	--->		Mn	+		CO	III
FeO	+		C	--->		Fe	+		CO	IV

Thermodynamic (59-65) study indicates that the columbo-tantalite carburation at low oxygen and carbon monoxide pressure lead to the separation of the Ta and Nb from Fe and Mn through the formation of tantalum and niobium carbides and the reduction & volatilization of iron and manganese metals as indicated by figure 11.

Figures 12 schematize the plasma furnace used in for the study of small quantities of columbo-tantalite. A new specially designed plasma refrigerated reactor is shown by figure 13. This water refrigerated reactor is used for the recovery of vapocondensates and residues of the treatment. Brass is the main construction material for this apparatus.

Penouta's columbo-tantalite agglomerates are treated in both reactors. Argon is used as a plasmagene gas and the average temperature during the treatment is about 2000 °C. The sample weight is 50 to 100 grams. Transfered arc is initiated between the torch and the upper part of the sample's graphite crucible. The melted sample climbs the crucible's wall to the top of the crucible. After the treatment, the vapocondensates and the residues are examined by XRD, SEM and microprobe.

Figure 14 presents the molten sample **A**, the climbed carburized Ta & Nb products **B** and the top rich tantalum carbides **C** after their treatment in the refrigerated plasma reactor. **A** is a recrystallized columbo-tantalite. The B phase composition is $Ta_yNb_{(1-y)}C_x$ where $x<1$. Ta_2C, TaCx and NbCx are the essential compounds of **C**. The vapocondensate composition is a recrystallized columbo-tantalite.

Figure 15 shows a schematize presentation of the B layer obtained in using the plasma furnace (figure 12). The layers 1 and 2 of this figure are composed of a carbide rich in Ta, Nb and Mn while the third one is rich in Ta and Nb compounds. The fourth layer is essentially composed of tantalum carbide and contained needles of Al and Ta compounds. Global analysis of these four layers indicates an increase of the Ta and Nb content from 55.5 to 88.2 %. With the actual refrigerated plasma reactor, full mass balance was not possible because of the failure of total recovery of vapocondensates. However it seems that the recovered residues Ta and Nb content is higher and consists mainly of carbides of these elements.

5. CONCLUSIONS

1. Echassières primary concentrate main tantalum and niobium bearing minerals are microlite and tantalo-columbite. Concentrates of Golpejas and Penouta contain columbo-tantalite. Up to 15 % of the total tantalum and niobium content of these concentrates are present in the

cassiterite as microinclusions and can't be recovered by the mineral processing. These elements will be concentrated in the tin slag during the metallurgical processing of cassiterite.

2. The average tantalum and niobium oxides content of the Penouta tailing is about 3 times that of the original ore. Some 2000 tons of Ta, Nb, W, Sn, Ti,... are ready to be processed.

3. Using the classical magnetic separation, it was possible to recover almost 100 % of the columbo-tantalite from the primary concentrates.

4. After the classical magnetic, electrostatic and gravity separation, the concentrate microlite content was about 30 %. Associating heat treatment and size classification to the classical mineral processing, it is possible to obtain a concentrate having $\geq$ 65 % of microlite. Using superconductor magnetic separator leads to a slight amelioration.

5. Chlorination of Golpejas and Penouta columbo-tantalite permits the selective concentration of the major part of the tantalum compounds in the residue. The volatile metal chlorinated compounds are condensed and a partial separation of these elements was possible. The chlorination of the Echassières tantalo-columbite is total and not selectivite. This is probably due to the presence of minerals containing Al or Ti compounds.

6. Carbochlorination of Echassières tantalo-columbite between 600 and 900 °C is selective while that of Golpejas and Penouta columbo-tantalite is not.

7. For temperatures less than 700 °C, selective chlorination of microlite was possible leading to the volatilization of tantalum and niobium chlorides and the concentration of Ca, U, Ba, Si, K, etc... in the residues.

8. High temperature carburation of columbo-tantalite leads to the formation of tantalum and niobium carbides. Part of the iron and manganese oxides is carburized and the rest is reduced to metals which are volatiles at this temperature range ($\geq$ 1550 °C).

9. Treatment of the columbo-tantalite in the plasma furnace leads to a similar results as that of 8.

Further extension of this research should be focused on :

A. Large scale experimentation of the chlorination and carbochlorination so as to explore the possible side reactions between the chlorinated compounds of different elements and their influence on the recovery rate of valuable elements and the selectivity of the chlorination reactions,

B. Separation of volatile metal chlorinated compounds using a predetermined temperature gradient,

C. Study of the chlorine degree of utilization and recycling during the chlorination process,

D. The optimization of the chlorination and carbochlorination process parameters in order to establish a mass and energy balance for a large scale experimentation,

E. Extending the plasma treatment using a feeding torch plasma,

F. Testing of different material with respect to their corrosion resistance in presence of chlorinated gas mixture in order to collect engineering data and to define the most adequate construction material for an industrial application of this process.

6. REFERENCES

1. SEABORG T.G.
"Our heritage of the elements",
Metallurgical Transactions A, 1980, 11A, p. 5-19.

2. "Matières Premières et Matériaux",
Agence Française pour la Maîtrise de l'Energie, 27, Rue Louis-Vicat, 75015 Paris, 10/83.

3. SCHUILING R.D.
"Tin belts around the Atlantic ocean : some aspects of the geochemistry of tin, a technical conference on tin" London, 1967, page 531 - 547, published by the International Tin Council and printed by Wijland and Leiteritz, Drukkerij's - Gravenhage, The Hague, Netherlands, 1968.

4. JONES T.S. and CUNNINGHAM L.D.
"Columbium and tantalum"
Minerals Yearbook, 1983, Volume 1, p. 273
Published by United States Department of the Interior, Bureau of Mines.

5. SANTOS MORANA M.
Technical director of "Centro Minero de Penouta",
Private communication, 4/88.

6. TCHUKHROV F.V.
Mineralogy, 1967, II, 3, p. 304, published by Nauka, Moscow.

7. CUELLIEZ F.
British patent, 1939, N° 507124.

8. KROLL W.J.
"The pyrometallurgy of halides",
Metallurgical Reviews, 1956, 1, 3, p. 291.

9. LIND R. and INGLES T.A.
"The chlorination of niobium ores and oxides"
U.K.At. Energy Authority, Ind. group, 1959, TN-106.

10. PINATTI D. G., PETOILHO J.C., BALDAN C.A. et FREITAS L.R. DE,
Brazilian Patent n° (11)(21) PI 7900175, 20.02.1980.

11. MAY S.L., TEWS J.L., HENDERSON A.W. and GRUZENSKY W.G.
"Extractive metallurgy of euxenite"
U.S.B.M., 1959, R.I. N° 5531.

12. WHALLEY B.J.P., INGRAHAM T.R. and MARIER P.
"The preparation of $NbCl_5$ from ore concentrates of columbium mining products limited, oka, que"
Department of mines and Technical Surveys Mines Branch Investigation, 1960, Report IR 60 - 123, Ottawa - Canada.

13. MAY S.L. and ENGEL G.T.
"Extraction of tantalum and columbium from ores and concentrates by chlorination"
U.S.B.M., 1965, R.I. N° 6635.

14. MCINTOSH A.B. and BROADLEY J.S.
"The extraction of pure niobium by a chlorination process, extraction and refining of the rare metals"
The Institution of Mining and Metallurgy, 1957,
p. 272 - 286.

15. MCINTOSH A.B.
"The development of niobium"
J. Inst. Metals, 1957, Vol. 85 - p. 367-372.

16. STEELE B. and GELDART D.
"Distillation of volatile chlorides as a mean of obtaining pure niobium, extraction and refining of the rare metals"
The Institution of Mining and Metallurgy, 1957,
p. 287 -294.

17. HENDERSON A.W., MAY S.L. and HIGBIE K.B.
"Chlorination of euxenite concentrates"
Ind. and Eng. Chemistry, 1958, Vol. 50, N° 4, p. 611-612.

18. FAIRBROTHER F., COWLEY A.H. and SCOTT N.
"The oxytrichlorides and oxytribromides of niobium (v) and tantalum (v)"
Journal of the Less-Common Metals, 1959, vol. 1, p. 206-216.

19. MILLER G.L.
"Tantalum and niobium"
1959, Butterworths Scientific Publications.

20. HENDERSON A.W.
"Chlorination of ores and concentrates as applied to extracting tantalum, columbium and tungsten"
Journal of Metals, 1964, vol. 16, p. 155-160.

21. JERE G.V., PATEL C.C. and KRISHNAN V.
"Thermodynamic considerations in the chlorination of different oxides constituting columbite (niobite) and tantalite"
Trans. Met. AIME, 1961, vol. 221, Aug. 1961, p. 866-872.

22. STEFANYUK S.L. et MOROSOV I.S.
"Kinetics and mechanism of chlorination of minerals (loparite, pyrochlore, zircon and euxinite)"
Traduction de Zhurnal Prikladnoi Khinii, 1965, vol. 38, N° 4, p. 729-735.

23. MEHRA O.K., ZAHED HUSSAIN S. et JENA P.K.
"Kinetics of the chlorination of niobium pentoxide with chlorine in presence of excess of graphite powder",
Transactions of the Indian Institute of Metals, March 1966, 53-56.

24. MEHRA O.K. et JENA P.K.
"Kinetics of the chlorination of tantalum pentoxide with chlorine in presence of excess of graphite powder",
Transactions of the Indian Institute of Metals, 12/ 1967, 210-212.

25. SRINIVASAN K. R. et JENA P.K.
"Kinetics of chlorination of the pentoxides of niobium and tantalum by chlorine and carbon".

26. OLSEN R.S. et BLOCK F.E.
"The chlorination of columbite in a fluidized-bed reactor". Chemical Engineering Process Symposium, 1970, Series 66 - 105, p. 225 - 228.

27. HABASHI F. et MALINSKY I.
"Technical niobium from pyrochlore",
CIM Bulletin, September 1975, 80-90.

28. HARRIS P.M. and JACKSON D.V.
"Investigations into the recovery of niobium from mrima hill deposit"
Trans.IMM - Sec. C, 1975, vol. 75, p. C95-C111.

29. MEUBUS P.
"High temperature chlorination kinetics of a niobium pyrochlore"
Metallurgical Transactions B. 10 B, 1979, N° 3, p. 93-101.

30. MEUBUS P.
"Chlorination kinetics of a niobium pyrochlore in the gas-solide phase"
Metallurgical Transactions B., 12B June 1981 p.241-247.

31. DONG HUI LEE,
"Recovery of tantalum and niobium values from tin slag by chlorination process".
Journal of the Korean Institute of Metallurgy and Mining Engineering, 1982, vol. 19, p. 209-214.

32. BROCCHI E. DE A.
"Reduction chlorination reactions of niobium and tantalum oxide containing materials"
Thesis, 3/1983, 270 pages, Imperial College of Science and Technology, London, United Kingdom.

33. BROCCHI E. DE A. et JEFFES J.H.E.
"Reduction chlorination of a Nb-Ta-bearing slag and a brazilian pyrochlore concentrate"
Miner. Process. Extr. Metall., Pap. Int. Conf. ; Pub.: Inst. Min. Metall., London, UK 1984, p. 161 -170.

34. SATO N. et NANJO S.
"Separation of niobium from ferroniobium by chlorination"
Metallurgical Transactions B.,16B, September 1985, p.639-644.

35. MOURA F.J., BROCCHI E.A. et KOHLER H. M.
"Kinetics of chlorination of niobium containing brazilian tin slag"
Pyrometallurgy 87, IMM Edition Nal Warner, 1987, p. 799-812.

36. MEYER-JOLY M.-CH.
"Valorisation du concentré mixte d'Echassières"
Thesis, 9/1988, 154 pages, Institut National Polytechnique de Lorraine, Nancy, France.

37. GABALLAH I.,ALLAIN E.,MALAU K.,MEYER M.-CH. et BLAZY P.
"Recovery of refractory metal oxides from tin slags"
Proceedings of the First International Conference on Hydrometallurgy "ICHM'88", Beijing, China, 10/1988, Edited by Zheng Yulian and Xu Jiazhong, Published by International Academic Publishers, p. 385-388.

38. GABALLAH I., ALLAIN E. et MEYER - JOLY M.-CH.
"Leaching of tin slags and subsequent chlorination of the tantalum and niobium concentrate"
Refractory Metals (Extraction, Processing and Applications) Edited by K.C. Liddell, R.S. Sadoway and R.G. Bautista, Published by TMS, 1991, p. 283-296.

39. MARIGNAC M.C.
"Recherches sur les combinaisons du niobium", Ann. Chim. Phys., 1866, vol. 8, p. 49-75.

40. LEVIN E.M., ROBBINS C. R. and MCMURDIE H.F.
"Phase diagrams for ceramists"
1964, vol. Is, p. 381.

41. SHIEH CH. - F. and GREGORY N.W.
"Spectrophotometric study of the vapors of iron (III) chloride and of mixtures of iron (III) chloride and aluminium (III) chloride"
Evidence for formation of mixed metal dimer molecules, J. Phys. Chem., 1975, vol. 79, N° 8, p. 828-833.

42. FOWLER R. M. and MELFORD S.S.
"$FeAlCl_6$, a volatile molecule formed by the reaction of aluminum chloride with ferric chloride"
Inorg. Chem. 1976, vol. 15, N°2, p. 473-474.

43. EGGERS H. - H., OLLMANN D., HEINZ D., DROBOT D.W. and NIKOLAJEW A.W.
"Sublimation and desublimation in $AlCl_3$-$FeCl_3$"
Z. Phys. Chemie, 1986, vol. 267, N° 2, p. 353-364.

44. BINNEWIES M.
"Gas complexes $MAlCl_5$ and MAl_2Cl_8, z. Anorg. Allg"
Chem., 1977, vol. 437, p. 25-32.

45. BINNEWIES M.
"Mass spectrometric investigations of the systems $FeCl_2AlCl_3$ AND $FeCl_2/FeCl_3$, Z. Anorg. Allg."
Chem., 1977, vol. 437, p. 19-24.

46. SCHÄFER H. and FLÖRKE U.
"Gaseous complexes of trichlorides, tetrachlorides, and pentachlorides with aluminium chloride"
Z. Anorg. Allg. Chem., 1981, vol. 479, p. 89 - 98.

47. M. SØRLIE and H. ØYE.
"Complexation and reduction - oxidation equilibria of titanium chlorides in gaseous aluminum chloride",
Inorg. Chem., 1978, vol. 17, N° 9, p. 2473 - 2484.

48. KREBBS B., JANSSEN H., BJERRRUM N.J., BERG R.W. and PAPATHEODOROU G.N.
"$NbAlCl_8$: a molecular dinuclear complex in the solid, melt, and vapor phases"
Synthesis, crystal structure, and Raman spectra, Inorg. Chem. 1984, vol. 23, p. 164 - 171.

49. GRUEN D. M. and MCBETH R.L.
"Vapor complexes of uranium pentachloride and uranium tetrachloride with aluminium chloride"
Inorg. Chemistry, 1969, vol. 8, N° 12, p. 2625 - 2633.

50. DEWING E. W.
"Gaseous complexes formed between trichlorides ($AlCl_3$ and $FeCl_3$) and dichlorides"
Metallurg. Trans. 1, 1970, N° 8, p. 2169 - 2174.

51. SCHÄFER H. and FLÖRKE U.
"Mass spectrometric measurements of the stability of the gaseous complexes MAl_2Cl_8 (M = Be, Fe, Zn, Cd, Pt). connection between the stability of the complexes MAl_2Cl_8 and the coordination of M and Cl in the solid dichloride",
Z. Anorg. Allg. Chem. 1981, vol. 478, p. 57 - 64.

52. PAPATHEODOROU G.N., MEISENHELDER J. and LOUTFY R.
"Vapor complexes of Fe (II) chloride with aluminum chloride",
J. Inorg. Nucl. Chem. 1981, vol. 43, p. 1056 - 1059.

53. EMMENGGER F. P.
"Stability of gaseous complexes between two - and three - valent metal halides"
Inorg. Chem. 1977, vol. 16, N° 12, p. 343 - 348.

54. UPADDHYA, K.; J.J. MOORE and K.J. REID
"Application of thermodynamic and kinetic principles in the reduction of metal oxides by carbon in plasma environmemt"
Metallurgical Transaction B., Vol. 17B Mar. 1986.

55. GARG. S.P., R. VENKATARAMANI and C.V. SUNDARAM
"Carbothermic reduction of refractory metal oxides"
Transaction of the Indian Institute of Metals.
Vol. 28, N° 4. August 1975.

56. WORRELL WAYNE L., CHIPMAN JOHN
"A thermodynamic analysis of the Ta-C-O, Cb-C-O and V-C-O system"
Transactions of the Metallurgical Society of AIME. Vol. 230, Dec. 1964.

57. HILBORN M.M., MUNZ R.J., BERK D., DROUET M.B.
"Evaluation of ferroniobium carbide production in a laboratory-scale plasma furnace"
Canadian Metallurgical Quarterly, N° 2 pp. 101-107, 1989.

58. MUNZ R.J. and CHIN E.J.
"Carbothermic reduction of niobium pentoxide and pyrochlorore in a tranferred arc argon plasma".
Canadian Metallurgical Quartely, Vol. 30,
N° 1, pp. 21-29, 1991.

59. PICHELIN G., A. ROUANET
"Vaporisation sous pression atmosphérique du système oxide de niobium-oxide de tantale"
Journal of the Less Common Metals, 153. 1989.
pp. 311-326.

60. SATA TOSHIYOKI
"High temperature vaporization of single oxides".
Refractories Japan, N° 4.34-233; 1982.

61. DJONA MAURICE
"Etude de la valorisation d'un système complexe à haute temperature".
CNRS, Odeillo. Université de Toulouse III,
Perpignan, France, 29/Juin./1987.

62. GUNNAR ERIKSSON
"Thermodynamic studies of high temperature equilibria"
Acta Chem. Scan.,25. N° 7.1971.

63. KELLOG H.H.
"Vaporization chemistry in extractive metallurgy"
Transaction of the Metallurgical Society of AIME
Vol. 236, May 1966.

64. JANAF THERMOCHEMICAL TABLES
J. Phys. Chem. Ref. Data 4:1 1975.

65. KELLOG H.H.
J. Phys. Chem. Ref. Data 7:793 1978.

Table I. Average chemical and mineralogical analysis of primary concentrate of Echassières as oxide weight percent.

SnO2	Ta2O5	Nb2O5	Total	Cassit.	Microl.	TaCb	Total	Others
46.4	4.9	4.2	55.5	48.9	5.1	5.4	59.4	40.6

Cassit = Cassirite Microl. = Microlite TaCb = Tantalo-columbite

Table II: Composition of microlite of Echassières primary concentrates, as oxide weight percent, obtained by microprobe.

Ta2O5	Nb2O5	UO2	WO3	CaO	Na2O	PbO	BaO	Ta2O5/Nb2O5
59.6	16.0	6.55	3.1	1.4	0.8	1.3	2.2	4.96

Table III: Columbo-tantalite composition of the three concentrates (as oxyde weight %) obtained by microprobe.

Origin	Ta2O5	Nb2O5	FeO	MnO	WO3	Ta2O5/Nb2O5	FeO/MnO	Ta+Nb/Fe+Mn
Echassières	23.5	53.3	4.1	14.5	1.54	0.52	0.38	4.14
Golpejas	35.4	43.0	10.7	6.0	n.d.	0.82	1.79	4.71
Penouta	33.5	28.3	4.1	15.4	n.d.	1.18	0.27	3.17

Table IV: Composition of casserite of the three primary concentrates, as oxyde weight %, obtained by microprobe.

Origin	SnO2	Ta2O5	Nb2O5	FeO	MnO	Total
Echassières	93.8	1.7	1.1	0.3	0.1	97.0
Golpejas	99.3	2.2	0.2	0.4	0.1	102.2
Penouta	99.3	1.9	0.1	0.2	0.1	101.5

Table V : Chemical analysis and specific surface area of tantalo-columbite concentrates.

Origin	% Ta2O5	% Nb2O5	% FeO	% MnO	Total	Sp.S.**	Observations
Echassières	16,7	44,3	2,0	12,3	75,3	1,5	= 15 % Topaze
Golpejas	28,9	38,8	>9,0*	5,1*	81,8	1,2	Rich in Fe& Ti
Penouta	33,5	29,0	4,1	15,4	82,0	0,5	

* values estimated from microprobe analysis

** Specific surface area m2/gr

Table VI : Semi-quantitative composition of residues and condensates during the chlorination of Echassières tantalo-columbite as a function of the temperature

T (°C)	Elements of the chlorination residue's	Elements of the condensates
	Initial	NB, Mn, Ta, Fe & Si, Al,Ti,Sn
500	Mn, Nb, Ta, Fe, & Si, Al, Ti, Sn	Nb, Cl, Ta, Fe, Mn
600	Mn, Ta, P, Nb & Si, Al, Ti, Sn	Nb, Cl, P, Fe, Ta, Mn
700	Mn, Ta, Nb, P & Fe, Si, Al, Ti, Sn	Nb, Cl, Mn, Ta, Fe
800	Ta, Nb, P, Si, Al, & Sn, Ti, Mn	Cl, Mn, Nb, Ta
900	Ta, Nb, P, Si, Al, & Sn Ti, Mn	Cl, Mn, Nb, Ta
1000	P, Al, Cl, & Ti	Cl, Mn, Ta, P, Nb, Al

Table VII : Idem table VI for the chlorination Golpejas

T (°C)	Elements of the chlorination residue's	Elements of the condensates
	Initial	Fe, Ti, Nb, Ta, Mn
500	Fe, Ti, Nb, Ta, Mn	Cl, Fe
600	Fe, Ti, Nb, Ta, Mn & K	Cl, Fe
700	Fe, Ti, Nb, Ta, Mn	Cl, Fe, Mn, Nb
800	Ti, Fe, Ta, Nb, Mn	Cl, Fe, Mn, Nb, & Ta
900	Ti, Ta, Nb	Cl, Fe, Mn, Nb, Ta
1000	Ta, Nb, Ti, & Fe	Cl, Fe, Mn, Nb, Ta, & Ti

Table VIII : Idem table VI for the carbochlorination of Echassières columbo-tantalite

T (°C)	Elements of the chlorination residue's	Elements of the condensates
	Initial	Nb, Mn, Ta, Fe & Sn, Ti, Al, Si
500	Nb, Mn, Ta, Fe, & Sn, Ti, Al, Si	Nb, Ta, Cl, Fe & Al, W
700	Ta, Mn, Nb & Fe, Al, Si, Sn, Ti	Nb, Fe, Cl & Ta, Mn, W
800	Ta, Mn, Si, Nb & Sn, Fe, Al, Ti	Cl, Nb, Mn, & Ta, Fe, W
900	Ta, Si, & Ti, Sn, Mn, Al, Nb, Fe	Mn, Cl, Nb & Ta, W, Ti
1000	Si, Ta, Al & Cl, Ti, Nb, Sn, Mn	Cl, Mn, Ta, Nb & Al

Table IX : Idem table VI for the carbochlorination of Golpejas columbo-tantalite

T (°C)	Elements of the chlorination residue's	Elements of the condensates
	Initial	Fe, Ti, Nb, Ta, Mn
300	Fe, Ti, Ta, Mn, Nb	Nb, Ta, Cl, Fe & Al, W
400	Fe, Mn, Ta, Ti, Nb	Fe, Nb, Ta, Cl
500	Mn & Ta, Nb, Si	Fe, Ta, Cl, Nb
650	Mn & Cl, Si	Ta, Fe, Cl, Nb, Mn

Table X : Semi quantitative composition of residues and condensates during the chlorination of Echassières microlite as a function of the temperature.

T (°C)	Elements of the chlorination residue's	Elements of the condensates
	Initial Ta, Nb, Sn, Fe, K, Ti	& (Mn, Al, Si)
200	Ta, Nb, Fe, Sn, Ti & (K,Mn,Al,Si,Cl)	Fe,Cl, & (Ti, Nb, Ta)
250	Ta, Nb, Fe, Sn, & (K,Ti,Mn,Al, Si,Cl)	Cl,K & (P, Fe, Al)
300	Ta, Nb, Fe, Sn & (K,Ti,Mn, Al, Si)	Cl, Nb,K,Fe & (Ti,Ta,Al,P)
400	Ta, Nb, Fe, Sn & (K,U,Ti,Mn,Si,Al)	Ta, Nb, Cl, & (Fe, P,Al,K)
450	Ta, Nb, Fe, K & (Ti,Ba,U,Sn,Mn,Al,Si)	Ta, Nb, & (Fe,Cl,K,Al)
500	Ta, K,Sn,Ca,U, & (Nb,Ba,Mn,Fe,Al,Si)	Ta,Nb, & (Cl,Fe,Al)
700	Cl,Ca,Si,Ba,K,U,Ta & (P,Nb,Al,Mn)	Ta,Cl,Nb & (Fe,K,U,Mn,Al)

Table XI : Idem table X for the carbochlorination of Echassières microlite.

T (°C)	Elements of the chlorination residue's	Elements of the condensates
	Initial Ta, Nb, Sn, Fe, K, Ti	& (Mn, Al, Si)
250	Ta, Sn, Nb, Fe, Ti & (Mn, Si, Al)	
300	Ta, Fe, Sn, Nb, K, Ti & (Al, Si, Mn,U)	Ta, Cl, Fe & (Nb, K)
350	K, Si, Ba, Ca, U, Fe & (Mn,Al,Nb,Ta)	Ta, Cl, Nb & (U, K, Fe)
400	K, Si, Ba, Ca, U & (Al, Fe)	Ta, Cl, Nb & (Fe, U)
450	Ca, Ba, Si, Mn, K, U & (Al)	Ta, Cl, Nb & (Fe, U)

Table XII : Possible gaseous complex binary chlorides synthesized during of the chlorination of columbo-tantalite or microlite.

Binary chloride	N	M Reference
N $N'Cl_6$	Al	Fe [41 - 43]
N $N Cl_5$	Al	Ca[44], Fe[45], Mn[44]
N $N Cl_6$	Al	Ti [46,47]
N $N Cl_8$	Al	Nb[48], Ta[46], U[49]
N N_2Cl_8	Al	Ca[44,50], Fe[45,51,52]
	Fe	Ba[53], Ca[53], Mn[44,50]
N N_2Cl_{10}	Al	U[49]
N N_3Cl_{11}	Al	Ca[50], Mn[50], Ti[47]

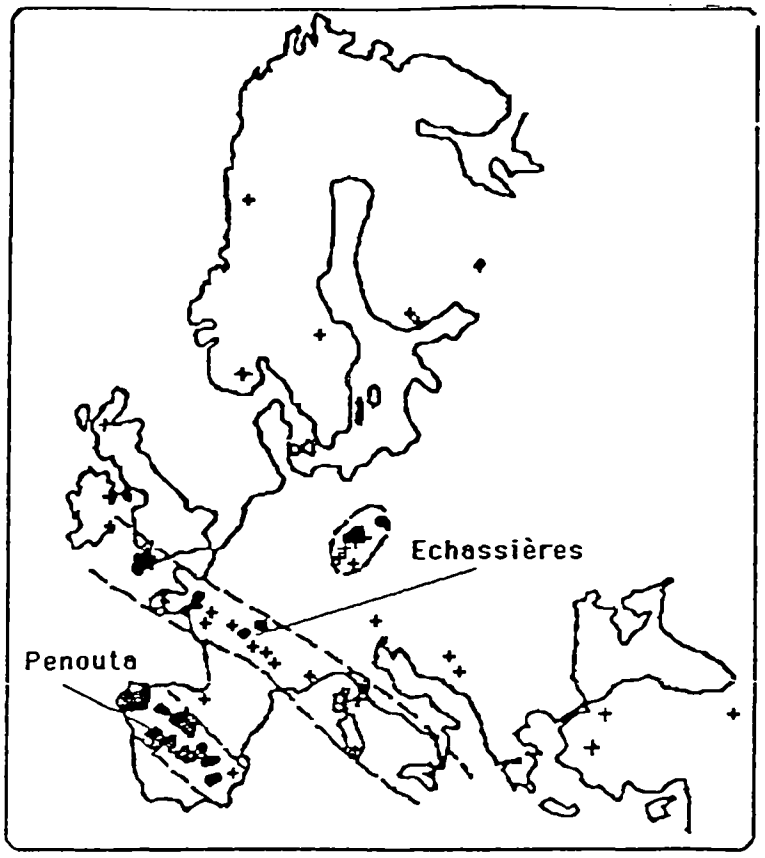

• Tin deposits(economic or marginal) + Uneconomic occurrence
--- Approximate limit of tin belts

Figure 1: Tin belts in Europe(3)

Echassières primary concentrate's size classification

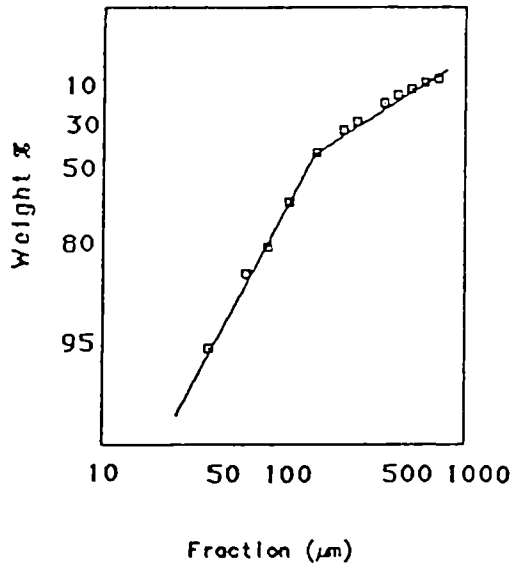

Figure 2: Rosin-Rammler curve.

Figure 3 : Flow sheet of Echassières (Allier, France)

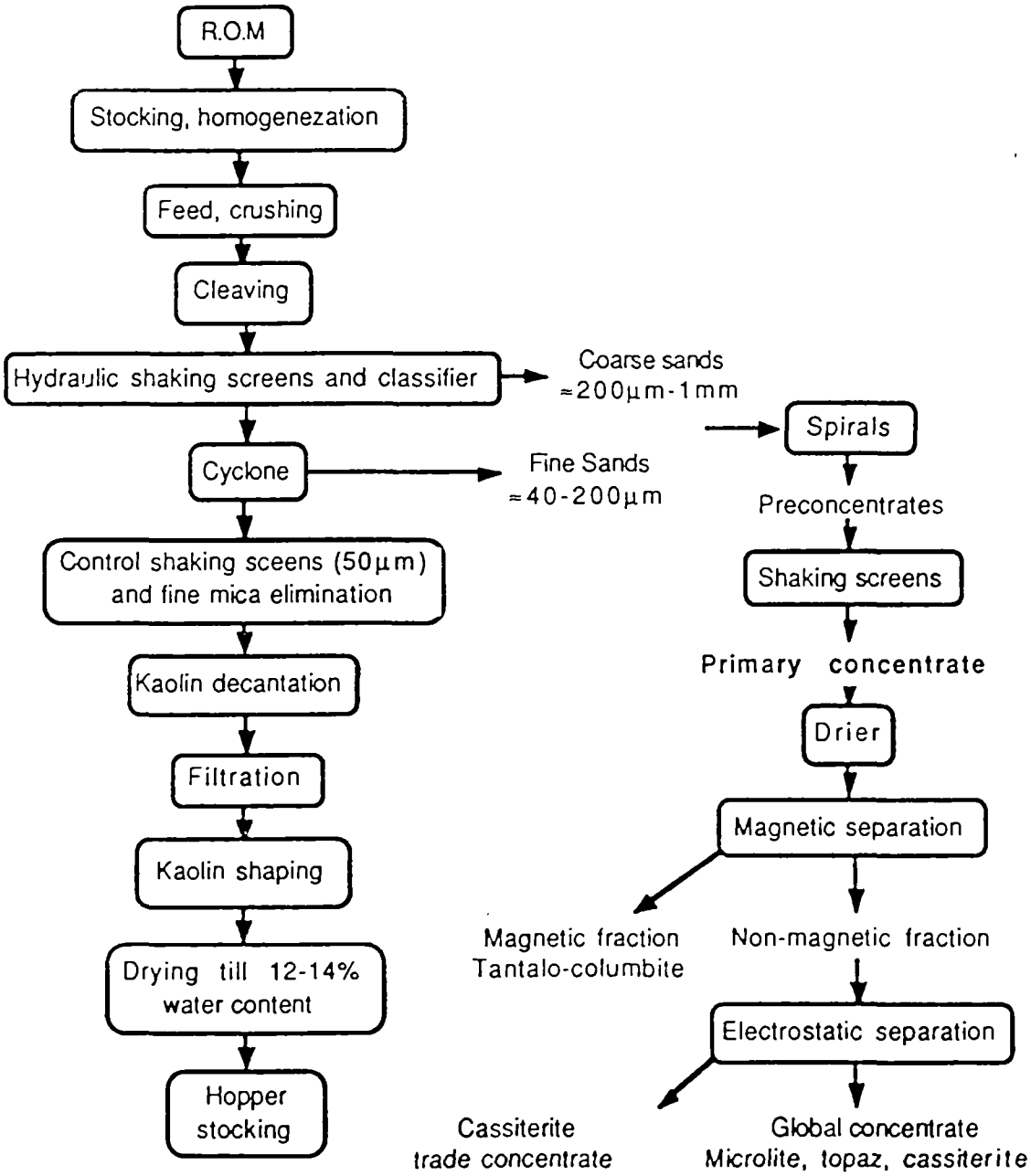

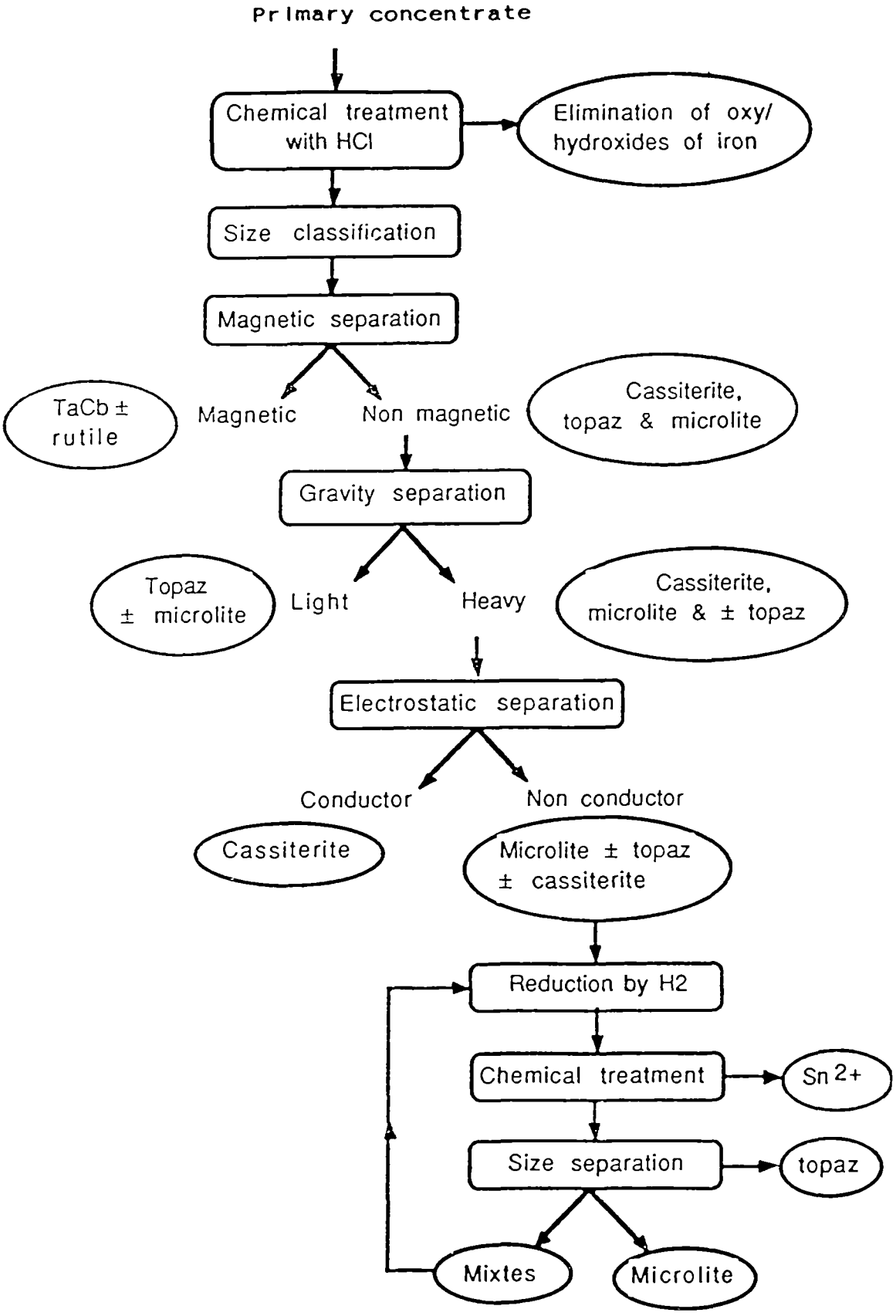

Figure 4 : Proposed mineral processing flow sheet.

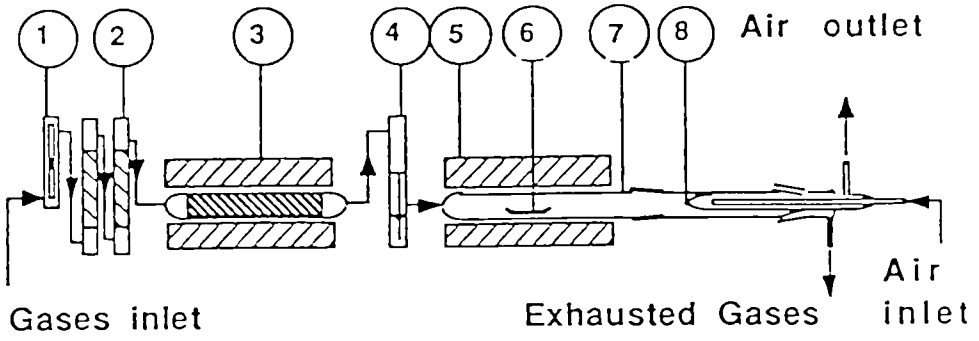

1. Flowmeter 2. P_2O_5 column 3. Carbon furnace 4. H_2SO_4
5. Furnace 6. Quartz boat 7. Quartz reactor 8. Condensation finger

Figure 5 : Chlorination apparatus

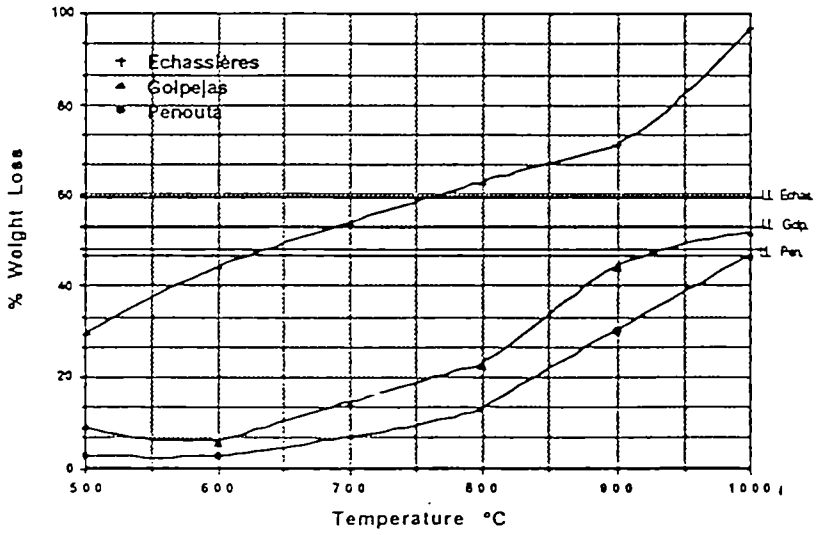

** LL : Theoretical calculated lower limit corresponding to the weight loss for the chlorination and volatilization of Fe, Mn, and Nb oxides.

Figure 6 : Comparison between the evolution of the percent weight loss of different concentrates of tantalo-columbite during their chlorination in horizontal experimental set.

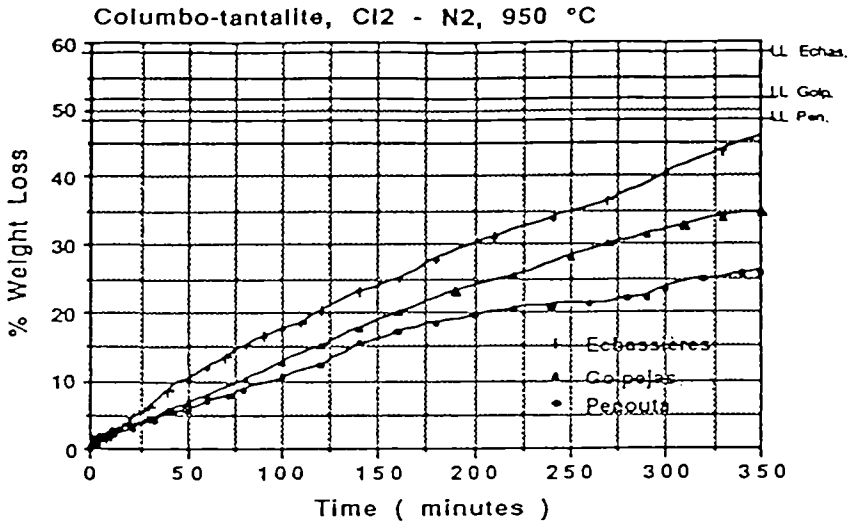

Figure 7 : Idem 6 for the vertical experimental set.

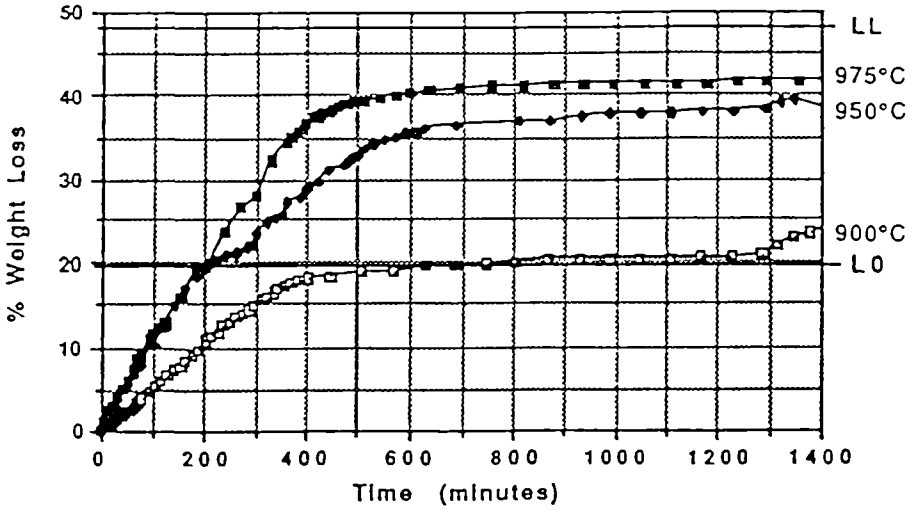

LO = Theoretical calculated lower limit corresponding to the weight loss for the chlorination and volatilization of Fe and Mn oxides

LL = Idem LO for Fe, Mn and Nb oxides

Figure 8 : % W.L. during the chlorination of Penouta columbo-tantalite in fuction of the time at different temperatures

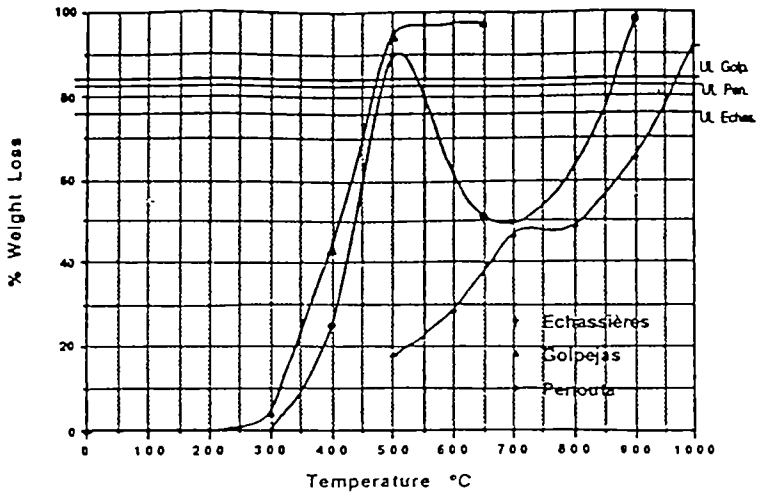

UL = Theoretical calculated upper limit corresponding to the weight loss for the chlorination and volatilization of Fe, Mn, Nb and Ta oxides

Figure 9 : Comparison between the evolution of the percent weight loss of different concentrates of tantalo-columbite during their carbochlorination in horizontal experimental set.

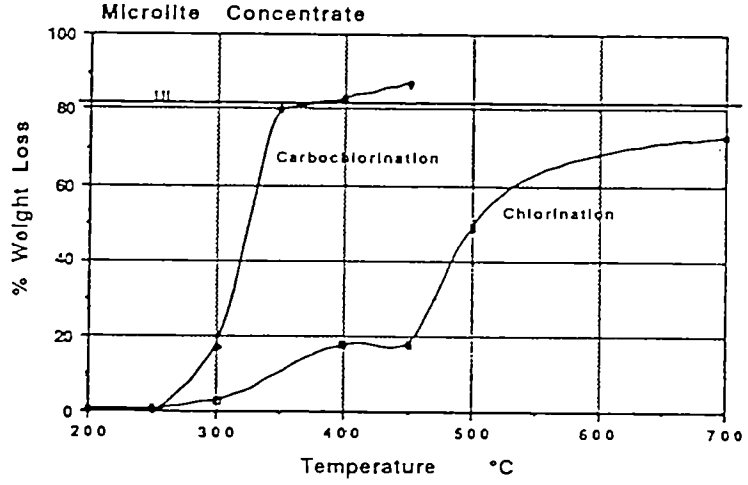

UL = Theoretical calculated upper limit corresponding to the weight loss for the chlorination and volatilization of Fe, Mn, Nb and Ta oxides

Figure 10 : Comparison of the evolution of the percent weight loss of microlite concentrates during its chlorination and carbochlorination in horizontal experimental set

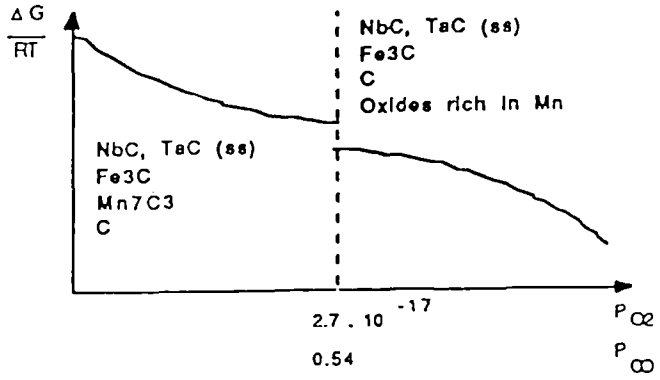

Figure 11 : Schematized evolution of Δ G/RT in function of the partial pressure of O2 and CO and predicted phases.

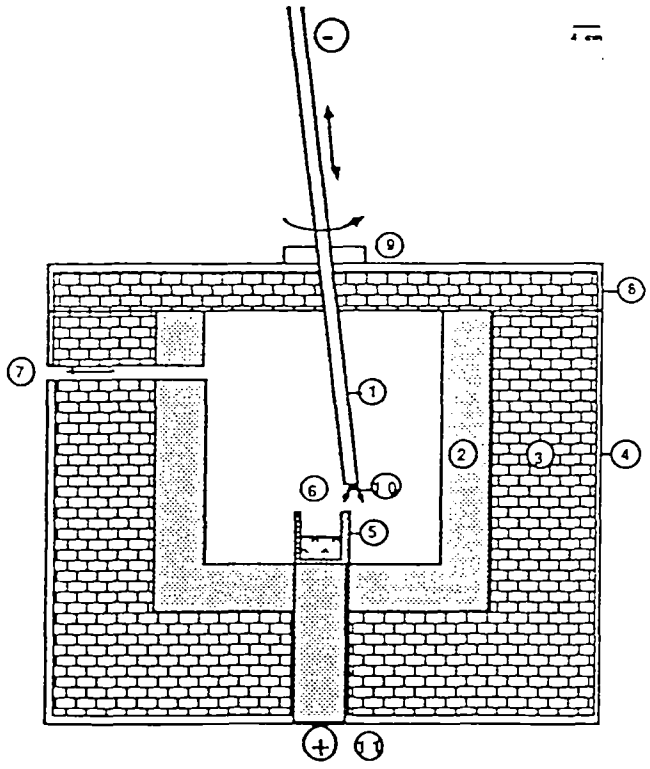

1. Vertical and precessional torch
2. Graphite furnace lining
3. Refractory cement
4. Steel external shell
5. Sample graphite crucible
6. Gas input
7. Gas output
8. water refrigerated cover
9. Refrigerated rotule
10. Cathode
11. Anode

Figure 12 : Plasma furnace.

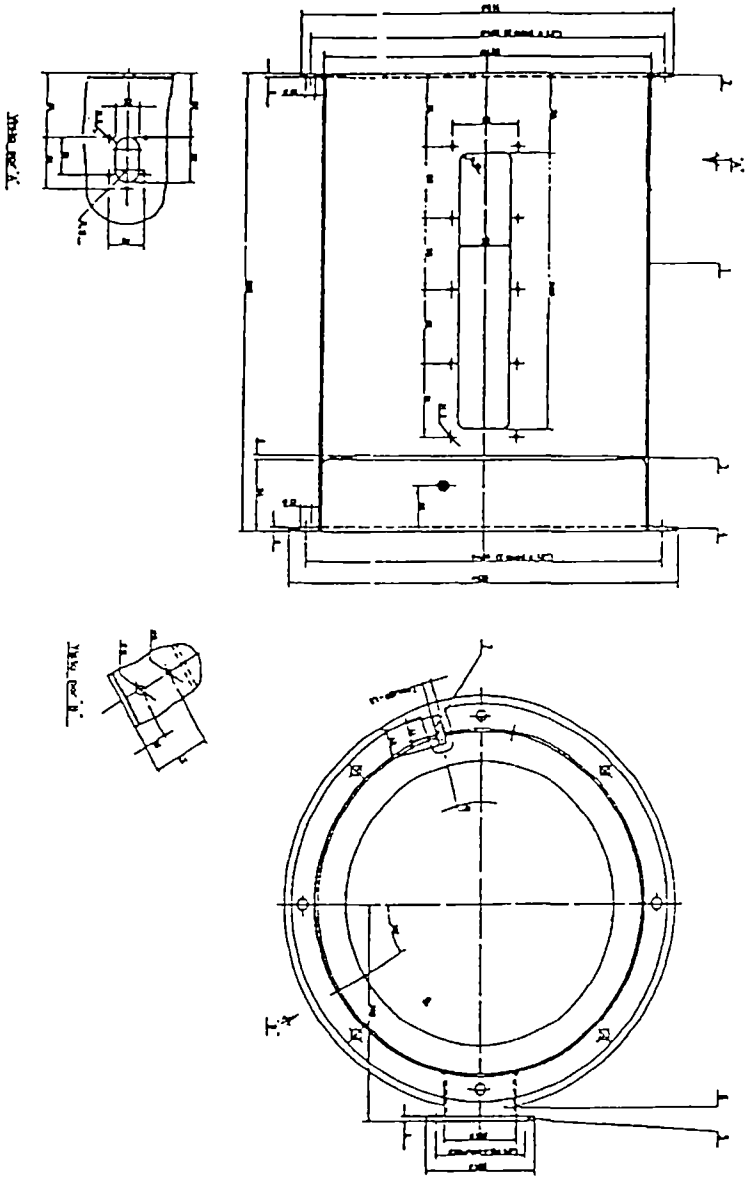

Figure 13 : Refrigerated plasma reactor.

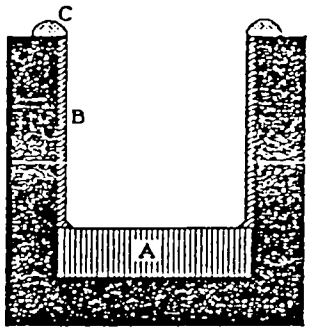

Figure 14 :

Molten sample and final products obtained by the apparatus described by (figure 13).

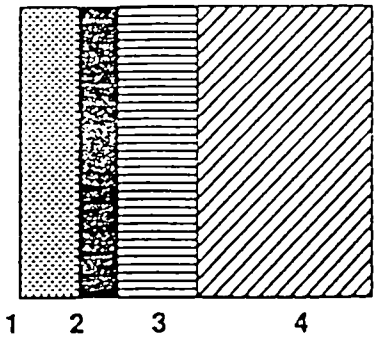

Figure 15 :

Schematic diagram of B obtained by the plasma furnace (figure 12).

RESEARCH AREA 3.2

HYDROMETALLURGICAL PROCESSING OF SULPHIDES AND OTHER ORES

RECOVERY OF NICKEL FROM NON-SULPHIDE SOURCES USING MICRO-ORGANISM ASSISTED LEACHING

Project Leader: D.J LEAK
K. R. K. Allbhal and A.W.L. Dudeney
Centre for Biotechnology and Mineral Resources Engineering Department,
Imperial College of Science Technology and Medicine, London, United Kingdom

Dr. S. Agatzini and P. Tzeferis
Metallurgy Department, National Technical University of Athens, Greece

Contract MA1M-0017-C(H)

1. INTRODUCTION AND OBJECTIVES

The aim of the work was to examine the application of microbially assisted leaching to the recovery of nickel from low grade laterites (non - sulphide ores). The specific objectives were :

i) To examine the mineralogy of the ores under test and establish any relationship between mineralogy and leaching characteristics.

ii) To examine the leachability of ores using commercially available 'chelating acids' of the types known to be produced from the metabolism of microorganisms.

iii) To establish the amenability of various ores to general acid leaching in shake flasks and columns using sulphuric acid as a control.

iv) To obtain and isolate from natural sources, various microorganisms with characteristics likely to be beneficial to the leaching process (e.g. acid tolerance, acid production and nickel tolerance).

v) To compare leaching with biologically produced acid mixtures with that obtained using the commercially available acids.

vi) To compare leaching with acids produced 'in situ' i.e. by growth of the organism in the presence of the ore, with a two stage process in which leaching is carried out with acids produced in the first stage.

vii) To examine the effect of growth substrate on biological acid production and the leaching process, including the use of substrates derived from process wastes (e.g. food or distillery wastes) available in the locality of the ores.

Six different samples of nickel laterite (from the Kastoria, Mantoudi, Triada, Litharakia, Kabia and Kukubajza deposits) were examined. The sample from Kastoria, was known to be of the garnieritic type, with the footwall being ophiolite. The deposit is located 10 Km to the Northwest of the town of Kastoria in Northern Greece. It had a relatively high nickel content. Examination of the ore in London gave 4.27 and 3.75% Ni, respectively, by fusion and direct acid dissolution. An acid resistant form is apparently present (probably nickel in solid solution in silicate). The lower value of 3.75% was taken to be a more appropriate target for an acid leaching project. The ore contained green, white and yellow-brown structures. Electron microprobe studies confirmed that most of the nickel was in form of garnierite, $(Ni,Mg)_3Si_2O_5(OH)_4$. The green fraction contained most of the nickel as low-magnesium garnierite and had chromite inclusions and abundant quartz. The white fraction contained high magnesium, low nickel, garnierite. The yellow-brown structures contained small concentrations of unidentifiable nickel. Minor effervescence with acid indicated the presence of small amounts of calcite. Detailed chemical analysis as well as screen analysis (Litharakia only) of the ore are shown in Tables 1 and 2 respectively.

The ore from Larco's Triada mine in southern Greece, was found by atomic absorption spectrometry to contain Fe, 14.0%; Mg, 2.1% and Ni, 0.88%. This low grade ore was obtained in relatively large quantities (40 kg) as a dark brown lumpy material of heterogeneous and complex mineralogy. Although uniform in colour, the ore particles were variable in size and hardness. Most of the nickel was found to reside in the more friable fraction with hard particles being almost barren of nickel. Electron microprobe analysis revealed that the nickel was bound mainly in the form of garnierite in a variable main fraction with large amounts of quartz and silicates.

The Mantoudi ore from Northern Euboea is known to be undergoing active laterisation (Agatzini, 1988) and has a soft friable structure. It has a varied colour - containing patches of green, brown and yellow. As this ore was not available in commercial quantities, and was only of interest for its microbial ecology, its mineralogical composition has not been examined in detail.

The Litharakia, Triada and Kabia deposits are sited 20 Km to the northeast of Halkis, the capital of Euboea island. These deposits have been known to consist of limonitic laterite with the footwall as ophiolite, rich in serpentine and the hanging wall of cretacious limestone.

Most of the experiments were carried out on the Litharakia ore due to its abundance. Also this could be considered the 'typical low grade' laterite found in Greece. Screen analysis of the Litharakia ore as well as chemical analysis of the Triada and Litharakia ores are shown in Tables 2 and 1 respectively.

Two further ores were examined towards the end of the project as part of a survey of leachability of Greek Laterites. These were Kukubajza and Kabia and their chemical analysis showed:

	Ni%	Fe%	Ca%	Mg%
Kukubajza	1.04	30.75	0.07	0.93
Kabia	0.85	21.08	0.66	2.14[1]

Further electron microprobe work was carried out on the Litharakia (low grade [LG]) and Kastoria (high grade[HG]) ores, ground to minus 100 mesh, to examine details of mineralogical associations. Although the samples were too fine grained and complex for comprehensive elucidation (much of the mass being below 1-2 μm, the resolution limits of the equipment), it was possible to obtain some useful information. Observable nickel was confirmed to be mainly in the form of garnierite {(poorly defined hydrated magnesium nickel silicate) $(Ni,Mg)_3Si_2O_5(OH)_4$} for the HG ore and chlorite $(Mg,Fe,Ni)_5Al(AlSi_3)O_{10}(OH)_8$ for the LG ore. Bulk minerals (with rough percentage modal proportions from electron dispersive x-ray analysis) were LG: fine mineral matrix, 44; aluminium silicate, 18; quartz, 15; calcite, 10; aluminium magnesium silicate, 8; and iron oxide/carbonate, 4 and HG: magnesium silicate, 41; quartz, 18; magnesium oxide/ carbonate, 15; nickel magnesium silicate, 11; fine mineral matrix, 6; calcite, 5; dolomite, 3; and calcium magnesium silicate, 1. Although the mineralogical composition of the matrix could not be determined, it is clear that the composition of the ores are extremely variable, as has been noted in their leaching behaviour. There are also large variations (not shown here) between different samples of LG (similarly HG), which highlight the need for careful selection and mixing to obtain representative and consistent samples for leaching work.

Images 1-8 show different features on 'elemental maps' (obtained from backscattered electron counts) of a selected single 256x256 (μm)2 area of an LG polished specimen: Image1 (I1), general view of all elements present (higher atomic numbers give brighter colours in the order red>yellow>green>blue): I2-I8, Fe, Cr, Si, Mg, Ni, Ca, and Al, respectively, views of individual selected elements (greater concentrations give brighter colours in the order

as above). Several identifiable mineral grains are present - but most are themselves complex (as are all the matrix particles). Of the elements considered, nickel has the highest atomic number, but only corresponds partly with the red on I1 (see also I6 below). I2 (Fe) shows (top left) two separate high grade particles surrounded by smaller particles containing less iron, together with varying concentrations of iron everywhere else except in quartz grains (bottom left - see I4). Several small chromite grains are evident (I3). Almost pure quartz (I4) is observed in grains of varying size (particularly top and bottom left), together with relatively high but variable concentrations of silicate minerals generally elsewhere. The large central grain is probably a complex aluminium iron silicate. Mg (I5) and Ni (I6) show considerable correspondence. Aluminium (I8) is found predominantly as silicates and is always present in the Ni (I6) and Mg (I5) rich zones indicating the presence of chlorite rather than garnierite. Calcium as quite pure calcite (I7) occurs in numerous individual small grains, but at a low concentration overall. I8 (Al) shows aluminium silicates occurring; excluding quartz - there is a close correspondence between I8 and I4.

2. EXPERIMENTAL

2.1 SOURCES OF STRAINS

A wide variety of organisms were used. A1, A2 and A3 which were commercial Aspergillus citric acid producing strains (obtained from the Commonwealth Mycological Institute at Kew Gardens). A* was an Aspergillus strain obtained from a culture collection in Greece. P2, P6, P14, P23 and P24 were strains obtained from The Federal Institute of Geo-Sciences and Natural Resources, Hannover, Federal Republic of Germany (courtesy of Dr. K. Bosecker) - all being species of Penicillia (Bosecker, 1988 and Carlile, 1988). F1 and B1 (Penicillium) were isolated at Imperial College from an actively laterising Greek ore.

2.2 MICROBIOLOGICAL MEDIA

For the biological screening experiments two types of media were prepared in distilled water. One was standard nutrient agar (and broth) and the second was Czapek-Dox agar (and broth). The reagents were all laboratory Analar grade. The formula for the Czapek-Dox (CD) medium was :

$NaNO_3$	0.20%
KCl	0.05%
$MgSO_4.7H_2O$	0.05%
$MgSO_4.7H_2O$	0.001%
Glucose	1.00%
$K_2HPO_4.7H_2O$	0.05%
Agar	1.5%

(For CD broth the same formula was used with agar excluded).

One percent standard nutrient broth was made according to the manufacturers instructions (Oxoid chemicals, plc). All media were sterilised at 120°C and 15 p.s.i. for 25 minutes.

2.3 ISOLATION OF MICROORGANISMS

Samples of the ore were cleaved to expose fresh faces from which a few milligrams were scraped onto prepared nutrient agar (NA) and CD plates using aseptic techniques in a horizontal laminar flow cabinet. Similarly, the NA and CD broths were also inoculated. After inoculation, the plates were incubated at 30°C, examined daily, and growth recorded. Isolates were obtained by sub-culturing from plates and by serial dilution of liquid cultures.

To investigate acid production methyl-red indicator was added to the agar at a concentration of 0.2 g/l. For creating a range of pH conditions a buffer system was established with citric acid and potassium hydrogen phosphate which was subsequently changed to potassium di-hydrogen phthalate to enable the study of citrate formation. For investigating nickel tolerance nickel chloride ($NiCl_2.6H_2O$) was incorporated in the agar. The buffer solutions were autoclaved separately from the media. From daily observations, if the organisms seemed promising (i.e. they produced acid metabolites in the presence of nickel on plates, thus changing the colour of the indicator from red to yellow), they were sub-cultured onto a separate plate of the same type, pH and nickel content as those on which they were originally grown. For the acid tolerance tests a series of plates were prepared at pH values 2.4, 3.4, 4.4, 5.4 and 6.4 and inoculated from the isolates.

The acid metabolites produced by the organisms in liquid media were tested qualitatively using high pressure liquid chromatography (HPLC) with a Waters 'fast-fruit juice' column containing a sulphonated resin packing. The procedure followed was that recommended by the manufacturers.

2.4 LEACHING CONDITIONS

The leaching tests were carried out in 250 ml flasks containing 10 g of ore in 100 ml leach solution. The flasks and contents were shaken at 25°C in an orbital incubator. Samples were taken at regular daily intervals by allowing the suspension to settle out and pipetting 0.5 ml of the supernatant for atomic absorption spectrometry. Liquid lost in this process and by evaporation was replaced by adding distilled water. The initial acid concentrations ranged from 0.1-0.5 M the latter representing the maximum concentration achievable through biological means.

2.5 BATCH BIOACID PRODUCTION

Bioacids were prepared in 250 ml flasks with modified Czapek-Dox (CD) medium as follows:

Composition (g/l)	Glucose 1	Glucose 2	Glucose 3	Sucrose	Molasses
Sugar	100	100	100	130	150
$NH_4H_2PO_4$	1.19	1.19	1.19	1.6	1.6
KCl	0.5	0.5	0.5	-	-
$K_2HPO_4.7H_2O$	-	-	-	0.25	-
$MgSO_4.7H_20$	0.5	0.5	0.5	1.2	-
$FeSO_4.7H_20$	0.01	0.01	49.8x10-6	49.8x10-6	-
$ZnSO_4.7H_20$	-	-	44.0x10-6	44.0x10-6	0.264
$CuCl_2$	-	-	21.2x10-6	21.2x10-6	-
$CuSO_4.7H_20$	-	-	-	-	0.24
$NaH_2PO_4\ 2H_20$	0.5	-	-	-	-
$NiCl_2.6H_2O$	0.4	0.8	1.6	-	-

Each flask and contents was sterilised at 15 psi for 15 minutes followed by inoculation with the desired organism and shaking in an orbital incubator at 30°C for time intervals in the range 22-60 days. Samples were taken at regular intervals (typically every 2-3 days) and placed in 1.5 ml Eppendorf tubes. Fresh sterile medium was added to replace the lost volume. The Eppendorf tubes were then frozen at minus 10°C (to prevent biodegradation) for later analysis by high performance liquid chromatography (HPLC). A Waters 'fast fruit juice' column containing a sulphonated resin packing was used following the manufacturer's recommended procedure.

2.6 COLUMN LEACHING

These experiments were carried out in fixed bed plastic trickle columns with variable heights. The leaching agent was sprayed at the top of a column at a specified flow rate. Leaching was carried out in several stages. Within each stage, the leaching agent was continuously recycled until the concentration of nickel within two consecutive cycles was the same. It was then replaced by fresh leaching solution with the commencing of a new stage. The weight ratio, solution:ore was maintained at 8:10 and the cycle time within the column was maintained at around 4 days for the Triada ore and around 2 days for the Litharakia, Kabia and Kukubajza ores.

3. RESULTS

3.1 MICROBIAL ISOLATES

The first phase of this project was to isolate indigenous micro-organisms present in samples of the Greek lateritic nickel ores and assess their potential for leaching nickel.

For the use of such organisms in the leaching process (whether 'in situ' or in a separate acid production unit), there were considered to be three basic pre-requisites.

1) Tolerance of the organism to high nickel concentrations.

2) Tolerance of the organism to acid conditions (i.e. low pH).

3) The ability of the organism to produce organic chelating acids.

Twenty five organisms including bacteria and fungi were isolated from the initial 'rock inoculum'. These isolates were purified by the above streaking techniques. Each was tested for its ability to:

1) grow at pH's other than that from which it had been isolated,

2) tolerate 40 p.p.m. of nickel, and

3) produce acid metabolites (on media and indicator plates).

Based on these tests, six organisms were deemed worth investigating further. Having isolated the organisms, an experiment was undertaken to assess their ability to grow at low pH. From the literature it is evident that hydrogen ion concentration plays an important if not dominant role in this type of leaching. In an actual process mineral acid might be added to maintain a low pH. Only two organisms (both fungi) B1 and F1 could grow optimally at low pH (3.3 - 4).

In earlier experiments, the nickel ion concentration was kept at 40 p.p.m. The isolates were now tested for their ability to tolerate higher nickel ion concentrations. They were inoculated on CD agar plates with nickel ion concentrations of 200, 400, 800, 1600 and 3200 p.p.m. incorporated. Most organisms failed to grow at any concentration above 200 ppm. Therefore, a process of serial acclimatization was undertaken whereby each organism was grown on media of progressively increasing (50 or 100 p.p.m steps depending on rates of growth) nickel concentrations. The pH in each case was that which was found to be optimum for a particular isolate. Having serially acclimatized the organisms, a much higher tolerance was obtained in most cases with a species (F1) being able to grow at 3200 ppm of nickel at its optimum pH for growth.

As liquid media are more representative of leaching conditions, the organisms were transferred from agar plates to liquid culture. The nickel tolerance was found to be half of that observed on agar plates. This lower tolerance probably reflects the poor diffusion of nickel in agar

plates allowing localised depletion; in a liquid medium the biomass will be completely surrounded by high levels of nickel at all times. However, after further stepwise transfers (1600 p.p.m. upwards for F1), F1 continued to grow healthily at the highest concentration. However the growth morphology of F1 changed from a mycelial form to discrete pellets in submerged culture at 3200 ppm nickel, and this pattern continued with further acclimatization to 6400 ppm.

Table 3 shows the results obtained when B1, growing at 1600 p.p.m. nickel on CD plates (and which did not grow immediately at 1600 p.p.m. nickel in liquid culture), was adapted to 1600 ppm in liquid-shake-flask cultures incubated at 30°C with various media. In the absence of Ni growth was profuse (++++) in all the media by day 8.

This indicates that B1 grows relatively well in complex media in the presence of nickel, possibly because constituents in these media can complex the nickel thus reducing its effective concentration. Alternatively, the presence of the extra growth factors in the extract might have stimulated the production of metal binding agents such as microbial polysaccharides which would bind the nickel. A third possibility is that rapid metabolism associated with the richer media facilitates the active expulsion of nickel and effective detoxification.

The P2, P6, P14 and P23 organisms were known to grow at 10000 p.p.m. nickel in a complex medium (Bosecker, K., 1988). However, when these organisms were transferred to CD media they did not grow above 3200 p.p.m. nickel, confirming that nickel tolerance levels are dependent on the composition of the growth media. Attempts were then made to try and cultivate these organisms for the production of chelating/mineral acids for leaching the ore. To ascertain which acids should be produced (biologically) the leachability of the ore with various commercial chelating/mineral acids was examined.

3.2 CHEMICAL LEACHING OF ORES

Before attempting to produce chelating acids by larger scale cultivation of the organisms, it was necessary to determine which were likely to be the most effective leaching agents. This was done by examining leaching of the ores with commercially available pure samples.

The leaching experiments were carried out with the following commercial acids (which could also be expected to be produced biologically): acetic(a), formic(f), lactic(l), sulphuric(s), citric(c), oxalic(o) and in combinations of citric plus sulphuric(c+s), oxalic plus sulphuric(o+s) and lactic plus sulphuric(l+s). All acid concentrations were 0.5 M total, representing (and in some cases exceeding) the maximum concentration likely to be available from

fermentation processes. These experiments were carried out with both the low grade (Litharakia) and high grade (Kastoria) nickel ores. The results are shown in Figs.1 and 2 for the low grade ore and high grade ore respectively. Important criteria were the rate of leaching, the extent of leaching and the existence of selective reactions.

For the low grade material, up to 40% of the nickel and 20% of the iron could be leached over a period of 12 days. The reactions were not complete after this period. For nickel, sulphuric acid was the most effective leaching reagent while, for iron, oxalic acid was the most effective. Mixtures of citric (or lactic) acid with sulphuric acid gave percent extractions of nickel equivalent to the sum of the effects of the acids employed separately. The analogous mixture with oxalic acid, however, gave very low extraction. The organic acids alone were relatively ineffective. For iron, only oxalic acid gave effective leaching, although mixtures of this acid with sulphuric acid appeared to be additive.

For the high grade ores roughly 55% of both iron and nickel was extracted over 15 days, although most of this was leached within the first 9 days. For nickel, sulphuric and citric acids (and mixtures) were the most effective. With oxalic and acetic, extraction fell after 6 days, presumably owing to precipitation of a nickel oxalate bearing compound. For iron, oxalic, citric and sulphuric acids (and mixtures) were effective. A mixture of 0.25 M of each of citric and sulphuric acids gave roughly 20% greater extraction than 0.5 M of either acid separately.

The above preliminary tests were carried out to investigate which acids would be appropriate for the leaching of the ores. However to obtain a more comprehensive understanding of the leaching parameters including the Ni:Fe ratios in solution as well as the maximum leachability of the ore, the leaching conditions were changed to examine the effects of acid concentration, leaching temperatures and different pulp densities (PD).

Leaching studies with Kastoria ore and citric acid at 25°C showed that in a 20 day leach the actual rate and final extent of leaching of both Ni and Fe, (measured as a percentage released from the ore) were dependent on pulp densities and citric acid concentration (Figs 3a, 3b and 3c). Thus a higher percentage leach was observed with a lower pulp density, using a fixed acid concentration, and a higher percentage leach was also obtained with a higher acid concentration with a fixed pulp density. It is interesting to note that the effect of pulp density was more dramatic at lower acid concentrations and this correlates with a distinct neutralising effect at the higher pulp densities, confirming the dominant role of hydrogen ion concentration in the leaching process. However after day 10 the pH in all the flasks remained fairly constant while leaching continued beyond day 20, indicating that other factors such as chelation also play a part.

The highest nickel extraction (1.5 M Citric acid, 5% PD, day 20) was about 43% whereas 1.5M sulphuric acid released approximately 65% in the same time. Only oxalic acid from those acids tested displayed any selectivity in leaching releasing a significant percentage of the iron but negligible nickel. This could be due to its reducing action on Fe^{3+} contained in the ore and the subsequent solubilisation of the Fe^{2+}. Additionally nickel oxalate is known to have a very low solubility.

It is evident from these studies on the Kastoria ore that besides sulphuric acid, citric acid had the most potential for nickel leaching. However none of the acids displayed any useful selectivity in nickel removal.

Litharakia ores were also leached with equimolar mixtures of organic acids, sulphuric acids and with a total concentration of 0.5 M. In this experiment a leaching time of 45 days was employed (instead of the 22 day cycle used earlier) in order to establish whether equilibrium could be achieved. The results showed, for nickel over 50% was leached with sulphuric acid (S) and citric plus sulphuric acid (C+S) within 15 days and, by day 34, equilibrium was apparently established at about 75% Ni extracted (S) and 55% (sulphuric plus lactic acid - results not shown). Unfortunately, at day 31, the flask of C+S broke and hence the performance of this combination of acids could not be ascertained fully. However, judging by previous experiments and the performance before day 31, it was assumed that C+S would have leached nearly as well as S alone. Citric acid alone removed 40% of the Ni and, although oxalic acid had the highest initial removal rate of about 30% Ni by day 3, by day 44 the figure was less than 4 % (based on Ni in solution). This was probably due to nickel oxalate precipitation. Oxalic acid may therefore be effective in nickel mobilization but does not release it in a soluble form.

As expected for iron, oxalic acid gave the highest percentage leached (27% at equilibrium) and a maximum of 20% removal was obtained with a mixture of sulphuric plus oxalic acids (results not shown). However, sulphuric acid and sulphuric plus citric acid mixtures leached only 7.5% of the iron present in the ore; while citric acid on its own leached less than 5%. It was clear that iron leached more rapidly initially, and equilibrium was established sooner, than in the case of nickel. However, significant selectivity for nickel was achieved with sulphuric acid, citric acid, and sulphuric-citric mixtures.

After day 45, the contents of all the flasks were centrifuged, washed twice, and releached with 0.5 M citric acid to examine further leachability of the ores with respect to nickel and iron. For nickel, fresh reagent

produced a negligible increase in extraction, and even that only with citric, oxalic+sulphuric and lactic acids. It is interesting to note that, for the material previously leached with oxalic acid, no further nickel was leached. This would seem to add credence to the suggestion that nickel oxalate was precipitating out and possibly forming an impermeable crust that encapsulated the nickel-containing mineral grains, thus preventing further dissolution.

3.2.1 Sulphuric (0.5 M) leaching of different particle size fractions of Litharakia ore

The friable nature of many of the ores meant that grading and size fractionation would not be out of question. To examine the possibility of upgrading the ore through an initial physical size separation, an experiment was undertaken to examine the nickel and iron contents, as well as leachability, of the various size fractions. After sieving the samples, all fractions were crushed to minus 100 mesh before leaching. The experimental conditions were the same as before, and the results are shown in Table 4. For both metals the leaching behaviour was similar in that the recovery of nickel and iron was greater and faster with the material derived from larger particle size fractions. The >9mm samples released 60% of the contained nickel by day 7, whereas the <0.15 mm released only 38% by day 15. In fact the nickel recovery decreased progressively with decrease in original particle size, possibly owing to ill-defined differences in mineralogy resulting from decreased protection from weathering for smaller particles. The fines contain little of the overall nickel, even though their percent Ni was not significantly different, because the main bulk of the original ore was >0.15 mm. For this particular ore, removal of fines (<0.6mm) prior to leaching would facilitate an effective improvement in nickel recovery - a conclusion which merits further investigation. For iron similar, but less pronounced, behaviour was observed.

3.2.2 Low molarity (0.1-0.4 M) organic/sulphuric acid leaching of Litharakia

Experiments were carried out to examine the effect of lower molar concentrations of acids on the leachability of the ore. For these, citric(c), equimolar citric+sulphuric(c+s) and sulphuric acids(s) were used in concentrations of 0.1-0.4 M in total. For nickel leaching (Figs 4a, 4b and 4c), with S and C+S, the leaching behaviour can be described as roughly 'additive' i.e., metal leached is proportional to acid concentration. Presumably, at higher acid concentrations, extraction would tail off as the solutions approached saturation. For the citric acid system the same general trend was observed but the increments were less regular. However it is possible that a more proportionate relationship would have emerged if leaching had proceeded to completion. The leaching behaviour for iron was similar.

Evidently a concentration of 0.2 M acid or greater is required to achieve a reasonable rate of leaching. In these closed systems, rough mass balance calculations show that acid consumption is the main limiting factor leading to cessation of leaching.

3.2.3 Kabia and Kukubajza ores

There are some differences between the ores from Litharakia, Kabia and Kukubajza. Kukubajza contains very little calcium (0.07%) and has a nickel content of 1.04%. It also has a very high Fe concentration of 30.75%. Kabia is apparently not too dissimilar from Litharakia except for the very high magnesium content (2.14%). As with the previous ores a variety of commercial acids that could be produced biologically were examined. Results are shown in Figs 5 and 6.

Kabia was very amenable to acid leaching, with over 95% removal of nickel and magnesium by day 9 with sulphuric acid. Citric + sulphuric acids and lactic + sulphuric combinations(0.5M in total) were nearly as effective with over 90% removal by day 14. Citric acid on its own released over 71% of the nickel by day 19, but more could probably have been released over a longer time course. The leaching behaviour of iron was not dissimilar to that of Litharakia with oxalic acid leaching 28% of the Fe by day 19, but otherwise relatively low percentages released indicating a high level of selectivity for Ni release with sulphuric and citric acids.

Calcium was almost completely leached with all acids except for oxalic and oxalic/sulphuric combinations, within the first day. It is most likely that precipitation of calcium oxalate could explain the behaviour with oxalic acid.

Kukubajza was also amenable to leaching with sulphuric acid. By day 11, 80% of the nickel was extracted. Sulphuric with lactic and citric combinations removed 70% of the nickel by day 19, but the leaching would have continued beyond that time. However, in contrast to Kabia with citric acid alone only 34% of the nickel could be leached. The leaching pattern for magnesium mirrored that for nickel, including the relatively poor response to citric acid, except that oxalic acid in combination with sulphuric proved to be highly effective for magnesium. For iron the greatest removal was with oxalic (17.5%) and with oxalic/sulphuric combinations (12%). However as previously observed with Litharakia and Kabia, iron leaching was poor with sulphuric citric and its combinations, giving a high selectivity of Ni compared to iron in these cases. This ore has very little calcium which could very easily be extracted with all acids except oxalic and oxalic/sulphuric combinations.

3.2.4 Inferences from Batch Leaching Experiments

It is evident from the above studies that the type of ore used has a considerable bearing on the applicability of organic or mineral acid leaching techniques. While sulphuric acid was the most rapid leaching agent in all cases, we have shown that citric acid, a well established product of fungal metabolism, could be equally effective over longer time periods in most instances. Combinations of microbially produced and mineral acids might be a feasible compromise when rates are too slow to be economical. With Kabia and Kukubaja ores acid leaching proved exceptionally effective releasing 95% of the contained nickel with a high level of selectivity of nickel over iron leaching (leachates were enriched for nickel by upto 20 fold compared to the ore content). Unfortunately these are not major deposits in Greece and would probably be uneconomical to process purely on the basis of size. The Litharakia ore, however, which comes from a major reserve also produced promising results particularly with respect to Ni:Fe selectivity in acid leaching. Problems due to acid neutralisation, probably due to calcite, were evident in this case so that in some instances leaching was stopping due to a rise in pH. However it was evident that further leaching could be obtained by replenishing the leaching solution. To better assess the potential for leaching this and other ores, it was necessary to look at the effect of continuous processes i.e. column leaching.

3.3 COLUMN LEACHING OF LATERITES

3.3.1. Litharakia and Triada ores with sulphuric acid

In the first set of experiments, Litharakia ore was leached with 0.5 M sulphuric acid in a series of columns ranging from 0.8 m to 2.2 metres in height. In 70 days nickel extraction of 70% was achieved with the Litharakia ore and from the trend, the reaction was still incomplete. This looks very promising as even with agitation leaching with 1.5 M sulphuric acid at 95°C a maximum of only 80% was extracted. Furthermore the high selectivity for nickel leaching compared with iron observed in shake flasks was again observed in column experiments. In a similar experiment with the Triada ore the selectivity for Ni compared with Fe was even greater, giving a Fe:Ni ratio of 2:1 in the leach liquor (in the ore it was around 30:1 and in agitation leaching experiments it was around 12:1), but the experiment could not be completed due to plugging problems encountered after 77 days (Fig 7). As already noted the cycle time in this experiment was twice that in the case of Litharakia column leaching. Hence in terms of total leach volume, the percentage metal release from Triada and Litharakia was similar. The selectivity for nickel compared to iron in column leaching was better than in agitation leaching possibly due to the larger particle size in which the iron minerals were engrained and hence

accessibility was reduced. In agitation leaching the particles are much finer. Cobalt leaching in the column experiments was similar to that of nickel, whilst chromium leaching was similar to that of iron.

3.3.2 Further Column leaching studies

The second series of column leaching experiments were conducted firstly to compare the use of citric acid, with sulphuric acid as a leaching agent in columns of Litharakia ore, and secondly to examine the leachability of the Kabia and Kukubajza ores with sulphuric acid in columns. Four columns were used:

Column	Ore type	Weight(kg)	Acid(0.5M)	Flowrate(l/d)
C1	Litharakia	10	sulphuric	4.0
C2	Litharakia	10	citric*	4.0
C3**	Kikubajza	3	sulphuric	1.25
C4**	Kabia	3	sulphuric	1.25

It had been observed in previous studies that ores with significant levels of calcite could suffer plugging in the early stages unless the pH was maintained at around 1. Hence an initial calcite stripping stage consisting of one cycle (ie 2 days) with 0.5 M sulphuric acid was introduced for all four columns. Additionally the citric acid in C2 was supplemented with sulphuric acid to reduce the pH to 1.

In the stripping stage the pH rose from an initial 0.58 to 3 in all cases even though the calcium was not removed entirely (except for C3 where the initial concentration was very low). The pH remained at around 1 for the rest of the period when used with sulphuric acid and around 2 with the citric acid column.

Leaching of the Litharakia ore with sulphuric acid displayed the same pattern as in the previous experiment with 75% of the nickel, 80% of the magnesium and 7% of the iron extracted by day 120. Calcium was leached steadily throughout, in contrast to the situation encountered with flask leaching in which most of the calcium was released in the early stages. This would seem to indicate that calcium either is not easily accessible due to the larger particle sizes or due to it being ingrained within a non refractory ore matrix.

In column C2 with citric acid the rate of leaching was about half of that in C1. A cycle which typically would take two days with sulphuric acid, took three days with citric acid. Plugging problems were often encountered but cleared with time (usually 24 hours). One of the reasons why plugging occurred could be due to the higher rate of calcium removal

and resulting precipitation. As with sulphuric acid leaching selectivity for nickel compared with iron was observed and the Fe:Ni ratios (Figs 8a, 8b, 8c and 8d) were also similar.

With the Kukubajza ore (Column 3) the leaching with sulphuric acid was very much faster than that of Litharakia as previously observed in the agitation leaching experiments. By day 21, 50% of the Ni was extracted and by day 60, this was up to 70% . In the same time span only 2 % of the contained iron had been leached. Although the % of iron in the ore is the highest (30%) the steady state stage concentrations (Fig 9b) were very much lower than that for the Litharakia ore in C1 (fig 9a). In fact the Fe:Ni ratio of the leachate was the lowest of all the ores used. By day 40 the ratio had reached approximately 1:1. This ore contains little calcium and it was no surprise that most of it was removed in the first stage.

As with the agitation leaching experiments, the Kabia ore proved the most amenable to sulphuric acid leaching. The stages were the shortest in the experiment and by day 40, 80% of the nickel had been extracted (fig 8a). Magnesium again leached rapidly (Fig 8b) suggesting that magnesium and nickel were from the same sites. Selectivity for nickel over iron was once again observed and the Fe:Ni ratio in the leachate was close to 1:1 by day 28. The behaviour of calcium was similar to that with the Litharakia ores.

3.3.3 Inferences from Column Leaching Studies

Column leaching experiments are lengthy to perform and require significant amounts of material. It has therefore not been possible to run a complete series of experiments including citric acid leaching of Kabia, Kukubajza and Triada ores, nor column leaching with biologically produced acids. However on the basis of the results available it can be concluded that acid leaching of laterites looks extremely promising and sets a precedent for progressing to heap leaching studies. Results with the most abundant Litharakia ore were particularly exciting. Nickel leaching approaching that for agitation leaching was obtained with good Ni:Fe selectivity. Citric acid also looks promising although the kinetics are slower. It is interesting to note that citric acid leaching was characterized by a fairly consistent yield per cycle whereas sulphuric acid produced an initial burst in the first cycle of a stage followed by rapidly decreasing yield in the latter stages. This may be indicative of different mechanisms at work.

Contained calcite is recognized as a problem, both in terms of wasteful acid consumption and also as a contributing factor to column plugging. It is believed that much of the calcite originates from the bed rock and could be removed by preliminary scalping operations. It has been noted that

plugging only occurs when the pH exceeds 1. Hence there may be some merit in using citric + sulphuric acid mixtures rather than citric acid alone, or, in amenable ores (eg Kukubajza) employing a sulphuric acid preleach before switching over to organic acids.

3.4 BIOLOGICAL LEACHING

Biological leaching was examined in both two phase systems in which the acids were produced separately and then added to the ore, and 'in situ', in which case the organisms were cultivated in the presence of the ore (ie the medium and inoculum were added to the ore).

3.5 THE TWO PHASE SYSTEM

3.5.1 Batch Bioacid Production

Nickel was added to some of the flasks in order to simulate conditions of a leaching operation in which leachate is recycled through the fermentor. Additionally, preliminary experiments had suggested that the presence of nickel could stimulate acid production.

The media used (Glucose 1, Glucose 2, Glucose 3, Sucrose 1, and Molasses) is described in the experimental section. These organisms and media were chosen as representative of the range of available potentially useful systems. The Glucose1 media was the same as that used in earlier experiments for isolation of the organisms. For Glucose2 medium the sodium hydrogen phosphate was omitted, as excess phosphate has been shown to inhibit the production of citric acid, an increased concentration of the latter was therefore possible. In Glucose3 the Fe concentration was decreased as earlier work in this department (King 1985) suggested that concentration of this element (and those of counterbalancing Zn and Cu) should be maintained at a lower value to maximize citric acid production.

3.5.2 Effect of media composition on acid production

Glucose 1 medium may be considered as the reference on which the effects of: i) added nickel, ii) reduced phosphate (glucose 2), and iii) reduced iron concentrations have been examined. In the absence of added nickel, the pH of the Aspergillus cultures dropped slowly, while that of the Penicillia dropped more rapidly. However citric and/or oxalic acid production appeared more slowly, once the pH had reached a low value. Hence the pH of the culture was not a reflection of citric or oxalic acid concentrations. Patterns of citric and oxalic acid were variable, but in all cases, the maximum citric acid concentration was greater than that of oxalic acid. In the case of the Penicillia it was evident that citric acid was behaving as an overflow metabolite, being produced initially but later degraded.

This was less marked with the Aspergillus strains. The rank order of increasing concentration of citric acid produced in this medium was P6 > P24 > A3 > P14 > P2 > A1.

Glucose 2 media appeared to increase citric acid and decrease oxalic acid production with A1 but had little effect on A3.

3.5.3 Effect of added nickel

In the Glucose 1 medium comparative results for nickel supplementation are only available for A1 and A3. The Aspergillus strains are fairly sensitive to nickel and even at 100 ppm a reduction in growth rate and rate of pH decrease was evident for these two strains. This appeared to stimulate citric acid production for A1, but was inhibitory for A3 (nb it is difficult in this case to distinguish inhibition of acid production from inhibition of growth). Higher nickel concentrations generally exacerbated the growth inhibition and consequently decreased the rate of citric acid accumulation. However with A2 (experiments done in Glucose 2 medium) this nickel concentration appeared to favour citric acid accumulation in long term (60 days) incubations. As samples were not taken between day 20 and day 60 it is impossible to say whether A2 in Glucose 2 medium, without nickel produced a similar maximum which subsequently declined (to zero by day 60). As expected higher levels of nickel reduced growth and citric acid concentrations of the Aspergillus still further.

With the Penicillia 200 ppm of nickel in Glucose 2 media appeared to reduce citric acid production rates compared with Glucose 1 media without nickel. However after longer incubations (60 days) P2 and P6 produced higher concentrations in Glucose 2 + nickel than the maxima seen in Glucose 1. It is interesting to note that growth and acid production in some of these strains of Penicillia (eg P14) was reduced by relatively low concentrations of nickel used (200 ppm). Although these strains can be adapted to high levels of nickel tolerance, the inocula for these experiments were taken from slants without nickel supplementation. The apparent loss of nickel tolerance indicates that the changes on "adaptation" are phenotypic rather than genotypic (ie do not result from stably inherited mutations).

3.5.4 Effects of alternative carbon sources

Sucrose: This medium was that previously used by King (1985) in this department for the production of citric acid using commercial strains of Aspergillus. As with Glucose3 it contained low concentrations of Fe and also low levels of phosphate and was employed without nickel addition. It is evident from Table 5 that the medium was only effective with

A3 where a rapid decrease of pH and high maximum citric acid concentrations (40 g/l) were obtained. All of the other strains produced a slow drop in pH and low maximum titres for citric acid. By day 32 the pH in all of the cultures had decreased to < 1.5

Molasses: Cane molasses and less frequently beet molasses are often used as cheap sources of sucrose for citric acid production. Using an edible grade molasses from Appleford Industries at 150 g/l (approximately 55 g/l sucrose) with copper and zinc added to counterbalance the iron present in the molasses, all of the strains were found to produce respectable maximum levels of citric acid (9-25 g/l), but also produced the highest concentrations of oxalic acid seen with the different media examined (Table 5). This is an undesirable characteristic of molasses fermentations as nickel oxalate is known to precipitate readily. It should also be noted that the pH in all these fermentations did not decrease as rapidly as with other substrates, nor reach the very low final values (<2) seen with other substrates. This was possibly due to the buffering capacity of the molasses. Additionally it should be noted that this molasses contained relatively high concentrations of iron, which in industrial citric acid production are reduced by precipitation. This was not done here and may have influenced the yield and nature of the products obtained.

3.5.5 Leaching of ores with biologically produced acids

An examination was made of the leaching characteristics of acids produced in the batch cultures from: Molasses (day 57) with A2, A2+Ni, A3+Ni, P6, P14 and P24; Sucrose (day 60) with A1, A2, A3 and P14; and Glucose2 (day 60) with A2+Ni, A3, A3+Ni, P2+Ni and P6+Ni. The contents of the flasks were filtered through Whatman 541 hardened ashless filters and 50 ml of the filtrate was added to 5 g of the non sterile ore (as used for the chemical leaching studies) in 250 ml flasks. The flasks and contents were shaken at 25°C in an orbital shaker. Samples were taken at 2-3 day intervals by allowing the suspension to settle out (and in some cases centrifuging) and pipetting 0.5 ml for atomic absorption spectrophotometry. Liquid lost in this process and by evaporation was replaced by adding sterile distilled water. Before the addition to the ore a sample of the filtrate was analysed to determine the initial concentration of Ni in the solution.

With the filtrates derived from the molasses medium (except that from A3) the suspensions did not settle out easily and hence had to be centrifuged. The results were generally consistent with the levels of leaching previously obtained with commercial citric acid. It is interesting to note, that the P14 system, which had one of the lowest concentrations in terms of initial citric or oxalic acid, removed the greatest amount of nickel (about 9%). A3+Ni , after day 15 had less Ni in solution than initially present

following a dramatic decrease after day 12 and the pH increased from 4.4 to 7.6. By day 20 the amount of Ni in solution was 46% of that which was found at day 0. It was evident that growth of the organism was reinitiating (presumably from spores remaining in the filtrate) and this new fungal growth was probably biosorbing the nickel from solution. Some drop in nickel concentration was also observed after long term incubation with other 'bioacids' and may also have resulted from reinitiation of fungal growth. It should also be noted that the extent of leaching in this case was not a reflection of the initial pH.

The trends with iron leaching showed some similarities. However, very little iron was leached with the filtrate from A2+Ni unlike the respective case for nickel leaching in molasses. Conversely, both iron and nickel were strongly leached by the filtrate from P14.

With the filtered bioacids originating from growth in the sucrose medium (day 60) organism A1 grew profusely in the presence of the ore thus causing poor settling characteristics in the latter and problems with interpretation of leaching characteristics. With A2 the settling characteristics were also very poor, although no signs of biomass growth were apparent. With A3 and P14, there was no apparent growth and no settling problems. Typical leaching profiles are shown in Figs.10a and 10b respectively with the sucrose medium. The filtrate from A3, which had an initial concentration of 11.8 g/l of citric acid and 0.64 g/l of oxalic acid, leached continuously at a pH of 1.7, and by day 23 had already removed 12% of the Ni in the ore. It should be emphasised that 11.8 g/l is only approximately 0.05 M citric acid and this level of leaching required much higher concentrations of commercial citric acid. Also it is interesting to note that the pH of all the initial filtered solutions was 1.8 but by day 3 the pH in the presence of the ore varied considerably, presumably because of variations in the suites of acids and the resultant buffering capacity in the different systems. For Fe the leaching trends were similar. From initial studies carried out with equimolar concentrations of commercial acids, oxalic acid leached the maximum amount of iron. However in the present experiment the filtrate from A2 which had the maximum amount of oxalic acid leached very little Fe. It is possible that a surface layer was retarding leaching.

With the filtrate from growth in Glucose2 medium, all of the organisms (with the exception of A3) grew in the presence of the ore. Good settling was obtained, however, in comparison with the sucrose or molasses media. The organisms formed a clump with the ore within a clear solution. At day 0, the Ni content of the filtrate (which initially contained 200 ppm Ni) from A2+Ni was 11 ppm., A3+Ni was 184 ppm, P2+Ni was 137 ppm and P6+Ni was 14 ppm. It is apparent that these organisms have a tendency to absorb the nickel. The

filtrate from P2+Ni, which had an initial citric acid concentration of 25.8 g/l (approximately 0.12 M) and a pH of 2.8-3.0, leached up to 27% of the Ni, whereas that from A2+Ni, which had an initial citric acid concentration of 40.8 g/l and 1.91 g/l of oxalic acid and a pH 1.8-1.9, leached only 17% of the Ni as determined by free Ni in solution. Also P6+Ni filtrate, which had an initial citric acid concentration of 33.9 g/l, leached only 9 % of the Ni. The probable explanation is that the organisms (in the case of A2 and P6) were absorbing the nickel, as is evident from the day 0 analysis. In the presence of the ore and the A3+Ni filtrate, the concentration in solution after day 3 fell below the day 0 level and by day 23 had reached 55% of the initial concentration of day 0. In the case of iron the leaching results were somewhat erratic. P2 filtrate did not leach much of the iron, whilst A2+Ni filtrate did. It would seem that the P2+Ni filtrate preferentially leaches nickel and not iron.

Comparison of the best leaching results on both the sucrose and glucose media is shown in Figs 10a and 10b for Ni and Fe respectively. Two commercial Aspergillus citric acid producing strains (A2+Ni andA3) and one Penicillium species P2 were apparently the best in terms of leachability of nickel, of which P2 showed superior selectivity for nickel compared with iron. However the extremely high initial rate of nickel leaching with the filtrate from P2 grown in glucose plus nickel is exceptional and the experiment requires confirmation before recommendation of P2 as the organism of choice is made. It is possible that some of the nickel recorded as leached was in fact released from the organism after transfer from the growth medium.

From these results it is evident that the effects of biologically produced acids are quite complex. Our current results indicate that biological nickel leaching with the metabolic products of heterotrophic fungi is not simply a reflection of citric acid concentration or pH. Rather the presence of citric acid in a well buffered environment appears to be a major criterion. Based on the concentrations of citric acid present, the biologically produced acids - e.g., from A2 and possibly P2 - would seem superior to commercial acids. On the laboratory scale the biosorption of nickel mentioned above can probably be avoided by finer filtration, but in a working system this facet would need more detailed consideration.

3.5.6 Sterile ore experiments

Owing to the incidence of renewed fungal growth during the leaching stage (and consequent biosorption of leached nickel) with P2 and A2, as well as the complex leaching pattern we believe that there were mechanisms involved in the process other than the direct effect of acid, namely:

- Mineral acid is produced (from the salts added to the media) even in very small amounts which can bring the pH down to around 2.

- Growth and consequent acid production initiates a few days after leaching has commenced, which could have arisen from the few spores remaining in the medium which were not recovered during filtration.

- Growth and consequent acid production appears a few days after leaching has commenced, due to the organisms present in the ore rather than spores from the filtered media.

- A combination of all the above.

To ascertain the importance of these mechanisms a series of experiments were conducted with sterilization of the ore with g radiation prior to leaching. Both the sterile and non-sterile ore experiments had the same mechanism for the addition of the leaching solution. The culture medium was centrifuged and filtered through a Whatman filter paper 541 and than added to the ore (ie spores could have got through). The aim here was to examine whether the leaching behaviour would be similar when the ore was sterilised, hence discounting the action of the organisms in the ore. It should be noted that due to time constraints, the effect of using both sterile medium and sterile ore was not examined.

With the non sterile ore and A2+Ni, the initial citric acid concentration was 40.8 g/l and after the leaching period had gone down to 9.58 g/l. The removal of nickel was only about 5% which was compatible with results obtained with commercial citric acid. A similar pattern was also observed with A3 in sucrose. However with P14, P23 and P24, the situation was quite different. Initially there was hardly any citric or oxalic acid produced but after the leaching there was 52.8, 20.2 and 37.9 g/l of citric acid produced with P6, P14, and P24 respectively. The leaching behaviour shows that there was concomitant nickel dissolution. P6 leached 30% of the nickel into solution and P23 removed up to 45% of the nickel. The leaching of Fe showed a similar pattern but with a smaller % removal.

With the sterile ore after day 51 (Table 6), up to 70% of the nickel had leached out with A3 (without nickel supplementation) concomitant with a slight increase in citric acid production, but as a comparison most of the Penicillia organisms performed far better than the Aspergillus strains with the exception of A3. High levels of nickel extraction coincided with either high initial citric acid concentrations or further production of citric acid, resulting from continued growth during the leaching process, which would seem to indicate that citrate is the prime agent for the extraction of the nickel.

Unfortunately a strict comparison cannot be made between the the sterile and nonsterile ores as the time allowed for the leaching in the non-sterile case was shorter than that for the sterile case (42 days and 51 days respectively). However it can be said that in the presence of the ore, the organisms seem to produce far more acid than in the culture medium on its own and that indigenous organisms (absent in the case of sterile ore) only play a minor and possibly insignificant role. Understanding the mineral/microbial interaction was beyond the scope of this project given the time restrictions. However one plausible argument could be that, once the organisms attach themselves to the surface of the mineral grains, a high metal ion concentration gradient is experienced which could be toxic to the organisms spurring them to produce more citric acid (possibly as a defense response) which subsequently leaches out more ions from the mineral grain.

3.6 'IN SITU' LEACHING

As explained earlier 'in situ' leaching as referred to here is different from the classical sense of hydrometallurgy. Here it refers to the addition of medium to the ore with an inoculum of organism. All strains were adapted to laterite by gradual acclimatization from 3 to 10% laterite in the culture medium.

The leaching tests were carried out in conical flasks containing known weights of ore and sucrose based culture medium. 5ml of fungal suspension grown from an inoculum grown in the same medium without ore was added. Prior to leaching and inoculation flasks containing the ore had been sterilised by autoclaving. Recoveries were calculated by taking into account the amount of ore and culture solution taken out during sampling.

Several microorganisms were studied namely; P2, A3, A, F1, A1, P6, and P24. The temperature was maintained at 30°C and the pulp density at 10%. To ascertain whether there had been any contamination during leaching cultures were examined by spreading onto agar plates. In these sets of experiments, sampling was continued until two consecutive estimates of nickel concentration were the same (up to a maximum of 48 days), rather than using fixed residence times. Samples were analysed for Ni, Co Fe, Ca, and Mg , and the results are shown in Figs (11 a-d).

Strains F1, A1 and P24 all gave low levels of nickel leaching and these experiments were terminated before the 48 day maximum. P6 leached nearly 30% of the nickel, but P2, A3 and A were by far the best strains in this context leaching between 55 and 65% within the 48 day period. It is

probable that leaching would have continued beyond that time, if the experiment had continued. Similar patterns of leaching were observed with all of the metals analysed, except that Aspergillus strain A (a strain obtained in Greece and only used in these studies) appeared to be particularly effective for cobalt and magnesium leaching.The pH profiles for most of these cultures typically dropped from an initial level of pH 7.5 to approximately pH 5, within 10 days, a period within which little leaching occurred. It is interesting to note that a much lower pH was achieved and maintained with strain F1 and yet the strain happened to be one of the poorest for leaching. This confirms that the effects observed are not primarily from hydrogen ion concentration. The pH of most of the cultures, notably including all of the good leaching strains, stayed fairly constant within the range pH 5-pH 6, during the time in which the bulk of the leaching took place (days 20-48).

At the end of the experiments the flask contents with A3 and P2 were filtered to separate solid residues (laterite + biomass) from the pregnant solution. The solids were leached with hot water in successive stages, until no nickel was obtained in the solution. It was then assumed that any remaining nickel, excluding that contained in the ore was that taken up by the fungal biomass. The solid residues were then heated at 700°C in a platinum crucible to get rid of the organic biomass and the ash was then leached with slightly acidic solution at 90°C and metal contents in solution analysed by AA. The filter cake was found to retain 2.5% of the soluble Ni for the strain P2 and 3.5% for the strain A3. 99% of the nickel was accounted for by this technique.

Cobalt extraction obtained by P2 and A3 was at about 55%. The behaviour was similar to that of nickel. Iron extraction was up to 22% for P2 and 33% for A3, where as chemical leaching with citric acid liberated only 10% iron. One possible explanation for this could be the production of oxalic acid, which releases iron by a reductive process:

$$Fe_2O_3 + C_2H_2O_4 = 2\ FeO + 2\ CO_2 + 2\ H_2O$$

The FeO is soluble and the pregnant solution contained 0.8 g/l of Fe^{2+} out of a total Fe of 2.8 g/l.

Calcium extraction surpassed 65%, however, at the end of the leaching experiments only 50% of the calcium was accounted for in the leach solutions. This was probably due to reprecipitation of calcium citrate which has a maximum solubility of about 0.1g/100ml of solution at 25°C.

Attempts were also made to use untreated Greek beet molasses as a feed medium. This substance had a very high ash content of more than 11.4%. The results highlighted the interdependence of substrate and organism for effective

leaching. Although P2 was again one of the best strains, A3 and A were poor. However A1 and F1 were effective in this medium. The leaching behaviour for nickel and cobalt was similar, but in the case for iron, A3 and A proved to be as or more effective than P2. The rates of leaching were generally lower than in a pure sucrose medium but it is likely that higher levels of nickel could have been released in a longer time period. It is suspected that inhibitory substances in the molasses reduced growth and metabolism, thereby decreasing production of chelating acids. Additionally metal ions present in the molasses could complex with the acids produced reducing their availability for leaching.

3.6.1 Inferences from Biological Leaching Experiments

Two possible process configurations may be envisaged if biologically assisted leaching is to be considered in a heap leaching operation, namely; (i) two stage leaching with biologically produced acids separated from the producing biomass, and, (ii) "in situ" leaching with the organisms contained in the ore. Although the work undertaken here is by no means comprehensive, it provides a guide to the benefits and potential pitfalls of both approaches.

The strategy adopted for the two stage process was first producing the acids biologically followed by a crude filtration, with the filtrate then being used for leaching. As a consequence of the incomplete removal of the biomass by crude filtration, fungal growth reinitiated during the leaching stage in many instances. Thus the "two stage" process also contained an element of "in situ" leaching, complicating the interpretation of results. While it might have been experimentally simpler to have removed the biomass completely by 0.45 μm filtration, this was considered unrealistic as a process option. Therefore in any two stage process the leaching mixture is likely to contain sugars and other nutrients sufficient to stimulate growth of indigenous or transferred organisms. Studies using sterile ore have demonstrated that the contribution of indigenous organisms is probably minimal under these conditions.

Despite the complication of the two processes operating concurrently, it is possible to draw a general conclusion that prior to regrowth of the fungus, and in those cases where growth did not reinitiate, the amount of leaching was consistent with the amount of citric acid present, ie there is no evidence for any other leaching factors operating under these conditions. However when growth is reinitiated, and also in some of the "in situ" experiments, leaching was considerably more efficient than observed in the "two stage" experiments. Although there is no data on acid concentrations for the "in situ" experiments, evidence for

the "two stage" experiments where growth reinitiated, suggests that contact between the ore and certain organisms stimulated citric acid production. While the bulk acid concentrations in themselves are not sufficient to explain the very high levels of leaching obtained, it is possible that if the ore particles are physically entrapped in, or bound to the fungal mycelium they could experience much higher localised acid concentrations.

4. OVERALL CONCLUSIONS

Slight modifications to the original objectives were agreed during the course of the project to include a more detailed mineralogical investigation of at least one ore as well as examining the leachability of a range of laterites from various sites in Greece. These were done at the expense of some parts of objective 7, notably the use of wastes in acid production. This topic was considered to be premature until the desirable conditions of a leaching process were fully understood.

Otherwise the majority of the above stated objectives have been met, although the results of 'in situ' leaching are limited and with more time would have been extended, particularly given the encouraging results obtained.

The following general conclusions have been drawn:

1) Greek laterites are generally amenable to low temperature leaching with nickel recoveries of > 70% achievable in column leaching experiments with sulphuric acid as the leaching agent

2) There was considerable variability in the ease of nickel leaching from the various ores. This may be partly explained by their (acid neutralizing) calcite content but differences in their mineralogy also played a part.

3) Sulphuric and citric acid leaching, especially in columns, showed a strong selectivity for nickel compared to iron. Mineralogical analysis of selected ores showed that nickel was generally present as Garnierite or Chlorite and electron microprobe analysis of the Litharakia ore showed that the nickel was dispersed throughout particles, usually associated with magnesium and aluminium, but critically showing little association with the bulk of the iron. Leaching of nickel was always accompanied by release of magnesium and it is assumed that the observed selectivity resulted from channelling along nickel and magnesium rich veins.

4) Of the potential chelating acids produced by the microorganisms, citric acid proved to be the most effective for nickel leaching. As a general observation citric acid is an effective leaching agent, although requiring a longer time scale than equimolar sulphuric acid, and should be capable of leaching high percentages of contained nickel. However problems of calcium citrate precipitation were encountered in column leaching experiments, which could lead to column plugging. This could be avoided if the pH of the leaching solution was maintained at ≤ 1.

5) Oxalic acid, a common fungal metabolite, should be excluded from the leaching process. It is extremely effective at leaching iron and also precipitates the leached nickel as nickel oxalate, which could cause plugging.

6) In a 2 stage process where the chelating acids were produced (biologically) separately and then applied to the ore, the extent of leaching was generally consistent with the levels of available citric acid.

7) Higher levels of nickel release were obtained when some of the organisms were grown in the presence of the ore ('in situ') than found in the comparable two stage processes, or could be explained by the bulk acid concentrations produced. This suggests contact between the ore and the organism is beneficial.

5. REFERENCES

1. AGATZINI S. (1988) National Technical University of Athens - Personal communication.

2. BOSECKER K. (1986) Proceedings of the Sixth International Symposium on Biohydrometallurgy, Vancouver B.C., August 21-24 1985, page 367.

3. BOSECKER K. (1988) Personal communication.

4. CARLILI M. (1988) Personal communication.

5. MCKENZIE et al, (1987) Int. Journal of Mineral Processing, **21**, 275-292.

6. ANON. (1988) Mining Journal, **311**, No. 7975, 1988, 14-15.

7. KOVATS J. (1960) Acta Microbiol. (Polish), **9**, 275-287.

Table 1: Chemical analysis of ores

Ore Component	Kastoria wt % (dried)	Litharakia wt % (dried)	Triada wt % (dried)
Ni	4.27	0.73	0.73
Co	0.028	0.043	0.056
Fe	5.72	19.36	26.9
Si	52.23	37.71	41.95
Mg	16.87	2.08	1.45
Ca	8.51	3.42	8.40
Cr	0.45	2.17	1.75
Al	0.18	15.49	7.10

Table 2: Screen analysis of Litharakia used in shaker flasks and column leaching

Shaker Flask studies Mesh Type	Partial Yield %	Column leaching Mesh Type	Retained wt %
150	0.00	4	10.25
-150+170	13.10	-4+6	11.54
-170+270	39.30	-6+20	43.81
-270+400	45.80	-20+80	22.48
-400	1.80	-80+200	5.34
		-200+270	1.18
		-270	5.40

Table 3: Growth of Penicillium Sp Strain B1 in media containing 1600 ppm Nickel

Growth medium	Mycelium present after 2 days	4 days	8 days	12 days
CD broth(1% glucose)	-	-	-	+
Malt extract(1%)	-	+	+++	+++
Yeast extract(1%)	+	++	+++	++++
1:1 malt and yeast extract (1% total)	+	+++	++++	++++

Table 4: Leaching with smaller size fractions of Litharakia Ore

Size(mm)	% of size in fraction	% of Ni in fraction	% of Fe in fraction	% removal Ni	% removal Fe
> 9	2.77	0.68	18.84	67.0	13.6
6 - 9	11.20	0.69	23.84	66.0	10.0
3 - 6	20.45	0.70	25.44	62.0	8.4
1.5-3	22.32	0.69	27.64	60.0	8.5
0.6-1.5	23.54	0.79	29.28	52.5	7.8
0.3-0.6	8.15	0.77	23.88	47.0	7.5
0.15-0.3	4.42	0.74	19.36	46.0	7.2
<0.15	7.42	0.74	17.32	42.0	6.9

Table 5: Maximum bio-acid concentrations* (g/l) achieved in different growth media

Microorganism	Glucose (citric acid)	Molasses (citric | oxalic)	Sucrose (citric | oxalic)
A1		5.01	
A1 + Ni		16.0	0.19
A2			2.91
A2+Ni	40.8	24.0	25.0
A3	9.84	17.0	40.0
A3+Ni	8.79	2.00	18.0
P2+Ni	25.8	23.0	
P6+Ni	33.9	17.0	0.24
P14+Ni		18.0	0.35
P23+Ni		24.0	4.50
P24+Ni		20.0	0.40

* results are given only for the acid (citric/oxalic) with the highest peak concentration during the period of study.

Table 6: Bioleaching of Sterile Ore

	citric(g/l)			oxalic(g/l)	Ni(%)*	Fe(%)*
Medium and organism	d0	d15	d51	d0	(day 51)	
Glucose with P2	38.8	64.3	80.0	2.70	-55.21	11.43
Sucrose with P23	3.18	19.17	45.0	0.29	9.69	1.03
Sucrose +200ppm Ni + P23	1.10	23.49	48.6	0.13	44.62	0.80
Sucrose +400ppm Ni + P23	3.18	18.50	85.0	0.21	-	7.75
Sucrose +800ppm Ni + P23	0.88	2.70	7.96	0.16	57.6	0.71
Sucrose with P6	4.83	21.33	26.32	0.13	13.03	1.78
Sucrose +200ppm Ni + P6	0.66	14.31	64.41	0.21	45.79	1.56
Sucrose with P24	11.9	77.4	74.6	0.08	35.49	3.37
Sucrose +200ppm Ni + P24	10.8	52.2	76.4	0.08	46.03	2.31
Sucrose(65g/l) + "" + A2	0.88	4.18	7.56	0.13	4.11	0.02
Sucrose(65g/l) + A2	0.66	9.86	12.42	0.08	16.28	0.66
Sucrose(130g/l) + A2	21.2	17.82	23.9	0.29	19.69	2.17
Sucrose +200ppm Ni +A2	1.1	18.36	24.3	0.13	39.49	1.34
Sucrose +200ppm Ni +A3	1.65	11.88	-	0.71	-	0.28
Sucrose(65g/l) + A3	17.8	12.02	20.66	0.29	43.63	3.56
Sucrose(130g/l) + A3	41.5	44.28	58.32	0.67	68.3	4.40
" (130g/l)+200ppmNi+A3	36.5	37.26	44.28	0.71	38.27	4.06

* measured as nickel/iron in solution and subtracting initial concentrations contained in the culture filtrate

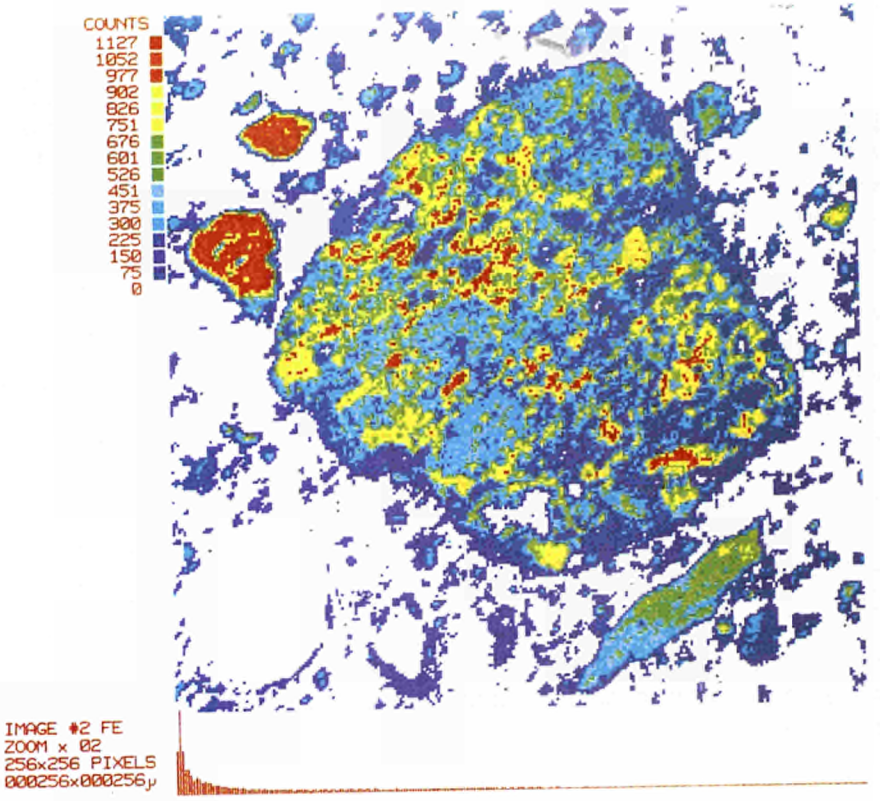
COUNTS
1127
1052
977
902
826
751
676
601
526
451
375
300
225
150
75
0
IMAGE #2 FE
ZOOM x 02
256x256 PIXELS
000256x000256µ

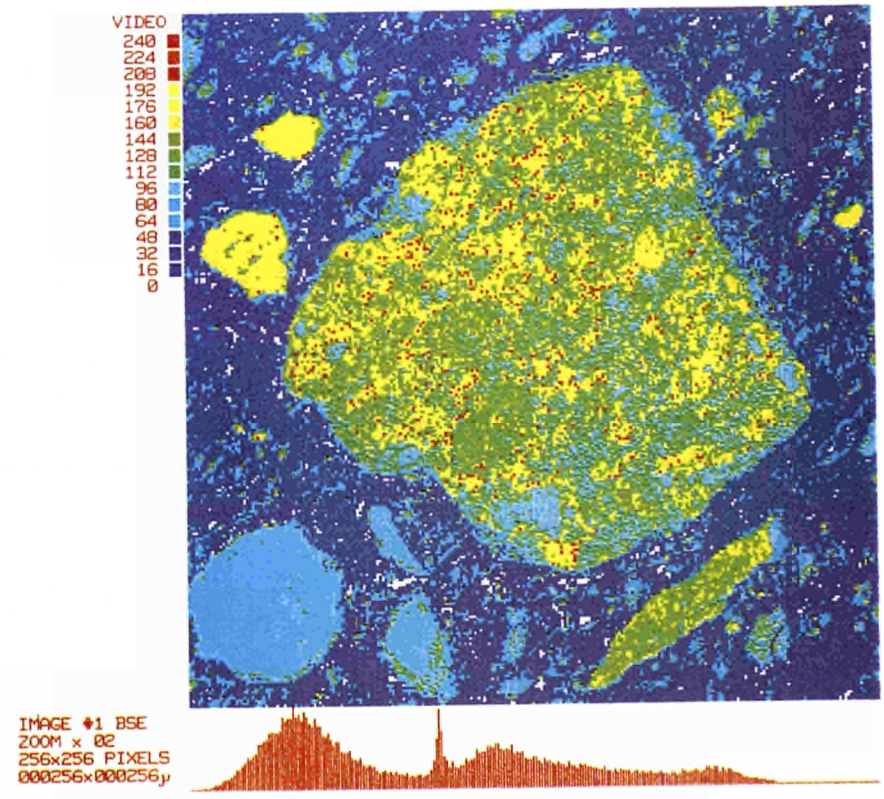
VIDEO
240
224
208
192
176
160
144
128
112
96
80
64
48
32
16
0
IMAGE #1 BSE
ZOOM x 02
256x256 PIXELS
000256x000256µ

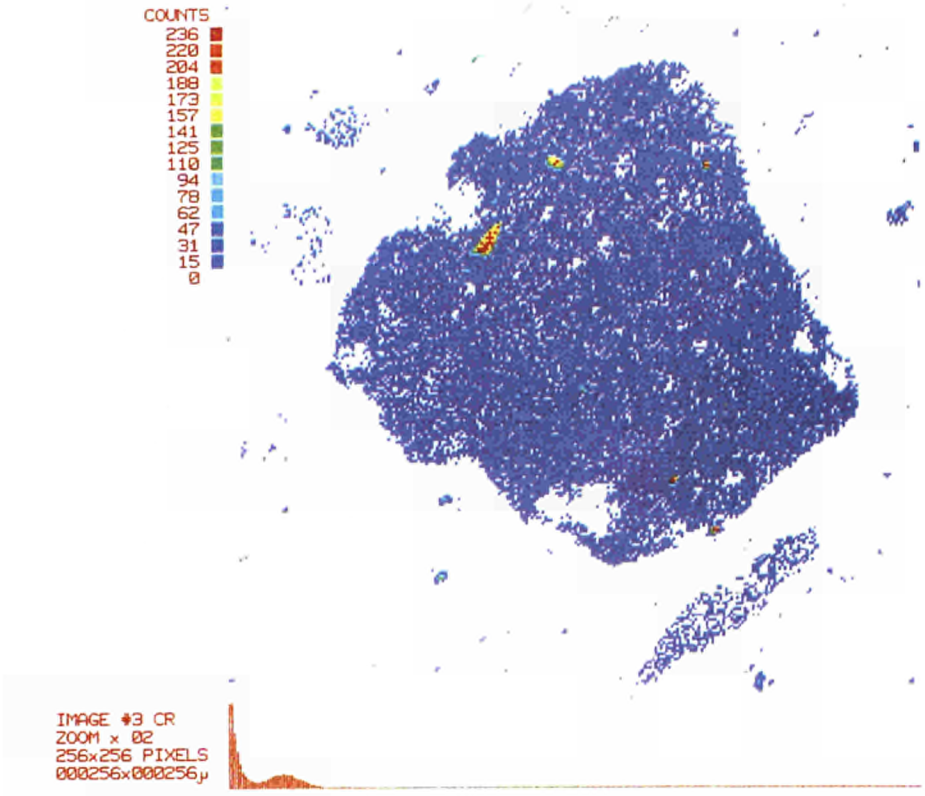
COUNTS
236
220
204
188
173
157
141
125
110
94
78
62
47
31
15
0
IMAGE #3 CR
ZOOM x 02
256x256 PIXELS
000256x000256µ

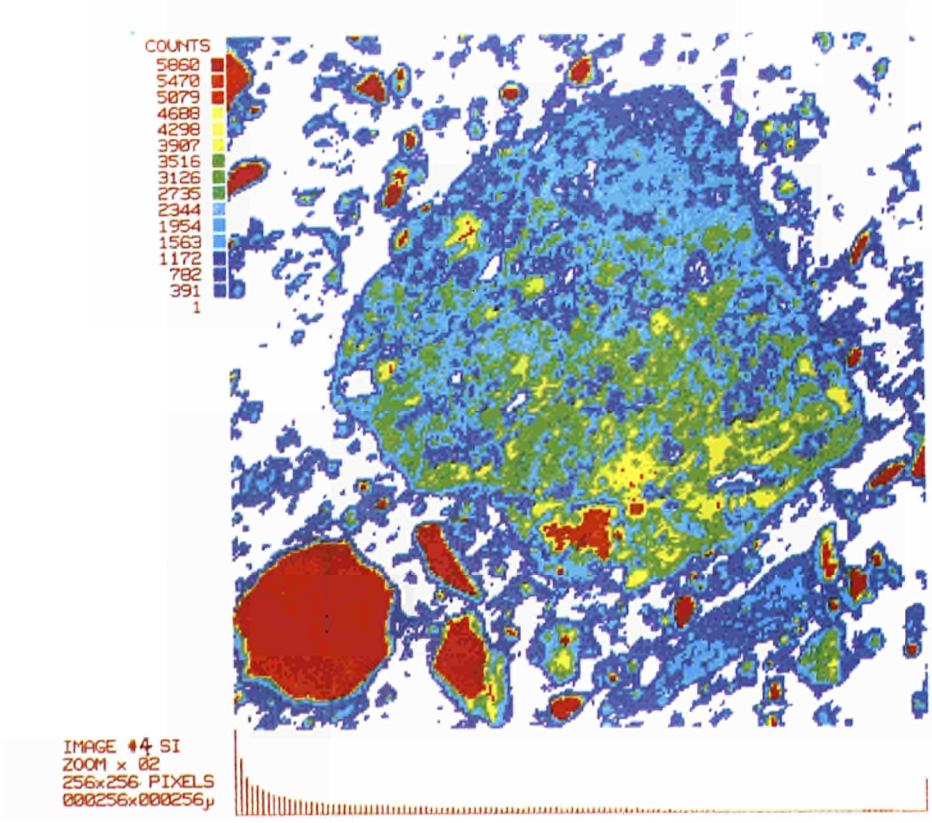
COUNTS
5860
5470
5079
4688
4298
3907
3516
3126
2735
2344
1954
1563
1172
782
391
1
IMAGE #4 SI
ZOOM x 02
256x256 PIXELS
000256x000256µ

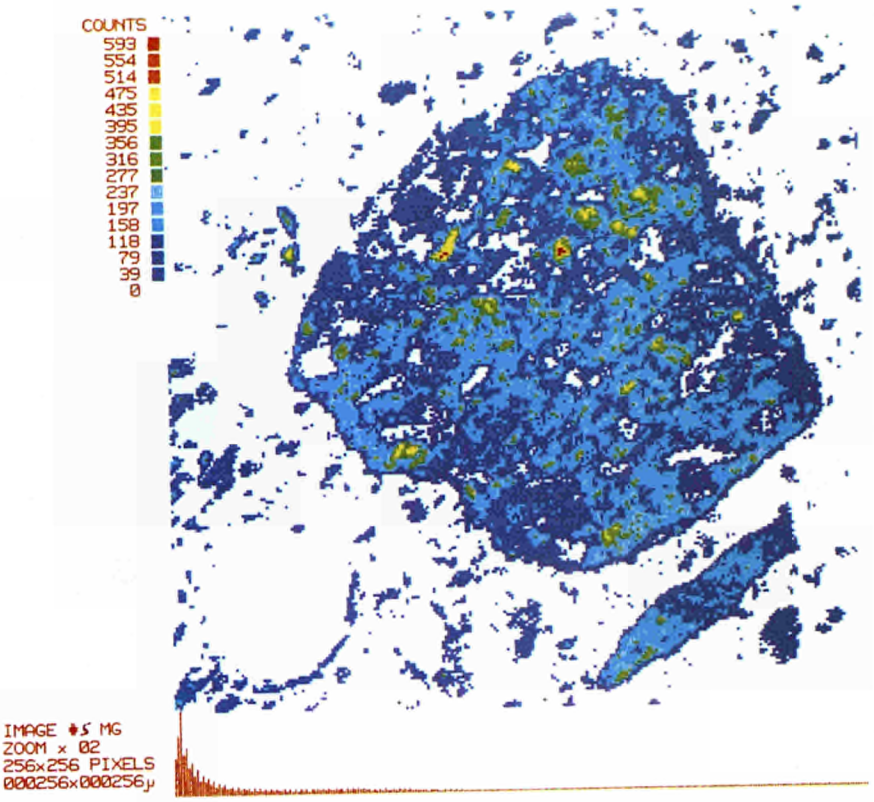
COUNTS
593
554
514
475
435
395
356
316
277
237
197
158
118
79
39
0
IMAGE #5 MG
ZOOM x 02
256x256 PIXELS
000256x000256µ

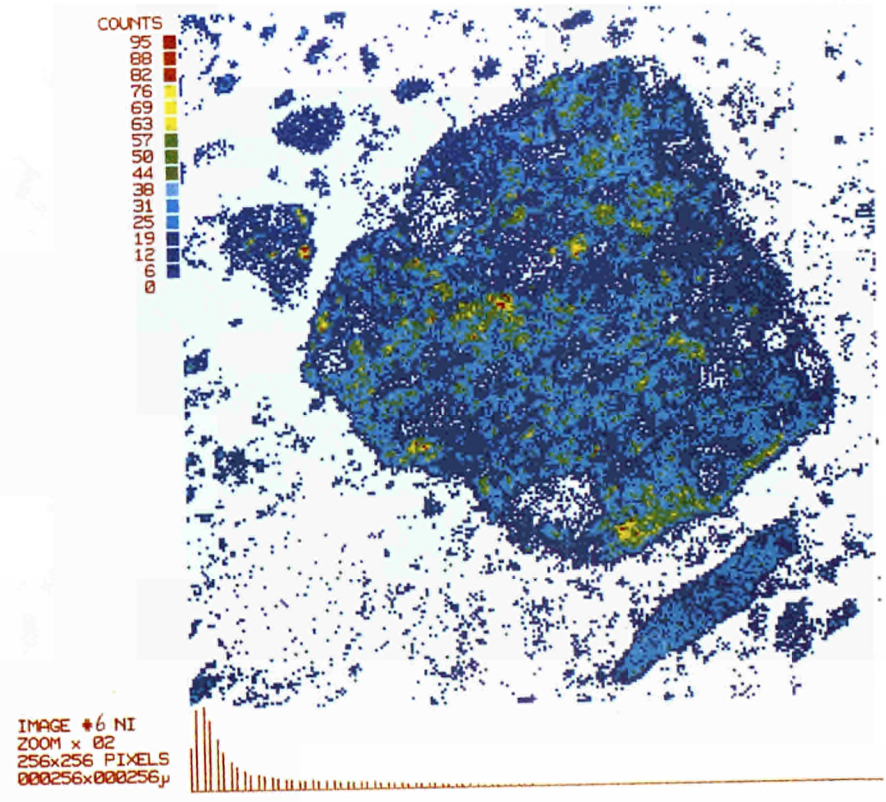
COUNTS
95
88
82
76
69
63
57
50
44
38
31
25
19
12
6
0
IMAGE #6 NI
ZOOM x 02
256x256 PIXELS
000256x000256µ

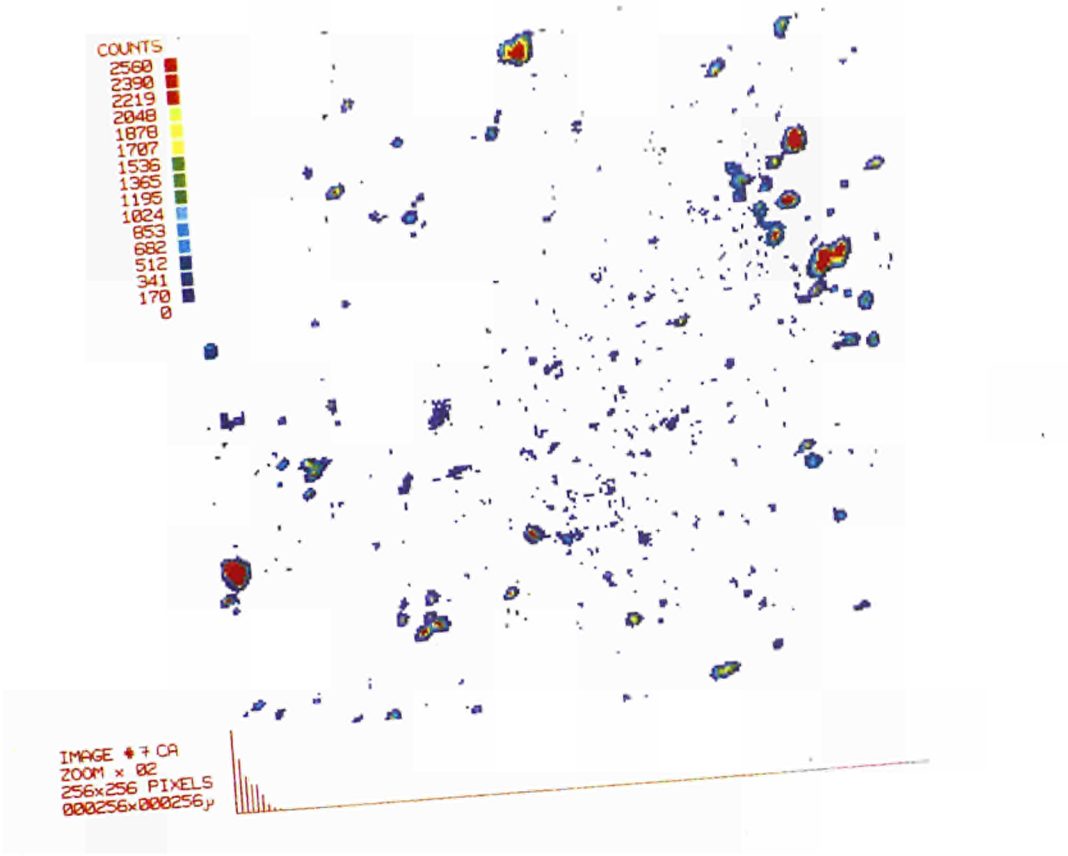
COUNTS
2560
2390
2219
2048
1878
1707
1536
1365
1195
1024
853
682
512
341
170
0
IMAGE #7 CA
ZOOM x 02
256x256 PIXELS
000256x000256µ

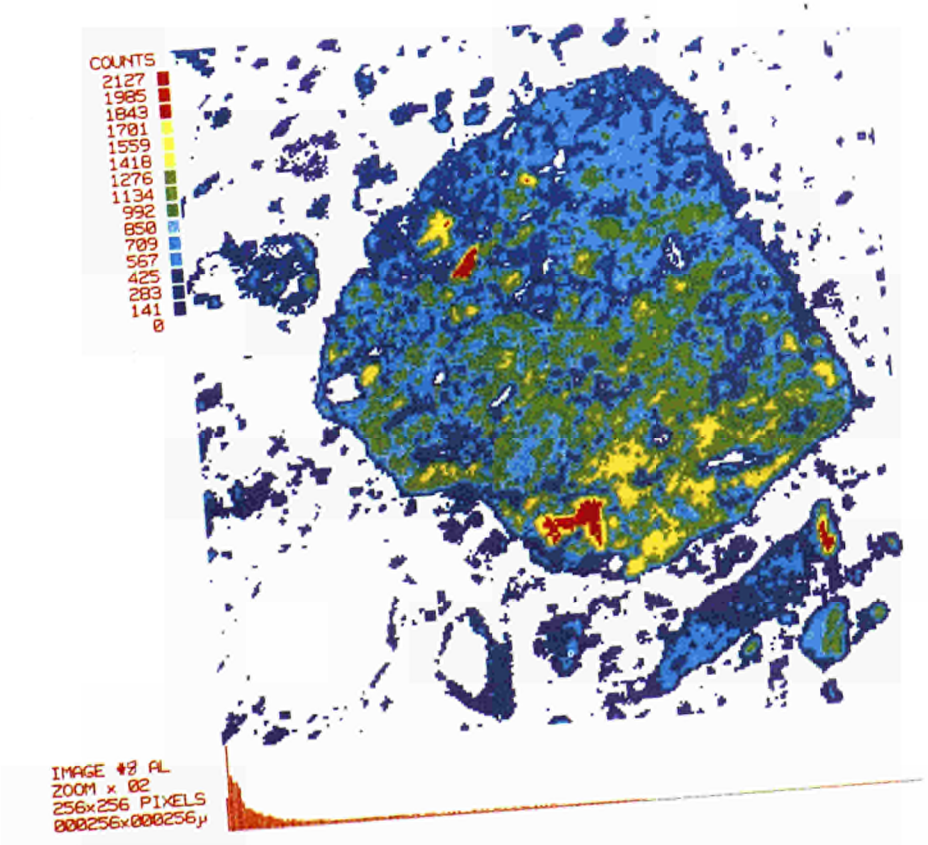
COUNTS
2127
1985
1843
1701
1559
1418
1276
1134
992
850
709
567
425
283
141
0
IMAGE #8 AL
ZOOM x 02
256x256 PIXELS
000256x000256µ

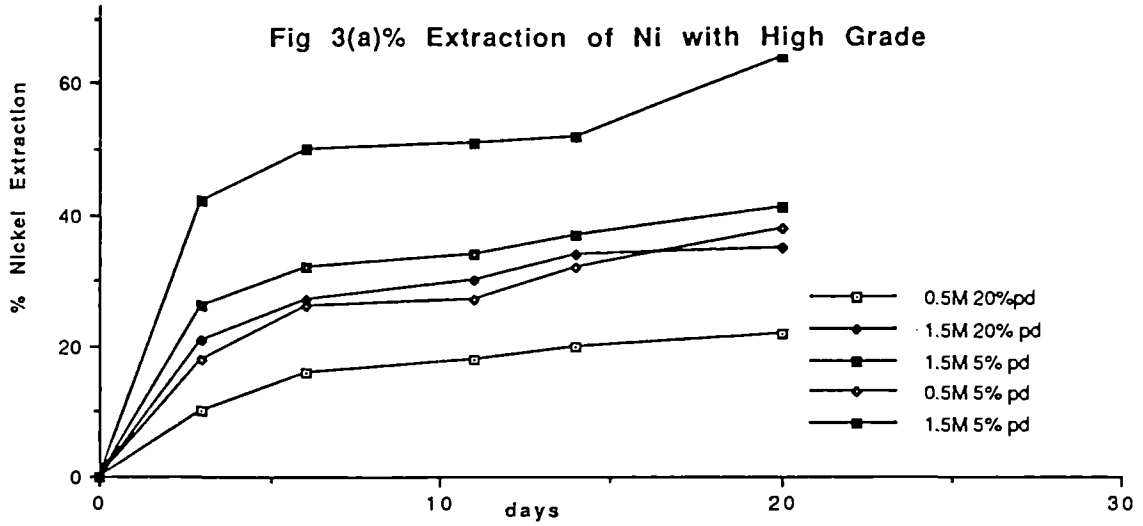
Fig 3(a)% Extraction of Ni with High Grade
% Nickel Extraction
60
40
20
0
0
10
days
20
30
0.5M 20%pd
1.5M 20% pd
1.5M 5% pd
0.5M 5% pd
1.5M 5% pd

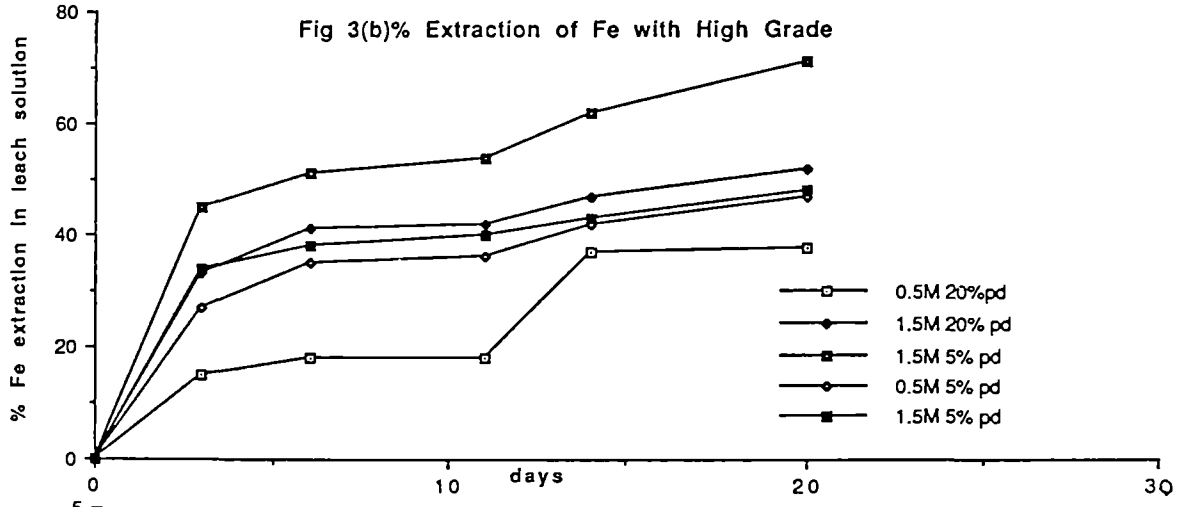
Fig 3(b)% Extraction of Fe with High Grade
% Fe extraction in leach solution
80
60
40
20
0
0
10
days
20
30
0.5M 20%pd
1.5M 20% pd
1.5M 5% pd
0.5M 5% pd
1.5M 5% pd

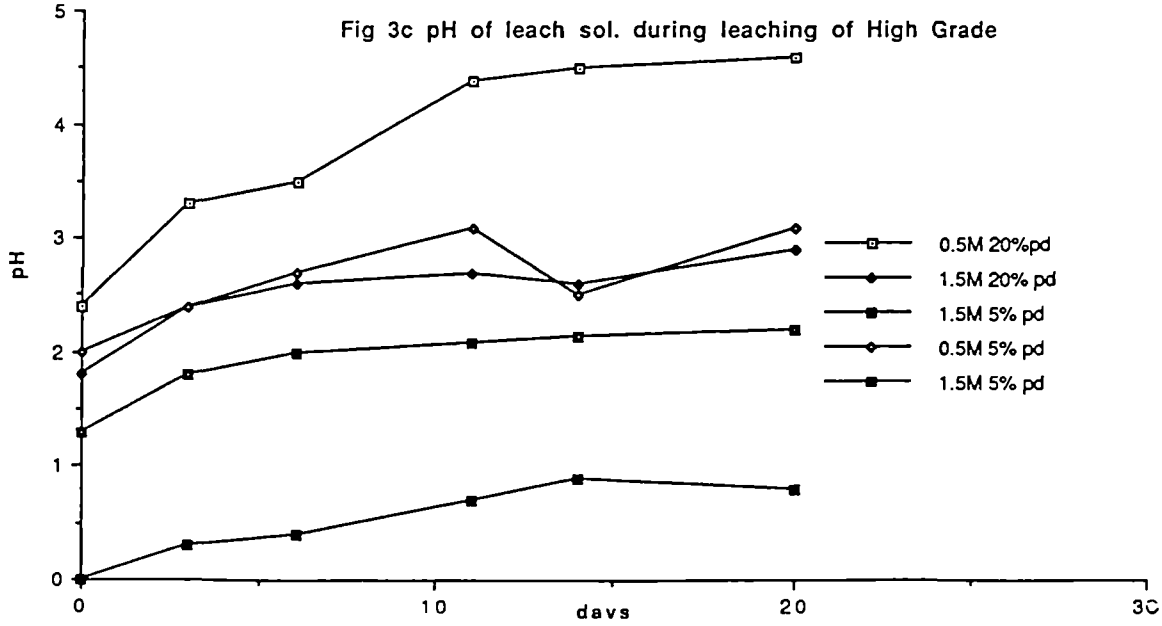
Fig 3c pH of leach sol. during leaching of High Grade
pH
5
4
3
2
1
0
0
10
days
20
30
0.5M 20%pd
1.5M 20% pd
1.5M 5% pd
0.5M 5% pd
1.5M 5% pd

Fig 4(a) Leaching of nickel - low grade ore

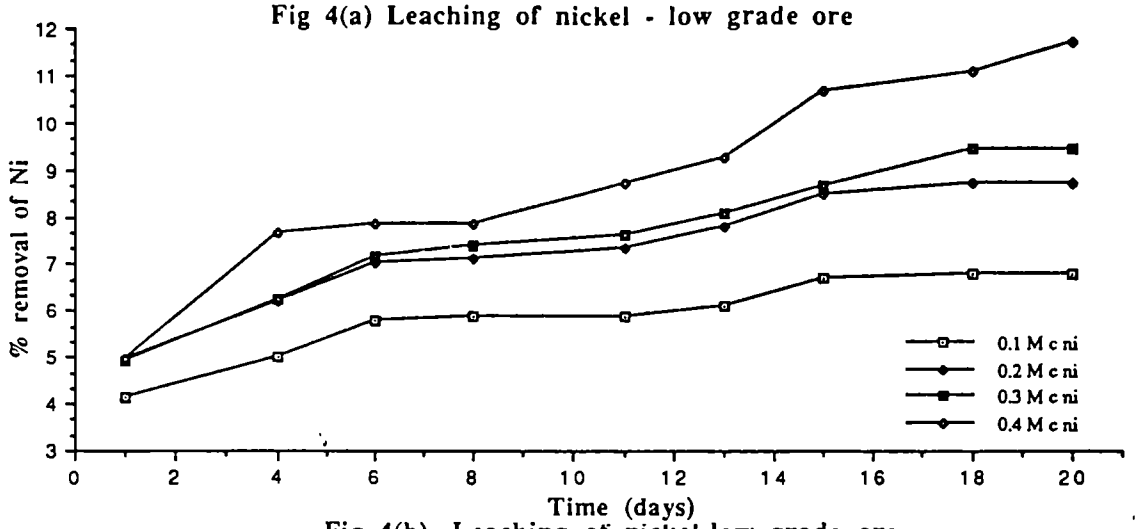

Fig 4(b). Leaching of nickel-low grade ore

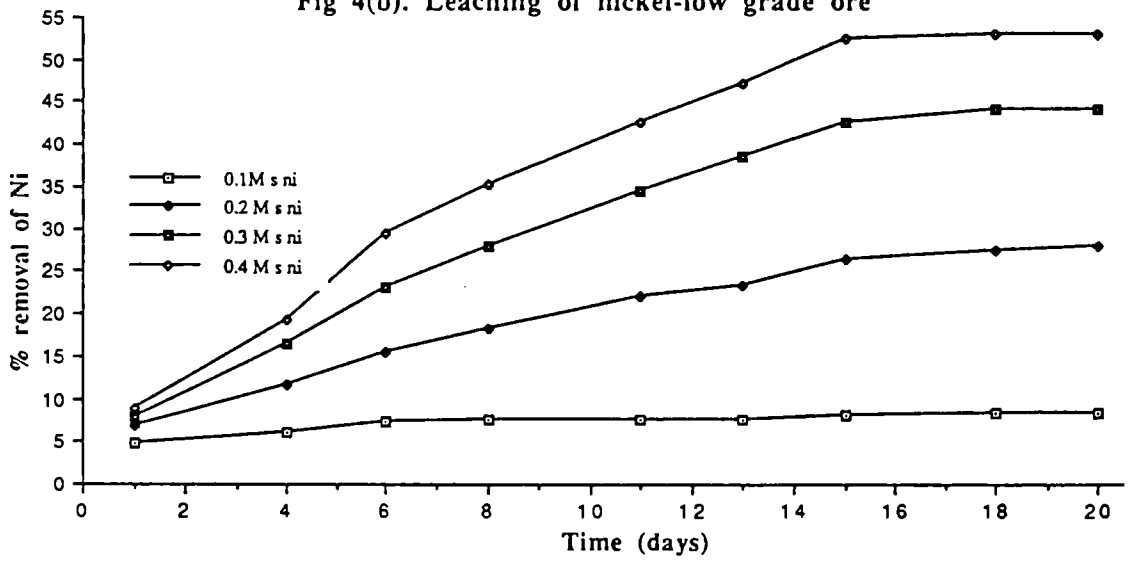

Figure 4(c). Leaching of Ni - low grade ore

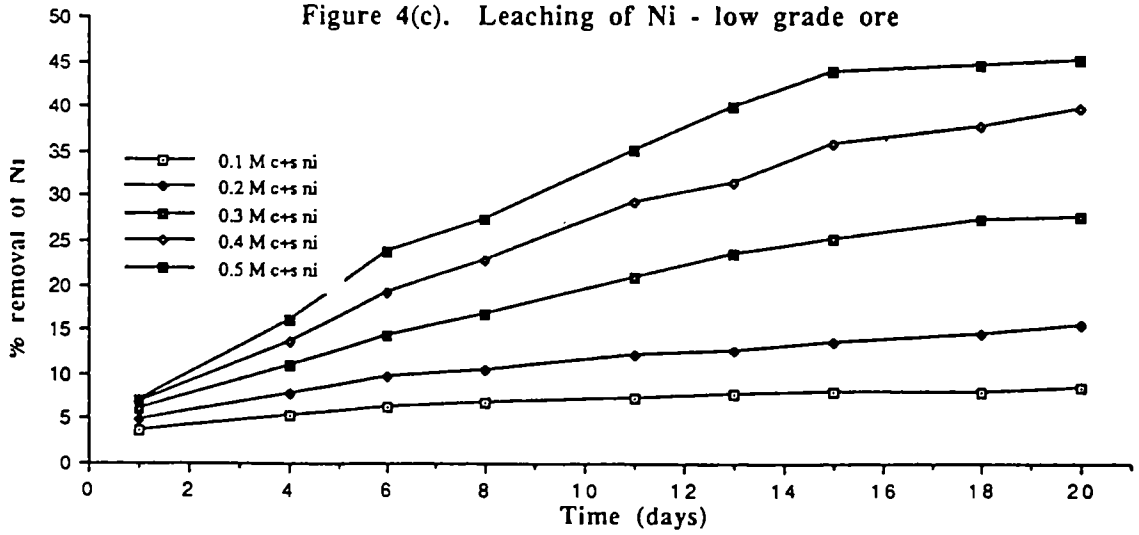

Fig 5(a) Leaching of Kabia for Mg

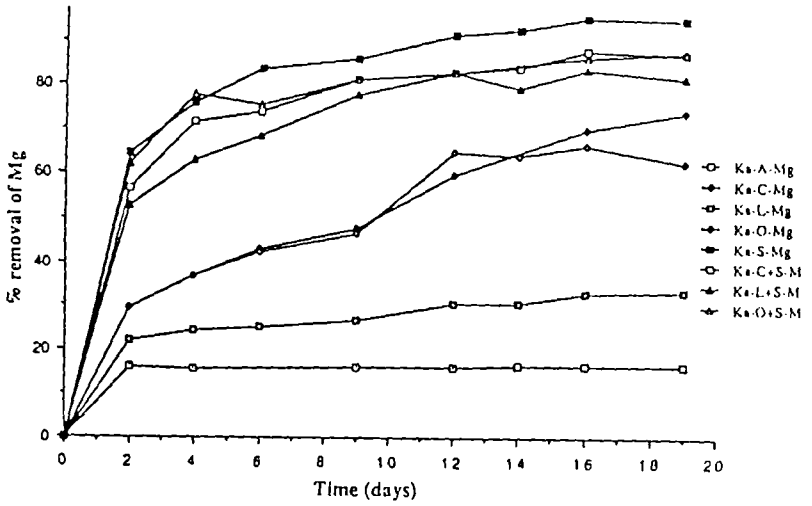

Fig 5(b) Leaching of Kabia for Ni

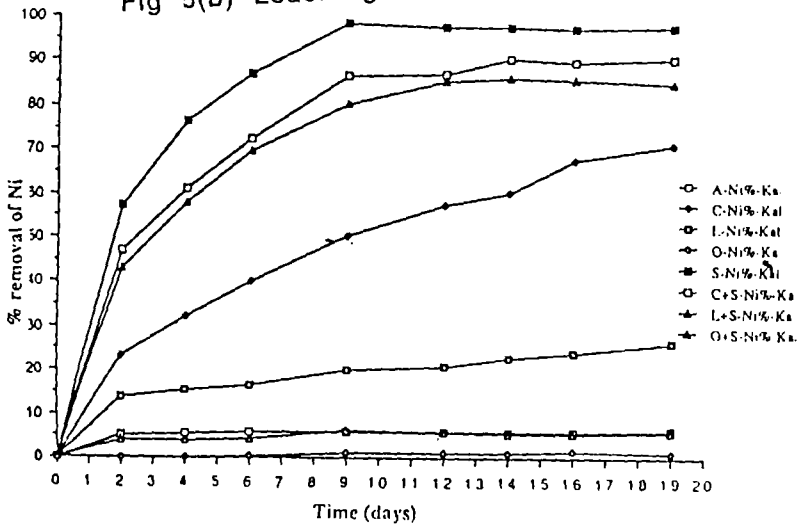

Fig 5(c) Leaching of Kabia for Ca

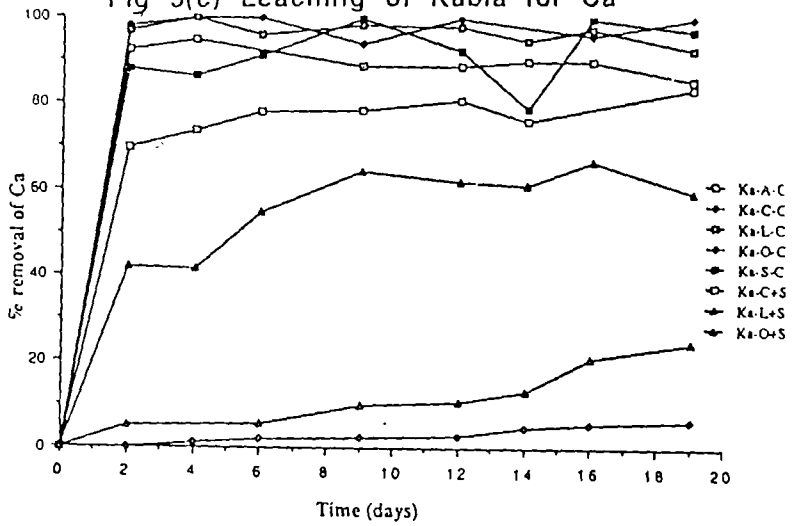

Fig 5(d) Leaching of Kabia for Fe

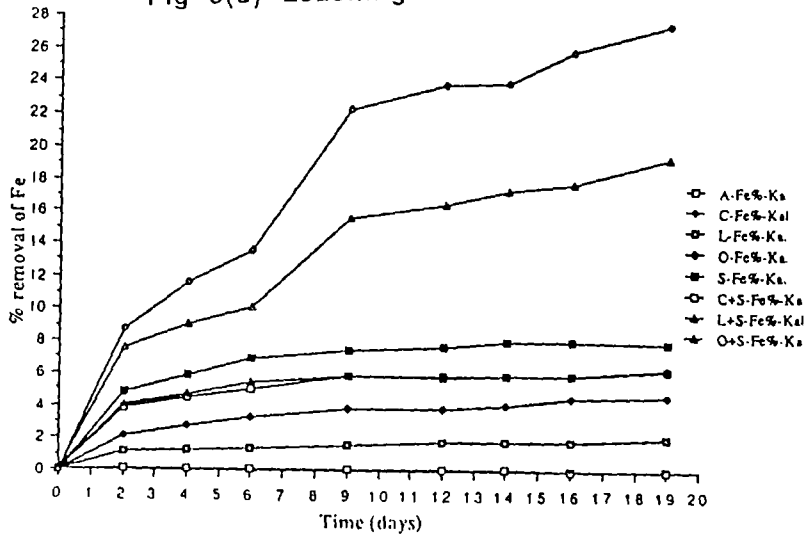

Fig 6(a) Leaching of Kukubajza for Mg

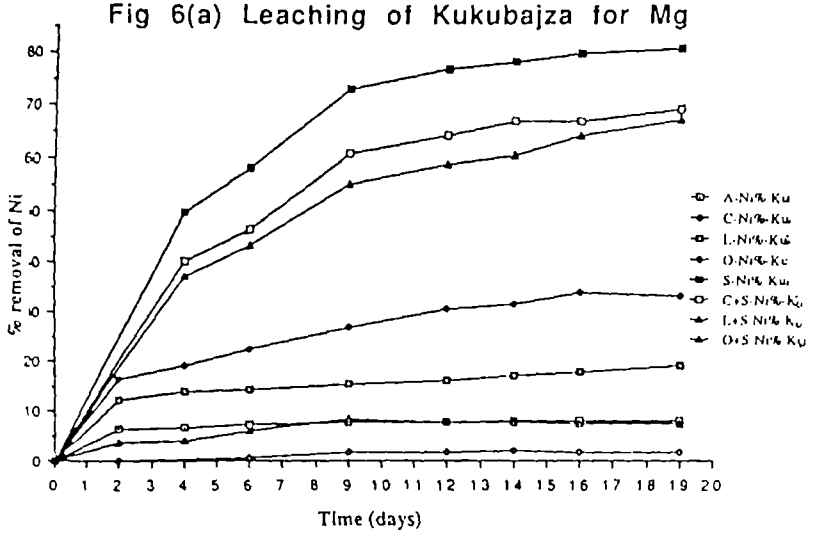

Fig 6(d) Leaching of Kukubajza for Fe

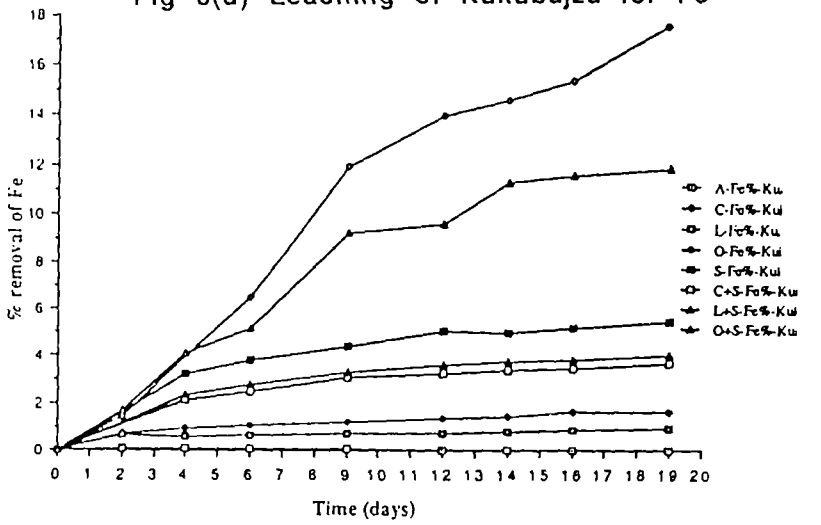

Fig 6(b) Leaching of Kukubajza for Ni

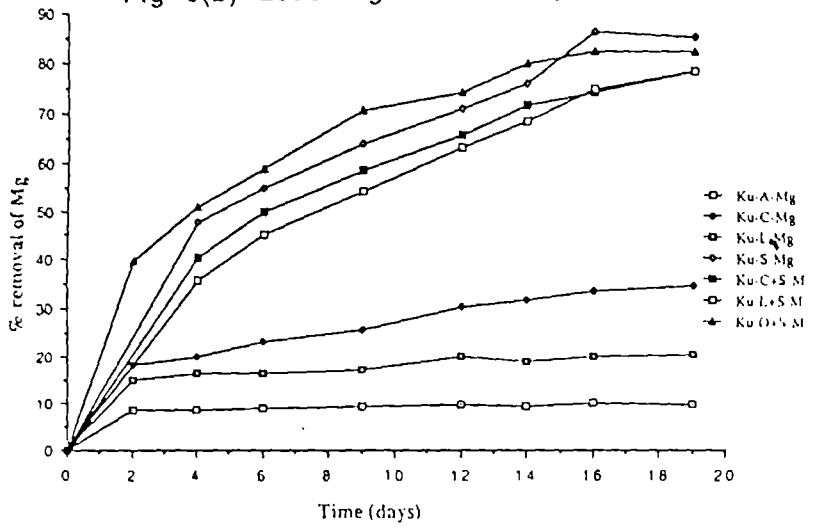

Fig 6(c) Leaching of Kukubajza for Ca

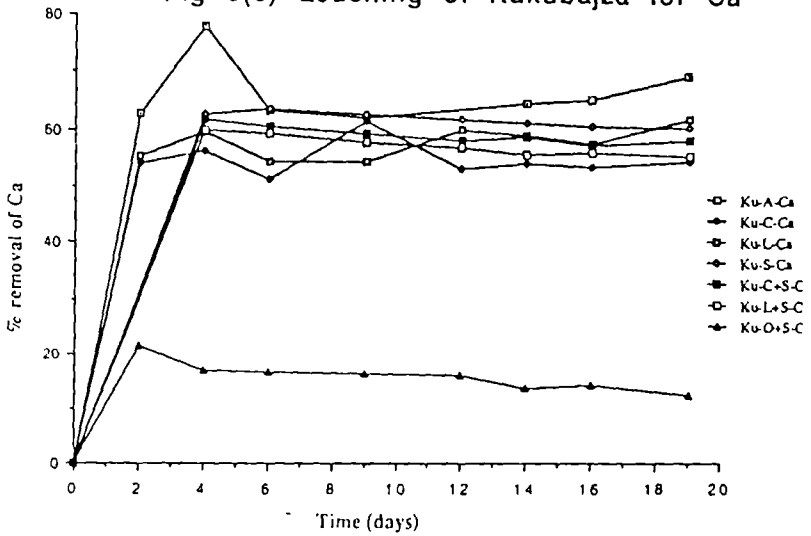

Fig 7 variation in Ni:Fe ratios during leaching of Triada

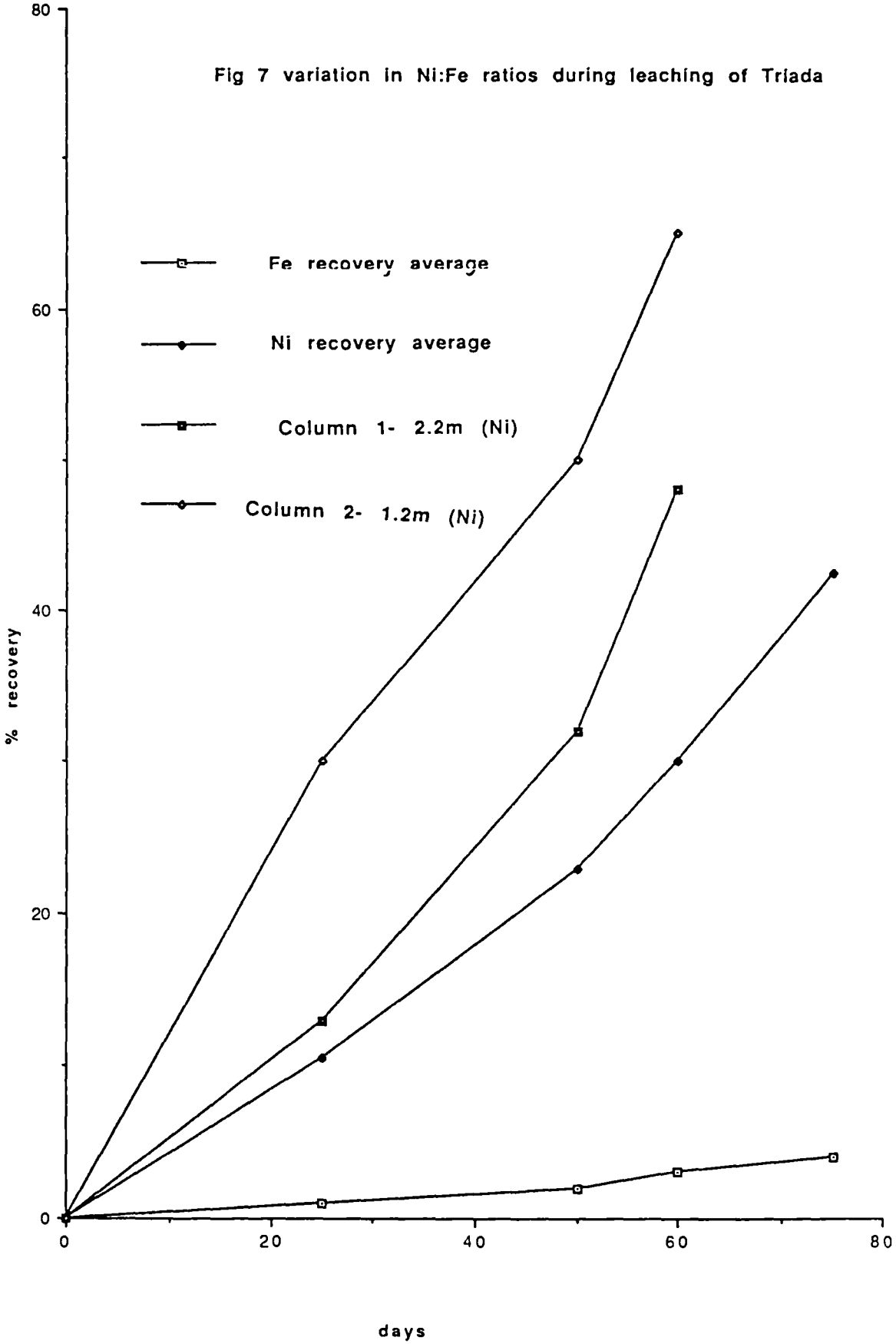

Fig 8(a) Leaching of Ni in Columns

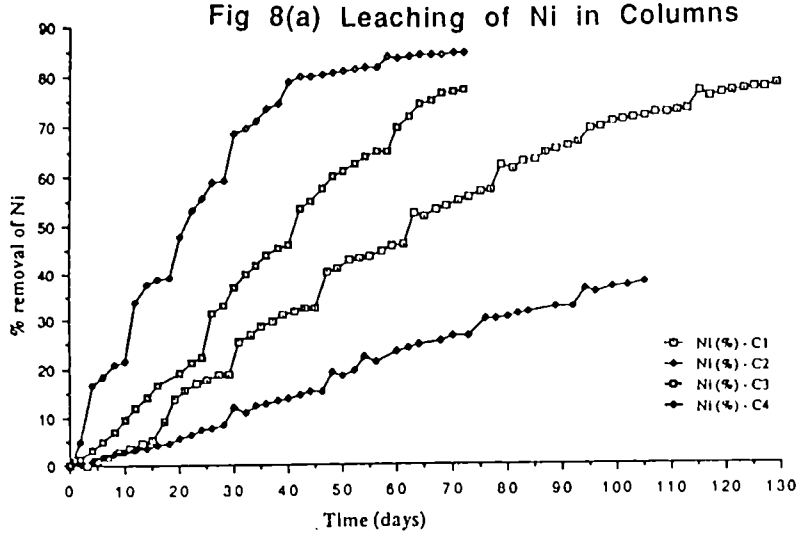

Fig 8(c) Leaching of Fe in Columns

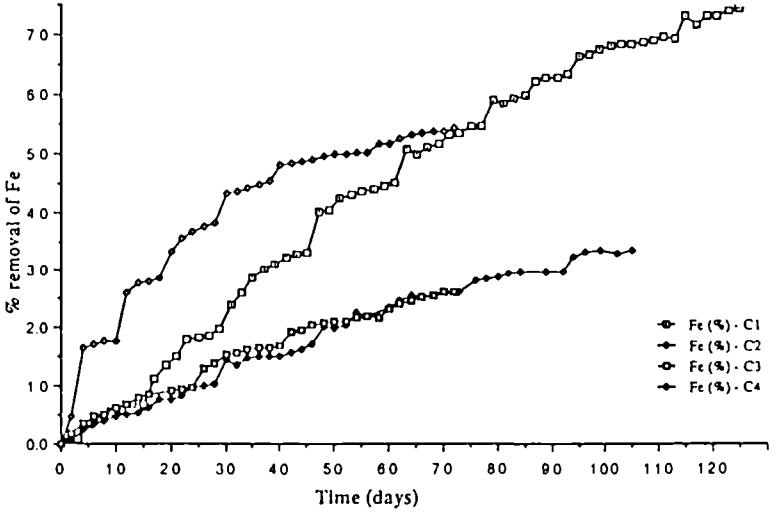

Fig 8(b) Leaching of Mg in Columns

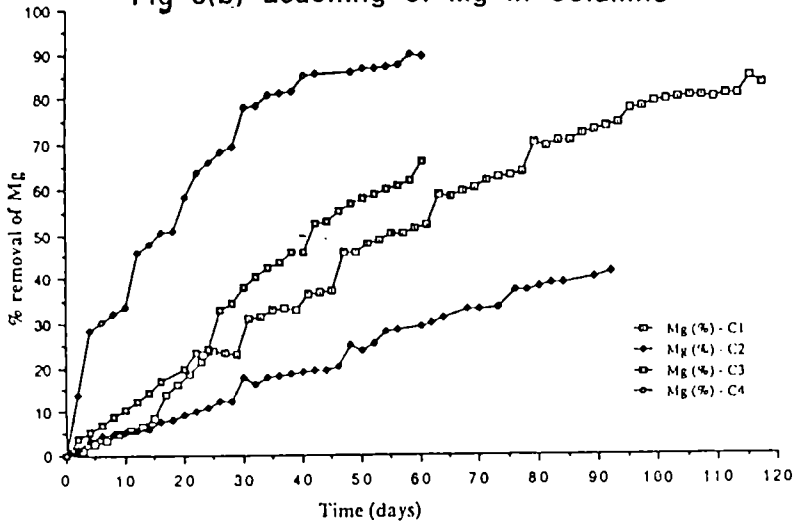

Fig 8(a) Leaching of Ca in Columns

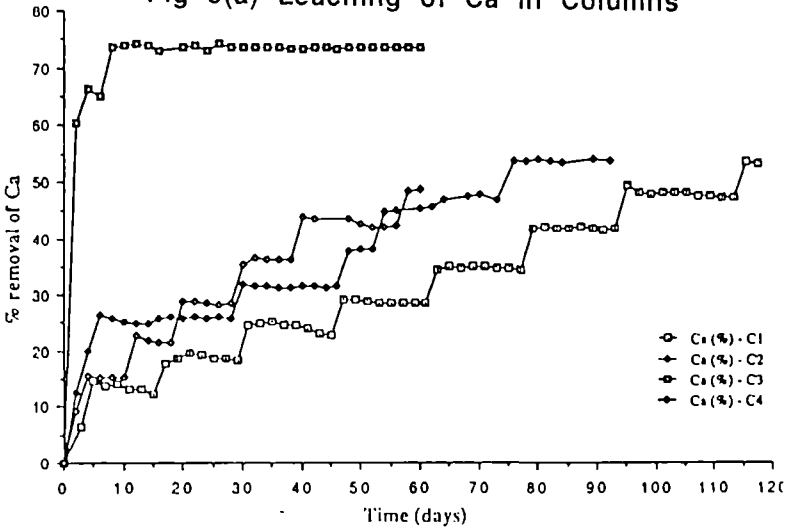

Fig 9(a) Steady State Concentrations C1-Sulphuric

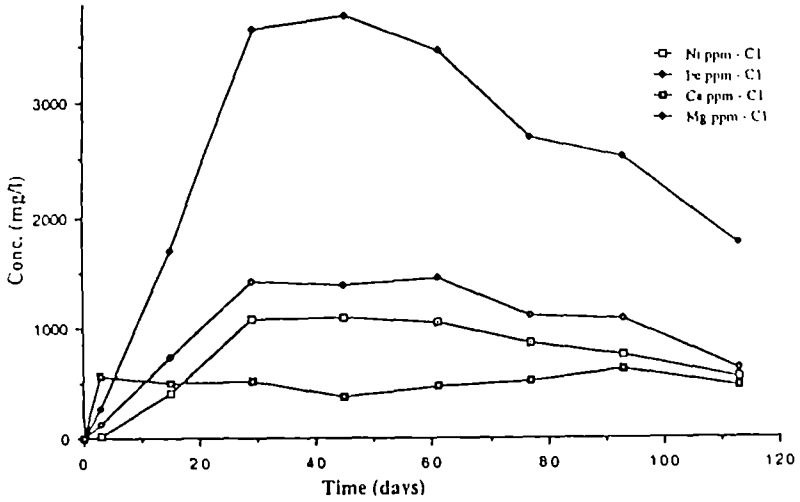

Fig 9(c) Steady State Concentrations C2-Citric

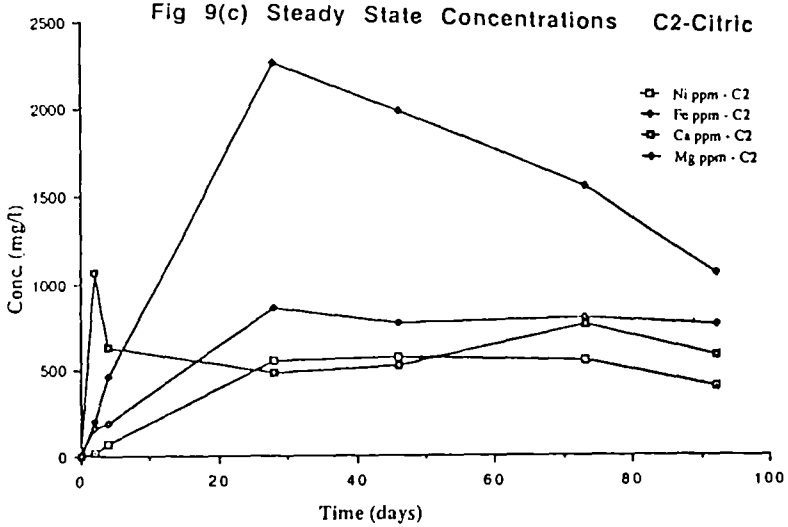

Fig 9(b) Steady State Concentrations C3-Sulphuric

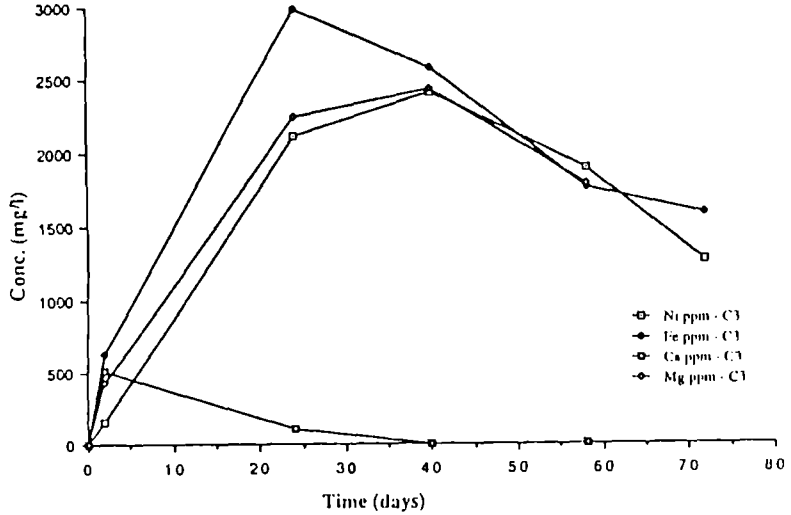

Fig 9(d) Steady State Concentrations C4-Sulphuric

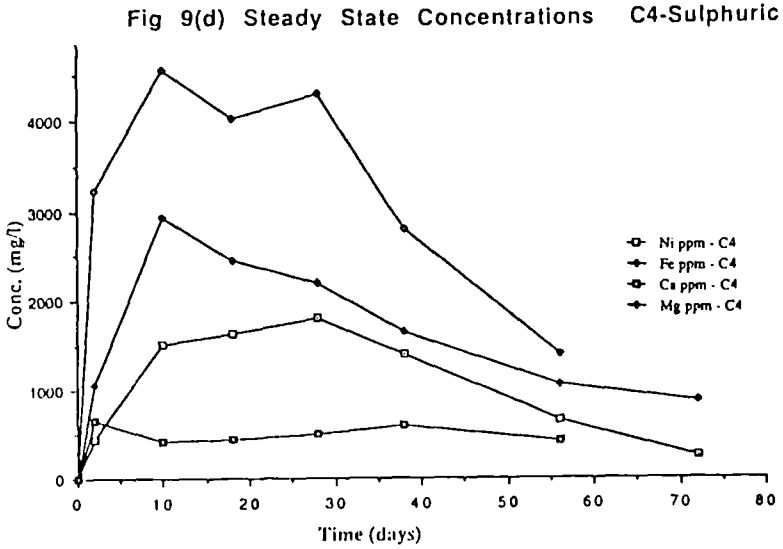

Fig 10 (a) Leaching of Ni with "bioacids" produced in Glucose-2 and sucrose medium with initial citric acid concs. of 40.8 g/l (A2), 11.8 g/l (A3) and 25.8g/l (P2).

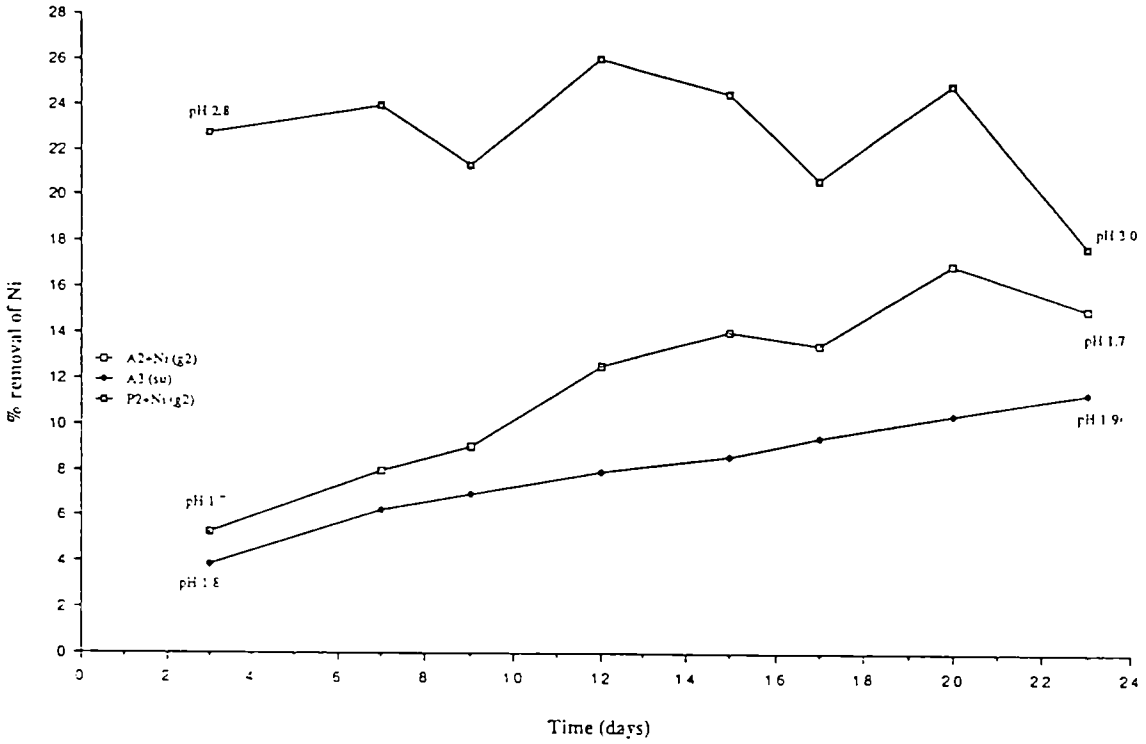

Fig 10 (b) Leaching of Fe with "bioacids" produced in Glucose-2 and sucrose medium with initial citric acid concs. of 40.8 g/l (A2), 11.8 g/l (A3) and 25.8g/l (P2).

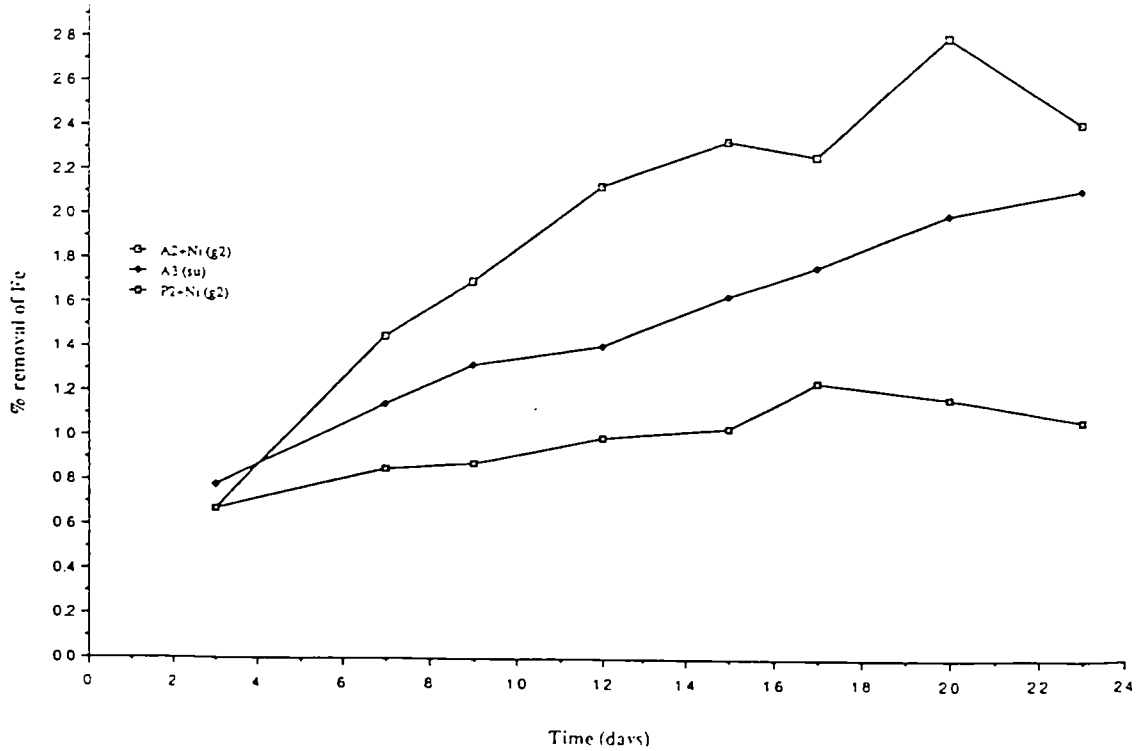

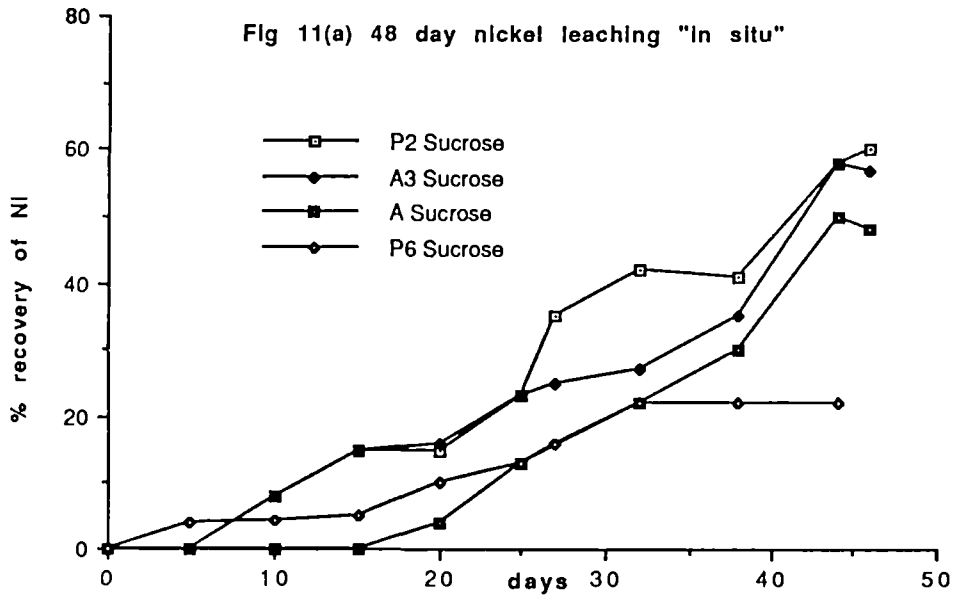
Fig 11(a) 48 day nickel leaching "In situ"
% recovery of NI
days
P2 Sucrose
A3 Sucrose
A Sucrose
P6 Sucrose
0
20
40
60
80
0
10
20
30
40
50

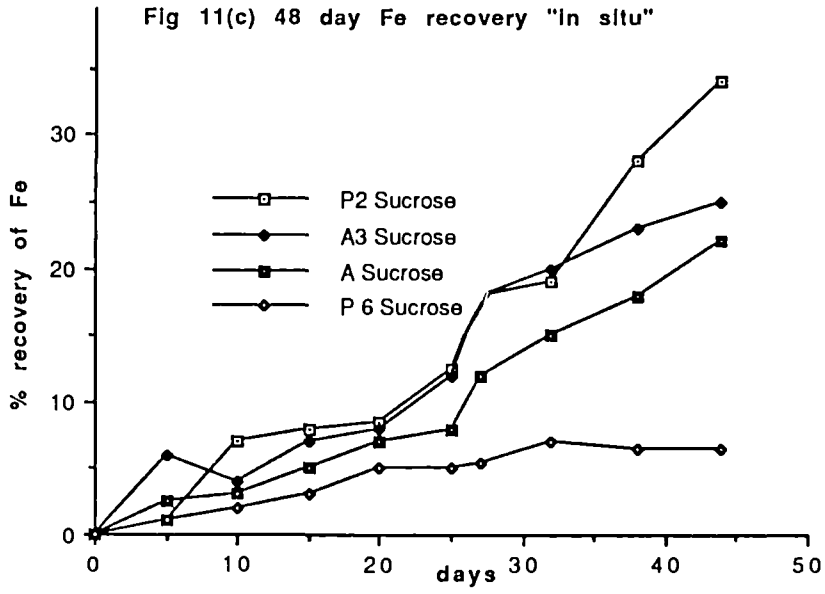
Fig 11(c) 48 day Fe recovery "In situ"
% recovery of Fe
days
P2 Sucrose
A3 Sucrose
A Sucrose
P 6 Sucrose
0
10
20
30
0
10
20
30
40
50

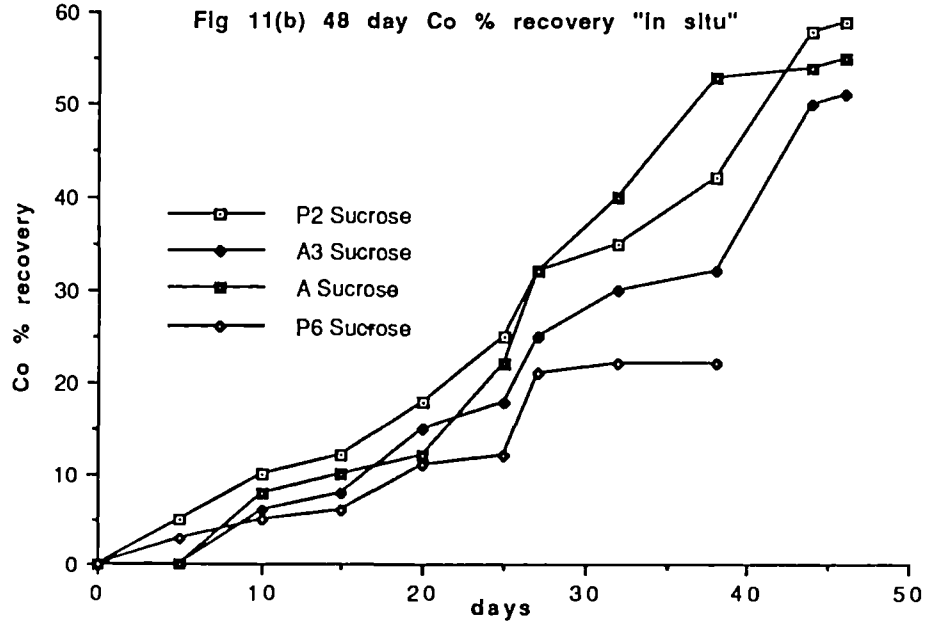
Fig 11(b) 48 day Co % recovery "In situ"
Co % recovery
days
P2 Sucrose
A3 Sucrose
A Sucrose
P6 Sucrose
0
10
20
30
40
50
60
0
10
20
30
40
50

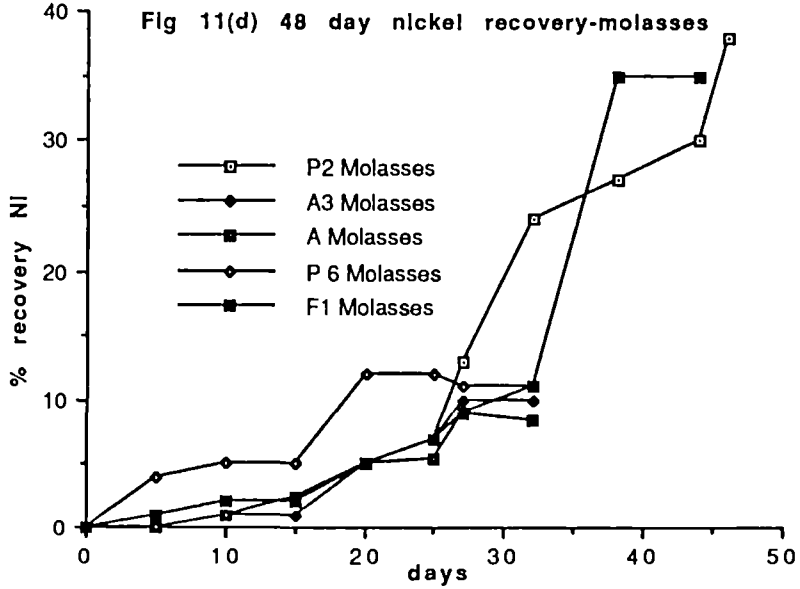
Fig 11(d) 48 day nickel recovery-molasses
% recovery NI
days
P2 Molasses
A3 Molasses
A Molasses
P 6 Molasses
F1 Molasses
0
10
20
30
40
0
10
20
30
40
50

THE USE OF LITHIUM-BEARING GEOTHERMAL FLUIDS FOR THE INDUSTRIAL PRODUCTION OF LITHIUM

Project Leader: Ch. FOUILLAC
Bureau de Recherches Géologiques et Minières (BRGM), Orléans, France

M. NICCOLINI
EUROMIN s.r.l., Trieste, Italy

Mrs MARABINI
Consiglio Nazionale delle Ricerche (CNR), Roma, Italy

Contract MA1M-0023-F

1. OBJECTIVE

This project had two main objectives :

- To estimate the lithium reserves contained in the French and Italian geothermal aquifers, either already in production or with a predicted development for the period 1995-2000.

- To develop a technique for the extraction of the lithium contained in French and Italian fluids.

2. INTRODUCTION

At present, lithium metal is mostly produced from silicate minerals. However, those countries that have no natural ore reserves containing lithium are planning to extract, or already produce, lithium from certain fluids enriched in this metal. For instance, in the USA lithium is produced in this manner at Silver Peak, Nevada (Li = 277 to 416 mg/l), at Searless Lake, California (Li = 70 mg/l) and from the Great Salt Lake, Utah (Li = 55 mg/l); in Chile, the Salar de Atacama contains 1500 mg/l Li. The metal is usually extracted as a carbonate, after evaporation of the solution and fractionated crystallization of the other salts.

Other lithium sources are presently being studied. Even though seawater has a low lithium content (0.14 mg/l), this resource is of interest to the Japanese; after all, the total lithium content is estimated to be $2,5 \times 10^{14}$kg. In the Middle East, the Dead Sea has aroused interest because

of its lithium content of 18 mg/l. Hydrothermal fluids also seem to be of interest, as in this case at least part of the extraction would be financed by geothermal production. The main sites where such research has been carried out are Hatchobaru, Arima, Onikoube and Othake in Japan, the Salton Sea in the western USA, Cerro Prieto in Mexico, and Wairakei and Broadlands in New Zealand.

During this study, we studied the potential for lithium production from fluids that are found within the territory of the European Community. An inventory was then made of those fluids that, because of their chemical composition, are likely to be of interest for the production of lithium. We then estimated the resources present in the French and Italian geothermal reservoirs. The various techniques for lithium extraction that are described in the literature, were reviewed with the intention to apply them to geothermal waters. Finally, experimental work has allowed to test on European geothermal fluids a lithium extraction technique during the precipitation of aluminium.

3. LITHIUM IN EUROPEAN GEOTHERMAL FLUIDS

3.1. SELECTION OF THE FLUIDS ON THE BASIS OF THEIR CHEMISTRY

Data were collected on the lithium contained in geothermal waters, and in water from springs and boreholes, the last from petroleum drilling in France, the United Kingdom and Italy. For each of these fluids, the chemical composition was studied.

For optimal extraction of lithium, the Na/Li ratio must be low, as sodium is a nuisance element for most extraction techniques. The data collected are presented in a log (Na/Li)/log (Li) diagram (Fig. 1). By way of comparison, we have plotted on the same diagram the fluids for which various authors have envisaged Li-extraction. In this case, the most interesting fluids are located in the top-left corner of the diagram. It can be seen that the six fluids presented all have a very high Li-extraction potential : the fluids from the geothermal field at Cesano (Italy), those from the Alsatian Trias in France, the water from South Crofty mine in Cornwall (U.K.) and, finally, the two waters from the French Massif Central (the Croix-Neyrat borehole and the Coren spring).

Even though less enriched in lithium than those cited above, the fluids from the Latera geothermal field in Italy have a Na/Li ratio that makes them much more interesting than the Japanese fluids. The fluids found in sedimentary rocks, in France and the U.K., have higher Na/li ratios, but they are still competitive when compared with other, non-European, fluids for which lithium extraction is planned. However, the fluids contained in the Triassic rocks of Italy have a chemistry that severely restricts the choice of suitable extraction techniques.

3.2. LITHIUM RESERVES IN THE TRIASSIC AQUIFERS OF ALSACE, FRANCE

The high lithium content of the fluids of the Triassic rocks of northern Alsace, has led us to further study of this potential resource. This study covered the Buntsandstein and Muschelkalk formations, both of which are dissected by normal faults into blocks of several kilometres. The study area covers about 900 km^2, centred on the oil field of Merckwiller-Pechelbronn.

The data consulted, which are mostly from oil exploration, made it possible to study the geometry of this area, where the top of the Buntsandstein was taken as reference level (Fig. 2). Temperature and pressure data were studied, and a rough map was drawn of the total salinity (TDS) from existing compilation data and 30 available measurements. The lithium concentration was deduced from the following equation, based on available data :

$$\log(Li) = 0.069\ t + \log(TDS) - 4.4077$$

This made it possible to draw a map of the lithium grades in the study area (Fig. 3). The following hydrodynamic data were also established :

- cumulative average productive height in the two reservoirs : 100 m;
- average porosity : about 6 %;
- average transmissivity : about 10^{-3} m^2/s.

The combination of these data made it possible to estimate that about one million tons of lithium reserves are contained in the study area (about 200,000 tons for the block diagram of Fig. 2). On the other hand, the type of available data, which mostly derive from oil-well tests, make it very difficult to evaluate the stock that can actually be mobilized.

3.3. THE LITHIUM RESERVES IN THE ITALIAN AQUIFERS

The potential reserves contained in four Italian geothermal fields were studied : Torre Alfina, Latera, Cesano and Campi Flegrei.

At Torre Alfina, the salt content of the fluids is very low and the lithium content is thus equally low.

For the evaluation of the lithium reserves at Latera, the following parameters were used :

- reservoir volume : 4 km^3;
- effective porosity of the reservoir : 5%;
- extractable volume of the fluid : 0.2 km^3;
- average lithium grade : 10 mg/l;
- potential lithium reserves : 2000 tons.

In the case of Cesano, the evaluation was based on the reservoir located around a single well, with the following parameters :

- reservoir volume : 0.7 km^3;
- effective porosity of the reservoir : 5 %;
- extractable volume of the fluid : 0.03 km^3;
- average lithium grade : 250 mg/l;
- potential lithium reserves : 7500 tons.

The parameters of the shallow geothermal reservoirs at Mofete and San Vito (Campi Flegrei) were estimated as follows :

- reservoir volume : 0.25 km^3;
- effective porosity of the reservoir : 5 %;
- extractable volume of the fluid : 0.01 km^3;
- average lithium grade : 25 mg/l;
- potential lithium reserves : 250 tons.

4. THE TECHNIQUES FOR LITHIUM EXTRACTION

Various techniques for the extraction of lithium are described in the literature, whose aim is the application to sea water, including that from the Dead Sea, or geothermal waters. However, not all these techniques were used on fluids of the same chemical complexity as those found in France and Italy (see the publications by Dang and Steinberg, 1978; Schultze and Bauer, 1984; Abe and Chitrakar, 1987; and Sakamoto et al., 1987). The main techniques known are :

- extraction through precipitation of aluminium, used in our experiments;
- adsorption on inorganic ion-exchange material;
- extraction with organic solvents;
  extraction on cation-exchange resins.

The use of crown compounds, in a technique deriving from solvent extraction was also contemplated. Such compounds, the simplest of which is illustrated in Figure 4, are capable of trapping those alkaline ions in their center that normally are not affected by the traditional complexing agents. We have drawn up a, non-exhaustive, list of 83 crown compounds that are specific for lithium.

Such products could be incorporated in a membrane, which would cause them to transport lithium selectively through this membrane, from a geothermal fluid to a receiving solution, as is shown in Figure 5. This technique is inspired by that of the transport through biological membranes. According to the properties of the compound, which govern the metal transfer, such transport can be down-hill, meaning that the energy necessary for this transport

is provided by the metal gradient that exists between the two aqueous phases. Another method is the coupled membrane transport process, in which case the transport is directed by electric or light energy, or by the concentration gradient of another chemical element.

This extraction technique could be applied to solutions with a high lithium content and a relatively low Na/Li ratio, as are found in the Triassic rocks of northern Alsace, the Massif Central and Cesano. The reason is that the selected crown compounds are not exclusive complexing agents for Li, but can also act, albeit more weakly, on sodium ions.

5. EXPERIMENTAL STUDY OF LITHIUM EXTRACTION FROM GEOTHERMAL FLUIDS

5.1. SPECIFIC ELECTRODE FOR LITHIUM

The classical methods to assay for lithium (atomic absorption and ion chromatography) can in some cases be difficult to apply, for which reason we considered it to be useful to develop a more flexible tool. The specific electrode answers such requirements, particular those of analytical rapidity. We, therefore, proceeded to manufacture a membrane for an electrode specific to lithium, such as was proposed by Kimura et al. (1987). The ionophore is the crown ether 6.6-dibenzyl-14-crown 4.
The composition of the membrane is as follows :

-	6.6-dibenzyl-14-crown 4	1.0 %
-	o-nitrophenyl-octyl-ether	70.3 %
-	potassium tetrakis	0.7 %
-	PVC	28.0 %

which was then adapted to the body of a Philips IS electrode.

The results obtained shown that the use of a specific electrode is quite promising, as it can assay the lithium content in solutions that are not too heavily mineralized, such as certain geothermal or other fluids. However, when the ionic strength of the solutions to be assayed becomes too high, it is necessary to use the technique of measured additions. This is a rapid technique, but the continuous monitoring of the changes in lithium concentration of the solution is no longer possible.

5.2. LITHIUM EXTRACTION THROUGH ALUMINIUM PRECIPITATION

Tests of the lithium extraction by means of aluminium precipitation were carried out on two reconstituted fluids with lithium content (Table 1), one from the Alsatian Trias (Cronenbourg), the other Italian (Cesano). This is one of the best known techniques for the extraction of lithium, which has been extensively tested for geothermal fluids (Yaganase et al. 1983; Schultze, 1984; Yoshinaga et al., 1986; and Rothbaum and Middendorf, 1987).

5.2.1. The experimental procedure

The experimental procedure is described on figure 6. Aluminium is added to 150 cm^3 of the solution as $AlCl_3.6H_2O$ solid. The pH is adjusted by adding potassium hydroxide and the solution is stirred and maintained at a constant temperature during the entire experiment. The pH is periodically measured and 10 cm^3 of the solution are sampled to assay the lithium content and, in certain cases, the aluminium content. The reaction time varies from 5 minutes to 6h 30 min, and is counted from the moment the pH is adjusted. At the end of the experiment, the sample is filtered and the solid phase is kept for analysis and for study by means of X-ray diffraction. The influence of three parameters, temperature (20°, 50° and 80°C), pH and Al content, on the extraction of lithium was then studied.

5.2.2. Results and discussion

Adding potassium to the solution increases its turbidity, and a non-settling gel is formed. The aluminium precipitates in fact as an amorphous hydroxide and carries the lithium along with it. In every case, precipitation was rapid and after 10 minutes the aluminium concentration had stabilized. The chemical composition of the solutions and the precipitates is shown in figures 7 to 12 and in Table 2.

The upper part of figures 7 to 12 shows the residual lithium concentration in the geothermal solution, and the lower part shows the evolution of the pH values. In general, the Li concentration decreases rapidly after adding the aluminium and KOH, after which it reaches a stationary level.

Other extraction tests described in the literature, mention that the process is affected by various parameters, such as the type and the concentration of the aluminious phase, the presence of certain salts, pH, and temperature.

In the case of a secondary use of geothermal fluids, it is necessary to effect the extraction at high temperatures; the tests carried out for this study indicate that such high temperatures favour the extraction. This highly promising result is in straight contradiction with the observation made on other geothermal fluids by Yaganase et al., 1983, and Yoshinaga et al., 1986. Furthermore, the extraction kinetics also increase with increasing temperature.

Another factor that influences the extraction of lithium is the aluminium content of the fluid; regardless of the temperature and the fluid, the extraction rate increases with an increasing Al/Li ratio (Fig. 7, 9 and 10). It is thus interesting to note that a high extraction rate of 50 % can be obtained with an initial Al/Li ratio of 1, and more than 95 % of the Li is extracted when the initial Al/Li ratio is 2.76. This means that it is not necessary to

consume vast quantities of aluminium to extract the lithium from the Cronenbourg and Cesano fluids. By way of comparison, tests carried out on the Waraikei fluids from New Zealand, give the same extraction percentage when the initial Al/Li ratio is as high as 66.5 (Rothbaum and Middendorf, 1987).

The influence of the pH was studied at 80° C, for a pH range of about 5 to 9. This is shown on figures 11 and 12. For the two fluids, the lithium extraction rate increases with the pH, but there seems to be no optimal pH value for this process, as was also observed for other fluids (Yoshinaga et al., 1986). In any case, the extraction rate seems to increase with the pH up to a certain level, after which further pH increases have no further effect (Fig. 11). The influence of the Al/Li ratio therefore seems to be more important than that of the pH. It should also be noted that high extraction rates are obtained when using the same pH as is found in the untreated geothermal solution, which means that the extraction of the lithium contained in such fluids will not change the reinjection procedure for the geothermal fluid.

The Li-extraction results obtained on the Cronenbourg and Cesano fluids, through studying the three parameters Al/Li ratio, temperature and pH, are very encouraging. It is possible to extract the lithium in a few minutes without cooling the fluids and at a pH that is close to that of the original fluid, and by using very moderate amounts of aluminium.

The solid precipitate phase contains Al, Li, Ca, K and Na; the anions were not assayed. This solid phase is amorphous and very rich in water, and the lithium is adsorbed on its surface. Washing tests with distilled water have shown that, except for Al and Li, all chemical elements are concentrated in the aqueous phase that remained in contact with the solid. This means that it is quite easy to obtain a very clean phase containing aluminium and lithium by simple washing.

Two reasons seem to explain the encouraging results that were observed and both concern the solid phase :

1. - The low silica concentrations avoid the formation of an aluminium silicate, which would not have carried along the lithium.

2. - The high chloride concentrations in the two fluids would slow down the transformation of amorphous aluminium hydroxide into a crystallized phase, such as gibbsite or bayerite (Fripiat and Pennequin, 1965), which absorbs lithium much less easily (Yaganase et al., 1983).

A few differences depend on the fluid from which the lithium is extracted, as can be seen on figures 7 to 12. The most important of these concerns the rate of extraction at 20°C (Fig. 13). For experiments carried out at the same pH, and regardless of the Al/Li ratio, the lithium extraction is greater from the Cronenbourg fluid than from the Cesano one. One can explain this phenomenon by looking at the adsorption mechanisms; the surface of the aluminous phase consists of amphoteric sites ≡ Al-OH that can react as follows (Rakonotarivo et al., 1983):

$$\equiv Al\text{-}OH_2^+ \quad <-----> \quad \equiv Al\text{-}OH + H^+ \qquad pKa = 6.37$$
$$\equiv Al\text{-}OH \quad <-----> \quad \equiv Al\text{-}O^- + H^+ \qquad pKa = 10.30$$

where the pKa are given at 25°C.

The experiments were done at a pH between the two pKa values, and ≡Al-OH is the dominant species that can react with a cation (C^+) like lithium, or with an anion (A^-), according to the two reactions :

$$\equiv Al\text{-}OHC^+ \quad <-----> \quad \equiv Al\text{-}OH + C^+$$
$$\equiv Al\text{-}OHA^- \quad <-----> \quad \equiv Al\text{-}OH + A^-$$

The presence of certain anions in the Cesano fluid can thus explain the behaviour of the lithium. Fluorides are known to react with aluminium and, in this case, could well adsorb on aluminium trihydroxide. Later leaching tests of the solid have at any rate shown that hydrofluoric acid can desorb the lithium.

The tests were carried out on reconstituted fluids that are thus devoid of any particles. It is, however, known that certain particles, such as montmorillonite, can adsorb on the aluminium trihydroxide, which would greatly hinder the lithium extraction. For that reason, it appears to be necessary to filter the fluids before beginning the extraction process; we have thus studied how the tangential microfiltration technique (TMF) can be best adapted to the specific conditions of geothermal exploitation. The flowsheet of a TMF pilot installation is presented on Figure 14.

6. CONCLUSIONS

Several geothermal waters that are found within the territory of the European Community, have chemical compositions that render them of interest for the potential extraction of lithium. The most attractive fluids are those from the Alsatian Trias, the geothermal field at Cesano, the South Crofty mine in Cornwall, and several waters from the Massif Central; a little behind these are the waters from the geothermal field at Latera.

Estimates were made of the lithium reserves contained in three of these fluids. The two reservoirs in Italy (Cesano and Latera) would contain, respectively, 7500 and 2000 tons of lithium. In northern Alsace, it is estimated that a 15 x 15 km block of Buntsandstein and Muschelkalk reservoirs contains about 200.000 tons of lithium. However, in view of the available data it is not possible to evaluate the amount of lithium that could in reality be mobilized.

Tests to extract the lithium through the precipitation of aluminium, have given very encouraging results for the Cronenbourg and Cesano fluids. The lithium is adsorbed on amorphous aluminium trihydroxide; this adsorption is quite efficient at high temperatures and at a pH that is close to that of the original solutions. Moreover, quite modest amounts of aluminium are consumed. It is possible to eliminate all other elements that remain in contact with the precipitate by washing with distilled water, which leaves just the lithium and the aluminium in the solid phase. The presence of fluoride ions in the solution can hinder the lithium extraction, but the reverse of this medal is that the same fluorides can be used to desorb the lithium, in order to recover it after its extraction from the geothermal fluid.

7. REFERENCES

1. ABE M. and CHITRAKAR R.
"Synthetic inorganic ion-exchange materials. XIV. recovery of lithium from seawater and hydrothermal water by titanium (IV) antimonate cation exchanger"
Hydrometallurgy, 19, 1987, 117-128.

2. DANG V.D. and STEINBERG M.
"Preliminary design and analysis of recovery of lithium from brine with the use of a selective extractant"
Oklahoma Geological Survey Circular, 79, 1978, 99-107.

3. FRIPIAT J.J. and PENNEQUIN M.
"Evolution de la composition et du poids moléculaire des hydroxydes d'aluminium et de fer purifiés par dyalise"
Mémoires présentés à la société chimique de France, 1965, 1655-1660.

4. KIMURA K., OISHI H., MIURA T. and SHONO T.
"Lithium ion selective electrodes based on crown ether for serum lithium assay"
Analytical Chemistry, 1987, 59, 2331-2334.

5. RAKOTONARIVO E., BOTTERO J.Y., THOMAS F., POIRIER J.E. and CASES J.M.
"Electrochemical modelling of freshly precipitated aluminium hydroxyde. Electrolyte interface"
Colloids and Surfaces, 33, 1988, 191-207.

6. ROTHBAUM H.P. and MIDDENDORF K.
"Lithium extraction from Waraikei geothermal waters"
New Zealand Journal of Technology, 2, 1986, 231-235.

7. SAKAMOTO H., KIMURA K. and SHONO T.
"Lithium separation and enrichment by proton-driven cation transport through liquid membranes of lipophilic crown nitrophenols"
Analytical Chemistry, 59, 1987, 1513-1517.

8. SCHULTZE L.E. and BAUER D.J.
"Recovering lithium chloride from a geothermal brines"
Depart. Int., Report of Investigations, 1984, p. 8883.

9. YAGANASE K., YOSHINAGA Y., KAWANO K. and MATSUOKA T.
"The recovery of lithium from geothermal water in the Hatchobaru area of Kyushu, Japan"
Bulletin of the Chemical Society of Japan, 56, 1983, 2490-2498.

10. YOSHINAGA T., KAWANO K. and IMOTO H.
"Basic study on lithium recovery from lithium containing solution"
Solution of the Chemical Society of Japan, 59, 1986, 1207-1213.

	Cesano	Cronenbourg
Na	63570	32200
K	21370	3978
Ca	43	4600
Mg	12	145
Li	350	220
NH_4	12	-
Fe	0,7	5,2
HCO_3	1900	305
SO_4	91010	508
B	13800	-
Cl	37010	61415
F	100	4,6
SiO_2	130	235

Table 1 : Chemical composition of the Cesano and Cronenbourg fluids; the concentrations are expressed in mg/l.

Echantillon	Al %	Li %	Ca %	K %	Na %
Cesano, 20°C					
16	7,62	0,04	0,056		
112	4,48	0,027	0,011		
124	4,5	0,042	0		
Cesano, 50°C					
512	1,57	0,11	0		
524	2,8	0,17	0		
612	1,43	0,14	0,36		
624	2,82	0,18	0,008		
Cesano, 80°C					
712	2,1	0,25	0		
724	3,3	0,22	0,006		
812	2,6	0,23	0		
824	4,5	0,26	0		
912	1,1	0,16	0,009		
924	2,7	0,2	0		
Cronenbourg, 50°C					
535	2,5	0,18	0,28	1,1	2,02
624	2,18	0,2	0,57	1,67	4,18
Cronenbourg, 80°C					
351	4,2	0,11	0	1,67	
435	3,9	0,16	1	1,43	
815	2,89	0,29	0,66	0,94	2,71

Table 2 : Chemical composition of the precipitates obtained during the various lithium-extraction experiments using aluminium precipitation, from the Cronenbourg and Cesano fluids.

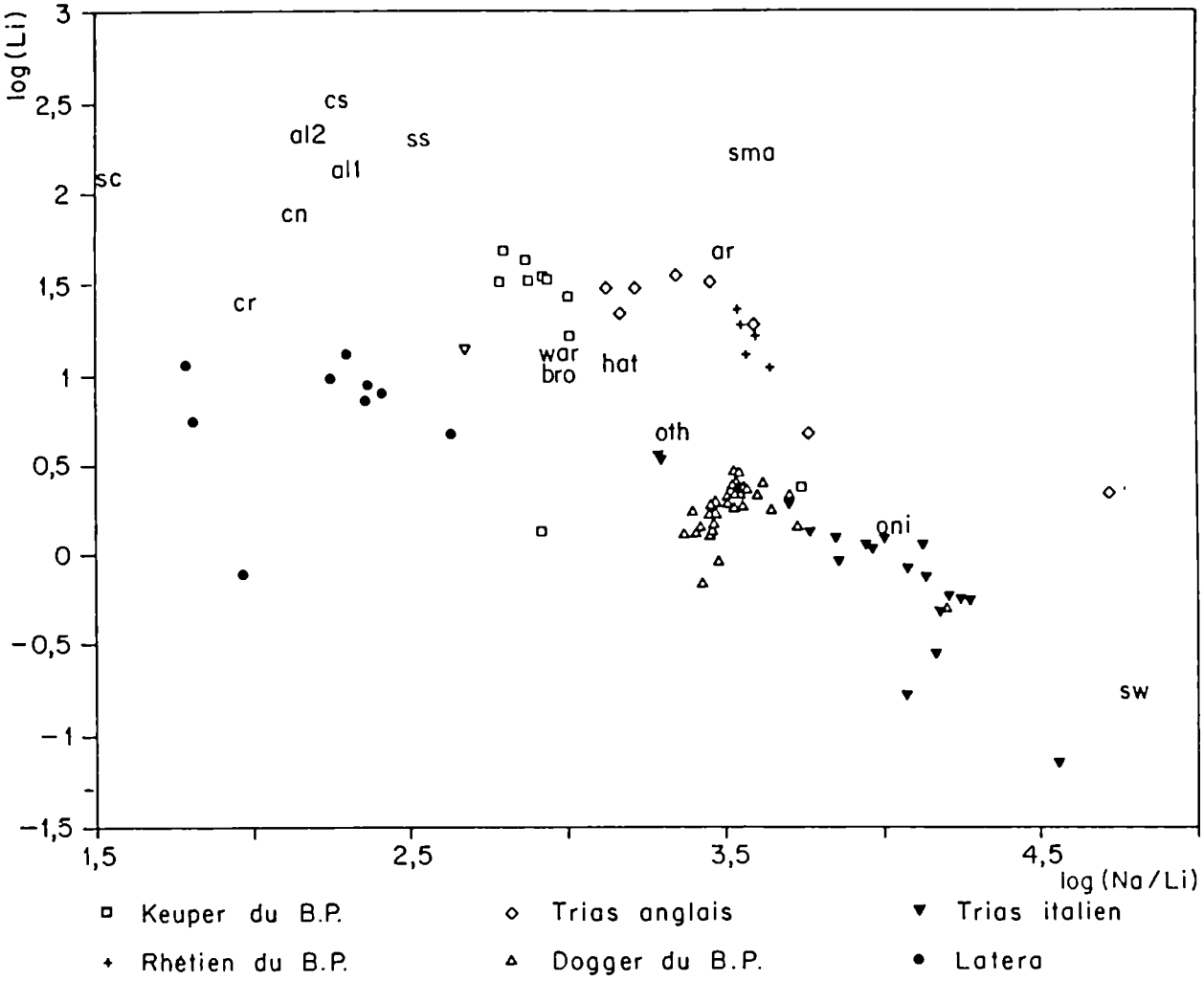

Figure 1 - Lithium concentration versus the Na/Li ratio of geothermal fluids and oil fields;
ar = Arima, oni = Onikoube, hat = Hatchobaru, oth = Othake, ss = Salton Sea, sma = Smackover, bro = Broadlands, war = Waraikei, sw = sea water, al = Alsatian Trias, sc = South Crofty

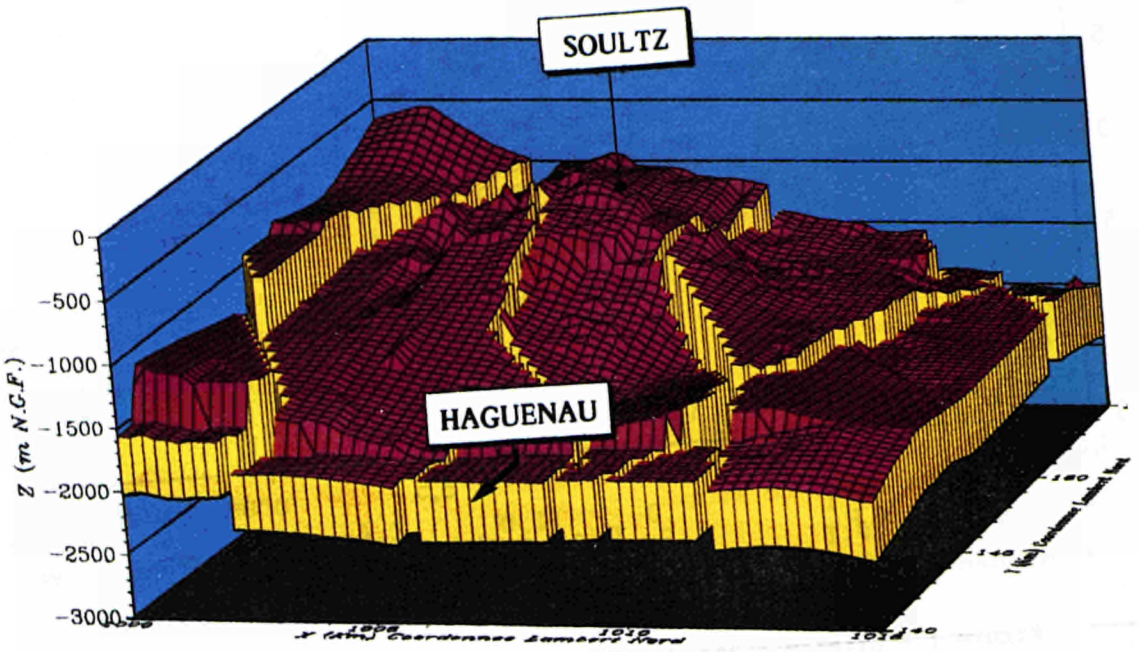

Figure 2: Block diagram of the top of the Buntsandstein in the Soultz-Hagenau area, northern Alsace

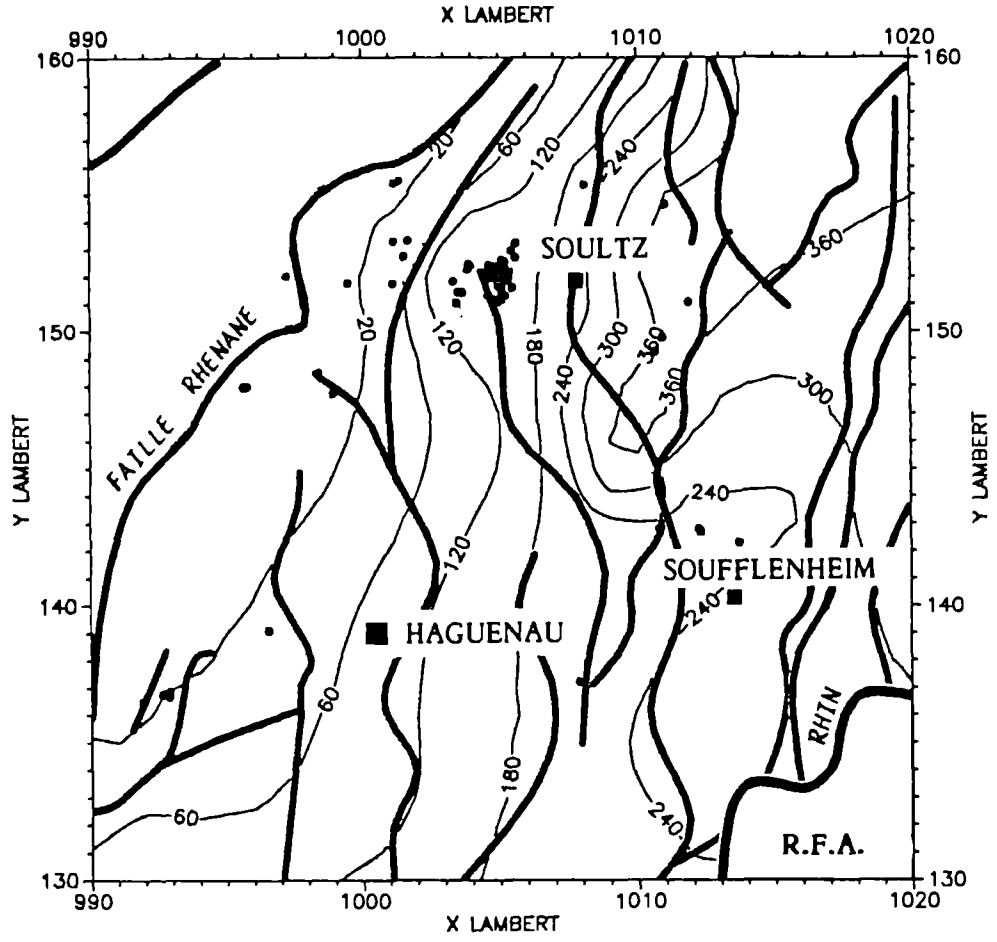

Figure 3: Lithium distribution in northern Alsace

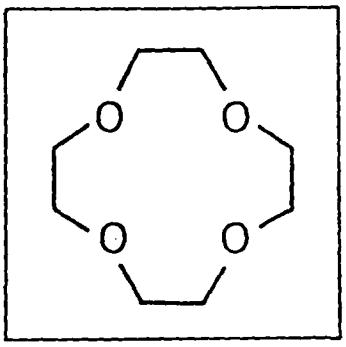

Figure 4 - The crown ether 12C4

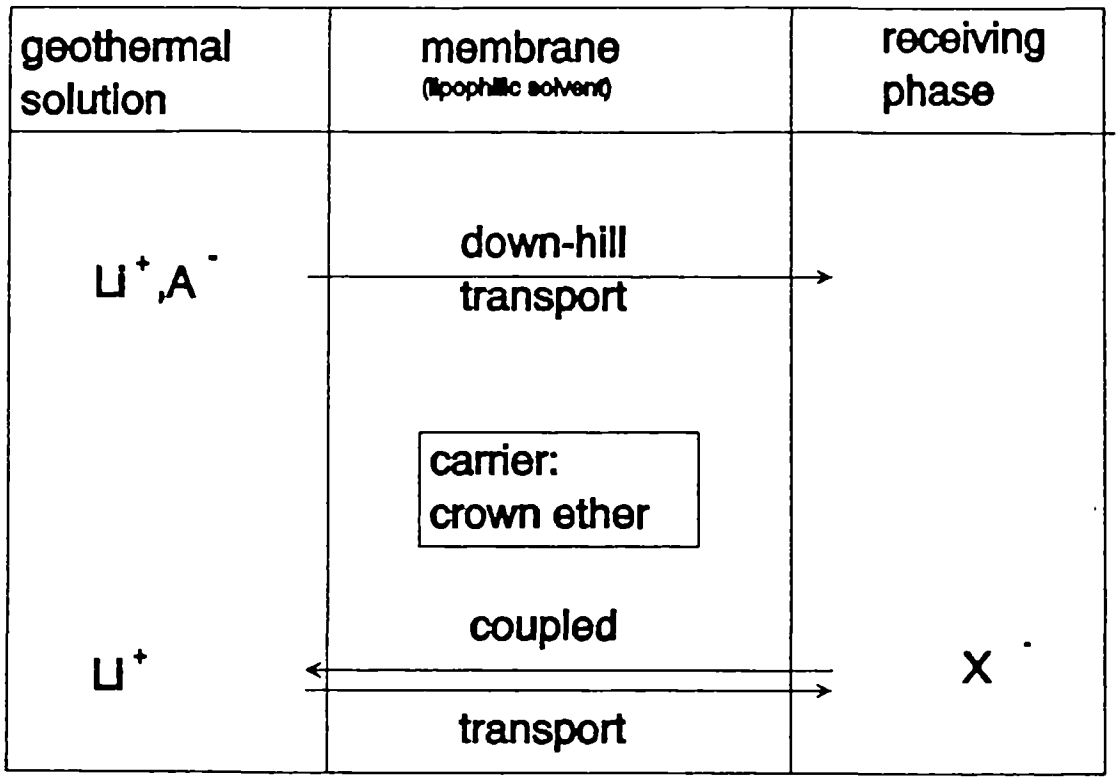

Figure 5 - The various processes of membrane transport

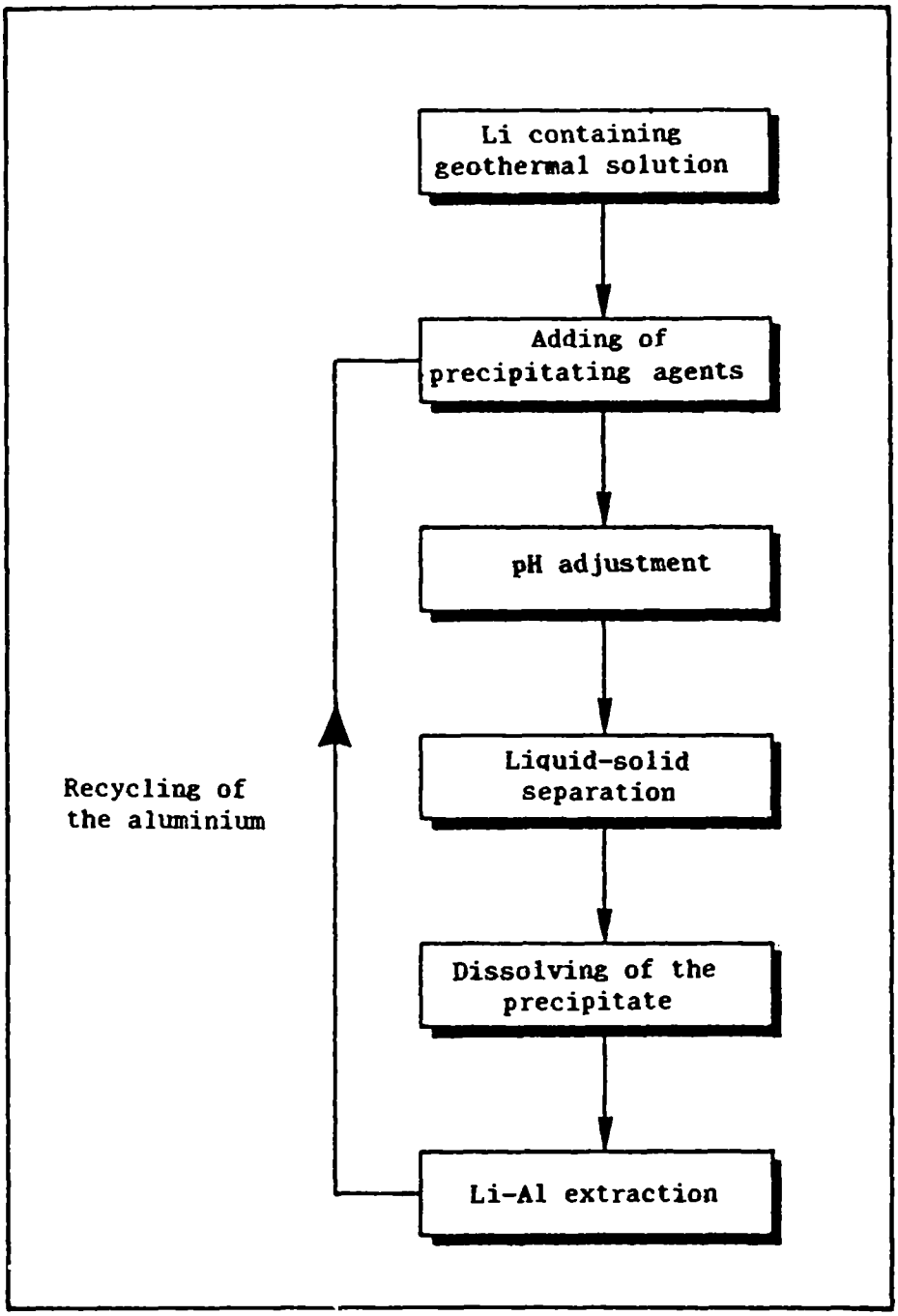

Figure 6 - The principle of lithium extraction through aluminium precipitation

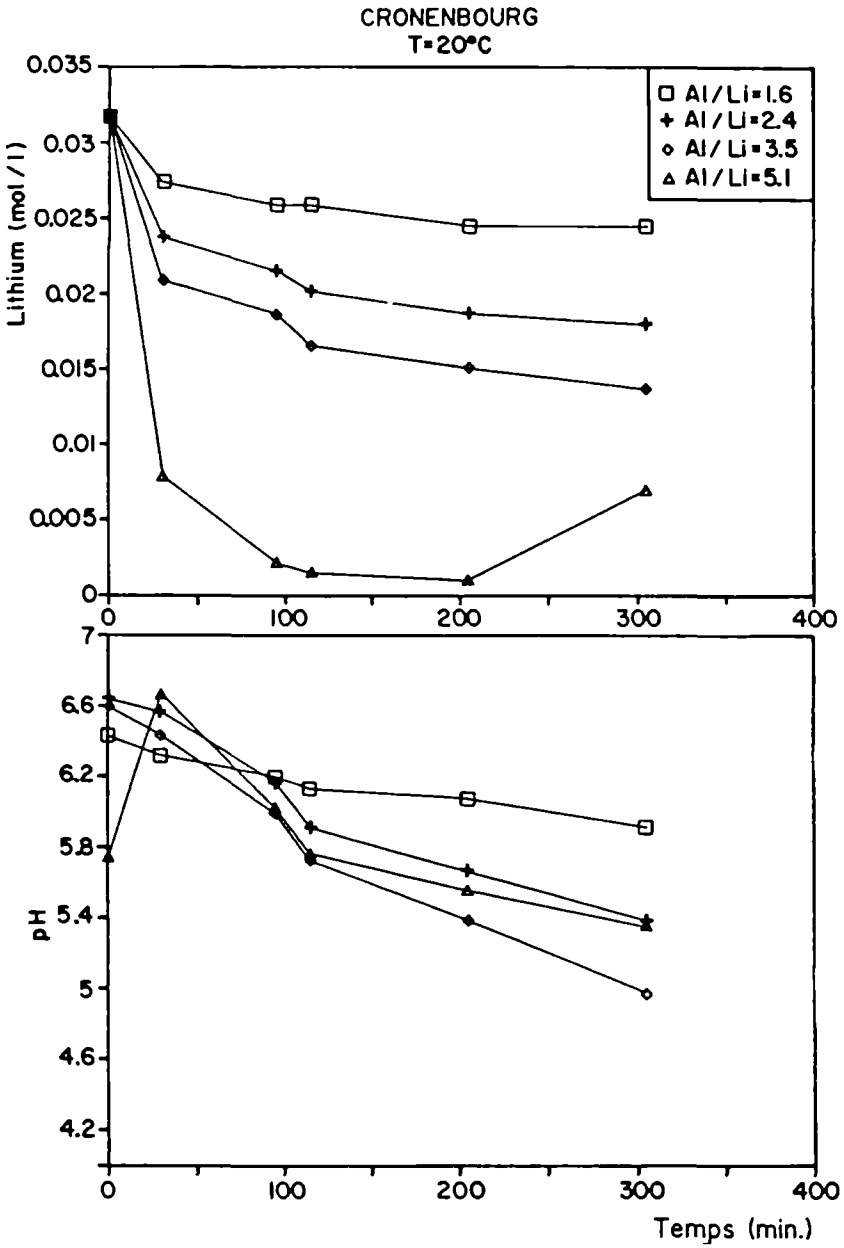

Figure 7 - Residual lithium concentration and pH in the Cronenbourg fluid, as a function of time and at 20° C

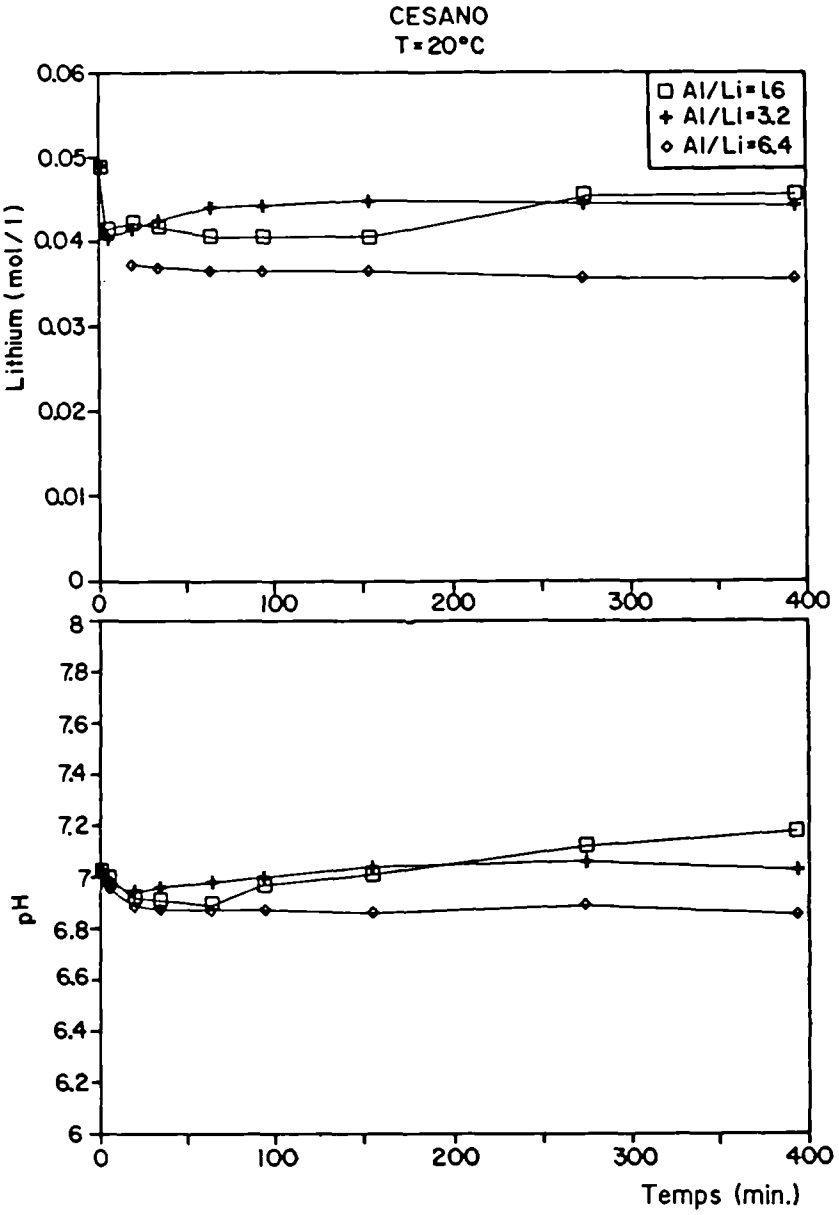

Figure 8 - Residual lithium concentration and pH in the Cesano fluid, as a function of time and at 20° C

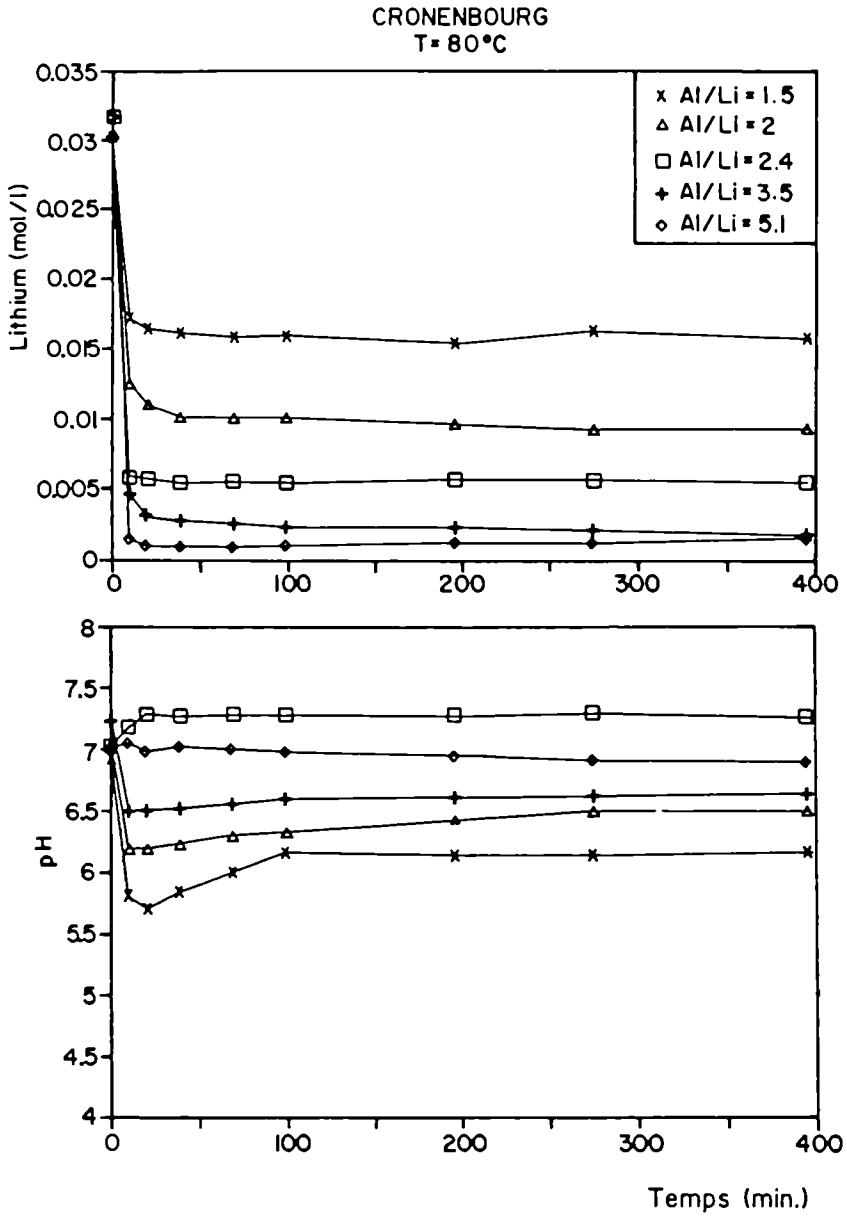

Figure 9 - Residual lithium concentration and pH in the Cronenbourg fluid, as a function of time and at 20° C, showing the influence of the Al/Li ratio

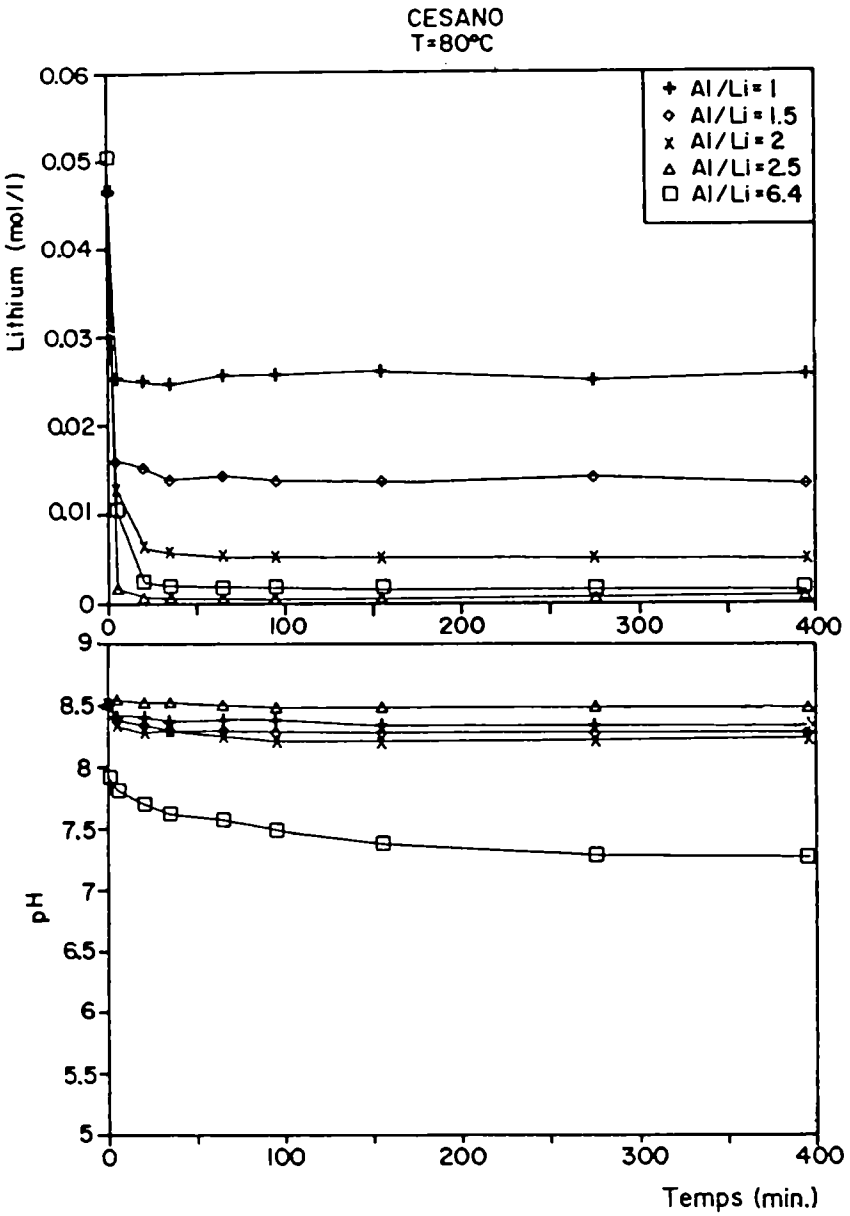

Figure 10 - Residual lithium concentration and pH in the Cesano fluid, as a function of time and at 20° C, showing the influence of the Al/Li ratio

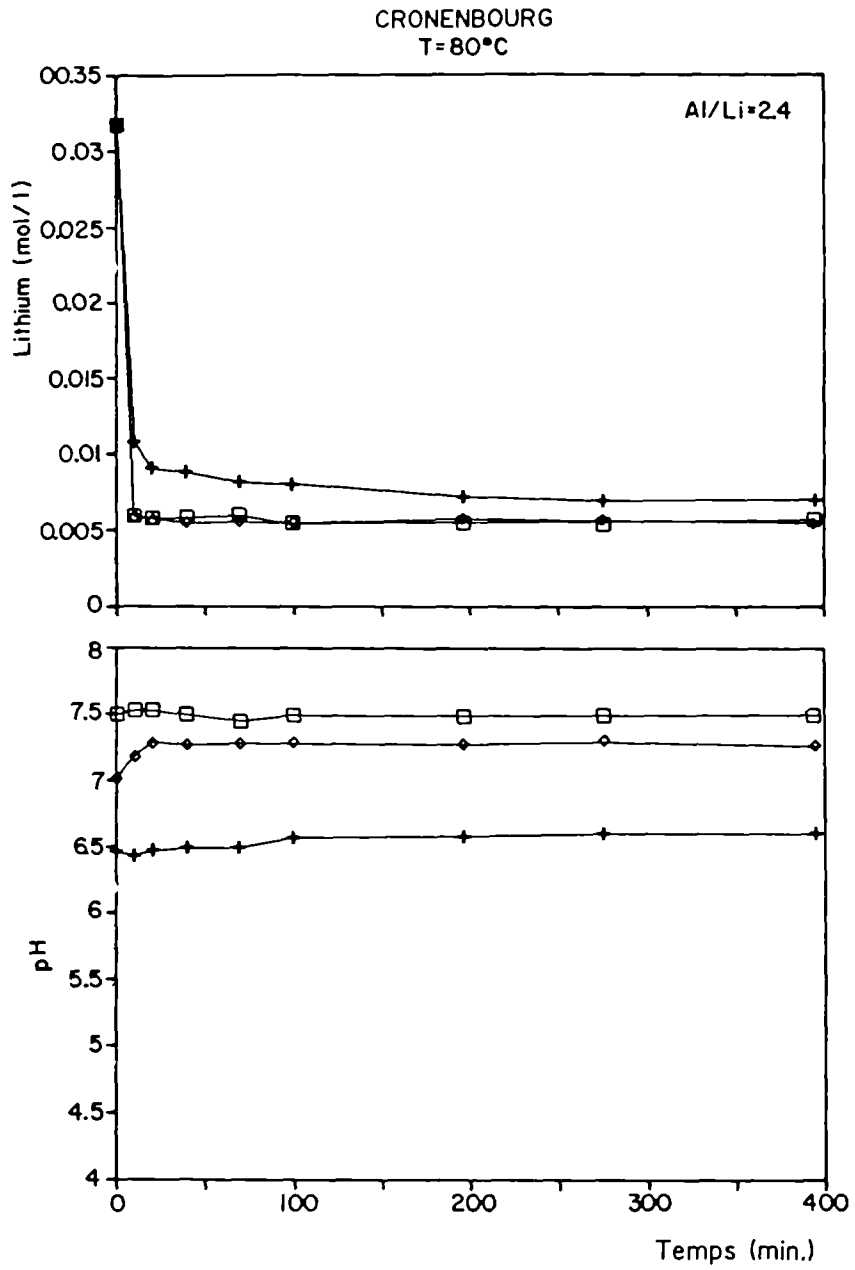

Figure 11 - Residual lithium concentration and pH in the Cronenbourg fluid, as a function of time and at 20° C, showing the influence of pH

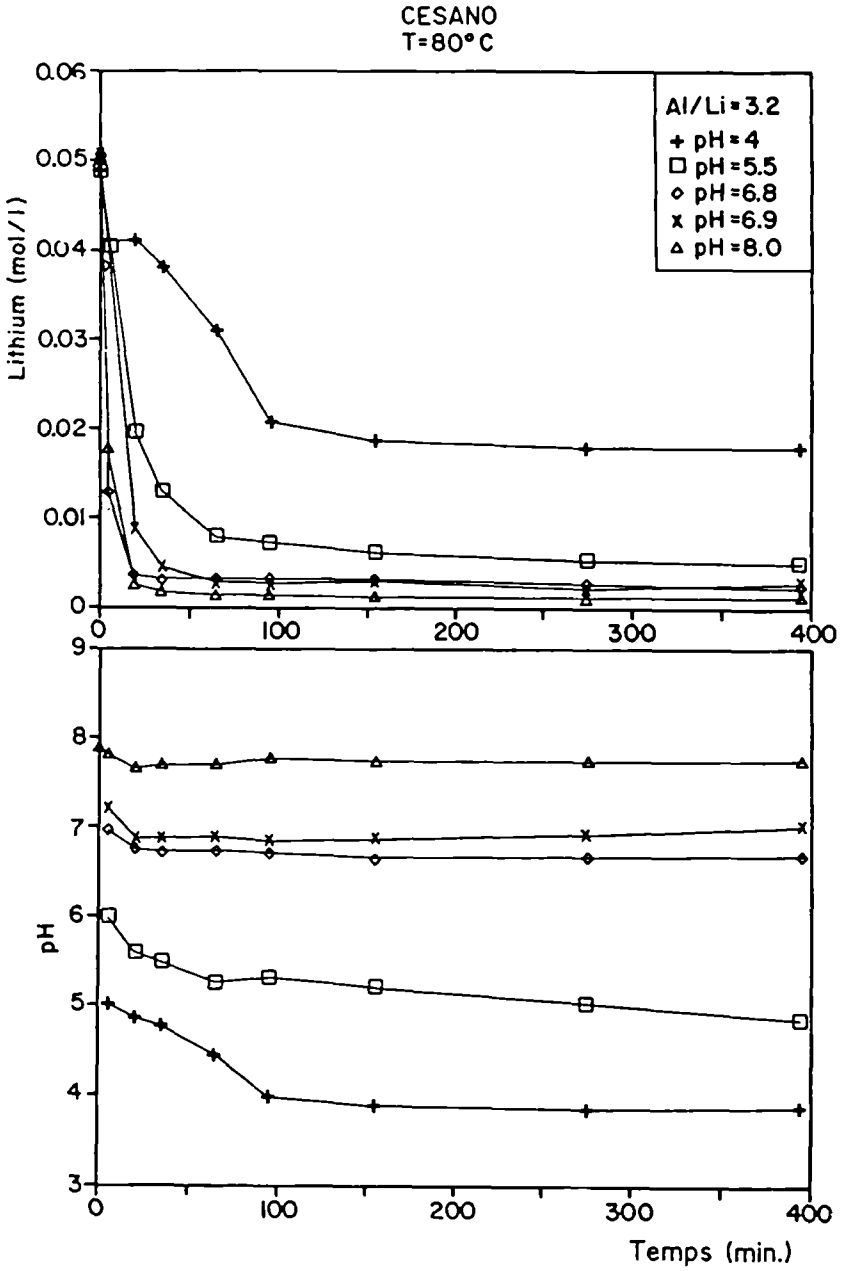

Figure 12 - Residual lithium concentration and pH in the Cesano fluid, as a function of time and at 20° C, showing the influence of pH

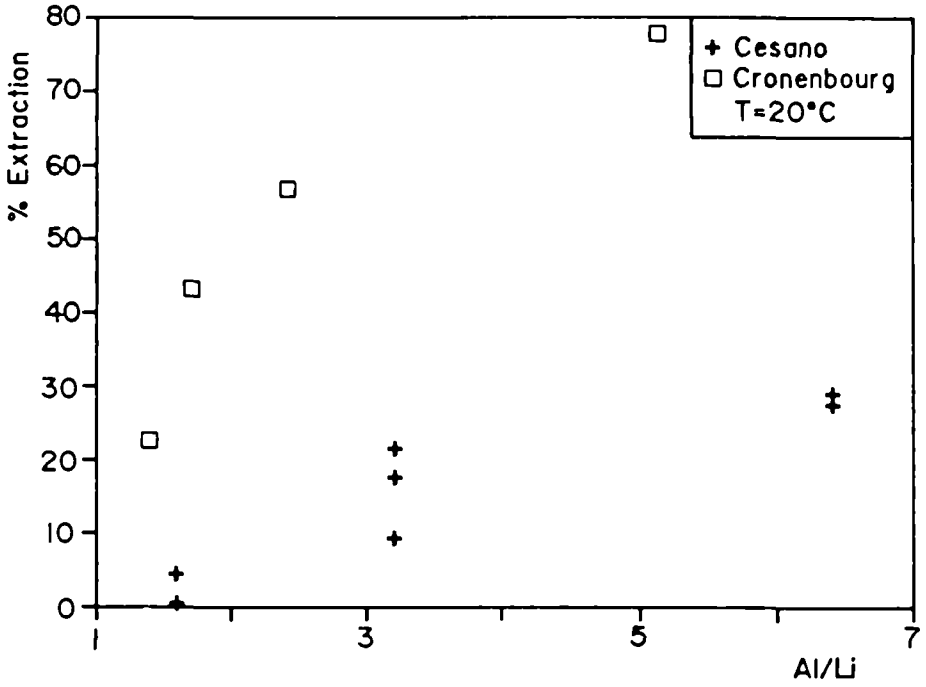

Figure 13 - Extraction percentage at 20° C of the lithium contained in the Cronenbourg and Cesano fluids, as a function of the Al/Li ratio

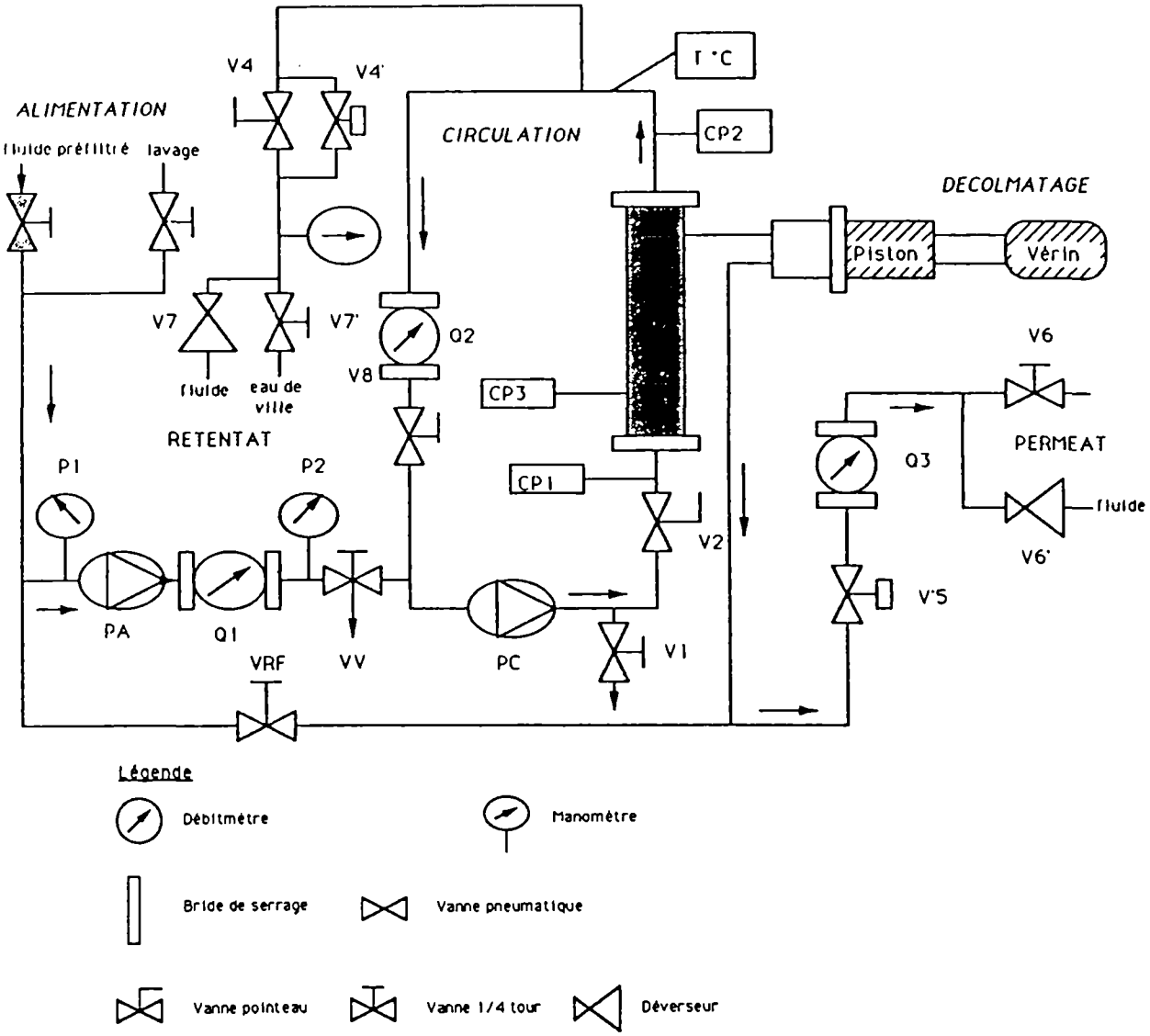

Figure 14 - Flowsheet of the TMF (tangential microfiltration) installation

A STUDY OF HYDROMETALLURGICAL TREATMENT OF COMPLEX SULPHIDE ORES BY LEACHING WITH FERROUS CHLORIDE AND OXYGEN IN A HIGHLY CONCENTRATED AMMONIUM CHLORIDE AQUEOUS SOLUTION

Project Leader: J.L. LIMPO
CENIM, Madrid, Spain

J.M. FIGUEIREDO
LNETI, Lisbon, Portugal

Contract MA1M-0045-C

1. OBJECTIVES

The objective of this research was the study and development of a process for the treatment of bulk concentrates of pyritic complex sulphide ores. The proposed process was based on an oxidizing leaching in a highly concentrated ammonium chloride aqueous solution by using oxygen as oxidizing agent. This study comprises the solubilization of metal values by a double step leaching, as well as the pregnant solution treatment for their recovery. Based on the experimental data, the process simulation and its economical evaluation are also performed.

2. INTRODUCTION

The treatment of complex sulphide bulk concentrates, based on an oxidant leaching in a concentrated ammonium chloride solution by using ferrous chloride and oxygen as oxidant agent, had already been preliminarly studied at CENIM (1,2). In this process, at the same time that the metal values solubilization (Zn, Cu, Pb and Ag) occurs, iron is precipitated mainly as goethite. This is an important feature of the process, because iron-free leaching solutions can be obtained. However, the initial added iron increased the volume of produced residues. This would make the solid-liquid separation more difficult and would lead to higher metal losses in the entrained leaching solution. Besides, losses of lead and silver might be produced by precipitation in the form of their respective jarosites. The use of ferrous chloride has also the disadvantage of necessaryly implying a complex treatment to regenerate leaching solution. The consideration of all these aspects led to the evaluation, in the first place, of the possibility of reducing ferrous chloride concentration to the lowest levels, in order to minimize those disadvantages.

Certain studies made with this aim were carried out at CENIM since this project application date until it started. These studies were completed within the first two months of this contract, which began on April 1988, and led to the conclusion that ferrous chloride can be completely eliminated if a small initial amount of copper is present in leaching solution. Consequently, all the research work has been conducted based on these conclusions.

Three bulk concentrates have been tested, from the Spanish side, Sotiel and Aznalcollar, and from the Portuguese side, Ajustrel.

Table 1 shows their chemical composition for the most significative elements. Mineralogical composition is similar for all three bulk concentrates and major constituents are sphalerite, chalcopyrite, galena and pyrite.
The leaching study has been systematically performed in parallel on the three bulk concentrates. This study comprises the bulk concentrate neutral leaching, the acid leaching on the residues of the neutral leaching, and the study in a double step, neutral and acid, of the bulk concentrates leaching. The next step has been the study of metal values recovery from the pregnant solutions and the simultaneous regeneration of the leaching solutions, specially the recovery of zinc and copper by solvent extraction. The experimental work has been completed with the study of certain solubility diagrams, such as those of copper and zinc diamine chlorides. These solubility studies had to be performed due to the scarcity of solubility data for the ammonium chloride medium at the leaching conditions used. The knowledge gained with the experimental work has been incorporated into the simulation work, on which the process economical evaluation has been based.

This report summarises the work reported in detail in the final report corresponding to the present contract (3). Part of the work has also been reported elsewhere (4,5,6,7,).

3. LEACHING

3.1 NEUTRAL LEACHING

Temperature, partial pressure of oxygen, initial concentration of copper, sulphate concentration, pulp density, stirring and leaching time have been the studied variables in the neutral leaching. The results show a similar behaviour of the three concentrates, however there is a higher leaching rate in the case of Ajustrel concentrate. Complex sulphide leaching with oxygen in concentrated ammonium chloride solutions easily produces metal values solubilization, provided that there will be in solution a certain concentration of copper. In the presence of this metal, the leaching rates are high, even in the case of using mild operation conditions for oxygen pressure and temperature. As an example, the evolution with time of solubilized zinc, copper, lead and silver during a leaching test is shown in figure 1.

Simultaneously with the metal solubilizations, some other transformations occur, which change the composition of the solution and give to this leaching medium their own characteristics. Leaching mechanism takes place through complex reactions, however, it happens as if everything will be only performed through the two following final reactions:

$$MeS + 2NH_4^+ + \tfrac{1}{2}O_2 \longrightarrow \underset{\downarrow}{S} + Me^{2+} + H_2O + 2NH_3$$

$$MeS + 2O_2 \longrightarrow SO_4^{=} + Me^{2+}$$

According to this, besides non ferrous metal solubilization, ammonia and sulphates are produced into the leaching system. Figure 2 shows the evolution with time of ammonia and sulphate concentration for the same test. Their respective proportions depend on the used operative conditions. The temperature is the variable which has a larger influence on leaching. The figures 3 and 4 show the change of solubilized metal percent as a function of time for several leaching temperatures in the range of 85-125 °C. There is no apreciable influence of oxygen partial pressure on leaching rate in the tested pressure range of 1 to 5 bars (figures 5 and 6). There is a slight increase in leaching rate from 1 to 2 bars, but above this pressure, there is no influence. A very efficient stirring is needed to ensure an oxygen transfer rate to the solution, similar to that one of the cuprous ions formed. However, stirring velocities above this value have no influence on leaching kinetics.

During all leaching time, the pH of the solution is practically constant. Its value is naturally kept close to the neutrality, 6 to 7. As a consequence of this high pH value, a high purity outlet solution is produced, which contains only the non ferrous metal values of interest. This is specially valid in the case of iron, and the obtained leaching solutions are iron-free. Other minor elements as As, Sb, Sn and Bi also remain in the leaching residue, and only traces are detected in solution. This is a very important characteristic of this leaching system, being advantageous to the treatment of the pregnant solution.

Attack mechanism and reactions in neutral leaching have been studied. The results obtained show that the chemical attack of the different sulphides is made through Cu^{2+} ions and, the oxygen has only a role in order to regenerate the original system by oxidizing the meanwhile formed Cu^{+} ions. To know deeper the reactions and the mechanisms which take place, a systematic study of leaching of each of the mineralogical species by Cu^{2+} in the absence of oxygen has been carried out. Experimental results show that 75 % of sulphur from sphalerite, chalcopyrite and galena is obtained under the form of elemental sulphur and 25% as sulphate. This agrees with the attack mechanism suggested by Lotens (8) for the oxidant agents, in which one electron is transferred.

3.2 ACID LEACHING AND TWO STEP LEACHING

During the neutral leaching, some insoluble basic salts of copper and lead may be formed. Consequently, important losses of these metals may occur if no additional steps are included in the leaching operation. Therefore, it is necessary to perform the leaching operation according to a treatment scheme with two separate steps. A first neutral leaching step in which most of metal sulphides are solubilized (70-90 %) and, a second one of acid leaching, in which the basic salts of copper and lead are dissolved and where the first step residue is spent.

The study of acid leaching operation has been carried out in parallel on the neutral leaching residues of the three bulk concentrates. The studied variables have been: temperature, oxygen partial pressure, initial copper concentration, initial sulphate concentration and ratio of initial acid concentration to metals non extracted in neutral leaching. The obtained results for each of the three bulk concentrates are similar and show that, the existence of a minimum initial acidity is necessary to ensure the solubilization of all basic compounds from neutral leaching. An excess above this value has practically no influence on the recovery yields, but it has considerable effect on the composition of obtained residues.

Two step leaching on the three bulk concentrates has been also studied. Neutral leaching has been carried out by contacting the bulk concentrate with the solution, which has been produced in the acid leaching of previous runs, whereas the residue from first neutral leaching step was spent in the second step of acid leaching. The pregnant solution from neutral leaching was used for the recovery of metal values. The experimental results show that recovery yields for Zn, Cu, Pb and Ag are constantly higher than 95 %.

3.3 LEACHING RESIDUES

The leaching residues has been studied also in order to determine the correlation between composition and the experimental test conditions. In this study, special emphasis has been put on the jarosite formation, in each of the two leaching steps, for different conditions of temperature, oxygen partial pressure, leaching solution composition and leaching time. To identify the composition of residues different techniques have been used, such as X ray diffraction, thermogravimetric and thermodifferential analysis, and quantitative determination of sulphate, ammonium, lead and silver. The obtained results show that there is no jarosite formation in the neutral leaching. Jarosite is only produced during the acid leaching. In this step, ammonium jarosite is precipitated, but losses of lead and silver due to the respective jarosite formation were not detected. Ammonium jarosite formation is only determinated by the initial acid concentration in the acid leaching step.

In practice, at equal initial acidity values, the other variables have no influence on jarosite formation. However, adjusting the initial amount of acid, the ammonium jarosite formation can also be avoided.

4. SOLUBILITY DIAGRAMS

Solubility data for the leaching medium and the conditions used were very scarce. Therefore, it has been necessary to perform a systematic and detailed work on the changes of every reaction product solubility as function of temperature and of medium composition. The lead chloride solubility as a function of temperature for the systems $PbCl_2$-NH_4Cl-H_2O and $PbCl_2$-NH_4Cl-$ZnCl_2$-H_2O has been studied. The results show that temperature and ammonium chloride concentration have a strong positive influence on the solubility of lead chloride. On the contrary, the presence of zinc has a strong negative effect. The influence of temperature, as well as of the zinc and ammonium chloride concentration on silver chloride solubility for the systems AgCl-NH_4Cl-H_2O and AgCl-NH_4Cl-$ZnCl_2$-H_2O is similar to that one of lead chloride.

In this process, the initial pulp density has to be limited to safety levels. The main cause for that limitation is not the lead and silver chloride solubility, but the solubility of zinc and copper amines, specially the latter one. For both metals the less soluble amine is the diamine, which crystallizes under the chloride form. The solubility diagram of the system $ZnCl_2$-NH_4Cl-NH_3-H_2O has been studied at six different temperatures between 30 and 60 °C. In all tested compositions the solid phase in equilibrium with the solution was $Zn(NH_3)_2Cl_2$. The obtained results show that solubility values are independent of ammonium chloride concentration, while there is a great solubility increasing when temperature increases. For copper, two system $CuCl_2$-NH_4Cl-NH_3-H_2O and $CuCl_2$-NH_4Cl-$ZnCl_2$-NH_3-H_2O have been studied. The isotherms of cupric chloride diamine have a similar shape to those ones of zinc, but solubility values are much lower. In this case, solubility diagram is more complex, due to the presence at low $(NH_3)/(Cu^{2+})$ ratios values of another phase solid, copper oxychloride $Cu(OH)_{1.5}Cl_{0.5}$, which still has a lower solubility than that of the diamine. Finally, a mathematical model have been developed in order to describe the ionic equilibria for this type of complex solutions, which will enable the correct interpretation of the experimental data.

5. SOLUTION TREATMENT

One of the main features of this process is the presence in the pregnant solution of ammonia in the form of metal amines. This ammonia allows the recovery of solubilized metals by solvent extraction, by acting as neutralizing agent for the acid released during this operation. Before

solvent extraction steps, the sulphate produced during leaching may be eliminated using lime. This reagent, besides precipitation of sulphates, generates ammonia, compensating the ammonia deficit in the process. The studied variables have been temperature (between 50 and 100 °C) and different levels of calcium and sulphate solution concentration. The results show that in a concentrated ammonium chloride medium, the solubility of gypsum is only slightly affected by temperature. However, a minor increase in solubility with temperature was observed. This is clearly in opposition to the behaviour of gypsum in sulphate medium.

5.1 ZINC RECOVERY BY SOLVENT EXTRACTION

Acidic extractants can extract zinc from aqueous media and among them the most suitable is the di(-2-ethylhexyl) phosphoric acid (DEHPA). A concentration of about 0.6 M (20% v/v) was used, diluted in a kerosene type diluent with a flash point above the working temperature. As modifier a decyl alcohol was used. Equilibrium distribution data at 50°C for zinc, between zinc chloride solutions 6 M in chloride and a 0.6 M DEHPA organic solvent, were obtained at different pH levels, ranging from pH 2 to 6 every 0.5 pH unit.

Other cathionic species, which are also present in leaching pregnant solutions, like copper, calcium and lead may also be extracted. Copper coextraction is pH dependent, reaching a maximum at pH range 3.5 - 4 and a minimum at pH range 5.5 - 6. Lead coextraction is the lowest one of the three metals. Calcium is highly coextracted, but its residual concentration in aqueous phase is reduced by the presence of sulphate to less than 1g/1. Coextracted impurities can be removed out of the organic phase by scrubbing with zinc solutions, usually zinc chloride. The method is very effective for copper and calcium, which can be reduced up to a few ppm in organic phase. Lead is more difficult to be eliminated, but its content is usually low. Chloride ions are also impurifying the organic phase. Chloride uptake is probably of mechanical origin and will be dragged by the organic stream. Chloride ions are also impurifying the organic phase. Chloride uptake is probably of mechanical origin and will be dragged by the organic stream. Chlorides can be considerably reduced by washing with water, and after three successive contacts, its contents is very low, less than 0.05 g/l.

Continuous solvent extraction runs in a mixer-settler battery were performed very satisfactorily. This operation shows the feasibility of the process under a continuous basis. Some final impurification at trace level remains in the organic phase, and the loaded electrolyte will be always contaminated. Therefore, additional purification operations to remove the last traces of metallic elements and chloride ions shall be incorporated in order to reach the specifications for zinc electroysis.

5.2 COPPER RECOVERY BY SOLVENT EXTRACTION

Cupric ions are extracted by oxime or oxine based extractants. LIX 65N and LIX 622 diluted in kerosene 200/260 at 10 to 20% concentration have been studied with this purpose. As above, tests were performed at 50°C and at 6 M chloride concentration. Because of the highly concentrated chloride solutions and of the presence of self released HCl, copper extraction can be limited in a high extent, which is specially evident for LIX65N in acid solutions. The aqueous solution for copper recovery is the zinc SX raffinate and a concentration of about 4-5 g/l zinc is contained in this solution. Zinc has a positive influence on copper extraction. This is due to the decrease in chloride availability for copper complexing with increasing zinc concentrations.

When cuprous to cupric oxidation by oxygen or air takes place in a ammonium chloride medium, an equimolecular amount of ammonia is produced, which is used to neutralize part of the released HCl during copper extraction. In these conditions, a 10% LIX 65N in kerosene can extract copper with good recoveries. In a simulated countercurrent batch test with 2 extraction stages and a phase ratio of O/A = 1/2, the performance was excellent. Copper recovery is easier than that one of zinc and there is no interference from other metallic species. Chloride organic impurification is about ten times lower than in the case of zinc-DEHPA.

6. SIMULATION AND ECONOMICAL EVALUATION OF THE PROCESS

The modelling and simulation work was undertaken aiming at the development of computational system(s) which would meet two major project requirements, namely :

i) Act as test-bed for the testing and screening of concepts and assumptions which emerged in the course of the experimental work, while also ensuring the required validation and integration of the experimental data gathered for the various operations and concentrates.

ii) Provide a framework for process analysis (including economic evaluation) and sensitivity tests on selected parameters and indices.

As a result of the work carried out on the SPEEDUP package (Prosys Technology Ltd, Cambridge, U.K.) in a VAX/VMS computing environment (Dec-Digital Equipments, Ltd) the following systems were developed :

A. Simulation model for the global process with simplified extraction operations models.

B. Simulation model for the Zinc/DEHPA full extraction operation, including stripping, scrubbing, other ancillary operations, as well as electrowinning.

C. Ibidem for the Copper/LIX full extraction operation.

D. Process analysis calculation model, which is an extension of A, with added sizing, costing and economic evaluation units.

The decision to develop systems B and C separately from A was dictated by the complexity and specific characteristics of the extraction operations, namely the predominance of equilibrium counter-current stages and closed-loop streams. The most complex example is to be found at the zinc extraction equilibrium stage, due to the upstream position of this operation with regards to the copper extraction. A total of thirty equilibria are contemplated, which range from the zinc and copper amines and chloride complexes, zinc, copper and calcium extraction reactions, metal sulphates dissociation, DEHPA dimerization, etc.

The global steady state conditions obtained for the Portuguese and Spanish concentrates, under the assumed reference conditions and for 20000 Kg/h are depicted in Tables 2-7.

Figure 8 shows under schematic form the computational system for the full process economical analysis. The process simulation model conveys the information on stream flows, feeds, consumables and products to the other units shown in this figure, by means of specially designed computer files which provide the required interfacing. Several other required inputs include corrective and upgrading factors and indices, which are common to conventional project engineering practises, as well as parameters which define the financial setup for economic evaluation.

In Tables 8 and 9 are summarized the main cost and profitability indices. Figure 9 presents the cumulative cash flow for Portuguese and Spanish concentrates for the reference concentrate unit costs of 26889 pta/ton and 37406 pta/ton estimated for a Discounted Cash Flow Rate of Return (DCFRR) adjusted to 20 percent. In both cases a pay-back time of 6 years is obtained. It can be concluded by the observation of these tables that while the capital investment is similar for the Portuguese and Spanish concentrate based plants, the revenue is more favourable in the case of the latter. The comparison of the total productions costs, while suggesting higher costs for Spanish concentrate, is partly hindered by the method applied for the estimation of the concentrate reference cost. Since this is a major factor in the production cost, it is more conclusive to draw a comparison from the concentrate break-even prices, which are also found to favour the Spanish concentrate, 51046 instead of 38317 pta/ton for the

Portuguese one, both in absolute terms and in relation to the respective reference unit costs which suggest, in addition, a greater investment safety margin. The break-even price is estimated by dividing the difference between the annuity of invested capital (based on a depreciation time of 15 years and on an interest rate of 20% p.a.) and the total manufacturing costs per the annual feeding rate of bulk concentrate (160000 t/y). Because of the uncertainty associated to many of the underlying cost factors and assumed reference values these conclusions were qualified by systematic sensitivity testing to plant capacity (±50%), price of bulk concentrate and electricity unit charges.

7. CONCLUSIONS

The experimental work undertaken during these two years of research has clarified most of the open questions and problems that initially have been assumed. In fact, the knowledge about the reaction mechanisms, solubility diagrams and equilibrium conditions of the different steps of the process is now much deeper and complete. Besides, the behaviour of the three different bulk concentrates as a function of the experimental conditions is known and may be extrapolated for other similar materials.

All this information as a whole, allowed to precise the different steps of the process, and to choose the most convenient operating conditions. The ensemble of these steps has led to the establishment of a hydrometallurgical process diagram for the treatment of complex sulphides (figure 7).

Under a technical point of view, the developed process is specially appropriate for the treatment of polymetallic complex sulphides. The most important characteristics are indicated as follows :

- High recovery yields for Zn, Cu, Pb and Ag, always over 95%;
- Mild operating conditions applied for leaching steps, avoiding the need of specially expensive equipment;
- Very pure solutions are obtained during the leaching. They are iron free and other common contaminant elements as As, Sb, Sn and Bi, are present only at trace level;
- Natural regeneration of leaching solution for metal value recoveries. Reagent consumptions in the process are low, being oxygen, lime and process water, the only significant ones;
- No losses of lead and silver will occur as jarosites. Additionally, and adequate acidity control during the acid leaching step, completely avoids ammonium losses due to ammonium jarosite formation.

As a complement to the development of a new process for the recovery of non-ferrous metals, a profitability study was conducted in an attempt to reveal, in economic terms, the relative merits of the proposed technological solution addressing two different types of concentrates, the Aljustrel Portuguese concentrate and the Aznalcollar Spanish concentrate. The conclusions drawn from the estimated profitability indices while pointing out to a better performance of the Spanish concentrate, also suggest a marginal advantage of the Portuguese concentrate both for an incremental plant capacity and aggravated electricity charges. However, the decisive importance and uncertainty associated to most costs and prices, particularly those related to the metal quotations, inevitably associated with market fluctuations, would justify more numerous and extensive sensitivity tests, which would be instrumental in identifying the most dominant factors and quantifying the associated uncertainty. Some of these factors might either be of a technological nature (e.g. reaction extents) and require further research, or be economic and justify some effort in producing more accurate estimates.

As a final conclusion it is believed that the global project objectives have been fully achieved. A new process has been developed experimentally together with highly integrated and responsive computational systems, which not only effectively capture and reveal the complexities of the proposed technological solution, but can also offer a considerable potential for the investigation of alternative production strategies and be a powerful aid for process scaling up.

8. REFERENCES

1. J.L. LIMPO and L. LUIS
"Lixiviacion de minerales sulfurados polimetalicos en soluciones de cloruro ferroso con oxigeno"
6 Asamblea General del CENIM. Madrid. Octubre, 1985.

2. J.L. LIMPO, A. LUIS, A. HERNANDEZ Y F.Y. ALGUACIL
Patente Española N° 545698 (1985).

3. "A Study of hydrometallurgical treatment of complex sulphide ores by leaching with ferrous chloride and oxygen in highly concentrated ammonium chloride solution"
Final report. Madrid : CENIM (1990).

4. J.L. LIMPO, J.M. FIGUEIREDO, S. AMER and A. LUIS
"Tratamiento hidrometalurgico de sulfuros complejos en soluciones de cloruro amonico : proceso cenim-ineti"
7° Congreso Nacional de Ciencia y Tecnologia Metalúrgicas. CENIM. Madrid (1990).

5. J.L. LIMPO, A. LUIS and C. GOMEZ
"Reacciones y mecanismos de ataque de los sulfuros metalicos en soluciones de cloruro amonico"
7° Congreso Nacional de Ciencia y Tecnologia Metalúrgicas. CENIM. Madrid (1990).

6. J.L. LIMPO, J.M. FIGUEIREDO, S. AMER, A. LUIS Y A. DE LA CUADRA
"Perspectivas tecnico-economicas del proceso cenim-inetI"
7° Congreso Nacional de Ciencia y Tecnologia Metalúrgicas. CENIM. Madrid (1990).

7. S. AMER, A. LUIS and C. CARAVACA
"La extraccion del cinc por el acido di(-2-etilhexil) fosforico de medios fuertemente clorurados"
7° Congreso Nacional de Ciencia y Tecnologia Metalúrgicas. CENIM. Madrid (1990).

8. J.P. LOTENS and E. WESKER
"The behaviour of sulphur in the oxidative leaching of sulphidic minerals"
Hydrometallurgy, 18 (1987) 39-54.

9. J.L. LIMPO, J.M. FIGUEIREDO, S. AMER Y A. LUIS
Patente Española N° 8902487, (1989).

TABLE 1

Constituent	Analysis (wt %)		
	Sotiel	Aznalcollar	Aljustrel
Zn	33.5	29.6	19.5
Cu	3.4	3.8	8.3
Pb	7.8	9.9	6.1
Fe	17.1	16.5	21.3
S	34.6	33.8	36.3
As	0.28	0.28	0.30
Sb	0.32	0.40	0.13
Bi	0.01	0.12	0.02
Ag	0.018	0.023	0.012

Table 2 - Process mass balance for the Portuguese concentrate (20000Kg/h)

Reference :	20000 Kg/h			
Concentrate :	PORTUGUESE			
Main Feed :				
Zn	60.246	Kmol/h	3938.860	Kg/h
Cu	26.046		1655.236	
Pb	5.941		1231.077	
Ag	19.370 E-3		2.089	
Other Feeds :				
O_2 *	156.894	Kmol/h	5020.608	Kg/h
Air **				
O_2	55.039		1761.262	
N_2	207.053		5801.630	
CaO ***	69.458		3895.217	
NH_4Cl	25.023		1338.746	
H_2SO_4	0		0	
NH_3	2.975		50.573	
Cu	0.475		30.184	
Zn	6.401		418.526	
Water :				
Process	1467.528		26415.511	
Evaporated	987.901		17782.212	
Cooling	34779.549		626031.888	
Products :				
Zn	63.248	Kmol/h	4135.156	Kg/h
Cu	26.108		1659.170	
Pb	5.819		1205.799	
Ag	15.819 E-3		1.706	
Losses :				
Zn	3.399	Kmol/h	222.230	Kg/h
Cu	0.413		26.250	
Pb	0.122		25.278	
Ag	3.551 E-3		0.383	
Residue :				
Final Residue			12594.762	Kg/h
Gypsum	58.965	Kmol/h	10150.295	

* 80 percent reactive
** Dry air
*** 85 percent reactive

Table 3 - Process mass balance for the Spanish concentrate (20000Kg/h)

Reference :	20000 Kg/h			
Concentrate :	SPANISH			
Main Feed :				
Zn	90.784	Kmol/h	5935.488	Kg/h
Cu	11.931		758.223	
Pb	9.580		1984.929	
Ag	41.969 E-3		4.527	
Other Feeds :				
O_2 *	155.587	Kmol/h	4978.774	Kg/h
Air **				
O_2	24.959		798.678	
N_2	93.892		2630.860	
CaO ***	66.541		3731.610	
NH_4Cl	21.931		1173.301	
H_2SO_4	0		0	
NH_3	2.425		41.221	
Cu	0.260		16.519	
Zn	10.431		681.986	
Water :				
Process	1692.364		30462.561	
Evaporated	1297.178		23349.202	
Cooling	47436.761		853861.697	
Products :				
Zn	95.678	Kmol/h	6255.425	Kg/h
Cu	11.993		762.1420	
Pb	9.483		1964.841	
Ag	34.598 E-3		3.732	
Losses :				
Zn	5.537	Kmol/h	362.049	Kg/h
Cu	0.198		12.600	
Pb	96.948 E-3		20.088	
Ag	7.371 E-3		0.795	
Residue :				
Final Residue			10285.171	Kg/h
Gypsum	56.495	Kmol/h	9725.044	

* 80 percent reactive
** Dry air
*** 85 percent reactive

Table 4- Process heat balance for the Portuguese concentrate

System Heat Load :
Added (+) / Removed (-)

Hot Acid Leaching :	Heat =	-601216.214	Kcal/h
Copper Reduction :	Heat =	55962.308	Kcal/h
Lead Cristalization :	Heat =	-6.056 E6	Kcal/h
Losses in the Circuit : (Delta T = 5.0 °C)	Heat =	1.170 E6	Kcal/h
TOTAL :	Heat =	-5.431 E6	Kcal/h

Table 5- Process heat balance for the Spanish concentrate

System Heat Load :
Added (+) / Removed (-)

Hot Acid Leaching :	Heat =	663767.893	Kcal/h
Copper Reduction :	Heat =	26568.649	Kcal/h
Lead Cristalization :	Heat =	-2.938 E6	Kcal/h
Losses in the Circuit : (Delta T = 5.0 °C)	Heat =	1.195 E6	Kcal/h
TOTAL :	Heat =	-1.053 E6	Kcal/h

Table 6 - Portuguese concentrate: non-ferrous metals solubilization and recovery yields

	Global Percentages	
	Solubilization	Recovery
Zn	97.139	94.900
Cu	99.723	98.443
Pb	99.932	97.947
Ag	97.000	81.666

Table 7 - Spanish concentrate: non-ferrous metals solubilization and recovery yields

	Global Percentages	
	Solubilization	Recovery
Zn	96.508	94.529
Cu	99.982	98.374
Pb	99.994	98.988
Ag	96.000	82.436

Table 8 - Cost Estimation (Portuguese Concentrate)
Plant Capacity : 160000 ton/year
Concentrate cost : 26888.7 pta/ton

Fixed Capital Investment (1)	13.35 E9	pta/yr
Working Capital (2)	2.92 E9	pta/yr
Total Capital Investment (1+2)	16.27 E9	pta/yr
Total Production Cost	10.30 E9	pta/yr
Total Revenue	14.26 E9	pta/yr
Concentrate Break Even Price	38316.67	pta/ton
Service Life	15.00	yr
Startup Year	3.00	yr
Project Yime	18.00	yr
DCFRR	20.00	Perc.

Table 9 - Cost Estimation (Spanish Concentrate)
Plant Capacity : 160000 ton/year
Concentrate cost : 37405.8 pta/ton

Fixed Capital Investment (1)	13.46 E9	pta/yr
Working Capital (2)	3.48 E9	pta/yr
Total Capital Investment (1+2)	16.94 E9	pta/yr
Total Production Cost	12.16 E9	pta/yr
Total Revenue	16.24 E9	pta/yr
Concentrate Break Even Price	51046.71	pta/ton
Service Life	15.00	yr
Startup Year	3.00	yr
Project Yime	18.00	yr
DCFRR	20.00	Perc.

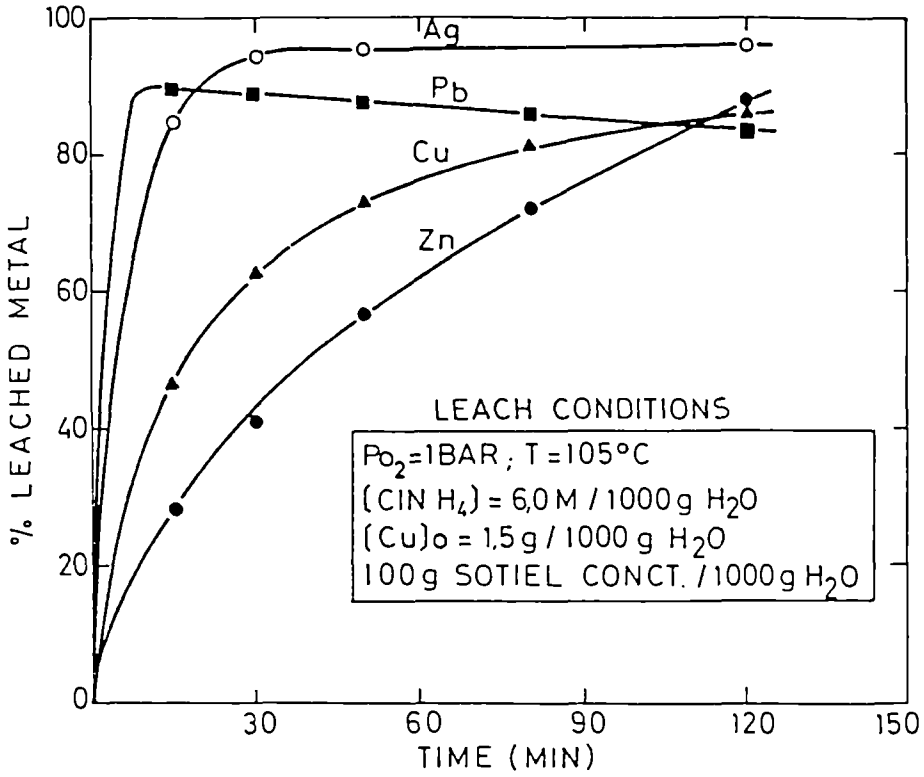

FIG. 1.- METAL EXTRACTION AS A FUNCTION OF TIME

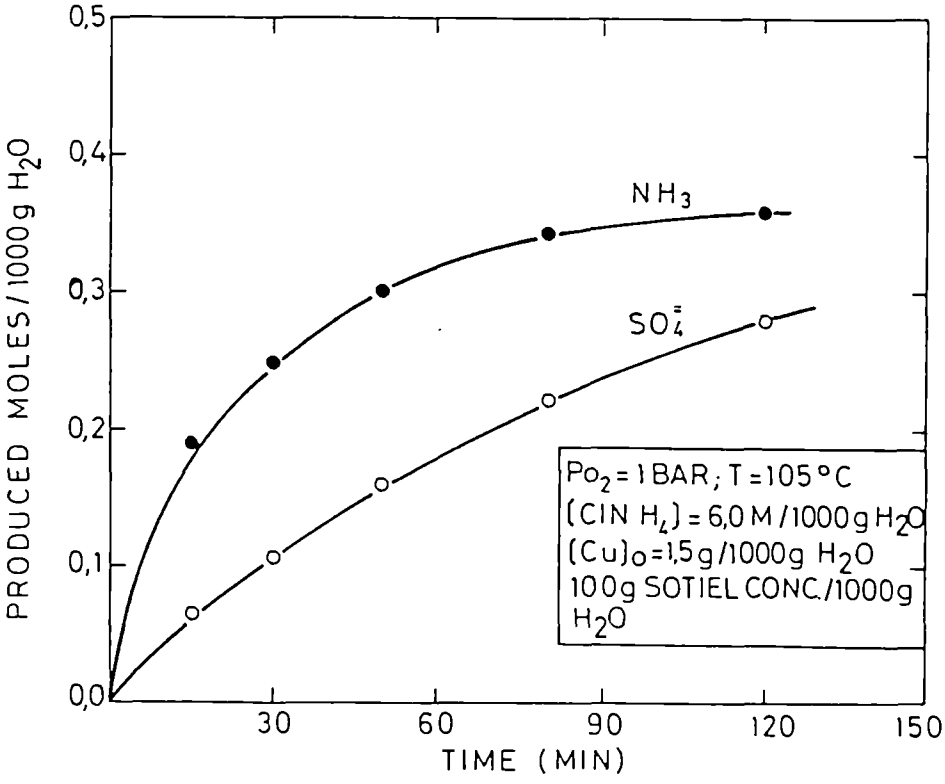

FIG. 2.- AMMONIA AND SULPHATE PRODUCED VERSUS TIME.

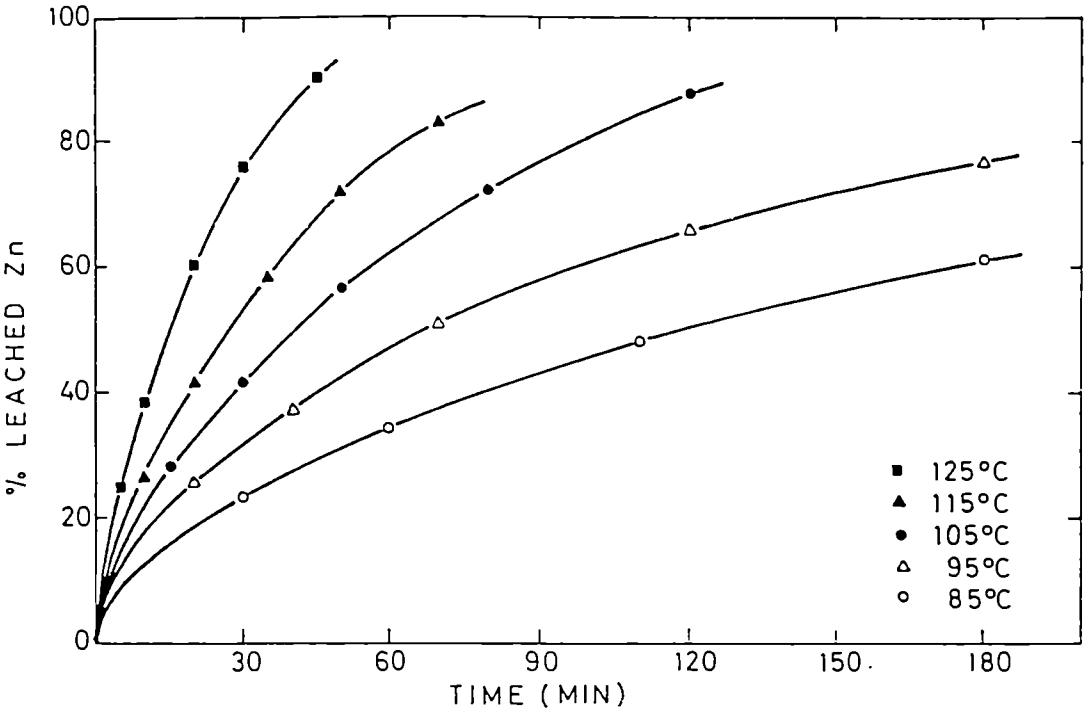

FIG.3.- EFFECT OF TEMPERATURE ON ZINC LEACHING KINETICS.
LEACH CONDITIONS:
Po_2=1 BAR ; [CIN H_4]=6,0 M / 1000 g. H_2O ; [Cu]o = 1,5 g /1000 g H_2O;
100 g. SOTIEL BULK CONCENTRATE / 1000 g H_2O.

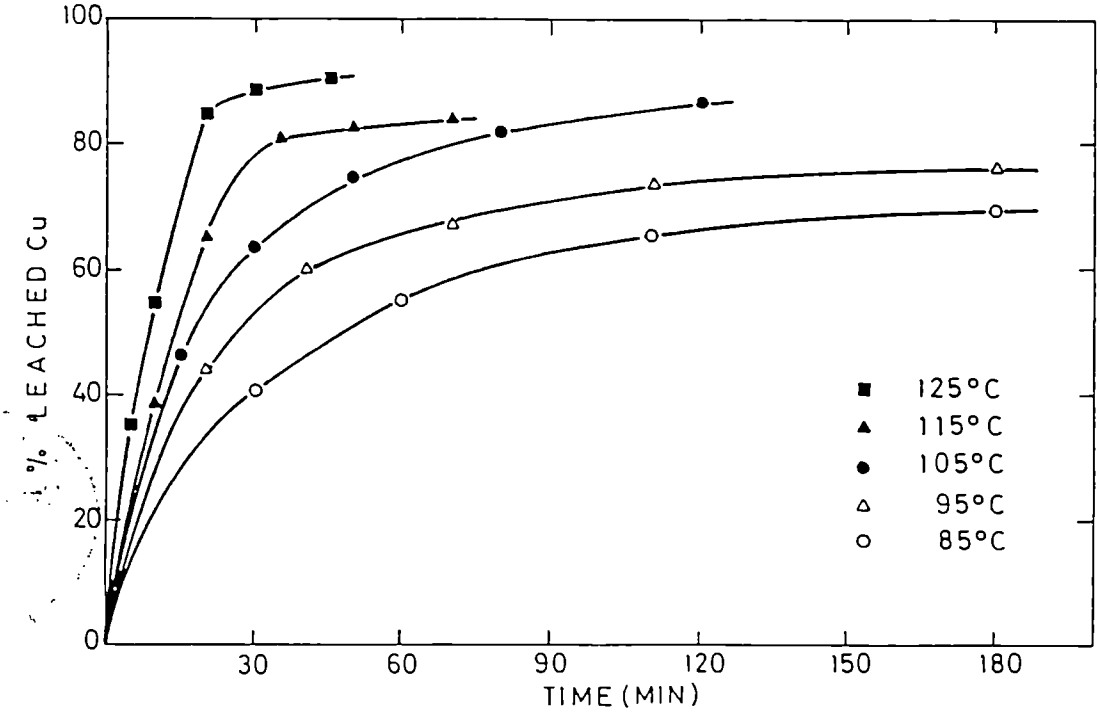

FIG.-4.- EFFECT OF TEMPERATURE ON COPPER LEACHING KINETICS.
LEACH CONDITIONS:
Po_2=1BAR; [CIN H_4]=6,0 M/1000g H_2O; [Cu]o = 1,5 g / 1000 g H_2O
and 100g SOTIEL BULK CONCENTRATE / 1000g H_2O

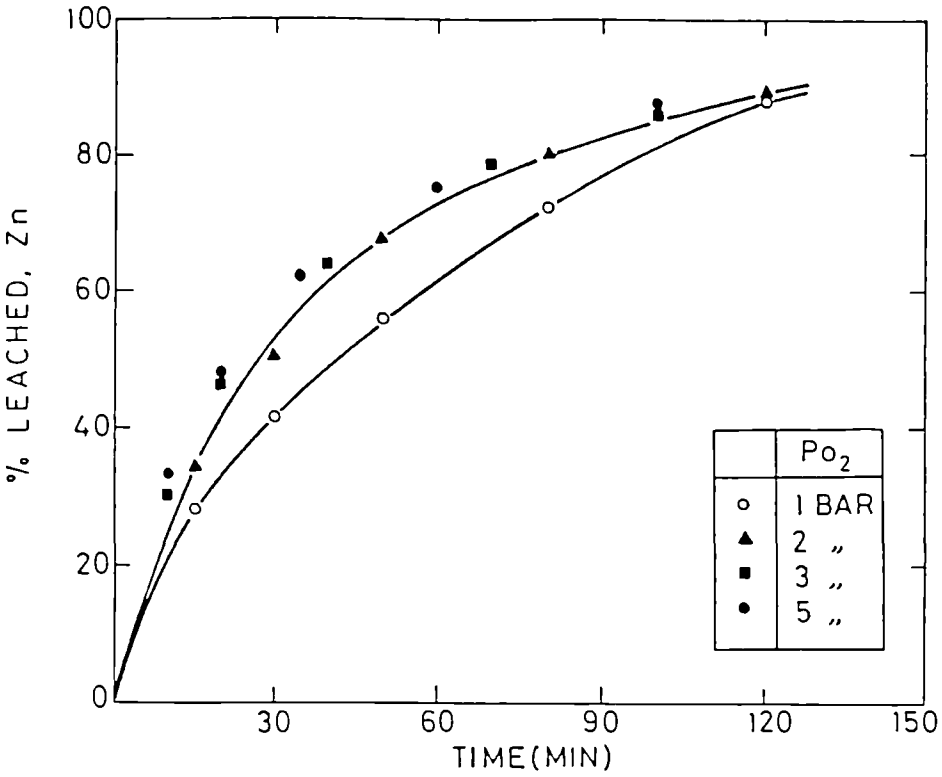

FIG. 5.- EFFECT OF OXYGEN PRESSURE ON ZINC LEACHING KINETICS
T = 105 °C ; [CIN H_4] = 6,0 M / 1000 g H_2O ; [Cu] o = 1,5 g / 1000 g H_2O ;
100 g SOTIEL BULK CONCENTRATE / 1000 g H_2O.

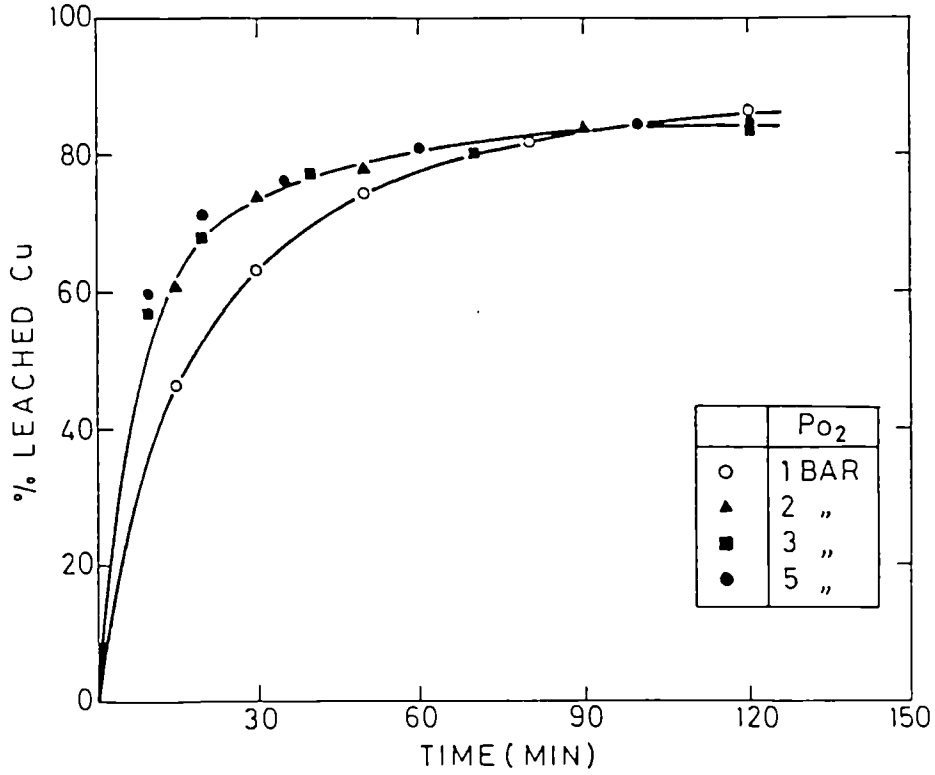

FIG. 6.- EFFECT OF OXYGEN PRESSURE ON COPPER LEACHING KINETICS
T = 105 °C ; [CIN H_4] = 6,0 M / 1000 g H_2O ; [Cu] o = 1,5 g / 1000 g H_2O ;
100 g SOTIEL BULK CONCENTRATE / 1000 g H_2O

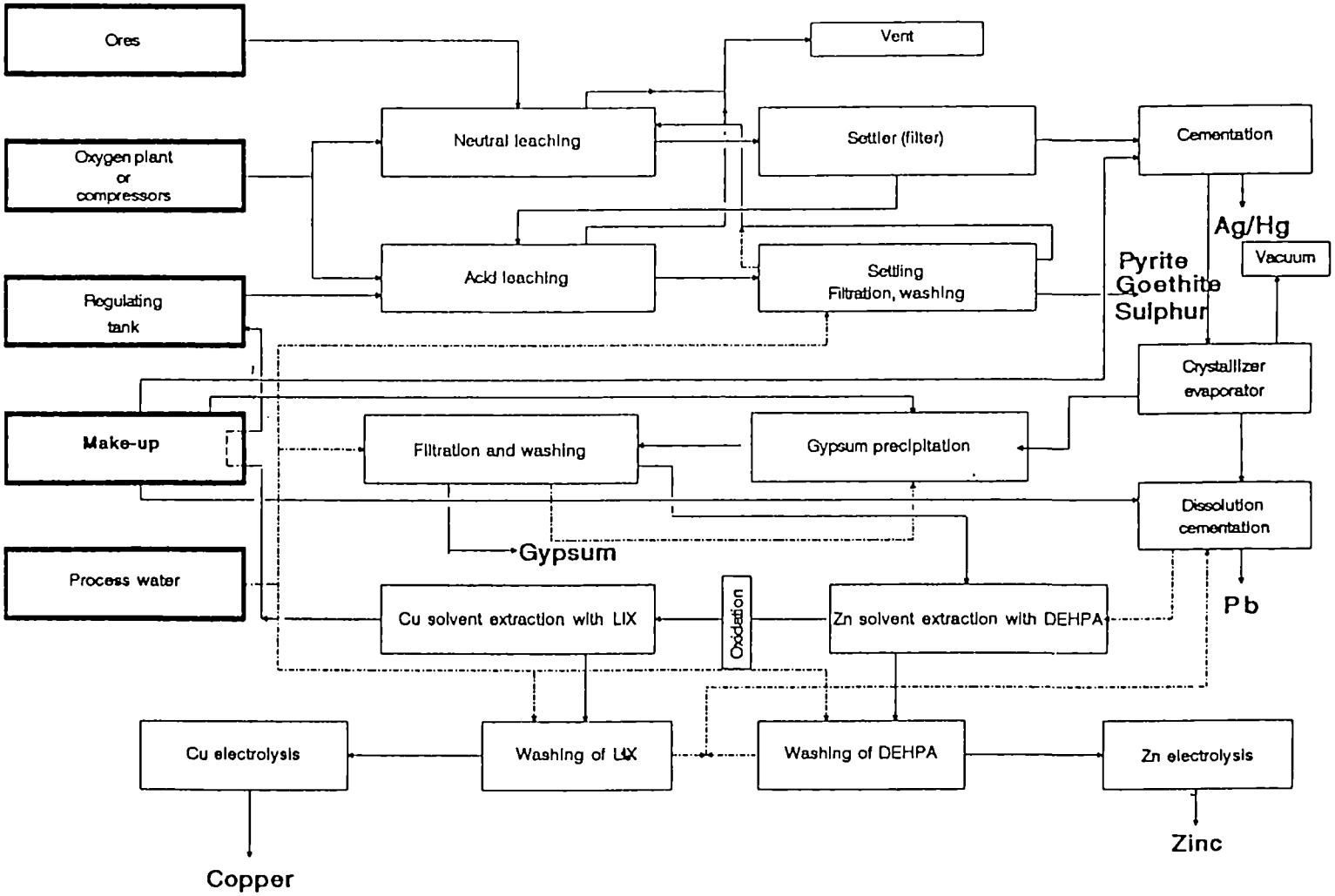

FIGURE 7.- FLOW DIAGRAM OF CENIM-LNETI PROCESS FOR COMPLEX SULPHIDE TREATMENT

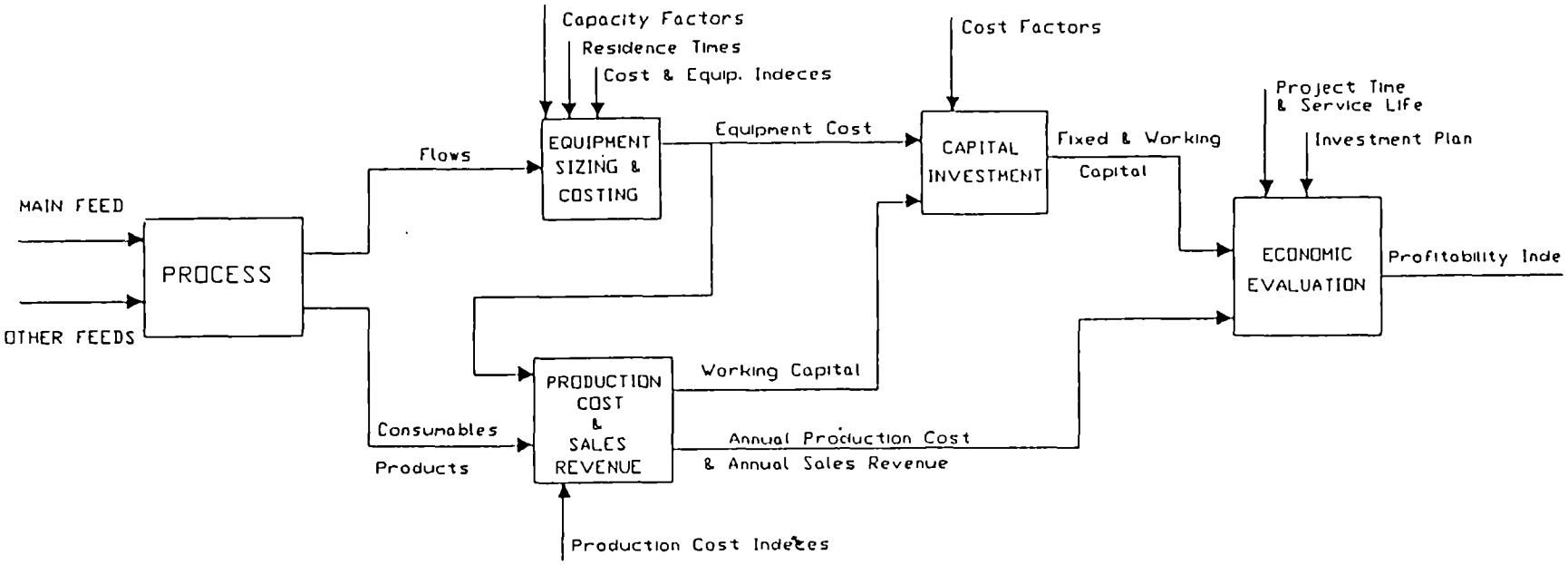

Figure 8 - Schematic representation of the computational system for full process analysis.

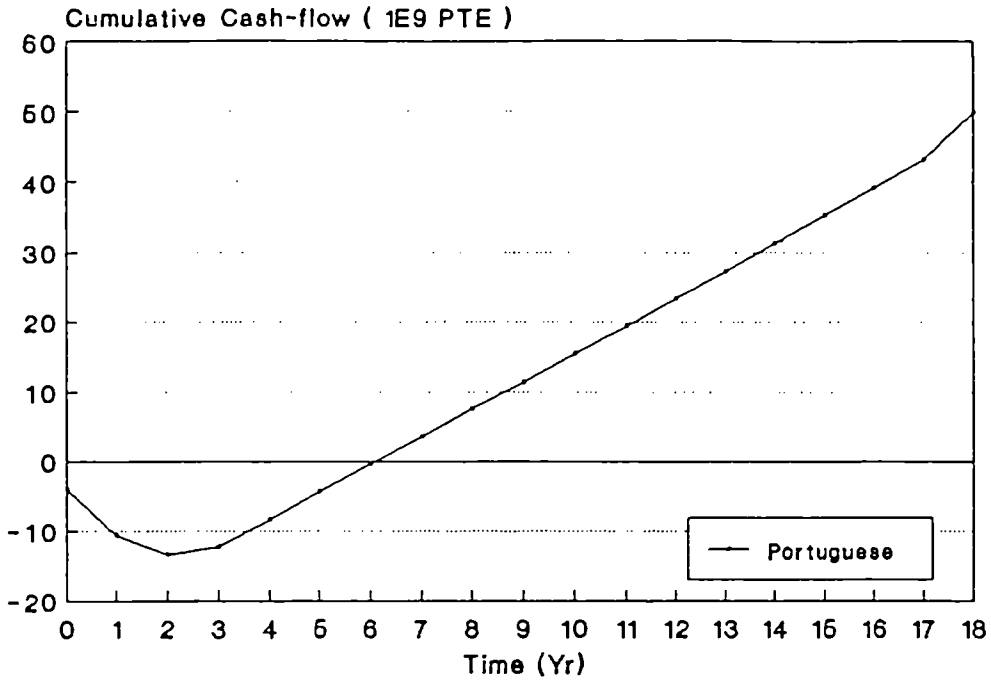

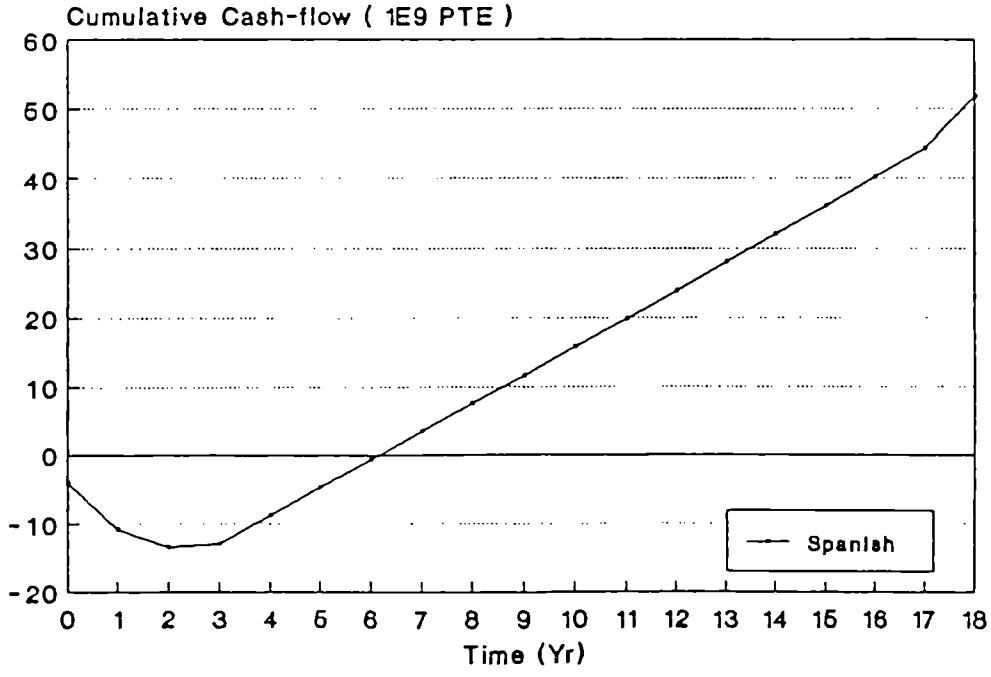

Figure 9 - Process Cumulative Cash-flow at the reference concentrate price for the Portuguese and Spanish concentrates.

IRON CONTROL BY HYDROLYTIC STRIPPING IN COMPLEX ORE PROCESSING - PART 1

Project Leader: A.J. MONHEMIUS
Royal School of Mines, Imperial College, London, United Kingdom

A. Gaunand
ARMINES, Paris, France

Contract MA1M-0052-C

PREFACE

This report summarizes the work performed at Imperial College whereas the next report summarizes the work done at Armines under the above mentioned contract.

1. OBJECTIVE

The main objective is to improve the knowledge of the various mechanisms having a role in the iron stripping operation which is contained in complex ore solutions.

2. INTRODUCTION

Hydrolytic stripping is a novel process which offers the possibility of removing iron from aqueous leach liquors as a stable oxide product in an uncontaminated form, thus avoiding the residue disposal difficulties of the Jarosite process and Goethite processes. The overall chemistry of the process is represented by Equation (1), which shows iron, dissolved in an organic phase as a carboxylate salt, being reacted with water at elevated temperatures to produce iron oxide by hydrolysis with re-formation of the carboxylic acid in the organic phase.

$$2\ FeV_3(Org) + 3\ H_2O \xrightarrow{HEAT} Fe_2O_{3(s)} + 6\ HV_{(org)} \quad (1)$$

Over the last few years, the reaction kinetics and other aspects of the hydrolytic stripping process have been investigated in the Hydrometallurgy Research Group at the Royal School of Mines, Imperial College[1]. It was found that, although detailed study could be made of the kinetics of the reaction, reproducibility of the particle sizes of the iron oxide products and the solid-liquid filtration characteristics was very difficult to attain with the batch experimental systems used. This was thought to result mainly from variability in the homogeneous nucleation of iron oxide crystallites.

In the present study, the results of experiments carried out in a purpose-built, continuous pressurised reaction system show that the reaction kinetics and particle size distribution of samples are to a great extent reproducible, indicating that steady state conditions prevail in the continuous reaction system. Thus the problems of poor reproducibility with the batch reaction systems can be overcome by the use of the continuous miniplant reaction system.

A detailed investigation of the market potential for hematite powders has shown that it is desirable to use the precipitated hematite as a pigment, taking into consideration market sizes and economic value, together with the physical and chemical properties of the precipitates, such as particle size, colour and purity. The responses from pigment manufacturers following assessment of the initial hematite solids produced by the hydrolytic stripping reaction with water, however, suggested that the colour shade of the solids needed to be modified to achieve higher economic value.

Formic acid solutions were then used, replacing water as the hydrolysing agent. The relationship between iron stripping efficiency with formic acid and reaction time was established at 105-145 °C for organic solutions loaded via Ca/Fe exchange extraction (Equation 2)

$$3\ CaV_{2(org)} + 2\ FeCl_3 = 2\ FeV_{3(org)} + 3\ CaCl_2 \quad (2)$$

Similar experiments were carried out with organic solutions loaded via Cu/Fe oxidative extraction (Equation 3), the latter being a method by which iron can be extracted from cuprous-ferrous solutions, similar in composition to those produced by chloride leaching of complex sulphide ores.

$$4\ CuCl + 2\ FeCl_2 + 3/2\ O_2 + 6\ HV_{(org)} = 4\ CuCl_2 + 2\ FeV_{3(org)} + 3\ H_2O \quad (3)$$

It was found that higher temperatures were needed to strip iron from organic solutions loaded via Cu/Fe oxidative extraction and that the activation energy of this reaction was higher than that found when the organic phase was loaded via reaction (2).

The use of formic acid had a significant effect on the kinetics of the precipitation reaction and, consequently, on the particle sizes, morphology, crystalline structure, and hence colour shade, of the hematite produced. Moreover, it was found that good gas dispersion in the reactor was crucial to achieve fast reaction rates with formic acid, and that with such a reactor, it was possible to produce a series of hematite powders of different colour shades, ranging from dark brown to dark purple to bright red, by varying the experimental conditions.

The experimental results were used to make a preliminary economic evalution of a process flowsheet which integrates hydrolytic stripping for iron removal with a chloride leaching process for treatment of complex sulphide ores. This exercise revealed that the loading of iron into the organic phase by oxidative extraction (equation (3), above) accounted for 50% of the capital cost of the plant, because of the long residence time required for the transfer of iron into the organic phase. It was concluded that, unless a method to catalyse this reaction can be found, the economic viability of the application of hydrolytic stripping in the processing of complex sulphide ores is not promising.

2. CONTINUOUS AUTOCLAVE SYSTEM

A continuous autoclave miniplant system, which is illustrated schematically in Figure 2.1, was constructed to carry out the hydrolytic stripping reaction. The autoclave (capacity 2L) was divided internally into four compartments. The mixture of organic and aqueous phases was pumped under pressure into the top of the autoclave and the slurry of liquid and precipitated solids was collected via a line near the bottom of the vessel into a second holding autoclave, which could be connected to an on-line pressure filter or a collecting vessel through a three-way valve. Two timer-controlled valves on the discharge line made it possible to maintain a stable flow from the pressure vessel according to the residence time required.

A 100L reaction unit was installed complete with heating and stirring facilities for preparation of large quantities of Fe-loaded organic solutions, which were used to feed the continuous autoclave system. Solutions of Versatic 10, a tertiary carboxylic acid (HV), in a diluent, Escaid 110, (33% by volume) were used throughout this work.

3. HYDROLYTIC STRIPPING WITH WATER - VERSATIC SOLUTIONS LOADED VIA Ca/Fe EXCHANGE

The Versatic acid solution was preloaded with calcium and then interchanged with ferric iron by exchange extraction to produce iron-loaded Versatic solutions (see equation (2)). The exchange reaction came to completion in a few minutes.

A series of seven experiments were conducted under identical experimental conditions to verify the consistency of the reaction kinetics and the particle characteristics of the solids produced. The concentrations of iron remaining in the organic phase after the replicate reactions were 1.2 $\pm$0.7 g/l, from initial concentrations in the loaded organic phases of 17 to 20g Fe/l. The solids precipitated in these

runs had a mean maximum size of 21.4 $\pm$4.1 μm, the amount of $\leq$1.2 μm in the solids was 5.8 $\pm$2.7%, and there were two invariant peak size bands at 3.0-3.9 and 6.4-8.2 μm, in which the largest weight percentages of the samples were found. It was therefore concluded that not only the reaction kinetics, but also the particle size characteristics of the iron oxide solids, were largely reproducible, indicating that the reaction proceeded under steady-state conditions in the continuous reaction system.

From the results of a series of factorially-designed experiments, it was shown that the reaction time did not significantly affect the maximum particle sizes of the precipitated iron oxide solids; however, an increase in reaction time caused a decrease in the proportion of particles of $\leq$1.2 μm. As the reaction temperature was increased, the maximum size of the solids decreased, while the percentage of particles $\leq$1.2 μm increased. An increase in the aqueous-organic ratio caused a very slight increase in the maximum sizes of the solids. There was no evidence of variation of the two peak size bands (3.0-3.9 and 6.4-8.2 μm) with any of these variables. X-ray diffraction measurements indicated that virtually all the peaks in the diffraction pattern could be accounted for by those belonging to synthetic hematite.

The colour of the hematite powder produced was deep brown. Assessment of this material by pigment manufacturers indicated that modification to a lighter, reddish shade was required to achieve a higher economic value. This led to the investigation of the use of formic acid solution for hydrolysis and morphology modification.

4. HYDROLYTIC STRIPPING WITH FORMIC ACID - VERSATIC SOLUTIONS LOADED VIA Cu/Fe OXIDATIVE EXTRACTION

The oxidative solvent extraction process for extracting iron from artificial leach liquors containing Cu and Fe was investigated. These liquors were of similar composition to those produced in the MINEMET process, one of the processes developed for the recovery of copper and zinc from complex sulphide ores[2]. The reaction involved in oxidative extraction is shown in Equation 3. Loadings of up to 30g/l of iron in the organic solution could be achieved in two and half hours by this method.

4.1 REACTION KINETICS

The kinetics of the hydrolytic stripping with 0.8M formic acid of solutions loaded via Cu/Fe oxidative extraction are presented in Figure 4.1. A laboratory-scale autoclave of

300 ml internal volume, fitted with a gas dispersion shaft/impeller assembly, was used for these experiments. The activation energy of the reaction was estimated as 156 kJ/mole, which indicates a considerable temperature effect on the reaction rate.

The hydrolytic stripping kinetics of organic solutions loaded via Ca/Fe exchange extraction by formic acid solutions were also investigated. These results are presented in Figure 4.2: the activation energy of the reaction was estimated as 90 kJ/mole. It may be seen that the reaction temperature can be about 40°C lower in the latter system to achieve the same reaction rates as organic solutions loaded via Cu/Fe oxidative extraction. This illustrates that the preparation method of the Fe-loaded organic solution has a marked effect on the reaction kinetics.
The effect of formic acid concentration in the aqueous phase can be seen in Figure 4.3, which shows that the reaction rate increases with formic acid concentration. Similarly, an increase in the aqueous-organic ratio at the same formic acid concentration results in an increase in the reaction rate - Figure 4.4. An experimental run done with an organic solution which was made by dilution of the Fe-loaded organic solution in half from from 21g Fe/l to 10.5g Fe/l showed a drastically lower reaction rate. It was concluded that it is necessary to load the organic phase to sufficiently high concentrations to achieve fast stripping reaction rates.

4.2 CHARACTERISATION OF THE HEMATITE SOLIDS

From the X-ray diffraction patterns of the solids produced by reaction of organic solutions loaded via Cu/Fe oxidative extraction with formic acid , it was seen that although these solids could be identified as hematite, the widths of the diffraction peaks decreased with increasing reaction temperature, revealing that the hematite produced at 185°C had a well-formed crystalline structure and large crystal size, whereas the solids precipitated at 150°C consisted of less ordered crystallites of various sizes with the hematite crystalline structure only partly formed. The solids produced at 170°C lay between these two extremes, but the diffraction profiles were much better defined than those at 150°C.

The solids produced at 150°C ranged in size from sub-micron up to 5 μm (Figure 4.5), and individual particles had circular, angular or elongated shapes. These solids were dark purple in colour. The solids produced at 185°C were sub-micron in size, with a predominant part of about 0.5 μm (Figure 4.6). The morphology of these particles was more or less spherical. This uniformity in both particle size and shape, which resulted in a bright reddish colour, was quite

different from the material produced at 150°C, and also from those materials produced from organic solutions loaded via Ca/Fe exchange extraction.

X-ray diffraction patterns of the powders precipitated by formic acid solutions from organic solutions loaded via Ca/Fe exchange extraction showed that crystalline hematite was the sole product at reaction temperatures of 105 and 120°C. The material formed at 145°C, however, showed a tendency for transformation the structure from amorphous to crystalline with reaction time. At 3.5 minutes, only a few broad X-ray peaks were observed, whereas the solids collected after 20 minutes reaction showed sharp diffraction profiles due to crystalline hematite, as well as the broad peaks seen in the earlier samples. Thus much of the amorphous structure and microcrystallites were transformed to ordered hematite crystal during the residence in the reaction system.
The maximum sizes of the solids precipitated at 120 and 130°C were 13.6 and 8.2 μm, respectively, and the size band which had the largest weight percentage was 3.0-3.9 μm. Increases in reaction temperature resulted in a shift towards smaller particle size. When the reaction time was increased from 3 min to 9 min, the size distribution of the solids became more uniform, with an increased weight percentage in the peak size band at the expense of the fractions in both the maximum size band and the sub-micron part.

4.3 HYDROLYTIC STRIPPING IN 2L BATCH AUTOCLAVE

Attempts were made to carry out hydrolytic stripping campaigns using formic acid in the continuous autoclave system with organic solutions loaded via Cu/Fe oxidative extraction. However it was found that the iron stripping efficiency was much lower than when using water as the hydrolysing agent. Investigations revealed that the reasons for this were that the design of the multi-stage system within the pressure vessel did not allow for recirculation and dispersion of the gas phase. These equipment limitations forced a return to a batch system in order to carry out larger scale experiments. Thus a 2L batch autoclave fitted with a gas dispersion shaft/impeller, similar to that used in the 300ml autoclave, was used. The reaction rate was enhanced significantly compared to that obtained in the continuous reaction system; however, it was still lower than that achieved in the 300ml autoclave. It was concluded that good gas dispersion is essential in order to ensure that the reaction occurs in the chemical reaction controlled range. This is an important factor to be taken into account in designing a suitable industrial reactor for the hydrolytic stripping reaction. With the correct type of reactor it should be possible to vary the reaction rate by

changing the formic acid concentration, thus obtaining fine particles, uniform in size and of the right colour shades to meet market demands

The hematite powder produced in the 2L autoclave had a larger particle size range (up to 5 μm) and a slightly deeper red colour shade than that produced in the 300 ml autoclave at the same temperature. Assessment of this product by a pigment manufacturer showed that it was a considerable improvement on the previous products and was commercially acceptable, although it did not achieve the quality of that produced in the 300 ml autoclave, presumably because of the poorer gas dispersion in the larger autoclave.

The hematite solids produced were largely hydrophilic in nature, since they tended to concentrate and settle quickly in the aqueous part of the two-phase system. This characteristic should make possible a two-stage liquid solid eparation on an industrial scale, involving settling to give an intial organic/aqueous phase separation, followed by a solid/aqueous phase separation at a reasonable filtration rate.

5. PRELIMINARY ECONOMIC EVALUATION OF THE PROCESS

A conceptual flowsheet for the solvent extraction/hydrolytic stripping process has been designed with the objective of integration with chloride leaching processes for copper extraction from complex ores, such as the MINEMET process[2], as shown in Figure 5.1. A preliminary economic evaluation of this process based on a plant producing 12,500 ton/annum iron oxide, which would result from a production of 10,000 tons/annum copper, assuming a chalcopyrite feed, indicated a total capital cost of about 8.8 million, of which the solvent extraction section accounted for 50%. The operating cost was estimated as 2.34 million per annum, which is equivalent to 187/ton of iron oxide produced. This of course has to be off-set by the capital and operating costs of the current alternative technology, which is goethite precipitation, together with the ever-rising costs of disposal of such precipitates. This cost estimation should only be taken as "order of magnitude" in its precision; however, it reveals that the solvent extraction of iron into the organic solution from the leach liquor accounts for a major part of the total capital and operating costs because of long loading times resulting from the slow rates of oxidative extraction. Significant increases in extraction rates would lead to major savings in the costs of iron oxide production by hydrolytic stripping.

6. CONCLUSIONS

1. It is possible to produce hematite powders of different colour shades and particle sizes by the hydrolytic stripping process, suitable for sale into the pigment market. The colour shade and particle size of the hematite depends on the preparation method of the iron-loaded organic solution and the rate of precipitation. Higher rates favour precipitation of fine powders of brighter red shades, while lower rates tend to produce coarser powders of deeper brown appearance.

2. The rate of precipitation of hematite during hydrolytic stripping can be controlled by varying the reaction temperature, and by using formic acid solutions instead of water as the hydrolysing agent. It is essential to have good gas dispersal in the reactor when using formic acid in order to achieve a chemically-controlled reaction and fast rates of precipitation.

3. The solvent extraction section accounts for more than half of the capital and operating costs of an industrial scale plant if the hydrolytic stripping process is combined into "MINEMET-type" processes for copper recovery from complex ores, where iron is loaded into the organic phase by the oxidative extraction method.

7. REFERENCES:

(1) A. J. MONHEMIUS, Final Report, CEC Contract MSM 094UK, 1985.

(2) J. M. DEMARTHE and A. GEORGEAUX, "Hydrometallurgical treatment of complex sulphides", Complex Metallurgy '78, M. J. Jones, ed., IMM London 1978, p 113.

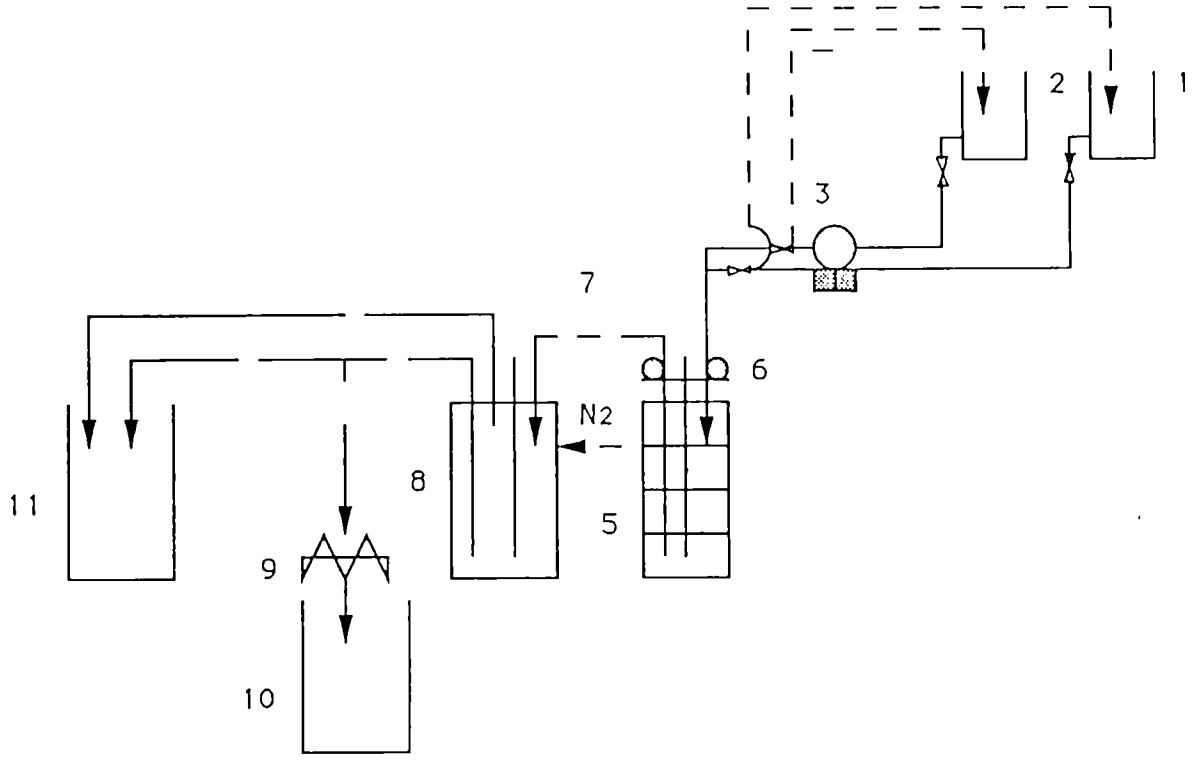

1. Organic solution tank;
2. Aqueous solution tank;
3. Pressure pump;
4. Relief valves;
5. 2L four stage autoclave;
6. Connectors;
7. Air-activated relay valves;
8. 3.5L stirred holding tank;
9. Pressure filter;
10. Liquid collecting tank;
11. Reservoir

Figure 2.1 Flowsheet of the continuous autoclave miniplant system

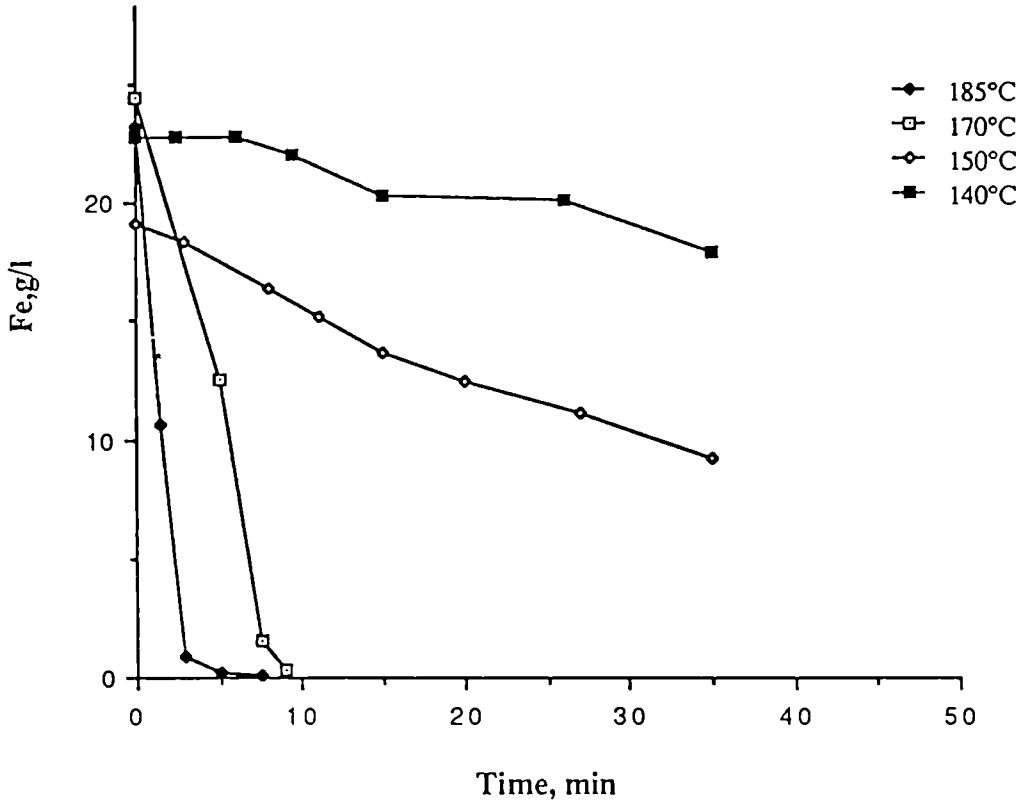

Figure 4.1 Effect of temperature, Cu/Fe oxidative loading

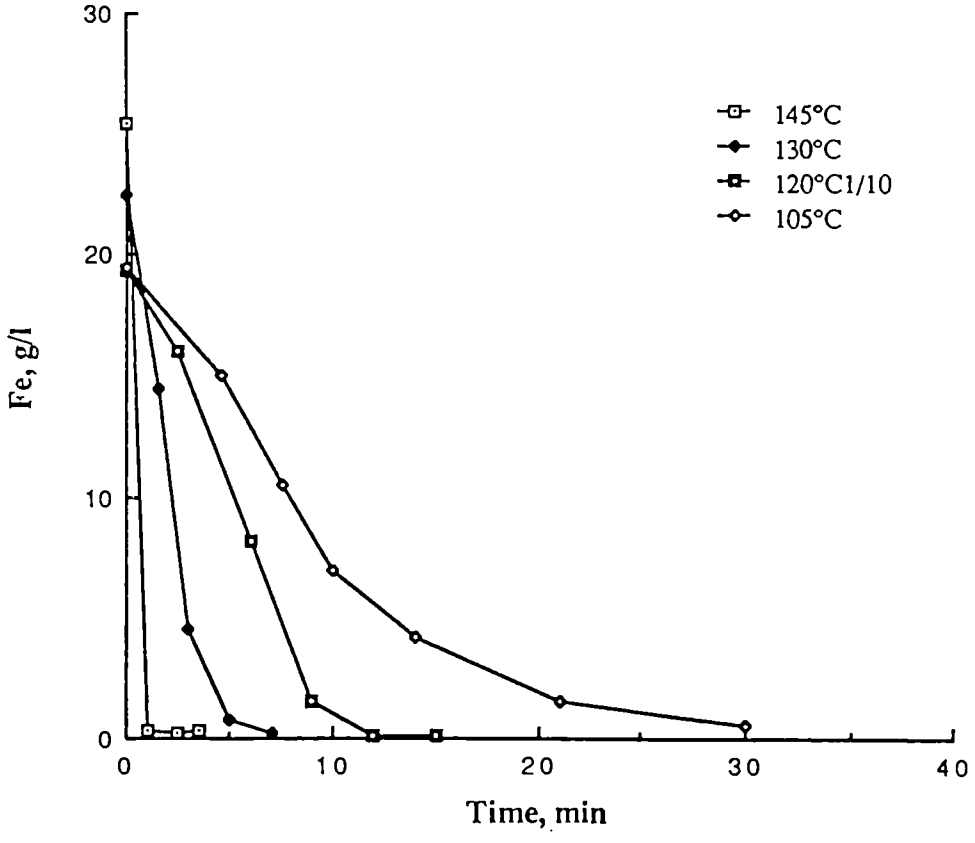

Figure 4.2 Effect of temperature, Ca/Fe exchange loading

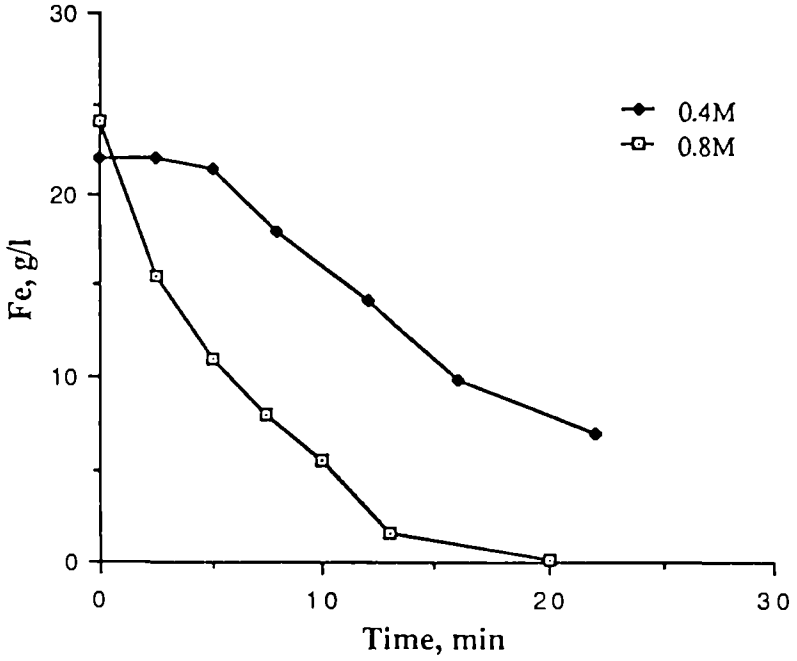

Figure 4.3 Effect of HCOOH concentration,120°C,Vaq/Vorg=1/10

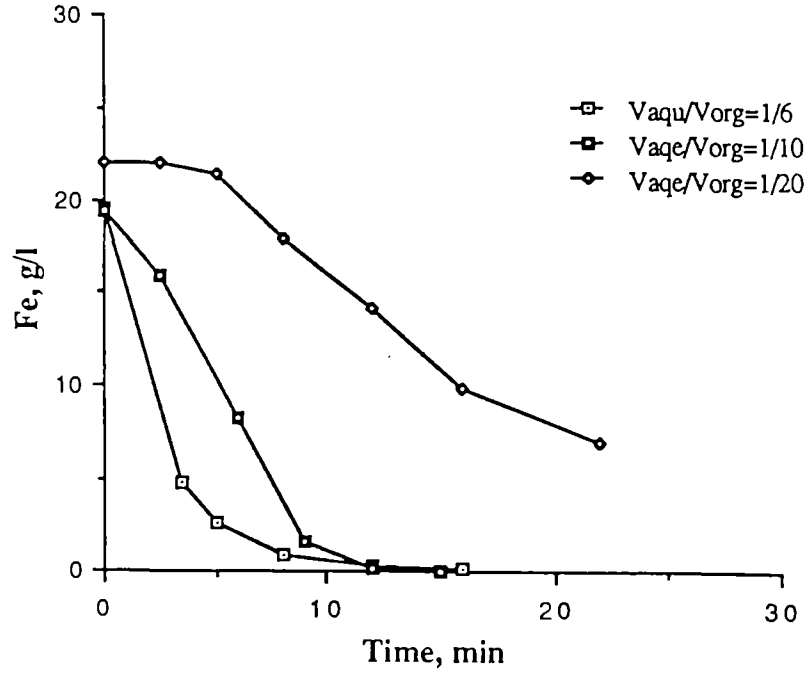

Figure 4.4 Effect of Vaq/Vorg ratio, 120°C,0.4M HCOOH

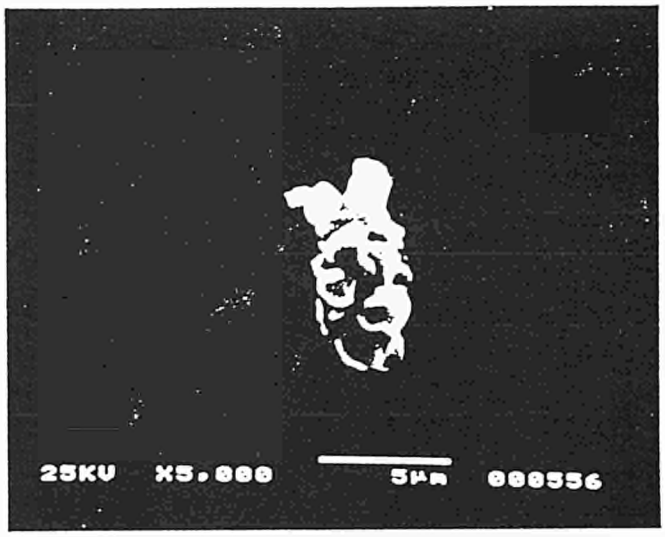

Figure 4.5 SEM micrograph of solids produced at 150°C from organic solution loaded via Cu/Fe oxidative extraction

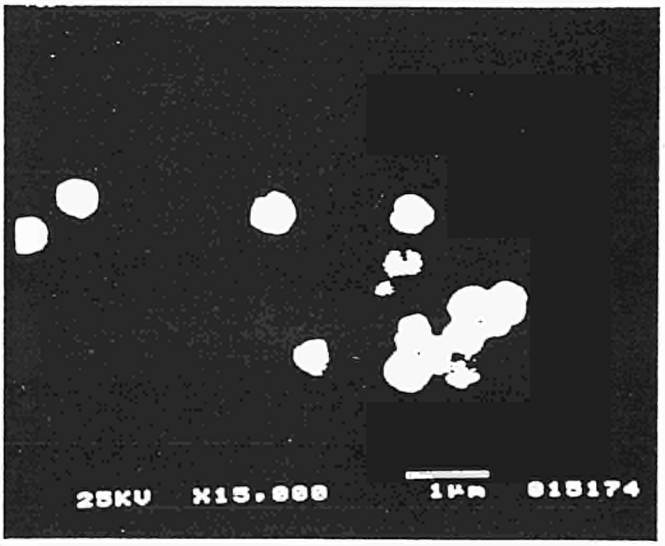

Figure 4.6 SEM micrograph of solids produced at 185°C from organic solution loaded via Cu/Fe oxidative extraction

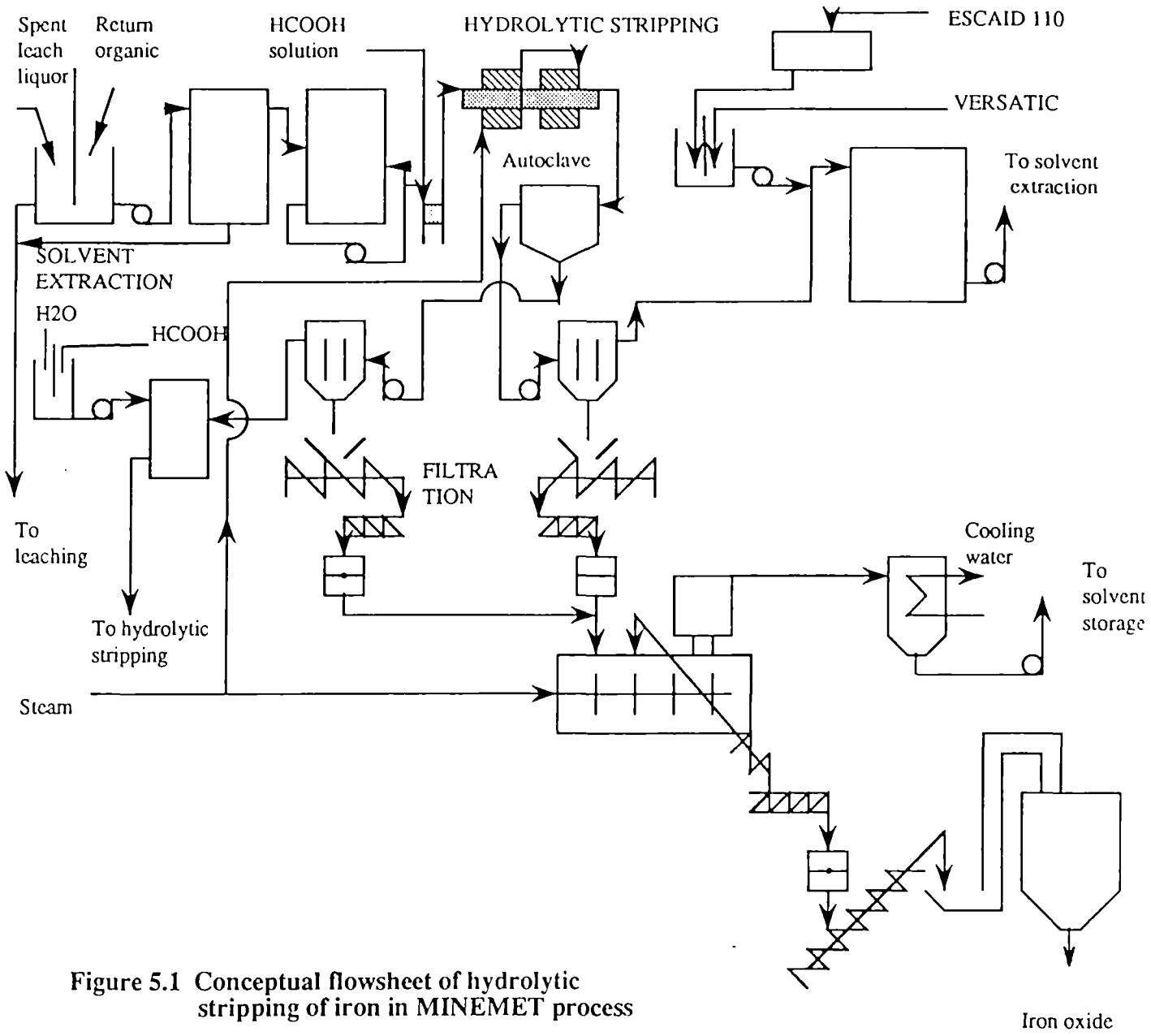

Figure 5.1 Conceptual flowsheet of hydrolytic stripping of iron in MINEMET process

IRON CONTROL BY HYDROLITIC STRIPPING IN COLPLEX ORE PROCESSING - PART 2

Project Leader : A.J.MONHEMIUS
Royal School of Mines, Imperial College, London, United Kingdom

A. Gaunand
ARMINES, Paris, France

Contract MA1M-0052-C

PREFACE

This report summarizes the work performed at ARMINES whereas the previous one summarized the work done at Imperial College under the above mentioned contract.

1. OBJECTIVE

To extend the novel iron oxidation extraction technique already used for iron elimination from solutions typical of a first hydrometallurgical process to those encountered in other processes; to test the sensitivity of iron extraction kinetics to both hydrodynamical and chemical conditions.

To provide new experimental information on iron extraction kinetics from acidic and chloride media by solutions of the carboxylic acid chosen for the novel elimination technique ; to build up an expression for the rate of this liquid-liquid extraction.

To gather in a set of mass balance equations the laboratory knowledge on expressions for the rate of chemical reactions and mass transfer parameters involved in both oxidations and extraction mechanisms, in order to predict their development in gas-aqueous-organic contactors for iron elimination in hydrometallurgical liquors.

2. INTRODUCTION

Iron removal is a very important step in the hydrometallurgical processes recently proposed for the treatment of poor copper-lead-zinc sulphide ores. Indeed, the high iron content of these ores and its association with copper in chalcopyrite lead to its substantial release in the leach liquors, in spite of the leaching reagents chosen in the processes - cuprous chloride for the Minemet process (Demarthe and Georgeaux, 1978), ferrous chloride for the Cuprex process (Dalton and Price, 1986); its accumulation in the flow-sheets would poison several organic extractants,

like D2EHPA (di-2-ethylhexylphosphoric acid) used for zinc extraction. So far, the widely adopted methods used in industry for iron removal are the Jarosite and the Goethite processes, which both involve precipitation of the two species mentioned by hydrolysis. However, the first one requires addition of ammonia and yields a 35 weight % iron precipitate, while the second may lead to simultaneous precipitation of cupric oxychloride (Demarthe and Georgeaux, 1978).

Several studies carried out in the laboratory on the copper oxidizing extraction step in the Minemet process (Levy et al., 1981; Renon et al., 1982; Gaunand and Papassiopi, 1985; Gaunand, 1986) suggested to use a similar technique for iron elimination: in gas-liquid-liquid reactors, the ferrous and/or cuprous chloride of the leach liquors are oxidized by air, and the resulting ferric species is partly extracted with a carboxylic acid, here Versatic acid 10 (a branched C10 monocarboxylic acid available from Shell Chemicals), diluted in Escaid 110 (a solvent available from Exxon), just enough to equilibrate the amount released at leaching by the ore. Carboxylic acids are usually chosen for removing contaminant iron from process streams because of their low cost, their selectivity for Fe(III) over most other base metals owing to the low pH required and their thermal stability. The acidity resulting from extraction is consumed by the oxidation reactions, so that the extraction equilibrium is shifted in the direction of iron-loading and there is no need of neutralizing reagent (Gaunand et al., 1987). The experiments achieved on cuprous-ferrous solutions, typical of Minemet process liquors, in an oxygen-aqueous-organic semi-batch stirred reactor, simulating a co-current operation, showed the efficiency of the novel technique: very good iron/copper selectivity, good and rather fast loading of the organic solution, without neutralizing reagent (75 % of iron extracted within 30 minutes from a 14 g/dm^3 ferrous and 0.17 mol/dm^3 cuprous solution, for equal volumes of aqueous organic solutions)(Gaunand, Bouboukas et Renon, 1987). Under the phase of the work concerned by this EEC contract, the sensitivity of iron elimination to hydrodynamical parameters: gas flow, stirring speed, and initial concentrations of ferrous species, hydrochloric acid and Versatic acid was investigated in the same three-phase stirred reactor. Especially, the new chemical conditions were chosen to test to which extent the technique was applicable to leach liquors of another chloride hydrometallurgical process, the Cuprex one (Dalton and Price, 1986), using iron (III) instead of copper (II) as leaching reagent, and with air instead of oxygen, because of its cheapness.

Kinetics of Fe (II) oxidation by oxygen in cupric chloride and concentrated NaCl solutions were already studied in the laboratory in a stirred gas-liquid reactor (Gaunand et al.,1987; Bouboukas, 1985). It was found that it involved

the rate of Fe (II) oxidation by Cu (II), followed by the oxidation of the cupric chloride resulting by dissolved oxygen. But no work had been done on the extraction side of the process. The thermodynamics of solvent extraction with carboxylic acids have been investigated in numerous studies from the 1950s onwards, together with other extractants for hydrometallurgy, which shows their complexity. Poullion and Doyle (1988) reviewed the previous extraction models including (a) partial hydrolysis and complexation of the metal by the ligands in the aqueous phase - Doyle (1988) suggests successive hydroxo-bridgings leading to the presence of polycations $Fe_p(OH)_q^{(3p-q)+}$; (b) extraction of carboxylate complexes containing OH groups; (c) polymerisation of the carboxylate complexes and their solvatation by carboxylic acid molecules. But publications related to the extraction kinetics by carboxylic acids were few. The second objective was then to study Fe(III) initial extraction kinetics from concentrated chloride solutions, first in a known interfacial area cell or Lewis cell, then in the stirred dispersion reactor used for the three-phase runs. Varying the ferric species, initial hydrochloric and Versatic acid concentrations allowed to find an expression for the rate of interfacial iron-carboxylate formation (Gaunand, 1990).

The third logical step led to gather chemical kinetics and mass transfer quantitative information previously elaborated, to develop the set of mass balance differential equations and the corresponding routine for a simulation of initial oxidizing extraction experiments in the semi-batch reactor, only from flow, stirring and initial concentrations data, both for Minemet-type and Cuprex-type liquors. Simulation and experimental results were then compared, to estimate the degree of prediction of the kinetic phenomena taken into account and of their relevant parameters.

This report summarises the work reported in detail in the 4 intermediate reports and the final report of the EEC contract.

3. EXPERIMENTAL WORK

3.1 IRON OXIDIZING EXTRACTION IN A STIRRED SEMI-BATCH REACTOR

The 0.102 m internal diameter standard reactor is provided with a water jacket for temperature control (45°), a Rushton turbine for mechanical stirring and calibrated capillaries for the gas feed. The reactor was first flushed with water-saturated argon and filled, after stopping argon flow, with 0.25 dm^3 of aqueous solution then 0.25 dm^3 of organic solution. Stirring then air injection were finally started. The pH was recorded with a glass and standard Ag/AgCl double electrode. Aqueous ferrous and organic iron concentrations

were measured after decantation of small volumes of emulsion automatically sampled, the first one by titration with $K_2Cr_2O_7$ solutions, the second by atomic absorption spectrophotometry. The initial concentrations were chosen close to those of the Cuprex process leach liquors, i.e. 1 to 2 mol/dm^3 for ferrous species and consequently 4 to 4.8 mol/dm^3 for the overall chloride concentration, 0.4 mol/dm^3 for cupric species, no addition of ferric or cuprous chloride, 0 to 0.02 mol/dm^3 for initial HCL. The Versatic acid concentration was varied between 10 vol% and 60 vol %. Stirring was varied between 1000 and 1400 rpm and the air flow between 1.22 and 3.85 dm^3/min.

3.2 IRON EXTRACTION KINETICS IN A KNOWN INTERFACIAL AREA CELL AND IN THE STIRRED REACTOR

A 0.079 m internal diameter and thermostatted standard glass reactor was provided with two independent impellers, in order that the stems of the stirrers did not cross the interface. Four equally spaced vertical Teflon baffles prevent vortexing and the stability of the interface was obtained thanks to a Teflon plate and ring. The iron load of the organic phase was continuously analysed by spectrophotometry (wavelength 315 nm) on a short residence time circulating loop also provided with a water jacket and hot water circulation. Thanks to thermostattation, the solutions in the reactor were at 45 °C, controlled within 0.3° C, which was needed owing to the high sensitivity of extraction kinetics to temperature, shown by a few experiments at 25 °C. The spectrophotometer on line was calibrated by sampling the organic phase at the end of each run and titrating iron at 25 °C with a second spectrophotometer. The pH was recorded with a glass and standard Ag/AgCl double electrode.

Just before use, the hydrogen ion concentration of the ferric chloride solution was titrated by soda at the experiment temperature (most of time 45 °C) after iron complexation by sodium fluoride. Both aqueous and organic solutions were heated at temperatures slightly higher than 45 °C, 0.2 dm^3 of the aqueous solution was settled in the reactor and its pH and temperature recorded. When the pH was stabilized, 0.2 dm^3 of the organic solution were gently poured in the reactor and stirring was started. The initial extraction rate was studied as a function of temperature -25 to 45 °C, stirring speeds - 100 to 200 rpm, and concentrations :

0.03 to 0.6 mol/dm^3 for Fe (III)
0. to 0.02 mol/dm^3 for initial HCl
1. to 5. mol/dm^3 for chloride ions
20 to 50 vol.% of Versatic acid

The same ferric extraction by Versatic acid was then achieved in the stirred reactor used in part 31 and followed by automatic sampling, and titration of extracted iron by atomic absorption spectrophotometry after decantation. Were varied the stirring speed - 1000 and 1400 rpm, the airflow - no flow and 1.22 dm^3/min, the organic phase volume - 200 and 250 cm^3, and concentrations :

0.035 to 0.06 mol/dm^3 for Fe(III),
0.003 to 0.006 mol/dm^3 for initial HCl
1. to 5. mol/dm^3 for chloride ions
30 and 40 vol.% of Versatic acid.

at 45°C and a chloride concentration of 4 mol/dm^3

4. RESULTS

4.1. IRON OXIDIZING EXTRACTION IN THE STIRRED SEMI-BATCH REACTOR (figure 2)

The initial iron extraction rate slightly increased with ferrous species concentration - 10 % increase for 2 mol/dm^3 instead of 1 mol/dm^3. It appeared to be quite insensible to the increase from 0 to 0.01 mol/dm^3 of initial HCl concentration and only reduced of a third for 0.017 mol/dm^3 of HCl. The increase of Versatic acid concentration from 20 to 60 vol.% was no more effective on the initial extraction rate. Increasing the stirring speed from 1000 to 1400 rpm led to a 65% increase of the extraction rate, and increasing the air flow from 1.22 to 3.85 dm^3/min led to a 25% increase of the extraction rate.

For the same variations, the initial ferrous species oxidation rate showed a 85% increase with ferrous species concentration, a 100% increase when HCL concentration is brought from 0 to 0.005 mol/dm^3, then a decrease for a higher HCl concentration, a very slight decrease with Versatic acid concentration, a 80% increase with stirring speed and a 70% increase with the air flow.

These results suggest that the extraction rate may be enhanced by increasing both stirring and air flow, but not ferrous or Versatic concentrations.

4.2 IRON EXTRACTION KINETICS IN A KNOWN INTERFACIAL AREA AND IN THE STIRRED REACTOR

A 6% reproducibility on extraction rates has been obtained thanks to a particular care taken to aqueous solutions preparation and hydrolysis.

The high sensitivity of initial iron extraction kinetics to temperature (25°C to 45°C) corresponding to an estimate of 80 kJ/mol for the energy of activation, indicates that, for both stirring speeds at 200 rpm, the extraction is controlled by a chemical reaction at the interface.

The extraction rate, with corrections to take into account the inverse third order with respect to $10^{(-pH)}$ found further, appears to be independent of stirring speeds in the ranges investigated - 100-250 rpm in each solution, i.e. independent of transport processes. This corroborates the previous assumption of a chemical kinetic controlled regime. Both stirring speeds are then set at 200 rpm for the following experiments.

The main result consists of a strong decrease of the rate of extraction r when the ferric chloride concentration is increased from 0.05 mol/dm^3 to 0.6 mol/dm^3 in 4 mol/dm^3 total chloride and 0.005 mol/dm^3 HCl solutions, because of the simultaneous increase of actual acidity coming from Fe(III) hydrolysis, as shown by pH measurements. Increasing the HCl concentration from 0 to 0.02 mol/dm^3 in 0.3 mol/dm^3 Fe(III) and 4 mol/dm^3 total chloride solutions leads in agreement to a drastic drop of the rate of extraction. A first order with respect to Fe(III) concentration and an inverse third order with respect to $10^{(-pH)}$ are inferred from both kinds of results.

Varying the total chloride concentration $[Cl^-]_T$ on the range 1 to 5 mol/dm^3 yields extraction rates within the same experimental range of error, with only a slight decrease for $[Cl^-]_T$= 1 mol/dm^3.

Finally, a second order with respect to the Versatic acid concentration is found from experiments with 20 to 50 vol.% versatic concentrations.

The variations found from the 42 data at 200 rpm stirring speeds, excepted the experiment at $[Cl^-]_T$ = 1 mol/dm^3, suggest that the rate of iron extraction may be represented by the empirical expression :

$$f = k \frac{[Fe(III)]_T[RH]^2}{10^{-3pH}}$$

where k = 0.306 x 10^{-9} mol/m^2.s is an average on the 42 data and s = 0.137 x 10^{-9} mol/m^2.s = 0.45 k is the standard deviation on k (see figure 1).

The kinetics in the stirred dispersion reactor showed a good reproducibility and the same qualitative influence of Fe(III), HCl and Versatic acid concentrations than those obtained in the known interfacial area cell. It was also found that air injection slightly increased extraction, which indicate that an hydrodynamical coupling is added to the chemical one in a gas-liquid-liquid contactor. The quantitative treatment of these data is in progress.

4.3 SIMULATION OF THE COUPLING OXIDATION AND EXTRACTION PROCESSES IN A STIRRED SEMI-BATCH REACTOR

The evolution of all the concentrations for the oxidizing extraction of a copper-iron solution in a semi-batch reactor only depends on four kinetic processes : oxygen mass transfer, Cu(I) oxidation by dissolved oxygen, Fe(II) oxidation by Cu(II) produced by the previous process, as shown by Bouboukas (1985), and Fe(III) extraction by Versatic acid. Accordingly, the evolution of the concentration of four species will be given by a system of four differential equations, the four other concentrations being calculated by electronentrality and overall copper, iron, Versatic acid balances.

It is known that Cu(I) oxidation kinetics occur in the slow reaction regime (Gaunand, 1986; Pani, 1987), depending on the product k_La (oxygen mass transfer coefficient x specific interfacial area available for oxidation - s^{-1}); k_La was taken from previous measurements in the laboratory using the system Cu(I)-O_2 (Pani, 1987; Bouboukas, 1985). As mass transfer coefficients at liquid-liquid interfaces are usually better in stirred dispersion reactors than in Lewis cells, the specific aqueous-organic interface a_{LL} (m^{-1}) was the only hydrodynamical parameter considered for extraction; a_{LL} was inferred from stirring speed and reactor geometry data, thanks to literature correlations.

The rate of Cu(I) oxidation by dissolved oxygen was expressed as a function of Cu(I), O_2 and H^+ concentrations, in agreement with Papassiopi studies (1985). The kinetic constants for the reversible Fe(II) oxidation by Cu(II) were those found by Bouboukas (1985). The previous expression found for initial extraction rate was combined with equilibrium measurements to build up an expression for the initial stripping rate, then by difference an overall extraction rate. Finally, a series of pH measurements at 45°C in HCl-4 M NaCl solutions yielded an estimate of the ratio $10^{(-pH)}/[H^+]$, assuming it remained constant during oxidizing extraction experiments.

On a qualitative point of view, the simulation led to pH variations in agreement with experiments : an immediate maximum of pH for Minemet-type liquors, thanks to 0.15 mol/dm^3 Cu(I) oxidation, against an immediate pH decrease followed by a slow increase for Cuprex-type liquors, corresponding to the delivery of acidity by extraction, thanks to immediate 1 mol/dm^3 Fe(II) oxidation by Cu(II). On a quantitative point of view, the iron oxidation and extraction kinetics showed a fairly good agreement (see figure 2).

5. CONCLUSIONS

The novel iron oxidization extraction technique already used for iron elimination from liquors typical of Minemet hydrometallurgical process, where the leaching reagent is cupric chloride, was tested on those encountered in Cuprex process, using ferric chloride as leaching reagent. For mean values of hydrodynamical conditions and concentrations: 45° C, atmospheric pressure, 1 kW/m^3 brought by stirring, an air flow of 1.22 dm^3/min, 1 mol/dm^3 Fe(II), 0.4 mol/dm^3 Cu(II), 4 mol/dm^3 chloride, 30 vol.% Versatic acid in Escaid 110, 13% of the aqueous iron were extracted in 130 minutes. Using pressurized air or oxygen instead, and a counter-current (both gas and organic solution upwards) continuous operation will improve this yield.

The kinetic study of iron (III) extraction from acidic and chloride media by Versatic acid solutions in a known interfacial area cell showed the paradoxal decrease of the extraction rate for higher iron concentrations, because of an important production of acidity by iron (III) hydrolysis and a high sensitivity of extraction to the pH, which leads to a minus third order with respect to $10^{(-pH)}$ in the rate expression elaborated.

A set of mass balance equations was written and solved numerically to simulate the development of oxidations and iron extraction in the oxidizing extraction experiments achieved in the stirred semi-batch reactor. For this purpose, the separately elaborated quantitative informations on the rate of chemical reactions and on mass transfer parameters were used. Good agreeement was found considering the lack of accurate thermodynamical representations for both aqueous (especially iron hydrolysis equilibria in chloride media) and organic solutions. Such a tool is useful to predict both iron oxidation and extraction yields in gas-aqueous-organic contactors for iron elimination in hydrometallurgical liquors.

6. REFERENCES

BOUBOUKAS G.
"Contribution à l'étude de l'extraction oxydante du fer : oxydation de solutions ferreuses en présence de cuivre et en milieu chlorure concentré"
Thèse Doctorale ENSMP, 1985.

DEMARTHE J.M., GANDON L., GEORGEAUX A.
"A new hydrometallurgical process for copper"
Proc.Int.Symp. on Copper Extraction and Refining A.I.M.E. Las Vegas (Edited by Yannopoulos J.C. and Agarwal J.C.) vol.43, pp. 825-848, 1978.

DALTON R.F. and PRICE R.
"The cuprex process - a new chloride-based hydrometallurgical process for the recovery of copper from sulphidic ores"
Proc.Int.Symp. on Iron Control in Hydrometallurgy. Toronto (Edited by Ellis Horwoood), pp. 466-476, 1986.

DOYLE F.M.
"The physical chemistry of the precipitation stripping process for removing iron (III) from carboxylate solutions with dilute sulphuric acid"
Hydrometallurgy 20, 65-85, 1988.

GAUNAND A.
"Extraction of Fe (III) in concentrated NaCl solutions with versatic acid : kinetics in a known interfacial area cell"
Joint CANMET/EEC seminar on complex sulphide ores, Athens, Greece, November 5th and 6th, 1990.

GAUNAND A. and PAPASSIOPI N.
"Oxidation of Cu (I) by oxygen in concentrated NaCl solutions - II. Kinetics in a known interfacial area cell"
Chem. Engng Sci. 40, 1985, 1533-1538.

GAUNAND A., BOUBOUKAS G. and RENON H.
"Iron elimination in cupric chloride hydrometallurgical processes by oxidizing extraction"
Chem. Engng Sci. 42, 1987, 1221-1227.

GAUNAND A. and ISCARIOT E.
"Extraction du fer (III) en milieu chlorure concentré par l'acide versatic 10 dans l'escaid 110"
Rapport N°3, EEC contract MAIM.0052.C(H), 1990.

LEVY P.E., BARATIN F. and RENON H.
"The oxidation of Cu (I) by oxygen gas in concentratd NaCl solutions"
A kinetic study. Chem. Engng Sci. 36, 1981, 1475-1485.

PANI F.
"Hydrodynamique et transfert de matière en réacteurs agités gaz-liquide et gaz-liquide-liquide : application à l'extraction oxydante du cuivre par l'extractant lix 65n-hs" 1987.

POUILLON D. and DOYLE F.M.
"Solvent extraction of metals with carboxylic acids-theoretical analysis of extraction behaviour"
Hydrometallurgy 19, 1988, 269-288.

RENON H., GAUNAND A., LEVY P.E., KAMEN A. and PAPASSIOPI N.
"Proc. Nato advanced school hydrometallurgy"
Cambridge, U.K., 1982, 15-18 September.

Figure 1. Representation of iron extraction rate at 45°C by equation (1). Standard conditions: $N_A = N_O = 700$ rpm. $[Cl^-]_T = 4$ mol/dm3; [Fe(III)] = 0.3 mol/dm^3; [HCl] = 0.005 mol/dm^3; [RH] = 30 vol.%. : [HCl] = 0.0035 or 0.005 mol/dm^3. [Fe(III)] = 0.03 to 0.6 mol/dm^3 and other standard conditions (20 data). + : [Fe(III)] = 0.3 mol/dm^3; [HCl] = 0.002 to 0.01 mol/dm^3 and other standard conditions (6 data). : [Fe(III)] = 0.05 mol/dm^3; [HCl] = 0. to 0.02 mol/dm^3 and other standard conditions (7 data). : [Fe(III)] = 0.05 mol/dm^3; [HCl] = 0.0035 mol/dm^3, [RH] = 20 to 50 vol.% and other standard conditions (5 data). : $[Cl^-]_T$ = 1 to 5 mol/dm3 and other standard conditions (5 data).

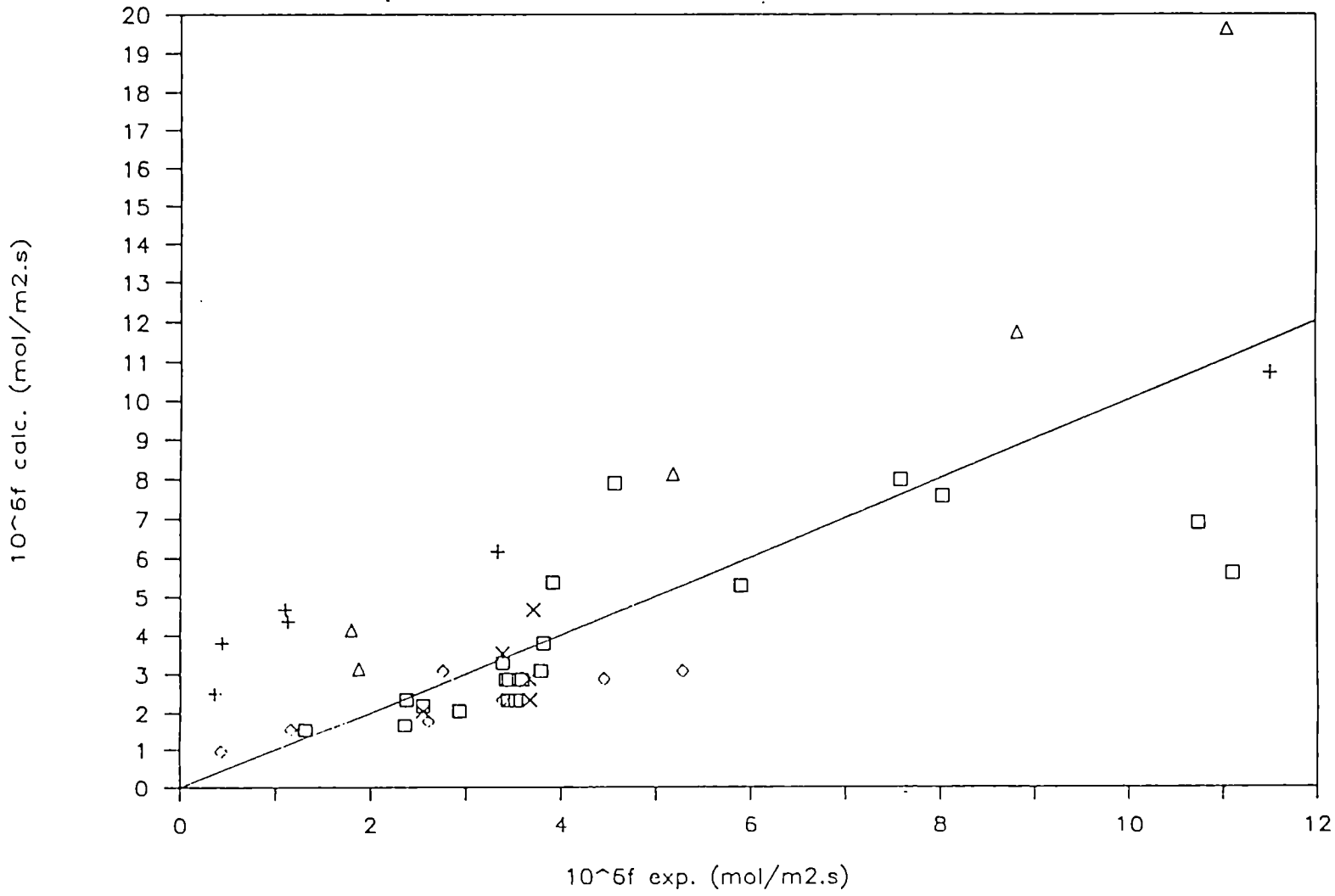

Figure 2. Simulation of iron oxidizing extraction kinetics in the semi-batch gas-liquid-liquid stirred reactor. N = 1000 rpm. Air flow Q_G = 1.22 dm^3/min. Temperature 45°C. Aqueous phase: $[Cl^-]_{T3}$ = 4 mol/dm^3 ; $[HCl]_{initial}$ = 0.005 mol/dm^3 ; [Fe(II)] = 1 mol/dm^3 ; [Cu(II)] = 0.4 mol/dm^3; V_{A3} = 0.25 dm^3. Organic phase : 33 vol.% of Versatic acid 10 in Escaid 110 ; V_O = 0.25 dm^3. + : experimental concentrations ; dashes : $(pH_{exp}+0.3)$.

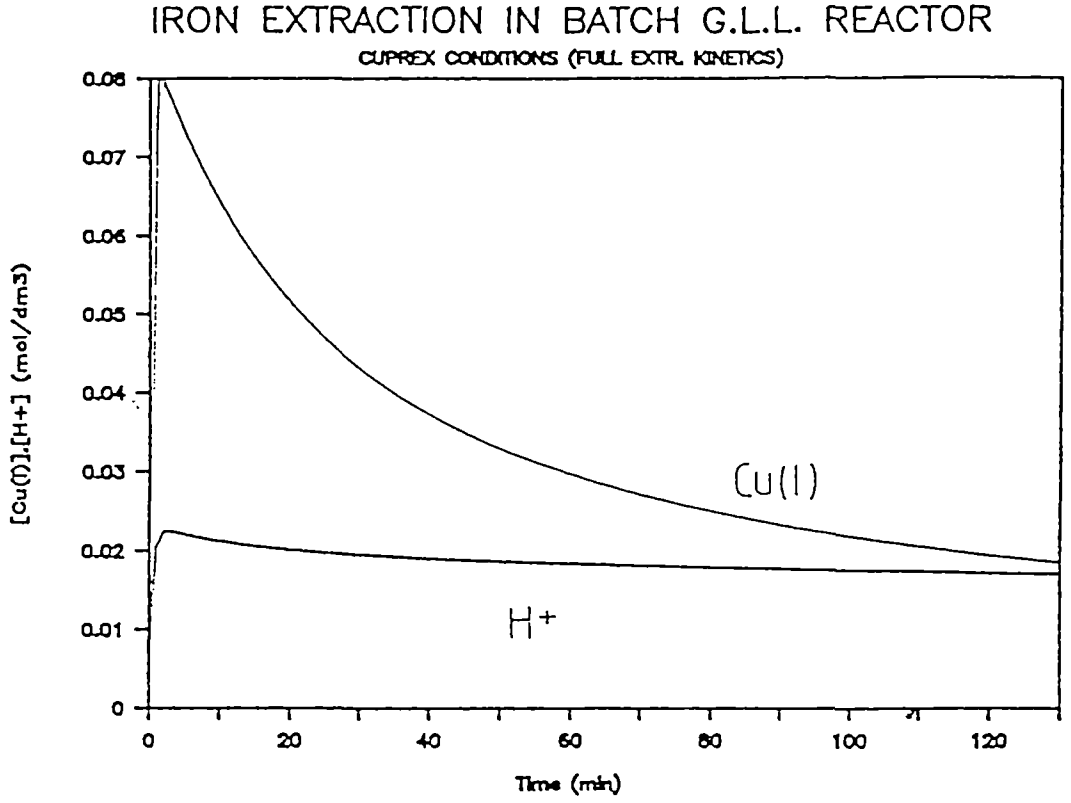

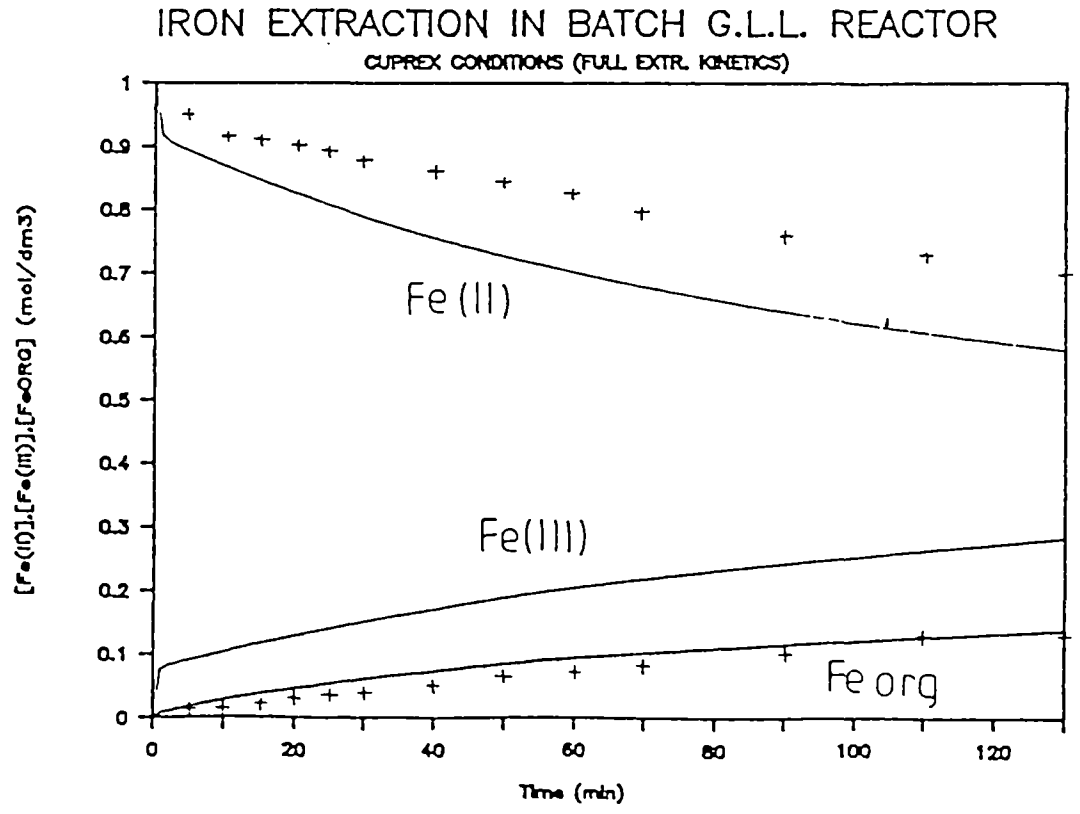

Fig. 2 (continued)

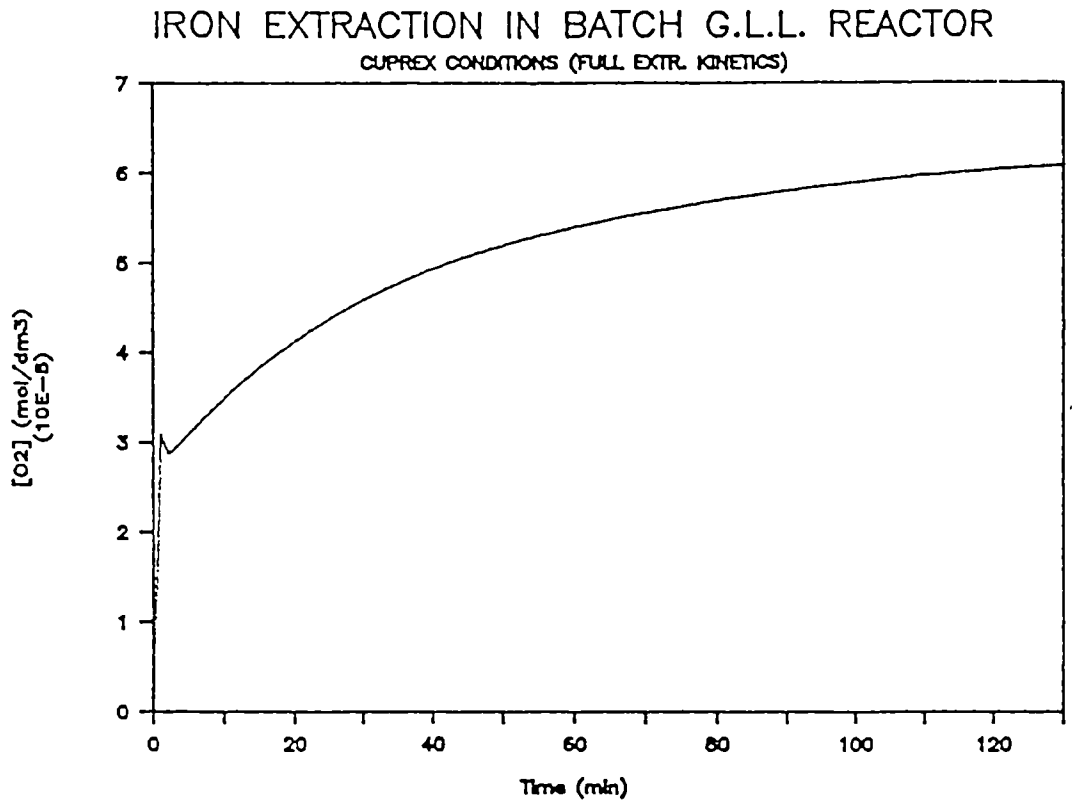

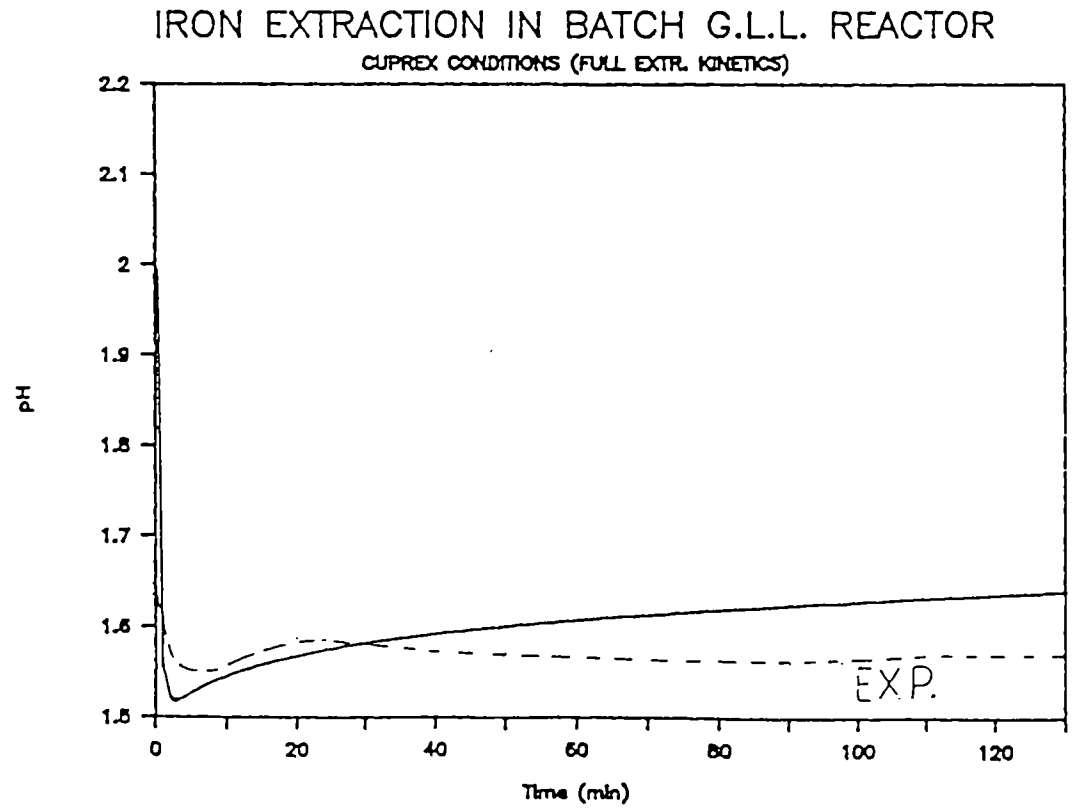

THE USE OF NOVEL BIO OXIDATION TECHNIQUES IN THE HYDROMETALLURGICAL TREATMENT OF MIXED SULPHIDE ORES

Project Leader: T. ERRINGTON
Davy McKee Limited, Stockton on Tees, United Kingdom

Aegean Metallurgical Industries S.A. (METBA), Athens, Greece

Contract MA1M-0069-C

1. OBJECTIVE

Aegean Metallurgical Industries of Greece (METBA SA) have undertaken the exploitation of the mixed sulphide ores of Greece including the Olympias arsenical pyrite concentrate produced at the Olympias Mine in Chalkidiki, Northern Greece. This concentrate is produced by differential flotation of the Run-of-Mine ore containing Pb, Zn, and pyrite to produce galena, sphalerite and pyrite concentrates.

Due to the highly refractory nature of Olympias pyrite concentrates, an oxidative pre-treatment step is required to render gold amenable to the subsequent cyanide leaching. The Sherritt Gordon aqueous pressure oxidation process was selected as the process route for the commercial exploitation of this resource. Bacterial oxidation was considered as a process alternative even at the final selection stage, but aborted because of the lack of industrial applications. Due to the foreseen economic and environmental advantages of this technique METBA has decided to further investigate its potential application in the future either along or in conjunction with the aqueous pressure oxidation process.

Based on the above Davy Mckee of England and METBA have undertaken a joint research project the aims of which have been to evaluate the mode of gold occurrence within the Olympias pyrite concentrate and to examine the effects of applying bio oxidation techniques as an alternative pretreatment for the liberation and subsequent recovery of gold by conventional cyanidation processes.

State of the art analytical techniques were used to identify the mode of gold occurrence within the concentrate and several parameters critical to the operation of bio oxidation processes were evaluated.

2. INTRODUCTION

Davy McKee (Stockton) Ltd (DMS) have been involved since 1979 with the evaluation and development of bio oxidation processes for the treatment of sulphidic ores culminating in the application and grant of USA, European and Australian patents for a process utilising bacteria for the recovery of gold from sulphidic, more particularly arsenopyritic, ores and concentrates.

Aegean Metallurgical Industries SA (METBA) have undertaken the exploitation of the mixed sulphide ores of Greece including exploitation of the gold reserves found in the pyrite concentrate produced by the Olympias Mine at Chalkidiki, Northern Greece. The Sherritt Gordon aqueous pressure oxidation process will be used, however, the use of bio oxidation techniques are still under evaluation as a means of expanding gold production capacity either as an independent technology or in conjunction with the pressure oxidation process.

The mineralogical investigations have been carried out by BRGM of France using state of the art techniques with the bio oxidation testwork being carried out by both DMS and METBA in order to determine the optimum conditions of operating a bio oxidation process.

Further studies have been carried out into the specific problems associated with the use of bio oxidation particularly with respect to the requirements of downstream processing and environmental implications.

The results of this study have been used to develop a basic bio-oxidation plant design basis and conceptual process flowsheet. A basic evaluation of the capital costs of the bio-oxidation process in comparison with the roasting and pressure oxidation processes has also been completed.

3. TESTWORK PROGRAMME

The testwork programme was divided into four phases of activity that may be briefly described as mineralogical investigations; initial bio oxidation amenability tests; optimization of bio oxidation process parameters; determination of mechanism of bacterial attack and definition of basic plant design parameters.

The following summary details the testwork programme that has been carried out covering the four phases of activity as noted above:

I) Depending on the analyses to be carried out, and the specific minerals to be examined, the study was effectuated on samples from run-of-mine ore, galena,

sphalerite and pyrite concentrates produced at the Olympias industrial flotation plant. Bulk chemical analysis of the as-received ore and concentrates samples is shown in Table 1.

Polished sections of all samples were prepared, for the various analyses to be effectuated.

Optical microscopy was employed to determine the major minerals present and examine the occurrence of visible gold.

For quantitative model analysis the optical image analyser Cambridge Quantimet 900 was used coupled with Scanning Electron Microscope (SEM). For SEM analysis a Cambridge Stereoscan 250 instrument was employed with Lemont backscattered electron detector. Electron Microprobe Analysis (EPMA) was conducted with a Cameca microbeam Camebax. The methods used to locate gold within the pyrite concentrate and define its mode of occurrence included: Laser ablation coupled with Inductively Coupled Plasma Mass Spectroscopy (ICP/MS), Ion microprobe (SIMS), and Mössbauer Spectroscopy.

For Laser ICP/MS analysis the Plasmaquad PQ_2 + ICP/MS equipment was used. To complement the above technique the ion microprobe Cameca IMS 3f installed at the Western Ontario University Canada was employed. The specific methodologies developed for gold analysis at trace levels within pyrite and arsenopyrite matrices are presented within the text of the report. Mössbauer measurements were organised by Ph Marion (Marion 1988) and conducted by F Wagner at the University of Munich (Wagner 1986, Wagner 1988).

Surface morphology of pyrite minerals after bacterial oxidation was examined with SEM. Polished sections of the as-received pyrite concentrate (d_{85} -85 μm) were observed before and after being placed in the bio-oxidation reactors for different time periods. Polished sections of the bio-residues (d_{95} -38 μm) were also prepared and examined under SEM to assess the actual degradation of pyrite matrix after bacterial oxidation.

II) Preliminary laboratory flotation tests on the Olympias concentrate to separate pyrite and arsenopyrite mineral phases and to evaluate the associated gold distribution and provide samples for the bio-oxidation testwork.

III) A three phase evaluation of the bio-oxidation process to identify the mechanism of bacterial attack on the sulphide mineralisation of the Olympias pyrite and to determine the overall gold recovery attainable utilising bio-oxidation techniques (figure 1).

iv) Batch bio-oxidation testwork using air sparged pachucas to assess the effect of the following parameters on bio-oxidation performance.

Ferrous iron concentration in the nutrient medium
pH
Redox potential (EMF)
Pulp density
Retention time
Particle size

v) A preliminary study of the effects of bio-oxidation by surface examination of mineralogical samples before and after treatment by bio-oxidation to show zones where mineral dissolution has occurred. In parallel, similar examinations have been carried out on bio-oxidation residue samples to show areas of preferential attack.

vi) Determination of the bio-oxidation mechanism prevalent in the attack of the Olympias pyrite thus allowing development of the basic process flowsheet that is applicable for treating this material on a large scale.

vii) Cyanidation of untreated Olympias Pyrite concentrate to give base data for gold recovery.

viii) Total oxidation dissolution of the sulphide mineralisation using nitric acid digestion techniques. This allows determination of the maximum gold recovery achievable by oxidation of the sulphide minerals thus indicating the quantity of gold associated with sulphide mineralisation and, by difference, the gold associated with non-sulphide mineralisation.

ix) Cyanidation of bio-oxidation residues to determine the relationship between gold recovery and level of sulphur oxidation. The effect of retention time is also included in terms of gold recovery obtained and the level of sulphur oxidation achieved.

x) An evaluation of the effects of neutralisation on liquid effluents from bio-oxidation (bio leachate) to determine limestone and lime consumptions required. Further examination of the stability of precipitates produced from the neutralisation of bio-oxidation liquors and cyanidation.

xi) A detailed evaluation of the thickening and filtration characteristics of the bio-oxidation residue produced from the treatment of the Olympias pyrite material to assist in the determination of downstream plant requirements.

4. GENERAL CONCLUSIONS

4.1. OVERALL CONCLUSIONS

The results of the mineralogical analysis carried out by BRGM support the general findings of both Davy McKee and METBA with respect to the mode of gold occurrence within the Olympias pyrite concentrate matrix, emphasising that gold is mainly associated with arsenopyrite and arsenic rich inclusions in the pyrite lattice.

Optical observations of polished sections before and after bacterial oxidation indicate the preferential attack of boulangerite and arsenopyrite compared to pyrite. The variation in gold and silver recovery under different oxidation conditions indicates that the gold and silver values are segregated into different mineral phases.

The preferential attack of boulangerite and arsenopyrite may be attributable to ferric iron attack, while pyrite oxidation is also associated with direct bacterial contact with the mineral surface. Preferential arsenopyrite dissolution becomes more evident at higher pulp densities. However, increased arsenic levels in solution may hinder bacterial activity at pulp densities in excess of 15% solids.

It is evident that arsenopyrite dissolution requires an initial ferric iron concentration in solution but that the redox potential of the system may be lower than that required for pyrite dissolution. Further, it has been shown by the testwork that an optimum pH range around 1.2 may exist for the bio-oxidation system utilised. However, further evaluation is required to determine the effect of pH control on the performance of the bio-oxidation system.

In summary, the testwork has indicated that a residence time distribution of between 5 and 8 days is required, for the system examined, to achieve the desired degree of sulphur oxidation and hence gold recovery. However, due to the preferential oxidation of arsenopyrite and the different conditions required for selective arsenopyrite and pyrite oxidation, the actual residence time employed for any given system will be a function of the pyrite, arsenopyrite ratio and gold distribution between these two mineral phases.

In the case of the Olympias pyrite, mineralogical examination and interpretation of the bio-oxidation testwork results shows that approximately 75-80% of the total contained gold is associated with the arsenic-rich mineral sites. Thus, to treat this materials using bio-oxidation techniques, a system designed to preferentially oxidise the arsenopyrite and arsenic-rich mineralisation is required to achieve gold recoveries of the order of 80% without the need for high total sulphur oxidation values. This means that a system designed for high pulp densities with low retention

times at high ferric iron concentrations and redox potential is desirable. However, the operation of such a system will be highly dependent upon the economics of the process. If gold recoveries higher than 75-80 % are necessary from an economic viewpoint, then consideration must be given to the additional plant costs that would be associated with extended retention times required to recover the remaining 25% of the total contained gold that has been shown to be associated with the less easily oxidised pyrite mineralisation.

4.2. MINERALOGICAL CONCLUSIONS

The mineralogical investigations carried out on the Olympias pyrite have produced the following conclusions:

i) With the analytical techniques used, gold has been detected in both the pyrite and arsenopyrite fractions. In both cases, a heterogeneous arsenic and gold distribution was noted (figure 2).

ii) The gold concentration associated with the arsenian pyrite inclusions was higher than that noted in "true" pyrite.

iii) In arsenian pyrite, gold enrichment was observed around boulangerite inclusions. However, gold was not observed within the boulangerite inclusions.

To qualify the above, it should be noted that the free boulangerite grains observed within the concentrate were not analysed for gold.

iv) Mössbauer spectrometry has shown that gold is contained mostly within the arsenopyrite fractions. No distinction was made between gold contained within the arsenian pyrite and gold contained within the arsenopyrite phases.

Mössbauer spectroscopy has also shown that gold is present within the concentrate as an alloy with a heavy element. The scope of the investigation has not allowed for the identification of this alloy and heavy element.

Results obtained by SIMS (Secondary Ion Mass Spectroscopy) and laser beam coupled with ICP-MS indicate the occurrence of gold in both pyrite and arsenopyrite minerals (figure 3).

v) Combining all data available from modal analysis and from gold distribution calculations, it is deduced that gold concentration in arsenopyrite and pyrite amounts to 50-52 ppm and 21-22 ppm, respectively. Gold

concentration in boulangerite was calculated to average 45 ppm, however gold association with this mineral needs to be further investigated. The values given above are extreme values for each mineral.

It should be noted that pyrite refers to both arsenic-free and arsenian pyrite. As previously described, gold distribution within arsenian pyrite and arsenopyrite appeared quite heterogeneous.

The above data are consistent with those recently reported by Cook and Chryssoulis (1989), Cabri et al (1989) and Chryssoulis (1989) on refractory gold. Cook and Chryssoulis (1989) examined 12 sulphide-rich ore deposits. Although invisible gold concentrations in specific minerals varied considerably from deposit to deposit, a positive correlation between the concentrations of arsenic and gold in pyrite was shown to exist for most of the analysed ores.

Examination of some specimens originating from the Olympias deposit, indicated an average gold concentration of 36 $\pm$ 12 ppm gold in arsenian pyrite areas, while gold was only present at levels lower than 2 ppm, in pyrite containing less than 0.5% As in weight. It was reported that compositional zoning of As within the pyrite is widespread and the two types are closely intergrown. Arsenopyrite gold content was 49 $\pm$ 24 ppm.

The positive correlation between the gold and arsenic concentration within the arsenian pyrite, suggests that substitution of gold into the pyrite lattice might be facilitated by the presence of arsenic as suggested by Boyle (1979).

Note: The values given above are extreme values for each mineral Pyrite refers to both "true" pyrite (arsenic free pyrite), and arsenian pyrite.

4.3. BIO-OXIDATION CONCLUSIONS

The initial bio-oxidation testwork on the Olympias pyrite carried out in parallel by Davy McKee and METBA has produced the following conclusions:

I) The Olympias pyrite concentrate is highly refractory as only 4% gold recovery and 40% silver recovery is typically obtained on direct cyanidation of the untreated material.

II) Nitric acid digestion of the concentrate in which 96% sulphur oxidation was achieved has indicated that precious metal recovery in excess of 85% gold and 95% silver can be obtained.

iii) Bio-oxidation testwork has shown the amenability of the Olympias pyrite concentrate to this oxidation process with maximum gold and silver recoveries of 84% and 92% respectively being reported. The corresponding maximum degree of sulphur oxidation was 75%. (Figure 5).

iv) The testwork carried out to determine the predominant method of bacterial attack has suggested that the gold and silver values are segregated within different mineralisations. Further, evidence from the testwork suggests that the silver values are held in less refractory (more easily oxidised) mineralisation than that for the gold values.

v) It has been shown that the presence of ferric iron in solution increases the preferential dissolution of arsenopyrite as compared to pyrite.

vi) There is strong evidence to show that arsenopyrite oxidation will occur at lower redox potential than that required for pyrite oxidation (figure 6).

vii) The tolerance of the bacterial cultures used to low pH values and high arsenic concentrations (greater than 15 g/l) have been observed.

viii) Experiments to determine the effects of pH on bio-oxidation suggest that, for the system utilised, an optimum pH range of around 1.2 may exist.

ix) Preferential arsenopyrite oxidation becomes more evident at higher pulp densities, possibly as a result of higher ferric iron concentrations. However, there are some indications that, for the system utilised, bacterial action may be hindered by pulp densities in excess of 15% w/v.

x) It is evident from the cyanidation tests on the bio-oxidation residues that, for any given level of sulphur oxidation, the associated gold recovery may vary depending upon the prevailing oxidation mechanism.

xi) The recovery of silver by cyanidation may be limited by the suspected formation of jarosite compounds produced during bio-oxidation or, more likely, produced during the neutralisation stage prior to cyanidation.

xii) During the cyanidation tests, an average consumption of between 10 and 30 kg/tonne residue of sodium cyanide was observed.

xiii) In Downstream residue treatment the need for adequate washing of the bio-oxidation residue prior to cyanidation in order to minimise cyanide consumption has been shown. Testwork has demonstrated that thickening of the bio-oxidation residues prior to filtration is necessary with close control on washing and neutralisation steps to minimise jarosite compound formation. Conventional process equipment has been shown to be suitable for this duty.

Figures 7, 8, 9, 10 and 11 are included to support the above conclusions.

4.4. GENERAL CONCLUSIONS

Although the work carried out under the scope of this study has been limited to one concentrate type, the results are sufficiently encouraging to indicate that bio oxidation techniques may be applied to many pyritic ores and concentrates since the mechanisms of bacterial attack on arsenopyritic and pyritic materials have been clearly identified.

With this information it is possible to design a bio oxidation system to meet the requirements of a particular feed material with respect to retention time, pulp density, pH, Eh etc.

The economic viability of bio oxidation is a subject that requires further evaluation. Although it is a relatively straightforward exercise to compare bio oxidation as an independent treatment process to competing technologies such as roasting and pressure oxidation, this does not necessarily reflect the economic benefits of using bio oxidation as, for example, a pretreatment process to pressure oxidation where the techniques of bio oxidation are used solely to modify the sulphur feed rate to the pressure oxidation autoclaves.

It has not been possible within the scope of this study to carry out a detailed investigation of the economics of refractory ore processing technologies, but a brief evaluation based on the bio oxidation flowsheets developed during the execution of the study has allowed development of a brief comparative table given here as table 2.

Based upon the conceptual flowsheets and equipment lists presented in the report and table 2 there is evidence to support the conclusion that bio oxidation offers an economically viable alternative to conventional technologies for refractory ore treatment processes. However, further work is required to determine the implications of feed tonnage and the effects, if any, exhibited by the economy of

scale criteria. Further, the economic viability of incorporating bio oxidation technology as a pretreatment to pressure oxidation is a subject requiring a dedicated evaluation.

5. REFERENCES

Boyle, R W 1979: "The geochemistry of gold and its deposits". Geological Survey of Canada Bulletin 280.

Cabri L J and Chryssoulis, S L 1989: "Analytical techniques for determination of invisible gold in refractory ores", presented at GAC/MAC Annual Meeting, May 1989, Montreal.

Cabri L J et al 1989: "The nature of invisible gold in arsenopyrite" accepted for publication in Canadian Mineralogist.

Marion Ph 1988: "Charactérisation de minerals sulfurés aurifères: mise en oeuvre de méthodes classiques et nouvelles". Thèse de Doctorat d'état, Nancy.

Wagner F E, Marion Ph, Regnard J R, 1986: "Mössbauer study of the chemical state of gold in gold ores". Gold 10, vol 2: Extractive Metallurgy of Gold South Afr Inst of Mining and Metallurgy, Johannesburg 1986, pp 435-443.

Wagner F E, Marion Ph, Regnard J R, 1988: "A Mössbauer study of gold ores, mattes, roaster products and gold minerals", Hyperfine Interactions, vol 41 (1988) pp 851-854.

TABLE 1

CHEMICAL AND PARTICLE SIZE ANALYSIS
OF OLYMPIAS CONCENTRATE SAMPLE.

PARTICLE SIZE ANALYSIS		CHEMICAL ANALYSIS						
Mesh Tyler (µm)	Retained weight %	Fe %	S %	As %	Zn %	Pb %	Au ppm	Ag ppm
+80 (+180)	13.9	40.4	39.2	9.0	2.0	0.7	31.8	22.4
-80+115 (-180+125)	11.6	43.2	38.8	8.5	1.0	0.5	26.9	13.6
-115+170 (-125+90)	18.8	44.4	39.8	10.0	0.3	0.3	28.5	10.2
-170+250 (-90+63)	14.9	40.8	41.0	13.0	0.2	0.3	27.6	7.8
-250+325 (-63+45)	15.8	42.4	39.4	13.0	0.2	0.3	30.8	8.4
-325 (-45)	25.0	40.8	37.8	13.0	1.0	0.7	34.6	23.3
TOTAL	100.0	42.0	39.2	11.4	0.8	0.5	30.5	14.9

PARTICLE SIZE ANALYSIS		DISTRIBUTION						
Mesh Tyler (µm)	Retained weight %	Fe %	S %	As %	Zn %	Pb %	Au %	Ag %
+80 (+180)	13.9	13.4	13.9	11.0	37.6	19.7	14.5	20.9
-80+115 (-180+125)	11.6	11.9	11.5	8.7	15.1	11.3	10.2	10.6
-115+170 (-125+90)	18.8	19.9	19.1	16.6	8.2	12.3	17.6	12.8
-170+250 (-90+63)	14.9	14.5	15.6	17.1	3.6	9.2	13.5	7.8
-250+325 (-63+45)	15.8	16.0	15.9	18.1	3.4	10.4	15.9	8.9
-325 (-45)	25.0	24.3	24.1	28.6	32.2	37.1	28.3	39.0
TOTAL	100.0	100.0	100.0	100.0	100.0	100.0	100.0	100.0

TABLE 2

REFRACTORY ORE TREATMENT

CAPITAL COST COMPARISON

	No Acid Plant	Acid Plant	Acid Plant & Neutralization
ROASTING			
Concentrate Fluid Bed	100	115	130
Whole Ore Fluid Bed	105	120	135
Whole Ore Circulating Fluid Bed	90	105	120
HYDROMETALLURGICAL OXIDATION (CONCENTRATE)			
Autoclave			125
Autoclave and Chlorination			140
Bio Oxidation			130

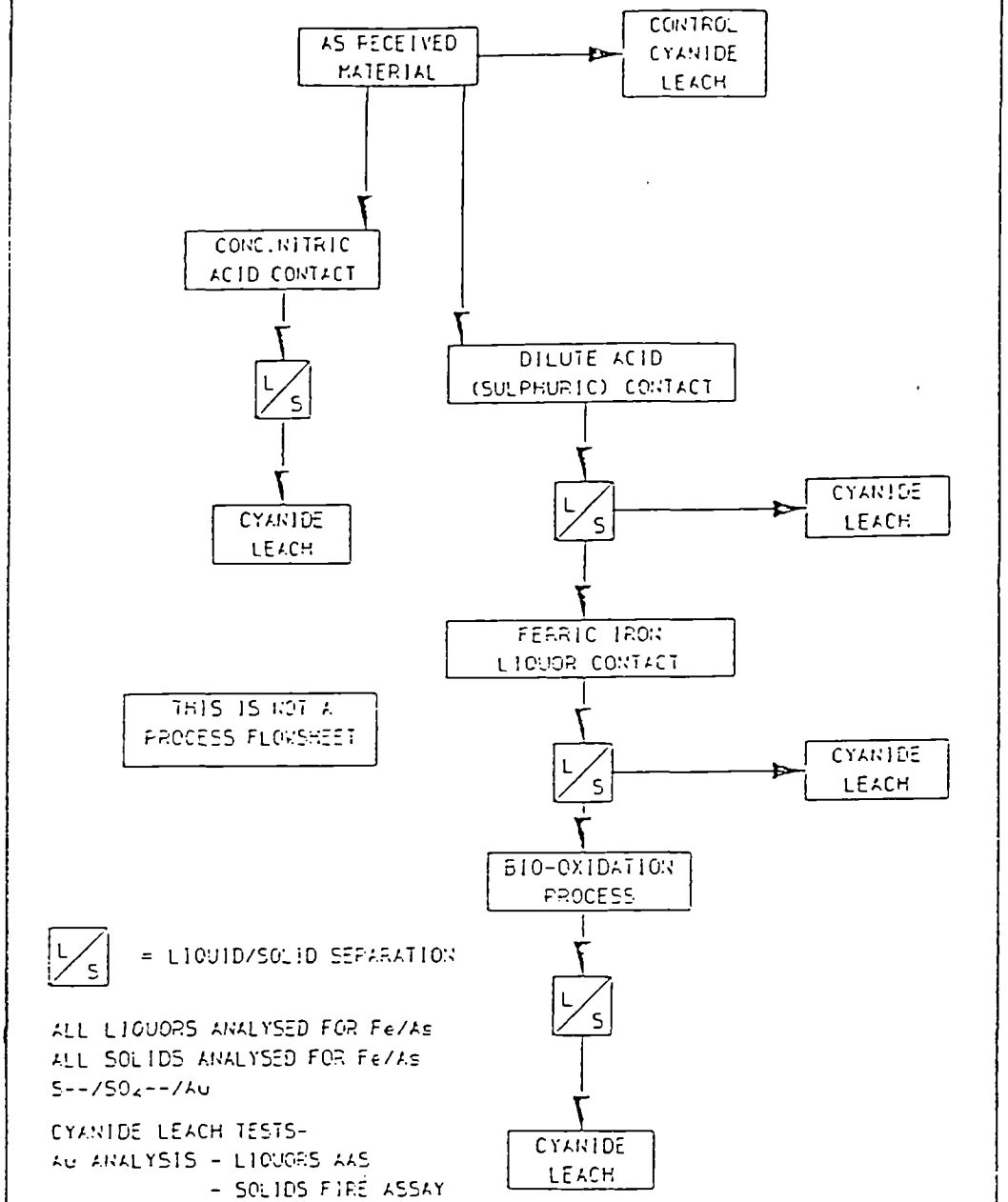

EXPERIMENTAL WORK PROGRAMME OUTLINE

Davy McKee
Stockton-on-Tees

Figure 1

Figure 2

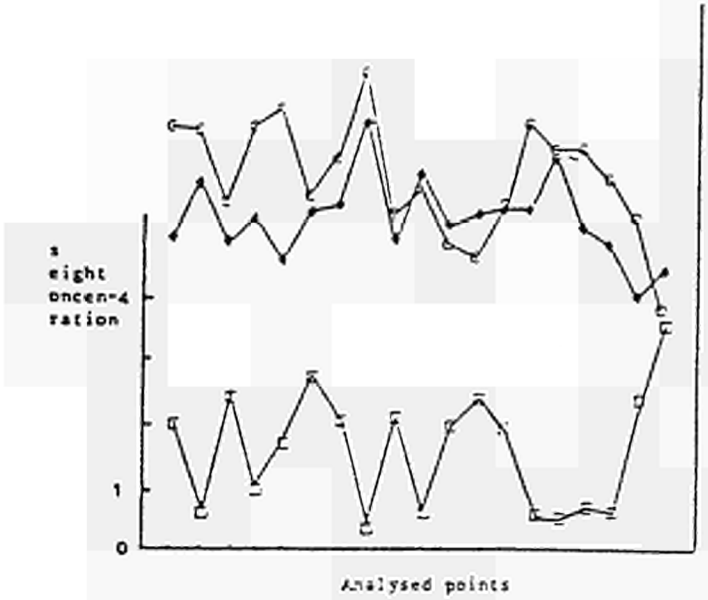

LINE PROFILE : PYRITE

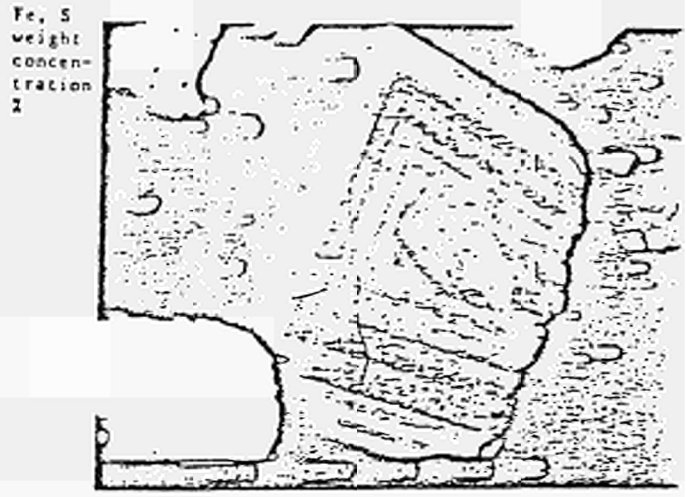

A - Pyrite

SEM images in backscattered electron mode

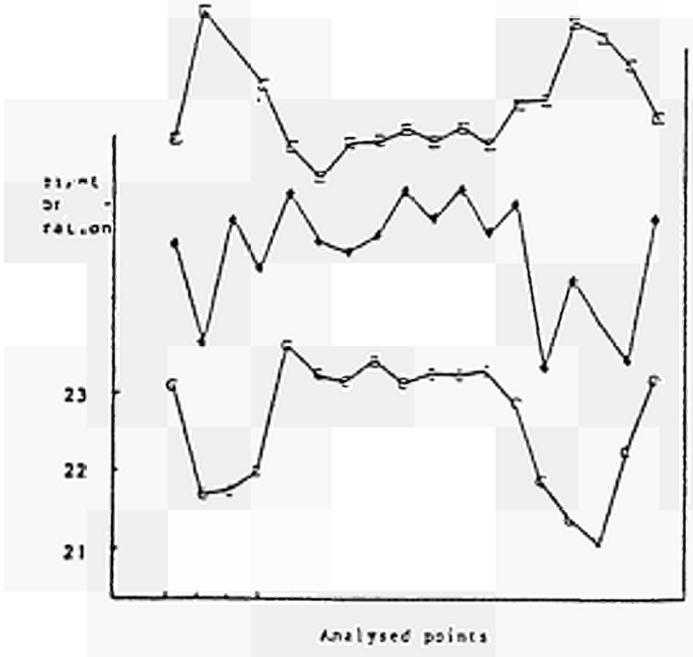

LINE PROFILE : ARSENOPYRITE

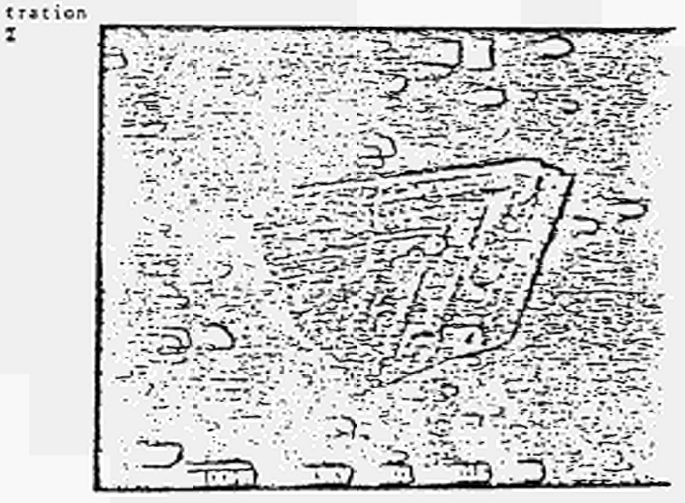

B - Arsenopyrite

Figure 3

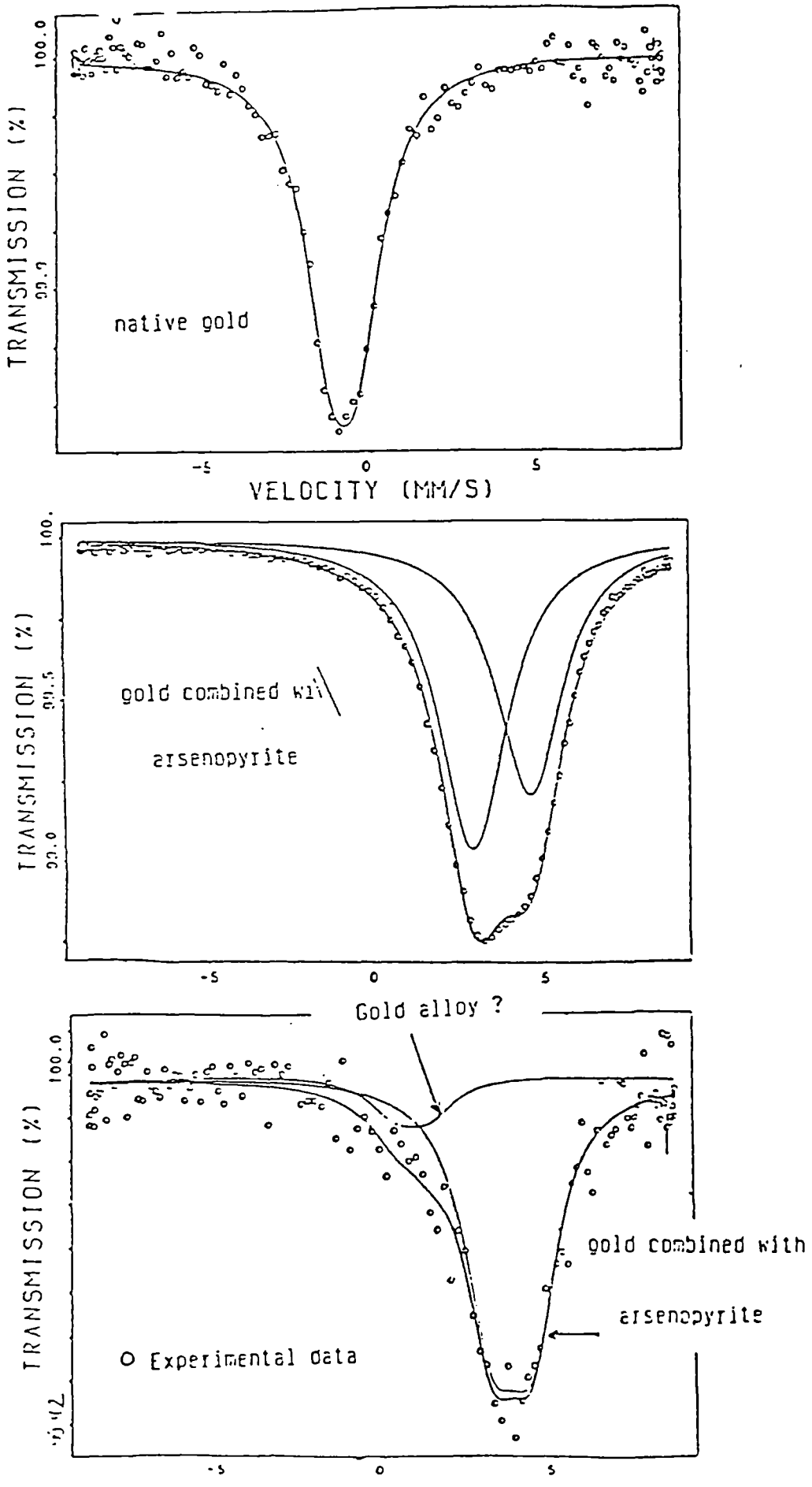
TRANSMISSION (%)
100.0
native gold
-5
0
5
VELOCITY (MM/S)
TRANSMISSION (%)
100.
gold combined wi
arsenopyrite
-5
0
5
Gold alloy ?
TRANSMISSION (%)
100.0
gold combined with
arsenopyrite
O Experimental data
-5
0
5

Figure 4

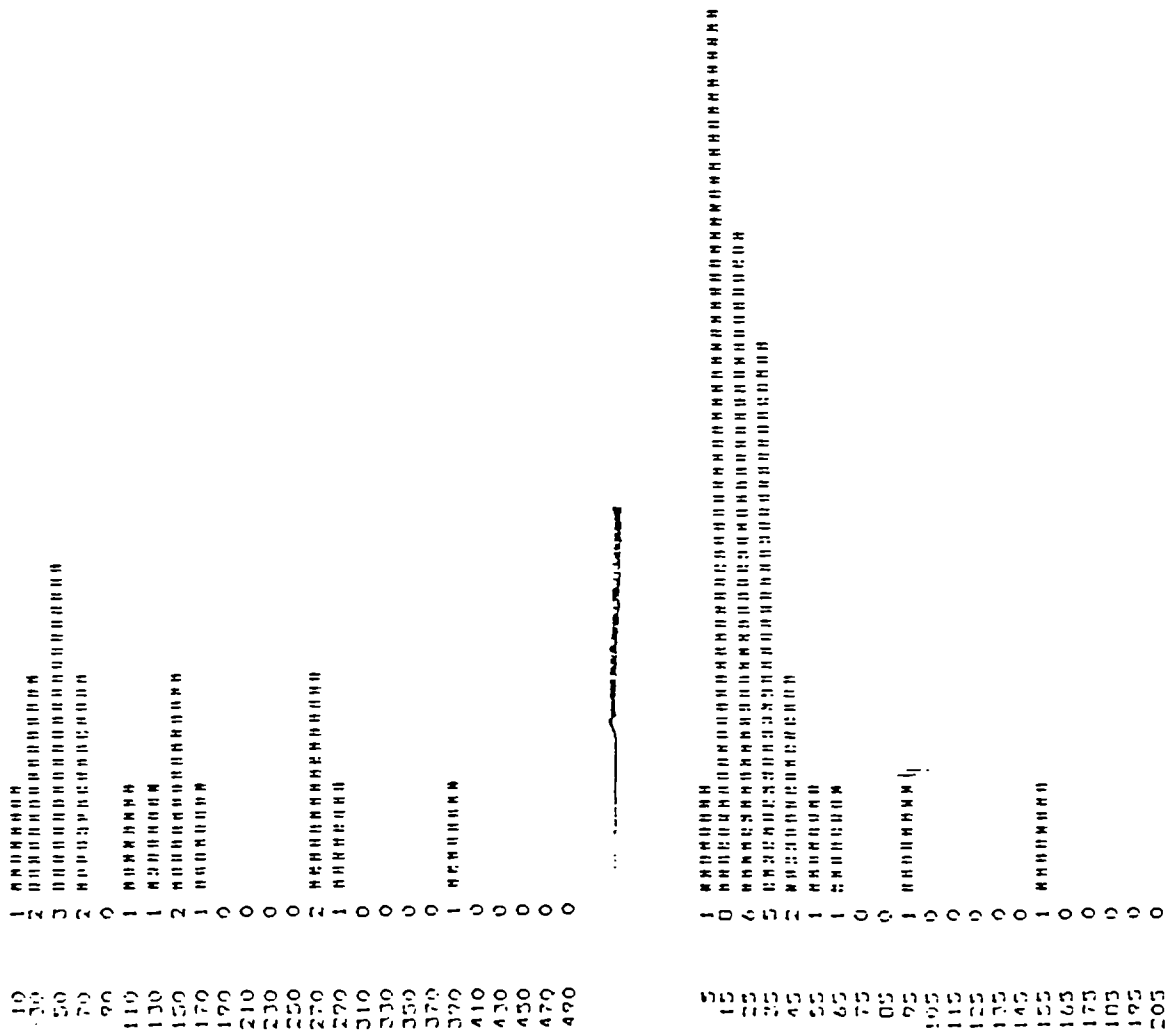

Figure 4 - Histogram distribution of gold concentrations obtained by SIMS analysis of arsenopyrite (a) and pyrite (b) minerals from an Olympias ore specimen.

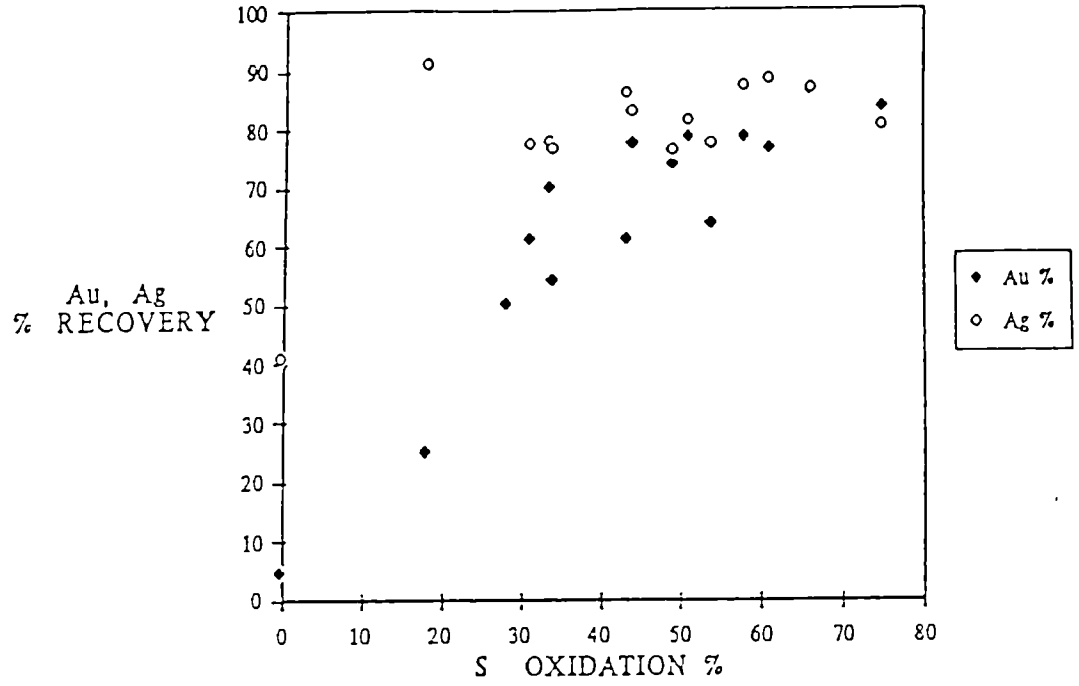

Gold and Silver Recovery vs Sulphur Oxidation in Olympias pyrites bioresidues.

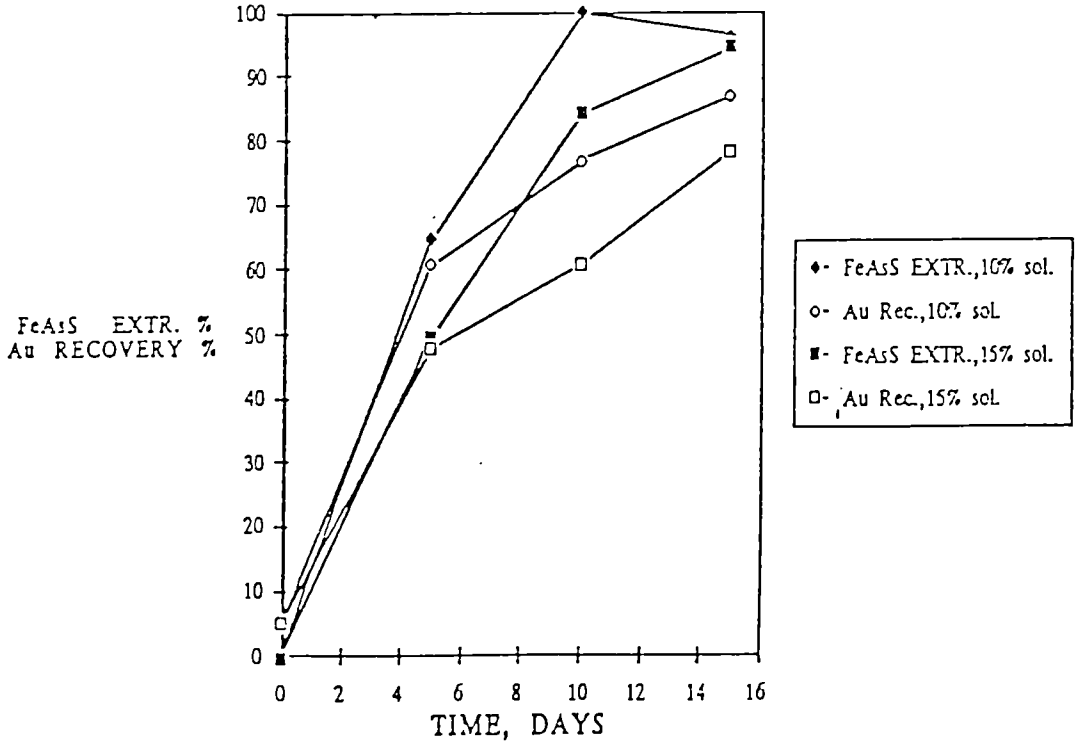

FIGURE 5 : FeAsS Extraction and Gold Recovery vs Time from Pachuca tests at 10% and 15% solids.

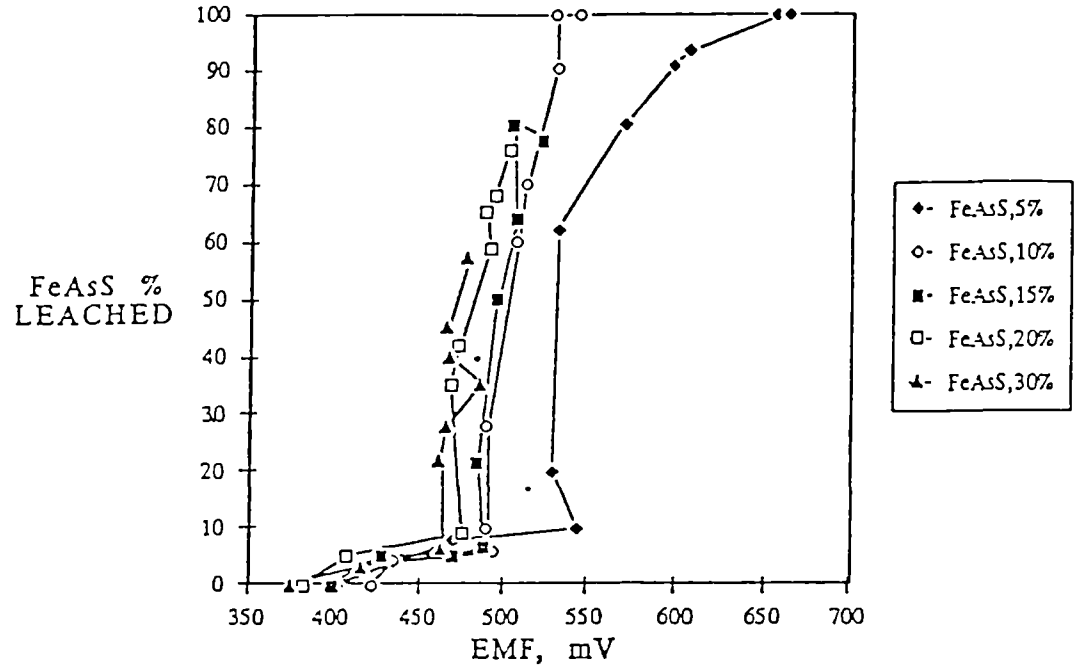

(a)

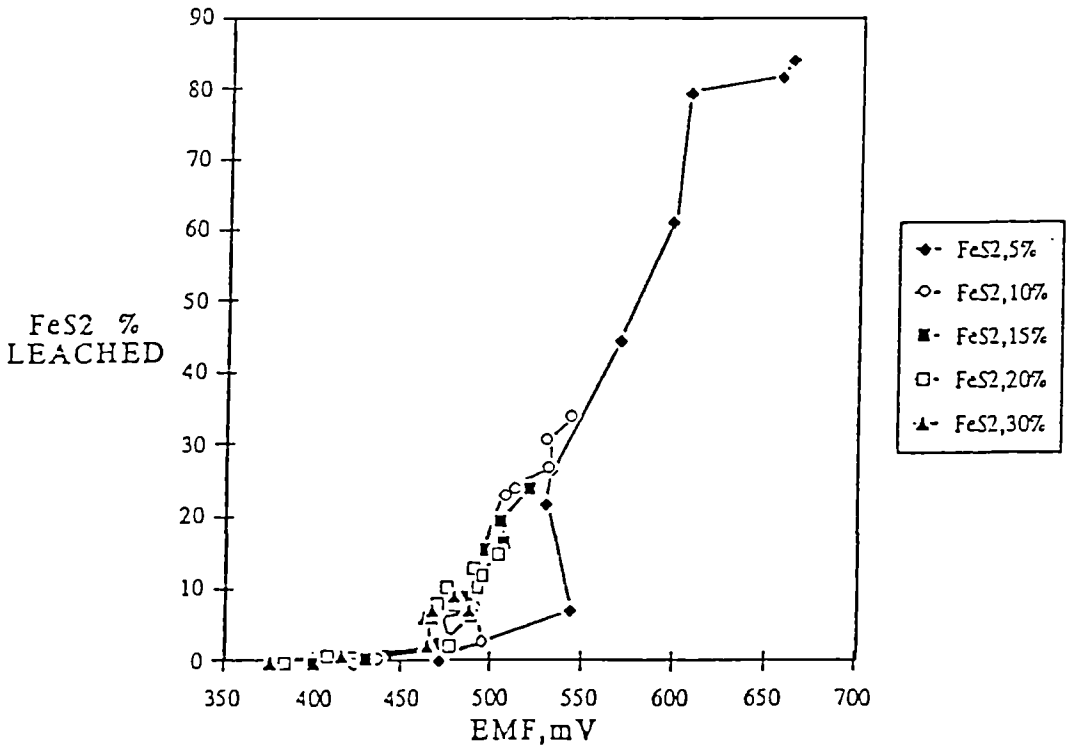

(b)

FIGURE 6: (a) FeAsS, (b) FeS_2 % leached vs EMF.
Pachuca tests PB1-PB5. Retention Time: 10 days.

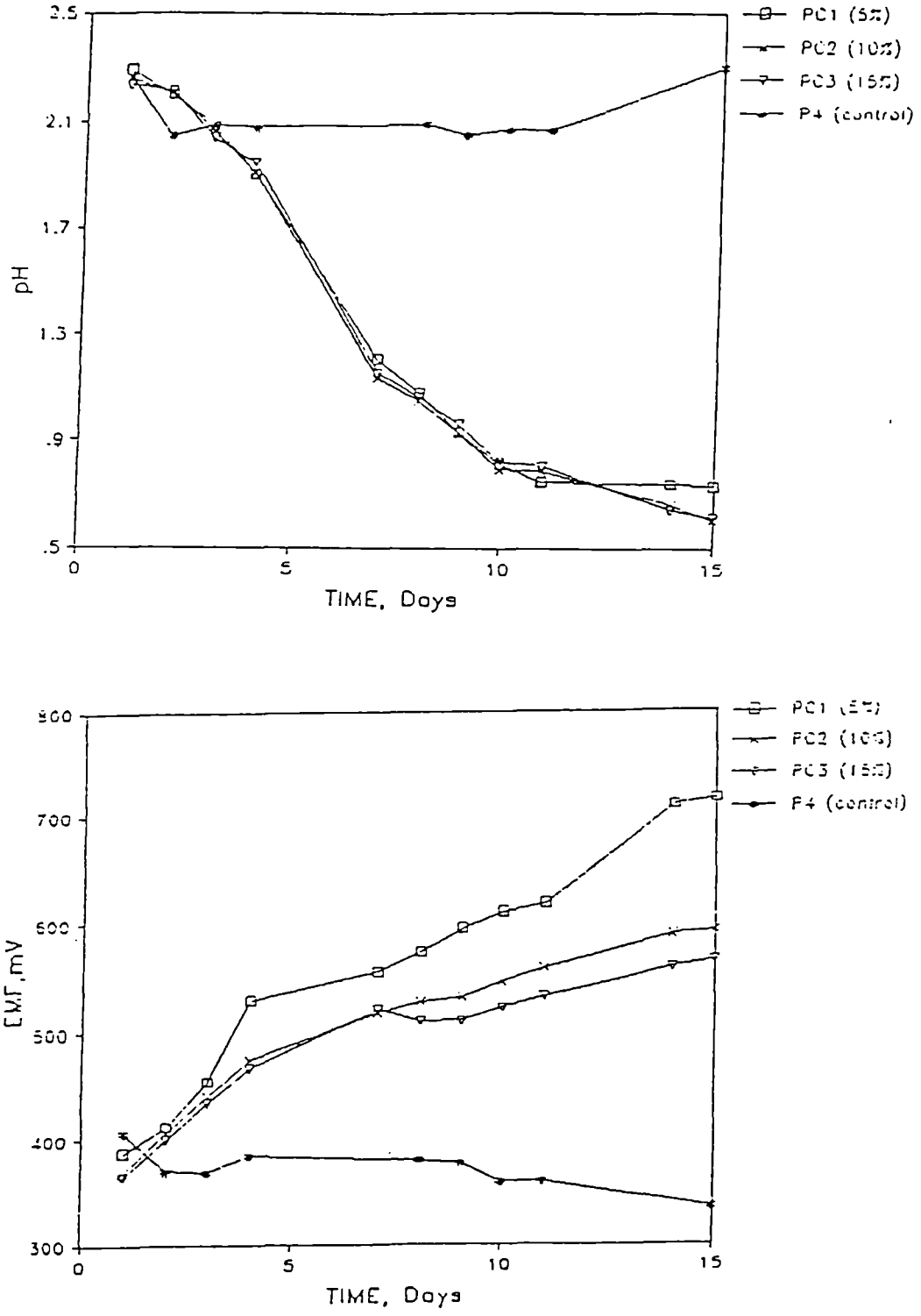

FIGURE 7 : (a) EMF and (b) pH vs time Pachuca tests : PC1, PC2, PC3 & P4. Retention time: 15 days.

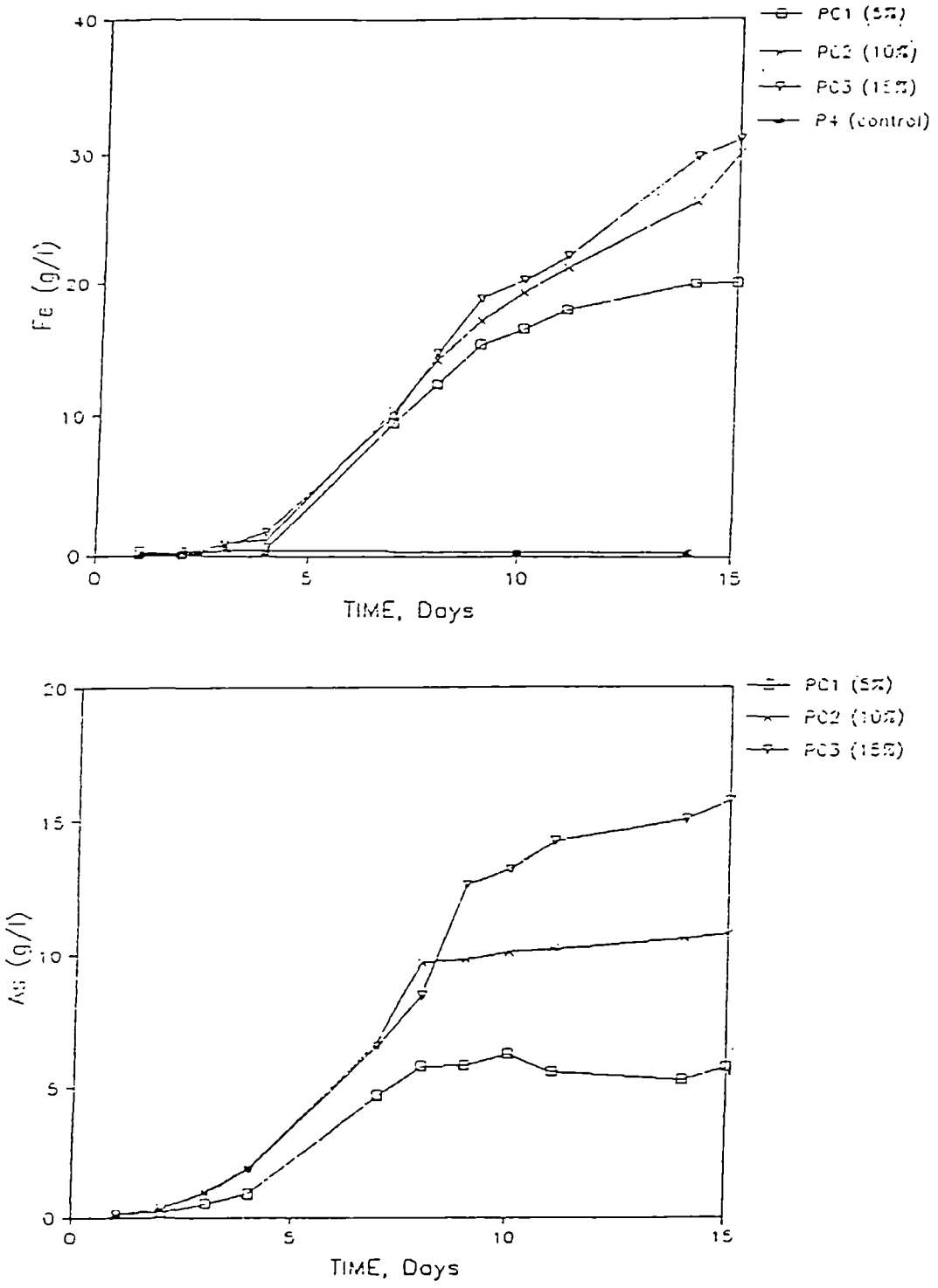

FIGURE 8 : (a) Fe and (b) As levels in Solution vs time. Pachuca tests : PC1, PC2, PC3 & P4. Retention time: 15 days.

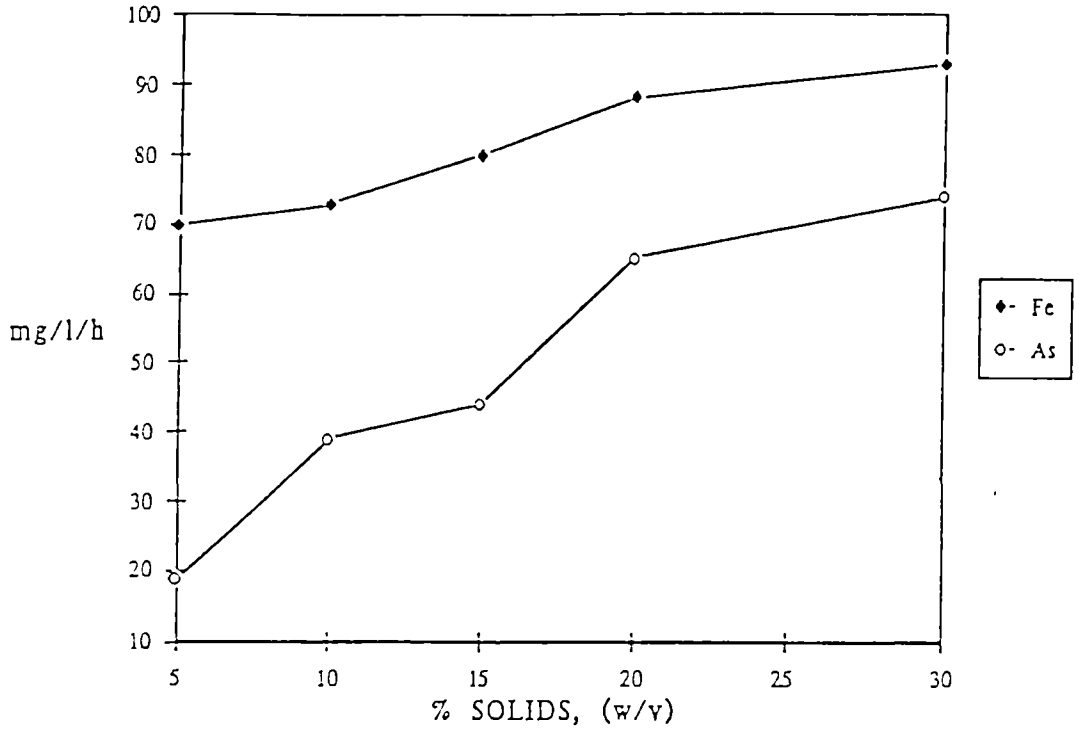

Fe and As average leaching rates vs pulp density.
Pachuca tests PB1-PB5. Retention Time: 10 days.

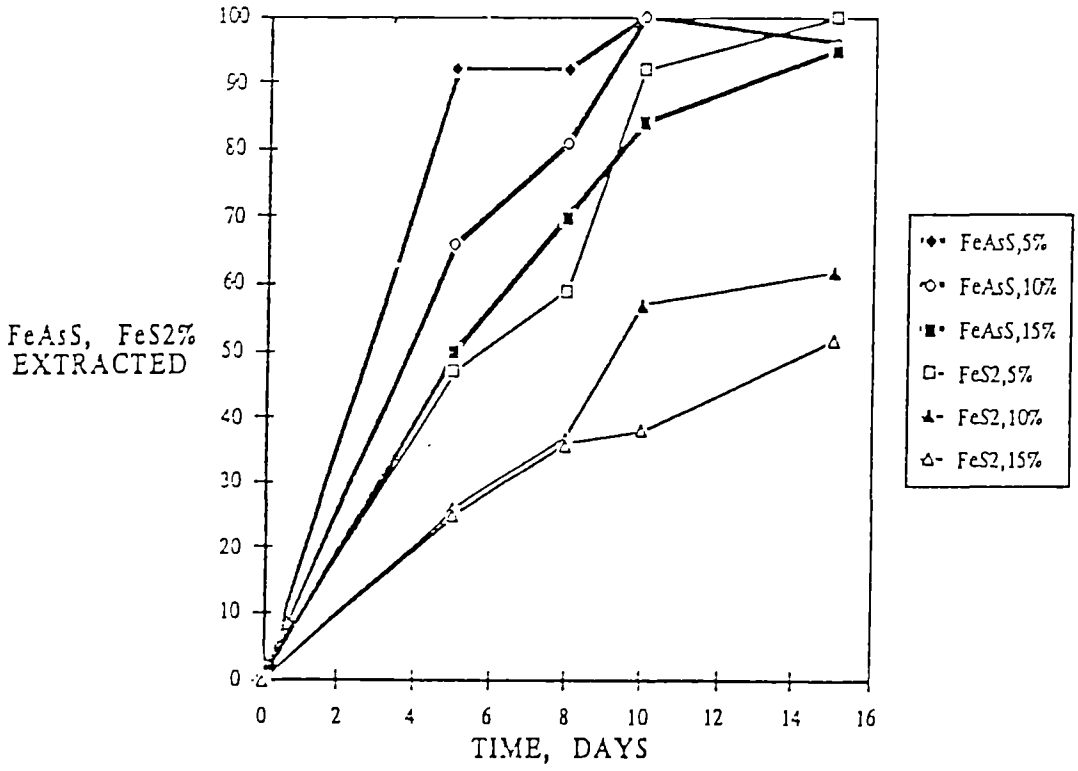

FIGURE 9: FeAsS, FeS2 % extacted vs time at different pulp densities.

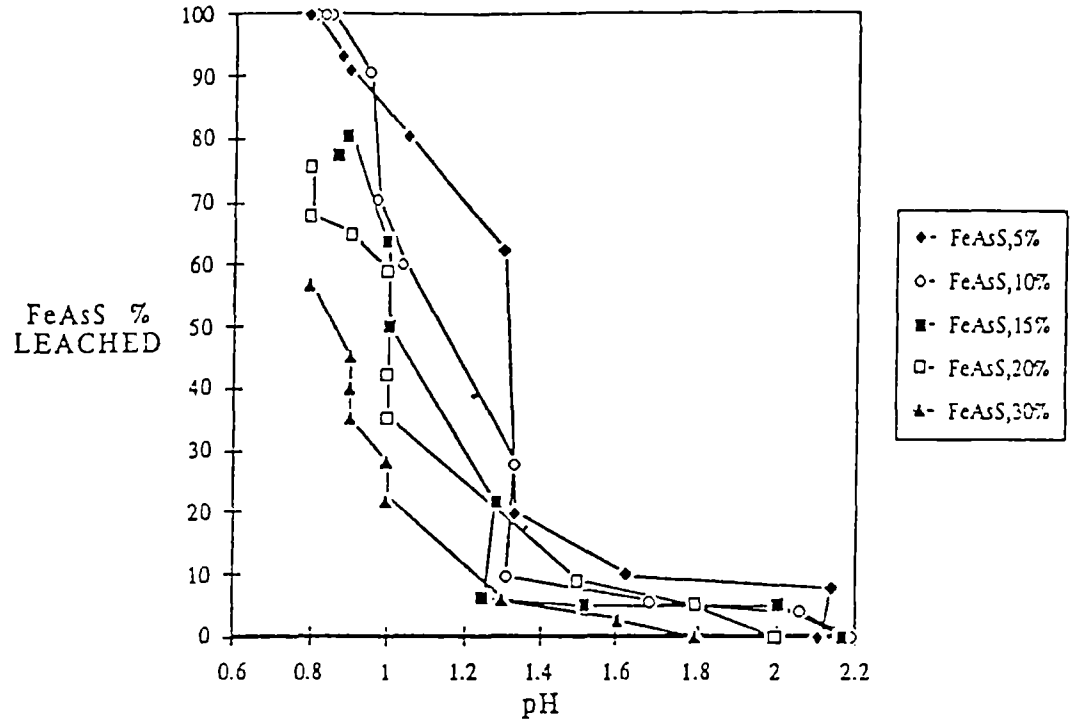

(a)

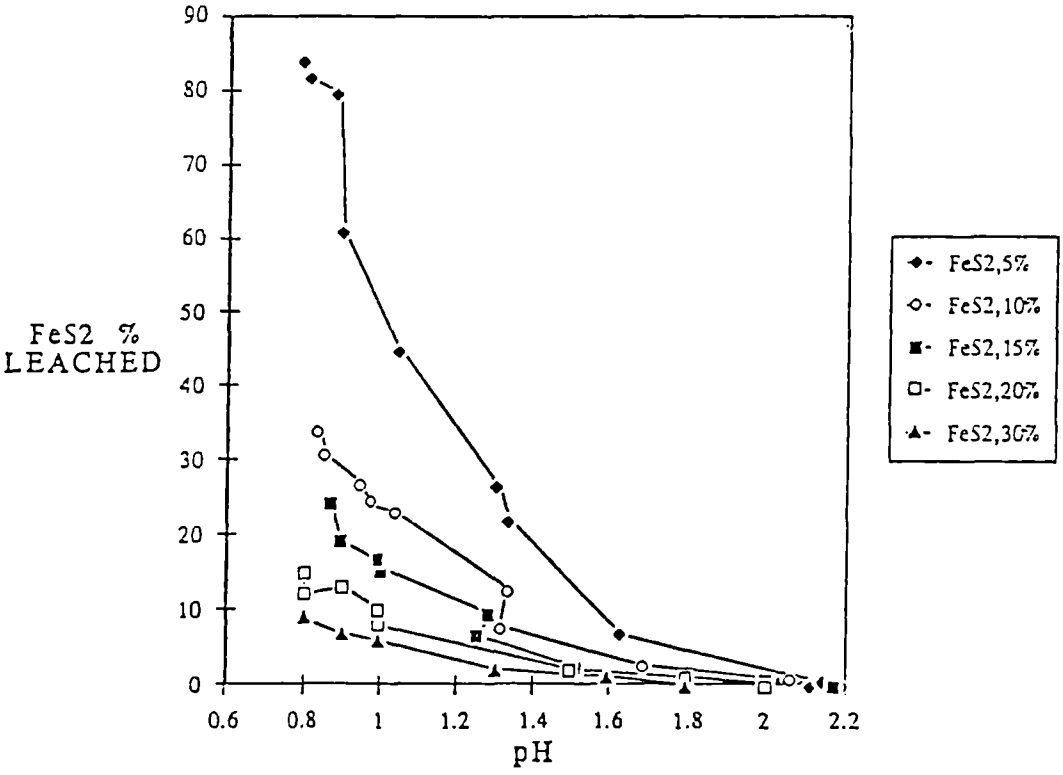

(b)

FIGURE 10: (a) FeAsS, (b) FeS_2 % leached vs pH. Pachuca tests PB1-PB5. Retention Time: 10 days.

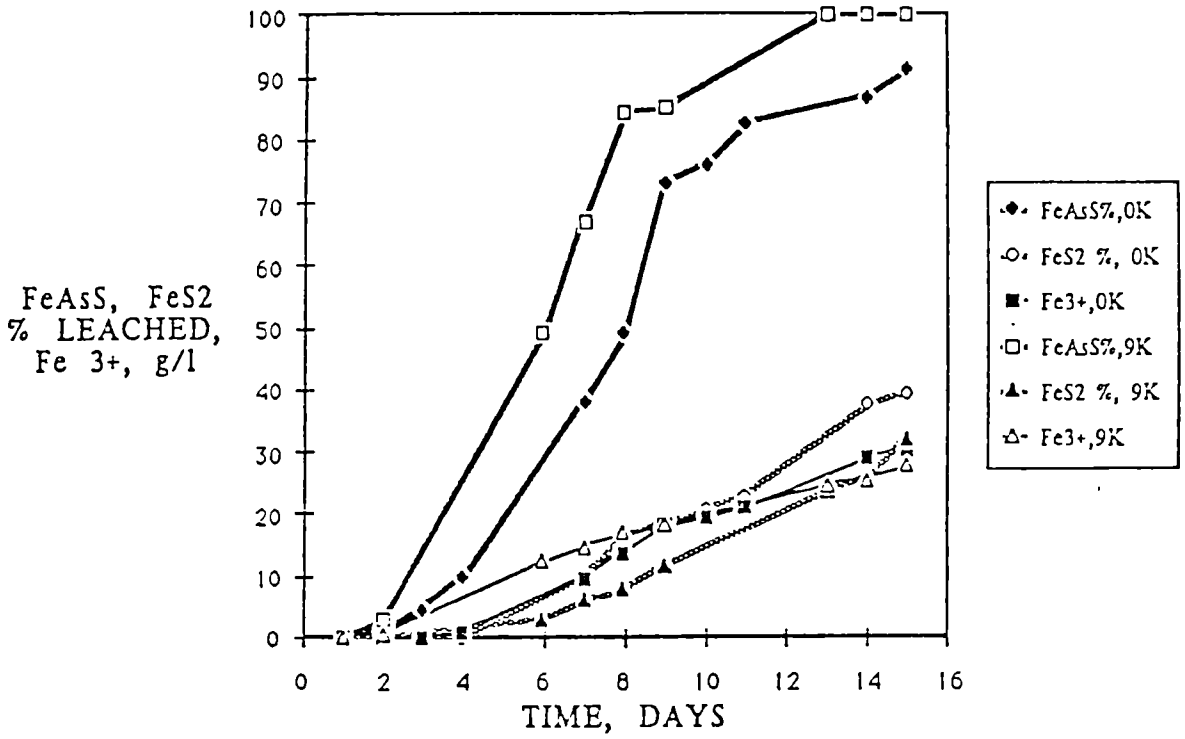

FIGURE 11: FeAsS, FeS_2 % leached vs time.
Pachuca tests PC3 (0K) and PE2 (9K). Retention Time: 10 days

RESEARCH AREA 3.3

PYROMETALLURGICAL PROCESSING OF SULPHIDES AND OTHER ORES

SIMULTANEOUS RECOVERY OF ZINC, COPPER AND LEAD AS METALS FROM COMPLEX SULPHIDES IN A SINGLE POLYMETALLIC SMELTING FURNACE

Project Leader: N A WARNER
School of Chemical Engineering, The University of Birmingham, United Kingdom

Mineral Industry Research Organisation, United Kingdom

RTZ Limited, United Kingdom

Billiton Research BV, Arnhem, Netherlands

Contract MA1M-0033-UK(H)

1. OBJECTIVE

The ultimate aim of the project was to demonstrate the technical viability of a process scheme to produce individual metallic products from complex sulphide ores. Complex sulphides generally relate to extremely fine-grained pyritic polymetallic base metal minerals of volcanic origin. The metals of economic value in these ores are copper, zinc, lead, silver, gold, tin, cadmium, indium, selenium and tellurium. The metals occur as constituents of the minerals chalcopyrite, sphalerite, galena, tetrahedrite and cassiterite. For a typical range of complex sulphides and pyritic ores the major base metal is usually zinc followed by lead and copper. For this reason the project was aimed at the feasibility of extracting these three metals pyrometallurgically without recourse to complicated separation procedures at the ore dressing stage.

2. INTRODUCTION

Theoretical studies and background laboratory work previously reported in papers stemming from research in the School of Chemical Engineering at the University of Birmingham (1) - (11) lead to the belief that there exists the basis of a technically viable process for direct smelting of zinc and lead sulphide ores using a Cu/Cu_2S intermediary. In order to pursue the project further it was therefore deemed necessary to construct and operate a pilot plant in which all the major aspects of the process route would ultimately be evaluated. In consequence a pilot plant programme was formulated and

activated under the sponsorship of a number of Mineral Industry Research Organisation (MIRO) member companies with financial assistance initially from British Technology Group (BTG) and the Department of Trade and Industry.

During Phase I of this programme, plant design and construction was carried out followed by a limited amount of commissioning work. Phase II has been supported by the MIRO members RTZ and Billiton, and BP Minerals before their absorption into RTZ, with a major research grant from the Commission of the European Communities. Detailed descriptions of the work carried out under the phase have been given both in reports to MIRO and at six-monthly intervals in reports to the CEC along with the final CEC report.

The metallurgical features that distinguish the process being developed at Birmingham University are:

1. The process is fully continuous and uses rapid reactions to simultaneously produce copper, zinc and lead in the one reactor.
2. Zinc metal is produced directly from zinc sulphide without going through the oxide phase. This feature is unique among smelting processes and reduces substantially the amount of purchased energy required for zinc metal production and, particularly, eliminates the need for energy in the expensive forms (i.e. D.C. electrical power or high grade metallurgical coke) which existing processes require for oxide reduction.

3. The need for submerged tuyeres or lances is eliminated. The oxygen requirements are provided by a number of top blow lances operating in the non-splash mode.

4. In-situ slag cleaning is possible because it is present as a moving layer only a few millimetres thick, thus ensuring good contact between reductant and oxidised slag components. Subsequent retention of the slag in the main circuit with matte flowing underneath should facilitate matte slag separation and contribute further to in-situ slag cleaning.

5. Transfer of heat from fuel combustion (e.g. natural gas) occurs across a relatively clean matte surface enabling efficient and highly intensive heat transfer to take place. In other matte-slag processes heat has to be transferred to matte through a layer of 10 cm or more of slag.

Table I focuses attention on zinc sulphide and compares the chemistry of the established technology with that of the reactions that are proposed for direct oxygen smelting. The

carbothermic reduction of the oxide produced in reaction 1(a) is the primary reaction of the zinc-lead blast furnace. The direct smelting route has certain thermodynamic limitations. If the temperature is sufficient, significant partial pressures of zinc gas and sulphur dioxide can coexist in stable equilibrium, but the problem is how to recover the zinc. Once the temperature is lowered in an effort to condense liquid or solid zinc, the reaction proceeds from right to left and zinc reverts to a mixture of ZnS and ZnO. That thermodynamic limitation can be overcome through two reactions in which copper and cuprous sulphide take part: reactions involved in 2(a) and 2(b) can be made to occur spontaneously in different regions of a reactor system, the net result being the direct smelting reaction.

For complex sulphide feeds containing similar proportions of copper, zinc and lead, direct smelting in the oxidising region under the top blow air/oxygen lances produces blister copper which collects in the furnace hearth. The solid charge is assimilated into the circulating matte under neutral or reducing conditions and then zinc and lead are produced by reactions (1) and (2) as the copper-saturated matte is exposed to the vacuum inside the RH vessel.

$$ZnS + 2Cu \longleftrightarrow Cu_2S + Zn_{(g)} \quad (1)$$
$$PbS + 2Cu \longleftrightarrow Cu_2S + Pb_{(g)} \quad (2)$$

Elemental zinc and lead together with some lead sulphide are flashed off, but as the gases cool from around 1200°C in passing to a zinc condenser (probably direct liquid zinc contact but possibly with molten lead), a lead sulphide mist or fog can be expected to form and equilibrium changes represented by reactions (3) and (4) can be anticipated, resulting in the formation of a sulphide/oxide dross in the condenser sump. This dross would be reverted but clearly it is imperative to limit the extent of SO_2 evolution within the vacuum vessel.

$$PbS_{(ls)} + Zn_{(g)} \longleftrightarrow ZnS_{(s)} + Pb_{(l)} \quad (3)$$

$$SO_2 + 3Zn_{(g)} \longleftrightarrow 2ZnO + ZnS \quad (4)$$

Both zinc and lead are preferably collected in molten zinc or Pb- Zn alloy, subsequent cooling of which yielding zinc 4* and zinc/lead bullion. Alternatively, it may be desirable to produce directly a refined zinc product with a lead content meeting Grade 1 specification. This involves vacuum re-evaporation from the circulating liquid zinc quench alloy without further energy input, but some decadmiumising would still be required to meet high grade purity standards.

* zinc 4 is a British specification grade (GOB = Good Ordinary Brand)

Table I Zinc Smelting Reactions

---

1 Established technology

(a) Roast reaction
(gas-solid reactor; fluid-bed or sinter roast)

$$ZnS + 3/2\ O_2 \ <--> \ ZnO + SO_4$$

(b) Carbothermic reduction

$$ZnO + 1/2\ C \ <--> \ Zn + 1/2\ CO$$

(c) Overall reaction

$$ZnS + 1/2\ C + 3/2\ O_2 \ <--> \ Zn + SO_2 + 1/2\ CO$$

2 Proposed direct smelting route

(a) $ZnS + 2Cu \ <--> \ Cu_2S + Zn$

(b) $Cu_2S + O_2 \ <--> \ 2Cu + SO_2$

$$ZnS + O_2 \ <--> \ Zn + SO_2$$

To enable reactions (1) and (2) to proceed it may be necessary in some cases to add metallic copper to the vacuum vessel, but normally the matte will be circulating at a rate sufficient for the mutual solubility of copper and copper sulphide to provide the requirement with no external movement of copper whatsoever.

Effectively, copper matte is a solvent for the other sulphides being smelted. Adding these to matte under non-oxidising conditions implies raising the solids to bath temperature followed then either by solid/liquid dissolution or melting. With both processes being strongly endothermic it is essential that efficient heat transfer conditions are established and again forced matte circulation is the key requirement not only to supply the heat but also to ensure rapid heat and mass transport by forced convection.

Both charge assimilation and the reactions occurring in the vacuum vessel are intensively energy consuming. Exothermic reactions however, also form part of the direct smelting sequence: the reaction in which cuprous sulphide is converted to copper is exothermic and any iron sulphide in the feed to the smelter has to be oxidised to form a slag, slagging reactions being strongly exothermic. The energy released in these reactions is transferred to the sites of the endothermic processes by means of the sensible heat contained in the circulating matte stream, so the minimum circulation rate needed is dictated by the thermal requirements and the temperature range over which matte can reasonably be handled.

3. EXPERIMENTAL WORK

Since the principle of the process route involves circulating liquid copper matte through two parallel adjacent hearth furnaces via a vacuum lift pump system similar to an RH vacuum degassing system in steelmaking, and with unit operations taking place in all these sections of the plant, the pilot plant necessarily needed to mimic this arrangement on a scale smaller than a proposed production plant but nevertheless large enough to be meaningful. Comments on size and design are given in the next section. The overall aims of a pilot plant programme can therefore be summarized as follows:

(i) To demonstrate that it is possible to heat and melt matte in the twin hearths and to contain this molten matte in the refactory-lined hearths. Both exothermic and endothermic chemical reactions take place in the system so that heat is required to raise the matte to temperature, to make up for the excess of endothermic over exothermic reactions, and to counterbalance losses to the surroundings. For the pilot plant direct electrical resistance heating was employed although commercially demand would probably be met by fossil fuel.

(ii) To demonstrate that the RH vacuum/gas injection system can circulate copper matte continuously around the circuit in a similar fashion to that achieved in steelmaking, and that the circulation rate is adequate to cope with heat transfer and process chemistry/engineering requirements.

(iii) To demonstrate the feasibility of rapid assimilation of Zn/Pb ore into the flowing matte as pellets and as concentrate.

(iv) To demonstrate satisfactory reaction to and evaporation of zinc metal in the vacuum vessel (and possibly Pb), at a rate commensurate with an economically high process output and yield.

(v) To demonstrate the technical feasibility of zinc condensation in massive form, minimising loss as fog. Similarly for lead.

(vi) To demonstrate the viability of the soft blow oxygen method for regeneration of copper metal from copper sulphide, and to determine the oxygen utilization efficiency.

(vii) To obtain as far as possible, given the scale limitations of a pilot plant, mass and energy balances which can be applied to process scale-up.

(viii) To demonstrate the feasibility of deoxidising the matte using carbon and/or pyrite in order to ensure minimum subsequent loss of zinc and lead as dross.

(ix) To demonstrate the ability to "clean" the slag by reducing copper oxide to copper and magnetite to wustite with carbon/pyrite thus maximising copper yield.

It was clear from the outset that given the limited manpower and timescale that it would not be possible to achieve all these aims during Phase II of the project. It was hoped however to achieve as many as possible, but particularly those associated with circulation and containment of matte, since it is not possible to simulate these in the absence of a pilot plant. As the work programme proceeded, the limitations on the aims became more clearly defined and in January 1989 therefore, the aims of the Phase II programme were re-assessed and firmed-up. It became clear that within the timescale and given the manpower constraints, it was unlikely that oxygen blowing could be introduced, and hence the revised aims were targeted at demonstrating circulation and adding high quality zinc concentrate with copper powder to study the zinc production system, leaving copper regeneration and the use of polymetallic ore for a further phase in the work programme. Slag cleaning and matte deoxidisation were also considered of lower priority in the Phase II programme although obviously of major importance to the total process route.

The pilot plant necessarily consisted of two hearth furnaces connected at one end via a RH vacuum lift system, and at the other by a weir. The first thing to be determined was the plant size and scale of operation. It was decided, initially at any rate, that a high grade zinc concentrate would be used on the grounds of simplicity and health and safety, and that consideration of lead production would be left until later. Also a reasonable zinc production rate was considered to be around 100kg/h. This in turn, together with predicted heat requirements, and mass and heat transfer considerations led to the size of the plant chosen.

Thus (Fig. 1 and 3) the plant consists of two refractory-lined rectangular hearths side by side but at different levels, with a vacuum lift pump (RH system) connecting the hearths at one end to transfer matte from the lower to the upper hearth, and a passage at the other

end to allow matte to flow back to the lower hearth under gravity, thus completing the closed loop. The hearths are contained within a stainless steel furnace shell with a detachable lid, and is designed to be gas tight. The furnace is vented to a caustic soda scrubber for removal of sulphur dioxide, water vapour and other gaseous products. The furnace shell is force cooled with ducted air to ensure that the melt freeze line is within the inner magchrome brick, which is backed by magnesite and superduty firebrick. No insulating brickwork is included in the design, so extensive forced ventilation cooling of the furnace room has been installed.

The twin hearths are internally approximately four metres long by 35 cm wide, and contain a known amount of copper saturated copper sulphide matte, or 'white metal'. The temperature of the matte is raised to about 1270°C,(ie 150°C of superheat above its liquidus temperature of 1120°C to ensure fluidity of the melt) by means of direct resistive heating. Electric currents as high as 7000 A are passed between graphite electrodes at either end of the hearths. In phase II of the programme power to each hearth was initially supplied by two 180 kVA welding transformers with parallel primary windings, and with their secondary windings in series, in order to supply sufficient voltage and thus power, to melt the matte. To facilitate pellet charging, the lower of the two hearths was designed so that matte depth at about 280mm was greater than the upper hearth at 150mm, and hence more heat is required to melt and sustain its temperature. It was found also, that in time, matte penetrated cracks in the brickwork, and the heat demand in this lower hearth increased markedly. Eventually it was found necessary to increase the power, first by doubling the transformer capacity, and later by inserting a third graphite electrode at the centre of the deep hearth. These modifications to the plant are covered in a later section.

The RH vacuum system (Fig 2) connects the hearths via two inclined snorkel legs, which are lowered into the molten matte immediately prior to circulation. Inert gas (nitrogen) is injected into the upleg of the vessel (in the deep, lower hearth) which, as it expands, forces the two-phase liquid upwards, into the main RH chamber. Under vacuum the entrained gas is evolved, and the melt returns to the shallow, higher hearth through the other leg, by gravity. The matte level in the shallow hearth therefore rises, and overflows a weir into a sloping brick-lined trough inclined downwards to the deep hearth and known as the matte crossover. In order to prevent matte freezing here as circulation progresses, electrical heaters have been installed, and also elsewhere in the furnace design. These include RH leg internal heaters and snorkel tip heaters to prevent the matte chilling as the snorkel legs are lowered into the hearths, and matte drawn

up into the vacuum chamber. Connected to the RH vessel is a second vessel to act as condenser for the zinc vapour. The condenser contains a cylindrical annular ring of molten lead; gas and vapour generated by the matte under vacuum impinges upon the steel surface of this cylinder, causing the zinc vapour to condense upon it.

Within the RH vessel-condenser connection, and the RH vessel itself, graphite hairpin heaters are installed to maintain the temperature of these components to prevent premature condensation of zinc, or matte freezing as it rises into the RH chamber.

The vacuum system is provided by a mechanical rotary pump/booster combination. Various water and nitrogen cooling circuits serve to prevent overheating of critical components. Incorporated into the plant is a vacuum-activated system for emptying the molten matte from the hearths into a holding vessel or 'dump tank', via a syphon pipe system.

Initially it was proposed that this dumping system would be employed after every trial, and the hearths refilled with matte. In the event, this has not proved necessary, as it has proved possible to reheat solidified matte. Nevertheless the dump system was retained for emergency purposes and for controlled emptying of the matte. Electrical heating of the syphon pipes and dump tank ensures transfer of liquid matte and ensures that no liquid water is present in the system which could cause an explosion.

A more detailed description of the main components of the pilot plant is given below.

3.1 FURNACE SHELL

The furnace shell is constructed with austenitic stainless steel type 304 L, in order to reduce the magnitude of induced electrical eddy currents. A sand sealing arrangement is employed to prevent gas leakage between the shell and the removable mild steel furnace lid. The top of the furnace casing has a trough running round the perimeter, being filled with free flowing sand.

Coverplates for the lid are bolted to flanges and provide maintenance access to essential equipment without the need to remove the lid. Lid removal is carried out by first raising it with hand-operated lifting jacks and then traversing the furnace by rolling the lid off using a hand operated winch.

3.2 FURNACE REFRACTORIES

In order to generate a freeze line of matte within the working lining of the hearth, it is necessary to tolerate high heat losses through the furnace walls, since an insulating (firebrick) outer course of bricks would cause matte penetration into the secondary lining. The temperature of the furnace wall is therefore dependent on the thermal properties of the refractory lining, which must also have good thermal shock resistance, and be chemically resistant to the melt.

Accordingly, Chrome-Mag and Mag-Chrome are used as the working lining for the base and sidewalls of the hearth, respectively. The secondary lining is constructed of magnesite which has a low thermal resistance and is chemically resistant to matte. Dense refractory fireclay bricks are used in the outer course and provide good heat conduction to the outer shell.

In the furnace roof area, dense low cement, cast refractory slabs are used as the hot working face, backed by insulating fireclay blocks covered with ceramic fibre refractory blanket.

3.3 MAIN FURNACE ELECTRICS

The matte itself acts as the resistive heating element, such that when a voltage is applied between submerged graphite electrodes at either end of each hearth, the power input for smelting is generated by the flow of current through the matte. Each hearth was initially independently heated via two transformers with their secondary windings in series from parallel primaries, supplied from two phases of the main three-phase incoming supply. This is discussed later in 'Plant Operation'. However, as noted above, this arrangement was modified for the deep hearth in order to obtain the power necessary to reach the required temperature.

The electrical connections to the graphite electrodes take account of the thermal expansion of the furnace. Each electrode is constructed in two parts, connected with a spigot joint (Fig. 4). The upper cylindrical section has a machined recess which is filled with lead metal. This section has a helically-wound heating element to melt the lead. The 5" diameter water-cooled electrode contact rod dipping into the lead is free to move in all directions. The rod passes through the furnace coverplate and is connected to either the transformer secondary output terminal (furnace snorkel end) or the bus bar returns (furnace syphon end) via water-cooled flexibles. The copper bus bar returns are located underneath the furnace lid, and take the form of thick-walled tubing along which nitrogen

gas is forcibly passed to maintain the copper at a cool, steady temperature. Each hearth contains a set of two bus bars, in parallel, which run the length of the furnace, and are connected to the copper electrode through its cover plate. A low melting point alloy is used to provide a gas tight seal between the furnace lid and bus bar conductor, and enables the copper to expand freely on heating.

The power to the hearths may be altered by manual adjustment of the coarse and fine voltage controllers located on the transformer (tap settings) and thyristor (dial) units respectively. The voltage and current flows for each hearth are indicated on a digital output recorder.

3.4 AUXILIARY HEATING CIRCUITS

There are a number of components and regions in and on the furnace assembly which are required to be at certain temperatures for optimum operation. Thus there exist some nine auxiliary heating circuits, detailed below:

(i) Busbar seals
Low melting point alloy heaters, parallel connected, two series of four heaters, across a fixed 35 volt supply. Temperature control is by thermal switches installed on each heater.

(ii) Liquid lead contact heaters
One 3 kW heater for each electrode, parallel connected in two series of two heaters. Temperature control by automatic/manual thyristor operation.

(iii) Matte crossover heater
A wire coiled heating element rated at 9.5 kW, supplied from a step-up transformer (240 to 330V) is utilised to preheat the inclined weir before matte circulation to prevent matte from freezing in the channel.

(iv) RH snorkel leg heaters
Two heating elements are connected in series to a 30 kVA transformer, with one element in each leg. Spirally wound, with a central return rod, they dissolve on contact with the molten matte, thus it is imperative that the snorkel legs are at their operating temperature prior to circulation, to prevent matte freezing within the leg.

(v) RH vessel main heater
The RH vessel is heated by radiation from a graphite hairpin electrode connected to a 180 kVA welding transformer itself supplied from two phases of the main supply. Power input control is via transformer taps and thyristor setting (cf main furnace electrodes). Copper contacts are water-cooled.

(vi) Vacuum crossover heater
A graphite hairpin heater was installed in the connecting duct between the RH vessel and zinc condenser, designed to prevent premature condensation of zinc. Power supply was from another welding linked to the same supply as the RH main heater, coarse control only. Later this system was modified.

(vii) Zinc condenser lead bath heater
Four heaters wired in parallel with thyristor control maintain the lead bath at its melting point.

(viii) Dump tank heaters
Maintain the temperature of the dump tank above 100°C to evaporate any moisture prior to matte transfer.

(ix) Dump tank syphon heaters
A separate heat circuit from (viii) but serving the same purpose.

3.5 THE RH VESSEL - ZINC CONDENSER VACUUM SYSTEM (Refer Fig. 5)

THe RH vessel consists of a refractory lined steel cylindrical shell, containing four graphite cyclones surrounding the hairpin heater. The vessel is connected to the furnace hearths by two snorkel legs which consist of double walled, refractory lined steel pipes. To preheat the leg before circulation, a sacrificial heating element is installed, which dissolves on contact with the molten matte. To protect the steel from overheating, the pipe is cooled by blowing nitrogen gas between the double wall, which is located in the lower, hotter region of the leg in close proximity to the matte. The upper part of the leg, above the furnace lid, is water cooled.

During the furnace heating operation the snorkel tips are kept a few inches above the matte surface in the hearth, to protect the refractories and heating elements. When the matte is molten, and both it and the snorkel legs are at the required temperature, the legs are lowered into the melt. Raising and lowering the RH-condenser system is achieved using manually operated geared winches. Level sensors on the snorkel legs ensure that the tips are submerged in the melt before circulation commences. The

RH vessel is connected to the zinc condenser by a horizontal flanged pipe. The vacuum offtake lines from the condenser feed back to a two stage 15 kW Edwards vacuum pump/booster combination, preceded by dust filters.

Injection of nitrogen lift gas into the RH snorkel upleg is through one of two spargers. A graphite sparger only was incorporated into the original design, but this has shown itself to be susceptible to fracture under the rigours of operation. Thus, a second sparger constructed from stainless steel tubing and castable refactory was installed to improve the reliability of the system. A fairly detailed experimental programme was carried out into sparger design, the majority of the work being described in the third progress report to the European Commission. Eventually, a design consisting of a nozzle made from castable refractory containing a narrow slot connected to the narrow bore stainless steel feed pipe was adopted. Modifications were also made to the external graphite sparger design, and the modifications to both spargers are described later.

Mass and heat transfer considerations led to the conclusion that matte circulation rates of around 1000-1500kg/min would be required. Theory, water modelling and analogy with 15-20l/min gas flow would be required to circulate at this velocity.

The internal diameter of the snorkel casting is approximately 70mm, designed to provide an adequate wall thickness of refractory needed to satisfy thermal requirements, but also of sufficient cross-section to permit adequate mass flow rates of molten matte to prevent it freezing in the pipe.

Were the vacuum to be applied without gas injection, the melt would be drawn up both snorkel legs to a certain height. This barometric height depends on the density of the matte and thus matte composition. At a matte density of 5.2 g/cm3 assumed for design purposes the raised matte level in the snorkel legs would fall short of the RH chamber (Fig.5). However, on injection of nitrogen gas into the upleg, the matte density in that leg decreases, thus increasing the matte level such that it enters the RH chamber. Here it is degassed, returning to its original density, and flows out of the chamber, via the snorkel down-leg. Thus, the nitrogen gas, by its own tendency to flow upwards, and its expansion due to the temperature of the system, provides the motive force for matte circulation.

The gas and spray generated within the RH chamber passes through the graphite cyclones, which serve to return entrained matte droplets to the molten stream, thus reducing carryover in the gas/vapour stream to the condenser.

Should the matte level in the RH chamber increase above a specified safe level, for instance due to large volumes of gas being entrained in the melt rising in the upleg, causing a low density two-phase foam to be generated, then installed level alarms and shutoff controls are employed to correct this situation.

3.6 NITROGEN GAS COOLING AND PROTECTION

As reported above, the furnace busbars and snorkel legs under the furnace roof are forcibly cooled with nitrogen gas supplied via a Roots Blower, fitted with two water cooled heat exchangers.

Protective gas blankets are also required for the furnace hearths and for the RH vessel, to prevent any oxidation of the matte and especially the graphite electrodes and heating elements. The nitrogen for this is supplied from standard 15-cylinder pallets, with separate circuits for the Roots Blower and the protective blanket.

3.7 PLANT OPERATION

3.7.1 Start up

After completion of the safety checks, the water cooling circuits are activated, along with the nitrogen cooling and protection blankets. The busbar seals heaters and liquid lead contact heaters are then activated, prior to feeding power to the main furnace hearth electrodes. Furnace hearth temperature rise should be between 20° and 50°C per hour. The initial heating rate will be about 20°C per hour, due to the large thermal mass and its electrical resistance when cold.

The remainder of the auxiliary heating circuits e.g. RH snorkel legs, matte crossover, RH vessel, vacuum crossover and zinc condenser, are then activated. Areas containing freshly cast refractory such as the snorkel legs should be held around 110°C for a few hours to drive off any moisture.

3.7.2 Furnace Heat-up

As the temperature of the furnace components increases, careful checks are made on the heating rate, and operation of the heating elements, adjustments being made as necessary. Regular monitoring and recorded checks are made on the various furnace parameters i.e. temperatures, electrical measurements, nitrogen and water flowrates and pressures, and any notes are made in a logbook.

Power input to the hearths is adjusted by coarse and fine controls i.e. the transformer tap settings and thyristor dials, respectively. Transformer tap settings may only be changed off-load, i.e. the power to the transformer is switched off before changing the tap, then power is restored, with the thyristor setting on minimum. This method avoids short circuits on the primary windings of the transformers, and consequent current surges exceeding the maximum demand limitations. Ammeters have been fitted to each primary phase of the incoming three phase supply so that current readings can be taken constantly, and maximum demand overload avoided. Prior to the modification involving the third electrode in the deep hearth, the current drawn from the blue phase supply far exceeded the red and yellow phases because of the particular method of phase tapping which was necessary with the given electrode configuration. Consequently very careful watch was kept on the blue phase current during this period, making sure that it did not exceed 900 amps. This resulted in red and yellow phase power being under utilized. With the third electrode, however, the new configuration allowed all three phases to be loaded more or less equally, and hence made better use of the power available. Also experience showed that by increasing the hearth temperature over a slightly longer period, the furnace refractories are allowed to absorb heat more evenly i.e. at a reduced heat transfer gradient, with resultant smoothness and increased controllability of hearth heating. Thus operational temperature can be sustained at a lower primary current level.

3.7.3 Matte Circulation

During the last few hours of the heating schedule, heating rates are balanced so that the heated components of the furnace achieve their operating temperatures at approximately the same time. The RH vessel and snorkel legs and the matte crossover must be hot enough to prevent matte freezing on contact, although the latter item is not too critical. The vacuum crossover and zinc condenser should also be at their target temperatures.

Matte levels are measured by depth probes to ensure sufficient depth for complete immersion of the snorkel tips. If required, more matte may be added in solid, granular form to either hearth by means of the combined sight/feed port above each hearth. Final matte temperature readings may also be taken via this facility to confirm the required superheat is available.

The vacuum receivers/filters are fully evacuated in isolation from the RH system, and the gas injection systems are activated. The flow of gas to the nitrogen protection of the RH, and the RH leg heating elements are switched off prior to manually lowering the snorkel legs into the melt. On confirmation of immersion by the snorkel tip level sensors, the system is exposed to the vacuum.

The system is designed such that the molten matte will be drawn up both legs, the gas injection 'lifting' the matte in the upleg into the RH chamber, where it is degassed before flowing into the shallow hearth through the downleg. This will cause the shallow hearth to overflow into the matte crossover, two graphite probes indicating a flow condition when contact is made between them by the molten matte. A further demonstration of matte circulation is obtained by observing the passage of silicon carbide chips across the matte cross-over between two special sight holes installed for this purpose.

In the trials carried out so far a charge consisting of a mixture of zinc concentrate and copper power has been added to the matte via a screw feeder. Although it was planned also to include pellet additions, the present programme ended before this could be achieved.

4. RESULTS

4.1 PILOT PLANT TRIALS

During Phase II, eleven pilot plant trials have been carried out. These have been detailed in reports to MIRO and in reports to the Commission of the European Communities, while the main text that follows concentrates on highlighting the more important points.

Whilst the early trials were primarily aimed at commissioning the various items of plant, the objective of each trial was to move as far along the process route as possible. Hence improvements in plant engineering and operations occurred throughout the whole trial programme. Although each of the trials terminated through the occurrence of some fault associated either with plant engineering or operation, each trial in turn contributed to advancing knowledge of the process route. It was notable that the majority of these failures concerned features which were necessary because of the scale of plant operation, and which would be absent in a commercial-sized plant. In turn these were mainly to do with the electrical heating systems.

The main electrical heating systems worked quite well, and the principal problems associated with their operation concerned an ever-increasing power demand as extra matte was added to the hearths to compensate for a continuing loss of matte to the refractory brickwork; indeed in trial 3, this loss was such that one of the RH snorkel tips

failed to make a liquid seal with the hearth. Extra transformer capacity was added to overcome the shortfall in the initial electrical arrangements, beginning with 1 transformer per hearth and ending with 4 on the deep side and 2 on the shallow side. Earth leakages and current short circuits were also encountered which led to very high transformer primary currents resulting in tripped circuit breakers and fuses, both in the laboratory and in the University sub-station. These faults were all corrected in turn. A further problem with the main heating circuits concerned out-of-balance phases in the original set-up which meant that one phase was loaded to a far greater extent than the other two, such that holding this below or at its maximum meant that the available power to the laboratory could not be fully utilized. Ultimately a third electrode was placed in the deep hearth so as to increase the power input to this hearth and at the same time obtain a better electrical balance between the three phases. This modification was very successful, although some short circuiting took place before the operation of the new arrangement was fully understood and optimized.

The most worrisome electrical feature involved the Fecralloy heaters employed to preheat the RH snorkel legs. These were a constant source of trouble, initially because of an inadequate design of the current-feeding leads. However even after this problem was solved by re-design, intermittent failure took place for a variety of reasons, mainly to do with structural integrity of the heaters and return current leads. A complete re-design and re-build of the snorkels is necessary to overcome this problem, and although this re-design was in hand, re-build had not been actioned by the end of the trials programme.

Another area developed during the trials programme was that of the sparging system in the RH up-leg. The original design of a perforated graphite tube external to the snorkel and fed by a graphite tube attached to the outside of the snorkel proved mechanically unsound (see previous section on plant design). Hence this was improved in design by reducing potential stresses and by including some steel protectors. In addition, and more successfully, an 'internal' sparger consisting of a slotted refractory nozzle and fed by a stainless steel tube, embedded in the snorkel refractory wall, was incorporated and this was nearer in design to the sort of sparger system used in steel degassing. The problem with the small pilot plant is of course much more sever than in a large degassing plant where very much more sparge gas is used, and hence larger dimensions are possible.

The production of fume in the trials, principally from lead which had been added to the hearths, led to a problem with the vacuum pump system, since fume found its way through the filters and jammed the pump mechanisms. This meant

that an otherwise very promising trail (trial 8) failed when the vacuum system tripped and refused to re-start. From this point on, following a complete overhaul of the vacuum pumps, a more efficient filter system was incorporated and the oil changed and the system cleaned after each trail.

The two most successful trials from the point of view of process engineering as opposed to plant engineering were trials 7 and 10 during which matte circulation was achieved. In trial 7 circulation continued for 48 minutes when a fire on a rubber bellows seal exposed the laboratory (and personnel) to escaping SO_2 , which resulted in an emergency shut-down.

In trial 10 circulation continued for 66 hours although owing to a leak in the RH system, full vacuum could not be maintained. Nevertheless, limited feed of the zinc concentrate was also carried out via a screw feeder arrangement. This was partially successful but the presence of a viscous slag layer meant that to obtain full assimilation of the concentrate, manual stirring of the matte had to be employed, thus limiting the amount of material charged to about 30 kg. Nevertheless, assimilation was demonstrated, and metallic zinc and lead were produced, although the major component of the deposits was lead oxide. The lead arose not from the concentrate, but from lead shot which had been added in earlier trials to assist in making electrical connections. The preponderance of oxide is due to the leakage of air into the vacuum system, but the absence of zinc oxide indicates that volatile lead sulphide has reacted with zinc to produce zinc sulphide, a reaction predicted by the theoretical evaluation of the process route. Thus, although the concentrate additions trial was not extensive, it demonstrated that the expected chemical reactions do take place.

The trials programme finally terminated when matte from the upper shallow hearth penetrated through the furnace brickwork into the lower deep hearth, and also caused an electrical short to the furnace case. There was no option therefore but to dismantle the furnace in order to determine the extent of the repair work necessary to re-furbish, should such a course of action be desirable. Quotations were therefore obtained for

(i) rebuilding the shallow hearth, leaving the deep hearth in its present condition, and

(ii) completely rebuilding both refractory hearths.

4.2 PILOT PLANT RESULTS IN RELATION TO PROGRAMME AIMS

Up to the end of phase II a number of the aims set for the programme were achieved. A great deal of the pilot plant work of course could be considered as commissioning of the plant, and this is particularly true of the various

electrical circuits involved. It was learnt that the solid matte can be raised to melting by passage of current directly through it, and that it was not generally necessary to employ a sacrificial conductor except where complete breakdown of current path had taken place. With successful melting it was also demonstrated that the matte could be kept molten in the hearths using the chosen refractory lining material without catastrophic failure. Clearly over the course of time matte penetration into the brickwork took place and in particular into gaps between bricks, cracks and fissures etc. However, when it is borne in mind that the plant was thermally cycled from the cold, fourteen times in phase II in addition to the cycling carried out in the initial tests in phase I, the plant behaviour in this respect could be said to be excellent. In a production plant, the thermal cycling load would be far less acute, and thus the pilot plant behaviour gives every confidence that satisfactory hearth lives could be achieved. It was very unfortunate that the final failure and breakthrough of matte occurred before the end of the phase II programme period, since it is highly probable that the remaining aims of the revised schedule would have been satisfactorily achieved. The various options which were (and are) available for continuation are discussed later.

The available heat in relation to process demand posed something of a problem, since not only were the usual problems of pilot plant operation faced i.e. heat losses form a far greater proportion of the total than on a production plant, but also the heat demand increased over that expected because of the extra matte which had to be added to the hearths to make up for loss to the refractories. Additionally, the decision to forego the use of oxygen during phase II meant that the chemical heat was all endothermic. These problems were largely overcome by increasing transformer capacity, and re-designing the deep hearth electrode system, and it was calculated that given the plant conditions after trial 10, after the steady state heat demand had been satisfied, between 87 and 109 kVA of power would have been available for pellet feed and chemical reaction, equivalent to a zinc production rate of between 25 and 50 kg/h. This would have been done had plant failure not occurred.

With respect to integrity of gas shrouding, the plant worked satisfactorily, and the shroud/waste gas cleaning system gave no problems. However, the absence of oxygen blowing meant that the system was not as fully loaded as it otherwise would have been. Local oxidation did take place when various parts in the furnace shell were opened for trouble-shooting purposes, and this served to show the importance of the furnace design with respect to gas tightness in relation to the quality of the matte charge.

After several attempts matte circulation was achieved on two occasions. In trial 10 this continued in a controlled manner for 6 1/2 h and ended only because of personnel fatigue, and not for any process reason, other than the leaking vacuum system, which was making further feed additions rather pointless. The sparge gas flowrates in relation to circulation rate agreed with the predictions from theory and model experiments, giving confidence to production plant design. Sparger design still requires some work for the pilot plant, but of course as mentioned above,the larger the plant size the easier this becomes.

The concentrate feed system worked well enough but the presence of a viscous slag meant that assimilation could hardly be described as rapid. It did however, underline the importance of ensuring that the charge is fed into the matte below the slag layer. If this is done, rapid assimilation seems possible as indicated by the single pellet experiments carried out in trial 11 before the plant failure.

The one trial in which concentrate was added did demonstrate that zinc sulphide does react and zinc metal evaporate as predicted. The small quantity added however, did not allow quantitative assessment to be made of either rate or yield. Similarly, although unintended the lead reaction was also seen to take place. Indeed the analytical results suggest that the reactions between copper and zinc or lead sulphide, and the evaporation of lead sulphide followed by its reactions with zinc vapour to give lead and zinc sulphide, all took place to a certain degree. In spite of the air leakage into the RH vessel very little zinc oxide was found in the condenser deposits, supporting the notion that zinc reacted with lead sulphide and that most of the oxygen was gathered by lead in the condenser, although zinc oxide was found in the RH slags. The preponderance of very fine powder also underlines the problem of fog formation which clearly requires further attention. In summary, the limited information available demonstrates that the required reactions do take place and underlines the necessity for their quantification and control. Clearly detailed mass and energy balances are not possible but none of the observations made are inconsistent with the theoretical work previously carried out.

Most of the revised programme aims were therefore achieved, even though those concerning the chemical reactions were only on a qualitative basis. The longer term aims associated with oxygen blowing and copper regeneration, and which include the problems of matte deoxidation, have yet to be tackled, and this underlines the desirability of continuing the work programme, since so far, nothing has been discovered which casts doubt on the undoubted theoretical promise of the process route.

5. CONCLUSIONS

The phase II pilot plant programme has now ended with the important engineering aims set out in the revised annexe to the European Community Contract being achieved. These involved demonstrating that copper can be heated, melted and maintained at temperature in the twin-hearth furnace system, which is central to the process route. Further, that the system can be maintained under inert atmosphere conditions without unwanted oxidation of matte and with due regard to the safety of personnel and to contamination of the environment. That the copper matte can be circulated via the RH type vacuum lift pump system, at a rate commensurate with the heat and mass transfer requirements dictated by the process chemistry of the zinc and lead production reactions, and that this circulation can be maintained with minimum control operations over a long period of time. Assimilation of Zn ore in concentrate form was also demonstrated to a reasonable degree, and the production of zinc metal on a very limited scale was achieved indicating that the proposed reaction system is possible with the geometric configuration of the hearth furnaces and RH system chosen.

The trials programme ended prematurely when matte from one hearth broke through the refractory brickwork to the other, although the behaviour of the refractory hearths over the whole of the period was considered to be excellent. The premature end meant that only a start had been made on quantifying those aspects of the process engineering associated with the chemical processes involved. Further, the programme itself had not attempted to study those parts of the total process route involving the oxygen blow. However, the progress made to date underlines the view that further testwork should be carried out preferably by instituting a further pilot plant programme, but alternatively by isolating each of the outstanding problem areas, and investigating in a series of stand-alone programmes.

6. REFERENCES

1. WARNER N.A. "A Method of Recovering Non-ferrous Metals from their Sulphide Ores", British Patent 2 048 309, (1983), U.S. Patent 4 334 918, (1982), European Patent 0 016 595, (1984).

2. WARNER N.A. "Direct Smelting of Zinc-Lead Ore", Trans. Instn. Min. & Metall. (Sect. C: Mineral Process Extr. Metall), 92, (1983), C147-152.

3. WARNER N.A. "Towards Polymetallic Sulfide Smelting", Complex Sulfides - Processing of Ores Concentrates and By-products, (T.M.S. AIME Warrendale Pa., 1985), 847-865.

4. WARNER N.A. "Countercurrent Gas Treatment of Metallurgical Melts", UK Patent No. GB 2193975 B.

5. MWANSA J.C. and WARNER, N.A. "Natural Convective Heat Transfer between Single Ore Pellets and Molten Copper-Nickel Mattes", In African Mining, IMM, London 253-266 (1987).

6. JONES T. and WARNER N.A. "Top-blowing Requirements for Direct Polymetallic Smelting". Pyrometallurgy '87. IMM London 1987, 605-626. (1987)

7. WARNER N.A. "Thermal Recovery of Sulphide Materials", UK Patent Application, 8810855.0 (1988).

8. WARNER N.A. "Advanced Technology for Smelting McArthur River Ore" , Minerals Engineering, 2, 3-32 (1989).

9. HANNA R.K. and WARNER N.A. "Process requirements for the direct condensation of both zinc and lead as metals in the polymetallic smelting of Zn-Pb-Cu sulphides". Proceedings of Non-ferrous Smelting Symposium, Port Pirie, Australia, 227-236 (1989).

10. SHENG L.J., ARMITAGE J.W. and WARNER N.A. "Prediction of fog formation during lead-zinc condensation", Trans. Instn. Min. & Metall. (Sect. C: Mineral Process Extr. Metall.) 99, (1990), 183-187.

11. HANNA R.K. and WARNER N.A. "Liquid Phase Mass Transfer in Top-Blown Open-Channel Flows", Trans. Instn. Min. & Metall. (Sect.C: Mineral Process Extr. Metall.) (1991). (In press)

Fig. 1

Schematic Plan Diagram of Pilot Plant
(approximately to scale)

Hearth Length = 4m
Width = 35 cm

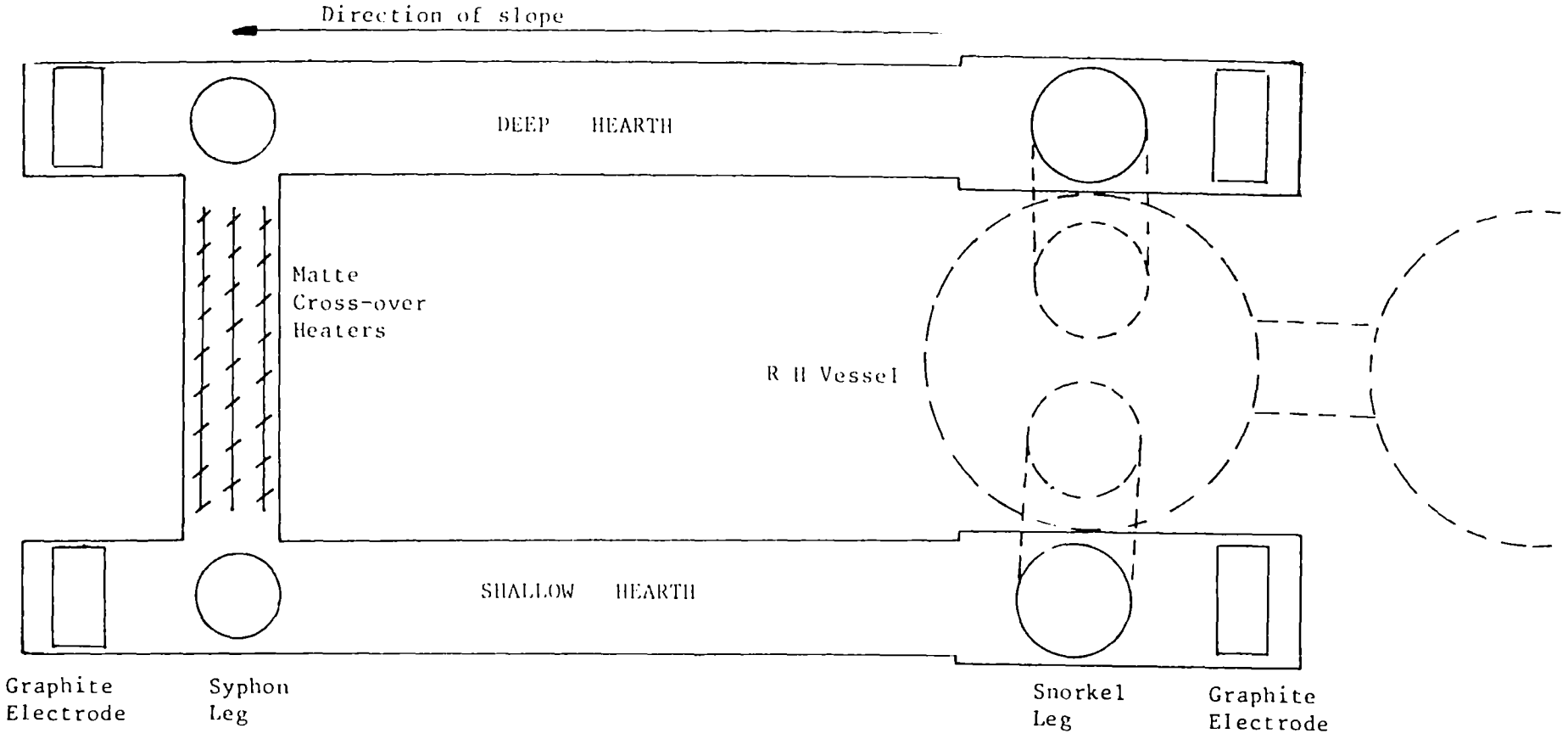

Fig.2

Vacuum Vessels

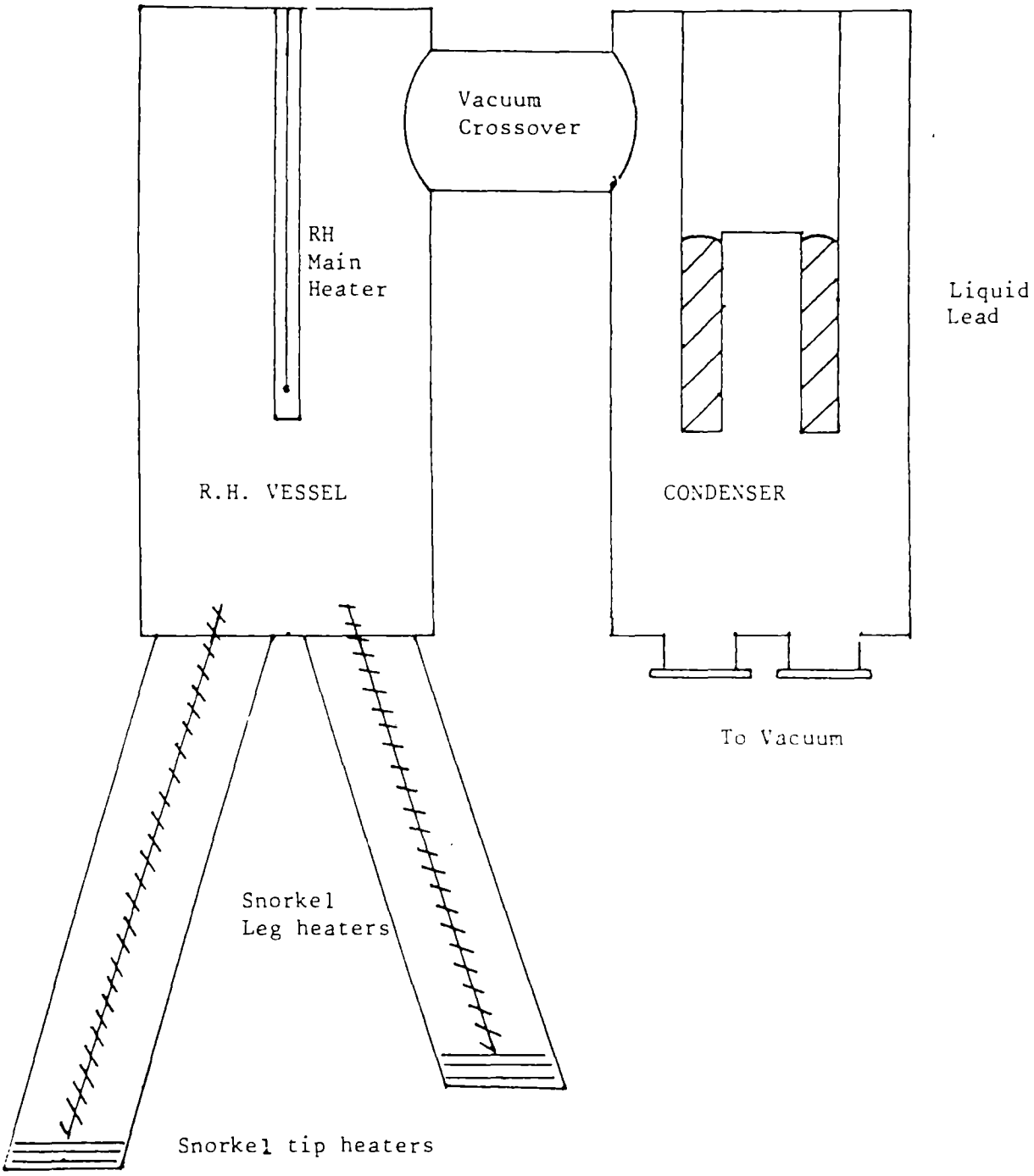

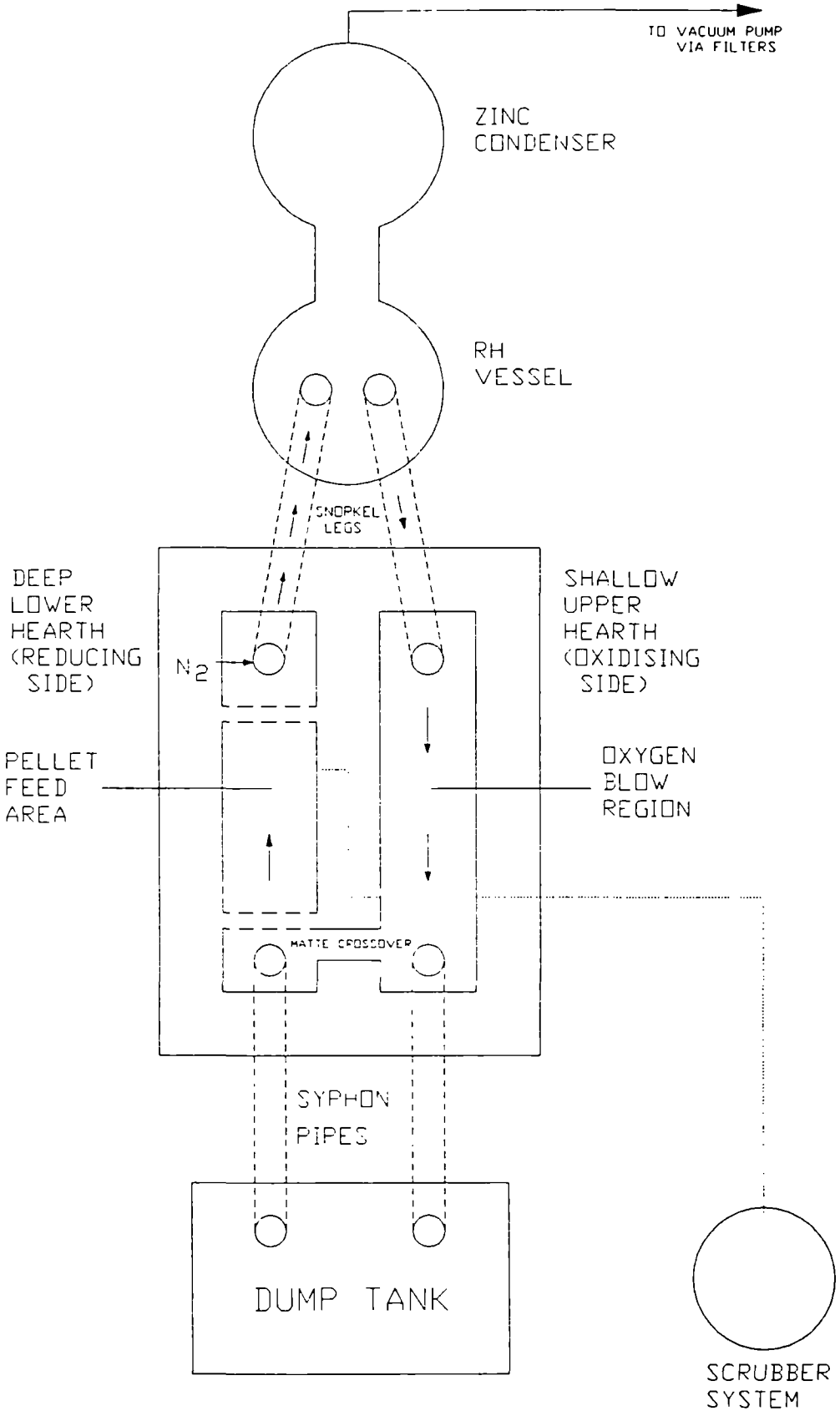

FIGURE 3. SCHEMATIC OF SMELTER

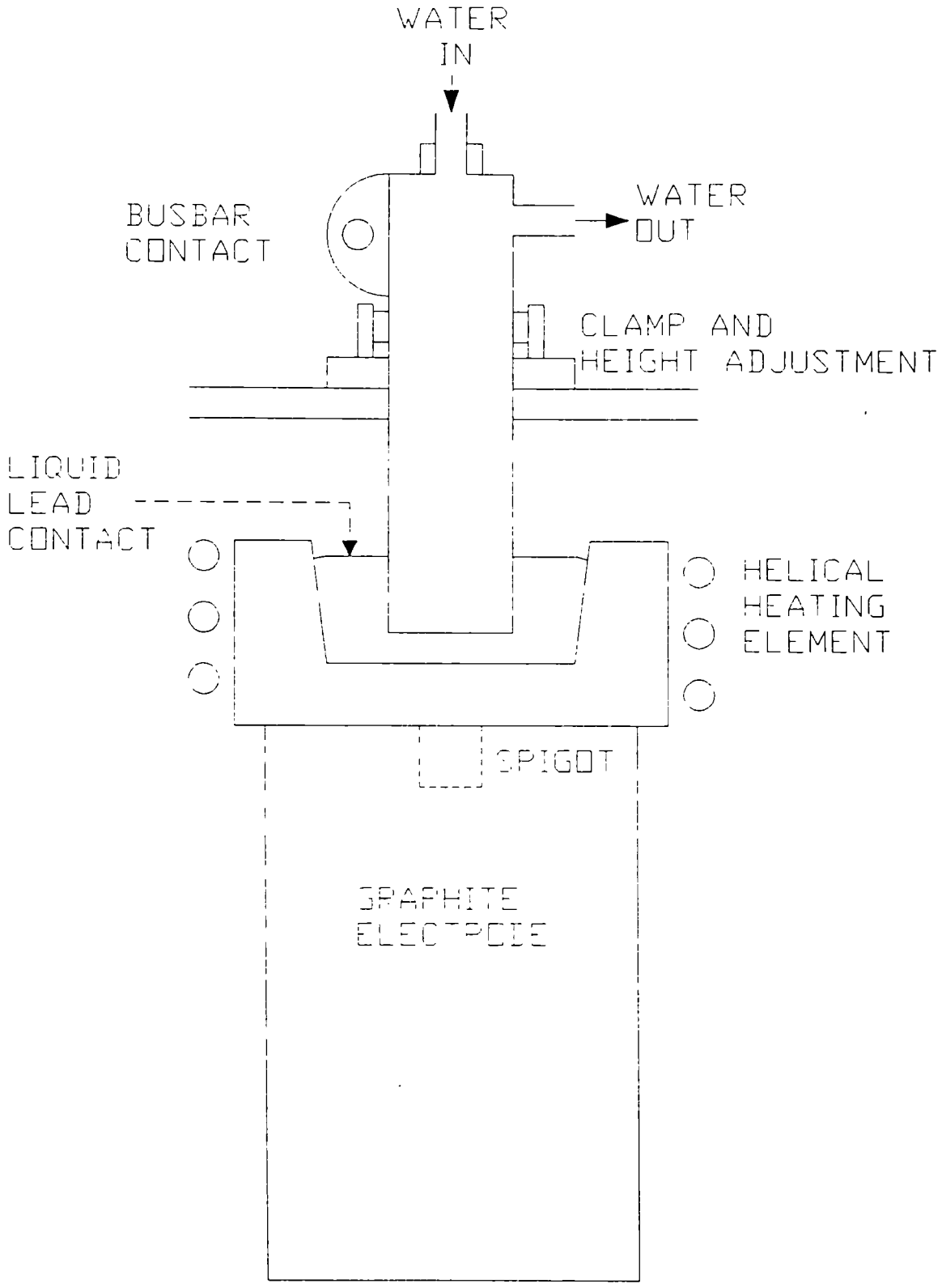

FIGURE 4 SCHEMATIC DIAGRAM OF HEARTH ELECTRODE

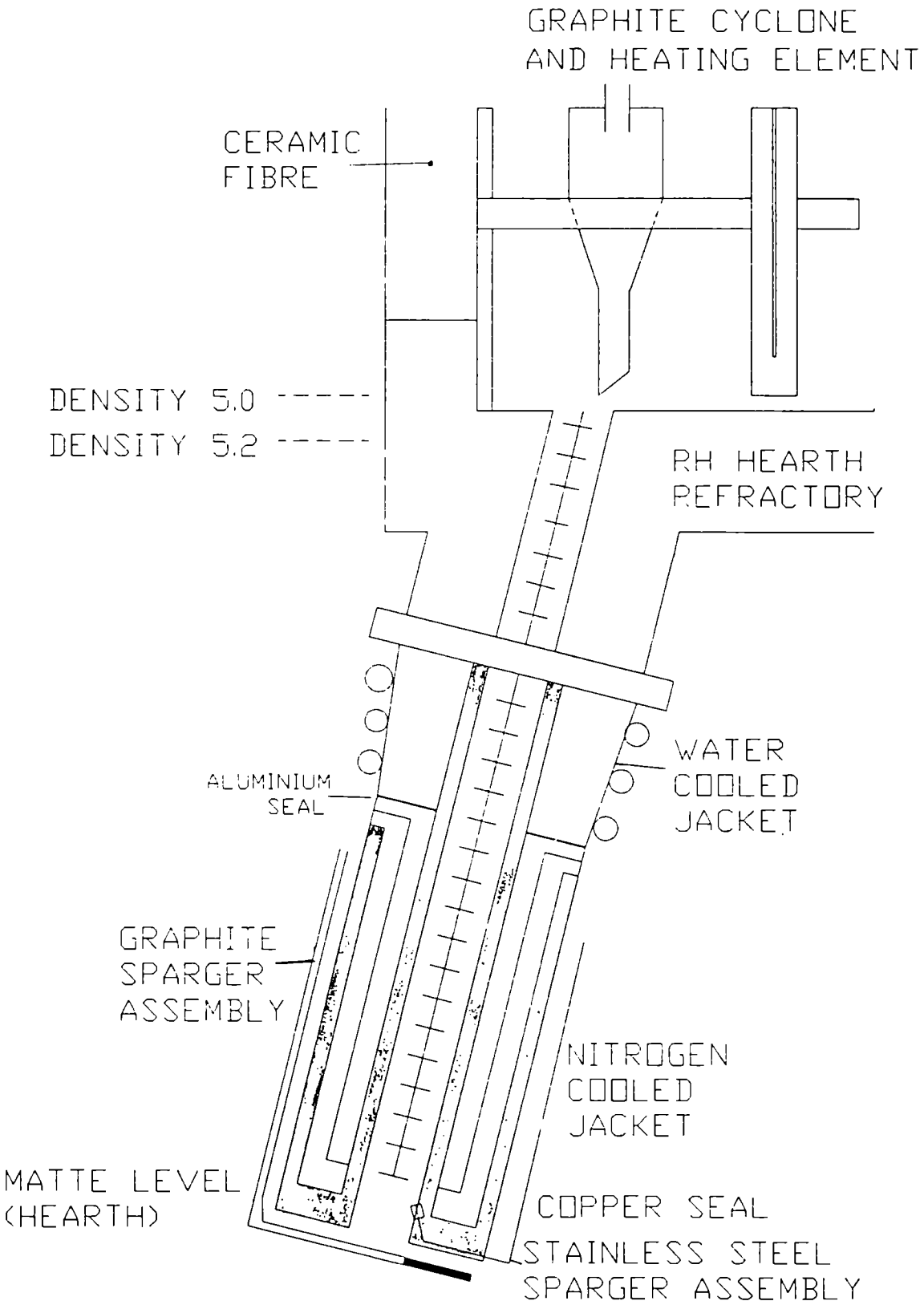

FIG.5 RH SNORKEL LEG ASSEMBLY

THE BEHAVIOUR OF COPPER IN THE ZINC IMPERIAL SMELTING FURNACE

Project Leader: M. DURETZ
Métaleurop Recherche, Trappes, France

Contract MA1M-0074-C

1. INTRODUCTION

The Imperial Smelting Furnace (ISF) was developed in Great Britain during the 1950's as a process which could produce zinc from a blast furnace. It is now an efficient means of producing zinc and lead from lower grade materials both of primary and secondary origin.

Since the mid 1970's, the main zinc plants have progressively changed the high grade concentrate mix towards low grade and mixed concentrates supplemented by oxidized materials and electrolytic leach residues. These changes, made for economic reasons (competition with classical zinc electrolysis plants), gradually increased in particular the amount of copper entering the furnace. This was notably the case at Berzelius (Metallgesellshaft : 2,000 t since 1973), Avonmouth in Great Britain, Cokle Creek in Australia. For Metaleurop, the plant at Noyelles-Godault was for a long time limited to smaller quantities from 1,000 to 1,500 t due to common processing of both lead coming from Imperial Smelting process and from lead Blast Furnace without specific copper extraction (total permitted input : 2,000 t).

The higher copper input to the ISF creates problems occurring, on the one hand, after the recovery of the zinc in the condenser and, on the other hand, after the furnace is tapped. The latter is due to the premature cooling of lead bullion and separation of copper while still in the ladle.

These problems will need to be solved if the ISF is to handle increased amounts of copper, so as to give to the ISF operators a definite advantage over the electrolysis plants. It is worth to recall that these plants are not suited for processing sphalerite concentrates (ZnS) containing large amounts of copper : their copper recovery is low and, most important of all, these operations necessitate the use of highly expensive zinc powder to separate copper from lead by cementation.

These were the motivations by which Metaleurop Recherche and Berzelius joined in a common research program. The objective of this program is to enable two ISFs of the European Community (Noyelles-Godault and Berzelius) to treat all the zinc-copper concentrates on the world market i.e. 10,000 t of copper each Imperial Smelting Furnace.

2. SHORT DESCRIPTION OF THE COPPER BEHAVIOUR IN THE MAIN STAGE OF THE ISF PROCESS - OBJECTIVES OF THE PROGRAM

The Imperial Smelting Process comprises :

a) A roasting operation in a Dwight Lloyd sintering machine in which the main sulfide minerals are oxidized. At that stage, the copper minerals contained in the concentrates, Cu_2S, $CuFeS_2$ and CuS are mainly converted to oxides.

b) A reduction step in the Imperial Smelting furnace : the sinter is reduced by imposing a very low oxygen potential over the entire shaft which allows to recover the zinc as a vapour at the top of the furnace. The sinter feed consists mainly of lead, zinc, copper and iron oxides. Copper is readily reduced into metallic form, then dissolved in the lead bullion collected in the heart of the furnace.
But, as the ISF feed may contain briquettes of leach residues or non ferrous oxidized dusts which as a whole are less mechanically resistant, part of the copper may be carried over to the condenser. Part of this copper passes into the zinc phase and goes to the zinc refinery.

c) A recovery of the lead bullion by discontinuous tapping into a forehearth which separates the speiss phase (Fe-As alloy) from the lead : at this stage, copper remains entirely in the lead bullion.

d) A decopperizing step of the lead bullion which is processed in kettles by lowering the temperature, with production of copper drosses which are removed generally by a mechanical way : most of the copper goes into the drosses.

e) Eventually, a copper drosses processing unit.

At the present day, steps (c) and (d) are batch operations. The decopperizing step is very slow and requires big kettle capacities since the furnace is tapped discontinuously. The main part of the research program has focused on adapting or improving stages (c) and (d) in order to outbust the overall copper recovery and allow the processing of burdens with copper contents as high as possible.

3. COPPER BALANCE IN AN ISF (Berzelius plant)

In an ISF, copper in the charge can be contained in the sinter or in hot briquettes. Part of this copper will be reduced in the shaft as well as zinc or lead, and will be found in the lead tapped at the bottom of the furnace. The other part will be entrained, mainly by mechanical carry-over, and will reach the condenser and divide between the liquid zinc and the condenser by-products. In order to have an evaluation of this copper quantity, an industrial copper balance has been done in the Berzelius plant.

3.1. TOP OF THE FURNACE : CU BALANCES CONDENSERS AND REFINERY

Copper oxide (CuO) is reduced to copper metal by coke in similar manner as ZnO and PbO. Volatilization of metallic copper is insignificant, so that the main amount of copper goes with the lead to the furnace bottom. So, only the mechanical carryover of fine particles of sinter and hot briquettes in the offgas system is to be made responsible for the copper content in furnace zinc (Ca. 0.06 % Cu), blue powder (0.05 - 0.1 % Cu) and pump sump dross (0.2 % Cu).

Temperatures predominating in the condenser and separation system (about 450 °C) favour a much greater solubility of copper in zinc than in lead (figures 1 and 2). So, almost all the copper entering the zinc separation system is bled off with the zinc ; the copper content in the lead remains below 0.1 %. This has been confirmed by the observation of the copper distribution in some qualitative tests : the fines of hot briquettes and sinter were mixed in either lead or zinc. The analysis of lead did not change, whereas in zinc metal (GOB and SHG) an enrichment of Cu, Zn and Pb was observed.

To see the influence of carryover of feed material into the condenser on the Cu content of zinc, it is necessary to find an indication for the amount of carryover. A good indication is the amount of pump sump dross.

The figure 3 shows the Cu content of sinter and hot briquettes at Berzelius for the years 1987 and 1988. The variation in sinter is not so wide as in the briquettes, because the hot briquettes are produced from secondaries coming from very different producers.

In the figure 4, the amount of pump sump dross is plotted against the sinter/hot briquettes ratio. If this ratio is increasing, this means less hot briquettes, the pump sump dross production is decreasing. This confirms that the higher amount of fine material in the hot briquettes is generating more carryover and finally more pump sump dross. Moreover, the increase in pump sump dross leads to a higher Cu content in zinc as visualized on the figure 5.

The conclusion is that the carryover of hot briquette fines influences the Cu content in furnace zinc more significantly than the volatilization from the furnace, which should be very low and more or less constant.

A mass balance for the zinc refinery is showed in figure 6. Nearly 90 % of the input in the refinery in form of furnace zinc is leaving the plant as metal for sale. Hard metal, dross, foam, lead, dust and cadmium fill the balance to 100 %. The copper distribution is shown in figure 7. Nearly 50 % of the copper in the furnace zinc is leaving the plant with the metal.

3.2. BOTTOM OF THE FURNACE : HANDLING OF LEAD BULLION AT LOW Pb/Cu RATIO

Over 90 % of the copper input goes with lead and slag to the furnace bottom. So, any increase in the copper input to the furnace will first affect the lead-slag system.

Lead and slag are tapped simultaneously out of the ISF and separated in a forehearth. The slag is granulated whereas the lead bullion is collected in kettles with 100 t capacity for decopperizing. The latter is done only by cooling : at lower temperatures, less copper can be dissolved in lead, so that a layer of copper dross is created on top of the lead bath and can be removed mechanically.

During a period of five weeks, the ISF was operated with low lead but constant copper througput. The lead to copper ratio in sinter is usually at a value of 10, it was now decreasing to 4. The result was an increased copper content in lead from 5 - 6 % for normal operation to more than 12 %.

To manage with this high copper content, it was necessary to operate the forehearth with a very precise temperature control to avoid temperatures below 990 °C (figure 2). At lower temperatures, a separation of copper rich phases and the formation of accretions are possible.

Such accretions formed during the period of investigation in colder parts of the forehearth. As a matter of fact, the lead production per ton of zinc being reduced to below 100 kg in comparison to more than 300 kg for normal operation, a much longer time was required to fill up a decopperizing kettle. During that time, especially when no stirring was possible, copper dross was formed as a crust on top of the lead bath, which could not be handled as usually.

To overcome this problem was very easy. After decopperizing, the lead was tapped only up to 50 %. This copper free lead was used to dilute the lead bullion coming from the furnace, so that the copper content was in a range of 5 - 6 % as usually. At that point, the copper dross formation showed no

difference with the standard operation although the production of dross was 2.5 times higher. Of course, this was only considered as a temporary solution ; as a matter of fact, it requires to double the capacity of the decopperizing kettles, which is wished to be avoided.

3.3. INVESTIGATION ON CONTINUOUS TAPPING

Another way of working considered, at the beginning of the study, to handle lead bullion with high copper content, was to tap the ISF continuously. This process, based on the continuous tapping of lead bullion developed by Asarco for lead blast furnaces, was first tried in an ISF by Cokle Creek on July 1985. From the informations available on this operation, one can mention the following difficulties :

* This way of working is acceptable for blast furnaces working continuously. Since the clean outs for the ISF occur every 10 to 15 days, which means a shut down of the furnace for 8 to 10 hours, the continuous tapping does not work in conditions of good efficiency.

* The zinc reduction, which is rather slow, takes place partly from the slag, which must therefore remain in front of the tuyeres for as long as possible. This requires a shallow crucible, which has an effect on the blast pressure. With a continuous tapping, the residence time for the slag may drop from 1h30mn - 2h to 1/2h. In such conditions, the zinc losses in the slag should be higher. This has been observed in Cokle Creek (8 % Zn in the slag, vs 7 % with discontinuous tapping).

* Despite the rather small residence time (1/2h), a complex technology is needed at the furnace bottom in order to maintain a slag height above the hearth. This leads to risks of speiss accretions which have to be absolutely avoided.

Cokle Creek has been developing this process since 1985. A lot of efforts have been exerted with no real success. The operators have been obliged to make very expensive modifications : lower the tuyere level in order to brass more vigorously the slag and maintain an adequate temperature in the hearth, build an additional Cowper heat exchanger in order to raise the blast temperature above 1,000 °C, and equip the lower part of the casing with copper blocks in order to freeze any speiss-slag leak. Furthermore, private communication from Cokle Creek operators indicates that these people are considering now a slag fuming in order to reach an acceptable zinc recovery.

Considering all these points, Metaleurop and Berzelius have decided to postpone all the development efforts regarding a continuous tapping for the ISF.

4. THE DECOPPERIZING STAGE

The decopperizing step at the bottom of an ISF aims at a copper recovery in the form of dry and fine powder, called dross, which can then be easily removed from the lead bullion. As already said, at the present day, this step is a batch process. The overall operation is very slow and therefore requires rather big kettle capacities.

4.1. DESCRIPTION FOR THE BERZELIUS AND NOYELLES-GODAULT OPERATIONS

At Berzelius, the lead bullion is tapped at 1,200 °C from the forehearth of the ISF into a ladle, then poured into a kettle and allowed to cool down. At this step, the lead bullion is somewhat quenched at an unknown temperature. The filling and the cooling of the kettle take several hours depending on its capacity. Because solubility of copper decreases as the temperature falls, "rough dross" or skims separate out on the surface. As the temperature reaches 380 °C, the kettle content is vigorously stirred again in order to lower the amount of entrained metallic lead in the skims and produce the final dross. They are then removed for further processing.

At Noyelles-Godault, decopperizing of the lead bullion is processed in a 70 tons kettle by quick cooling and high speed stirring leading to the production of fine drosses which are removed by suction. One of the characteristics of this process is its compactness due to the lack of room at the bottom of the furnace. The mean profile of an operation has been established. It shows that there are five steps (figure 9) : filling of the kettle ; drossing time during which stirring cools the lead and produces fine drosses ; suction time ; emptying time ; waiting time.

Today, the kettle can treat only 40 % of the ISF lead bullion. The capacity is limited for two reasons :

* It is not possible to receive the whole tapped lead in the kettle : the maximum allowed temperature obliges to leave in the kettle cooled lead from the previous operation.

* No lead from the following tap goes into the kettle because the sum of times of tapping, drossing, suction and emptying is longer than the time between two taps.

4.2. INCREASING THE CAPACITY OF THE DECOPPERIZING KETTLE

One can admit that the times of suction and emptying are not likely to be reduced. At the present time, the drossing time is not mastered. It can range from 45 mn to 160 mn. The difficulties come from the drying of "wet drosses" which may appear during drossing.

The checking of many parameters such as temperature and composition of the lead bullion, as well as special trials of different ways of stirring and cooling, did not give us any solution to the problem. On the other hand, analysis of lead during the operation showed that the decopperizing of the bullion was achieved quite fastly and that there was no decantation problem. So the only constraint for emptying is to do it at a temperature giving an acceptable copper content.

With all these observations we can imagine a new way of working whose typical profile is given on figure 10. It should allow to process up to 50 % of the ISP bullion in one kettle. That procedure was tested, but bad conditions regarding lead production (low lead production, low temperature of the lead, low copper content) did not allow us to confirm the feasibility of that process. Nevertheless, this trial showed that it is possible to remove the dross every two taps only and to have a quasi-continuous suction of the dross during operation.

That operating way was then adopted when the copper content of the lead bullion was high enough (above 3 %). One possible way to treat the whole production would be to invest a second kettle, but because of a lack of room in the Noyelles-Godault plant, it was decided to orientate the research towards an increase of the decopperizing kinetics by finding new operating means. Therefore, investigations were undertaken on the fundamental mechanisms of the decopperizing stage.

5. FUNDAMENTAL STUDIES OF THE DECOPPERIZING OF THE LEAD BULLION

5.1. THE MINERALOGICAL STRUCTURE OF THE COPPER DROSSES

The copper drosses may appear in two forms : a raw dross and an oxidized dross, as sketched in figure 12. Oxidized dross differ from raw dross by their much finer grains, and by the fact that almost all the metallic lead is transformed into PbO.

A mineralogical characterization of the dross has been done, using microprobe analysis. The table 1 shows the average composition of the main phases, and the table 2 shows the component phase balance for the oxidized dross. One deduces that the final copper content of the dross depends on how much lead is trapped and oxidized during the removal of copper drosses from the kettle. For Noyelles-Godault, this result means that close attention should be paid during the stirring and suction steps.

5.2 LITERATURE SURVEY

A literature survey dealing with the decopperizing of lead has been done on the fundamental aspects : equilibrium phase diagrams relative to the chemical composition of lead bullion, and studies on the mechanisms of the germination of copper species in lead bullion at low temperatures.

The equilibrium diagrams in the Pb-Cu-X systems (X = S, As, Sn, Sb) (ref. 7) show that the stability areas have similar shapes in all the diagrams. From the stability regions of the phases Cu_xX_y where X = S, As, Sn and Sb, the affinity of these species can be ranked accurately and the following rule can be retained :

S > As > Sn > Sb (where > means "has a greater affinity for Cu than").

The studies reported in the literature about germination in the systems Pb-Cu-Sb, Pb-Cu-As and Pb-Cu-Sn when lowering the temperature (ref. 8 to 10) show that the seeds are mainly formed between 600 and 700 °C for Pb-Cu-As and Pb-Cu-Sb systems and between 450 and 550 °C for Pb-Cu-Sn system. At higher temperatures, all the diagrams show an increase in the copper content close to the one given by the solubility diagram of the Pb-Cu system.

5.3. FUNDAMENTAL STUDIES OF THE DECOPPERIZING METALEUROP RECHERCHE EXPERIMENTS

From the industrial operation characteristics, the literature survey as well as the mineralogical drosses structure, one can figure out that the drossing operation is based on the following mechanisms :

* Germination step in which the impurities such as copper are expelled.

* Aggregation and growing step in which the previous crystals gather and collect at the surface.

* Oxidation and drying step in which, because of the stirring, some oxidation occurs. The forces are favourable to the dross formation.

Specific laboratory experiments were carried out in order to investigate the kinetics of germination and coalescence at temperatures ranging from 400 to 700 °C. The procedure was as follows : after melting and homogenization at 1,150 °C during 30mn, the samples (200g) were poured into a crucible maintained at the aimed temperature ; at the end of the experiment time, the crucible was quenched in water ; the samples were cut and divided in 3 parts (top, center, bottom) for chemical analysis and microscopic observations.

In a first series of experiments, the following lead bullion composition was chosen : 94 % Pb, 5 % Cu, 1 % Sn. This choice provides advantages regarding the samples preparation and does not take into account the eventual combined influences of the other impurities such as As and Sb. These impurities have been investigated only once the influence of temperature and time had been known.

The results are illustrated for a time of 30mn at several temperatures in the figure 13. One can notice a clear tendency to a growing of the aggregates as the temperature increases and so in each part of the sample. In the middle of the sample and especially at 700 °C, one can observe a rather dendritic coalescence instead of the globular coalescence in the upper part.

The influence of the time at 700 °C is illustrated in figure 14. One can see that the coalescence of the crystals can give a unique crystal of more than 8 mm diameter for a time of 2h30mn.

The results of the influence of temperature and time on the crystals sizes and shapes have been summarized in the figures 15 & 16 for the upper and middle parts of the samples. For a given time, the higher the temperature, the larger are the crystals sizes. For a given temperature, the time favours the crystals coalescence or "growing". But is seems that a very long time (2h30mn) disfavours the aggregation.

The composition evolution of the copper grains remarkably corresponds to those of the composite species between 400 and 700 °C surrounding the initial composition in the copper corner of the Cu-Sn diagrams (see figure 17) ; that is to say : α and β Cu phases for 600 and 700 °C, and Cu phases for 400 °C. Consequently, one can see that the quenching temperature has fixed the composition of the grains which can or cannot gather afterwards.

A second series of trials have been performed with synthetic lead bullion containing 3.5 % Cu and 2.5 % Sn. The temperature variations were from 400 to 600 °C whereas the quenching time was kept constant at 30 mn. From the coalescence and morphology points of view the results were the same than those with less tin in the lead bullion.
On the contrary, the composition of the copper phases changed quite a lot (figure 18). As the phase (Cu_4Sn) is still present, one can see clearly the role played by the demixtion phenomena and cooling velocity. This is illustrated in figure 19 where the demixtion zone for the lead compositions (hatchured zone) spans the temperature interval 750 to 800 °C.

Higher quenching temperatures set a lower cooling rate which allows a higher demixtion rate, creating a bigger quantity of liquid rich in copper. The observations at 600 and 700 °C show a greater coalescence of the copper grains and this is due to the phenomena described above.

All these results have also been checked on industrial bullions and the same conclusions were drawn.

5.4. PROPOSITION FOR A NEW FAVOURABLE DECOPPERIZING PROCESS

Regarding the objective of compactness and improvement of the kinetics of the decopperizing process, one favourable scheme would be :

* A lead bullion composition which promotes a strong proportion of copper Cu_3X during the demixtion step as shown in the ternary diagram (Pb-Cu-X (= AS + Sb + Sn) (figure 20).

* A rather slow cooling in the 700 - 800 °C temperature range in order to impose high demixtion rates. This step should be short (less than 5 mn) and would allow to reach a 0.5 % copper content in the lead bullion, suitable for the further refining steps.

* A following quenching at 400 °C of the lead bullion in order to succeed in the drossing/drying step, or a separation step of the copper rich phase and then a quenching in order to produce a fractional product.

One can imagine, in the case of Noyelles-Godault, an intermediate small ladle which realizes the demixtion step in front of the present kettle. But this requires to develop new materials for the lead stirring at 800 °C.

The separation of the copper rich phase from the lead bullion and its cooling also necessitates new investigations which have not been performed in this study.

6. CONCLUSIONS

1. The copper at the top of the furnace originates mainly from carryover of fine materials charged, and is transferred mostly in the zinc phase which goes to the zinc refinery. It does not cause too many problems if the physical quality of the charge is high enough.

2. The ISF can not be economically operated with a continuous lead tapping since these new investments, as shown by Cokle Creek in Australia, are heavy and do not bring very important improvements. In particular, the slag zinc content remains in average above those of furnaces running with a discontinuous tapping.

3. However Berzelius has shown that the ISF can accept during short periods, amounts of copper in their input corresponding to a content up to 12 % in the lead bullion. For longer periods the decopperization of this bullion has to be improved.

4. As in Noyelles-Godault, but with a corresponding kettle capacity of 140 t and a special tapping procedure, it is possible to decopperize continuously by quenching the raw lead tapped from the furnace. The copper dross is then a powdery material, and can be handled easily, regardless to the initial copper content.

5. The kinetics of copper separation from lead is increased by a higher temperature, but the current technology can not accept it, because the materials used (for stirrers, pumps,...) do not resist to the corrosion by lead at 700 - 800 °C.

6. In consideration of this, a new proposition for a favourable scheme of decopperizing has been given. It comprises a rather slow cooling in the 700 - 800 °C temperature range in order to impose high demixtion rates and a following quenching at 400 °C of the lead bullion in order to succeed in the drossing/drying step, or a separation of the copper rich phase and then a quenching in order to produce a fractional product. This step necessitates to develop new materials for the lead stirring at 800 °C.

7. REFERENCES

1. BRYSON J.L., GRAY P.M.J.
"Recovery of copper in the Imperial smelting furnace"
Trans. IMM, section C, vol 77, June 1968, pp. 72-84.

2. EMERY A.C., HARRIS C.F., ROBSON A.W.
"The role of zinc-lead blast furnace in processing complex sulfides"
Complex Sulfides '85, ed. Zunkel A.D.,Boorman R.J., Morris A.E., Wesely P.J., pp. 635-642.

3. ADAMI A.O., FIRKIN G.R., ROBSON A.W.
"Treatment of complex materials and residues in the Imperial smelting process"
Complex Metallurgy '78, PP.36-42.

4. TEMPLE D.A., JOHN G.O.
"The treatment of complex zinc/lead/copper ores in the Imperial smelting process"
CIM Bull., vol. 64, Feb. 1971, pp. 58-66.

5. HANSEN M.
"The constitution of binary alloys"
2nd Edn., Mc Graw-Hill, 1958.

6. MACZEK H.
"The economics of processing complex sulfides concentrates in the Isf"
Complex sulfides '85, ed. Zunkel A.D., Boorman R.J., Morris A.E., Wesely P.J., pp. 773-782.

7. DAVEY T.R.A.
"Phase systems concerned with the copper drossing of lead"
IMM publication, May 1963.

8. KRYSKO W.W.
"Die entkupferung des bleies - parts 1 & 2"
Erzmetall, vol. XVII, 1964, pp. 285-340.

9. KRYSKO W.W.
"Die entkupferung des bleies - parts 3 & 4"
Erzmetall, vol. XIX, 1966, pp. 12-20.

10. KRYSKO W.W.
"Die entkupferung des bleies mit schwefel - parts 5 to 7"
Erzmetall, vol. XIX, 1966, pp. 121-127.

Phases	S %	Pb %	Ag %	Sn %	Sb %	Fe %	Ni %	Cu %	Zn %	As %	TOTAL
Impure Copper	-	0,16	0,26	15,0	19,6	0,05	1,42	62,8	0,10	0,89	100,20
α - Copper	-	0,16	0,12	0,67	3,75	0,07	0,38	92,0	0,10	2,52	99,77
$Cu_{1,87}$ S	21,1		0,13					78,5	0,09		99,73
$(Zn_{0,87}$ $Fe_{0,07}$ $Cu_{0,06})$ S	33,1					4,10		3,70	58,5		99,40
PbO		91,3						0,48			91,78*

* plus 7.67 % of oxygen

TABLE 1 : Compositions of the phases contained in the copper drosses

Phases	% mass	Mass of each element								
		S	Pb	Ag	Sn	Sb	Fe	Cu	Zn	As
Metallic Pb	1		1,0							-
PbO	51,6		47,1							
Metallic Cu	34,6		0,05	0,07	3,21	4,60	0,02	25,8	0,03	0,53
ZnS	5,5	1,82					0,23	0,20	3,22	
Cu_{2-x} S	1,2	0,25						0,94		
Fe - As	1,9						1,38	0,12		0,39
Oxides	4,6				1,09		0,20		1,07	
Total	100	2,07	48,15	0,07	4,30	4,60	1,83	26,52	4,32	0,92

TABLE 2 : Sharing of the elements in the different phases contained in the copper drosses

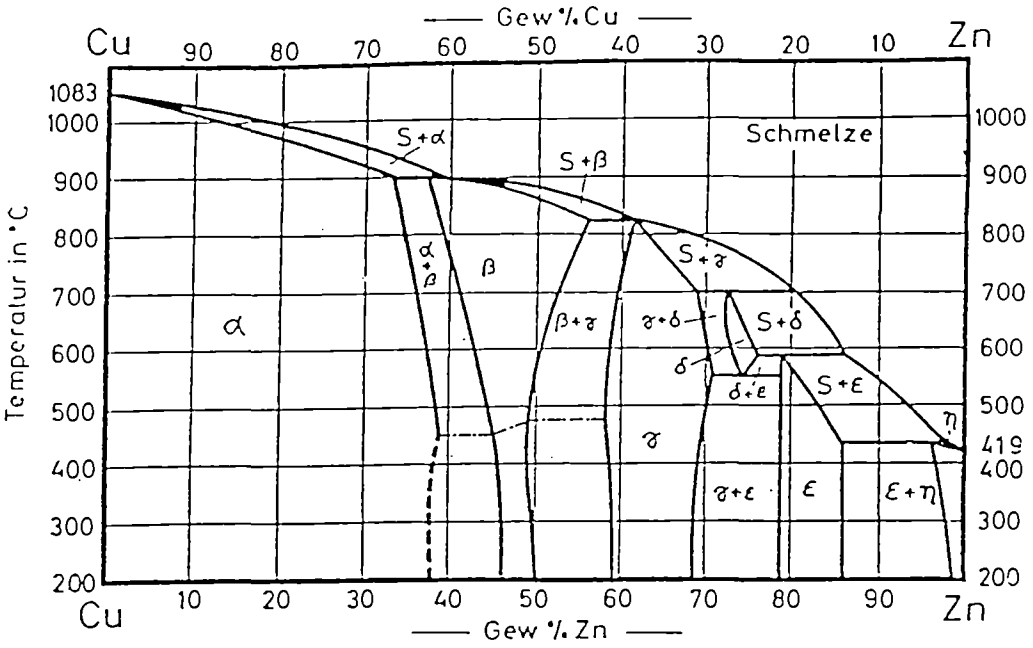

FIGURE 1	Cu- Zn	

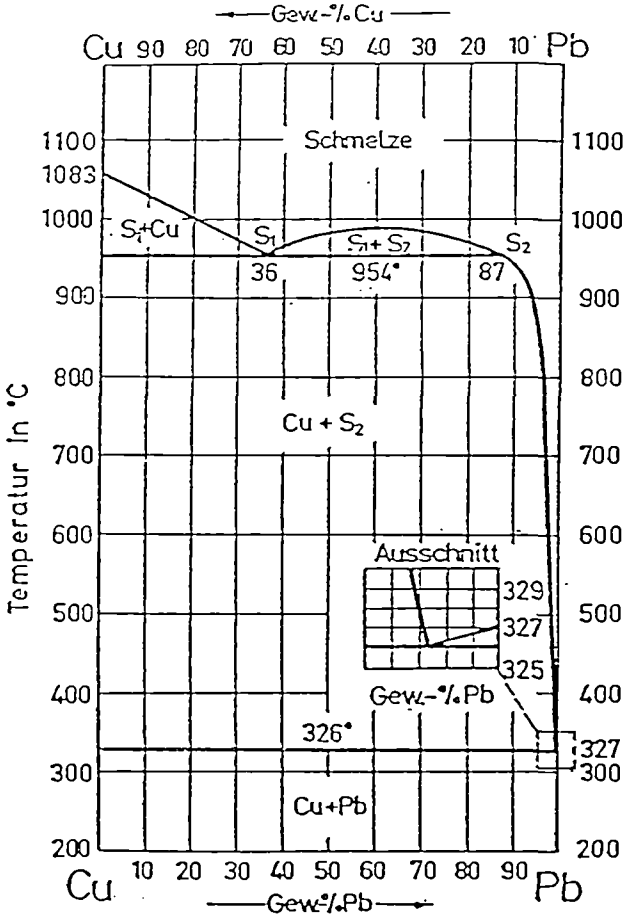

FIGURE 2	Cu-Pb	

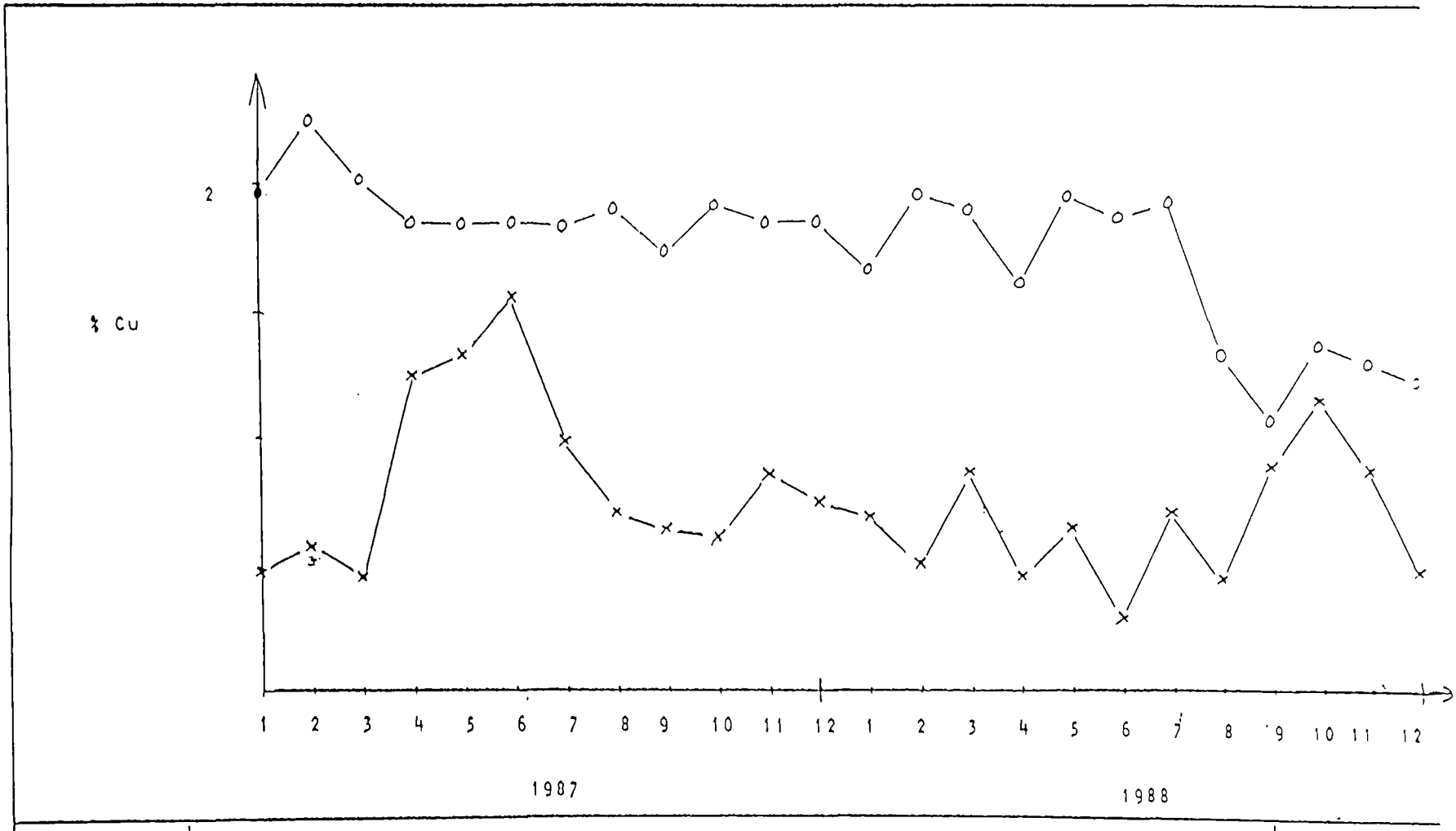

Berzellus Metallhütten GmbH

FIGURE 3.

Kupfergehalt im Sinter (O)

Kupfergehalt in den Heißbrikotts (x)

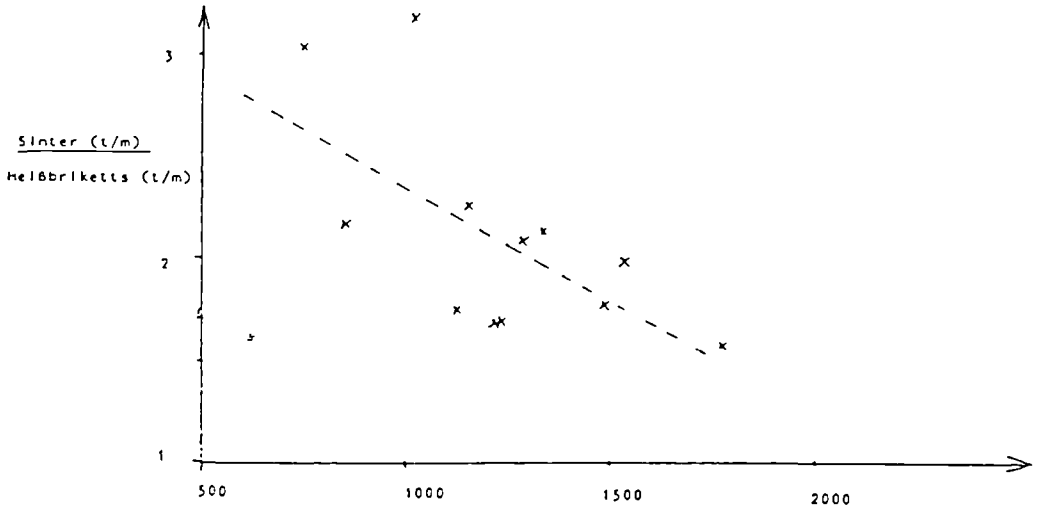

FIGURE 4

Berzelius Metallhütten GmbH	Einfluß des Verhältnisses von Sinter/Heißbriketts in der Charge auf den Entfall von Pumpensumpftraß

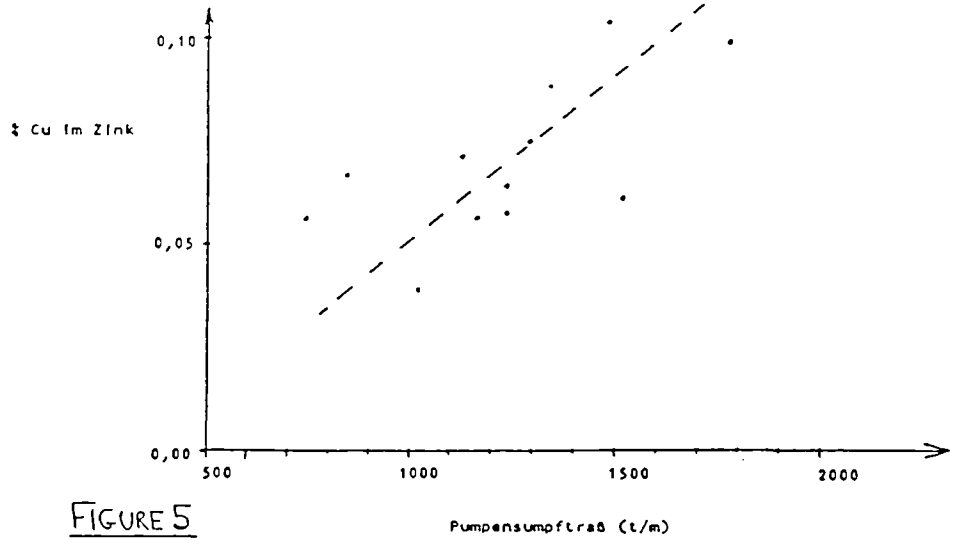

FIGURE 5

Berzelius Metallhütten GmbH	Einfluß des Pumpensumpftraßentfalls auf den Kupfergehalt im Rohzink

Massenverteilung Feinzinkanlage

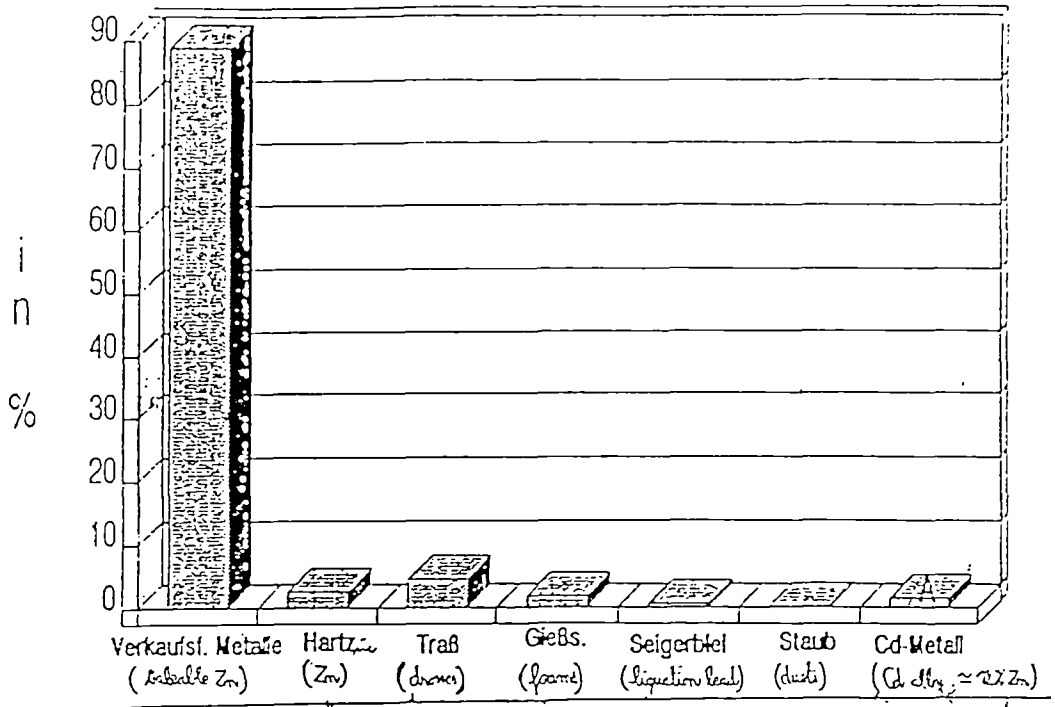

Berzelius Metallhütten GmbH | FIGURE 6 | Massbalance Zinc Refinery

Cu-Verteilung

in %

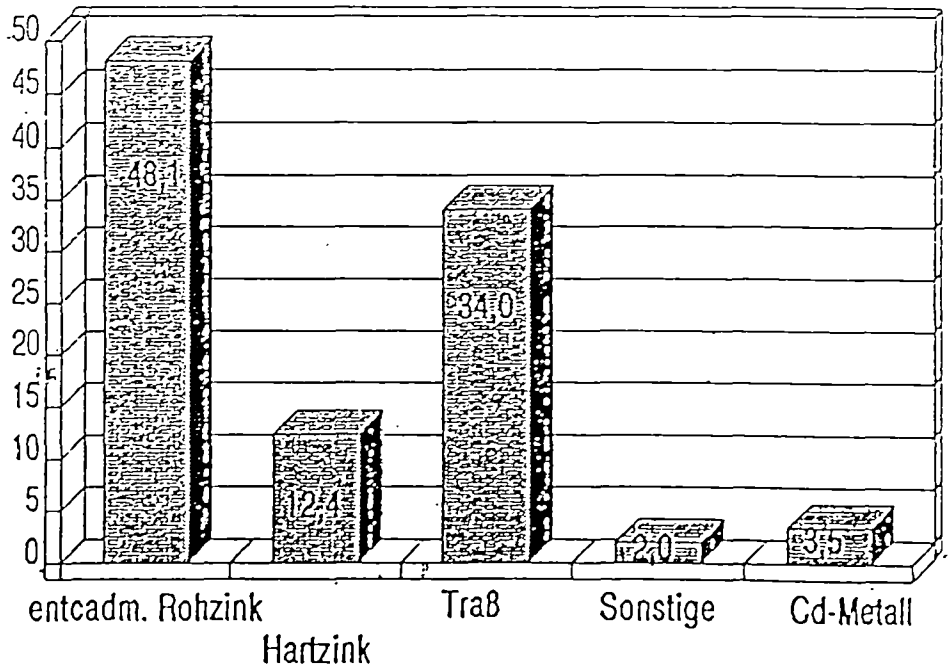

Berzelius Metallhütten GmbH | FIGURE 7 | Copper Distribution in the Zinc-Refinery

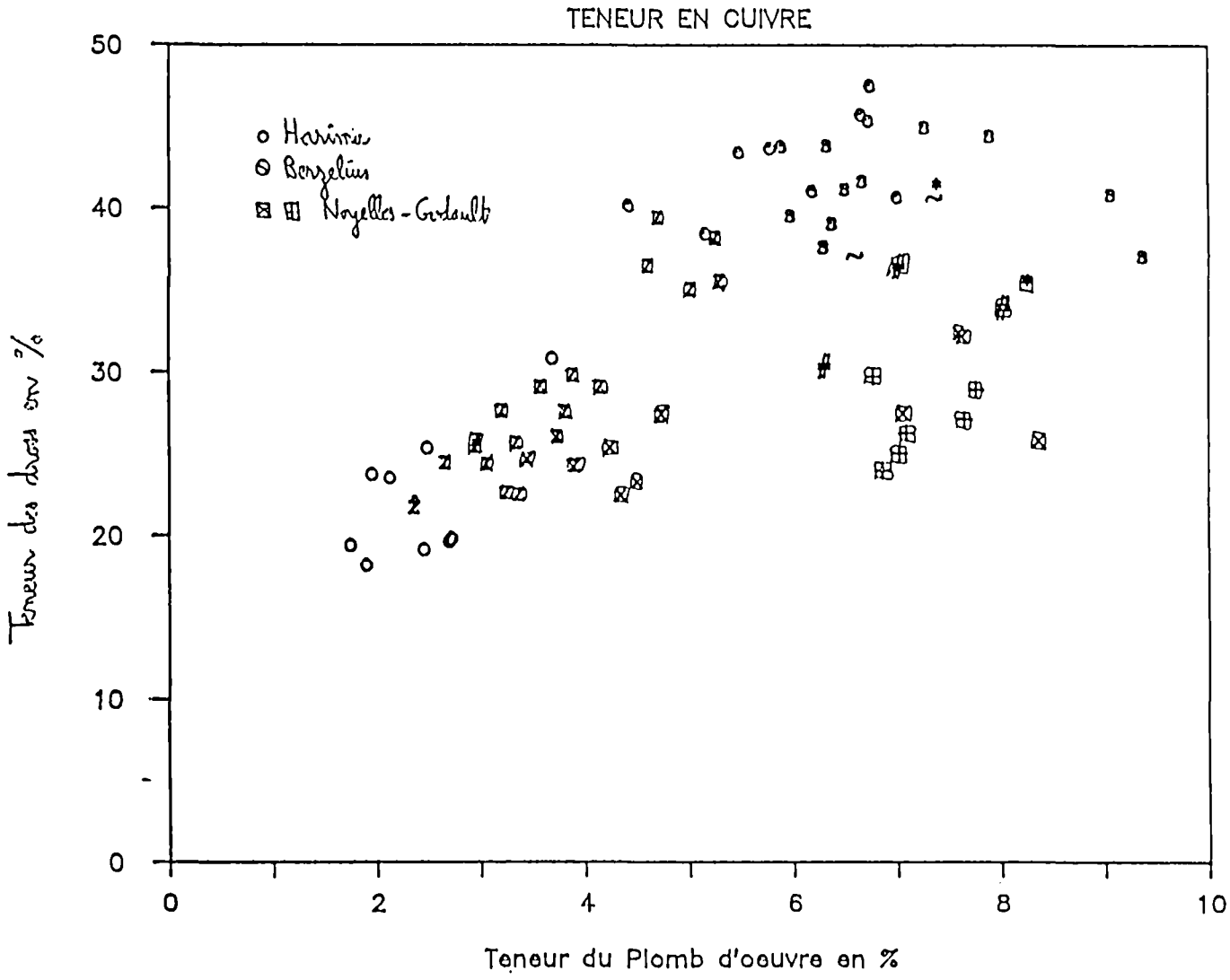

FIGURE 8 : CORRELATION BETWEEN THE COPPER CONTENTS IN THE LEAD BULLION AND IN THE COPPER DROSSES, FOR DIFFERENT ISF

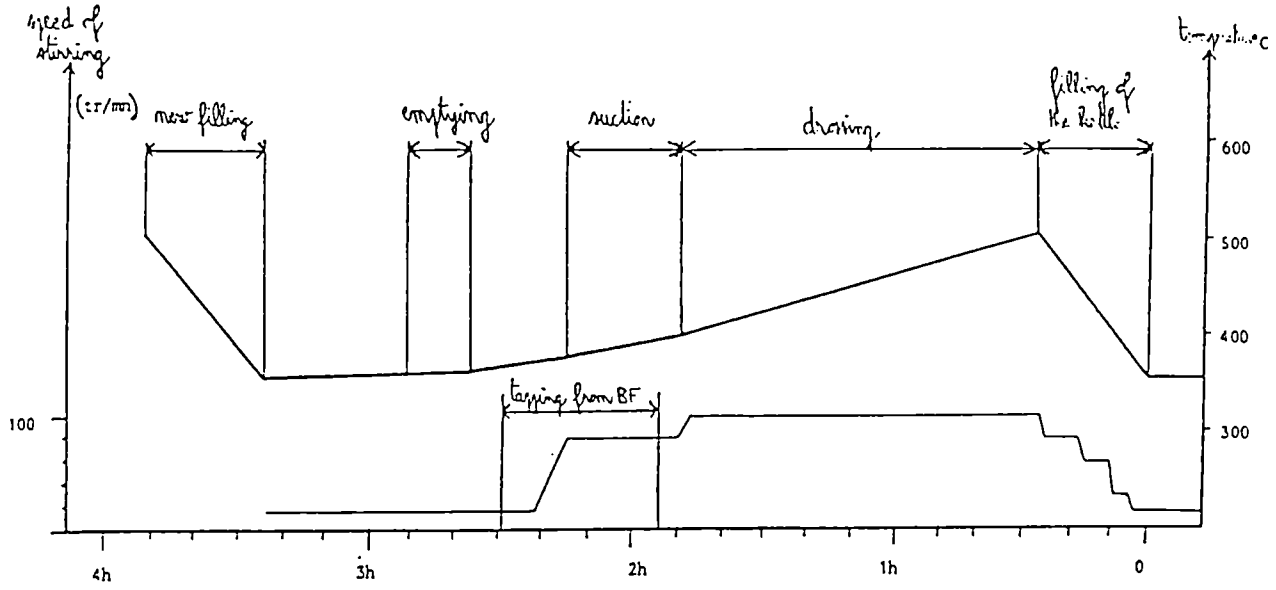

FIGURE 9 : Decopperizing of the lead bullion from ISF in Noyelles-Godault (in the 70 t kettle)

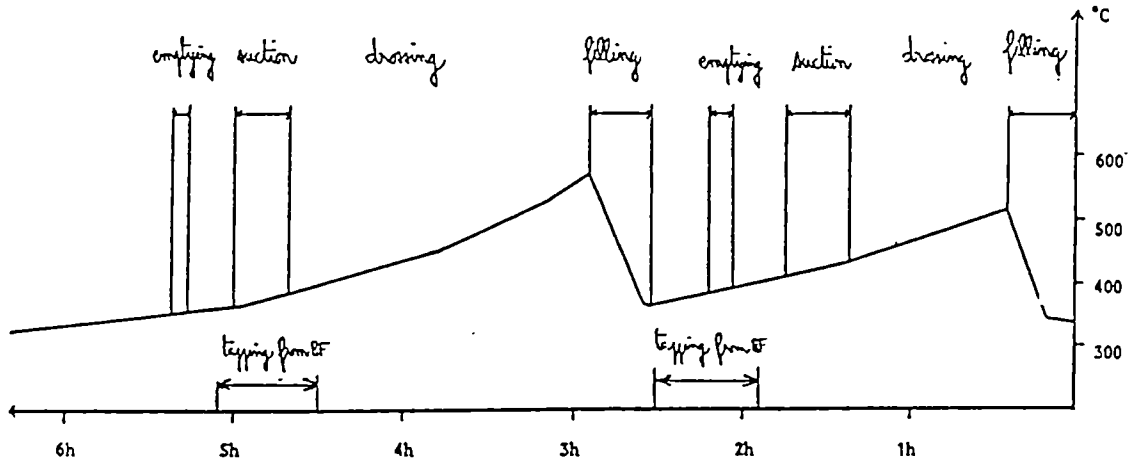

FIGURE 10 : Proposed timing for the treatment of 50 % of the ISF lead bullion (to be compared with figure 9)

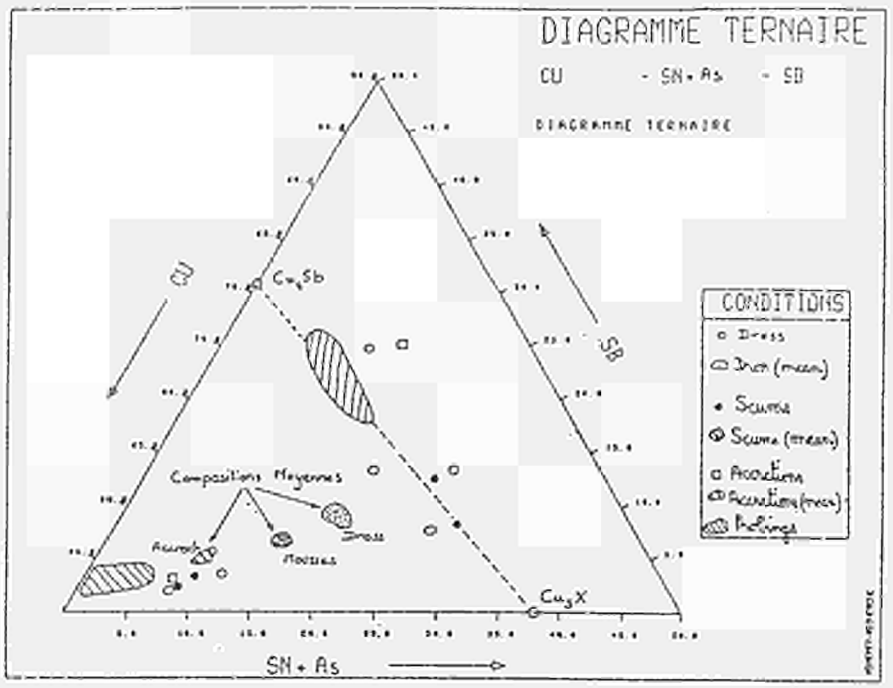

FIGURE 11 : Composition of copper drosses and other products of the drossing operation

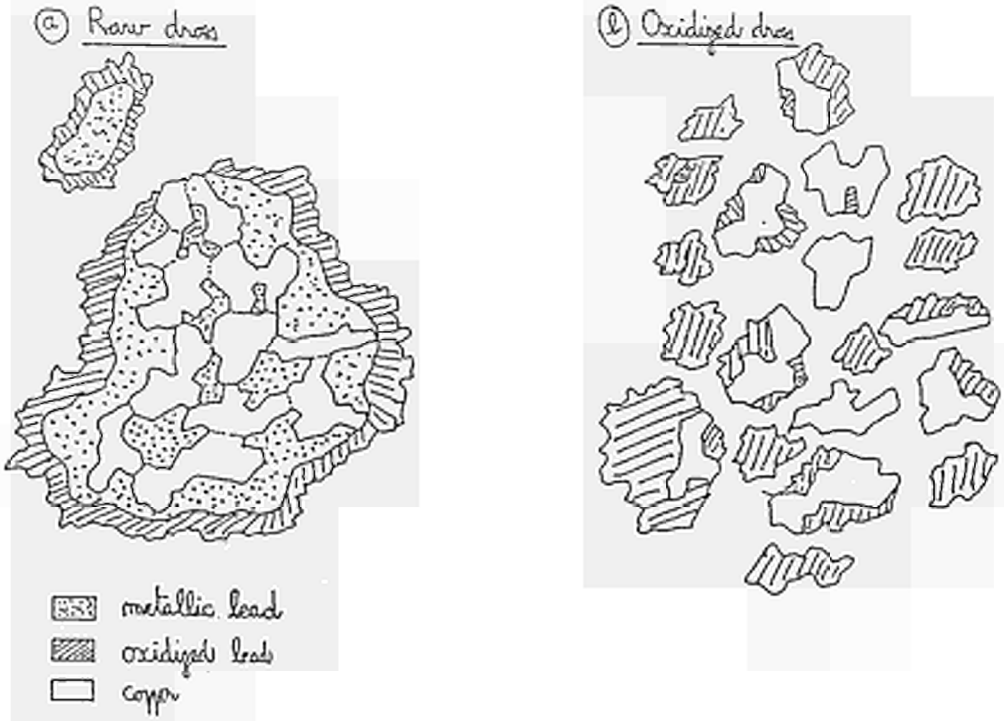

FIGURE 12 : Mineralogical structure of the copper drosses

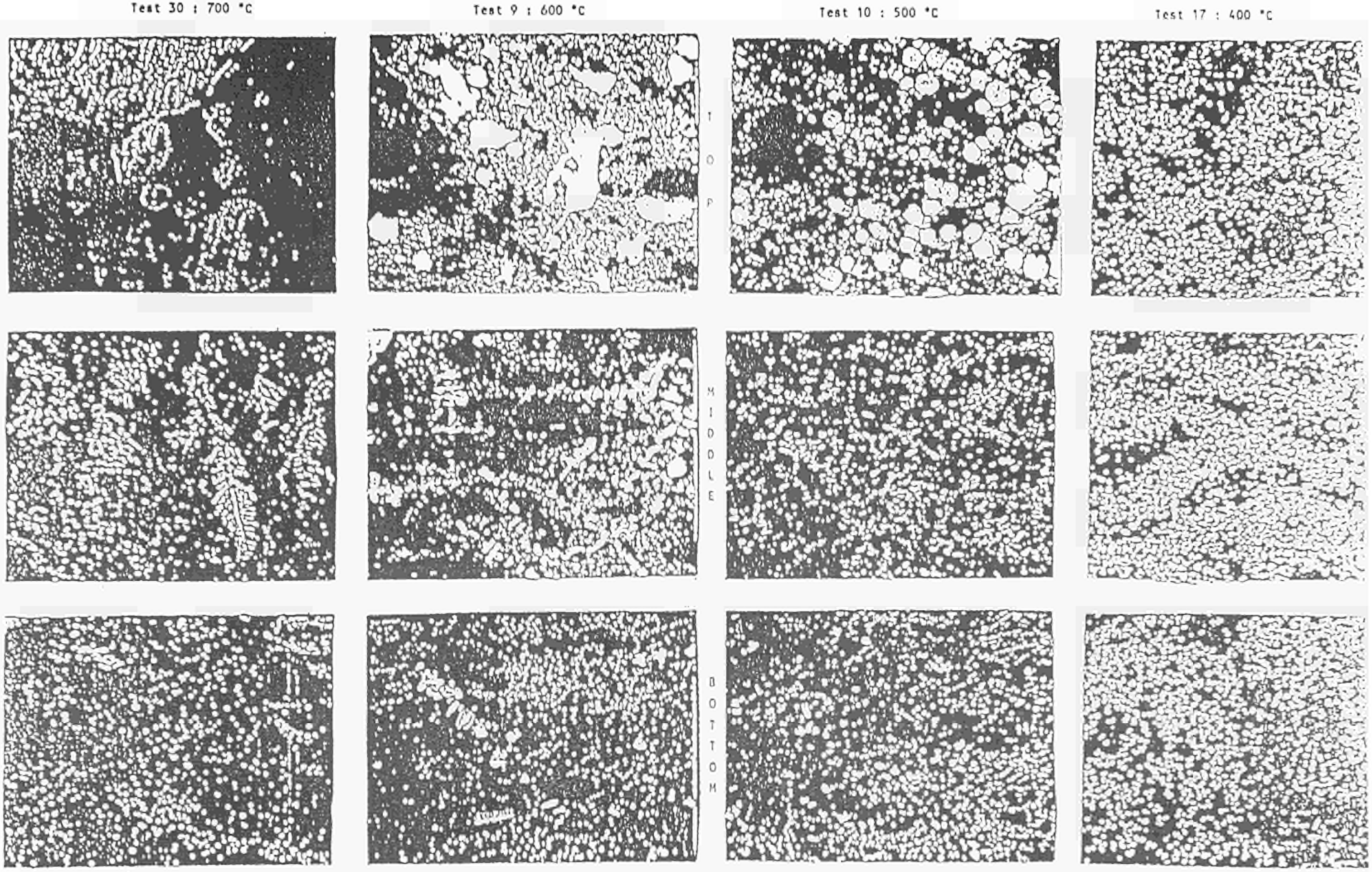

FIGURE 13 : INFLUENCE OF TEMPERATURE

Quenching time : 30 mn

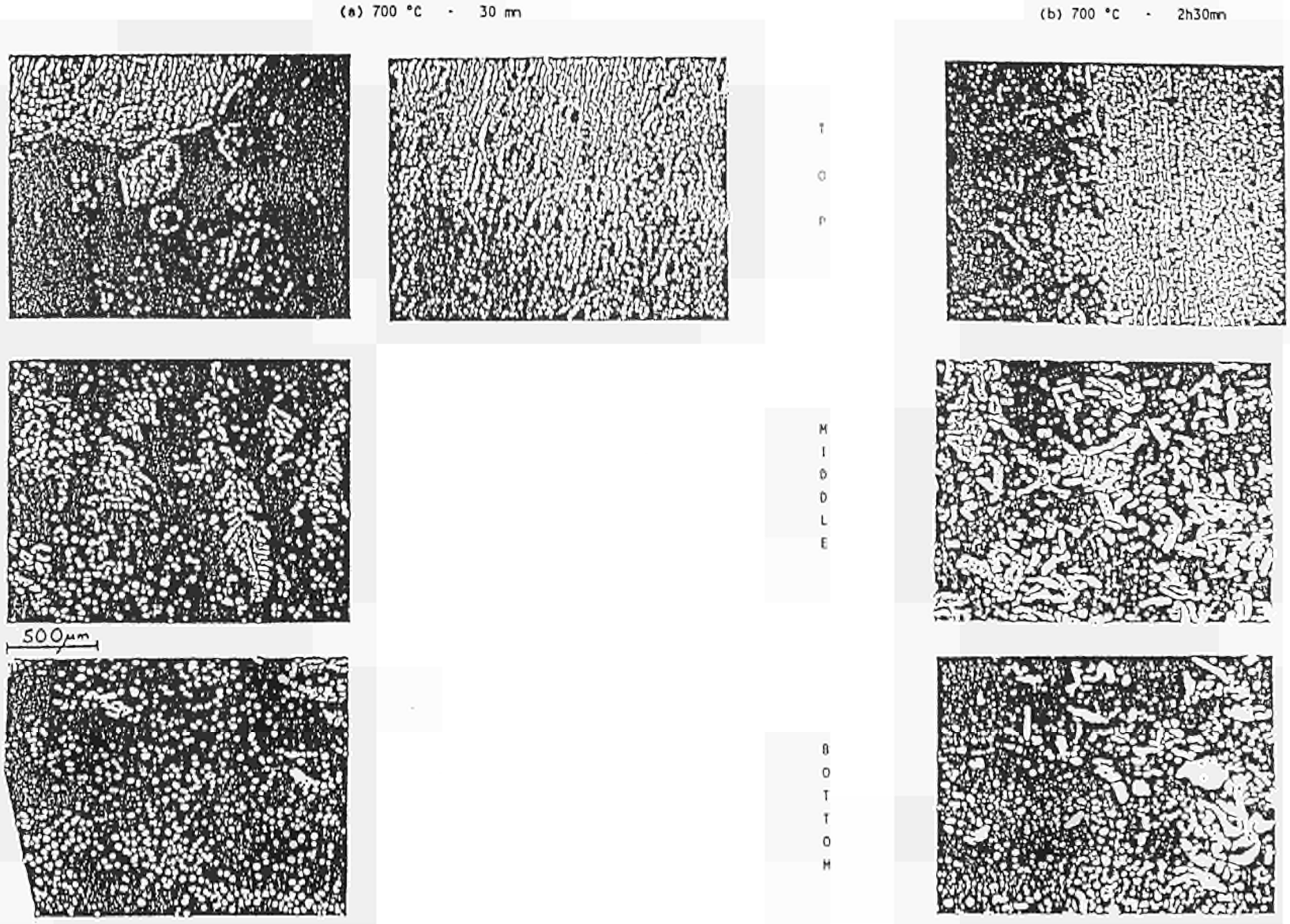

FIGURE 14 : INFLUENCE OF THE QUENCHING TIME ON THE MORPHOLOGY OF THE COPPER DROSSES

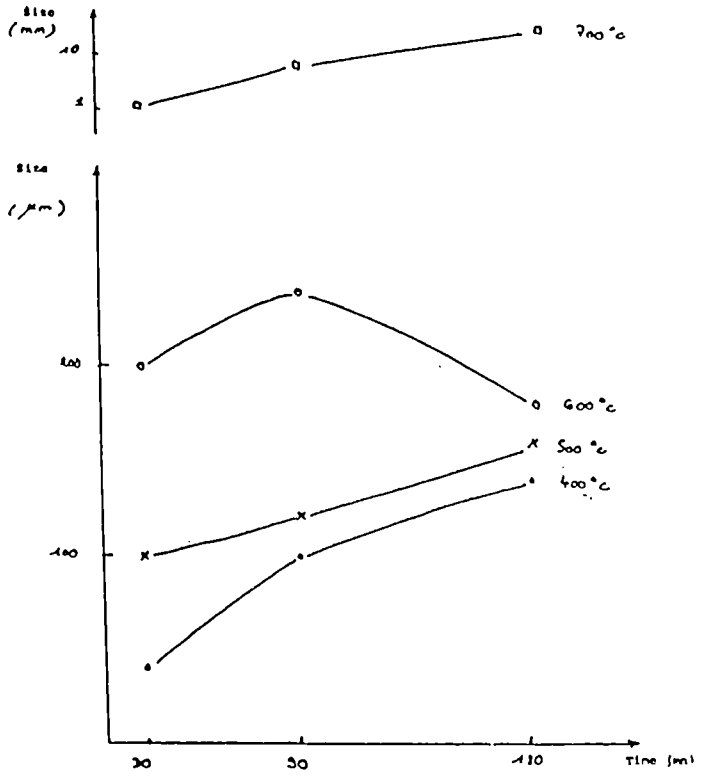

FIGURE 15 : CRYSTALS SIZES IN TERMS OF TIME AND TEMPERATURE
TOP OF THE SAMPLE

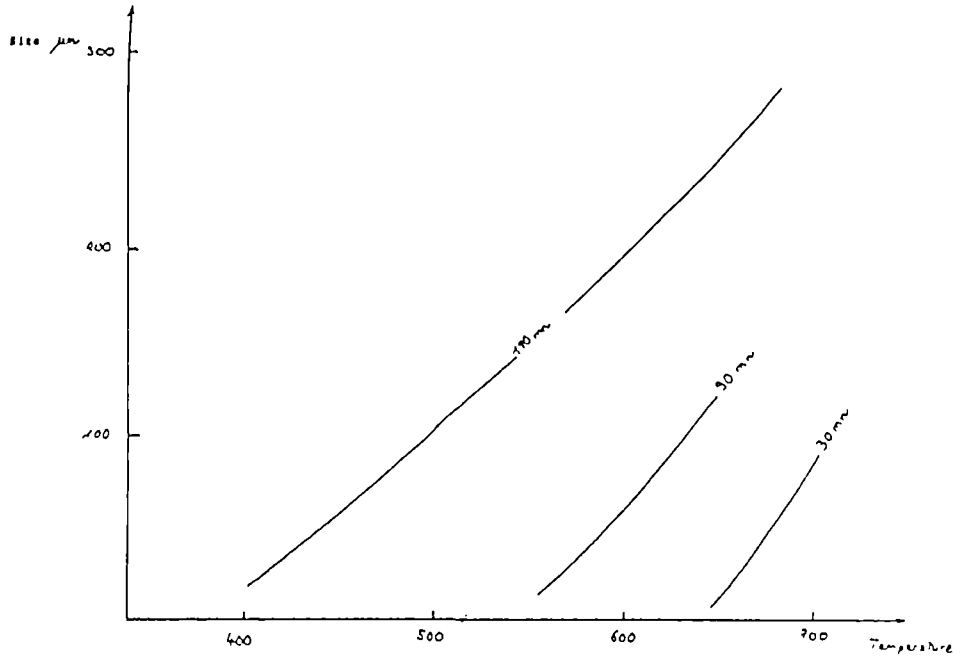

FIGURE 16 : DENDRITIC CRYSTALLIZATION
MIDDLE OF THE SAMPLE

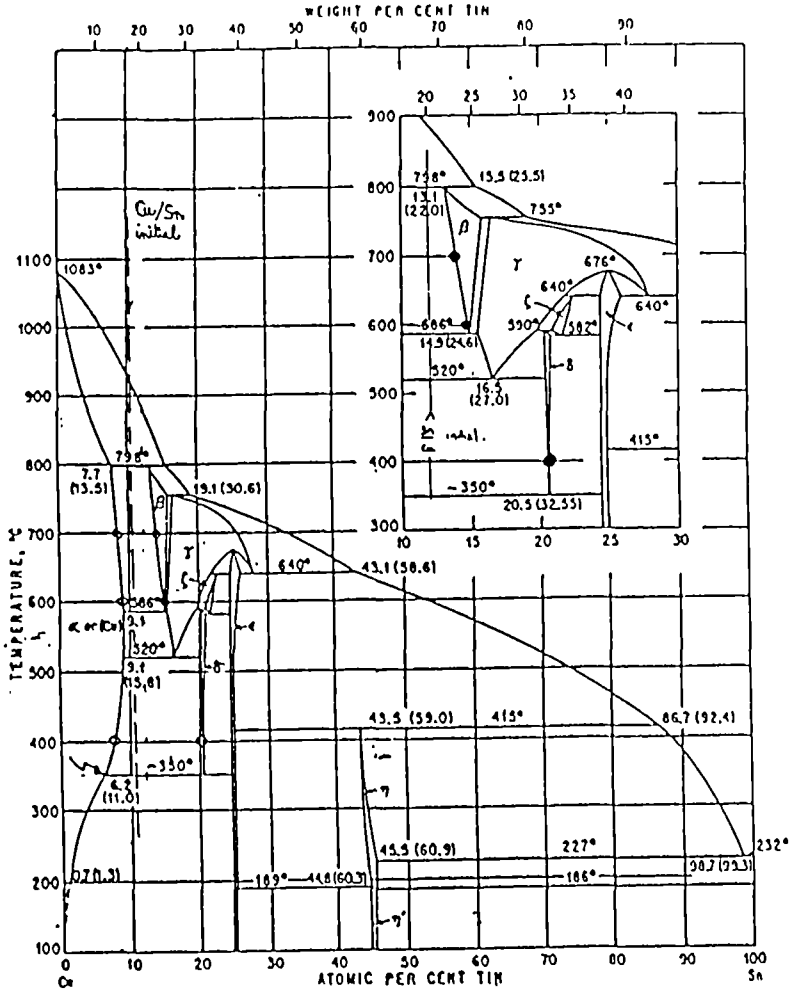

FIGURE 17 : EVOLUTION OF THE COMPOSITION OF PRECIPITATED Cu-Sn PHASES WITH THE TEMPERATURE
INITIAL COMPOSITION OF THE LEAD BULLION : 5 % Cu & 1 % Sn

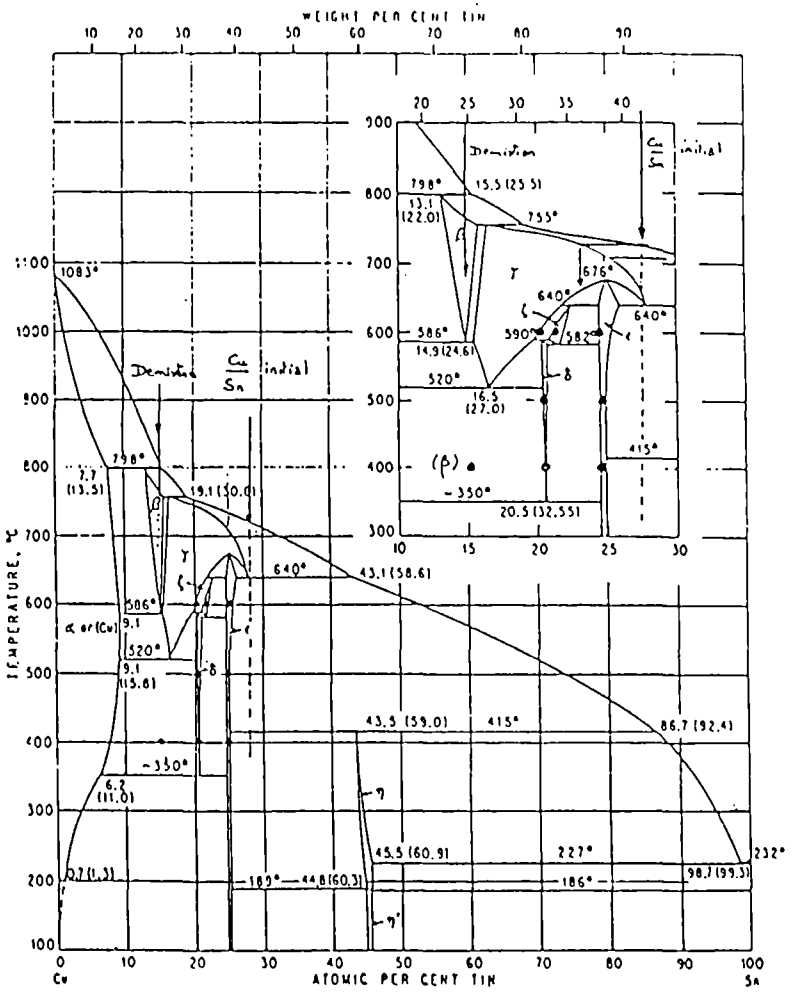

FIGURE 18 : EVOLUTION OF THE COMPOSITION OF PRECIPATED Cu-Sn PHASES WITH THE TEMPERATURE
INITIAL COMPOSITION OF THE LEAD BULLION : 3.5 % Cu & 2.5 % Sn

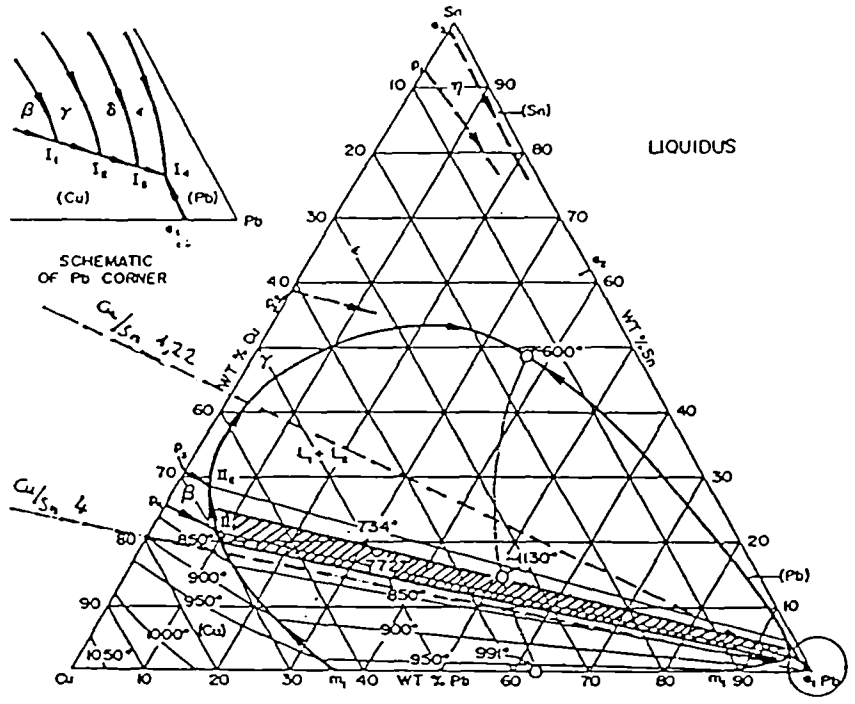

FIGURE 19

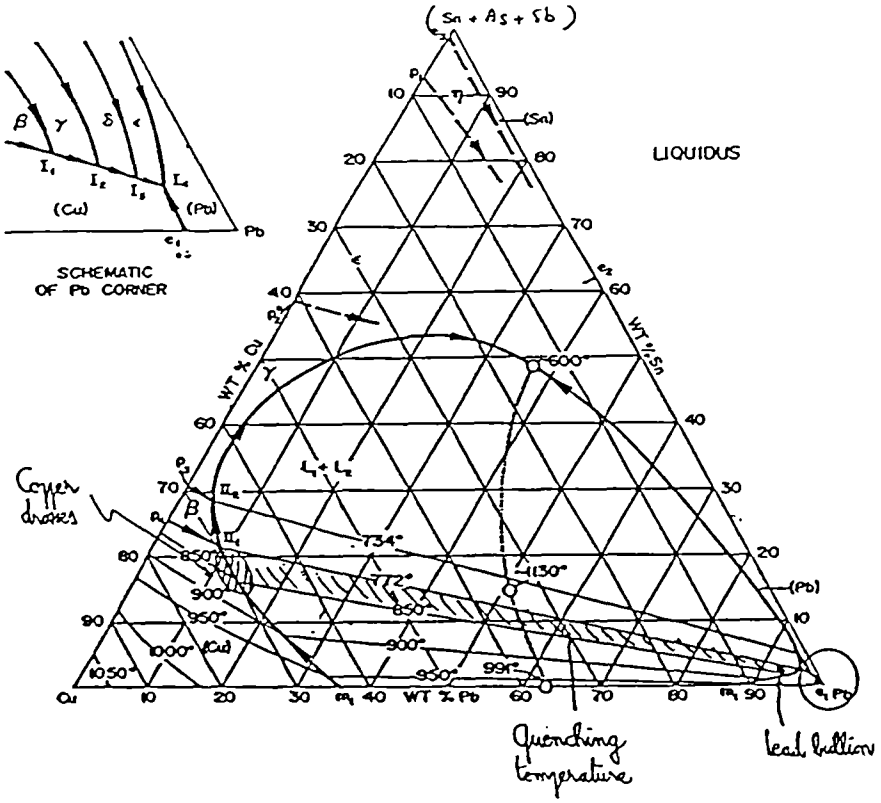

FIGURE 20 : New proposed decopperizing process

RESEARCH AREA 3.4

TREATMENT OF MINING WASTE AND METALLURGIC RESIDUES

RESIDUAL ULTRA FINE PYRITE AS A RAW MATERIAL FOR NON FERROUS METALS RECOVERY AND SIMULTANEOUS SULPHURIC ACID PRODUCTION

Project Leader: Jacques DUPONT
S A P E C, S.A., Portugal

G. HERMIA, A. VAN LIERDE, L. EVRARD
Université Catholique de Louvain, Louvain-la-Neuve, Belgium

Contract MA1M-0020-P

1. OBJECTIVE

New specific tailings are under way to be produced in Portugal. These tailings are directly related to the sulphides of non ferrous metals ores processing and consist in ultra fine residual pyrite issued from the ore beneficiation.

These residual pyrites which are considered as a tailing, could possibly be a cheap raw material for sulphuric acid production, and would replace in the same proportion the elemental sulphur imported into the Common Market.

In addition, but it is not always the case, other valuable elements could be recovered at a low cost from the residual pyrite.

But because such tailing material is unusually fine, laboratory and pilot plant tests are required to find out the specific behaviours and properties for the purpose to be able to bring the preliminary backgrounds in order to indicate the possible and most suitable ways for processing of such type of raw material.

2. INTRODUCTION

The main characteristic of the sulphides deposits in Portugal is the extreme dissemination of the valuable elements in the ore, which necessitates a very fine milling for acheaving an acceptable recovery of these elements.

Similarly, the residual pyrite is also exceptionally fine the K_{80} of samples showed variance between 16 and 28 microns.

It is a matter of fact, that this residual pyrite is much finer than the other flotation pyrites and even than the residual pyrites coming from the complex sulphide flotation plants on the Spanish side of the Iberian pyrite belt.

A good example is the residual ultra fine pyrite from the Corvo copper mine which started production late in 1988. The copper content in the Corvo deposit varies between 6 and 14 per cent and chalcopyrite is the essential copper mineral. This chalcopyrite is exceptionally disseminated in the pyrite matrix, and as a consequence of that, the copper remaining in the residual pyrite could be relatively high, despite the extremely fine milling.

In that case, the flowsheet of a commercial unit would basically comprises the following stages :

1) the dewatering of the residual pyrite slimes.

2) the conditioning of the dewatered product for further operation.

3) the sulphatizing roasting in fluidized bed, with waste heat recovery, in order to produce SO_2 for sulphuric production and transform the valuable elements in soluble sulphates.

4) the leaching in slightly acid sulphate solution with the recovery of the valuable elements.

It has to be pointed out that the waste heat recovery is one of the major input in the new suphuric acid plant.

On the other hand, if the dry solids of the ultra fine pyrite are between 80 and 90 %, the material is very sticky and becomes a compact mud impossible to handle.

In addition the 99 to 100 % dry solids, a dry dusty ultra fine material, are not suitable because of roasting problems.

When dry feed is required pelletization has to be carried out. Thanks to the granulometry of the material, pelletization can be performed without any binder.

A further drying makes the pellets very strong. Then pelletization would be an additional cost to the process, which would be better to avoid.

The dewatering and the conditionning of the material are the key points of the process.

It is clear, that it is possible to operate the roasting with pyrite slurries. But because of the ultra fine granulometry of this material, the viscosity of the slurry starts to increase tremendously at 70 - 75 % of solids, higher viscosity makes more difficult to secure correct distribution of the feed into the roaster. Also, there are two major disadvantages with feed slurries :

- the high humidity of SO_2 gas which would disturb the dry dust collection and waste heat recovery.

- the loss of an important portion of the waste heat recovery.

The zone between 90 and 96 % of dry solids would have to be explored for getting a good filter cake which can be handled conveyed properly and stored without any subsequent agglomeration, and also securing an easy feed distribution of such cake into the fluidized bed roaster. Such a processing can give low investment as well as low operation cost.

3. LABORATORY AND PILOT PLANT WORK AND RESULTS

3.1. DEWATERING

3.1.1. Laboratory tests on Corvo residual pyrite

Laboratory tests have been operated on Corvo residual pyrite.

The main topics of the hydrocycloning, thickening and filtration tests are as follows :

- selectivity of hydrocycloning is acceptable : about 2/3 of the fraction below 1 u is passing into the overflow despite the fact that this represents only 22 % of the flow;

- filtration of the hydrocyclone overflow is difficult; filtration rate is slow and cake is sticky and very wet, 28 - 30 % moisture;

- thickening of the hydrocyclone overflow is very poor; after 24 hours, the thickening underflow contains only 26 - 28 % dry solid; nevertheless, settling rate is not too bad;

- filtration of the hydrocyclone underflow is good; the cake has good mechanical properties, its moisture is normal and there was no solid in the filtrate;

- by eliminating the finest part of the feed which represents 10 to 14 % of the solid content in the feed, the filtration properties have been improved, and vaccuum filtration can be considered, as a possible alternative to filters press;

- the filtration of the hydrocyclone overflow is not feasible. Nevertheless if it contains sufficiently valuable elements the following could be considered : thickening and drying in lagoon, solution which would be possible in Alentejo (Portugal), especially in the summer

period; drying in fluidized bed indirect heating would be probably a too expensive way because of the exceptionally high moisture, but it works.

3.1.2. Laboratory and pilot test on Aljustrel residual pyrite

a) Short description of the main physical properties related to representative sample :

- particle size characteristic :

below	1 microns	:	8 %
	K 50	:	14 Microns
	K 80	:	27 Microns

- viscosity has been tested by torsion viscosimeter, and the results are indicated here after on Table I

This shows the following points :

- due to much finer particle size distribution, the viscosity of the pulp is considerably higher than when compared with normal flotation pyrite which is not ultra fine.

- below 70 % of dry solids, the viscosity of the pulp is quite low. Consequently, pumping, mixing, spraying and keeping the pulp homogeneous are easy and requires low power.

- above 70 % of dry solids, the viscosity of the pulp starts to increase substantially and upon reaching 74.5 % of dry solids increases dramatically.

- at higher dry solids than 78 %, the products become rapidly more and more muddy and very sticky.

The pulp is thixotropic and this property increases with increasing dry solids content.

Therefore fs high dry solids is required, high speed mixing has to be used as well as powerful mixing in order to prevent any settling time in the whole volume of the pulp.

b) Laboratory filter press test.

At 72% the specific dewatering rates are $1,18 \times 10^6$ and $3,3 \times 10^5$ s/m^2 at a pressure of 1 and 4 bar respectively.

At 79% the specific dewatering rates are $3,8 \times 10^6$ and $1,24 \times 10^6$ s/m^2 at a pressure of 1 and 4 bar respectively.

With a pulp at 79 % dry solid, the filtration cake has 0,46, a medium compression coefficient, while at 72 % dry solid, the filtration cake has 0,63 which is a low compression coefficient. A better distribution of the solids is carried out during the filtration with a lower solids content pulp.

c) Pilot filter press test

A typical filtration sequence is indicated in Table II. From this, it could be anticipated a rate of production cake 170 to 200 kg per hour and square meter at about 93 % Dry solids in a commercial filter press equiped with cake squeezing and final compressed air belowing through. The expected time of sequential cycle would be :

filtration	:	8'
membrane squeezing	:	1'
dehydration by compressed air	:	16'
idle time	:	5'
		30'

3.2. FILTER CAKE CONDITIONING

The ultra fine residual pyrite is very reactive. Consequently, the storage period of the filter cake has to be short because this material reacts rather rapidly with the atmospheric agents agglomerating the mass.

After the storage and before the roasting, the pyrite filter cake has to be treated in a desintegrator in order to destroy the lumps and limit the remaining clumps which have occured during the filtration handling and storage.

It could be worth to mention also that good filter cake have been produced by mixing dry ultra fine pyrite with pulp of the same material, which permit to adjust the dryness of the cake.

3.3. ROASTING TEST IN PILOT PLANT

After the dewatering, the second topic is related to the conditioning and afterwards the roasting of the Corvo ultra fine residual pyrite.

The capacity of the SAPEC's pilot roaster is rather high. So, in order to prepare suitable filter cake quantity for the roasting, an indirect way was used. The pyrite stored under water in the drum is repulped with water.

A part of the slurries is dryed in fluidized bed by indirect heating. Free flowing pyrite is afterwards mixed to with pulp to correct moisture of the filter cake. Pellets generated during the mixing were desagregated. This is indicated on flow sheet I.

The Corvo ultra fine residual pyrite contains rather high remaining copper. Sulphatizing roasting tests have been developped in order to produce at the same time SO_2 for sulphuric acid production on recoverable copper by leaching in slightly acid solution.

Chemical and particle size analysis are indicated in table III and IV.

The major topics of the roasting testing campaigns are :

Point 1

Thanks to an appropriate fluidization velocity and an adequate particle size distribution of the fluidized bed, the fluidization and consequently the sulphatizing roasting in the bed have been improved and the copper recovery increased.

Point 2

Increasing the roasting temperature from 595° C to 620° C decreases the soluble iron of the cinders. So concerning the cinders from the cyclone, which is the most important part of such ultra fine pyrite, the soluble iron decreased from 13,55 % to 4,84 % and 5,17 %.

As far as the recovery of copper is concerned, this is a little lower : 95,47 % instead of 97,03 % for the cinders from cyclone.

It is interesting to note that this excellent recovery of the copper on a tailing of copper ore flotation, could be still improved if residual sulphides of the cinders are floated, after the leaching operation.

Point 3

By lowering the excess of air from 37 % to 16 % no particular undesirable effect was observed. It is obvious that the lowest excess of air in a safe and stable operation has still to be defined.

Point 4

The residence time of the cinders coming from the underflow of the fluidized bed is long. Despite this fact the ferrite formation is low, since the recovery of the copper is 88,48 % at 37 % excess of air and 94,67 % at 16 % excess of air, for this portion of the cinders.

Consequently, the kinetics of ferrite generation is quite low at 620 °C if the partial pressure of SO_3 in the fluidized bed is sufficient.

Point 5

The dust collected after the hot cyclone in the gas circuit is too sulphatised. Consideration has to be made in a commercial plant, to recycle such material into the roasting cycle.

Point 6

The high reactivity is due essentially to the high specific surface of this kind of material.

Point 7

The examination of the cinders has shown :

- the exceptional high and uniform microporosity;
- the absence of any fusion nor sintering;
- the presence of copper-iron sulphate compounds.

It is surprising that, although no sintering occurs, particle size increases during the roasting creating exceptionally high porous cinder.

Remark

If the level of valuable elements, other than sulphur, is too low, no subsequential recovery after the roasting has to be considered and the roasting would be a dead roasting at moderate temperate, i.e. around 800 °C. Nevertheless, regarding the high reactivity of this type of material, attention has to be paid to prevent and erratic sulphatisation of the cinders.

4. CONCLUSIONS

4.1. Before undertaking this research program, it was not possible to answer the following questions :

- Is it possible to operate at a commercial scale the dewatering of such fine material?

- Is the pelletization required for the roasting feed?

- Is the recovery of valuable elements feasible?

Today, the information is available as follows :

- The dewatering in filter press with cake squeezing by membrane followed by compressed air can be considered as a commercial unit.

- The pelletization would be superseded.

A sulphatizing roasting if very smooth can secure an excellent recovery of copper by leaching and if it is required other valuable elements except lead. In the case of only sulphuric acid production the dead roasting has to be contemplated.

4.2. Recommendation for processing the Portuguese ultra fine pyrite

The filtration of the raw Portuguese ultra fine residual pyrite is feasible, even without any previous hydrocycloning to eliminate the finest particles.

Pressure filtration is required because of the specific cake resistance.

Membrane squeezing and blowing air through the cake is essential for reaching sufficient low residual moisture in the cake.

Nevertheless, if in the residual pyrite the proportion of submicronic particle size is high and finer than what have been tested, unexpected difficulties in the filtration operation can be foreseen.

In that case, a hydrodynamic treatment before the filtration would be useful for eliminating a portion of these undesirable submicronic particles.

As far as the filtration feed is concerned, the viscosity of the pulp has to be kept in low range, that means below 70 % of dry solids for securing a uniform filling in the filter chambers.

The blowing air is the slowest operation in the sequential cycle of the pressure filtration. So the blowing has to be limited to the highest acceptable residual moisture reached.

Therefore automatic sophisticated press filters, with membrane for cake squeezing, air blowing through the cake and filter cloth washing are suitable for making a smooth work.

An adequate pulp, not too viscous, has to be prepared in a surge mixing tank. Heavy agitation has to be operated in the whole volume of the pulp.

Before the roasting, the filter cake has to be treated in a desintegrator in order to destroy the lumps and limit the remaining clumps.

The roasting has to be carried out in fluidized bed roaster in dead roasting conditions if the valuable elements are no worth of recovery. But if remaining valuable elements as copper, gold are to be recovered then sulfatizing roasting is recommended because it is a more economic way for recovery.

The specific rate of the roaster is similar to others already in operation for ultra fine pyrite, and consequently information about it is available. But more attention has to be paid to the boiler elements installed in the SO_2 gas circuit in the case of waste heat recovery with sulfatizing roasting.

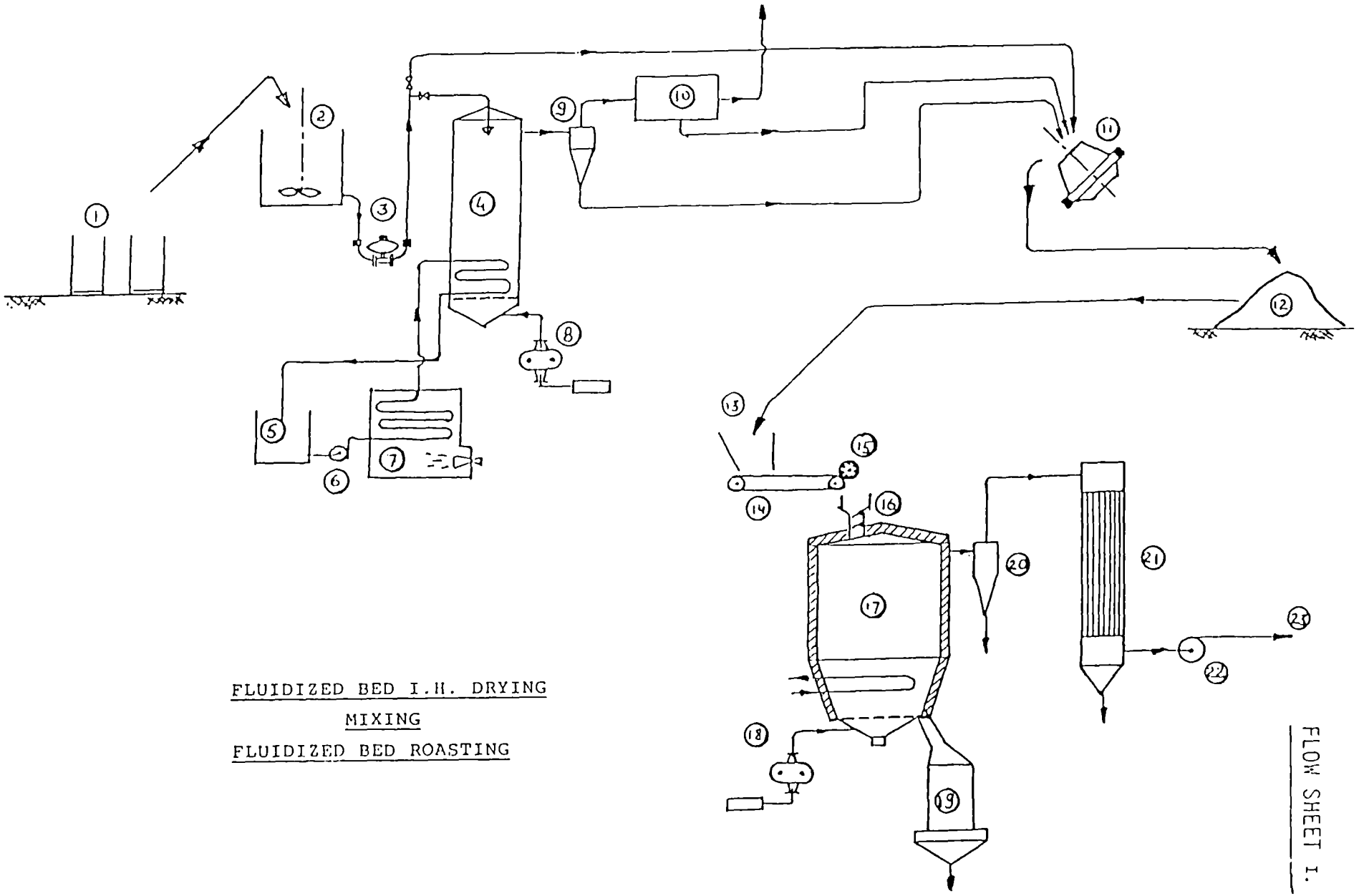

FLUIDIZED BED I.H. DRYING

MIXING

FLUIDIZED BED ROASTING

FLOW SHEET I.

Speed r.p.m.	47	94	188	375
Dry solids %	Viscosity centipoise			
50	5	6	7	10
60	6	8	10	20
69	10	17	23	40
74	40	83	117	140
77.5	110	178	277	570

Table I.

	Cumulative filtrate volume cc.	Time
Filtration 4 bar	1.800	30"
	2.995	1'
	3.845	1'30"
	4.069	1'45"
Cake squeezing 4 bar	4.503	2'
	4.568	2'30"
	4.611	4'
Dehydration by c. air	4.780	4'30"
	4.869	4'
	4.943	6'
	5.006	7'
	5.059	8'
	5.115	9'
	5.171	10'
	5.219	11'
	5.250	12'
	5.301	15'
	5.351	20'

Table II.

CORVO, ULTRA FINE PYRITE

$S_{tot.}$	:	42.8 %	d. b.
S_S^{--}	:	42.13	
S_{SO4}	:	0.74	
Fe	:	37.61	
Cu	:	2.14	
Zn	:	0.21	
Cd	:	0.001	
Ph	:	0.11	
Co	:	0.017	
Ni	:	0.006	
Mn	:	0.053	
As	:	0.26	
Sb	:	0.03	
Hg	:	14	p.p.m.
Tl	:	33	"
Ag	:	25,4	"

CHEMICAL ANALYSIS - TABLE III.

Min.	1	microns	9,4 %
"	2	"	15.5
"	4	"	30.3
"	8	"	52.9
"	16	"	78.5
	32	"	96.5

PARTICLE SIZE ANALYSIS - TABLE IV.

PYROMETALLURGICAL TREATMENT OF RESIDUES AND PRECIPITATES FROM HYDROMETALLURGICAL ZINC RECOVERY IN A C.C. SUPPLIED ELECTRIC ARC FURNACE

Project Leader : J. KRUGER
Institute of nonferrous metallurgy and electro-metallurgy,
University of Technology Aachen, Germany

Budelco B.V., Budel-Dorplein, Netherlands

Preussag A.G. Metall, Goslar, Germany

Contract MA1M-0037-C

1. OBJECTIVE

In the previous project RNF-0004 D "Treatment of residues and precipitates of hydrometallurgical zinc winning by DC electric arc melting" /1/ conducted before mainly in an electric arc furnace two possible process variants have become visible :

either : recovery of lead, zinc and silver by volatilization in a common flue dust

or : the production of a silver-containing lead bullion and a flue dust containing only lead and zinc.

Further more an inert slag is produced in both cases which can easily be dumped or used for different purposes. Because of the rather small test scale (10 kg) a final assessment of both variants was not possible.

Therefore, large scale tests (up to 800 kg) were made to investigate, which of the process possibilities mentioned above is more suitable to treat the residues from hydrometallurgical zinc winning.

Significant process data for an economical evaluation of a selected process were expected from the testwork such as :

- energy consumption,
- electrode consumption,
- distribution of rare metals such as Ge, Ga and In in the process products metal, slag and fluedust

2. INTRODUCTION

In hydrometallurgical zinc winning zinc concentrates are processed with about 10 % of iron. During roasting iron reacts with zinc forming zinc ferrites ($ZnO.Fe_2O_3$ which

are insoluble in weak sulfuric acid. To avoid zinc losses of about 15 % and more, the neutral leach residue (NLR) is leached again at higher temperature and higher acid concentrations. Under such conditions most of the iron content is dissolved, too. For the iron-zinc separation from the solutions three different iron precipitation processes are commercially used :

- the jarosite process,
- the goethite process and
- the hematite process.

The chemical compositions /4-8/ of such residues (table 1) show that only hematite can be sold (e.g. to the cement industry). For the other two materials there exist no application, they have to be dumped.

Per tonne of zinc 0.95 tonne of jarosite and 0,7 tonne of goethite are produced, which makes about 1 million tonnes of jarosite and 350.000 tonnes of goethite per year that have to be dumped in Europe.

Because of the environmental regulations, it is absolutely necessary to avoid dumping of such materials in future. They will have to be treated either by a hydrometallurgical or a pyrometallurgical process. Such a process has to be successful, otherwise new ways for the iron-zinc separation have to be found. In this way a pyrometallurgical treatment of the neutral leach residue could be a promising alternative.

Several attempts for a hydrometallurgical treatment have been performed until now, but none of them has been proven yet. Therefore in the institute of nonferrous metallurgy of the University of Technology of Aachen it was tried to smelt jarosite under reducing conditions in an electric arc furnace.

3. EXPERIMENTAL WORK

3.1 EXPERIMENTAL SETUP AND DESCRIPTION OF THE TESTWORK

The modified experimental setup for the smelting tests is presented in figure 1. A detailed description of the reconstruction of the existing DC arc furnace is given in the first interim report dated February 1989/2/.

The smelting capacity of the installed electric arc furnace was increased to 1 tonne of jarosite corresponding to a bath depth of 85 cm.

The electricity supply consists of a 5 kV transformer (350 kVA) and a rectifier (Verithyr ABB). This unit supplies a direct current of 5234 Amperes with a maximum voltage of 54 V and for alternating current 4290 Amperes of a maximum voltage of 110 V.

The off-gases, which are produced during smelting, pass through a hot cyclone and are dedusted in a pocketfilter with a filter area of 140 m^2. The nearly complete dedusted gases are further treated in a venturi scrubber where SO_2, CO_2 and fine fluedust particles are washed out. In the installed off gas cleaning system 5000 M^3/h flue-gas can be treated.

For feeding the furnace semicontinuously a rotary disc feeder was installed on a platform above the furnace. The feeder is capable to feed continuously 30 - 200 kg jarosite/h.

At the beginning of the tests the arc is struck against some iron swarf (ca. 1 kg). Afterwards a small amount of slag with a small grain size (10-20 mm) is charged and melted down. Subsequently charging of residue, coke and fluxes starts after a short holding time of about ten minutes.

During smelting the temperatures of the bottom electrodes, of the electrode cooling system and of the furnace wall are measured continuously. Furthermore the off-gas temperature in the cyclone and before entering the pocketfilter is controlled, too. The power input (MVA), the voltage (V) and the current (kA) can be monitored at the control desk and are plotted.

The feeding operation itself is controlled visually. If there is unsmelted material on the surface of the bath the charging is interrupted until all material is smelted. Then new charge material is fed into the furnace.

After charging of all the material the melt is kept at a constant temperature for at least one hour. For tapping the taphole is burnt with oxygen and the melt is tapped into a ladle which is arranged in a casting pit.

All products are weighed and test samples for the chemical analysis are taken from :

- the slag,
- the fluedust,
- the scrubbing water,
- the scrubber sludge and
- the metal phase, if present

to enable the calculation of a mass balance.

The total power consumption and electrode consumption are determined, too.

Except of one all tests were carried out at AC current. Problems with the rectifier resulted in a delay of about four months. Furthermore, the complicated chemical analysis of the large number of samples takes a lot of time and has not been finished yet.

3.2. FEED MATERIALS

During the testwork four different types of Jarosite from Metaleurop Weser Zinc in Nordenham and Budelco B.V., Budel-Dorplein in the Netherland were tested (table 2).

Main differences exist in respect to the contents of lead, zinc, germanium, cadmium and thallium.

Regarding the content of lead and thallium the Jarosite from Budelco B.V. is characterized by higher values, the contents of zinc, germanium and cadmium are somewhat lower. At Metaleurop before iron precipitation a lead silver residue is separated from the leach because they are treating zinc concentrates high in silver. At Budelco no lead silver residue is produced because only concentrates with lower contents of silver and lead are treated there.

Fluxes for smelting were sand with a content of SiO_2 of about 99.7 % and lime with a content of CaO of about 96 %. Metallurgical coke with a C_{fix} value of about 90 % was used as reductant.

4. REDUCTANT

The input and the output materials and the experimental data of the smelting tests are listed in table 3.

In tests 1, 3 and 4 Jarosite from Metaleurop with an iron content of 24.8 % and in test 6 with an iron content of 25.2% was used. The Jarosite from Budelco with an iron content of 19.9 % was used during the test 2 and 5. In the tests 8 and 9 the iron content was 25.2 %.

Except of test 2 and 3 the temperature of the melt was tried to be kept constant at about 1400 to 1450°C. In the test 2 the temperature of the melt was 1600 °C and in test 2 1500°C. In the test 4 it was tried to lower the temperature to about 1350 °C. But in this case it was impossible to keep the charging velocity constant at about 40 kg of Jarosite plus fluxes per hour.

During all tests the desired composition of the slag lies in the Olivine region in the system $FeO-SiO_2-CaO$.

To improve the reducing conditions of the slag lies in the Olivine region in the system $FeO-SiO_2-CaO$.

To improve the reducing conditions in test 8 and 9 ferrosilicon (75 % Si) was added at the end of the smelting period.

During test 8 the ferrosilicon was just added to the smelt and pushed under the surface. In test 9 the smelt was stirred after charging the ferrosilicon. Al tests except no. 9 were run at AC current.

During all tests slag and fluedust were produced. In addition, a metal phase was received in tests 2, 8 and 9. Because of the large number of data, all the results and mass balances of each single test are not listed, but only a summary concerning the chemical composition of the slags (table 4), the flue dusts (table 5) and the metal phases (table 6).

In table 8 the distribution of the metals between the produced phases (slag, flue dust and metal phase, if present) are listed.

In table 8 the specific data concerning energy and electrode consumption are summarized.

4.1 SLAG

For the tests at a temperature of about 1400 °C the chemical composition of the slags shows, that the lead content is always in the range from 0.1 to 0.5 %. The zinc content of the slags depends on the degree of reduction. At 1400 °C the lowest value that was achieved is greater than 1 %.

Concerning the valuable metals the results show that the silver content in slag is always between 30 to 50 ppm. The germanium concentration is between 30 to 100 ppm and the Indium concentration can reach values of about 200 ppm, if this element is present.

Concerning further minor elements it can be noticed that cadmium and thallium are volatilized nearly completely. The arsenic concentration reaches values from 50 to more than 200 ppm and the bismuth concentration reaches the values of the input material (100 ppm). The sulfur content depends on the slag composition. Figure 2 shows that under reducing conditions the sulfur in the slag is proportional to the iron content of the slag. Furthermore a dependency from the CaO content of the slag can be seen. The equation for the calculation of the sulfur content of the slag (figure 3) fits only for slags with medium FeO-contents.

The slag from test 2, which was performed at an average temperature of about 1600 °C is very clean compared to the other slags. The lead and zinc content are only 0.1 % and the content of minor elements is always lower than 40 ppm (except of bismuth). The sulfur content is only 0.7 %.

4.2 FLUE DUST

The chemical composition of the flue dust shows the flue dust as a valuable product of the process.

The content of lead and zinc amounts to more than 50 % in nearly all tests and therefore it is supposed to be no problem to treat this flue dust either in pyro- or hydrometallurgical processes.

The highly volatile elements such as cadmium and thallium are enriched to values of more than 0.1 %, the concentration of arsenic can reach values over 1 %. The factor for the enrichment of the valuable elements lies for silver between 2 and 4, for germanium between 4 and 10 and for indium between 3 to 5. The total values are for germanium 200 to 600 ppm, for indium 200 to 800 ppm and for silver 100 to 800 ppm.

The sulfur content of the flue dust is always higher than 10 % and reaches values up to 18 %. The analysis of sulfate in the tests 1 to 3 shows that most of the sulfur is in the sulfidic form.

4.3 METAL PHASE

During the test 2, 8 and 9 a metal phase was produced (table 6). In test 2 this phase was produced because of the high addition of coke and the high temperature of the melt.

In the tests 8 and 9 ferrosilicon (respectively 18 and 12 kg) was added.

The chemical composition of the metal phases shows that in test 8 only small amounts of the ferrosilicon reacted with the melt. The metal phase consists mainly of iron and silicon. But even in this case when the reaction of ferrosilicon and the melt was not very complete the metal phase acts as a collector for the valuable metals and arsenic. Some sulphur was found in the metal phase, too.

The chemical composition of the other metal phases is similar, although the test conditions under which they have been produced were different.

Both phases are characterized by high contents of sulfur (around 15 %) and an iron content between 72 and 73 %. They show certain similarity with matte. In the same way like the metal phase from test 8 they act as a collector for silver, germanium, indium and arsenic. The lead content is relatively high compared to the lead content of the corresponding slags (between 1,3 and 5,4 %).

4.4 DISTRIBUTION OF THE ELEMENTS

The distribution of the elements on the different phases are listed in table 7. The values are calculated from the mass balances of the single tests and refer to the analysed values in the products.

In respect to the mass balances it must be noted, that even if tests have been performed with a melt of about 700 kg, there are big deviations especially for the minor elements. These deviations are due to the low concentrations of these elements in the materials

The data show, that the high volatile elements like cadmium, thallium and lead (as PbS or PbO) can be found in the fluedust nearly completely.

In the presence of a metal phase, lead shows the tendency to collect in the metal phase, but only up to 12 % in maximum (test 9).

Zinc is distributed equally between the products (slag and flue dust). Only at higher temperatures or stronger reducing conditions (using ferrosilicon) zinc is volatilized to more than 80 %. If no metal phase is present, arsenic is volatilized to more than 70 and up to 80 %. But in case of a metal phase about 40 % of the arsenic can be analysed in this phase.

Concerning the valuable elements the data show that silver is distributed between slag and fluedust fifty/fifty. If a metal phase is present, more than 50 % can be analysed in it, and the silver content of the slag is much lower. If a metal phase is formed, the behaviour of germanium and indium is quite similar. Without a metal phase it seems that both elements tend to be kept in the slag.

4.5 PROCESS DATA

From the data of the testwork several specific data have been calculated for the reducing smelting of jarosite in an electric arc furnace.

The specific values are summarized in table 8. As the amount of charged materials differs very much for the different tests the specific values are always calculated for the jarosite (dry) and the total input (dry) (except coke addition).

The values for the specific energy consumption show that the consumption lies between 2000 and 2500 kWh per tonne of jarosite and 1500 to 2000 kWh per tonne of charged material.

These values are very high, but in an industrial process it would be possible to reduce the energy consumption further because under industrial scale conditions heat losses are much smaller.

The specific electrode consumption varies between 6 and 15 kg/t of charged material. For the jarosite input values are calculated in the range of 9 to 18 kg/t.

5. CONCLUSIONS

The results of the smelting tests show, that it is possible to treat jarosite in pyrometallurgical process successfully. At a temperature of 1400 °C and the addition of ferrosilicon slag, fluedust and a metalphase are produced.

The slag is nearly clean and there should be no problem by deposing the slag. The flue dust is high in lead and zinc, and contains higher amounts of the volatile elements. The metal phase formed during the process is high in sulfur (14 %) and acts as a collector for the valuable elements like silver, germanium and indium and for arsenic.

In respect to the sulfur content of the slag the results show that it is necessary to produce such a metal phase, because the sulfur content of the slag is directly proportional to the iron content. Even if a metalphase with such a composition is not a valuable product, there should be no problem to treat this material in the sinter machine lead shaft furnace.

Concerning the energy and the electrode consumption the following values were obtained from the testwork:

energy consumption : 2000 - 2500 kWh/t of jarosite (dry)
electrode consumption : 8 - 15 kg/t of jarosite (dry)

The values are very high, but it can be expected that the values for the energy and electrode consumption will decrease strongly in industrial scale processes.

6. REFERENCES

1. KRÜGER J.
"Treatment of residues and precipitates of hydrometallurgical zinc winning by DC electric arc melting"
EC-No. RNF-004 D, Final report.

2. KRÜGER J.
"Pyrometallurgical treatment of residues and precipitates from hydrometallurgical zinc recovery in a DC supplied electric arc furnace"
Contract N° MA1M-0037-C(BA)
1/2 interim report.

3. KRÜGER J.
"Pyrometallurgical treatment of residues and precipitates from hydrometallurgical zinc recovery in a DC supplied electric arc furnace"
Contract N° MA1M-0037-C (BA)
3/4 Interim report.

4. KNOBLER R.R., et al.
"The new zinc electrolysis and treatment of the national zinc company"
Erzmetall 32 (1979), pp. 179 - 116.

5. RÖPENACK A.
"Rückstandsfreie hydrometallurgische zinkgewinnung durch das hämatitverfahren"
Erzmetall 42 (1989), S. 125 - 129.

6. STEINTVEIT G.
"Electrolytic zinc plant and residue recovery"
Det Norske Zinkkompani a/s
AIME World Symposium in Mining and Metallurgy of Lead and Zinc, Vol.II, Ed. Cotterill; Cegan, Aime, New York, 1970, pp. 223-246.

7. WUTHRICH H.R., A.V. RÖPENACK
The electrolytic zinc plant of ruhr-zink Gmbh, Datteln
Aime, New York, 1970, pp. 247-268.

8. MASSON N.J.J., K.J. TORFS
"Aufarbeitung von laugenrückständen der zinkelektrolyse"
Erzmetall 22 (1969), Beiheft B 35-B 42.

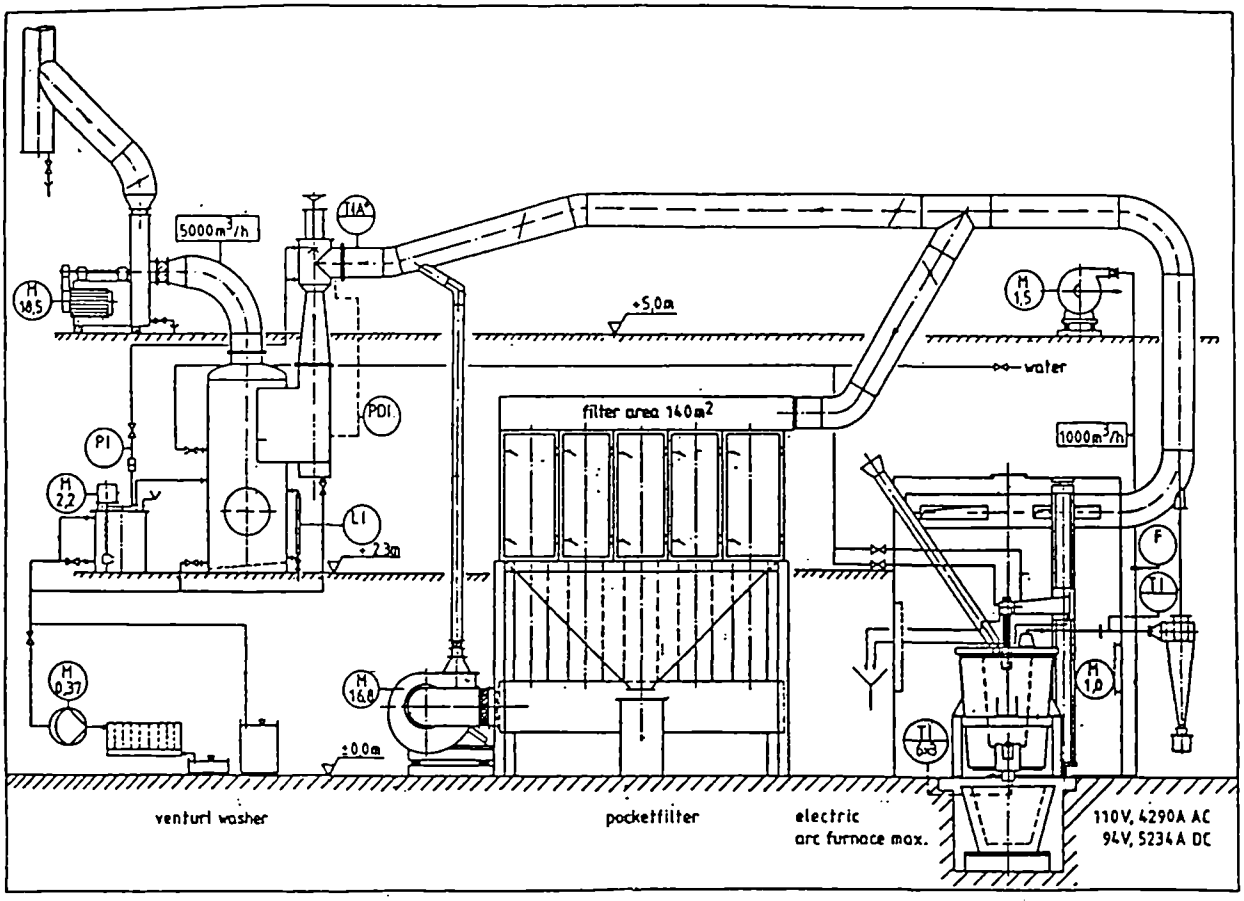

Figure 1: Experimental setup

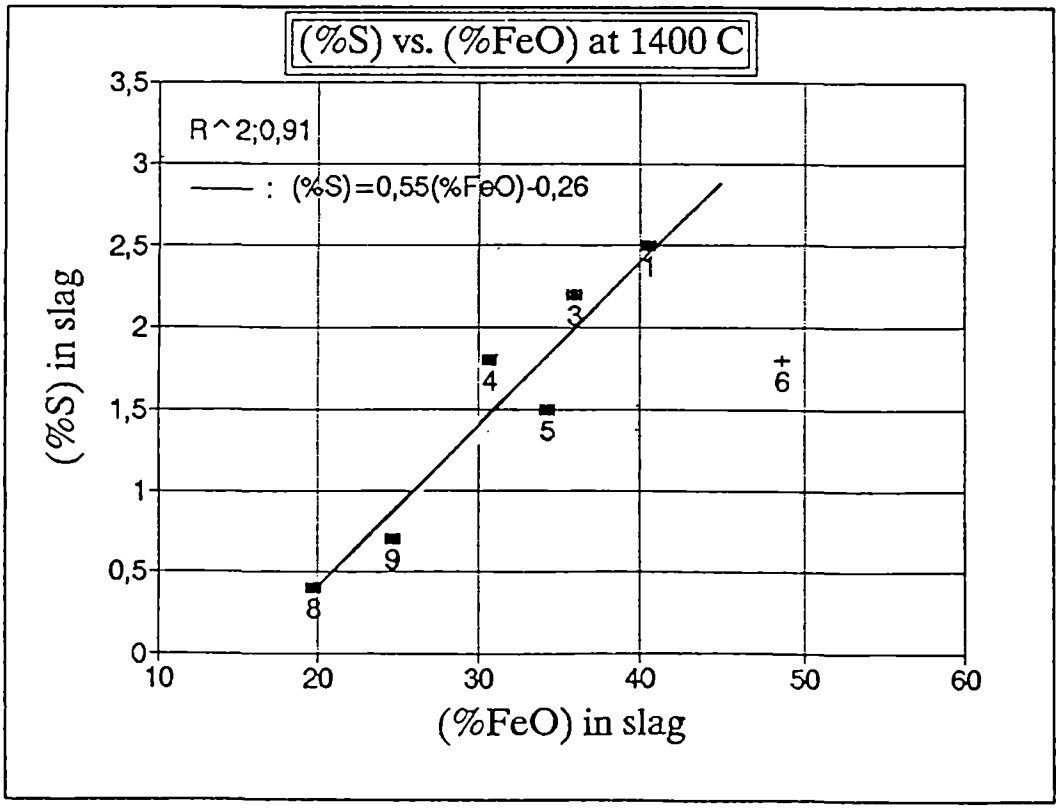

Figure 2: Sulfur content vs. (FeO) content in the slag at 1400°C

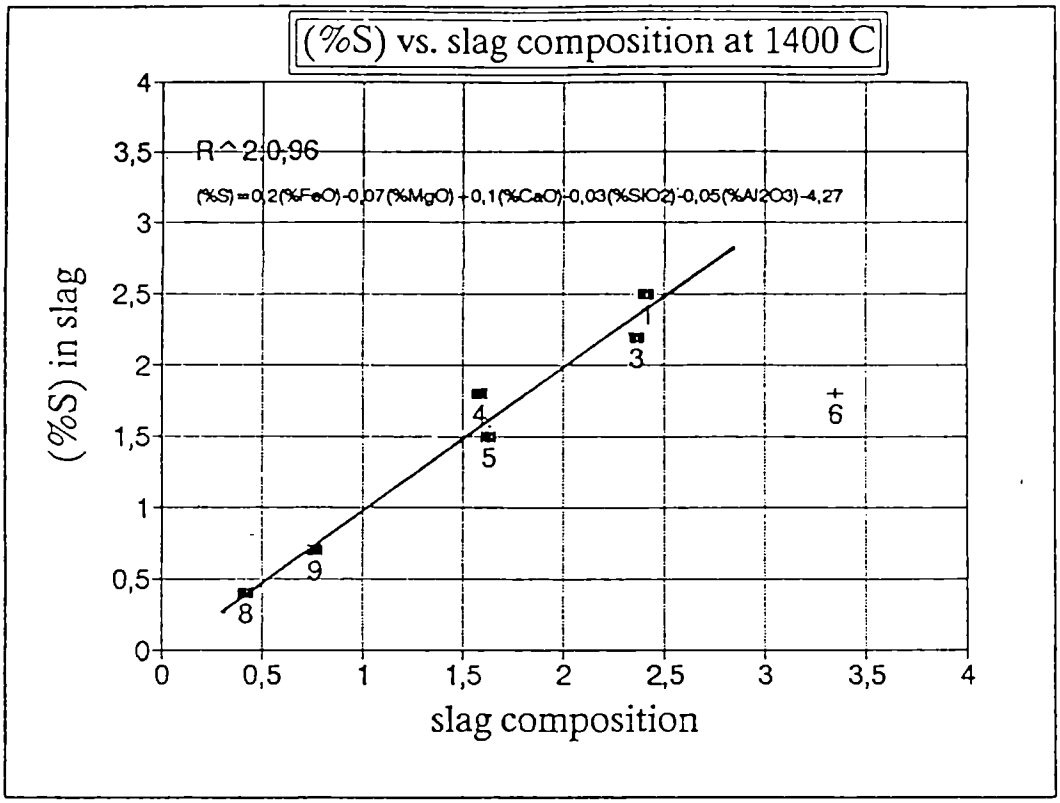

Figure 3: Sulfur content in slag vs. slag composition at 1400°C

residue	jarosite	goethite	hematite	neutral leach residue
formula	X(Fe(SO4)2(OH)6)	FeOOH	Fe2O3	
theoretical composition:				
Fe(%)	36, 3	62, 8	69, 9	
S(%)	13, 9			
real composition:				
Fe(%)	20–25	40	60, 0–65, 0	
Zn(%)	1, 8–5, 4	2, 4–7, 0	1, 0	20, 0–30, 0
Pb(%)	1, 8–5, 0	1, 0–2, 0	0, 1	2, 5–7, 5
S(%)	12, 0	5, 0	3, 0	7, 0
humidity (%)	50	50	10–15	44
amount(wet) (t/tZn)	0, 9	0, 7	0, 27	0, 11
application	disposal	disposal	cement industry	
technology	simple	expensive	very expensive	

Table 1: Comparison of the different residues and precipitates from hydrometallurgical zinc winning /4-8/

company		Metaleurop Weser Zink GmbH	Metaleurop Weser Zink GmbH	Budelco B.V.	Budelco B.V.
Fe	(%)	24, 8	29, 2	19, 9	25, 2
Fe3+	(%)	24, 4		19, 5	
MgO	(%)	0, 4	0, 1	0, 3	0, 4
Al2O3	(%)	1, 3	1, 0	0, 9	0, 8
SiO2	(%)	6, 3	4, 1	5, 1	4, 0
CaO	(%)	0, 8	0, 8	4, 6	1, 9
Pb	(%)	2, 4	2, 3	5, 0	5, 8
Zn	(%)	5, 4	5, 0	1, 8	2, 6
Ag	(ppm)	143	101	168	250
Ge	(ppm)	105	95	10	31
In	(ppm)	280	1	195	50
As	(ppm)	2800	2200	2400	3400
Cd	(ppm)	650	610	370	300
Tl	(ppm)	25	132	78	58
Bi	(ppm)	110	8	110	36
C	(%)	0, 8	1, 1	1, 0	1, 1
S	(%)	9, 5	11, 5	12, 0	12, 6
SO4	(%)	28, 4		35, 8	
NH4+	(%)	1, 8		1, 5	

Table 2: Chemical composition of different types of jarosite /2,3/

No. of test		1	2	3	4	5	6	8	9
current		AC	AC	AC	AC	AC	AC	AC	DC
jarosite from		M.E.	B.B.V.	M.E.	M.E.	B.B.V.	M.E.	B.B.V.	B.B.V.
input:									
jarosite (dry)	(kg)	593, 0	665, 8	843, 5	782, 4	830, 0	634, 5	726, 9	726, 9
metallurgical coke	(kg)	42, 0	84, 5	67, 5	76, 8	54, 4	63, 1	59, 5	69, 5
lime	(kg)	30, 4	33, 7	138, 0	142, 1	89, 3	5, 6	162, 8	74, 4
sand	(kg)	24, 5	56, 1	83, 6	100, 8	115, 0	90, 9	161, 5	90, 6
slag	(kg)	13, 0	9, 0	11, 0	50, 0			21, 5	
iron swarf	(kg)	1, 5	1, 0	1, 0	1, 1		1, 5		
ferrosilicon	(kg)							18, 0	13, 2
output:									
slag	(kg)	350, 0	380, 6	710, 0	570, 0	700, 0	415, 0	703, 2	453, 0
fluedust (filter)	(kg)	44, 5	96, 4	126, 0	118, 2	130, 0	25, 5	54, 5	81, 6
fluedust (cyclon)	(kg)							0, 45	7, 7
sludge (dry)	(kg)	2, 5	1, 0	0, 5	143, 1				
metalphase	(kg)		98, 4					20, 0	72, 0
scrubber water	(l)	800, 0	800, 0	1500, 0	1800, 0	s. V4	1200, 0	1600, 0	800, 0
energy consumption	(kWh)	1155, 0	1658, 0	1937, 0	1784, 0	1712, 0	1474, 0	1758, 0	1640, 0
electrode consumption	(kg)	5, 3	7, 6	11, 0	7, 1	7, 2	10, 6	13, 0	10, 6
total time	(h)	11, 8	13, 3	19, 0	26, 0	21, 2	19, 5	23, 5	17, 3
charging time	(h)	9, 5	10, 5	17, 9	23, 9	20, 0	15, 3	22, 2	16, 6
bath temperature at tapping	(°C)	1436, 0	1700, 0	1500, 0	1462, 0	1483, 0	1400, 0	1400, 0	1400, 0
bath depth	(cm)	58, 0	64, 0	85, 0	83, 0	85, 0			

Table 3: Experimental data of the smelting tests

		slag V1 M.E.	slag V2 B.B.V.	slag V3 M.E.	slag V4 M.E.	slag V5 B.B.V.	slag V6 M.E.	slag V8 B.B.V.	slag V9 B.B.V.
Fe	(%)	31, 5	11, 3	27, 9	23, 9	26, 6	37, 8	15, 3	19, 1
Fe3+	(%)	1, 1	0, 4	1, 0	0, 5	0, 6			
MgO	(%)	3, 9	5, 9	2, 0	1, 4	2, 4	3, 5	4, 5	7, 1
A'203	(%)	7, 8	19, 5	12, 3	11, 1	10, 0	3, 9	7, 0	2, 3
SI02	(%)	18, 4	27, 4	24, 6	29, 1	27, 6	27, 4	24, 7	28, 3
CaO	(%)	7, 7	15, 1	17, 5	19, 2	13, 6	4, 1	25, 3	21, 3
Pb	(%)	0, 4	0, 1	0, 3	0, 2	0, 6	0, 4	0, 2	0, 2
Zn	(%)	3, 1	0, 1	2, 5	1, 8	1, 6	1, 9	1, 2	1, 1
Ag	(ppm)	47	14	50	20	44	32	10	47
Ge	(ppm)	65	5	100	26	32	60	7	34
In	(ppm)	190	34	200	100	120	3	3	4
As	(ppm)	110	10	540	100	350	46	100	100
Cd	(ppm)	19	10	20	100	100	16	100	100
Tl	(ppm)	1	1	4	100	100	14	5	3
Bi	(ppm)	130	110	100	120	150	1	1	1
C	(%)	1, 1	0, 1	0, 1					
S	(%)	2, 5	0, 7	2, 2	1, 8	1, 5	1, 8	0, 4	0, 7
SO4	(%)	0, 5	n.d.	0, 3					
amount	(kg)	350	380, 6	710	570	700	403	703, 2	453, 0

Table 4: Chemical composition of the slags

		flue dust (filter) V1 M.E.	flue dust (filter) V2 B.B.V.	flue dust (filter) V3 M.E.	flue dust (filter) V4 M.E.	flue dust (filter) V5 B.B.V.	flue dust (filter) V6 M.E.	flue dust (cyclon) V8 B.B.V.	flue dust (filter) V8 B.B.V.	flue dust (cyclon) V9 B.B.V.	flue dust (filter) V9 B.B.V.
Fe	(%)	4.3	5.1	3.6	3.5	1.8	4.6	6.9	3.1	11.5	3.3
Fe3+	(%)				0.2	0.1					
MgO	(%)	3.5	0.8	0.7	0.9	0.5	0.3	0.4	0.5	0.7	0.3
Al2O3	(%)	4.2	1.7	2.3	1.0	0.7	0.9	1.0	0.8	1.0	0.8
SiO2	(%)	6.0	5.4	5.4	12.9	2.8	6.3	1.4	2.6	5.8	3.2
CaO	(%)	3.4	8.0	1.7	25.9	12.3	2.1	1.0	6.3	3.0	2.6
Pb	(%)	14.0	26.2	13.3	5.6	32.3	23.1	13.0	36.0	38.5	28.7
Zn	(%)	22.3	14.7	18.7	9.9	13.5	31.9	50.5	15.2	11.9	28.2
Ag	(ppm)	339	373	220	93	356	390	180	675	784	307
Ge	(ppm)	450	200	600	184	188	308	65	164	103	230
In	(ppm)	790	710	700	160	500	250	31	406	357	239
As	(ppm)	13800	8000	8000	2800	10000	10700	4200	12000	3000	10700
Cd	(ppm)	4700	3100	3700	1800	3100	4600	100	2500	1500	3500
Tl	(ppm)	214	500	330	460	720	1385	4	617	181	1017
Bi	(ppm)	420	390	300	140	460	148	55	413	275	211
C	(%)	2.1	3.0				0.8	0.8	1.5	3.0	1.0
S	(%)	13.5	11.2	11.9	5.6	10.7	18.4	4.9	14.6	14.8	17.9
SO4	(%)	8.9	10.2	6.6							
NH4+	(%)	1.4	0.2	1.2							
amount	(kg)	44.5	96.4	126.0	118.2	130.0	25.5	0.5	54.5	7.7	81.6

Table 5: Chemical composition of the flue dusts

		metal phase V2 B.B.V.	metal-phase V8 B.B.V.	metal-phase V9 B.B.V.
Fe	(%)	73, 3	82, 2	72, 2
Pb	(%)	1, 3	0, 4	5, 4
Zn	(%)	0, 1	0, 2	0, 3
Ag	(ppm)	556	141	944
Ge	(ppm)	50	132	149
In	(ppm)	320	7	38
As	(ppm)	4400	3900	10300
Cd	(ppm)	10	100	100
Tl	(ppm)	3	1	10
Bi	(ppm)	110	1	19
C	(%)	0, 1	0, 1	0, 1
S	(%)	15, 3	2, 2	13, 6
SiO2	(%)		9, 5	1, 9
amount	(kg)	98, 4	20, 0	72, 0

Table 6: Chemical composition of the metal phases

no. of test	1	2	3	4	5	6	8	9
Fe	98/2	35/4/60	98/2	97/3	98/2	99/1	86/1/13	61/3/36
Pb	18/80	1/94/5	11/89	15/85	9/91	22/78	7/93/0	3/85/12
Zn	52/48	3/96/1	43/57	47/53	40/60	49/51	50/50/0	17/82/1
Ag	52/47	6/37/57	56/44	51/49	40/60	57/43	15/79/6	18/26/56
Ge	53/46	7/74/19	48/52	75/25	47/53	75/25	30/54/16	34/43/23
In	65/35	11/60/29	62/38	15/85	56/44	16/84	8/91/1	7/83/10
As	5/94	1/63/36	27/73	21/79	15/85	6/94	9/81/10	3/53/44
Cd	3/96	1/99/0	3/97			5/95		
Tl	3/97	1/99/0	6/94			14/86	9/91/0	1/98/1
Bi	70/30	45/42/12	65/35	80/20	63/36	10/90	3/97/0	2/91/7

Table 7: Distribution of the metals on the different phases (slag/flue dust/metal phase) (%)

No. of test		1, 0	2, 0	3, 0	4, 0	5, 0	6, 0	8, 0	9, 0
current		AC	AC	AC	AC	AC	AC	AC	DC
type of jarosite		M.E.	B.B.V.	M.E.	M.E.	B.B.V.	M.E.	B.B.V.	B.B.V.
input (jarosite)	(kg)	593, 0	665, 8	843, 5	782, 4	830, 0	634, 5	726, 9	726, 9
input (total)	(kg)	691, 5	797, 9	1209, 4	1212, 7	1120, 0	732, 5	1090, 7	905, 2
met. coke addition	(kg)	42, 0	84, 5	67, 5	76, 8	54, 4	63, 1	59, 5	69, 5
spec. coke addition (jarosite input)	(kg/t)	70, 8	126, 9	80, 0	98, 2	65, 5	99, 4	81, 9	95, 6
energy consumption	(kWh)	1155, 0	1658, 0	1937, 0	1784, 0	1712, 0	1474, 0	1758, 0	1640, 0
spec. energy consumption (jarosite input)	(kWh/t)	1947, 7	2490, 2	2296, 4	2280, 2	2062, 7	2323, 1	2418, 5	2256, 2
spec. energy consumption (total input)	(kWh/t)	1670, 3	2078, 0	1601, 6	1471, 1	1528, 6	2012, 3	1611, 8	1811, 8
electrode consumption	(kg)	5, 3	7, 6	11, 0	7, 1	7, 2	10, 6	13, 0	10, 6
spec. electrode consumption (jarosite input)	(kg/t)	8, 9	11, 4	13, 0	9, 1	8, 7	16, 7	17, 9	14, 6
spec. electrode consumption (total input)	(kg/t)	7, 7	9, 5	9, 1	5, 9	6, 4	14, 5	11, 9	11, 7
charging time	(h)	9, 5	10, 5	17, 9	23, 9	20, 0	15, 3	22, 2	16, 6
average charging velocitiy (jarosite input)	(kg/h)	62, 4	63, 4	47, 1	32, 7	41, 5	41, 6	32, 7	43, 8
average charging velocitiy (total input)	(kg/h)	72, 8	76, 0	67, 6	50, 7	56, 0	48, 0	49, 1	54, 5
average bath temperature	(°C)	1430, 0	1600, 0	1500, 0	1450, 0	1450, 0	1430, 0	1430, 0	1430, 0

Table 8: Specific data of the experimental testwork

OPTIMIZATION OF THE ANACONDA PROCESS FOR THE ELECTROLYTIC RECOVERY OF ZINC FROM ZINC SULPHATE SOLUTION BY TREATING THE LEACH RESIDUE

Project Leader: F. LECHER
Métaleurop Recherche, Trappes, France

Contract MA1M-0043-C

1. OBJECTIVES

To find alternative ways of performing the iron bleed of electrolytic zinc plants, through new routes of treating the Neutral Leach Residue. With the aim to test processes which enable to produce, at low operating costs, iron residues more easily dumpable than the present ones.

2. INTRODUCTION

Most modern electrolytic zinc plants around the world are working on the following scheme:

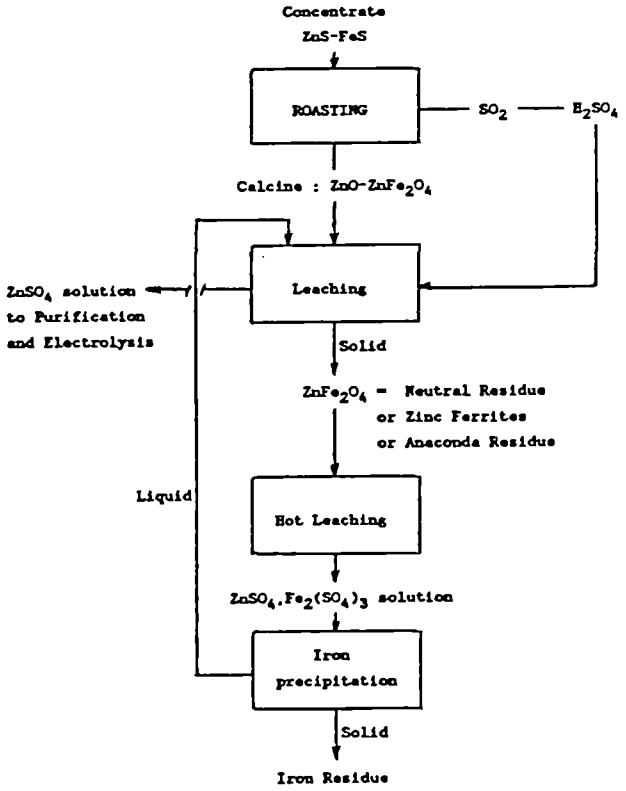

With this kind of scheme, high zinc recovery is obtained (>95%) but iron is leached with Zn at the hot leaching and have to be precipitated from the solution for bleed. Depending on precipitation conditions, 3 kinds of iron residues can be obtained: jarosite, goethite, hematite (as produced at Metaleurop, ex Preussag plant in Nordenham).

- Jarosite and goethite are leachable residues, they are at present stockpile in ponds for environmental safety: it can be forbidden in the future.

- Hematite is theoretically a not leachable residue, then it can be stockpiled or even sold easily: in practice, the residues are always impregnated by the solutions of the plant, making them not so easily dumpable.

So what we propose in this study is to look at the feasibility of changing the hot leaching and iron precipitation steps in present electrolytic zinc plants for a pyrometallurgical step (electric furnace smelting of the Neutral Leach Residue). With this, we have two objectives:

- To bleed the iron content of zinc concentrates treated in electrolytic zinc plant in a non leachable slag which can be easily dumpable or sold as inert material.

- To recover the zinc content of the Neutral Leach Residue in the fumes of the pyrometallurgical furnace, these flue-dusts being leached in a following stage for a total zinc yield of the plant >95%.

With this aim, we have performed tests at the laboratory smelting on samples of Neutral Leach Residue from Nordenham zinc plant, as it is described hereafter.

3. EXPERIMENTAL WORK

The tests were performed on the solid fraction of different neutral residue samples of Nordenham.

Average chemical analysis (sample: October 1988)

wt. %									ppm				
Zn	Pb	Fe	Ca	Si	Al	S^t	S (SO_4)	As	Cu	Cd	Ag	In	Ga	Ge
23.2	6.2	18.7	4.1	2.5	0.53	6.3	5.2	0.19	0.82	0.17	170	257	130	135

3.1. CONSTITUTING PHASES

Major phases:

- Franklinite [$(Zn,Fe)O.Fe_2O_3$]
- Gypsum [$CaSO_4.2H_2O$]
- Mn oxide
- Sphalerite (ZnS)
- Zincite (ZnO)

Minor phases:

- Cd-Pb-Ag silico-aluminates
- K-Na silico-aluminates
- Willemite (Zn_2SiO_4)
- Fe oxides
- Anglesite ($PbSO_4$)
- Plumbojarosite [$Pb(Fe,Zn)_6(SO_4)_4(OH)_{12}$]
- Amorphous SiO_2

On these kinds of samples, smelting tests were performed at the laboratory of Métaleurop Recherche, in an induction furnace (simulation of smelting in an electric furnace), in different reducing conditions in order to determine conditions for production of a clean slag and a good recovery of zinc in dusts.

4. RESULTS

They are contained in fig.1 and 2 (tests performed on samples of 100 g of dry Neutral Leach Residue).

- With low carbon (2 g) in the charge (oxidative conditions), fig.1 shows that smelting of zinc ferrites leads to the production of a SO_2 gas and of a slag $ZnO-FeO-CaO-SiO_2$. Then, zinc recovery is nearly equal to zero so a supplementary fuming step would be necessary for zinc extraction.

- With high carbon (20 g) in the charge (reducing conditions), 85% of the zinc input can be recovered directly in flue dust. Other products are an iron matte and an inert slag for disposal.

- Then reducing conditions were tested further because of the advantage of producing both an inert slag and of recovering zinc in one step. The partition of different elements between matte phase, slag and flue dust for different tests and different reducing conditions is given in fig. 2. Results of these tests are summarized hereafter.

- Smelting of a (100 g ME WZ ferrites + 19 g C) burden gives the following partition of the elements between the different phases:

Zn in the off-gases	90 %
Fe in the matte	70 %
Fe in the slag	30 %
S in the matte + slag	85 %
S in the off-gases (oxides + gases)	15 %
Pb in the off-gases	90 %
Pb in the matte	10 %
Ag in the matte	75-80 %

With a (100 g ME WZ ferrites + 16 g C) burden the following partition is obtained:

Zn in the off-gases	90 %
Fe in the matte	65 %
Fe in the slag	35 %
S in the matte + slag	70 %
S in the off-gases	30 %
Pb in the off-gases	90 %
Pb in the matte	10 %
Ag in the matte	75 %

The smelting of a (100 g ME WZ ferrites + 13 g C) burden gives:

Zn in the off-gases	70 %
Fe in the matte	35 %
Fe in the slag	65 %
S in the matte + slag	60 %
S in the off-gases	40 %
Pb in the off-gases	90 %
Pb in the slag	10 %

Less reducing conditions (+10 g C) give:

Zn in the off-gases	70 %
Fe in the slag	100 %
S in the slag	30 %
S in the off-gases	70 %
Pb in the off-gases	90 %
Pb in the slag	10 %

13-16 g C/100 g ferrites seem to be the optimum, in order to maximize the amount of Zn to the flue dust and to minimize iron quantities to the matte.

For further calculations, we have assumed the following partition of the elements between the different phases for the reducive smelting of zinc ferrites in an electric furnace (13-16 g C/100 g ferrites).

Zn in the off-gases	85 %
Fe in the matte	50 %
Fe in the slag	50 %
S in the matte + slag	70 %
S in the off-gases (15 % oxides, 15 % gases)	30 %
Pb in the off-gases	90 %
Pb in the matte	10 %

5. ELECTRIC FURNACE SIZE UP FOR THE REDUCING TREATMENT OF NEUTRAL LEACH RESIDUE

Assuming the partition above, and knowing the constitutive phases of Neutral Leach Residue and the possible reactions in reducing conditions, it is possible to calculate, through mass and heat balances, working conditions and size of an electric furnace for the treatment of zinc ferrites. Results of these calculations are summarized hereafter:

Electric furnace (NDH)*		
Working conditions		
Annual capacity	(t/y)	75,000
Residue	(t/h)	9.5
Zn	(t/h)	2.0
Energy		
Coke + Coal consumption	(kg/t residue)	135
Electricity	(MWh/t residue)	1.0
Gases		
Secondary air	(Nm^3/h)	34,000
Off gases flowrate	(Nm^3/h)	35,000 ($3,700\ Nm^3/t$ residue)
T	(°C)	927
CO_2	(%)	7
O_2	(%)	16
SO_2	(%)	0.2
Size of furnace (m^2)		100 - 150

(*) Size and working conditions for a furnace treating the Neutral Leach Residue of the Metaleurop Nordenham zinc plant (120,000 t/yr Zn)

6. CONCLUSION

6.1. COMPARISON OF DIFFERENT PYROMETALLURGICAL FURNACES FOR THE TREATMENT OF NEUTRAL LEACH RESIDUE IN REDUCING CONDITIONS

In the past METALEUROP (as Penarroya) monitored different furnaces in which Neutral Leach Residue was treated. The table hereafter gives a comparison of these treatments in front of the one in an electric furnace.

	Crotone's Cupola furnace	Electric furnace Nordenham	Surex Waelz kiln furnace
Working conditions			
Residue (t/h)	8.0	9.5	10.0
Zn (t/h)	1.0	2.0	1.7
Energy consumption			
Coke consumption + Coal consumption (kg/t residue)	460 (0.27 DM/kg)	135 (0.27 DM/kg)	600 (0.27 DM/kg)
Electricity (MWh/t residue)		1.0 (0.08 DM/kWh)	
Energy costs (DM/t)	125	115	162
Gases output flow rate			
Volume (Nm^3/h)	(55,000-70,000)	28,000	(55,000)
(Nm^3/t)	7,500	3,700	5,500
Temperature (°C)	900	900	600
SO_2 content (%)	0.17	0.20	0.06
Clinker or slag produced (t/t)	0.54	0.35	0.868
Matte produced (t/t)	0.14	0.2	
Ag content (g/t)	2,700	500	
Rendement Ag (%)	75	75	

The capacity of the three furnaces being in the same order of magnitude, comparison of working conditions by ton of Neutral Leach Residue treated is possible.

- Electric and Cupola furnace processes have the advantage of producing a silver bearing matte for silver recovery.

- Electric furnace process is very attractive because of:

  - less energy consumption
  - smaller gases output flow rate.

- Waelz kiln does not need any feed preparation. Electric furnace process needs only small feed preparation. Cupola furnace would need a larger one.

- So, electric furnace remains the most attractive and could be the most interesting to invest in at that time even if its investment cost is high.

FIGURE 1 : ZINC FERRITES

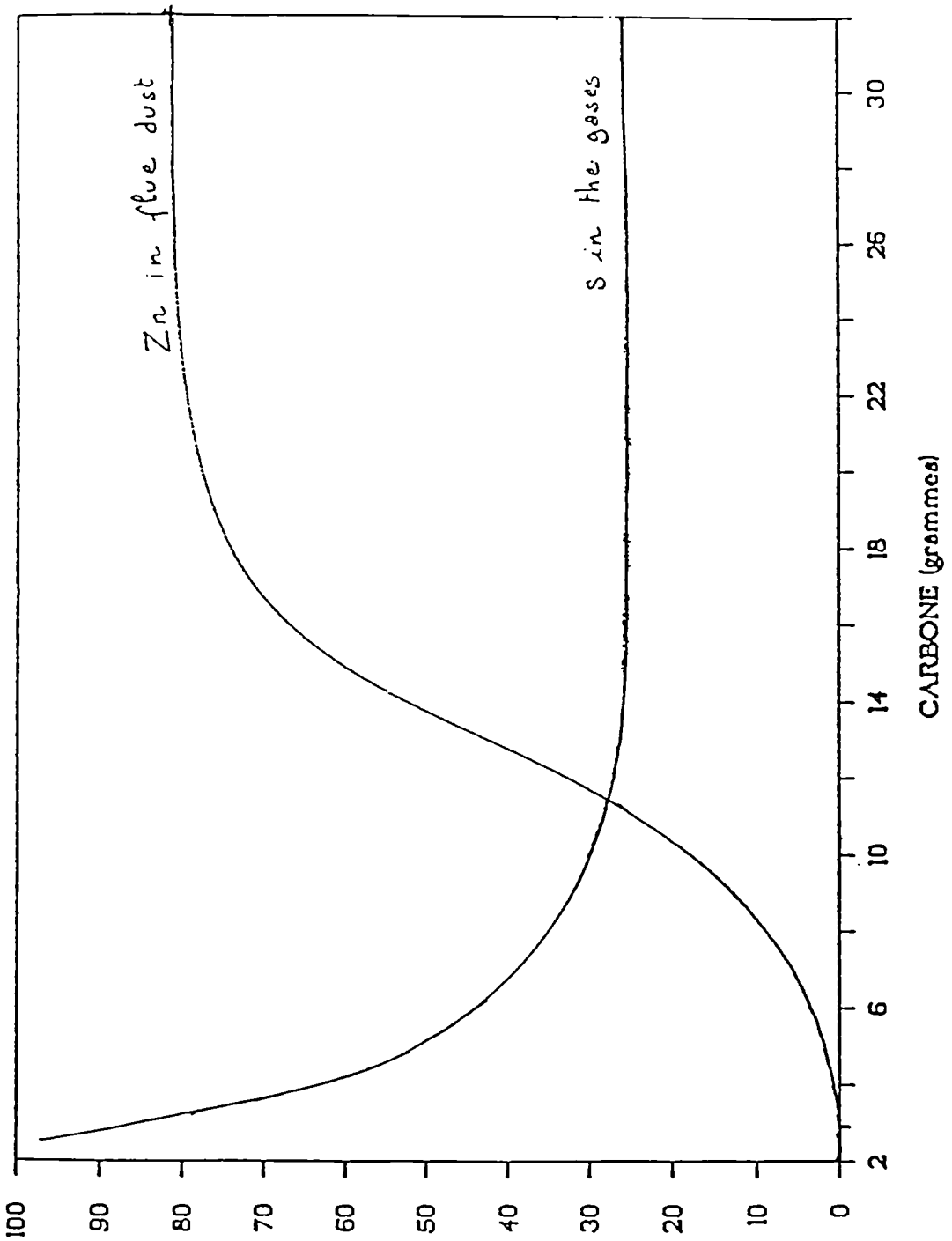

FIGURE 2 : ONE STEP SMELTING : Laboratory results

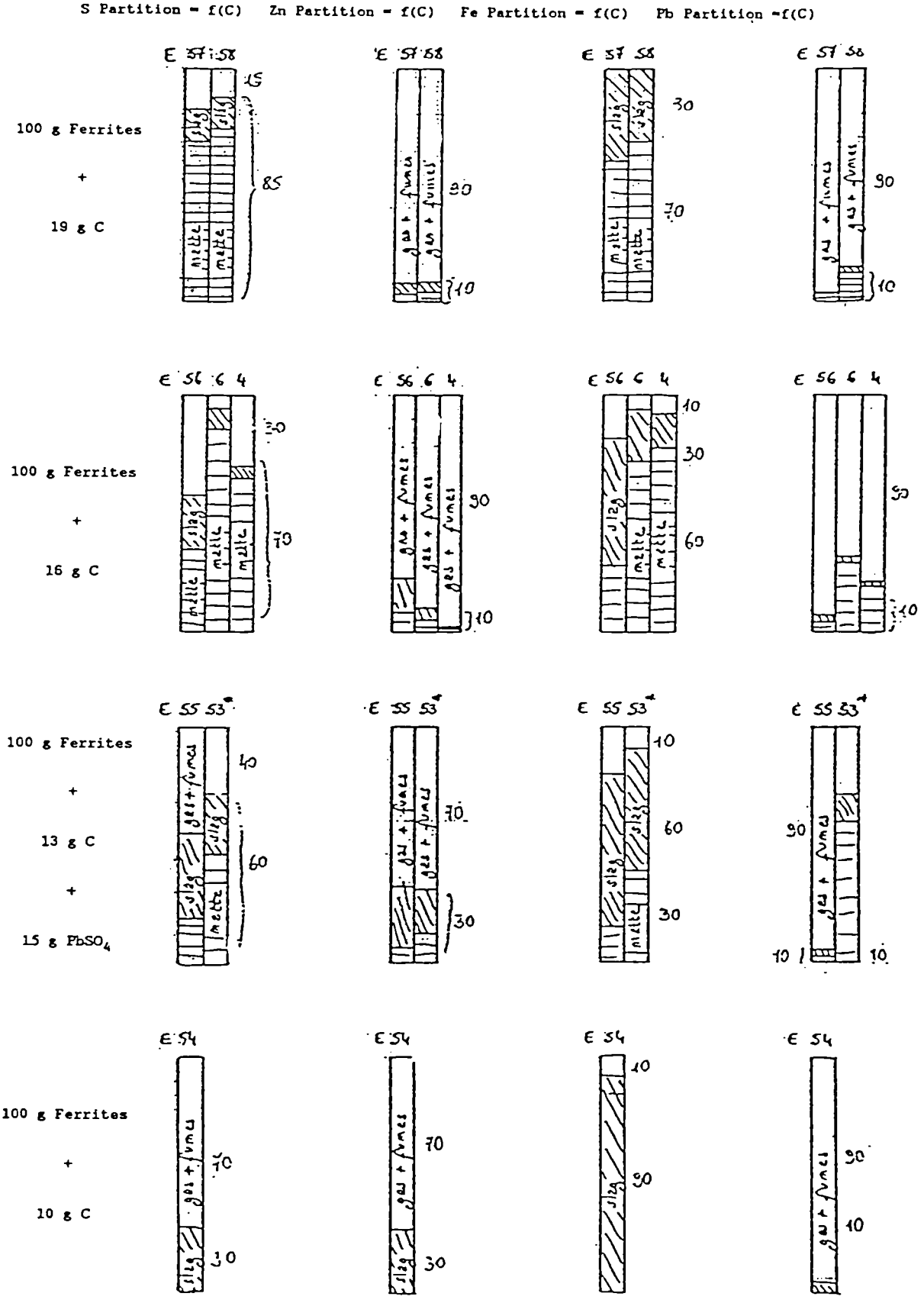

RESEARCH AREA 3.5

MODELLING AND CONTROL IN MINERAL PROCESSING

MODELLING OF AN AUTOGENOUS GRINDING AND FLOTATION PROCESS

APPLICATION TO THE INDUSTRIAL PROCESSING OF THE MOINHO COMPLEX SULPHIDE ORE

Project Leader: A. BROUSSAUD
P. CONIL, H. VEDRINE
Bureau de Recherches Géologiques et Minières, (BRGM), Orléans, France

C.F. MATOS, C.N. FERRAO
Empresa de desenvolvimento Mineiro, Lisboa, Portugal

Contract MA1M-0021-C (CD)

1. OBJECTIVE

To elaborate a steady-state simulator of the process developed by EDM to beneficiate the Moinho polymetallic sulphide ore (Portugal) and to provide it to the team in charge of the development of the process. The simulator is expected to assist the team in commissioning the full scale plant, and later on, in improving it.

To achieve this objective, intermediate but essential objectives were :

- to design and calibrate an operational model of autogenous grinding mills and pebble mills based on pilot scale experiments,
- to understand and model the influence of particle size and mineral liberation on the behaviour of the mineral species in flotation circuit, again based on pilot scale experiments,
- to insert unit operation models developed within the frame of the project in the USIM PAC simulation package previously developed by BRGM and to train the process engineers in using the software.

2. INTRODUCTION

The Molnho polymetallic ore contains copper, lead, silver and zinc. The deposit is located at Aljustrel, 200 km south of Lisbon (Portugal), and is part of the Iberian pyrite belt.

The process was developed at the Aljustrel pilot plant by EDM (Empresa de Desenvolvimento Mineiro) with a view to constructing an industrial plant with a capacity of 150 t/h. The commissioning of the plant is scheduled for 1991. The process on which this study is based, was determined from numerous pilot scale campaigns (35 campaigns amounting to 420 days of pilot tests) and includes two-stage autogenous grinding followed by differential flotation of copper, lead and then zinc with regrinding of the zinc middlings.

The pilot plant flowsheet for this process is shown in Figure 1.

The processing of the Molnho ore poses numerous technical problems essentially related to :

- the fineness of the ore, which necessitates a very fine grind of the order of 30 microns;

- the mineralogical complexity, with the number of minerals present, especially the copper- or lead-bearing minerals, being very high;

- the heterogeneity of the deposit which is reflected as much in the grade variations as in the textural variations or hardness variations;

- the relatively low grades (in the order of 1.15 ± 0.30% copper, 1.26 ± 0.2% lead and 3.5 ± 0.6% zinc).

Thus the processing requires very fine grinding, and flotation selectivity for the different metal-carriers in order to obtain satisfactory results is extremely difficult to achieve.

The laboratory tests and above all the numerous pilot experiments carried out on this ore have given EDM an extensive knowledge of differential flotation of complex ores and autogenous grinding. However, in spite of this expertise, the difficulties in processing the Molnho ore and the complexity of the flowsheet makes it very difficult to optimize the process and to evaluate the influence of process parameters on the overall process performances.

Therefore the partners decided to implement a steady-state simulator to assist the process engineers in :

- optimizing the circuits so as to find the best compromise between grade and recovery for each flotation circuit, and to select suitable settings (grind size, adjustment of the classifiers and hydrocyclones, etc...) in the grinding-classification circuit and in the regrinding circuit of the middlings from the zinc flotation;

- adapting the full scale plant to future objectives (changes in feed rate and particle size, changes in the price of the concentrates, etc...)

The partners initially expected that the simulator could be used for the design of the plant, but the schedule of the projects (the Moinho project and the research project) did not allow it.

3. THE SIMULATOR

3.1. STEADY STATE MINERAL PROCESSING PLANT SIMULATION

A steady-state mineral-processing plant simulator is basically software capable of predicting plant operation according to the characteristics of the feed and the circuit.

The prediction of water and ore streams of the plant operated at steady state under given conditions is called direct simulation, whereas the use of the simulator to back calculate some parameters of plant configuration (such as the required size of a piece of equipment) to obtain a given operation of the plant is called reverse simulation.

The main components of a simulator are usually :

- the simulation software, per se, which enables communication between user and simulator and coordination of calculations. As this is the only component visible to the user, it is often called the simulator. Advanced simulators, such as USIM PAC, offer many other capabilities for data input, display of results and data processing : establishment of material balance, model calibration, direct and reverse simulation, plant capital cost estimation (see Figure 2),

- mathematical models for unit operations, buried inside the simulator as subroutines. They constitute, however, the vital core of the system.

3.2. SPECIFICITY OF THE MOINHO PROCESS SIMULATOR

The USIM PAC software package is used as the shell of the simulator, but the elaboration of a simulator specific to the Moinho process required a research project to be carried out :

- no autogenous grinding model was available. It was therefore necessary to design, code and calibrate a model,

- the earlier pilot plant tests carried out by EDM indicated that mineral liberation plays an important role in the flotation of the Moinho ore. No flotation model taking into account mineral liberation was available and therefore investigations were needed to characterize and model the influence of mineral liberation in the flotation circuit.

4. ORGANISATION AND DEVELOPMENT OF THE RESEARCH

The research included the following phases :

- design an ore model
- collect experimental data in the pilot plant
- model the autogenous grinding circuit
- model the flotation circuits
- incorporate the models developed in the USIM PAC simulation software package
- train the process engineer and make the simulator available to them.

Modelling phases were the most important. They included many interactions between experimental work, mathematical modelling per se, and model evaluation. To keep this synthesis report clear, these interactions will not be described.

4.1. MODELLING THE ORE

Mathematical models cannot take into account in an integral manner the mineralogical and textural complexity of the ore. It is therefore necessary, before any modelling of a process, to model the ore, that is to say to define a simplified representation with a small number of minerals and particle size classes, and, for the Moinho ore, to define how mineral liberation will be taken into account.

Furthermore, and since it is only possible to carry out a complete quantitative mineralogical analysis for a very restricted number of samples, it must be possible to deduce the mineralogical composition of a sample from its chemical analysis. Mineralogical modelling must therefore include an algorithm for the reciprocal conversion of mineralogical composition/chemical composition.

For the Moinho polymetallic sulphide ore the principal minerals retained have been chalcopyrite, sphalerite, galena and a pyritic gangue. The chemistry-mineralogy conversion model consists of the following single equation :

Chalcopyrite content = 2.888 x copper content
Sphalerite content = 1.647 x zinc content
Galena content = 1.155 x lead content
Pyritic gangue + chalco. + sphal. + galena = 100%

In the grinding circuit the ore was modelled by 21 particle size classes, to allow a good description of particle size distributions as well of the feed (up to 250 mm) or the final product (d80 ± 30 μm).

In the flotation circuits, only 4 particle size classes were considered :

44-96 μm
23-44 μm
11-23 μm
<11 μm

It was decided for practical reasons not to try to describe the real textural complexity of the ore. Mineral liberation was taken into account by distinguishing two subclasses for each mineral and each particle size class :

- free (or liberated) particles made of one mineral phase only

- mineral born by locked carrier particles.

4.2. COLLECTION OF DATA AND CALCULATION OF COHERENT MATERIAL BALANCE

A sampling campaign at the Aljustrel pilot plant made it possible to measure the flowrates and the solids percentages and to take samples for each of the principal streams of the grinding circuit and the copper, lead and zinc circuits. Particular attention was paid to the rougher, scavenger and first cleaner banks, and also the cleaner bank after regrinding in the zinc circuit.

The raw experimental data, obtained during the sampling campaign, were inevitably affected by errors and thus were incoherent one with another. They had to be made coherent one with another. They had to be made coherent before they were used for model design and calibration and this was done by employing a data reconciliation algorithm.

To use such an algorithm, it is necessary first to evaluate the level of confidence which it is legitimate to allocate to each measurement. In this present case this evaluation was carried out with particular care in defining an error model for each measured value. Error models take into account the conditions under which the data were collected.

Finally, data were processed by the BILCO software previously developed by the authors research group. The BILCO software provides coherent estimates which satisfy mass conservation equations and which are also as close as possible to the measured values, weighed according to their individual accuracies. BILCO also calculates the accuracy of the estimates.

Estimates provided by BILCO have been proved to be always at least as accurate as raw experimental data, and are usually significantly more accurate.

Coherent material balances were established for each mineral, each particle size class. Additionally separate material balances were established for each textural sub-class (free and locked particles) for particles size classes # 2 (23-44 μm) and # 3 (11-23 μm) in the flotation circuits. The implementation of such material balances is an innovation and needed a specific methodology, described below.

4.3. SEPARATE MATERIAL BALANCES FOR THE FREE AND LOCKED PARTICLES

The main difficulty arises from the impossibility to directly measure particle liberation. Particle liberation can practically be observed on polished sections. This 2D (aerial) observation is biased : it systematically underestimates the proportion of locked particles because a number of locked particles are observed as free particles if the section shows one mineral only. Therefore a methodology shall include :

- 2 D measurements
- reconstruction of information on 3D liberation
- data reconciliation (processing by BILCO)

An additional difficulty comes out of the high cost of 2 D measurements. Such measurements can be done :

- with an image analyser. This is very costly and was done during the project only for a few main samples, partly with a Quantimeter 900 (Cambridge UK) and partly with a QEM-SEM System (CSIRO-Australia),

- or by optical evaluation. This was done for most of the samples with a Swift point counter at the Laboratory of the Directorate of Mines (Porto, Portugal).

The two methods give very different results because the definition of a free particle is different. This was verified for several samples, and abacus were created for conversion of optical evaluation into "image analyser" values. Of course, the relative accuracy of information provided by optical methods is lower and this was taken into account for the establishment of coherent material balances with BILCO.

4.4. MODELLING OF THE AUTOGENOUS GRINDING CIRCUIT

Two autogenous mill models, corresponding to decreasing levels of complexity have been realised and tested :

Level 3 (advanced model) : population balance model using a complete kinetic approach to describe each of the main phenomena occurring during autogenous grinding (fracture, chipping and abrasion),

Level 2 (simplified model) : based on a simplified kinetic approach for the description of the grinding of fine particles and on a direct calculation of the load of coarse particles.

4.4.1. Level 3 model of autogenous mill

Mathematical representation

This steady state model of the autogenous mill is a population balance model on a kinetic representation of breakage.

This mode of representation depends on a formalism identical to that of chemical engineering to describe milling :

- the filiation of particles during fragmentation, analogous to the stoichiometry of a reaction, is represented by a breakage matrix;

- the kinetic at which each particle size class undergoes fragmentation, analogous to a reaction velocity is described using a matrix termed the selection matrix;

- modelling the RTD (residence time distribution) makes it possible to represent the time during which the particles and their progeny are capable of undergoing fragmentation, and characterises the transport of the material in the mill.

The geometrical parameters of the mill are taken into account by a link between this approach and the energy available for milling, based on what has been carried out for ball mills (Herbst, Broussaud).

The equations serving as the basis for the model do not permit a direct analytical solution and so the model carries out an iterative computation. In fact, unlike ball mill, where the presence of a grate has little effect on the transport of the ore in the unit, the grate plays on essential role in the autogenous mill by retaining that part of the ore which acts as the milling material. In this respect the charge present in the mill corresponds to an equilibrium between the feed flow rate of the large particles, the speed of their comminution and the retention of their mass in the mill until the particles which are produced pass through the meshes of the grate. Computing this equilibrium involves calculating the circulating load of the ore rejected by the grate together with the quantity of material contained in the mill. In the algorithm used it requires the intervention of a time constant. The procedure corresponds to a semi-dynamic calculation which simulates the evolution of the hold up in the transient regime.

In order to limit the computation time and the number of iterations carried out it is desirable to start the computation with a description of the hold up which approximates to its reality. An automatic initialisation procedure for the particle size distribution of the charge has therefore been incorporated into the model.

The level 3 model consists of :

- a main structure, shown in Figure 3, based on a representation of the transport of the material in the mill, on the semi-dynamic simulation of arriving at the equilibrium of the hold up and on an energy-kinetics relationship, and

- a secondary description, which can be modified, corresponding to the modelling of the breakage and selection functions.

These components are dealt with in the following paragraphs.

Transport of material in the mill

The transport of material in the mill is represented by :

- N perfect mixers in series ;

- a classification function which models the role of the grate and which operates on the product leaving the last perfect mixer. Particles passing through the grate form the outlet from the mill and those rejected by it are recycled into the feed to the first mixer.

Breakage and selection matrices

The level 3 model utilises three breakage matrices, one for each breakage phenomenon, which essentially are fracture, chipping abrasion and three selection matrices. For simplicity each of these matrices will be denominated by the name of the preponderant phenomenon.

The breakage matrices

The matrices for breakage by fracture and chipping are modelled by functions of the following form :

$$B_{ij} = \emptyset \, (X_{i-1}/X_j)^{\gamma} + (1-\emptyset) \, (X_{i-1}/X_j)^{\beta}$$

where :

B_{ij} : value of the cumulative breakage function
X_i : mean dimension of the particles in the size function i
$\emptyset, \gamma, \beta$: parameters of the model, determined on the results of batch trials in a laboratory mill or on a pilot-scale plant.

For the breakage by abrasion matrix the model considers that when particles of a given size i are eroded their mass is distributed between the immediately smaller fraction i+1 and all the particle size distribution fractions of the fines (smaller than 1 mm). The distribution is a function of the variation of the volume corresponding to the passage of a sphere of mean diameter X_i to one of diameter X_{i+1} ;

mass fraction entering in fraction i+1

$$= (X_{i+1}/X_i)^3$$

mass fraction entering into all the fines fractions

$$= 1 - (X_{i+1}/X_i)^3$$

The selection matrices

The selection matrices for abrasion and chipping are modelled by functions of the form :

$$S_i = S1 \, X_i^{\alpha}$$

where :

X_i : mean dimension of the particles in the particle size fraction

S1 and α : parameters of the selection function

In the case of the fracture selection matrix a supplementary term represents the quantity of oversize particles present in the charge. This reflects the hypothesis that the kinetic of fracturing is proportional to the quantity of the milling charge.

The energy approach

The power drawn by the mill is calculated as a function of the characteristics of the latter. The forecasts of several empirical formulae have been compared with the experimental values of the powers drawn by the primary and secondary autogenous mills in the pilot-scale plant.

The equation :

$$P = 3.33.D^{2.3}.L.\rho.Vr.(1-0.5/2^{2-10Vr}).J.(1-0.937.J)$$

where :

P : power in kW consumed by the mill
D : internal diameter of the mill (m)
L : internal length of the mill (m)
J : fraction of the volume of the mill occupied by the slurry
Vr : speed of rotation, expressed as a fraction of the critical speed
ρ : density of the ore : 4.6 for the Mohno ore

giving the best results it has been retained and utilised in the model.

Link with the kinetic approach

The link between the kinetic approach and the energy approach is effected by the relationship between the parameter S1 of the selection functions and the power available for milling :

$$S1 = SE1.Pw/H$$

where :

Pw : power available for milling
H : charge of ore
SE1 : normalised parameter of the selection function

Initialisation of the hold-up

An automatic initialisation procedure for the particle size distribution of the charge has been incorporated in the model. This procedure is not necessary for the good functioning of the model but it does make it possible, by initialising the calculation of the charge with a

description of the latter which is near to reality, to reduce appreciably the duration of the iterative computation. It is derived from the work of Goldman and Barbery who used a formula, published by Austin and describing the particle size distribution of balls in a mill, in order to predict the particle size distribution of the charge in an autogenous mill.

4.4.2. Level 2 model

The differences between this model and the level 3 model came mainly from the simplifications of the grinding phenomena description.

The level two model considers that, in an autogenous mill, the main part of the grinding of the average and small size particles is realised by the coarse lumps. These coarse lumps, retained by the grate, are only subject to two phenomena, self-breakage and abrasion, which is predominant. When the mill reaches the steady state, the mass of lumps of the load corresponds to the equilibrium between the lumps mass flowrate entering the mill and the rates of lumps comminution.

For the comminution of coarse particles, as abrasion is the main phenomenon, this model considers that there is only one relationship between the rate of lumps comminution, the lumps size and the mill diameter. As a consequence, a direct calculation of the mass of the lumps hold-up can be realised, without the need for an iterative structure similar to the level 3 model one.

This model follows separately :

- from one side the coarse lumps behaviour, with a direct lump hold-up mass calculation, and

- from the other side the average and small particle behaviours, that are represented using a simplified kinetic theory where the product of the breakage function (particle progeny fragments distribution) multiplied by the selection function ("grinding rate") is described by one function only.

For these last particles, the mass transport inside the mill is described, as for the level 3 model, by a 2 mixers in series residence time distribution model.

Mill size (diameter, length) and settings (rotation speed) are taken into account, for the small and average sized particles, by a link between the simplified kinetic approach and the power available for comminution. For the lumps, there is a relationship between the "abrasion" rate and the mill diameter.

The main structure of this model is shown in figure 4.

4.4.3. Conclusions on the autogenous grinding modelling

The models of the autogenous mill have been built with the objective of making it possible to predict the performances of this unit as a function of the particle size distribution of the feed, taking into account the principal design and operational parameters (feedrate, geometry of the mill, speed of rotation, etc...). Another constraint was to simplify as far as possible the experimental methodology of utilising the model.

Level 3 model

The model which as been developed includes several original features, in particular the semi-dynamic computation of the charge, the separate follow-up of the angular and rounded products and the linkage between the energy consumed and the kinetics of grinding.

The validation test of the semi-dynamic computation of the charge, the separate follow-up of the angular and rounded products and the linkage between the energy consumed and the kinetics of grinding.

The validation test of the model shows that forecasts of operation at a feedrate and feed particle size distribution which differ considerably from those of the calibration point correspond in a satisfactory manner to the measured values.

However numerous facets of the model have still not been validated, in particular the possibility of scaling up, and additional research is still necessary.

Many aspects of autogenous milling are still imperfectly understood. In particular, and whilst the descriptions of the phenomena of comminution have already been the subject of in-depth work on the part of various authors, the subject of the transport of materials in the autogenous mill is still represented in a rather incomplete manner and call for additional study.

Although, the experimental methodology for model parameters estimation and model calibration is simpler for this model than those previously proposed, it still remains expensive (need for pilot scale continuous test) and difficult (high complexity of model calibration).

Level 2 model

Like the level 3 model, the level 2 model developed during this study includes several original features, the main one being its algorithm of direct calculation of the lumps hold-up.

The experimental methodology for utilising this model is much simpler than for the level 3 model and, at the opposite of the level 3 model, it may be adapted without a large amount of work to reproduce the autogenous grinding after a change of ore characteristics.

Therefore, this level 2 model seems to be of high practical value and quite promising for practical applications.

4.5. MODELLING THE FLOTATION CIRCUITS

Three flotation models corresponding to increasing levels of complexity have been successively tested :

First level : the flotation kinetics have been modelled for each of the minerals, without explicitly taking into account the influence of particle size and texturology

Second level: the influence of particle size was explicitly taken into account by defining flotation kinetics for each mineral in each of the four particle size classes.

Third level : taking explicit account of the texturology and particles sizes led to defining flotation kinetic for each of the minerals, by particle size class and by textural sub-class.

4.5.1. First modelling level

Basic model

The basic model considers two types of possible behaviour for the solids :

- hydrophobic particles flotation is described by a first order kinetic law;

- hydrophilic particles behaviour is interpreted as mechanical transportation by the water.

For the hydrophobic solids the model assimilates the flotation to a first order kinetic phenomenon with discrete distribution of the kinetic constrains. Three sub-populations are thus defined for each type of particle, one floating rapidly, one floating slowly and one not floating.

Since the flotation cells are assimilated to perfect mixers the cumulative recovery Rn for a given type of particles over the n cells of a bank, is :

$$R_n = Rinf \cdot [(1-\phi) \cdot \sum_{j-1}^{n} \{(K_r \cdot \tau j)/(\prod_{i-1}^{j} (1 + K_r \cdot \tau_i))\}$$

$$+ \phi \cdot \sum_{j=1}^{n} \{(K_1 \cdot \tau_j)/(\prod_{i=1}^{j} (1 + K_1 \cdot \tau_i))\}]$$

where for each type of particle considered :

Rinf : maximum recovery
Kr : fast floating kinetic constant
K1 : slow floating kinetic constant
Ø : proportion of the type of particle, capable of floating, floating slowly
τ_i : residence time in cell i

For the water the model considers a first order kinetic behaviour with a single kinetic constant. The cumulative recovery of water in the froth from n cells of a bank may be written :

$$RE_n = REinf \cdot \sum_{j-1}^{n} (KE \cdot \tau_j)/(\prod_{i-1}^{j} (1 + KE \cdot \tau_i))$$

where :

REinf : infinite recovery
KE : kinetic constant
τ_i : residence time cell i

Results and Interpretation

As an example the results are set out and discussed for the copper circuit.

The kinetic models make it possible, as is shown by Figure 5, to reproduce effectively, for the four minerals of the ore model, the flotation kinetics in the various circuits. Taking into account the level of uncertainty associated with the experimental data, it would be fruitless to seek models with a more sophisticated formulation without also making the influence of new parameters explicit.

The mechanical entrainment by water can be used to model the behaviour of sphalerite and gangue in the rougher bank.

Figure 6 shows, for these minerals, a constant carriage coefficient for all the cells of the bank.

On the other hand, figure 6 demonstrates that galena shows, like chalcopyrite, hydrophobic behaviour in the copper circuit. Only a kinetic model can account for its behaviour.

4.5.2. Modelling the influence of particle size

The flotation model used at this level is a two-parameter kinetic model, one kinetic constant and one maximum recovery, defined for chalcopyrite, sphalerite and gangue in each particle size class.

The following is the expression for the recovery of a mineral in a given particle size class :

$$RE_n = Rinf \cdot \left[\sum_{j=1}^{n} \left((K \cdot \tau_j) / \left(\prod_{i-1}^{j} (1 + K \cdot \tau_i) \right) \right) \right]$$

Results obtained at this level were frustrating. It was clear that the maximum recovery is smaller and flotation is slower for coarse particles (>44 μm) than for the others. Apart from that, the influence has not been possible at this stage of the modelling to interpret the results in a constructive fashion. The continuation or the study has shown that the influence of the mineral liberation is more important than the particle size per se.

4.5.3. Modelling the influence of mineral liberation

The flotation model used at this level distinguishes the behaviour of the minerals according to whether they are found in the form of free particles or in the form of locked particles. It is a two-parameter kinetic model (a maximum recovery and a kinetic constant) defined for free particles and locked particles for each mineral in particle size classes # 2 and # 3.

The recovery of a mineral in a given particle size class, in a bank of n cells, is given by the expression :

$$R_n = Rinf1 \cdot lib \cdot \left[\sum_{j=1}^{n} \left((K_1 \cdot \tau j) / \left(\prod_{i-1}^{j} (1 + K_1 \cdot \tau_i) \right) \right) \right]$$

$$Rinfn1 \cdot (1-lib) \cdot \left[\sum_{j-1}^{n} \left((K_{n1} \cdot \tau_j) / \left(\prod_{i=1}^{j} (1 + K_{n1} \cdot \tau i) \right) \right) \right]$$

where :

Rinf1 : maximum recovery for the liberated fraction
Rinfn1: maximum recovery for the non-liberated fraction
lib : fraction of mineral liberated
K1 : kinetic constant for the liberated fraction
Kn1 : kinetic constant for the non-liberated fraction
rl : residence time

The results of the mineral liberation analyses for the particle size class 44 μm are not significant. They have not, therefore, been taken into account in the modelling.

For the finer particle size class, technological limitations have not made it possible to carry out liberation measurements.

Results and Interpretation

The models make it possible to reproduce effectively the experimental kinetics, as shown by the example in Figure 7. The curves shown on Figures 8, 9 and 10 and the calibration results in Table 1 illustrate the influence of mineral liberation on the kinetics in the zinc flotation circuit.

Three types of behaviour can be clearly distinguished

- free particles of hydrophobic minerals float almost in their totality from rougher onwards,

- free particles of hydrophilic minerals float only slowly and very partially,

- locked particles, float only partly and slowly. There are clear similitudes between the behaviour of the different minerals (hydrophobic and hydrophilic) when they are carried by locked particles.

Figures 11, 12 and 13 illustrate the evolution of the proportion of each of the liberated minerals in the froth. One can clearly see from Figure 11 the fast drop in the proportion of liberated sphalerite in the froth of the scavenger concentrates (cells 3 to 5 of the bank). Most of the free sphalerite has been floated in the two rougher cells and there is practically nothing left other than the locked sphalerite at the entry to the scavenger bank.

This justifies the introduction of a mill for regrinding the scavenger concentrates.

Figure 14 demonstrates the regular increase of the proportion of the liberated pyritic gangue in the concentrates in the zinc rougher/scavenger bank. The proportion of gangue associated with the sphalerite or the chalcopyrite diminishes as the locked carriers of these minerals float, whilst the mechanical carriage by water, demonstrated at the first level of modelling, leads to an increasing proportion of liberated gangue in the concentrates.

Table 1 shows the activation of the sphalerite, the chalcopyrite and the non-liberated gangue after regrinding. This is no doubt due to the creation of new hydrophobic surfaces during the regrinding.

4.5.4. Conclusion on flotation modelling

The main result is that flotation kinetics are very dependent of particle liberation. Three kinds of behaviour are observed and modelled :

- free particles of hydrophobic minerals (chalcopyrite, sphalerite in the zinc circuit),
- free particles of hydrophilic minerals,
- locked particles.

The influence of particle size per se is much less significant. Flotation models developed are believed to be reliable enough to be used for the optimization of the process and the flowsheet.

They have the potential to be used also for the optimization and the adaptation of the full scale plant. However, they may need to be calibrated again with full scale plant data to account for scale factors not taken into account during the research.

5. RESULTS AND CONCLUSIONS

The detailed results of the research are presented in the final report of the research [1]. Only the main points are mentioned here in terms of their conformity to the objectives and their concrete value for the different parties.

5.1. CONTRIBUTION FOR THE PROCESS ENGINEERS OF THE MOINHO PROJECT

5.1.1. New knowledge concerning the ore and its processing

A first contribution from this study, even before its completion, consisted of an important increase in knowledge of the ore and of its processing.

The considerable work involved in the data collection (sampling the different streams of the pilot plant with 1,645 samples collected, 481 particle size analyses, 12,352 standard chemical analyses, and 153 semi-quantitative and quantitative mineralogical analyses) and data processing with advanced material balancing techniques prior to modelling has resulted in a description of the process with a detail never before obtained.

New understanding of the process related to :

- the selectivity of the grinding,
- the kinetics of the flotation of the minerals in the different banks (cf. figures 5 and 8),
- the influence of the mineral liberation on the performance of the flotation circuits.

5.1.2 Availability of a simulator

The main result of the study consists in providing the engineers in charge of the industrial project with a steady-state simulator of the process.

Function of the simulator

The simulator provided to the EDM process engineers has all the capabilities of the standard USIM PAC software package and additionally it includes the specific unit operation models developed during the research. EDM engineers were trained in using it.

The simulator is used for process optimization. It enables process engineers to predict the influence on the plant performance, of modifications in :

- the equipment setting (changes in the ball load of the regrinding mill, modification of the hydrocyclone settings, etc...),
- the plant flowsheet (recycling of streams, number of cells of the flotation banks, etc...)
- the size of the main unit of equipment.

Limitations of the simulator

Although the simulator is really a powerful and operational tool, it suffers from some limitations :

- the accuracy of the models is not as good as initially expected,
- the simulator does not include a model for column flotation.

The first limit comes out of the difficulties to get a stable enough operation of the pilot circuit and to take enough representative samples. This, and the fact that some aspects of the process are not fully reproductible, probably because of variation in ore properties which cannot be measured, makes it impossible to have perfectly accurate data to calibrate the models. It is clear that unit operation models cannot be more accurate than data used for their calibration. Despite of this limit, models are believed to be reasonably accurate.

The second limit is a more serious one for the process engineers : flotation columns were added to the process and will be key pieces of equipment of the full scale plant. Unfortunately the decision was made too late to be taken into account for the joint research project.

5.2. CONTRIBUTION FOR BRGM

5.2.1. Additional expertise in modelling

This study has enabled BRGM to acquire new expertise in modelling industrial mineral processing plants, especially in relation to :

- the autogenous mill through :
  - construction of two new and original autogenous mill models and a full methodology to use them (designed experiments, sampling, data collection and processing),
  - proving the validity of the models, understanding their limitations and defining areas of research which lead to more phenomological models in the future.
    For example the material transport in the mill is still represented in a fairly simple manner and requires further investigation, especially to take into account the presence of pebble ports or pebble extractors. The scaling up capabilities of the models remain also to be studied.
- flotation through :
  - the perfecting of a methodology to model the influence of particle mineral liberation on the flotation kinetics.

5.2.2. Development and use of the USIM PAC simulation software

The simulator produced for the study has enabled BRGM :

- to enrich the library of USIM PAC unit operation models with autogenous mills models. However, these models will not be available on a commercial basis until further research makes it possible to overcome the limitations mentioned before.

5.3. CONTRIBUTIONS FOR THE SCIENTIFIC COMMUNITY

The results of the research, and especially those related to the models developed and the methodology were made available to the world of mineral processing through 3 papers given in international conferences and published [2], [3], [4].

5.4. ASSESSMENT OF THE PROJECT

The initial objective was attained :

- a simulator of the grinding circuit and of the flotation circuits (copper, lead, zinc) was implemented and provided to the process engineers. The process engineers also received relevant training,

- innovative models were developed for autogenous grinding and flotation taking into account mineral liberation. The modelling of the influence of mineral liberation on flotation kinetics provided a significant improvement on the understanding of the process,

- the project was therefore really fruitful for both partners.

Although the simulator is operational, its value for the Moinho project is partly limited by the lack of column flotation models and the need for additional research on the modelling of autogenous grinding.

6. REFERENCES

1. CONIL P., VEDRINE H., BROUSSAUD A. , DE MATOS C.F., FERRAO C.N.,
   Modelisation du procédé de broyage autogène et de flottation différentielle du minéral sulfure complexe de Moinho (Portugal).
   Application au développement industriel du projet.
   Rapport final.
   Bureau de Recherches Géologiques et Minières, rapport n° 30786, 1990.

2. CONIL P., MATOS C.F., BROUSSAUD A., FERRAO C.,
   Modelling of the autogenous grinding of the Moinho (Portugal) complex sulphide ore.
   SAG Conference 1989, September 25-27, 1989.

3. VEDRINE H., BROUSSAUD A., CONIL P.,
   Modelisation de la cinétique de flottation d'un minéral sulfure polymétallique.
   Industrie Minérale - Mines et Carrières - Les techniques - Mars-Avril 1990.

4. VEDRINE H., BROUSSAUD A., CONIL P., MATOS C.F.,
   Modelling of the flottation kinetics of a polymetallic sulfide ore.
   To be presented at the AIME Congress, 1991, SME annual Meeting, and Exhibit. February 25-28, Denver 1991.

		Particle size classes (µm)	Kinetic constants in min^{-1}		
			rougher	1st cleaner	cleaner after regrinding
SPHALERITE	free	-44 +23	0.258	0.700	1.480
		-23 +11	0.618	0.622	1.890
	locked	-44 +23	0.226	0.237	0.324
		-23 +11	0.232	0.242	0.452
PYRI GANG	free	-44 +23	0.032	0.033	0.041
		-23 +11	0.037	0.061	0.050
	locked	-44 +23	0.121	0.077	0.539
		-23 +11	0.205	0.107	0.283
CHALCOPYRI	free	-44 +23	0.169	0.141	0.019
		-23 +11	0.204	0.192	0.500
	locked	-44 +23	0.084	0.063	0.263
		-23 +11	0.076	0.067	0.105

TABLE 1 - Kinetic constants. Zinc flotation circuit

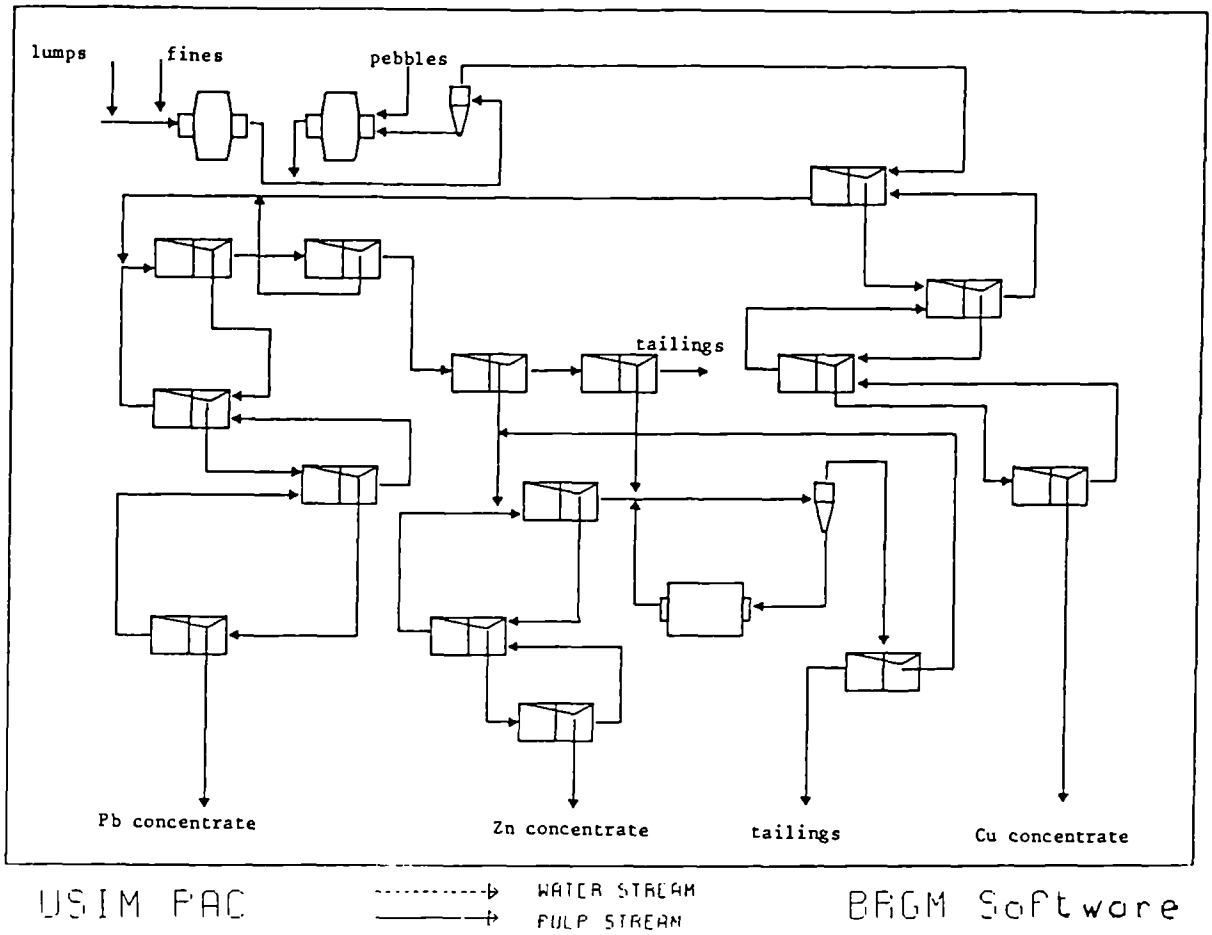

FIGURE 1 - PILOT PLANT FLOWSHEET

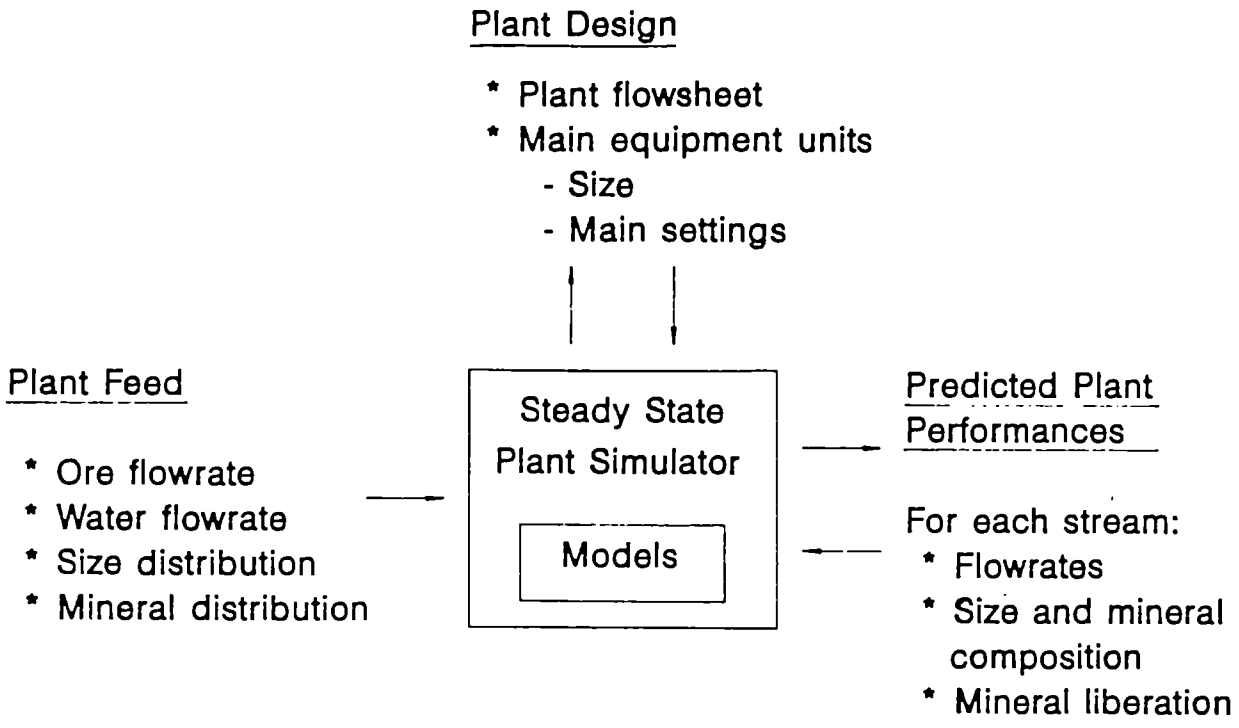

FIGURE 2 - FUNCTIONS OF A STEADY STATE PLANT SIMULATOR

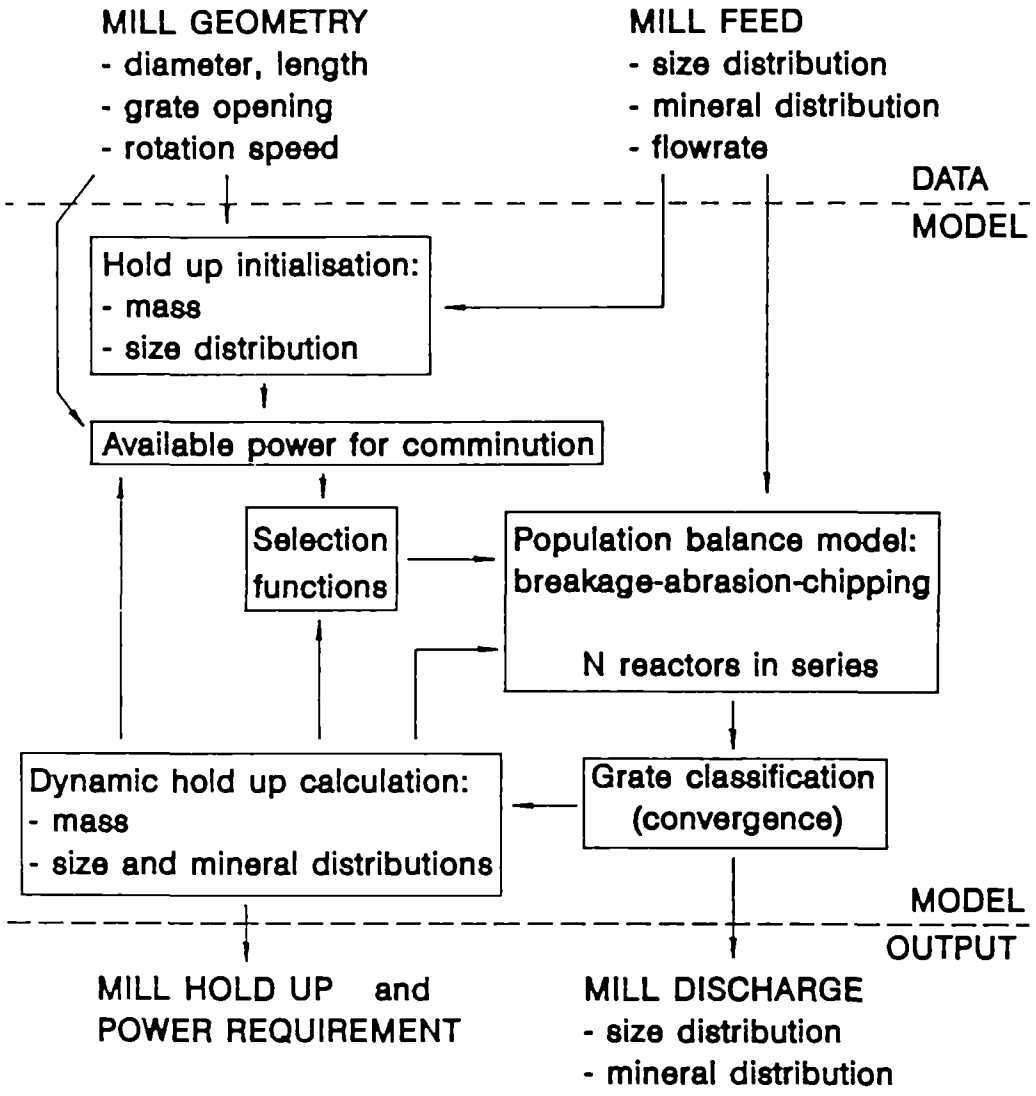

FIGURE 3 - SIMPLIFIED REPRESENTATION OF THE STRUCTURE OF LEVEL 3 AUTOGENOUS MILL MODEL

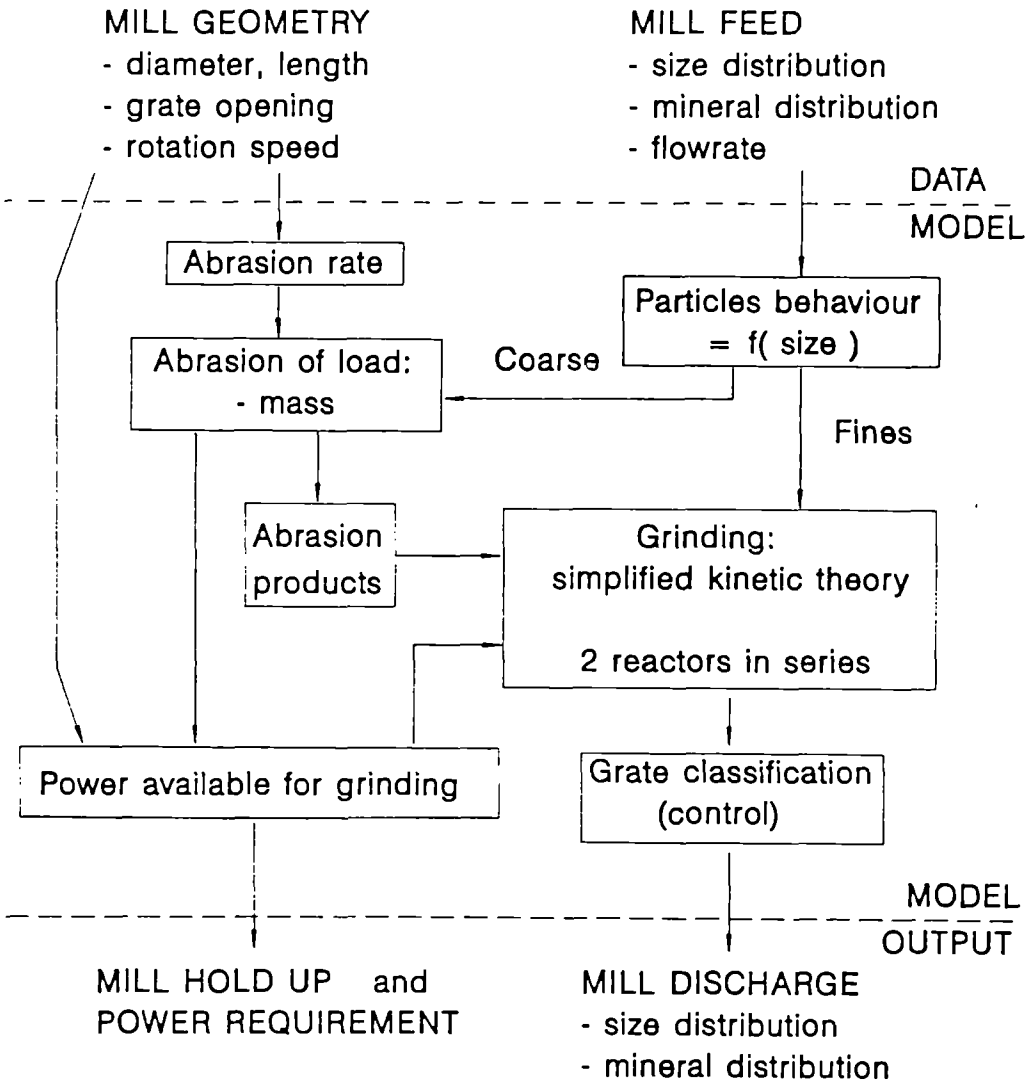

FIGURE 4 - SIMPLIFIED REPRESENTATION OF THE STRUCTURE OF LEVEL 2 AUTOGENOUS MILL MODEL

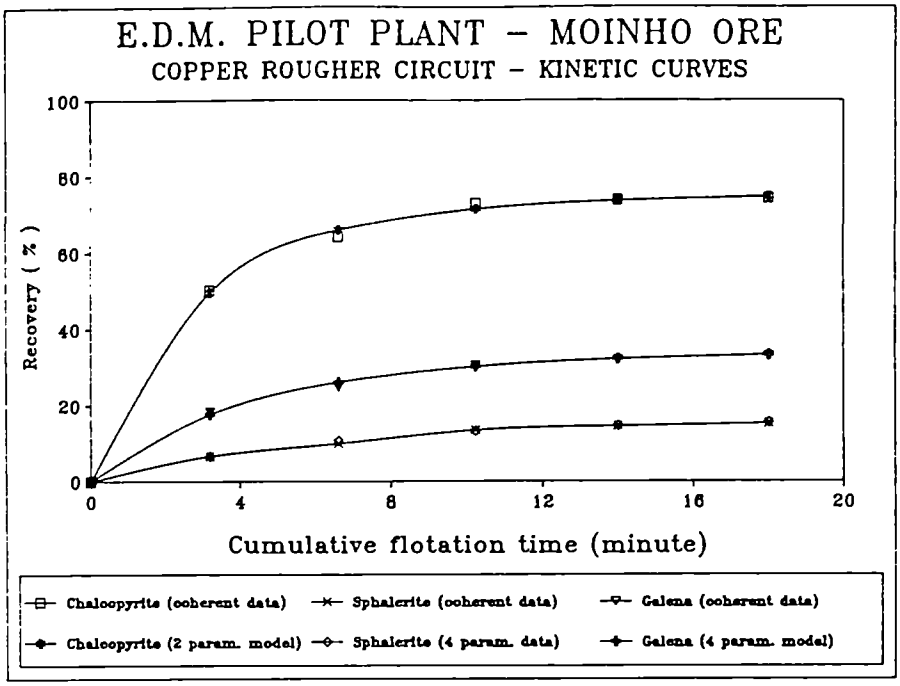

FIGURE 5

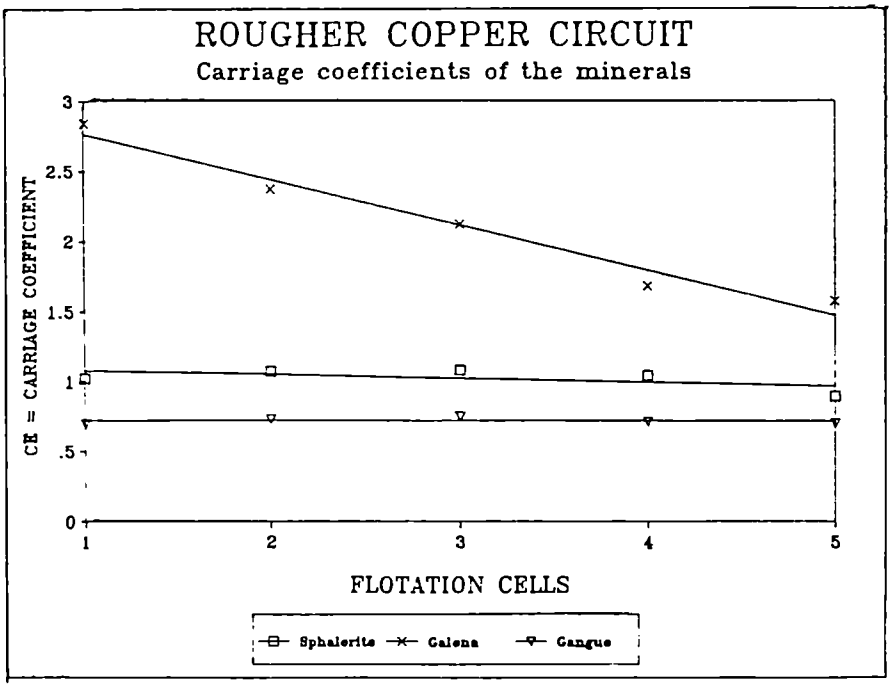

FIGURE 6

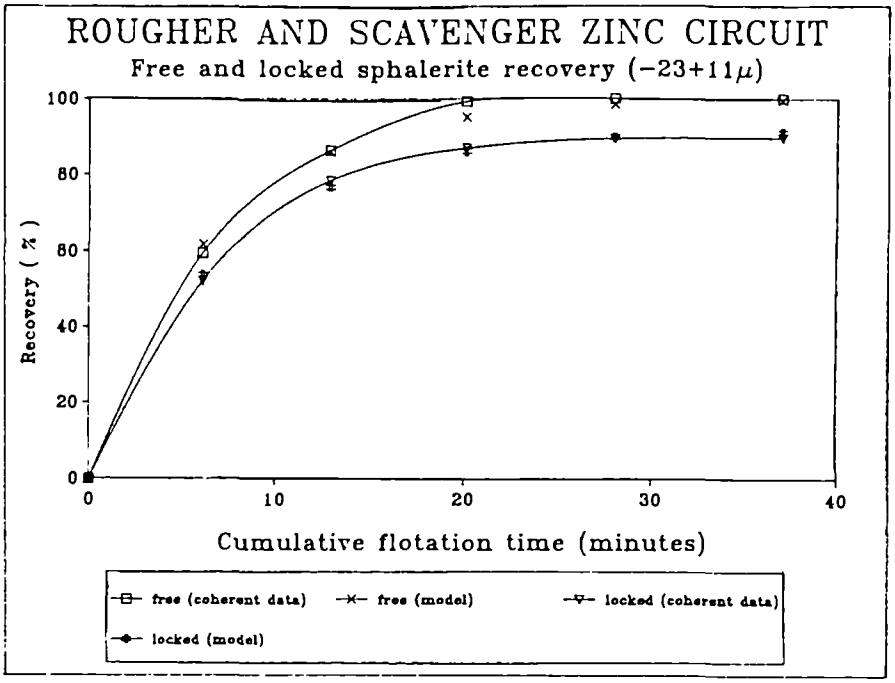

FIGURE 7

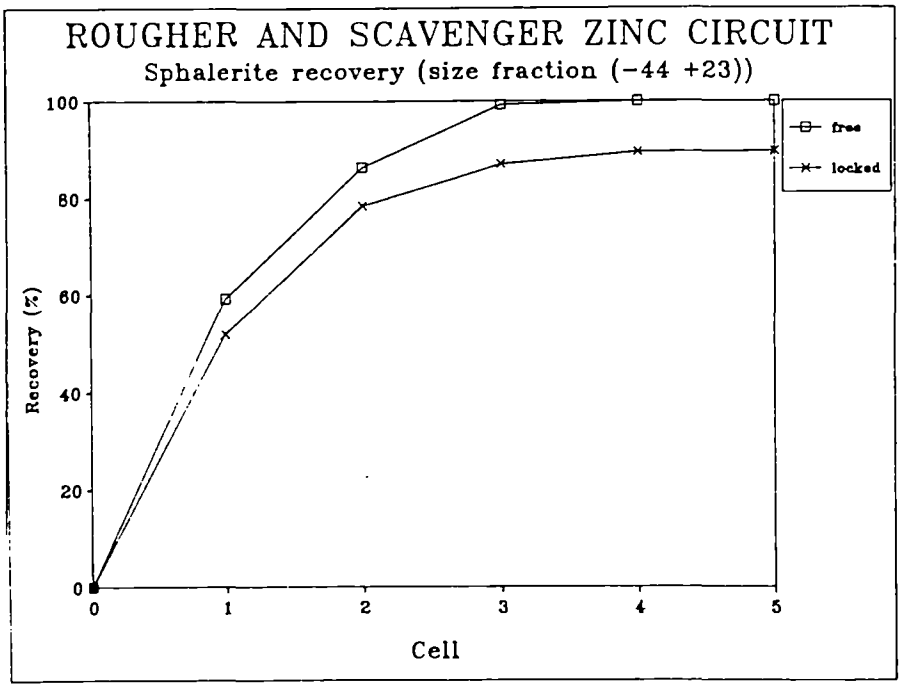

FIGURE 8

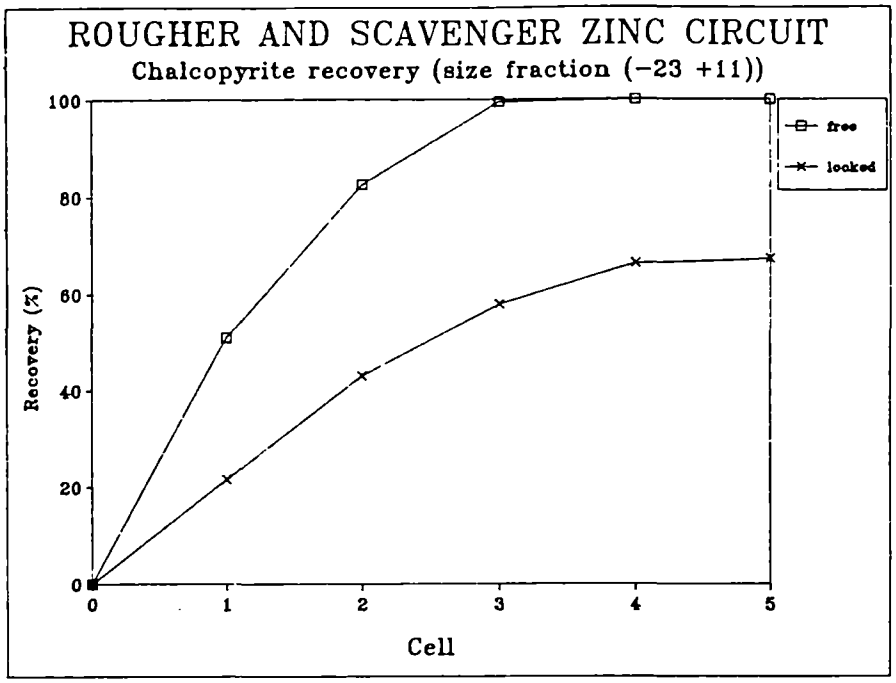

FIGURE 9

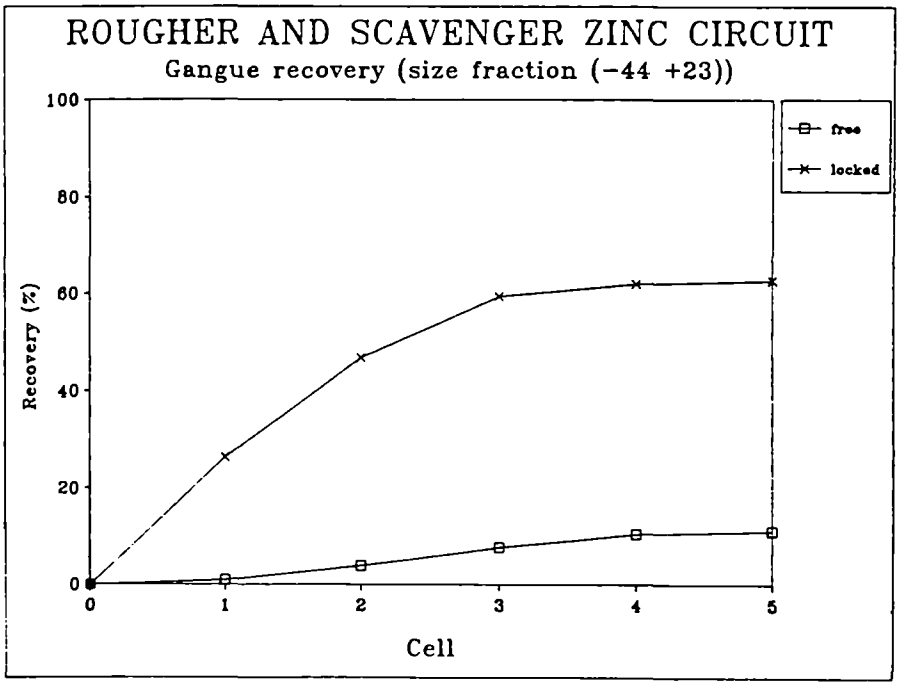

FIGURE 10

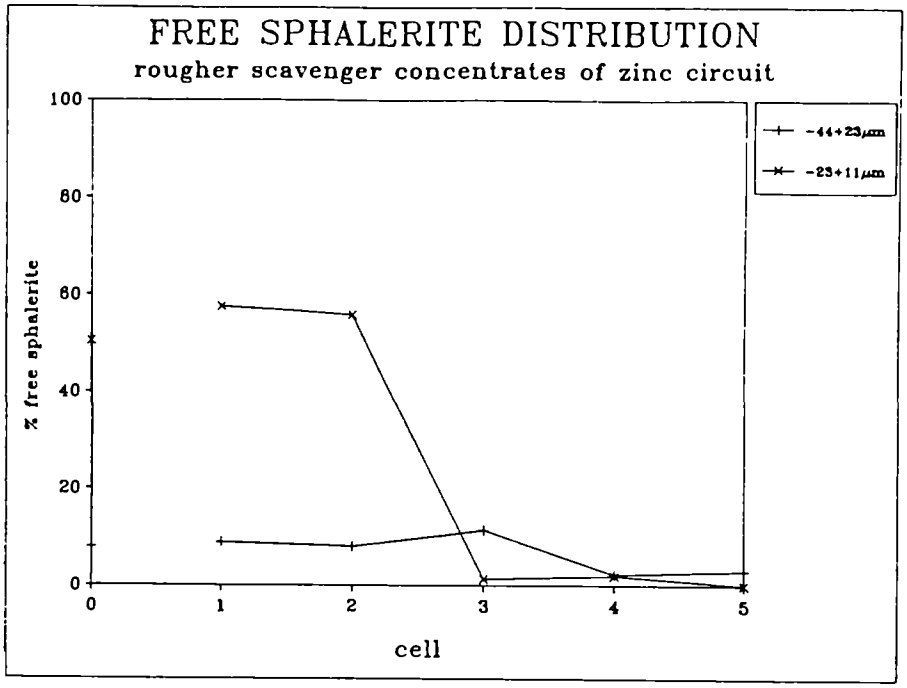

FIGURE 11

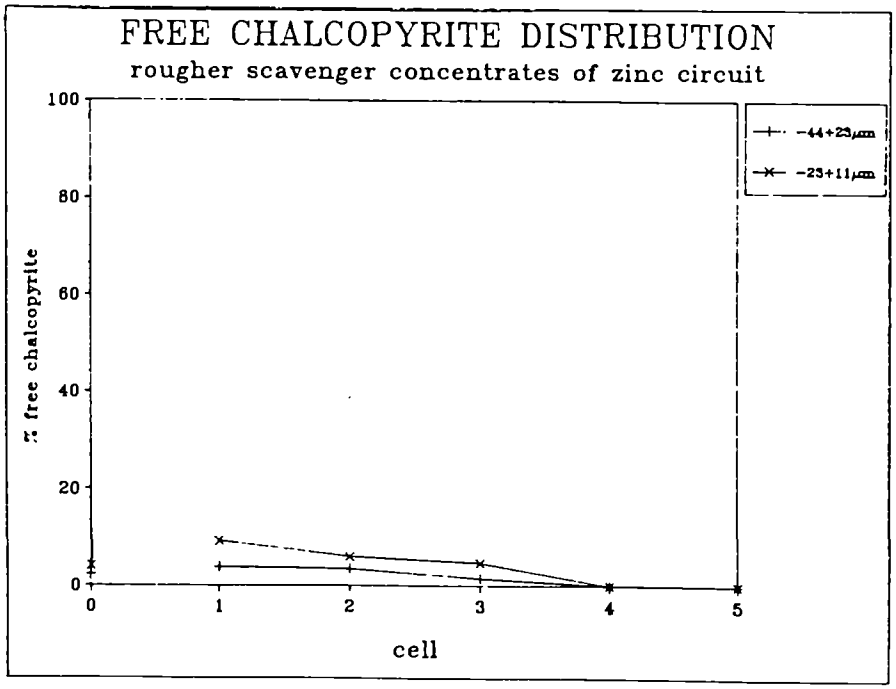

FIGURE 12

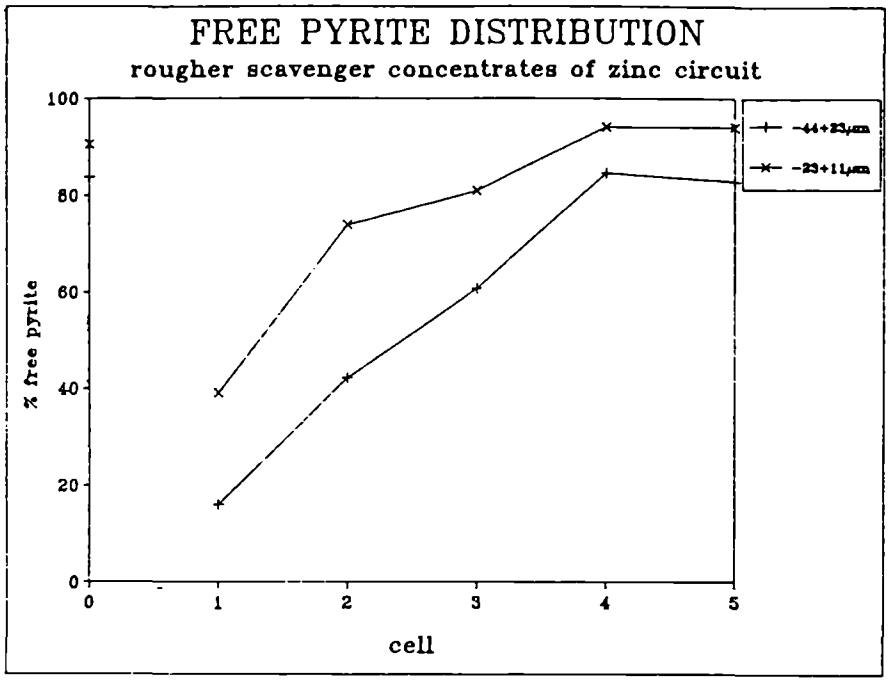
FREE PYRITE DISTRIBUTION
rougher scavenger concentrates of zinc circuit
% free pyrite
100
80
60
40
20
0
0
1
2
3
4
5
cell

FIGURE 13

DEVELOPMENT OF AN INTEGRATED COMPUTER-BASED METHOD FOR PLANT ENHANCEMENT

Project Leader: P. TUCKER
Warren Spring Laboratory, United Kingdom

Contracts MA1M-0047-UK and MA1M-0077-UK

1. OBJECTIVE

The objective of the project was the development and validation of a suite of mathematical (and other computer-based) techniques, for use in the mineral processing industry, for optimising plant performance.

2. INTRODUCTION

This report summarises the technical results from contracts MA1M-0047-UK and MA1M-0077-UK of the Third EC Raw Materials Programme. These contracts form two phases of a collaborative project between Warren Spring Laboratory (WSL), Beralt Tin and Wolfram SA (BTW) and Carnon Consolidated Ltd. (CCL).

The techniques were developed within an overall methodology which is practical to use on site in industrial mineral processing operations, with the emphasis on solving problems of direct relevance to producing plant: to improve plant efficiencies, to increase mineral recoveries and product grades, and to maintain this improved performance. The techniques were validated on the industrial-scale operations at BTW (Panasqueira mine) and the Wheal Jane plant of CCL.

3. RESULTS AND DISCUSSION

3.1. METHODOLOGY

The parallel application of computer simulation backed up by computer-aided process analysis comprised the formal methodology behind this project. The methodology can be thought of as being analogous to a control loop; process simulation and modelling providing the forward planning part of the cycle and material balancing (data reconciliation) completing the main return (analysis) branch of the cycle. Data enhancement and expert systems can provide for accelerated analyses an diagnostics. These concepts are portrayed schematically in figure 1.

3.2. MODELLING AND SIMULATION

3.2.1. Development of New Models

The work undertaken on this contract has resulted in seven new unit process models being developed and included within the WSL process modelling package. The new models comprise:

(i) Generic shaking table model
(ii) Reichert cone model
(iii) Generic classifier model (Spiral and Rake)
(iv) Generic crusher model (Cone and Rolls)
(v) Duplex concentrator model
(vi) Multi-g separator model
(vii) Mineralogical model of flotation/flotation tables

which complement the existing suite of models covering Spiral concentrators (both multiport type and sluice type, also specialist coal separators), Hydrosizers, Jigs, Dense media cyclones (a generic model covering both DMS and Triflo units), Pinched sluice, Hydrocyclones and Grinding mills.

In developing the new models, emphasis was given, wherever possible, to developing a generic approach that would satisfactorily model a class of devices rather than just one specific device within that class. This (new) approach was accomplished through developing a general main model function which would fit every device within the class simply through a structured scaling of a set of adjustment (model) parameters contained within the function. This scaling was facilitated either through the incorporation of a "user-specified" switch parameter or by exploiting the inherent properties of the normal model parameters used in the model function. (These "normal" parameters serve firstly to calibrate the model for a specific ore under specific operating conditions and secondly, through their systematic variation, to describe how performance then varies with a change in those operating conditions. The latter role is formulated in terms of an auxiliary model). The switch parameter concept was used to account for table geometry and duty in the shaking table model, whereas different allowed ranges of parameter values were used to differentiate between spiral and rake classifiers and different modes of parameter variation (i.e. different auxiliary models) distinguished the cone and rolls crushers.

The main model functions were able to fit all measured data sets to better than +/- 8% (shaking table) down to +/- 1.5% (spiral classifier), with the scale of variation more indicative of the variale quality of the raw data rather than of any inherent differences in quality of individual models. All models developed fully describe the relationships between particle size, SG and process performance as the essential minimum. The degree to which the other operating variables can and have been accounted for varies from model to model. The classifier model, for

example, fully accounts for the complete set of operating parameters (i.e. feed rate, pulp density, washwater, geometry, screw speed, angle and weir height). The shaking table model explicitly accounts for all the variables that can vary or are adjusted in normal operation (i.e. feed rate, pulp density, wash water and tilt) and implicitly handles other important dependencies as well (e.g. feed classification, heavy mineral concentration of the feed etc.). The crusher models simply account for the single most-important operating variable, gap size. The Duplex and MGS models are slightly more limited, restricting their coverage to the most dominant operating variables only. No auxiliary relationships proved possible for the Reichert cone. The flotation model was developed on different fundamental principles to the gravity process models, using a distributed coefficient approach with an array of discrete coefficients (rather than an analytical function) being used to depict the flotation response. The external formulation of the model was however designed to be fully consistent with the gravity model format. The flotation model was consistent with the gravity model format. The flotation model was again of "generic" type with equal applicability to flotation tables.

Within the individual models, the major innovation was with the shaking table model. Here, the introduction of a "ranking" of the constituent size/SG fractions and relating their point of discharge from the table (and therefore their recovery) by abundances as well as rank order was a significant development over previous gravity modelling approaches (e.g. partition curve models where recoveries were considered to be direct functions of size and SG). This new approach enabled competition between individual size/SG fractions to be modelled directly. Competition (or particle crowding effects) are of prime importance in shaking table separation. An example of model fit to measured data is shown in figure 2.

3.2.2. Industrial Application

Beralt

A full process audit of the Barroca Grande plant at Beralt was undertaken for the three-fold purpose:

(i) To provide a base-line against which any improvements resulting from this project could be quantified.

(ii) To identify the specific areas where process efficiencies could be improved.

(iii) To provide data for model development, calibration and validation.

The results confirmed that the plant was already operating very efficiently with overall WO_3 recoveries between 83% and 86% at grades of around 10% (fines section) and 25% (slimes section). The audit also provided data far beyond that normally collected at the plant. It provided quantitative data on the mass flows in every stream, and the tungsten, copper and arsenic partitioning around the whole circuit. The tungsten partition is summarised in figure 3. The audit highlighted two potential problem areas where further attention could be profitably applied. Firstly, in the fines section where irregular performances were identified. Secondly, slimes section tungsten losses were high, amounting to over 4.5% of the total tungsten fed to the plant.

A combined computer-based sensitivity analysis of the fines section coupled with a more detailed experimental study of circuit variability was used to assess the significance of the observed feed fluctuations to the section. The sensitivity analysis (a suite of simulation predictions) established that the hydrosizer provided sufficient buffering (or desensitising) to provide a reasonably consistent final concentrate even if there were gross fluctuations elsewhere in the circuit. The computer results were validated in the experimental study, from which it was also concluded that wide fluctuations in fines circuit feed grade do occur, and can occur over fairly short time scales (< 1 hour) as well as on a day to day basis. The most sensitive area within the circuit was the table treating the -5mm + 2.5mm material (which bypassed the hydrosizer). Feed grade fluctuations, at this point in the circuit, (i) have direct knock-on implications to the local tailings grade, (ii) were the dominant influence on the final concentrate grade and (iii) effectively controlled the overall grade of the fines circuit coarse tail, although this grade always remained within tolerable limits (<0.13% WO_3). Action was taken. A rolls crusher was installed to treat this 2.5 - 5mm material which was then classified along with the -2.5mm material prior to tabling.

BTW already recognised the need to redesign the slimes section. During the course of the contract, changes were progressively made introducing Duplex concentrators firstly for final concentrate cleaning and lately for the first roughing operation. Repeat audits confirmed progressive improvement with concentrate grades rising to 40% WO_3 with circuit recoveries increasing to better than 90% for the +45 um fraction and to 30-60% for the finer material. A sensitivity analysis showed large fluctuations in circuit feed were effectively buffered in the circuit. The study also led to a recommendation that a middlings retreatment table should be installed. Installation of the second Duplex has liberated one of the installed tables which can now be used to effect this recommendation.

At the end of the project, the plant was achieving an overall 86% WO_3 recovery with slimes concentrate grades up to 55% WO_3.

Carnon

Simulation studies at Wheal Jane were concentrated on the primary gravity circuit. Prior to the contract, significant improvements, (worth circa 120,000 per annum) had been made on the recommendation of simulation results (Ref. 2). The simulation studies on this contract continued the programme of progressive improvement. Firstly, a simulation was undertaken to assess whether spiral concentrators would be more suitable than shaking tables for treating the coarsest hydrosizer product (i.e. from spigot 1). The results were negative. Secondly, simulation studies were used to investigate the significance of an imbalance in loadings between the two installed hydrosizers; an equal balance being difficult to maintain in practical operation. Results showed that the effects of a slight imbalance were not critical. Thirdly, simulation was used to predict the most beneficial assignment of tables to each hydrosizer spigot product. Predictions for a 30 tonne per hour operation are summarised in figure 4. If the (then) current pool of 19 available tables were to be maintained, then the practised configuration of 5-4-4-6 was confirmed as the best solution. It was however shown that significant benefits could be gained by adding extra tables to spigots 2 (preferentially) than to spigots 3 and 4 respectively. Subsequent metallurgical monitoring at the plant is beginning to provide evidence which fully supports these predictions. The recommendations have now be followed as out of service tables were recommissioned and as tables from other duties become available because of changes in priorities.

General

The simulations undertaken at the two plants showed many parallels. Both looked at the same type of equipment and both employed multiple simulations (or sensitivity studies) to establish the relative merits and impact of a number of operating regimes. At Berait, investigations centred on the problems of fluctuating flows and variable feed grades. At Carnon, concern was more linked to the relative loadings within the circuit. The two together demonstrated the utility of the models themselves; the same models being used at both plants and with equal applicability despite very different feedstocks being treated. In each case options were assessed on the computer, without plant disruption, without time-consuming and costly testwork and prior to any capital investment being made.

The benefits achieved are, however, as yet very difficult to assess in terms of extra grades and recoveries achieved, as any results from simulation are inextricably tied up with each plant's other metallurgical improvement programmes.

This, far from obscuring the merits of the method, clearly illustrates its success in the positive conviction that both Beralt and Carnon have shown in deploying simulation as one (of many) metallurgical tools available to them and used by them for plant enhancement. The fact that the simulation methods were designed to parallel or complement traditional methodologies has facilitated their acceptance in this way. Their further success in a decision support role was demonstrated time and time again.

3.3. EXPERT SYSTEMS

3.3.1. Unit Process Diagnostics

An expert system for shaking table diagnostics was developed (i) to identify faults and inefficiencies in table performance and (ii) to advise on the best course of action to take in order to rectify such faults. The developed system (detailed in ref. 1) incorporates three levels of diagnostics. The level 1 diagnoses test the measured (or percieved) operating settings against the industry "rules of thumb" and manufacturers' operating ranges for "normal" practice. A total of 29 potential faults can be identified from application of these heuristics. The deeper levels expand the diagnostic capability. Here diagnoses are based not only on set-up information but also on visual indicators (e.g. mineal band behaviour) and on measured grade/recoveries. At the time of writing, in excess of 90 different faults can be identified at these levels.

The expert system was written in PROLOG and formulated in terms of IF-THEN-ELSE production rules. Delivery was on IBM PC or PS/2. A successfull strategy for knowledge elicitation was developed. Basic knowledge was supplied by the knowledge engineers (who were minor experts in the domain). This was supplemented by knowledge extracted from written sources. Higher level and local knowledge was then added by the industrial experts at Wheal Jane and Beralt.

The system was distributed to Wheal Jane, South Crofty, Beralt and Geevor mines for evaluation and validation. One of the positive successes (identification of inadequate shake frequency as the result of drive belt slippage) is documented in ref. 3.

The expert system analysis allows for periodic or responsive monitoring to be undertaken without calling on expensive, and time consuming, analytical procedures. It also allows the metallurgist and operator to check if any unusual "quirks" will have serious implications on performances, and will delineate potential problems for further attention. The system should identify the most likely cause of the problem and should advise on the most fruitful line of action (to eliminate its root cause rather than just to alleviate its symptoms).

3.3.2. Supervisory Systems

The objective was to develop a consultative (off-line) expert system to assist plant personnel in their control of the Wheal Jane tin concentration circuit. At present, the circuit is sampled, for monitoring purposes, three times per eight hour shift. Sample assays are analysed by a specialist metallurgist. Based on this analysis, the metallurgist initiates any remedial action that he thinks necessary. His decisions are based on a complex set of factual and heuristical rules which have been built up through experience. An expert system was developed from these rules (currently numbering 120). The rules are of the IF-THEN-ELSE type. Rules related both to assays values within a single monitoring round and to the change in values between rounds. In this way both immediate problems and longer term deteriorations can be detected. The computer displays results in a similar layout to that currently produced but draws attention to important and problem values by highlighting them in a contrasting or flashing colour. A remedial action report is generated where necessary. The system is written in PROLOG for an IBM PC implementation.

The benefits of the system are, firstly, it can serve as an assistant to the expert metallurgist effecting a significant saving of his time and, secondly, it provides expert support to the non specialist (e.g. plant operators) helping them to make decisions during the operational periods when a specialist is not available. Validation and testing will proceed outside the contract.

3.4. OTHER TECHNIQUES

The concept of data enhancement was developed, at WSL, immediately prior to this project being proposed. An innovative application, to simulate heavy liquid analysis had been developed. The technique centred on transforming (or enhancing) readily available data to provide data that would be in a more useful form for its application. The transformations were effected through the adoption of enabling assumptions coupled with the application of physical conservation laws. On this project, it became clear that another data enhancement application (this time to estimate mineral liberation in the course of comminution) would facilitate a practical solution to the complex problem of liberation modelling. Work, on the project, was directed to testing the applicability of the underlying assumptions and the reliability of the method. It was found that the errors in prediction of mineral distribution through enhancement were of the same order as the errors in the prediction of the size distribution through conventional modelling. The guarded success gives confidence that adequate liberation estimates can be obtained, and are

within the reach of production plant operators without the access to the sophisticated liberation measuring equipment found in research institutes.

Data logging software, for hand held portable computers, has been developed in support of process audit. Collected data is downloaded onto an IBM PC, on completion of the audit, for further processing (material balancing, etc.).

4. CONCLUSIONS

Individual components of a computer-based toolkit have been developed on this project, to complement and extend the range of techniques previously developed by WSL, and others, for application to mineral processing development investigations. The development of these techniques has enabled the methodology, graphically illustrated in figure 1, to be implemented practically on production plant. The techniques have been validated through case studies. As a result of these studies, benefit has accrued to the two industrial partners, most significantly in the form of quantified decision support. The emphasis has always been on the practicality of implementation. Data enhancement and expert system techniques have enabled significant benefit to be gained at a reduced analytical cost. Industrial confidence in expert systems, as a valuable technique, built up progressively throughout the project culminating in the whole plant supervisory system being specified and developed in the project extension.

The developed techniques are already being actively exploited by BTW and CCL. The simulation package has been additionally licensed to other industrial users and used extensively in consultancy (flowsheet development) studies carried out by WSL.

The future is now seen as one of refinement of the modelling and simulation techniques with the major growth area now being for further expert system development.

5. REFERENCES

1. TUCKER P., LEWIS K.A.: An Expert System for Shaking Table Diagnostics. Mineral Engineering, 1989, Vol 2, No 1, pp 87-92.

2. LEWIS K.A., WELLS A.P., TUCKER P.: Computer Simulation at Wheal Jane, Cornwall. Proc. Mineral Processing in the United Kingdom, Leeds (April 1989).

3. TUCKER P., LEWIS K.A.: Expert Systems: Their role in Mineral Processing in the UK. Proc. Mineral Processing in the United Kingdom, Leeds (April 1989).

4. NEWTON S.: Computer Mass Balancing for Plant Process Audit. Proc. Mineral Processing in the United Kingdom, Leeds (April 1989).

5. TUCKER P., WOOD P., LEWIS K.A.: Computer Optimisation of Shaking Tables. (In preparation for International Symposium on Gravity Concentration; Camborne 1990).

6. PEARL M., LEWIS K.A., TUCKER P.: A Mathematical Model of The Duplex Concentrator. (In preparation for International Symposium on Gravity Concentration; Camborne 1990).

7. LEWIS K.A., TUCKER P., WELLS A.P., LEJEUNE G.: Expert System Supervisory Control of the Wheal Jane Tin Concentrator. (In preparation for 2nd Conference on Personal Computers in Industrial Control; Stevenage 1990).

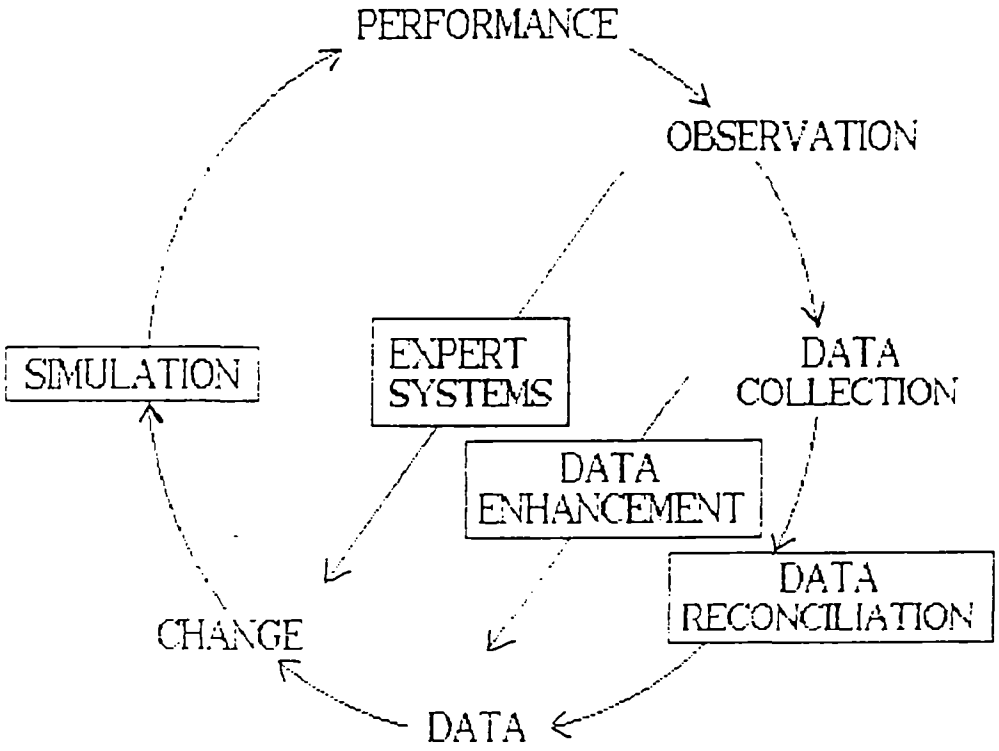

Figure 1. Methodology for plant enhancement.

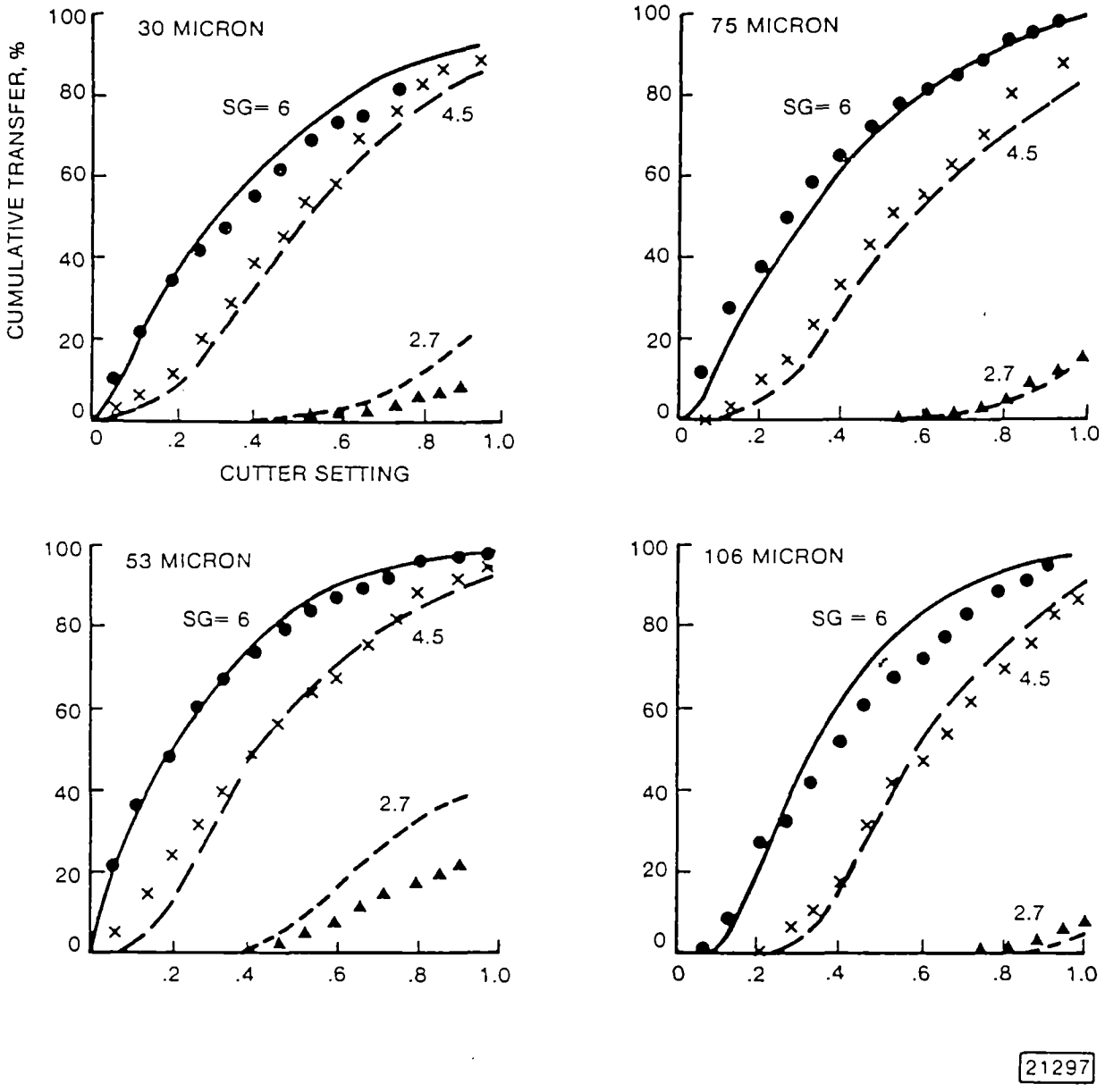

FIG. 2. SYNTHETIC ORE: MODEL FIT

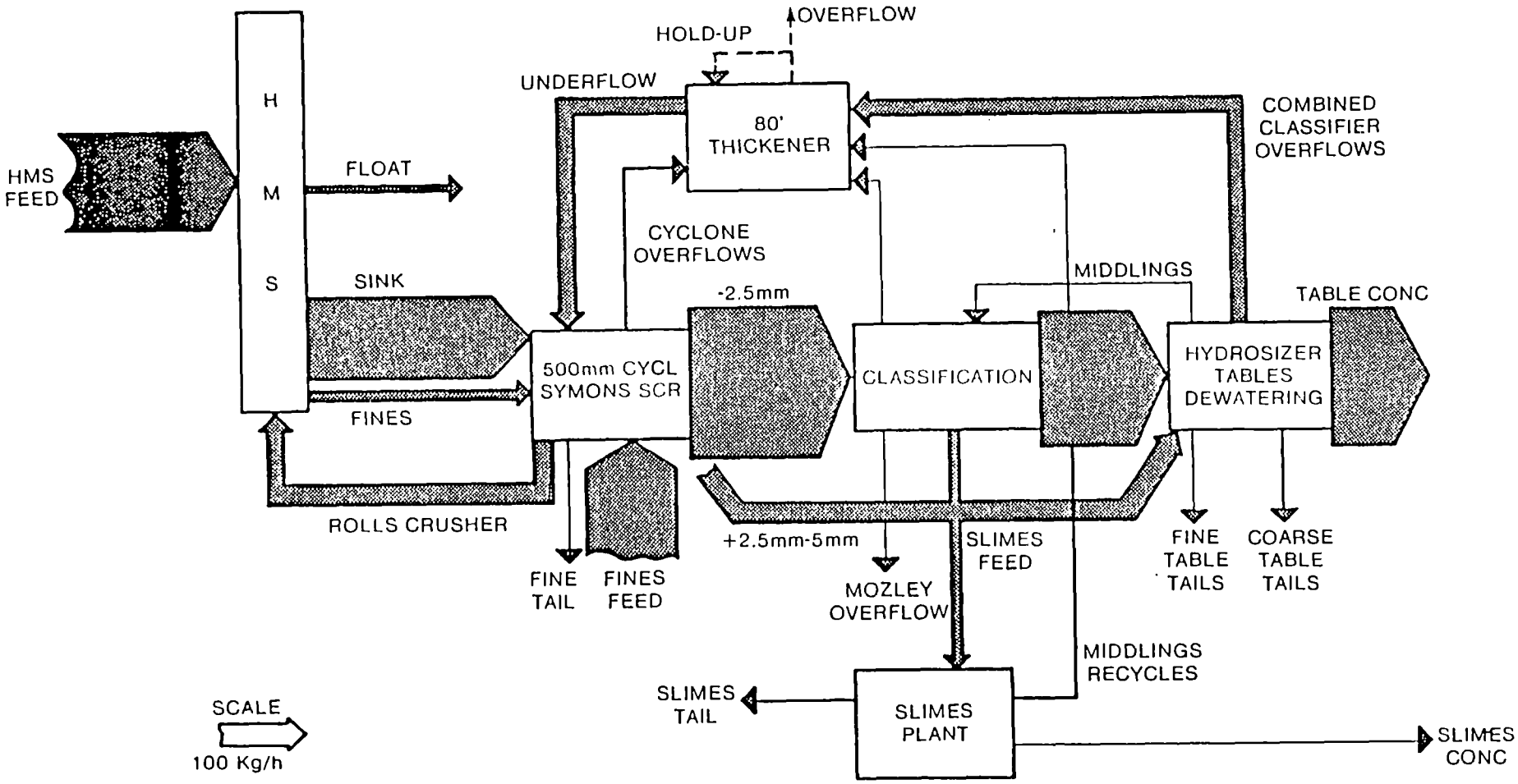

Fig. 3. Beralt WO3 Flows

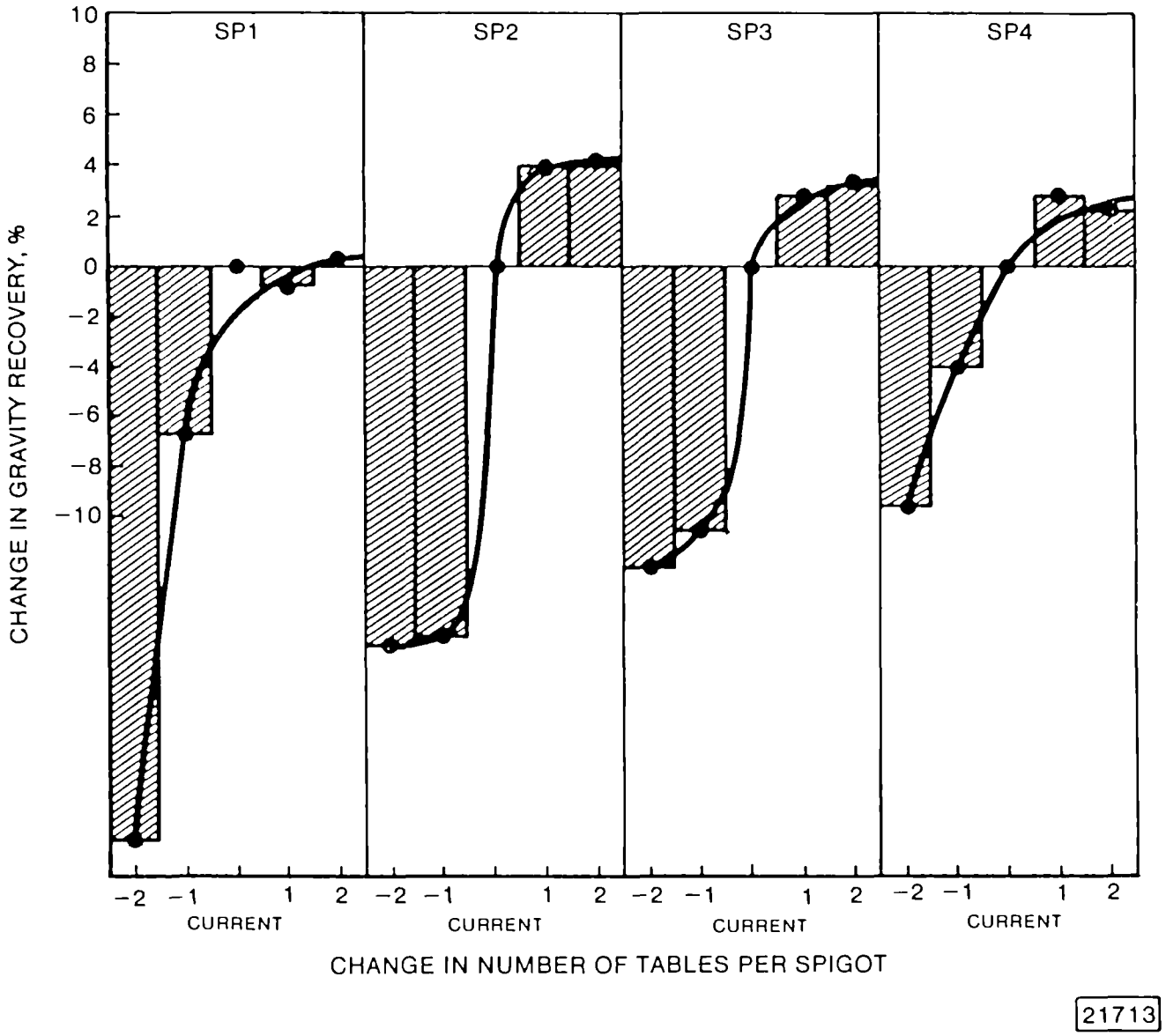

FIG. 4. WHEAL JANE TABLE ALLOCATION. 30tph

DEVELOPMENT AND APPLICATION OF A MODULAR, INTELLIGENT CONTROL SYSTEM FOR MINERAL PROCESSING PLANTS

Project Leader: A. BROUSSAUD
J.C. Guillaneau, O. Guyot, J.F. Pastol
Bureau de Recherches Géologiques et Minières (BRGM), Orléans, France

M. Jourdan, J.L. Maesen
Coppée Lavalin, Belgium

Contract MA1M-0058-C(CD)

1. OBJECTIVE

The objective of the project was to design, create and demonstrate an advanced control system for small and medium-size mineral processing plants, based on the use of on-line algorithms for plant simulation and diagnosis, and on-line Expert Systems.

2. INTRODUCTION

A common problem of the mineral processing industry is that unit processes are affected by a number of ore parameters which are difficult or impossible to measure with today's technology.

Difficulties in interpreting measurements are commonplace in conventional Process Control Systems. In many cases the information available consists of on/off boolean values representing the working status of equipment and analog values giving orders of magnitude of operating parameters.

Conventional process control systems which do not include process models and expert knowledge of the process are unable to use efficiently this information.

The system, here referenced to as ANPROC, designed and implemented during the research is the first attempt to interface a steady-state simulation package (a version of USIM PAC) with a process control system through an Expert System.

3. PLANNING AND ORGANIZATION

The initial project schedule included the following steps:

a. Specifications of the overall structure for ANPROC:
   - Expected fonctions of the system,
   - Fonctions interactions.

b. Definition of the different modules that are to be part of ANPROC:
   - Their own fonctions,
   - The communication aspects between the internal modules of the structure.

c. Hardware and software choices:
   - For the structure development,
   - For the Expert System development.

d. Development of the basic (internal) modules:
   - Database, communication modules.

e. Choice of the industrial target:
   - Configuration of the external modules: the USIM PAC simulator, the Expert System's knowledge base,
   - Integration of these modules into the structure.

f. Industrial tests.

The capabilities and the structure of the system have been defined by the two partners. The other tasks have been distributed between Coppée Lavalin, Belgium (computer environment and communication) and BRGM, France, (simulation and mineral processing).

The three first steps have been defined in common. Phase d. was mainly developped by Coppée-Lavalin which built an universal data base structure and communications modules.

BRGM was in charge of the phase e. for which an expert knowledge of modelling and simulation as well as of mineral processing was required to settle the basis of on-line use of combined simulation and expertise.

The test and industrial application, phases e. and f., were initially planned to be carried out on the Chessy complex sulfide ore project in France. The Chessy project has been unfortunately delayed and another target had to be chosen.

The Kaolins d'Arvor china clay company agreed to be the application target.

As they were not yet equiped with programmable controllers, a fore study consisted in installing a Process Control System. This was not explicitly part of the initial project, but was yet a compulsory step to test industrially the ANPROC system. It delayed very significantly the completion of the research project.

In parallel, a study of the application process (china clay separation circuit) has provided the basis for the configuration of a simulator of the separation circuit and the development of expertise to interpret simulation results in real time.

4. THE SYSTEM DEVELOPPED

4.1. HARDWARE STRUCTURE

The hardware structure of the system (see figure 1) basically consists of a conventional PLC (Programmable Loop Controller) level overheaded by two 386 hardened industrial microcomputers.

The first 386 microcomputer hosts a copy of the conventional process control software package which displays the process flowsheet and status (9 screens), stores data, displays archived data in different graphic forms.

The original feature of the system (on-line diagnosis module) is housed by the second 386 microcomputer (described figure 2) which should be physically linked to the first one and available for on-line process diagnosis.

The main software tools installed in the second microcomputer are a steady-state simulation package, a version of USIM PAC, and a commercial Expert System shell, working in "parallel", that is multitasking, in a graphic environment.

4.2. SOFTWARE STRUCTURE

The software configuration of ANPROC is modular (see figure 3). It is built around a central data base that hosts information coming from and going to other modules.

This structure can be configured by any advised user. Two main types of module can be defined.

- Interface modules: these are small programmes in charge of communication, that is data transfer and formatting, between the data base and external modules. One of these interface modules is also in charge of the display of a main screen menu and graphic results, as a front-end user interface.

- External modules: these are external software integrated and configured for the application as tools for process diagnosis. In our case, USIM PAC simulation software and NEXPERT OBJECT Expert System development shell.

WINDOWS 3.0 multitasking and graphic environment overheads all these modules, allowing dynamic data exchange, graphical display, and integration of existing exotic executable software.

5. INNOVATIVE ASPECTS OF THE SYSTEM

The system is characterized by:

1. The integration of preexisting tools:
   it would be useless to create software similar to preexisting packages.

2. The supervision of a simulator by an Expert System.
   The second point is really innovative and required the study of two modules.

5.1. ON-LINE PLANT SIMULATION MODULE

The main characteristics of the system are anticipation of events and diagnosis. Sensors generally provide very noisy information, and this is more true for mineral processing than for other industrial areas. Therefore, it is necessary to obtain a "model" of the process to be able to calculate non-measured values and to compare the predicted values with the measured ones.

Initially, a large number of "models" of the process were considered:

- a coherent material balance,
- a dynamic material balance (with Kalman filtering),
- a steady-state simulator, or
- a dynamic simulator.

The research focused on the on-line use of a steady-state simulator for predicting the future steady-state operation of the circuit after a modification of the ore or an operating condition, determinating the unmeasured streams of the plant, suggesting new set points for plant operation, and diagnosis of unit operation.

The simulator is also used for automatic calibration of the models, and comparison between simulated and measured values for the unit operation diagnosis.

5.2. ON-LINE EXPERT SYSTEM MODULE FOR DECISION-PREPARATION

From the standpoint of the user, the engineer or operator, the Expert System is a software which can, for example rapidly diagnose of the operational state or the cause of plant problems, and recommend actions to be taken or set points and settings to be adopted, and perhaps even automatically modify certain set points.

There are several advantages to exploring this area of use: the Expert System can simultaneously handle quantified data and more or less accurate data expressed in ordinary language. It is possible constantly and instantly to make available to operators part of the know-how of the best and

most experienced plant engineers and operators or simulation engineers. It is also possible for systems to be not, or only partly, physically linked to the process for small plants. Lastly, low-cost Expert System development packages usable on micro-computers are available on the market.

The rule-based modules (developed on the NEXPERT OBJECT commercial shell) in the ANPROC system are used for the general interface of the system, mostly based on graphics and on natural language dialogue. The most innovative point of this research is this combined use of an algorithmic module (simulation) and an Expert System. The knowledge base contains a part of the know-how of the operators and process engineers, some rules of "good sense" about the quality of the process data and mostly how to deal with the steady-state simulator, that is:

- which data is needed (from the process or the operator),
- how to run the simulator (for calibration or simulation),
- which are the most sensible values issued of the simulation which have to be shown to the operator or compared with the process values.

This combination of Expert System and simulator is illustrated in part 5 with the industrial application.

6. INDUSTRIAL APPLICATION

The Chessy sulfide ore project, which plant was the application target for ANPROC, has been delayed and the system was then tested in the china clay plant of the Kaolins d'Arvor, France. The system focuses on the separation unit of the plant where sensors and programmable controllers were not installed at the beginning of the project. A first task was to set up a classical control system based on the FIX software. It took a long time to be efficient and integrated, after which the following phases of the project could be settled.

The flowsheet figure 4 shows the separation circuit of the plant.

A long preliminary phase of knowledge extraction has revealed the main problem in this circuit and empiric rules to solve it. The knowledge base of the Expert System has been built around this target:

The plant flowsheet includes "BRGM sieving panels". These are static screens, patented by BRGM, with a nylon screening cloth that enables a sharp cut around 40 microns. They are efficient unless overfed, in which case they quickly become very inefficient and generate significant losses of china clay (contained in the size fraction below 20 microns). When such a problem occurs, the practical solution is to decrease the feed rate. Unfortunately it may take up to 30 minutes to solve the problem, and the decrease in the feed rate is sometimes too great, resulting in a loss of capacity.

Some rules were found to help prevent the problem, for instance:

> IF there is an increasing pulp density trend at the overflow of the secondary cyclones
>
> THEN there is a risk of saturating the sieving panels
>
> AND use the simulator to evaluate whether the risk is serious.

The use of a simulator for such a purpose then involves the application of:

1. Rules to evaluate the feed particle-size distribution (which is not measurable), based on the feed rate and the power drawn by the rake classifier.

2. Rules to evaluate the validity of the most recent calibration of the simulator (under steady-state conditions at a time when no trouble was observed).

The simulator then simulates the operation in steady-state using the present feed rates and estimates particle-size distribution. Subsequent rules applied are of the type:

> IF the predicted (simulated) value of the pulp density at the overflow of the secondary cyclones is above 1050 g per litre
>
> THEN the risk is serious
>
> AND use the simulator to find an optimal decrease of the feed rate.

A shematic overview of the reasoning of the Expert System is shown in Figure 5.

The development of the Expert System is not carried out by a group of two (a Knowledge Engineer and an Expert), as is often described in the literature. It is carried out by a team that includes plant experts (process engineers and operators), a simulation expert and a knowledge engineer, although the simulation expert has experience in artificial intelligence and knowledge engineering, and the knowledge engineer is also a simulation specialist.

The purpose is not to insert in the Expert System all existing knowledge about plant operation and use of the simulation package, but only the knowledge necessary to detect plant troubles as soon as possible (preferably before they occur) and to propose decisions to avoid them (based on simulations and heuristics).

As far as configuration is concerned, a customized simulator of the separation circuit has been developed, with USIM PAC, involving:

- selection of unit operation models,

- selection of average feed characteristics (size distribution, etc)

- calibration of the models according to different operating conditions and ore types.

7. CONCLUSIONS

The objectives of the project have been largely but not totally achieved.

A software structure (ANPROC) has been created. It handles information coming from a conventional process control system installed in a mineral processing plant and:

- uses steady-state simulation to foresee plant operation -
- uses expertise to analyse on-line data and simulation results
- provides on-line advices (decision proposals) to the plant operators through a user-friendly interface.

ANPROC is a flexible, configurable, real-time software structure which includes preexisting tools for process diagnosis. It takes into account steady-state simulation, empirical rules and sensors information to help operators, who have to make decisions for process improvements on-line.

The most innovative feature of ANPROC is the real-time supervision of a steady-state simulator (USIM PAC), by an Expert System. To use this capability, a simulator has to be configured for a given circuit and expertise on simulation of the circuit has to be extracted and expressed as a network of rules for the Expert System.

The initial objectives have been slightly changed. Instead of using separately and almost independently an Expert module and an algorithmic module (simulation), it was found more efficient to combine these tools for:

- dealing with the lack of sensors in the plant,
- providing the operators with clear and understandable advices.

The initial industrial target for this project was the base metals mine of Chessy (Rhône, France) but as the project has been delayed another site had to be found. The Kaolins d'Arvor (Morbihan, France) china clay plant agreed to be the application target although they were not yet equiped with a classical control system.

Thanks to the close cooperation of Kaolins d'Arvor, the application software has been developed. Simulations were done on the process and gave a good representation of steady-state operation. This study outlined a way to prevent plant inefficiency and gave the frame of expertise. The data base created, reading data from PCS recorded historic files, passes data to the Expert Sytem that processes it, either warning the user or running a simulation and then displaying diagnosis. Quite a large amount of such off-line tests were carried out.

The physical implementation (in real-time) is awaiting a global decision from the plant management concerning the automation of the whole process. Upon this decision depends the choice of a standard communication network which is a decisive hardware requirement to implement the system developed.

8. REFERENCES

A. BROUSSAUD, J.C. GUILLANEAU, J.F. PASTOL, M. JOURDAN, C. GHIBU, R. PERISSE : "Development and Application of a Modular, Intelligent Control System For Mineral Processing Plants"
CEC Seminar on mineral processing and extractive metallurgy Warren Spring Laboratories, Stevenage U.K. 1989, February 27th and 28th.

A. BROUSSAUD, J.C. GUILLANEAU, O. GUYOT, J.F. PASTOL, J. VILLENEUVE : "Methods and Algorithms to Improve the Usefulness and Realism of Mineral Processing Plant Simulators"
To be presented at the XVII International Mineral Processing Congress Dresden - Sept. 23-28, 1991.

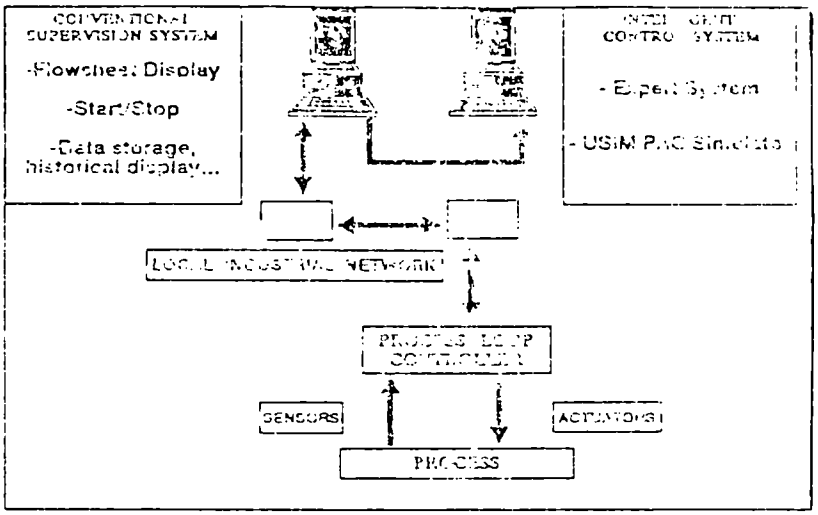

Fig. 1: Structure of the complete process-control system

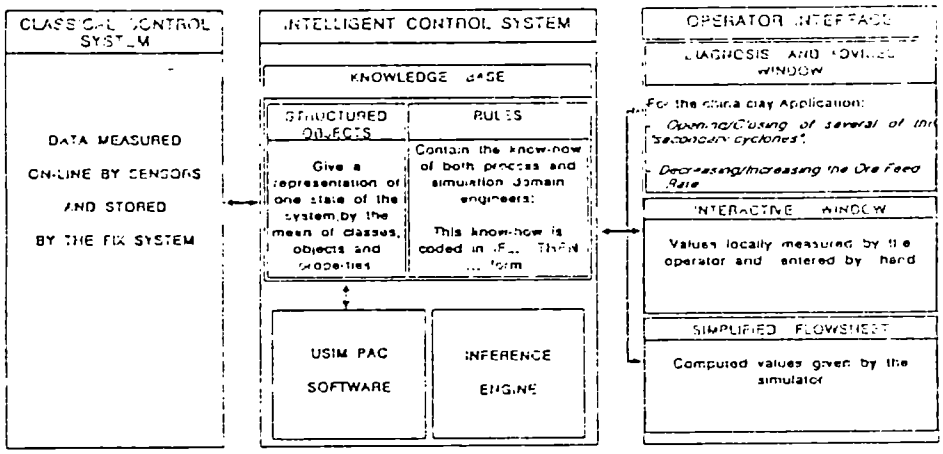

Fig. 2: Description of the intelligent control system modules

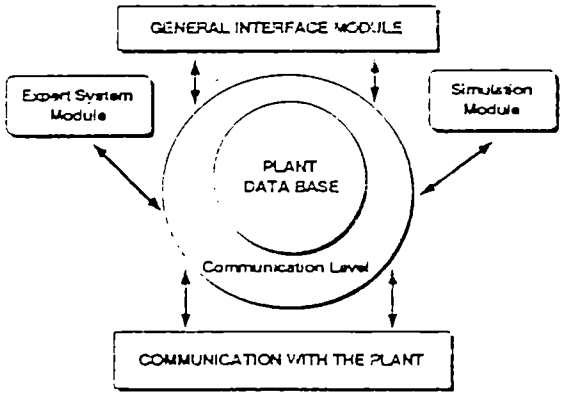

Fig. 3: Schematic description showing the communication between the modules

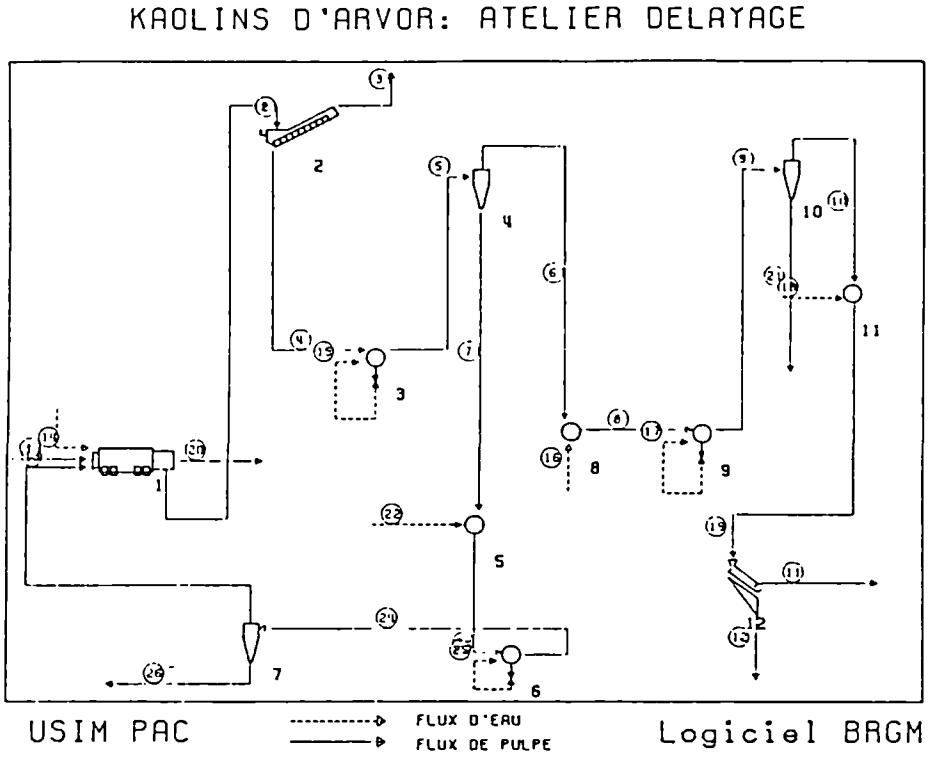

Fig. 4: Simplified Flowsheet of the China Clay Classification Circuit as Displayed by USIM PAC.

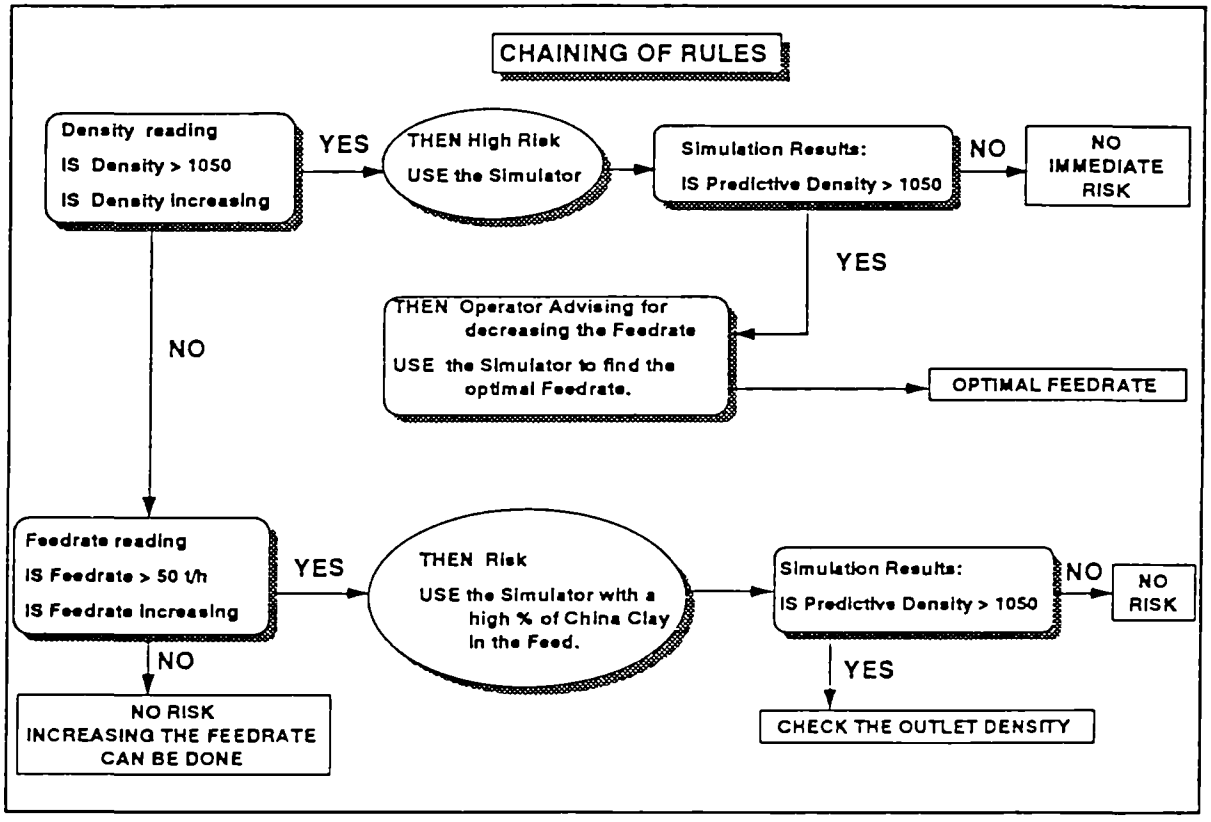

Fig. 5: Overview of the rules chaining

RESEARCH AREA 3.6

CHARACTERIZATION OF ORES AND MINERAL ANALYSIS

DEVELOPMENT OF NEW SENSORS FOR ON LINE ANALYSIS OF METAL AND ORGANIC IONS IN WATER. APPLICATION TO MODELLING AND AUTOMATIC CONTROL OF FLOTATION PLANTS

Project Leaders : J.J. PREDALI - J.P. BEUVELET
Metaleurop Recherche, Trappes, France

A. VAN LIERDE
Université Catholique de Louvain, Belgium

J. BESSIERE
Université de Nancy I, France

J. J. FOMBON
Cerac S.A., France

Contract MA1M-0042-C (CD)

1. OBJECTIVE

The aim of the present Research and Development program was to develop new sensors for flotation based on two techniques that are really promising in other fields, for accurate and rapid analysis :

- Double Pulse Normal Voltametry : presently an equipment has been patented by our company and is sold by Solea S.A. The objective is to adapt this technique for on line analysis agents of flotation and inorganic ions into industrial pulp.

- Dielectric methods with High Frequency to study the evolution of reagents absorbed on solid surfaces whose rate is determining flotation efficiency.

2. INTRODUCTION

The development of an efficient control of flotation needs rapid and low cost determination of the main parameters of the process. These parameters can be classified into two types :

- characterization of the solid : flow rate, pulp density, particle size distribution, chemical analysis;

- characterization of the liquid phase of the pulp : determination of inorganic and organic ions into solution.

If parameters of the first type are easy to determine using new manufactured equipments, these of the second type are not available on line and at low cost. However their control would be on asset for the modelling of the flotation process.

On the economical point of view, the development of new sensors would allow an efficient control of flotation, that means higher recovery of metals, lower cost of reagents for the plants of E.E.C. and other countries. It would also be a new development area for the electronic and computer industries.

Furthermore, these new sensors would allow better and cheaper control of trace metals of environmental waters to improve their quality.

In order to control the flotation process with these new sensors, two previous steps are necessary :

a. To acquire data using the new sensors which is the aim of this study,

b. To interpret the data collected in order to create a model.

Concerning data collection two complementary techniques were studied :

- Double Pulse Normal Voltametry for analysis of organic and inorganic ions.

- Dielectric methods with High Frequency to study the evolution on solid surfaces.

3. DESCRIPTION

The programme divided into four parts was mainly applied to sulphides flotation with two cases :

- Bulk flotation of a high grade zinc ore with low content in other sulphides (Saint Salvy ore).

- Differential Cu, Pb, Zn flotation of a pyritic ore with high pyrrhotite (FeS) content.

3.1. METHODOLOGY OF CONDITIONING THE SAMPLE

The main part of the work was the selection and adaptation of electrodes for the Double Pulse Normal Voltametry :

- Platinum disc electrode,
- Rotating disc electrode,
- Mercury drop electrode,

3.2. METHODOLOGY OF MEASUREMENT

This work was carried out first using synthetic solutions then applied to the pulps prepared with the ores.

Double Pulse Voltametry

Measurements of Cu^{2+} and Zn^{2+} ions, with or without potassium ethyl xanthate (KEX) which is the collector for the flotation of sphalerite (ZnS), during activation of the sphalerite adding copper sulphate ($CuSO_4$, $5H_2O$) into the pulp.

Dielectric methods

Measurements and interpretation of the activation by Cu^{2+} and S^{2-} and adsorption of the collector on the minerals (sphalerite, malachite).

3.3. APPLICATION AND INTERPRETATION OF THE MEASUREMENTS

Measurements of ions into solutions and adsorption data, correlated to flotation results, permit to select the Dielectric method to follow the flotation process.

3.4. TEST OF THE DIELECTRIC METHOD

This method was applied to follow the activation of malachite in a copper oxide ore and the activation of sphalerite in complex sulphide Cu, Pb, Zn ore.

4. RESULTS

The study permits to compare the two methods concerning the activation of sphalerite by copper ions.

The polarographic method shows that all the copper added ($CuSO_4$, $5H_2O$) until 900 g/t is adsorbed on the ore without appearance of equivalent quantity of Zn^{2+} ions. Over 900g g/t of copper sulphate added, copper in excess stays into the solution without adsorption on the ore. This

method permits to characterize the final state, but, as copper adsorption is very fast, it does not seem possible to use this method to follow the adsorption of Cu^{2+} on sphalerite and consequently to follow the flotation.

The dielectric method with high frequency gives two important results :

a) It is possible to follow the adsorption and the desorption of ions (Cu^{2+}, S^{2-}) and collectors on surfaces of pure minerals (sphalerite, malachite). Measurement of the dielectric constants of the initial non conductor sphalerite, during addition of copper ions, permits to follow the activation of the sphalerite.

   The dielectric method shows the increase of the conductivity of the malachite when sulfur ions are added. It could permit to determine the needed amount of sulphur to add in order to realize full activation of malachite. In this case, industrial application is easier, because most of the malachite ores do not contain conductor minerals, which could interfere with the measurement of activation.

b) Applications

   when the ore does not contain conductor mineral, the dielectric method could permit to follow "in situ" the activation of a mineral :

   - sphalerite by copper ions
   - malachite by sulphur ions.

   In front of a complex ore which contains conductor minerals (pyrite, pyrrhotite), measurement of the activation of the sphalerite is possible if sphalerite content in the ore is sufficient (Zn > 10 %). In this case, solids must be washed before the measurement is carried out.

   For example, we have observed a significant difference between the amount of copper sulphate needed to activate sphalerite at the laboratory (500 g/t $CuSO_4$, 5 H_2O) compared with the amount needed at the pilot plant (800 g/t) in order to achieve the same zinc flotation results. It could be explained because of the recycling at the pilot of the tailings from the cleanings of the previous copper and lead flotations where important amounts of pyrite and pyrrhotite depressants are needed (NaCN, Na_2SO_3). Excess of cyanide and sulphite ions could complex Cu^{2+} when copper sulphate is added for sphalerite activation.

5. CONCLUSIONS

Polarographic methods have not permitted to follow the activation of sphalerite by copper ions because the activation takes place very quickly and this method measures the final state when solids and solution are not at the equilibrium.

At the contrary, the dielectric method with high frequency permits to follow the adsorption of copper ions on the sphalerite surface by measurement of the conductivity. This could allow to adjust the amount needed of copper added, to float the sphalerite without excess of consumption in copper sulphate.

When the ore contains pyritic gangue minerals, the measurement of the conductivity of the activated sphalerite is more difficult but can be realized when zinc content is high enough and after a previous washing of the solid. The dielectric method has given satisfying results in order to control the activation of the malachite by sulphur ions.

This research programme could be followed by :

- the extent of the method to other cases, to follow the kinetics of reactions in order to control other processes.

- the development of an industrial apparatus.

6. REFERENCES

1. J.M. THIEBAUT, G. ROUSSY, K. CHLIHI and J. BESSIERE
"Dielectric study of the activation of blende with cupric ion"
J. Electroanal. Chem. (262) p 131-144 (1989).

2. J. BESSIERE, K. CHLIHI, J.M. THIEBAUT and G. ROUSSY
"Dielectric study of the activation and deactivation of sphalerite by metallic ions"
Int. J. Miner. Process., 28 (1990) 1-13.

3. J. BESSIERE, A. EL HOUSNI and J.J. PREDALI
"Dielectric study of the activation and deactivation of sphalerite by metallic ions and malachite by sulphide ions"
2nd Workshop on Flotation of Sulphide Minerals. Lulea, Sweden. June 90.

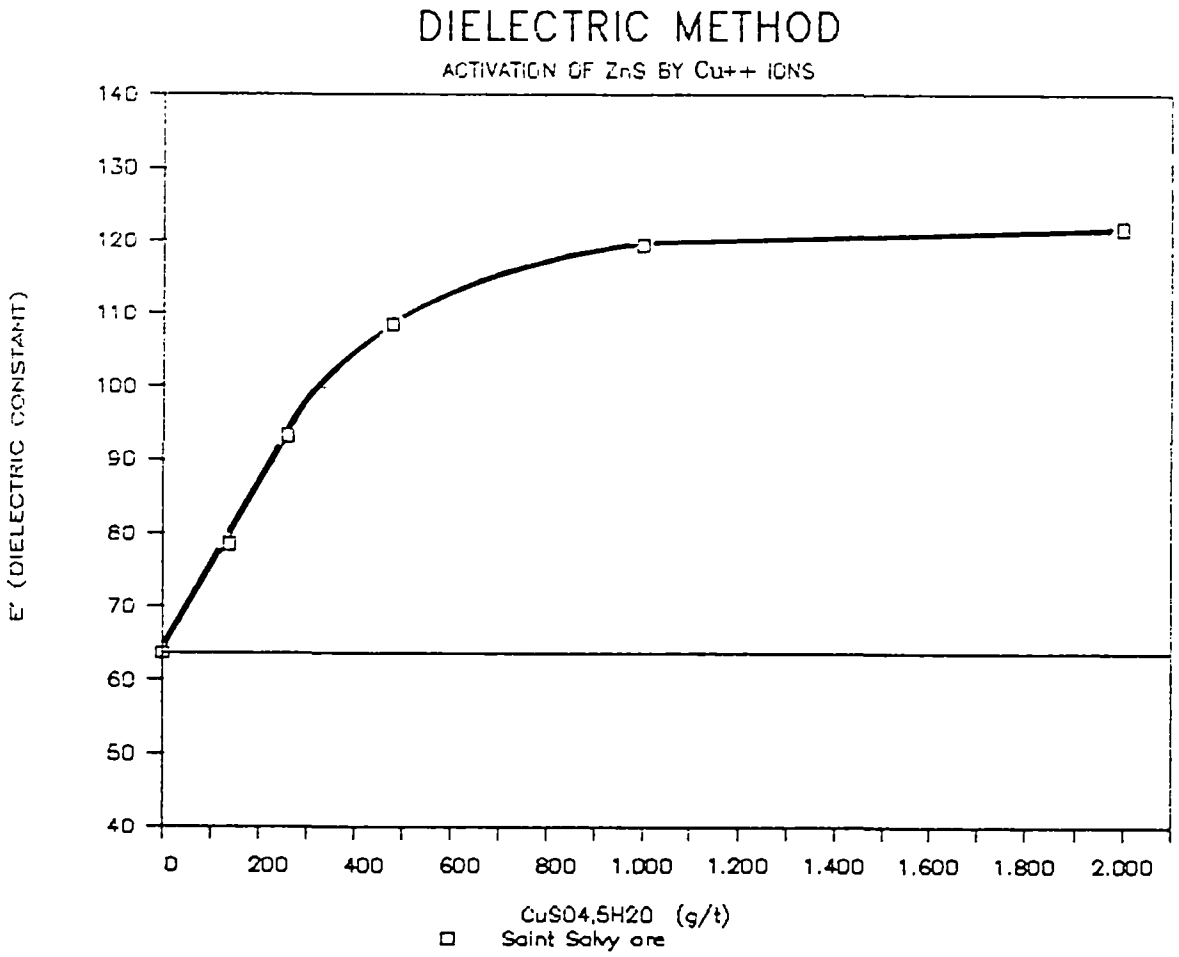

Solid in the pulp : 30 %

Conditioning : 15 minutes

Frequency : 1 MHz

Washing : No

QUANTITATIVE ANALYSIS AND AUTOMATION OF CaF_2 ORE FLOTATION VIA NEUTRONIC ACTIVATION

Project Leader: F. REGGIANI
Mineraria Silius S.p.A., Cagliari, Italy

V. BENZI
Università di Bologna, Italy

A. GARAGNANI, L. LEMBO
C.R.E. "E. Clementel, ENEA, Bologna, Italy

C. MUNTONI
Università di Cagliari, Italy

Contract MA1M-0061-C

1. OBJECTIVE

The aim of the project was to prove the operative feasibility of an "on line analysis" based on nuclear activation using 14 MeV neutrons. This on line analysis method was to be used to automate control of the flotation process for ores containing mostly fluorspar. The thermoluminescence technique was also forecast as a subsidiary method in those points of the flotation cycle where less precision is acceptable.

2. INTRODUCTION

The efficiency of a flotation cycle can be expressed by the relation:

$$E = \frac{c}{f} \times \frac{(f - t)}{(c - t)}$$

where parameters c, f, and t are the weight percentage of fluorspar present in the concentrate, feed and tailings respectively of the commercial fluoride. The automated control of a flotation plant requires "real time" quantitative analysis of the pulp at least in correspondence to the previous strategic points.

As is known, analysis with classical methods requires too long a time to be compatible with the running time of a flotation plant. Furthermore, the X-ray fluorescence analysis technique is intrinsically limited in its applicability in the case of light elements, among which fluorine and silicon are of specific interest.

Actually, in order to analyze on-line the fluorite and silicon concentrations in the flotation plant, a careful evaluation of actual conditions imposed by operative realities suggests the choice of neutrons as the exciting particles in nuclide activation. In this regard, a previous feasibility study, based on the Montecarlo simulation method, showed the effectiveness of 14 MeV neutrons. Figure 1 shows the simulated gamma spectra corresponding to feed concentrate and tailings in the fluorite cycle (1).

A first experimental test was carried out on three series of dry samples taken from the previously mentioned strategic points of the flotation cycle in the MINERARIA SILIUS plant (Table 1). The experiment has been performed at the University of Bari (Italy) with the assistance of Professor G. Skoff. The nuclides activation took place with 14 MeV neutrons generated by a 400 KV electrostatic accelerator by means of the reaction $2H^{+}(3H, 4He)n$; deuteron energy was on the order of 300 KV. The gamma counter was composed of an NaI(Tl) 4"x5" crystal. Calibration of the counting apparatus was carried out using CoCs samples, while for reference samples chemically pure CaF_2, $BaCO_3$ and amorphous silicon were used. Radiation, idle and counting times were 300, 60 and 60 seconds respectively; thus the total time for the analysis of each sample was 7 minutes, which is compatible with the running speed of the flotation plant.

As shown in Figures 2, 3, 4, the peaks concerning nuclides of interest are clearly defined and the general trend of spectra accord well with what was expected from the simulation model.

Unfortunately, on the quantitative side, these results appeared less satisfactory, and this seems to depend mostly on the use of chemically pure standards whose autoabsorption coefficient for gamma radiation is quite different from that of the sample analyzed. Moreover, it is to be pointed out that the electrostatic accelerator used is not properly suitable for application in an industrial plant.

3. EXPERIMENTAL WORK

On the basis of the experience gained our attention was mainly devoted to study a simple device for nuclear activation method based on so called "sealed tube" as a source of 14 MeV neutrons. At the same time, as far as the subsidiary method is concerned, the main interest was devoted to test the performances of commercial available thermoluminescence analyzers.

The "Laboratorio di Ingegneria Nucleare" of the Bologna University was working on the neutronic activation project and the "Laboratorio Applicazioni di Dosimetria" of the ENEA also located in Bologna, was charged with the thermoluminescence technique study.

An experimental test was carried out on dry samples with low and high fluorite content such as those of Table 1.

For nuclear activation analysis two different approaches were selected. The first method is based on simultaneous irradiation as well as simultaneous counting of the sample with unknown fluorite content and an appropriate standard with the same autoabsorption coefficient for gamma radiation. The second one is based on the determination of a calibration curve and monitoring of neutron flux by foil activation of thermal energy. In both cases a KAMAN neutron generator Model A-800 was used (Table 2; Figures 5, 6).

Dry powder samples weighing 100 g were irradiated for about 45 minutes, owing to the low neutron pulsed output, corresponding to a total of 8,000 pulses, giving an average neutron flux of about 3.8×10^6 $ncm^{-2}s^{-1}$. At the beginning, the activated samples were analyzed by a NaI(Tl) 3" x 2" scintillator (QUARTZ & SILICE) linked with a LABEN analyzer; subsequently a 3" x 3" Germanium detector, connected with multichannel analyzer CICERO SILENA plus MicroVax, was employed (Table 3).

The decay curves were obtained by measuring the gamma radiation peak at 511 KeV relative to positron decay of 18 F (Figures 7,8). The accuracy is found to be of few percent. Finally our attention was principally directed towards the determination of a reference curve giving the correlation between activity and fluorite concentration over the whole range of concentrate-tailing analysis.

As far as the thermoluminescence technique is concerned, great care was devoted both to test the performances of the SOLARO model analyzer by Vinteen and to elaborate a technical procedure for sample preparation.

The samples were thermally treated for 1 h at 400°C and then irradiated with ^{60}Co gamma radiation. The TL intensity was determined using samples of 10 mg submitted to pre-heating in an oven for 10 min. at 100°C. The heating rate of the reader was fixed at about $20°Cs^{-1}$. The double emission peaks between 200 and 300°C were taken to be the dosimetric reference signal. The best particle size for the samples was found to be 45-65 μm and can be achieved by means of standard sieves.

4. RESULTS AND CONCLUSIONS

As can be seen in Figure 9, the experimental data concerning the nuclear activation technique applied to samples whose CaF_2 concentration was ranging from 6% up to about 98% fit very well a cubic function, even in the case of a low number of experimental points. Clearly, the actual irradiation time (45 minutes) required by the KAMAN neutron source is too long with respect to the running time of a flotation plant; however, this situation could be greatly improved by using much more intense, commercially available, sources (Table 4).

Comparison between a) and b) in Figure 10 shows the improvement in the glow curves reproducibility achieved by the adoption of the appropriate particle size distribution. In Figure 11, the values of TL signal as a function of CaF_2 concentration, both in the tailing and concentrate, are shown. The responses are linear in both cases and the method seems to be valid for determination of variations of CaF_2 concentration of about 1%.

5. REFERENCES

B. Minetti-C. Muntoni:

- Automazione degli impianti di flottazione.
- Studio di fattibilità dell'analisi continua dei minerali attivati con neutroni da 14 MeV.
- Fisica e Tecnologia n.4 (31)1981.

L. Lembo et al.

- Measurements of CaF_2 concentration in fluorite ore using thermoluminescence techniques.
- Radiation Protection Dosimetry n.33 (187) 1990.

T A B L E N. 1

PROCESS POINTS	SAMPLE N°	WT % IN THE SOLID			
		CaCO3	CaF2	BaSO4	SiO2
Feed	1	6.63	44.01	6.60	25.19
	4	10.00	45.34	8.62	22.21
	7	7.63	52.03	8.28	18.28
Concentrate	2	0.69	97.07	0.69	1.09
	5	0.72	97.39	0.58	0.78
	8	1.08	96.10	1.23	1.01
Tailing	3	13.13	3.41	10.26	41.49
	6	15.88	3.41	11.56	45.30
	9	13.38	4.78	15.68	49.61

T A B L E N. 2

DATASHEET OF NEUTRON GENERATOR "SEALED TUBE" KAMAN MOD. A-800

PULSE INTENSITY	$(6.5 \pm 0.5) \times 10^7$ n/pulse
PULSE HALF-WIDTH	2.5 microsec
FREQUENCY	1 - 10 pulses/sec
N° MAX OF PULSES	2×10^5
DIMENTIONS	4" x 24"
WEIGHT	10 kg
SOURCE POSITION	7-3/8" (lower end)
SOURCE AREA	5 cm^2
NEUTRON ENERGY	14.3 MeV

TABLE N. 3

DATASHEET OF HARSHAW GERMANIUM SEMICONDUCTOR DETECTOR

DETECTOR

S.N.	: HPO 57		
Type	: High Purity Germanium		
Geometry	: one open ended coaxial		
Active Volume	: 60	cm^3	$\pm$ 5
Diameter	: 42	mm	$\pm$ 2
Length	: 50	mm	$\pm$ 2
P-core diameter	: 10	mm	$\pm$ 2
Diffusion depth	: 0,5	mm	$\pm$ 0,3

CRYOSTAT

Type	: 94	VD	
Diameter cap	: 85	mm	
Length cap	: 130	mm	
Window thickness	: 1	mm Al	
Detector-window distance	: 10	mm	
LN_2 dewar	: 34	LD	

ELECTRICAL

Preamplifier	: NB 21 G		
Coupling	: cooled FET		
High Tension	: 1500	V positive	
Current	: 50	pA/	1500 V
Capacitance	: 30	pF/	1500 V

GUATANTEED PERFORMANCE

Relative Efficiency (1.33 MeV)	: 10	%	
Absolute Efficiency (1.33 MeV)	: 120	x 10^{-6}	
Peak-to-Compton Ratio	: 33	:1	

Resolution:	E	FWHM	FWTM
	1332 keV	: 2,03 keV	4,17 keV
	"Pulser"	: 1,2 keV	---- keV

T A B L E N. 4

DATASHEET OF DIFFERENT NEUTRON GENERATORS COMMERCIALLY AVAILABLE

COMPANY	:	KAMAN (USA)		SODERN (FRANCE)	TECHSNABEXPORT (URSS)		
MODEL	:	A-801	A-711	GNT-02	ING-01	ING-02	ING-03
EMISSION	:	PULS.	CONT.	CONT/PULS.	PULS.	PULS.	PULS.
FREQUENCY (pulse/sec)	:	1-10	-	-	3	3	1
PULSE INTENSITY (n/pulse)	:	10^8	-	$2x10^8$	10^8	10^9	10^{10}
CONT. INTENSITY (n/sec)	:	-	$7x10^{10}$	$2x10^8/10^{11}$	-	-	-
N° MAX OF PULSES	:	$2x10^5$	(x)	(xx)	$3x10^6$	$5x10^5$	10^7
COSTS (ML)	:	65	170	600	47	64	(xxx)
RECHARGE	:	Y	Y	Y	N	N	N

(x) 200 hour; (xx) 1000 hour; (xxx) not yet known

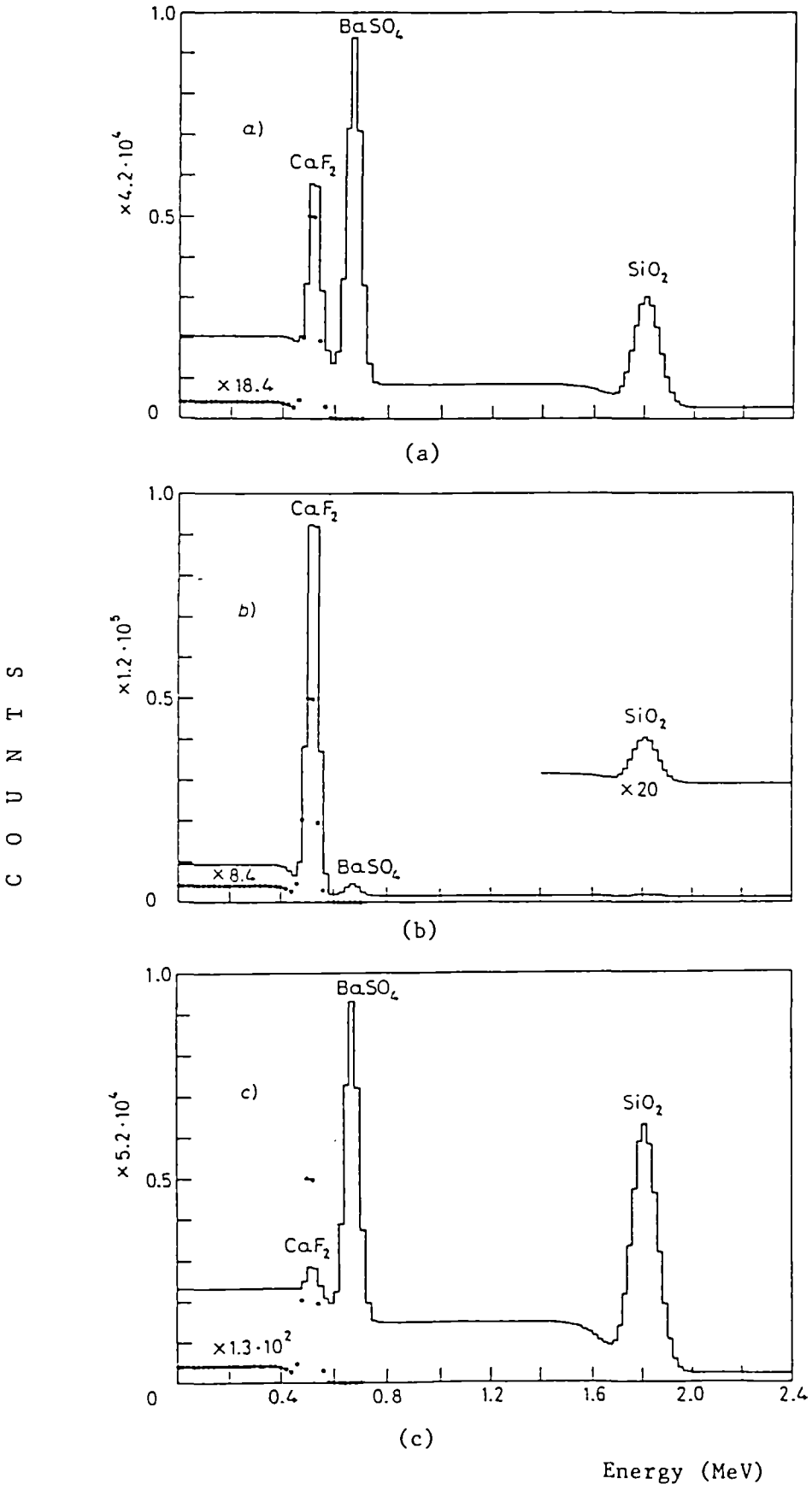

Fig. 1 - Gamma spectra simulation:
a) feed, b) concentrate, c) tailing.

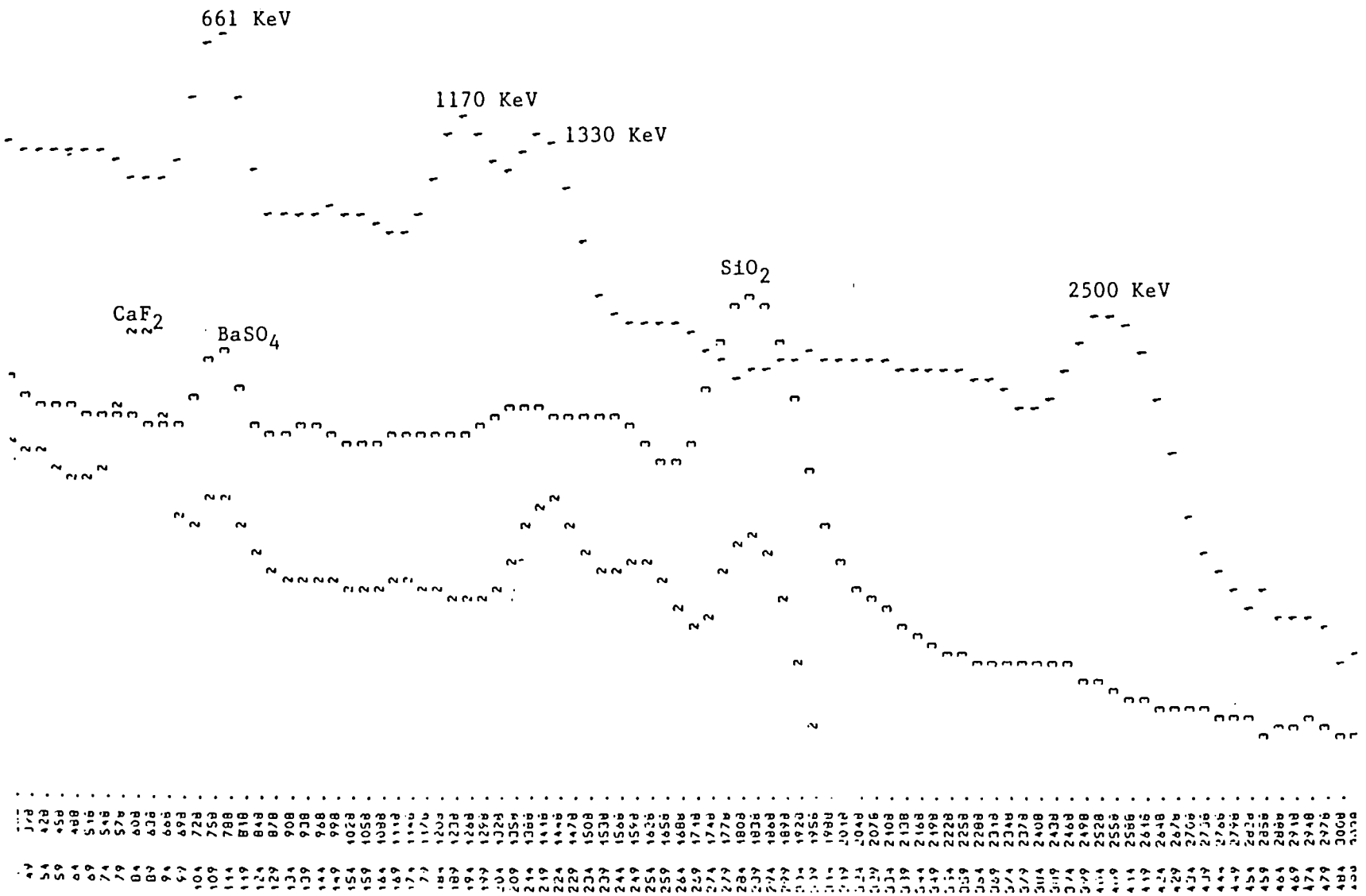

Fig. 2 - Gamma spectra of calibration standard CoCs(1), concentrate (2) and tailing (3) of fluorite.

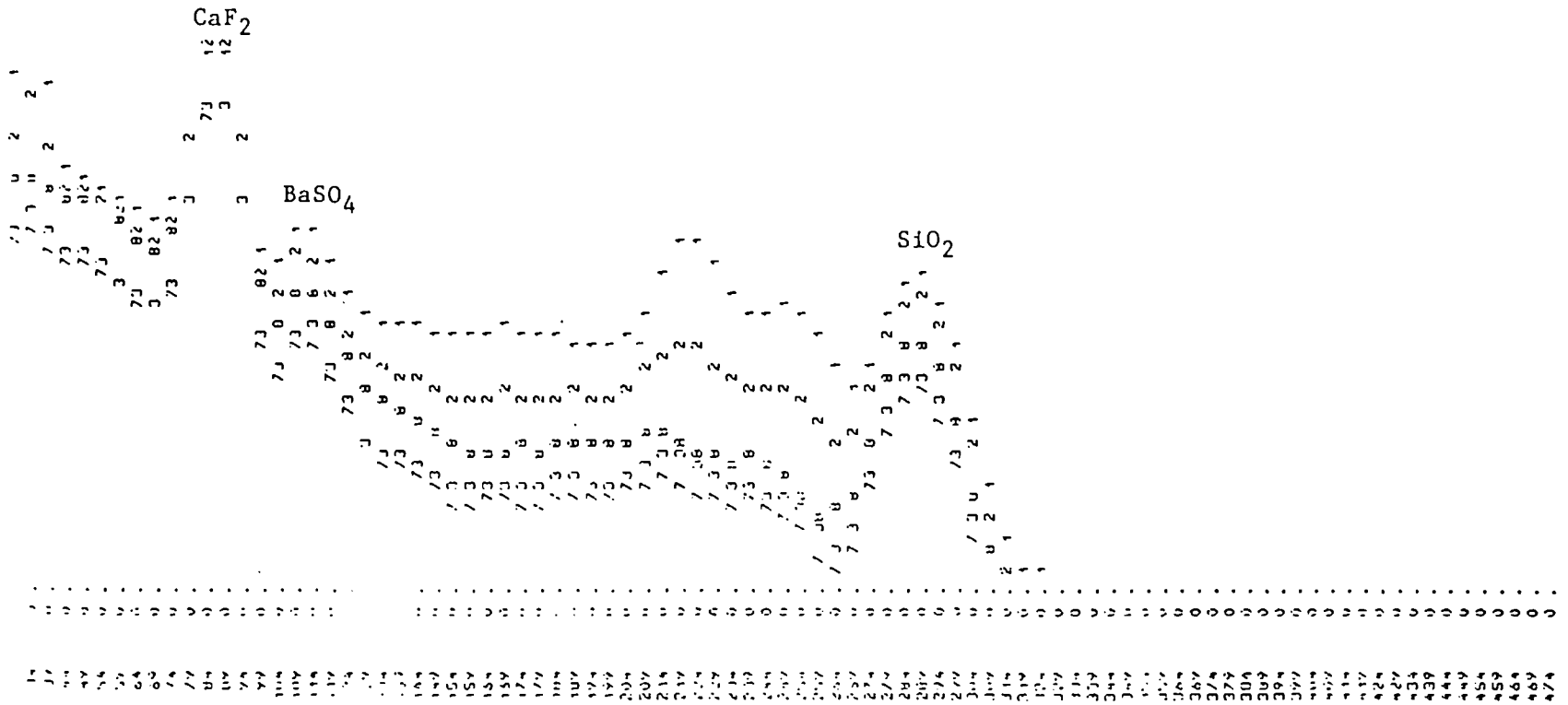

Fig. 3 - Gamma spectrum decay of fluorite concentrate.

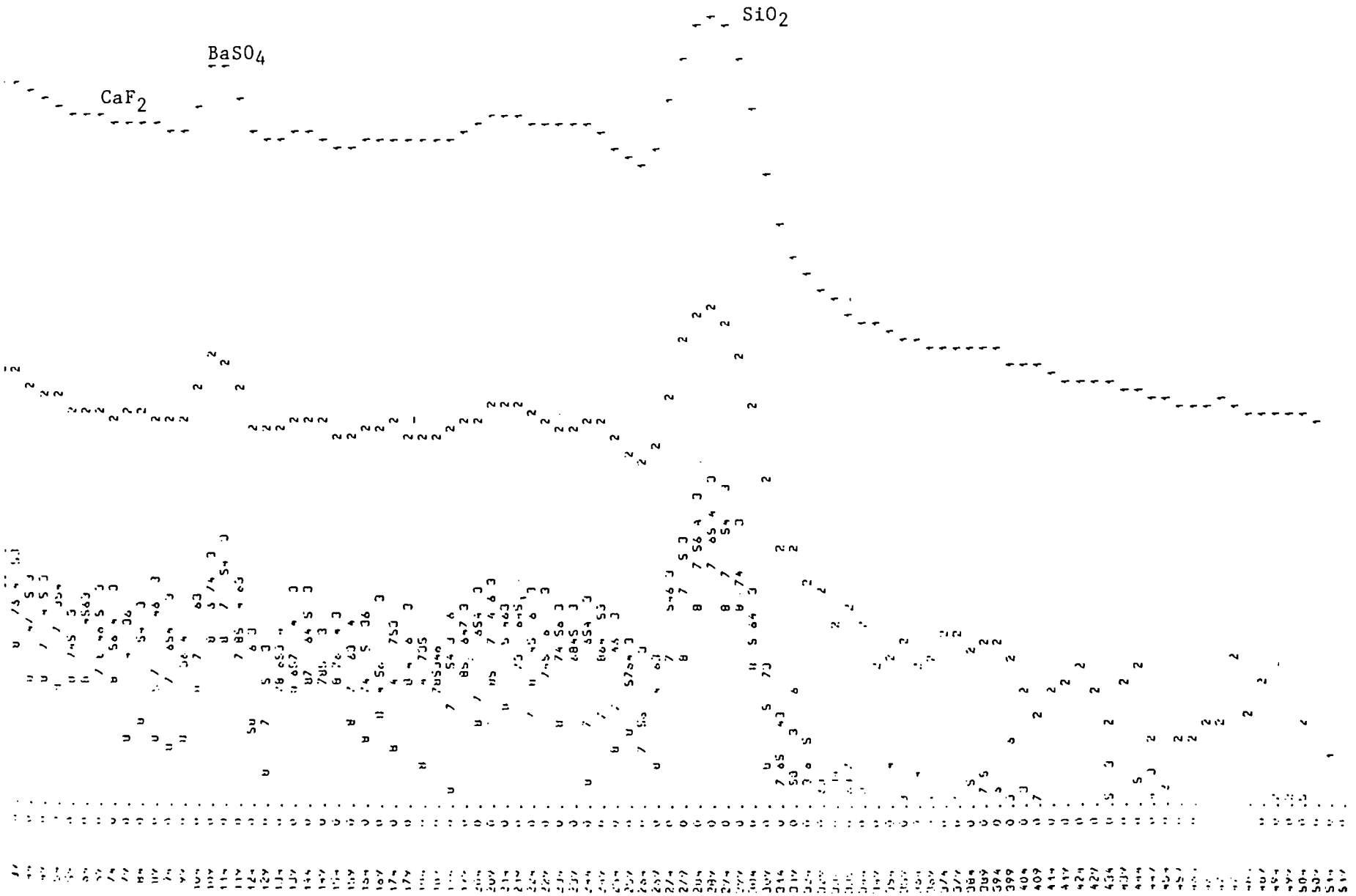

Fig. 4 - Gamma spectrum decay of fluorite tailing.

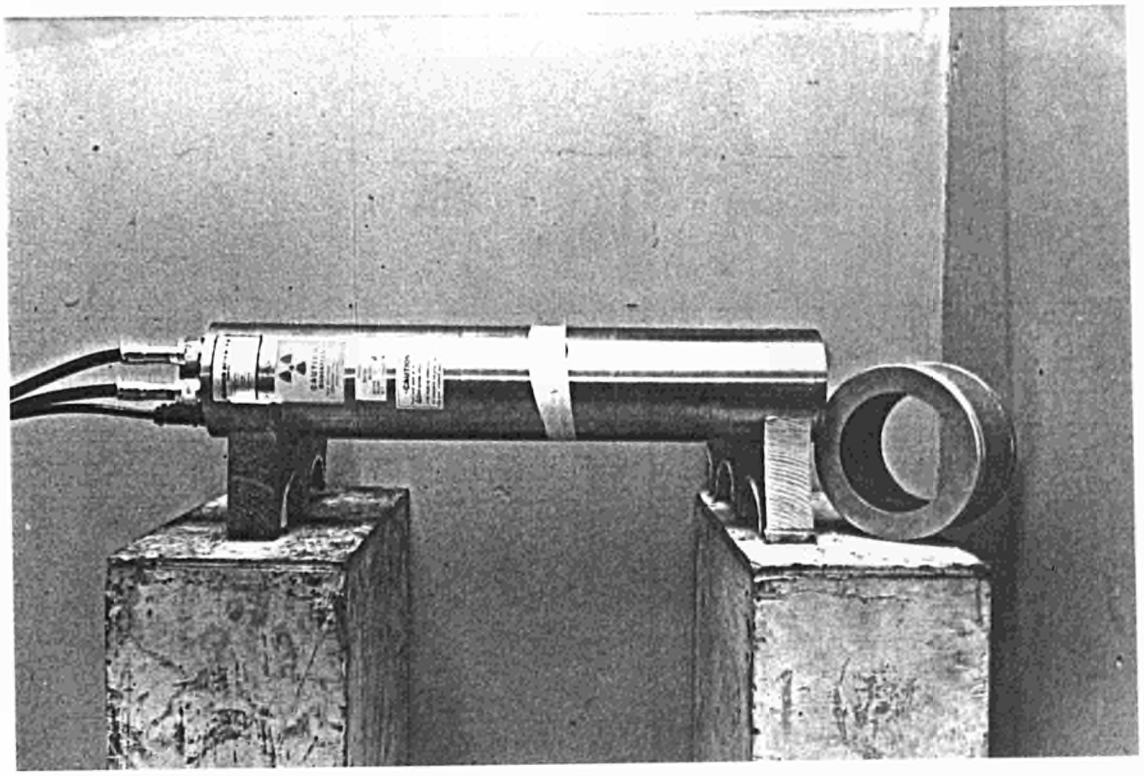

(a)

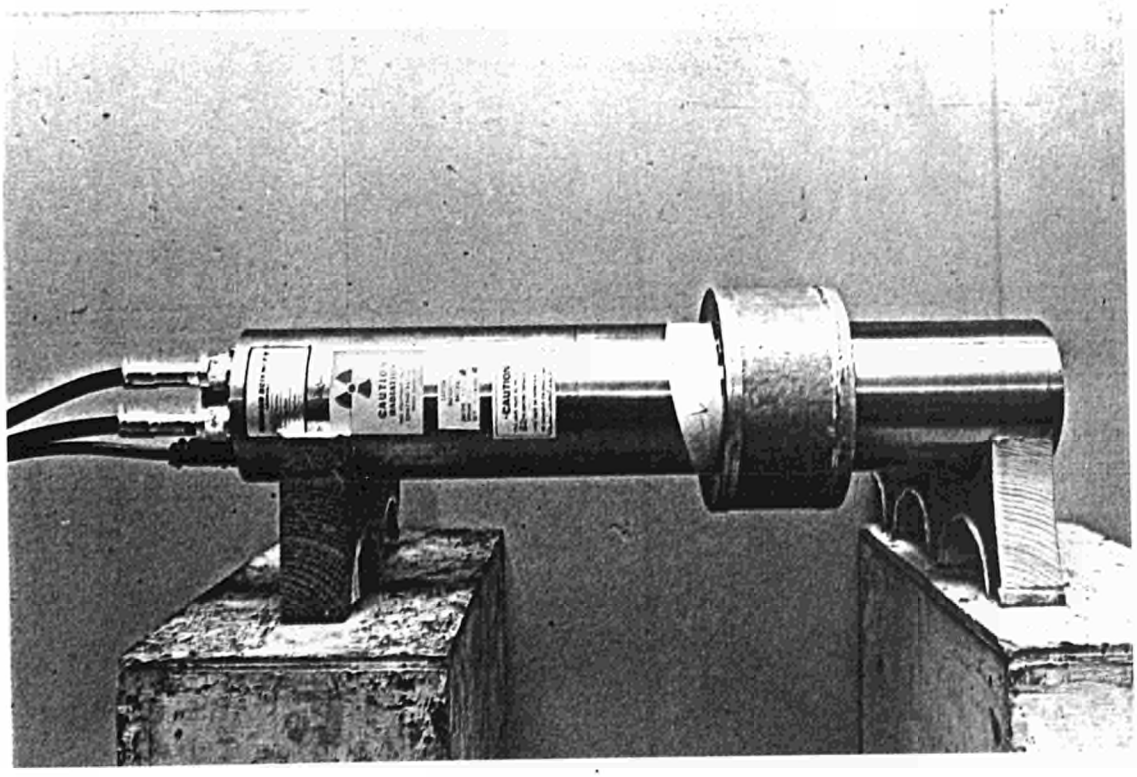

(b)

Fig. 5 - Neutrons generator KAMAN A-800 with sample-holder out of side (a) and in side (b)

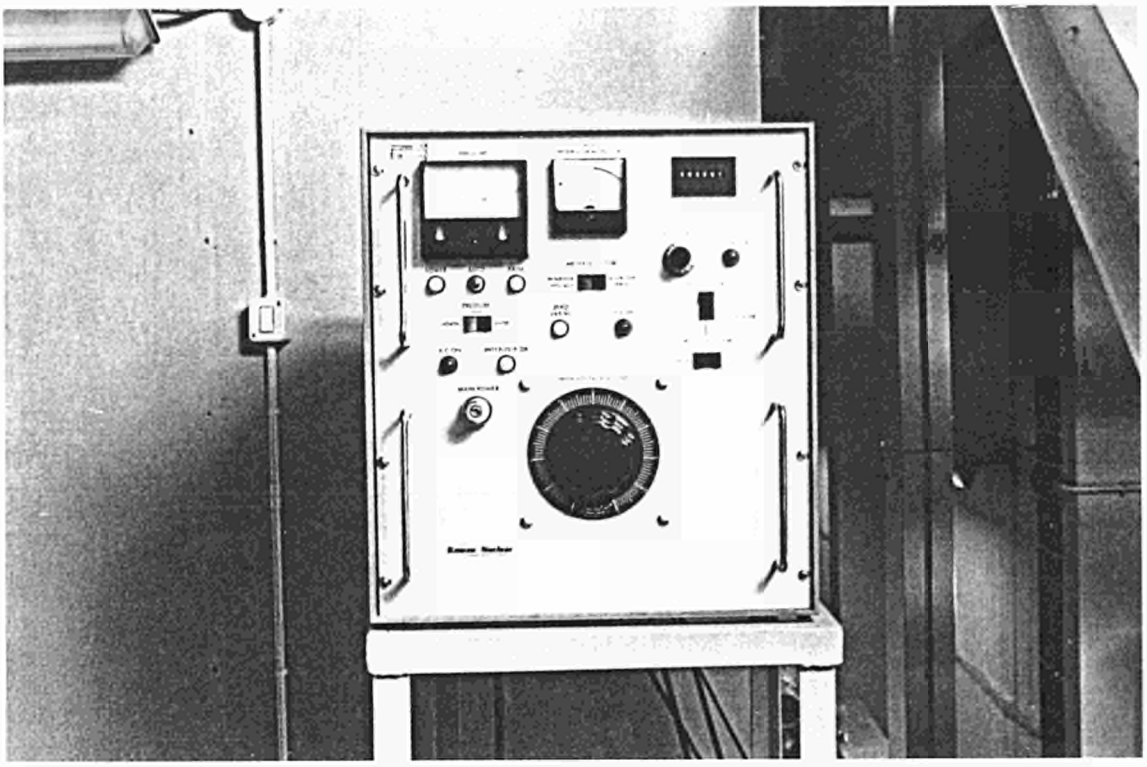

(a)

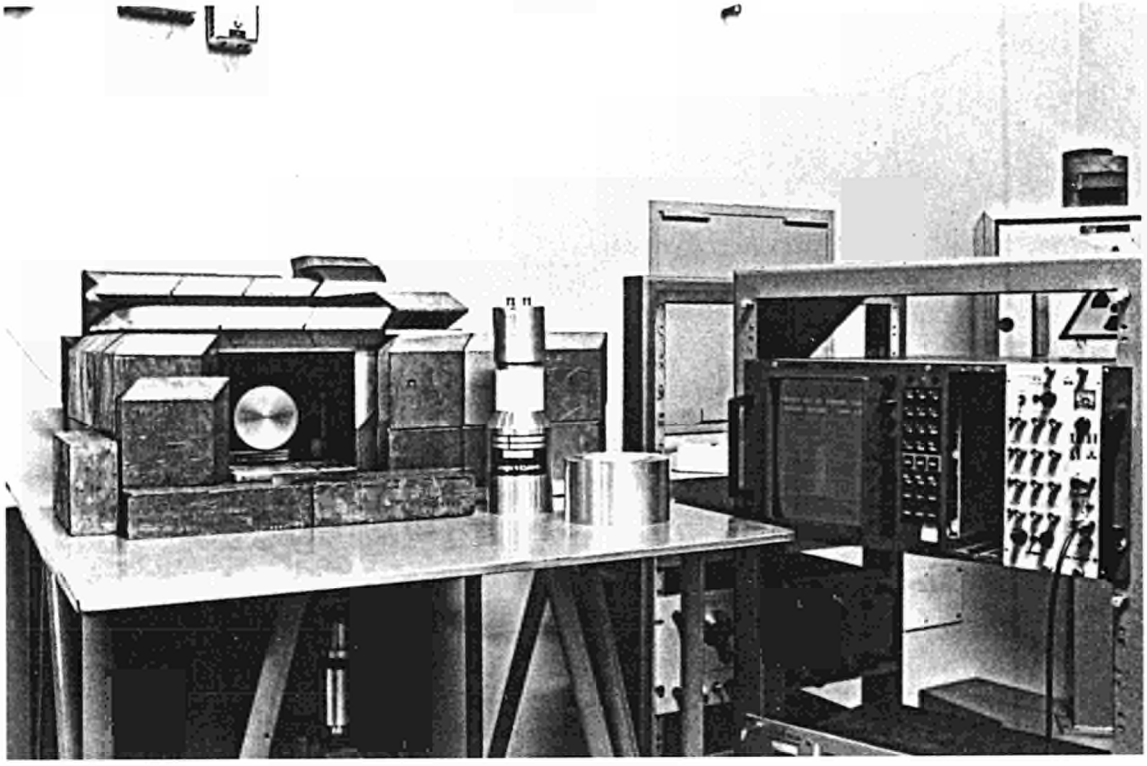

(b)

Fig. 6 - KAMAN console (a) and gamma counting device with NaI(Tl) scintillator.

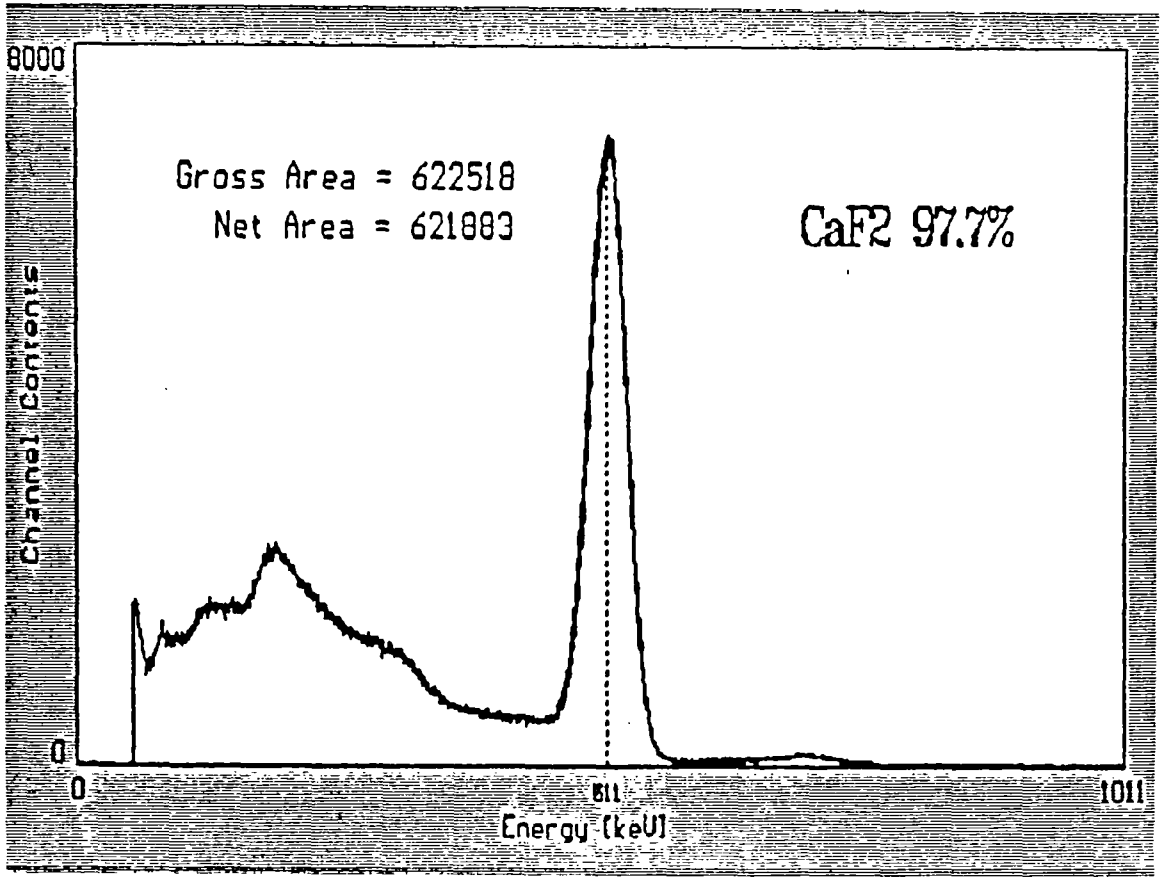

Fig. 7 - Gamma spectrum of fluorite concentrate

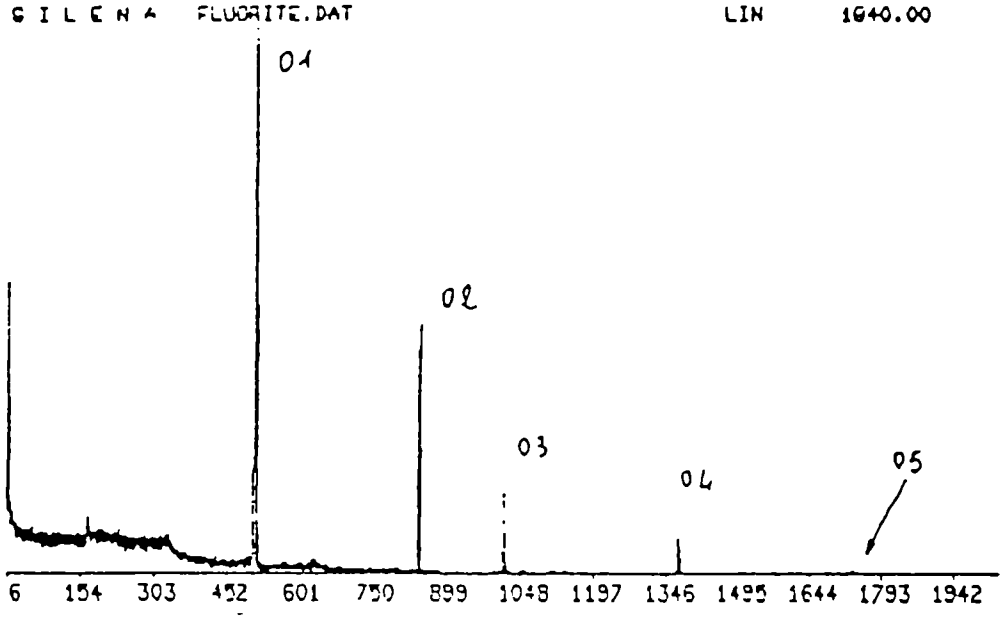

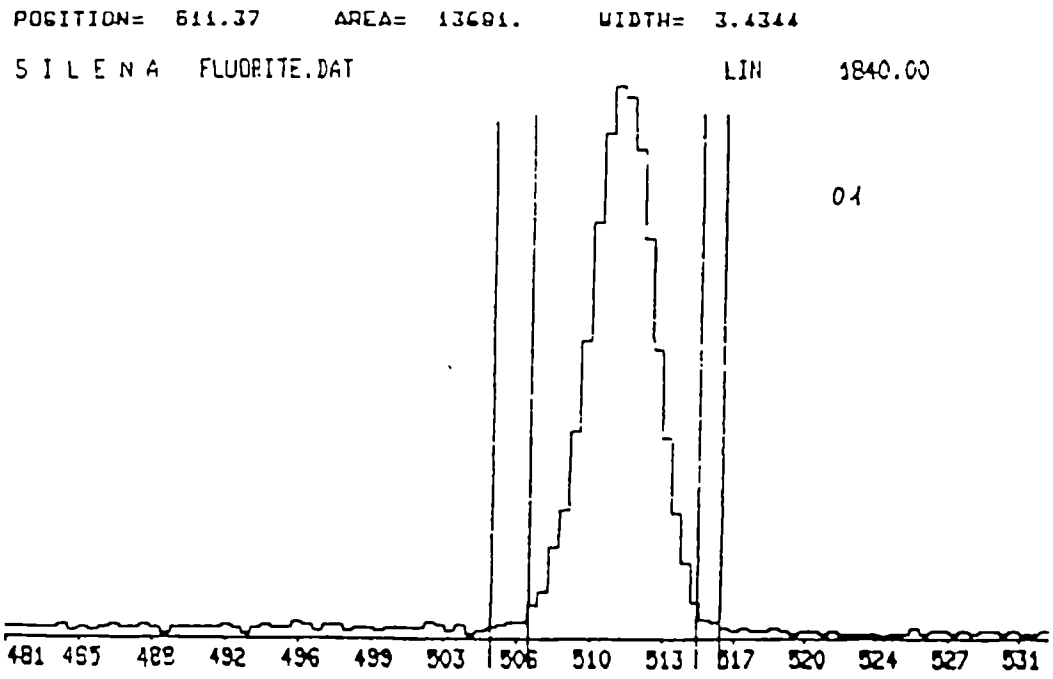

Fig. 8 - Area evaluation of fluorite.

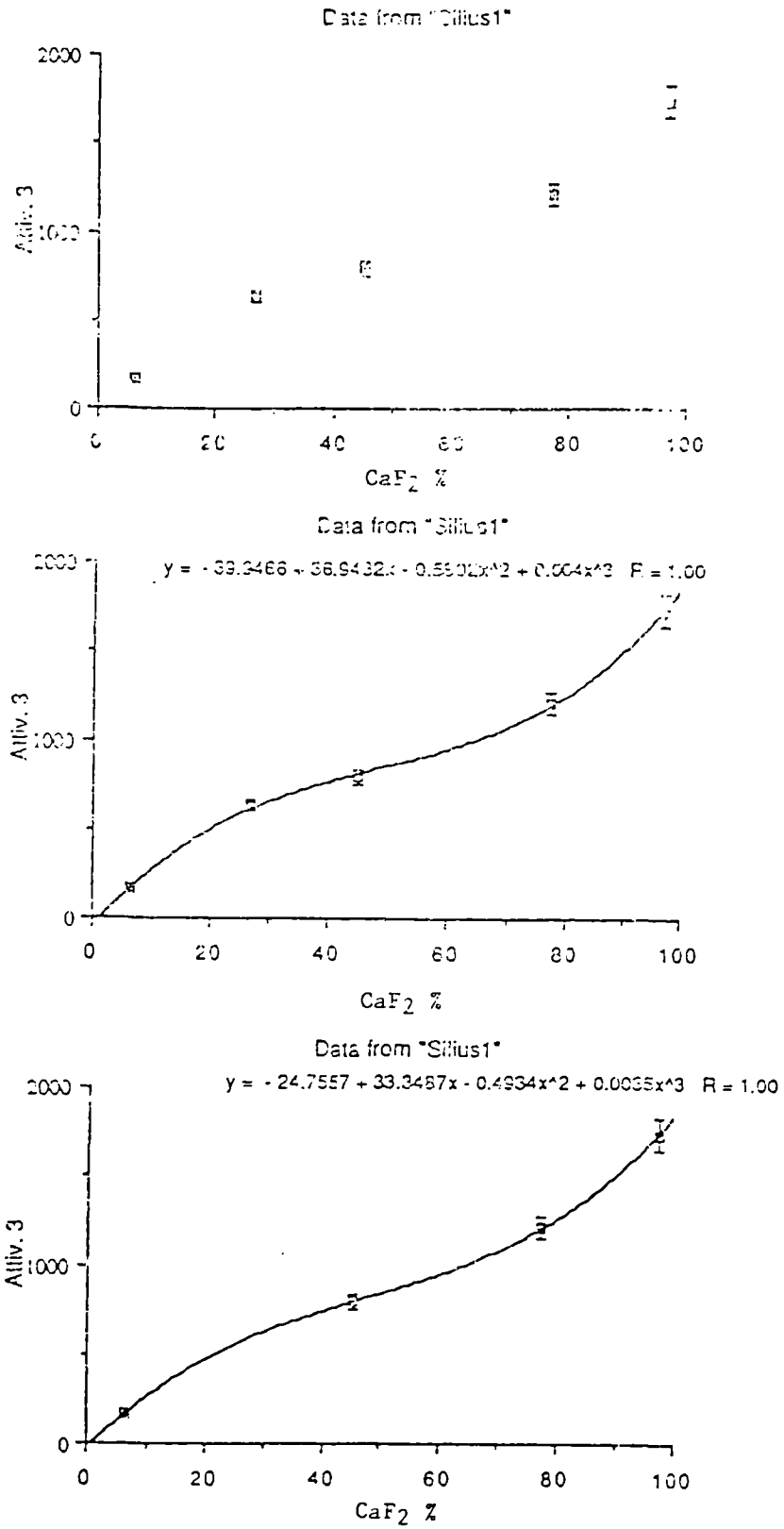

Fig. 9 - Reference curve for fluorite concentration.

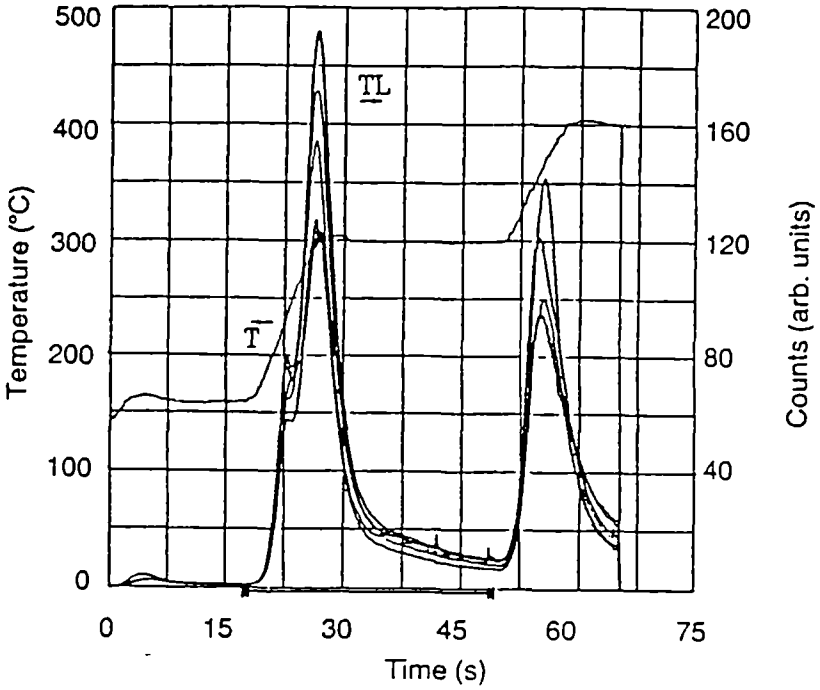

a) Without selection of grain size.

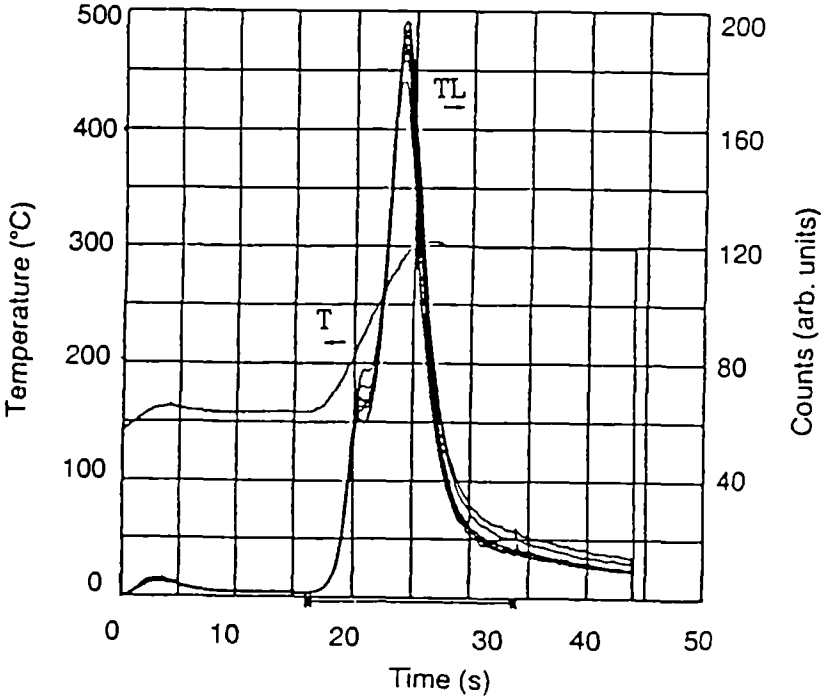

b) Grain size between 45-65 um.

Fig. 10 - Glow curves of tailing power (7,5% CaF_2).

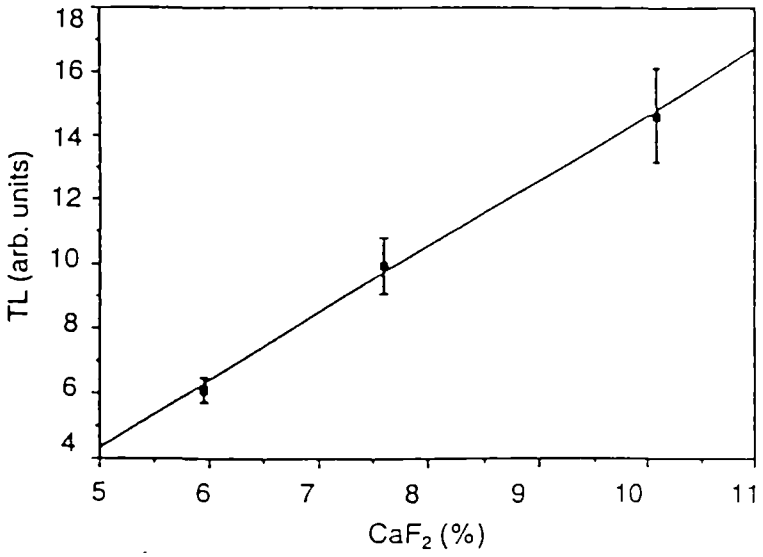

a) Tailing

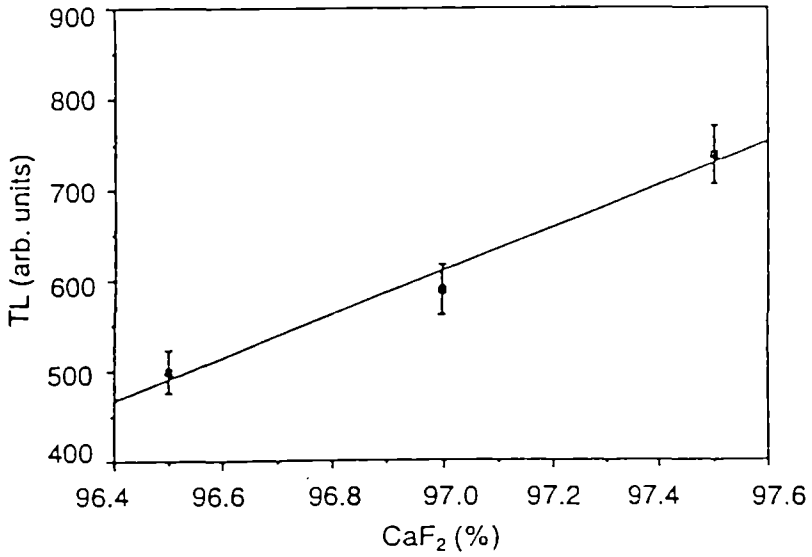

b) Concentrate

Fig. 11 - Thermoluminescence response as a function of the CaF_2 concentration.

ON-LINE ANALYSIS OF CEMENT RAW MATERIALS BY PROMPT GAMMA NEUTRON ACTIVATION ANALYSIS

Project Leader: J.L. PINAULT
Bureau de Recherches Géologiques et Minières (BRGM), Orléans, France

Laborlux S.A., Esch sur Alzette, Luxembourg

Contract MA1M-0066

1. INTRODUCTION

The operation of a cement plant involves systematic analysis of the raw materials. This is usually done on samples taken at different points in the material stream. The return time for this type of control is of the order of one to two hours, and it is carried out upon coarse, pre-crushed material, when the plant carries out a pre-blending, and always upon the fine-grained product destined for burning. The latter, commonly known as meal because of its fine grain size (a few μm) is heated by the kiln gases directly after grinding, which renders it virtually anhydrous.

On-line analysis enables a reduction in the equipment necessary for pre-blending or blending and a substantial improvement in the quality of the clinker by reducing the variations in composition of the material being fed to the kiln.

The subject of the present contract, the study of on-line analysis of cement raw materials by prompt gamma neutron activation (PGNA) analysis, comprises two distinct parts: analysis of the coarse, pre-crushed products, and analysis of the fine products before their introduction into the kiln. The achievement of these objectives was beset with a number of difficulties related to process control in general, i.e. the relatively short analysis time required to enable rapid reaction upon the process of fabrication, and the representativity and high accuracy of the analysis required.

The Bureau de Recherches Géologiques et Minières (BRGM), with many years experience in the use of neutron activation in boreholes, entered into association with the Société Luxembourgeoise de Laboratoires d'Analyses, d'Etudes et d'Essais de Matériaux (Laborlux S.A.), both for the definition of objectives and to find a cement manufacturer

to take part in the investigation. The company selected was Intermoselle, which has the particular feature of being operated in equal shares by three European companies of different nationalities - S.A. des Ciments Français, S.A. des Ciments Luxembourgeois and Dyckerhoff Zementwerke A.G. - and which evinced a willingness to participate in the integration and operation of the pilot scheme.

As far as the mechanical construction of the analyser was concerned, the Luxembourg company Paul Wurth S.A. agreed to invest in both design and realization.

PART 1 : ON-LINE ANALYSIS OF THE KILN MEAL

2. OBJECTIVES

The optimal functioning of a cement kiln and the production of good quality clinker both require rigourous control of the feed supplied to the kiln. The feed is a mixture of relatively heterogeneous raw materials (limestone and marl, as far as the Intermoselle clinker plant is concerned) and additives such as slag. The composition of the raw feed is generally described in terms of ratios, the most important of which, at the stage immediately before burning, the lime saturation, or KST ratio; this is the ratio $CaO/(2.8\ SiO2 + 1.18\ Al2O3 + 0.65\ Fe2O3)$, the value of which should be maintained between 1.04 and 1.10.

Under present conditions, the variations of the KST ratio on entry to the kiln are considered to be too large. One way of remedying this would be the on-line analysis of the meal feed on exit from the electrofilters (i.e. before blending), so as to be able to act on the set-point values of the analysers located upstream of the mill. Since the residence time of the meal is fairly short, of the order of 10-20 minutes, rapid and accurate analysis would make it possible to regulate raw material contents upstream of the silos. It nevertheless appeared judicious, during an initial period and for reasons of accessibility, to place the analyser downstream of the blending silos, in parallel with the conventional analytical system, so as to be able readily to compare results between the two methods.

3. DESIGN OF THE ANALYSER

3.1. BRGM PARTICIPATION: NUCLEAR ENGINEERING

Prompt gamma neutron activation analysis has many advantages. The most important of these are :

a) The large bulk of material to be analysed requires deep penetration of the radiation used; penetration using this method is some tens of centimetres, giving good representativity.

b) Multi-element analysis is possible. A wide range of elements can be analysed - H, B, Al, Si, S, Cl, Ca, Ti, Cr, Mn, Fe, Ni, Cu, Cd, REE, W, Hg, to quote only the most sensitive. This opens a wide range of possibilities, not only in the mining industry (s.l.), but also in the transformation industries. In particular, the cement industry offers an excellent opportunity, since the elements whose contents must be known for the control of fabrication processes (Si, Ca, Fe, Al and, for water contents, H) are readily activated.

Few concrete examples of the use of this method have so far been very successful, however. This is related mainly to the many technical difficulties encountered when attempting to reconcile analytical accuracy and precision, the shortest possible measurement time, robustness, cost of fabrication compared with conventional systems (sampling and laboratory analysis), and minimal maintenance.

However, the considerable success in recent years of the utilization of computation codes, both as an aid to designing analysers and for their calibration, opens up new possibilities. To this can be added recent work on signal processing which enables the maximum available information to be drawn from spectra. This constitutes the essence of the present contract - to utilise the enormous potentialities of the computation code to win the technological stakes.

The analyser was designed using the computation code Moca, developed by BRGM initially for the design and calibration of nuclear borehole logging tools (neutron-neutron, gamma-gamma, neutron-gamma) with the aim of simulating the spectral response of the analyser on pure products ($CaCO_3$, Fe_2O_3, Al_2O_3, SiO_2) which is necessary for deconvolution computations and for calibration of the analyser. This code also made it possible to dimension the analyser as regards to the nuclear probe and the container for the meal to be analysed. The major difficulty lays in the fact that the meal is virtually anhydrous, which renders it relatively transparent with respect to neutrons. Cylindrical symmetry was decided upon since this gives the best possible confinement of the neutrons. The level of activation necessary for accurate analysis can then be generated by a low-activity source. A large (6" x 8") NaI(Tl) detector was initially opted for essentially because of its relative insensitivity to temperature.

The spectrometry equipment (which will later be located near the control panel) is connected to a PC-compatible computer which processes the information in real time to give directly the values and the KST ratio as a function of time.

The meal flows around the detector, which is protected by a cylindrical polypropylene shield; this is a hydrogenated material that acts as a neutron moderator.

3.2 PARTICIPATION OF PAUL WURTH S.A.: MECHANICAL ENGINEERING

The Paul Wurth company designed, constructed and set up the analyser at Intermoselle.

The material to be analysed (dry meal before burning) is sampled at the output from an elevator. The feed pipe is kept full of meal so that the probe is always immersed. Extraction is effected by a variable rate rotary feeder that feeds the meal back into the main stream. The detector is air-cooled. The meal is fluidized by air-injection to facilitate its flow through the analyser.

4. THE FIRST TRIALS

The first comparisons between on-line analysis by neutron activation and XRF analysis of samples by Intermoselle were made at the end of 1989. They showed up certain divergences that were due essentially to a lack of sensitivity attributed to an observed constant very high background, itself owing to a lack of adequate protection of the NaI(Tl) detector against neutrons.

A number of innovations were then introduced into the spectral deconvolution software, taking advantage of the new spectral methods of signal processing. Reproducibility tests showed that relative errors on the KST ratio were close to 2% for an analysis time of one hour, which was in accordance with what we had predicted at the beginning of the contract.

Comparison of results nevertheless showed that the neutron activation analyses presented little variation. In particular, the increase in the KST ratio owing to a decrease in silica observed on certain days after shutdown of the mill were not, or only poorly detected by neutron activation analysis. This was first of all attributed to a sampling problem, but in fact, what we were seeing was the consequence of irregular flow of the meal through the analyser.

5. IMPROVEMENTS MADE BY CHANGING THE DETECTOR AND MODIFYING THE FEED MEAL

Feeding of the analyser was modified by moving the descending column, placing it between the sampler and the analyser, so that the meal is injected to the analyser at a point diametrically opposite that of extraction by the rotary feeder.

In order to reduce analysis time while maintaining the accuracy on the KST ratio, the 6" x 8" NaI detector was

replaced by a much denser (and therefore more efficient) 3" x 8" BGO bismuth germanate ($Bi_4Ge_3O_{12}$) detector, the reduction in diameter allowing increased protection against neutrons.

During the annual shutdown of the plant, tests were carried out for reproducibility making measurements both statically and dynamically (16 each), the latter with the analyser feed operating in closed circuit. This showed that both the problems of meal flow in the analyser and precision of measurement had been resolved. The relative standard deviation on the KST ratio was brought down to 0.99% for an acquisition time of one hour. The estimated standard deviations are 0.15% for SiO2, 0.05% for CaO, 0.01% for Fe2O3 and 0.10% for Al2O3 (if the acquisition time was a quarter of an hour, the standard deviations would be multiplied by two). The dynamic measurements showed a variation in the KST ratio more than five times greater than the estimated standard deviation for a single measurement, which is highly significant. These variations were confirmed by analysis of samples taken simultaneously and carried out by Laborlux because the XRF equipment was not available at Intermoselle.

6. CONCLUSIONS

Although we do not yet have enough results of comparison between PGNA analysis and analysis of samples, we now know that the difficulties encountered during 1990 have all been resolved. Testing will be resumed as soon as the plant starts up again, which will be during March. If the quality of the first results is confirmed, the analyser will be moved farther up the material stream, at the outlet from the electrofilters.

PART 2: FEASIBILITY STUDY OF THE ANALYSIS OF COARSE, PRE-CRUSHED MATERIAL ON A BELT-CONVEYOR BY PROMPT GAMMA NEUTRON ACTIVATION ANALYSIS, AIDED BY THE MOCA SOFTWARE PACKAGE

7. PURPOSE

At the beginning of this contract the analysis of coarse material was envisaged using an analyser similar to that developed for the meal, with sampling of the material transported on the conveyor being effected by the John B. Long Co.'s system, known to Laborlux, with introduction of the material into the analyser designed for the analysis of meal, followed by its extraction and return to the main stream. However, two problems arose during the course of the contract.

First, tests on the flow of material similar to that used by Intermoselle (limestone and marl) resulted in blocking in the analyser, owing to the rheological properties of the material, which are such that it will not pass through a space that has to be narrow in order for all the stream to take part in the neutron reactions.

Second, the Gammametrics system acquired by Ciments Belges CCB at the end of 1985 has been operating since 1989 on pre-crushed raw material. Although it has given satisfaction to its users, this analyser has not been widely adopted in cement plants because of its cost and because it cannot be used if the material is sticky.

In order to avoid falling into the trap of developing an apparatus destined for a small and highly competitive market, it was decided to study the feasibility of directly analysing material on the conveyor, with the aid of the Moca simulation code. Difficulties inherent in this approach are the problem of confining the neutrons within the transported material, and that of the correction of the intensities of the different characteristic radiations for inter-element effects (owing for example to the presence of water), and for variations in thickness and apparent density of the material, that is necessary for quantitative elemental analysis of the material.

The feasibility studies nevertheless gave positive results. However, the construction of a pilot would have taken something of the order of 24 months, which prevented any such undertaking in the framework of the present contract.

8. PRINCIPLE

The material is analysed while on a belt conveyor. The gamma radiation induced by the neutrons emitted by a 252Cf isotopic source is perceived by a detector placed below the belt. The analysis takes place while the belt is in movement, and the integration of the nuclear events is effected during a predetermined time, at the end of which the information is used to compute the contents of the various constituents. The analytical system functions by transmission - the emission of neutrons and the detection of the resulting radiation take place on opposite sides of the conveyor belt, thus, the entire thickness of the material on the belt takes part in the analysis. Two reflectors, placed on either side of the belt, ensure the confinement of the neutrons within the material. Their width is adapted to that of the belt.

The distinctive feature of this system is that direct elemental analysis of the material is performed without the material coming into contact with any mechanical part.

The correction model for converting the measured intensities into content values is based on the observation that all the constituents of cement raw materials ($CaCO_3$, SiO_2, Fe_2O_3, Al_2O_3, H_2O) can be determined from the characteristic radiation of one of their component elements (respectively Ca, Si, Fe, Al and H). The weight proportion O_i of each constituent can be calculated from the intensity I of the characteristic rays by the ratio $Oj = \mu_j.I_j/\mu_i.I_i$, the coefficients μ_i being calculated by the Moca code. This ratio is independent of the thickness of the layer of material, of apparent density and of inter-element effects provided that the material is statistically homogeneous.

9. OVERALL CONCLUSIONS

Analysis of meal :
A pilot is functioning satisfactorily. This should enable Intermoselle to continue its investigations into the utility of on-line analysis of hot products.

Analysis of pre-crushed material :
A system is proposed enabling direct analysis on belt conveyors. The construction of such an analyser would require about two years.

Analysers of these types would certainly find other applications in the various sectors of the mineral industry where on-line analysis for process control is or would be advantageous, such as direct analysis of ash in coal, control of sinter feed to blast furnaces, etc.

These analysers use a low-activity 252Cf isotopic source, which is of great interest as far as protection against radiation is concerned. In particular, the analysed material possesses no residual radioactivity after irradiation.

At the end of 1990, Laborlux carried out a market survey by mailing. The first replies indicate a growing interest in on-line analysis of solid material streams in the mineral industry. It would, however, be premature at this stage to draw any conclusions, especially as they will be strongly influenced by the concrete results obtained at Intermoselle.

RESEARCH AREA 3.7

INDUSTRIAL MINERALS

BENEFICIATION OF TALC-CHLORITES FROM PYRENEAN AND VALMALENCO ORES

Project leader: J.M. CASES
Centre de Recherche sur la Valorisation des Minerais, Nancy, France

L. Piga
Instituto per il Trattamento dei Minerali, Rome, Italy

Contract MAIM-0035-C

1. OBJECTIVE

1.1 ON PYRENNEAN TALC ORES

To achieve a direct beneficiation of talc-chlorite concentrates obtained either from the open pit mine or from a treatment using an optical sorter. In the future to extend this beneficiation method to concentrates obtained by flotation. Two different ways were chosen; wet micronisation and thermal treatments in order to design materials useable as reinforcement agents in the plastics industry, in high technology refractory compounds and as coating agents in the paper industry.

To study the possible beneficiation by flotation of some commercialized products, some coarse rejects resulting from air classification (40000 t/year) and some fine products resulting from the washing of the optical sorter by suppressing carbonates and iron rich minerals.

1.2. ON TALC ORES FROM VALMALENCO

Beneficiation by flotation in order to obtain samples enriched in talc and chlorite for subsequent use in the paper industry (recycled and non recycled papers) as pitch control agents, in the polyester mastics as fillers, in the anti-corrosive paints as fillers and in the formulation of ceramic pastes for tiling.

2. INTRODUCTION

Talc materials are commonly considered as products of low unit value but high place value. The beneficiation of such products tries generally to answer two questions: 1) How is it possible to eliminate undesirable impurities? 2) Is there any process that would open new channels to the mineral?

Here is considered the direct beneficiation of talcs either by wet micronizing or heat treatment. The possibilities to

obtain talc-rich or chlorite-rich concentrates with low amounts of impurities (carbonates, iron minerals) are studied. The separation processes are froth flotation, hydrocycloning or magnetic separation.

3. DIRECT BENEFICIATION OF PYRENNEAN TALC ORES

3.1. RESULTS

Three different samples were used for this study. A talc-rich ore (Talc 82%, Chlorite 12%), a chlorite rich ore (Talc 41%, Chlorite 55%) and a very pure Indian talc used as a reference.

The main results obtained can be summarized as follows :

- When the solid concentration is increased during wet micronization, the particles obtained are finer due to an increase in shear strains.

- By adding certain reagents during grinding, one can obtain either coarser products (addition of NaOH + KCl or Melamine) or finer products (addition of LiCl).

- An increase in the shear strains during grinding leads to more delaminated particles. The use of acidic conditions favours the delamination of talc samples.

- In the case of dry grinding, the analysis of the scale of rupture localization shows that :

Delamination following the 001 crystallographical plane occurs up to surface area values of around 5 m2/g.
A rupture parallel to the c axis then occurs and provokes a decrease in lamellarity for products with surface areas between 5 and 15 m^2/g.
For longer grinding times, attrition occurs. It produces very fine particles which are responsible for a large increase in surface area up to 80 m^2/g. [1].

- In the case of wet micronization, products with high surface area can be obtained without an important change in the crystallographical order of the products (this cannot be achieved through dry grinding).[2].

- For a better understanding of the rheological properties of the slurries, a modelling of the surface charge of talc minerals was performed. This modelling allows the determination of the pK of the different surface groups. It has been shown that in this type of studies, it is necessary to take into account the presence on the surface of precipitated (tridimensional condensation on the substrate) phases, $MgCO_3$ between pH 5 and 11 and $Mg(OH)_2$ in alkaline conditions.

- Measurements of the rheological properties have shown that most of the pulps present an age-fluidizing character. After grinding in the presence of a dispersant, the pulps are less visquous but exhibit an age-thickening character due to the decomposition of the dispersant.

- The rheological properties of the suspensions could certainly be improved after fully taking advantage of one of the discoveries made during this resarch program. The hydrophobicity of talc is not due to structural or chemical reasons but to the particular affinity of nitrogen (argon and krypton exhibit the same type of behaviour but less intense) for the basal faces of this mineral. [3],[4],[5].

- Statistical analysis was used to correlate the structural properties and the surface and morphological parameters of ground products with the mechanical properties of filled polymers. This approach yielded a simple modelling of the mechanical properties of the polymer and showed that the flexural strength and the deformation temperature were normally correlated but were anticorrelated with the impact strength. This means that a simultaneous optimization of these three parameters will be difficult to achieve. When talc is pure, the two first parameters are strongly dependent on the lamellarity of the particles.

- Studies dealing with the thermal treatment of talc ores are more advanced than it was expected from the initial program. They have shown that :

The dehydroxylation of the brucitic sheet of the chlorite occurs in two stages, the release of water is achieved only after the dehydroxylation reaction.
The dehydroxylation of the mica sheet is a rather heterogeneous reaction.
Some hydroxyl groups remain bound to the products obtained in the decomposition of talc.
By adding small quantities of different alkaline salts, it is possible to substantially decrease the different dehydroxylation temperatures.

In order to solve the problem relative to the origin of the talc hydrophobicity, a quasi equilibrium gas adsorption device (equipped with pressure sensors that work at low pressure) was developped ; it enables one to study the surface heterogeneity and the microporosity of adsorbents in satisfactory conditions.[6].

These studies have allowed "Talcs de Luzenac SA" to improve their knowledge of wet treatments. As a result they lead to different new investments in the plant :

- A unit for designing slurries for paper coating (7500 t/year)
- A wet microgrinding unit
- A drying unit for treating the products obtained after wet treatments.

3.2. FUTURE RESEARCH DEVELOPMENTS

A lot of important research still need to be carried out, which justify the demand for an extension of the present grant.

- Analysis of the dispersion mechanisms. Search for more efficient reagents to enhance the rheological properties of the slurries. It will then be critical to achieve the constancy of these properties over a period of more than a month, whatever the storage temperature between -5°C and +30°C.

- Detailed study of the mechanism of the dehydroxylation of the brucitic sheet in the chlorite in order to allow this mineral to be used satisfactorily as a reinforcement filler in polypropylenes.

- Detailed study of the dehydroxylation of talc and the mica sheet of chlorite for the design of high technology refractory materials. This study will also have to include a study of the conditions influencing the nature and the structural order of recrystallization phases.

4. BENIFICIATION OF PYRENNEAN TALC ORES BY FLOTATION AND MAGNETIC SEPARATION

Talcs de Luzenac SA provided commercialized products, coarse rejects from air classification processes and fine particles obtained after washing. The aim was to obtain, by flotation, products enriched in either talc and/or chlorite so that their mineralogy could suit different industrial applications such as high technology refractories, paper filling and coating, reinforcement of pastics...

Two different methods were used : magnetic separation (either high wet intensity or very high field obtained by a superconducting coil) and flotation.

4.1. SEPARATION IRON-TALC BY MAGNETISM

This study aimed at obtaining products with Fe_2O_3 content < 0,25%. All the talc samples studied have an intrinsic Fe_2O_3 content (substitution in the lattice) of 0.5 to 0.7%. It is thus impossible to achieve the desired values through a physical process.

Tests revealed that chlorite is not separated neither by high field nor very high field magnetic separation. This means that magnetic separation is not suitable for enriching the ores.

4.2. DIRECT FLOTATION OF TALC

For all the pyrennean samples studied, selective flotation using only a frother (natural hydrophobicity of talc) leads to concentrates with more than 90% talc content. Depending on each specific case successive flotation stages followed by recleaning stages of the floated products can be necessary.

4.3. CHLORITE-DOLOMITE SEPARATION

Three different processes have been tested for separating chlorite from dolomite.

- Size classification by a cyclone;
- direct flotation of dolomite using fatty acids as collectors;
- direct flotation of chlorite using cationic collectors;

The preliminary studies show that

- The products resulting from the cyclone have a low dolomite content and generally meet the desired requirements. The choice of the cyclone depends on the ore to be treated but generally it has a small cutting size (7 to 20 micrometers) and the overflow represents only a small weight percent of the initial feed.

- Flotation using fatty acids is rather inefficient in terms of selectivity; the use of depressing agents (sodium silicate, alginic acid, carboxymethyl cellulose...) did not result in any significant improvements. In any case, to obtain a positive result, talc has to be eliminated prior to any treatment.

- Amine flotation can be used only if the chlorite content is much lower than the dolomite one. This is unfortunately a rare case.

As a result of these studies, Talcs de Luzenac SA decided to invest in the building of a semi-industrial scale flotation plant (2500 t/year) for obtaining talc concentrates.

4.4. FUTURE RESEARCH DEVELOPMENTS

In the demanded extension of the grant, research will be focused on the most promising process i.e. the combination of size classification, using a cyclone, and flotation. To obtain good results it will be necessary to choose reagents capable of insuring a good selectivity of the separation chlorite-dolomite. This represents the last critical separation step for achieving a profitable talc flotation process. Interesting applications can then be found for a chloritic concentrate with a low content in silica and dolomite (less than 3%).

5. FLOTATION OF TALC ORES FROM VALMALENCO

Research was carried out on two different samples.

The most important part of this study was to design a method for obtaining the real mineralogical composition (unknown at the present time) of a very complex ore; this needs to be detailed enough to monitor and control beneficiation processes. This approach required the combination of very modern analysis methods and statistical methods such as principal component analysis. The average composition of the ore can be roughly described as follows : Talc 49%, Chlorite 19%, Carbonates 30%, Sulfur and Magnesite 2%.

The iron that needs to be eliminated is contained in almost all the minerals including magnesite (10% Fe_2O_3).

The liberation size is around 10-15 micrometers.

Low intensity magnetic separation allows the elimination of 20% of the total iron content.

Taking advantage of the differences in particle strength between talc and carbonates, it was possible, after attrition and flotation, to obtain a concentrate with the following composition : Talc 77%, Chlorite 18%, Carbonates 5,4%.

In this process the talc recovery is around 30% whilst the chlorite and carbonates recovery is 22% and 4% respectively. The talc and chlorite recovery could be increased up to 68% and 44% respectively by floating the ore using isoamylalcohol as a collector.

5.1. FUTURE RESEARCH DEVELOPMENTS

Future research developments will mainly focus on :

- Grinding by attrition and selectivity of different types of grinding.

- Finding reagents for obtaining talc-chlorite concentrates with a low carbonate content.

- Designing of a quick and easy method for controlling the aspect ratio (lamellarity of the particles) after grinding.

6. REFERENCES

[1] J. YVON, P. MARION, L. MICHOT, F. VILLIERAS, F. E. WAGNER. (1990) Development of mineralogy applications in mineral processing. Submitted European Journ. of Miner.

[2] J. . YVON, E. PAPIRER, J.M. CASES, P. ROLLAND, L. MICHOT, J.F. DELON, R. MERCIER, Y. GRILLET. (1990) Broyage de la muscovite et de substances talcochloriteuses en milieux liquides, caractérisation des solides fragmentés. In Press : Bull. BRGM.

[3] L. MICHOT, J. YVON, J.M. CASES, J.L. ZIMMERMANN, R. BAEZA (1990) Apparente hydrophobie du talc et affinité de l'azote pour ce mineral. C.R. Acad. Sci. **310** série II 1063-1068.

[4] L. MICHOT, J. YVON, F. VILLIERAS, J.M. CASES, J.L. ZIMMERMANN, R. BAEZA (1990) Apparente hydrophobie du talc et affinité, en particulier, de l'azote pour ce mineral. Journées de la société française de minéralogie et de cristallographie, Rennes 5-7 sept.

[5] L. MICHOT, J. YVON, J.M. CASES, J.L. ZIMMERMANN (1990) Affinity of nitrogen for the surface of talc. Relation to the natural hydrophobicity of this mineral. Presented to the "Fine Particles Processing Conference" San Diego. 15 p. To be published by Pergamon Press.

[6] L. MICHOT, M. FRANÇOIS, J.M. CASES (1990) Surface heterogeneity studied by a quasi-equilibrium gas adsorption procedure. Langmuir **6** 677-681.

IMPROVEMENT OF THE QUALITY OF REFRACTORY MINERALS SUCH AS ANDALUSITE

Project Leader: Ch. BISCARAT
DAMREC, Longueville, France

J.J. PREDALI
MINEMET RECHERCHE, Trappes, France

A. VAN LIERDE
Université Catholique de Louvain, Louvain-la-Neuve, Belgium

Contract MA1M-0070-C

1. OBJECTIVE

The aim of the proposed Research and Development work was to increase the quality of European Andalusites through:

- A better knowledge of the deposit with regards to the final quality of the concentrate.
- A better efficiency of the processes which will include new steps such as flotation.
- The objective of this project was also to decrease the production price.

The technical programme was twofold:

In connection with TECMINEMET (Department "Informatique et Infographie Minière"), correlation studies between mine sampling and plant mineralogical results were undertaken. A new, fast and efficient laboratory test, was developed from this research. It is now possible to forecast actual mineralogical composition and concentrate qualities for any ore type from mine cutting samples.

Flotation research and development:

Previous experiments carried out in 1986 by MINEMET RECHERCHE on behalf of DAMREC indicated that it was likely that the concentrate grade could be improved but in any case an extensive R and D programme was required:

- In connection with "UNIVERSITE CATHOLIQUE DE LOUVAIN" (Prof. Van Lierde) for fundamental flotation studies to improve the different steps of the process: pyrite removal and Andalusite/Biotite/Quartz differentiation.
- In connection with MINEMET RECHERCHE (J.J. PREDALI) for the application of the process to different tailings produced by DAMREC plants.

- In connection with MINEMET RECHERCHE (J.J. PREDALI) for the demonstration of the process through the use of an industrial flotation pilot plant to produce concentrates for commercial tests.

2. INTRODUCTION

Andalusite (Al_2O_3, SiO_2) is an industrial mineral of the sillimanite group (Kyanite, Andalusite, sillimanite) used as a raw material for the manufacturing of high alumina refractories for the ferrous and non ferrous industries (production of refractory bricks, refractory cement, etc...).

South Africa has the World's largest known reserves of Andalusite followed by France, with the Glomel Plant located in Brittany. This is the only domestic production of this material for the EEC.

The refractory characteristics of the sillimanite group of minerals is derived from their ability to form the refractory high-performance mullite phase (3 Al_2O_3, 2 SiO_2) at high temperatures. This phase combines high strength at high temperatures with resistance to physical and chemical erosion. Andalusite breaks down to form a mixture of mullite and vitreous silica (SiO_2) at 1380°C. The resulting mullite consists of an aggregation of interlocking crystals which remains dimensionally and chemically stable until the temperature reaches at least 1810°C.

South African production has an alumina (Al_2O_3) content above 60% and an iron oxide (Fe_2O_3) content below 0,8%. The Glomel's Andalusite is lower in alumina content (59%) and higher in iron oxide content (1.1%).

Foreseeable future demands for Andalusite will be for a high quality product: (plus 60% in alumina and minus 0.8% in iron oxide).

3. IMPROVEMENT IN THE KNOWLEDGE OF THE DEPOSIT

A computer programme has been developed to obtain a better method for exploitation of the open pit through the following steps:

- Drilling and laboratory study of the cuttings;
- Computerization of the data;
- Correlation between the quarry and plant data;
- Forecast of the plant results using the quarry data;
- Selection between mineralised and barren areas in the quarry;
- Optimization of the run of mine feed grade after primary crushing;
- New method of ore reserve calculation.

Finally, the studies above have allowed us:

- To determine the representative parameters of the quarry (cuttings before blasting) giving a good correlation with the plant results.

  To define:

  - The cuttings recovery method (drilling mest...)
  - The analysis storage and restoration (see figure 1),

  To choose the best laboratory improvement tests to answer the quarry problems,

  To determine the laboratory operating conditions (see figure 2) and make the correlation between the analysis of powder blasting and the plant results.

4. IMPROVEMENT OF ANDALUSITE RECOVERY AND QUALITY

Due to the necessity of obtaining large particles of Andalusite, a rather complex flowsheet has been designed for the plant (fig. 3).

Therefore, six middlings are produced by the different concentration operations and must be studied to define a process Andalusite recovery.

The study has started with the richest talling called F.G. (Talling no 3 - fig. 3) that contains 66% Andalusite, and muscovite, biotite, quartz, pyrite.

Later, other tailings were tested (see fig. 3):

- Andalusite G (Talling no 5)
- Electrostatic talling (Talling no 5)
- HMS talling - "White sand" (before and after concentration): (Talling no 4)
- Magnetic talling (before and after concentration): (Talling no 2).

5. STUDY OF THE DIFFERENT TAILINGS

All these tailings have been tested following the same procedure.

5.1. MINERALOGICAL STUDIES

- mineralogical determination,
- Andalusite liberation size : to give a high grade Andalusite concentrate with lower iron content.

In conclusion, all these studies above have allowed us to show:

- The main impurities to be eliminated out of these tailings : minerals with high iron content (such as pyrite, biotite, ilmenite, iron, oxide) and quartz.

- The liberation size of Andalusite to recover a high grade concentrate. In any case it seemed that a 250 microns milling was good enough to achieve a high grade concentrate.

5.2. MINERALOGICAL STUDIES

Improvement studies have been carried out (such as flotation, magnetic separation ...) to increase the grade of concentrate and define the parameters of the ore treatment process.

For the F.G. product (Tailing no 3, fig. 3) a flotation process has been developed and patented, with the following operations (fig. 4):

- Grinding,
- Pyrite flotation,
- Desliming,
- Andalusite flotation.

AT the same time, more detailed basic studies have been carried out in the "Université Catholique de Louvain" to determine the sensitivity of the process and define the range of variations of the main parameters.

5.3. BASIC STUDIES

The following basic studies have been developed:

- Kinetics of flotation for pyrite and Andalusite,

- Optimization of re-cleaning conditions,

- Influence on flotation (selectivity and yield) when using industrial water,

- Influence of the desliming size before Andalusite flotation,

- Influence and limit on flotation when recycling the industrial water,

- Collector concentration measurement method,

- Collector residual concentration in the various stages of the Andalusite flotation: evolution and tests,

- Andalusite recovery from the low grade tailings (direct flotation).

In conclusion, all these basic studies have given us a better knowledge of Andalusite theoretical flotation. Thus, it has been easier to understand the field problems of the flotation pilot plant.

In particular, they have permitted us to specify the mode of collector addition to the roughing and the cleaning method with one or two steps. As shown on figure 5, the characteristic curve of Andalusite flotation obtained by cleaning the rougher concentrate in two steps under the optimum operating conditions presents less selectivity than that observed in the best roughenings. On the other hand, when the rougher concentrate is not submitted to the cleaning, the flotation curve is clearly moved to the right: thus, batch Al_2O_3 recoveries corresponding to a concentrate of 59.5% Al_2O_3 are increased by about 10%. Such results require the addition in steps of about 95% of collector at the roughing stage and 5% for the cleaning steps. Let us note that the iron content of concentrates always remains below the maximum allowed: 0.8%.

Besides this, the research has helped us to solve major difficulties we met in the Glomel industrial pilot plant.

a) Influence of the use of Glomel water containing $CaSO_4$ and $FeSO_4$ in significant amounts.

   To keep the recovery at highest values in the case of high salinity it was necessary to increase the whole collector consumption (see fig. 6). The main problem is Fe^{+++} ions. These ions have a very harmful effect on the flotation selectivity that cannot be remedied by increasing the collector consumption.

   However recycling flotation water or a suitable treatment could cancel the major part of these problems.

b) Imperfection of cyclone desliming after pyrite flotation pulp before Andalusite flotation.

   To examine the action of the desliming cut size, numerous tests were made on the two ore samples. In all tests, the only modification of experimental conditions concerned the collector consumption. The main results are shown in figure 7.

c) Determining the collector consumption with the residual concentration of the collector on different points of the flowsheet (any consumption optimization is possible).

Finally, these tests allowed us to study the limits of the recovery process of Andalusites lost in the tailings of Glomel plant with a direct flotation process.

5.4. CONTINUOUS TESTS ON GLOMEL INDUSTRIAL PILOT PLANT

All the laboratory results have then been verified at the Glomel industrial pilot, for all the tailings involved.

- Material balance sheet installation,
- Testing and running the industrial pilot plant in Glomel with Andalusite tailings,
- Continuous double cycloning on the industrial pilot: study and installation.

6. PRECONCENTRATION OF THE GLOMEL PLANT'S TAILINGS

For the lowest grade tailings it is necessary to preconcentrate the Andalusite to have a high concentrate with the flotation process (Al_2O_3 content above 60% and Fe_2O_3 content below 0.7%).

6.1. WHITE SAND (H.M.S. Tailings; tailing no 2; see fig. 3)

A preconcentration by sieving at 0.63 mm is sufficient to preconcentrate the Andalusite.

6.2. MAGNETIC TAILINGS (Tailing no 2; see fig. 3)

Treatment on a new H.G.M.S. is sufficient to preconcentrate the Andalusite, it will then be necessary to test on the pilot plant and to make a feasibility study.

7. ELIMINATION OF THE COLLECTOR ABSORBED ON THE ANDALUSITE GRAINS

With standard direct flotation, the Andalusite collector remains adsorbed on the surface of the grains. It is then impossible to mix Andalusite and water.

The object of the studies was to find an efficient industrial method of eliminating the adsorbed collector from the surface of the Andalusite grains with:

- Laboratory studies and tests on dry and wet process.
- Continuous studies on the industrial pilot plant at Glomel.

8. REVERSE FLOTATION OF ANDALUSITE

We have studied the reverse flotation process of Andalusite.

The first laboratory results are encouraging. It appears however that the treatment process is very accurate.

Therefore it would be necessary to continue the laboratory studies and then set up a continuous control on the Glomel pilot plant to confirm defined parameters.

A patent on this reverse flotation process has been drafted.

Further studies

Under this contract we have studied various other treatment processes to improve the quality of the concentrates in particular: study of the elimination of the pyrite content of Andalusite KB- by pneumatic concentration.

9. RESULTS OBTAINED: INDUSTRIAL APPLICATIONS

Significant economic improvements for the processes have been achieved.

The following results have been obtained:

a) Quality improvement

Up to now Glomel high grade concentrates had the following characteristics: Al_2O_3: 59%; Fe_2O_3: 1.1%.

The products obtained after direct flotation show a very clear improvement: Al_2O_3: 60%; Fe_2O_3: 0.7%.

b) Increase of tonnage and yield of the Glomel plant

The recovery of Andalusite normally lost in high grade tailings through the use of direct flotation has enabled us to increase Glomel productivity and decrease production prices.

Through flotation of the Andalusite content in the tailings we could recover about 8 800 tons in 1990.

Due to this supplementary tonnage and equally to some productivity improvements due to a better knowledge of the quarry, Glomel could appreciably increase the tonnage sold:

In 1988: + 17 %
In 1989: + 6.3%

10. CONCLUSIONS

A new process using direct flotation has been developed for the Andalusite recovery.

Accurate laboratory studies have been carried out to define the main parameters of the Andalusite flotation process.

Continuous flotation tests have been carried out to check the process and produce concentrates for customers tests.

Finally, the whole studies and research have allowed us:

- To control the quarry exploitation.
- To improve and to regulate the concentrate quality.
- To optimize and increase the Andalusite recovery.
- To improve the whole plant process.
- To decrease the operating cost of sold products.

Direct flotation of andalusite

The studies and research completed in this project enabled us to back up the French patent and extend it to Europe and the principal mining nations (U.S.A., Canada, Australia etc...).

Reverse flotation

This project has enabled us to study reverse flotation. A patent has been drafted.

11. REFERENCES

PREDALI J.J., BISCARAT Ch., VAN LIERDE A.:
"Improvement in the quality of refractory minerals such as andalusite". Project report. Stevenage: 27-28 February 1989.

FIGURE LIST

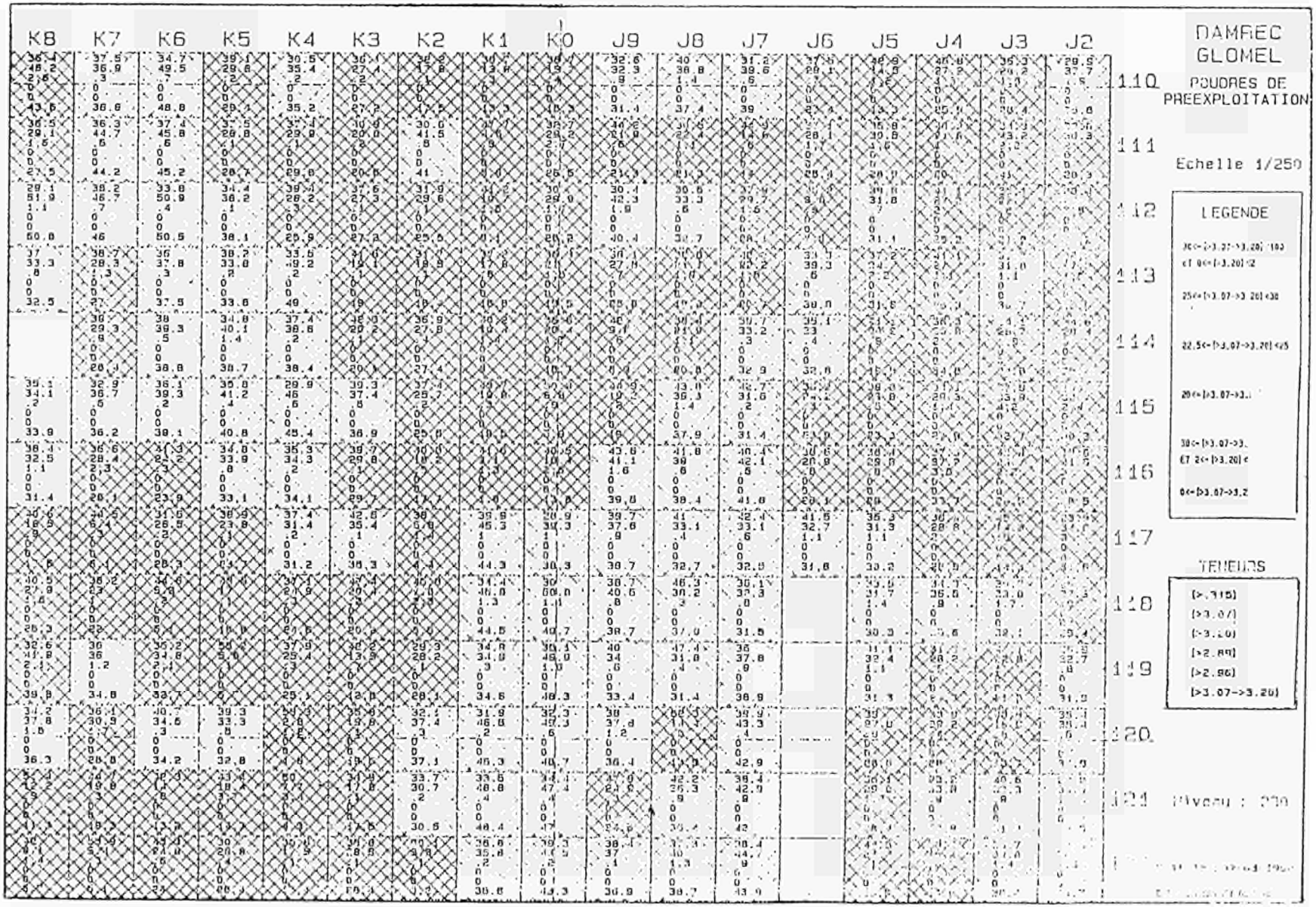
K8
K7
K6
K5
K4
K3
K2
K1
K0
J9
J8
J7
J6
J5
J4
J3
J2
DAMREC
GLOMEL
POUDRES DE
PREEXPLOITATION
Echelle 1/250
LEGENDE
TENEURS
(>.715)
(>3.07)
(>3.00)
(>2.89)
(>2.86)
(>3.07->3.20)
110
111
112
113
114
115
116
117
118
119
120
121
Niveau : 220

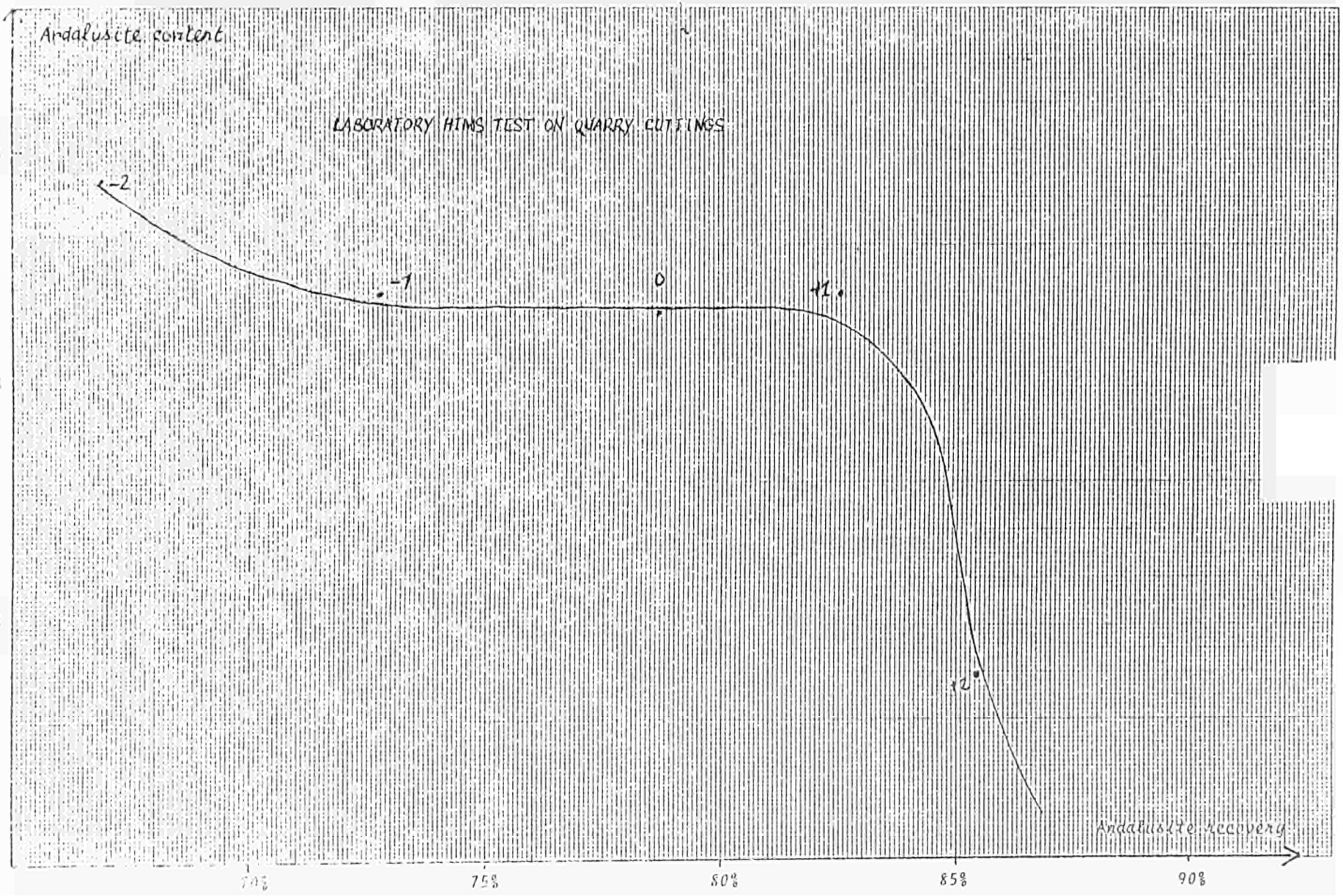
Andalusite content
LABORATORY HMS TEST ON QUARRY CUTTINGS
-2
-1
0
+1
+2
70%
75%
80%
85%
90%
Andalusite recovery

DAMREC _ GLOMEL PLANT

ANDALUSITE Flowsheet

ACTUAL FLOWSHEET

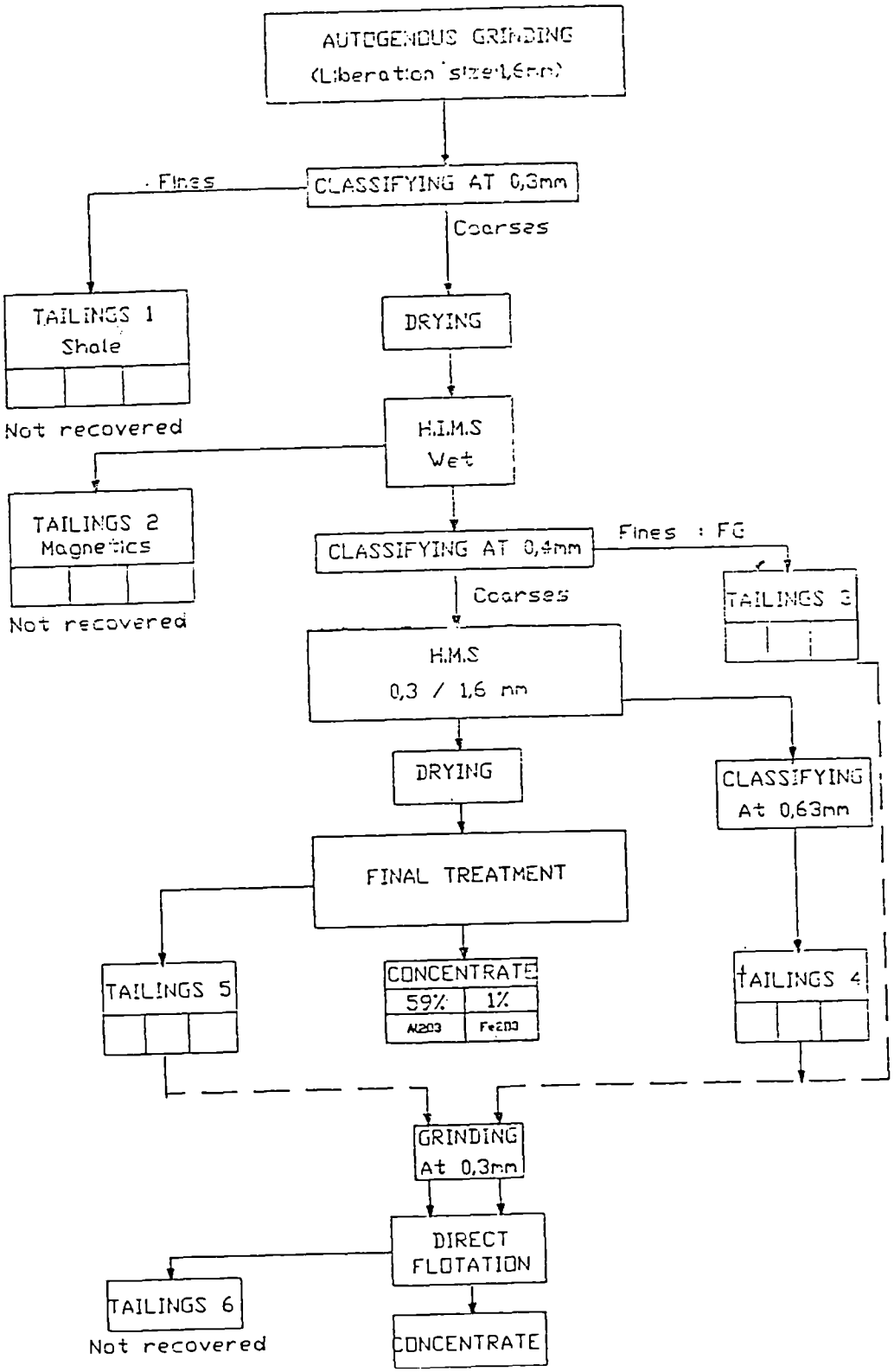

Figure 4 : Pilot flowsheet

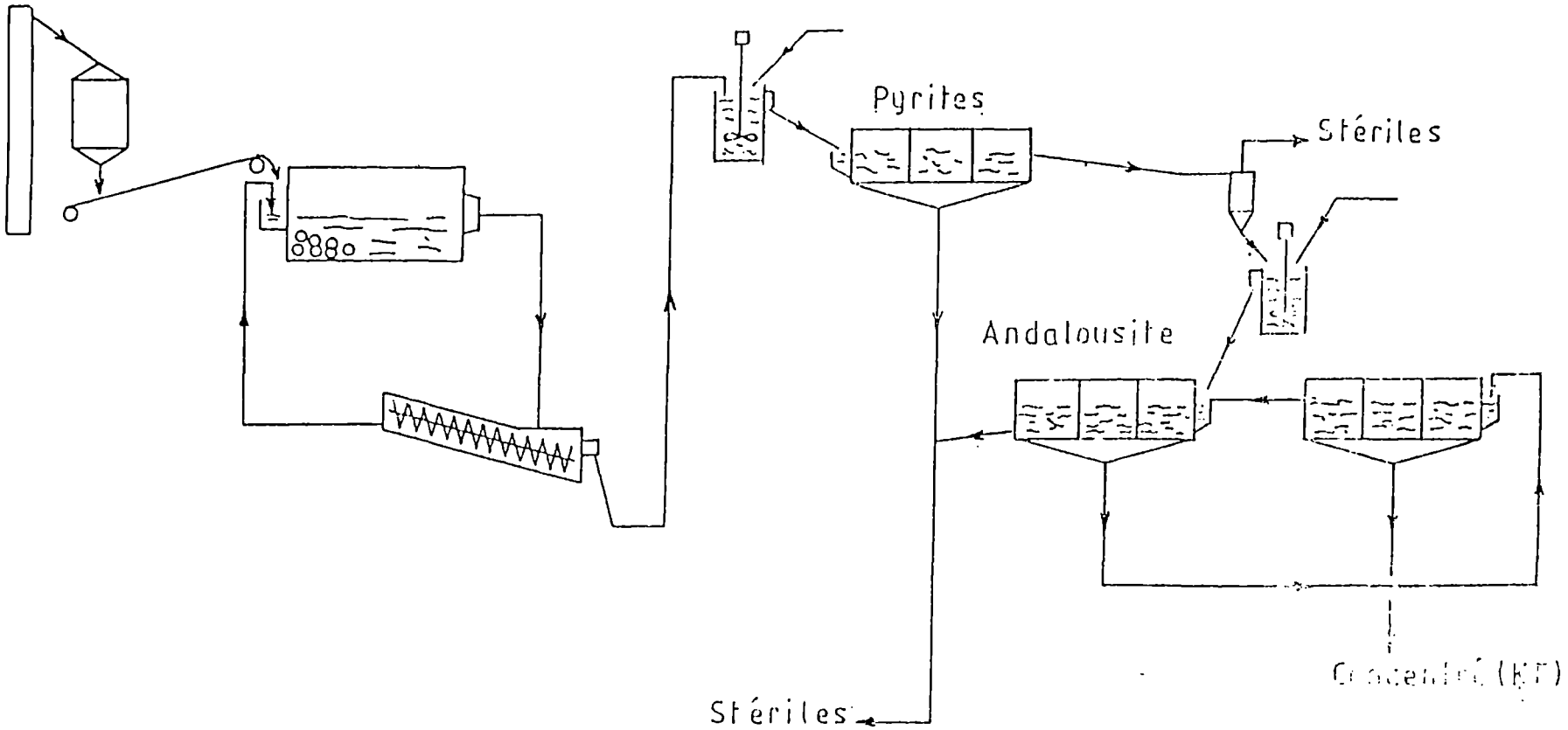

FIGURE 5

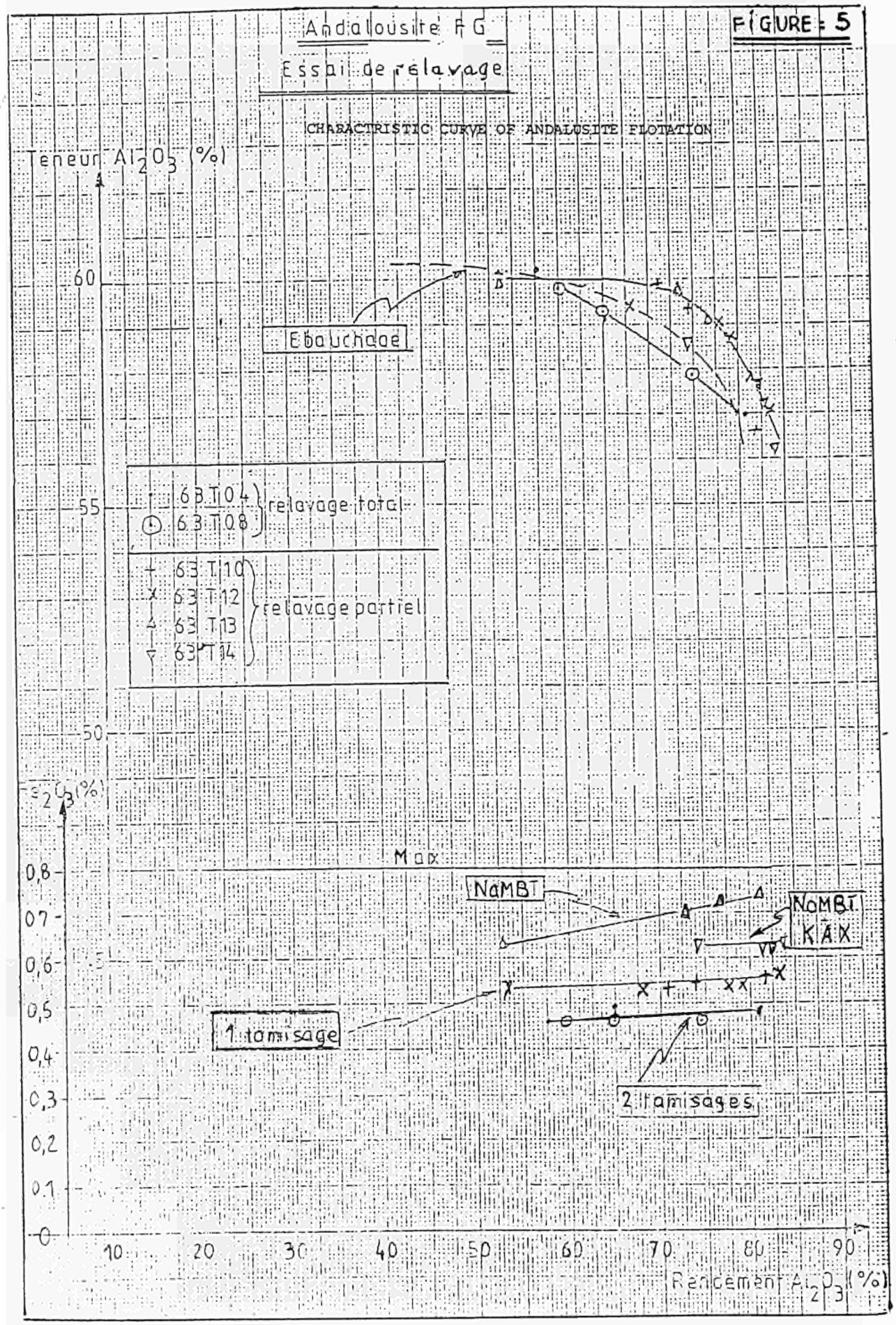
Andalousite FG
Essai de relavage
CHARACTERISTIC CURVE OF ANDALUSITE FLOTATION
Teneur Al_2O_3 (%)
60
55
50
Ebauchage
63 T 04
63 T 08
relavage total
63 T 10
63 T 12
63 T 13
63 T 14
relavage partiel
Fe_2O_3 (%)
Max
0,8
0,7
0,6
0,5
0,4
0,3
0,2
0,1
0
NaMBT
NaMBT KAX
1 tamisage
2 tamisages
10
20
30
40
50
60
70
80
90
Rendement Al_2O_3 (%)

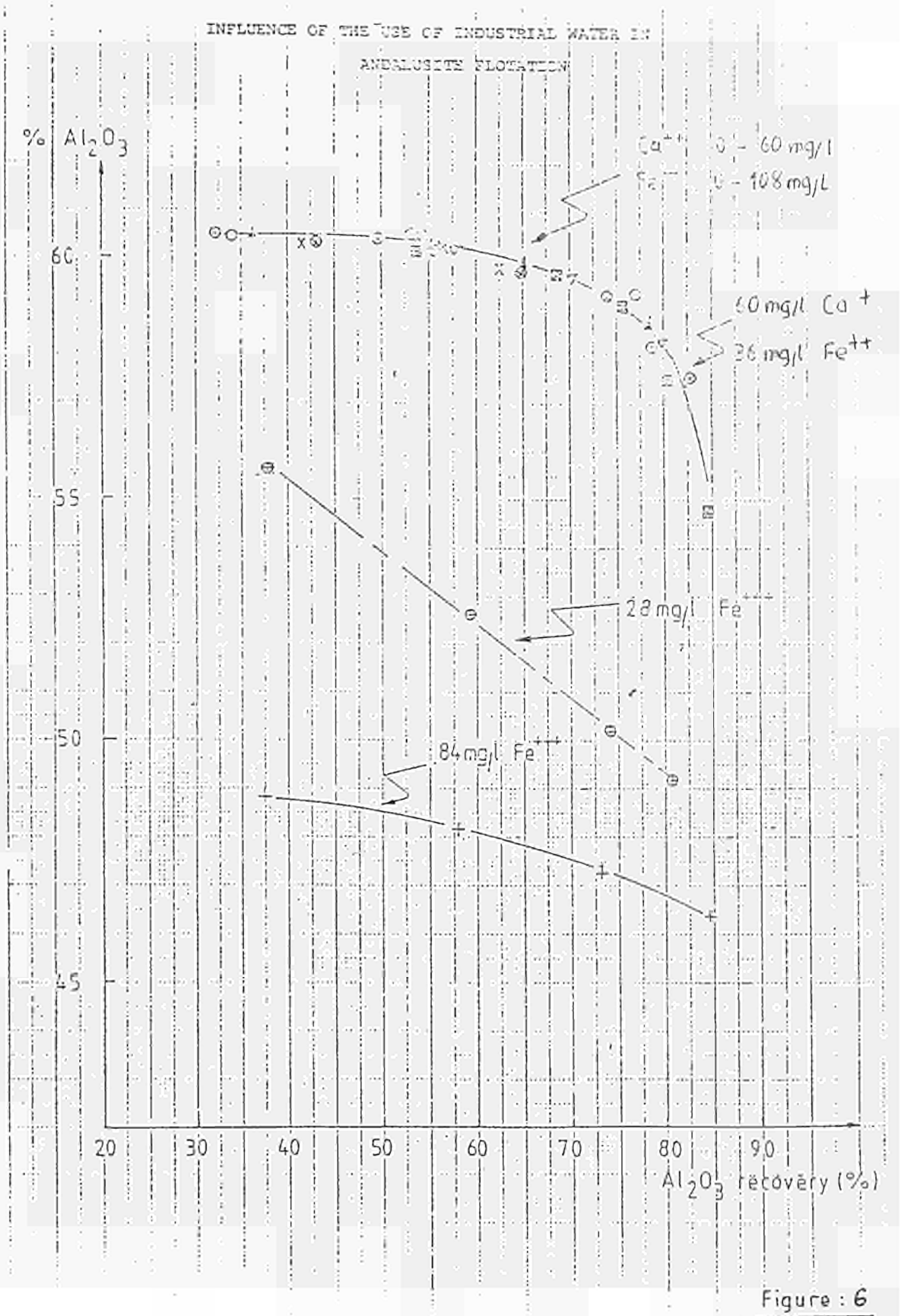
INFLUENCE OF THE USE OF INDUSTRIAL WATER IN
ANDALUSITE FLOTATION
% Al_2O_3
60
55
50
45
20
30
40
50
60
70
80
90
Al_2O_3 recovery (%)
Ca^{++} 0 - 60 mg/l
Fe 0 - 108 mg/l
60 mg/l Ca ++
26 mg/l Fe^{++}
28 mg/l Fe^{++}
84 mg/l Fe^{++}

Figure : 6

INFLUENCE OF THE DESLIMING CUT SIZE BEFORE ANDALUSITE FLOTATION

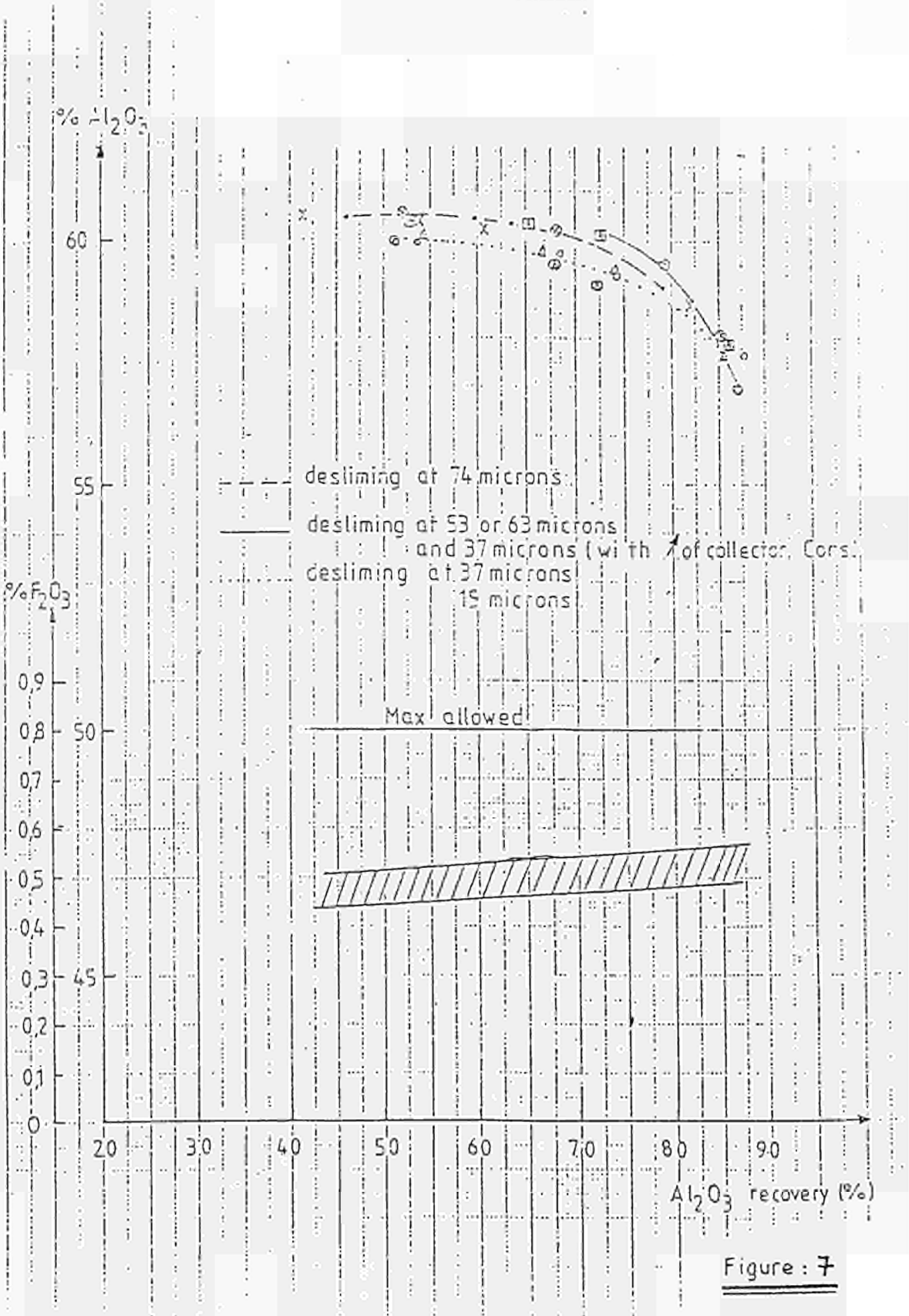

Figure : 7

European Communities – Commission

EUR 13647 – Summary reports of the R&D programme : Primary raw materials (1986-89) Volume III

Edited by M. Donato

Luxembourg: Office for Official Publications of the European Communities

1992 – X, 486 pp., 68 tab., 173 fig. – 21.0 × 29.7 cm

Resources series

ISBN 92-826-3796-4

Price (excluding VAT) in Luxembourg: ECU 48

This document contains the summary reports of cost-sharing R&D contracts funded under the Primary raw materials subprogramme of the Commission of the European Communities. This was part of the R&D programme on raw materials and advanced materials (1986-89).

The main objectives of the Primary raw materials subprogramme were to enhance the competitiveness of the European Community mining and metallurgical industries and to reduce European Community vulnerability for minerals, particularly those of critical or strategic interest.

This programme was funded with ECU 20 million for the period 1986 to 1989 of which ECU 17 million was allocated to research contracts. The balance was allocated to the management of the programme (staff, organization of contact group meetings, expert meetings, international cooperation and other costs).

The subprogramme comprised three research areas:

1. Research and development exploration

Economic geology, methods of geochemical and geophysical prospecting, remote sensing.

2. Mining technology

Rock fracturing, rock mechanics, support systems, problems associated with depth, robotics, methods of modelling and simulation, problems of small-size mines.

3. Mineral processing

Hydrometallurgy of complex sulphide ores, oxidized ores, refractory ores, mine tailings and metallurgical residues; modelling and control in mineral processing; industrial minerals.

Iron, fossil fuels and building materials were excluded from the programme.

Venta y suscripciones • Salg og abonnement • Verkauf und Abonnement • Πωλήσεις και συνδρομές
Sales and subscriptions • Vente et abonnements • Vendita e abbonamenti
Verkoop en abonnementen • Venda e assinaturas

BELGIQUE BELGIË

Moniteur belge / Belgisch Staatsblad
Rue de Louvain 42 Leuvenseweg 42
1000 Bruxelles / 1000 Brussel
Tél. (02) 512 00 26
Fax 511 01 84
CCP / Postrekening 000-2005502-27

Autres distributeurs /
Overige verkooppunten

Librairie européenne/ Europese Boekhandel
Avenue Albert Jonnart 50 /
Albert Jonnartlaan 50
1200 Bruxelles 1200 Brussel
Tel. (02) 734 02 81
Fax 735 08 60

Jean De Lannoy
Avenue du Roi 202 Koningslaan 202
1060 Bruxelles 1060 Brussel
Tel. (02) 538 51 69
Telex 63220 UNBOOK B
Fax (02) 538 08 41

CREDOC
Rue de la Montagne 34 Bergstraat 34
Bte 11 Bus 11
1000 Bruxelles 1000 Brussel

DANMARK

J. H. Schultz Information A/S
EF-Publikationer
Ottiliavej 18
2500 Valby
Tlf. 36 44 22 66
Fax 36 44 01 41
Girokonto 6 00 08 86

BR DEUTSCHLAND

Bundesanzeiger Verlag
Breite Straße
Postfach 10 80 06
5000 Köln 1
Tel. (02 21) 20 29-0
Telex ANZEIGER BONN 8 882 595
Fax 20 29 278

GREECE ΕΛΛΑΔΑ

G.C. Eleftheroudakis SA
International Bookstore
Nikis Street 4
10563 Athens
Tel. (01) 322 63 23
Telex 219410 ELEF
Fax 323 98 21

ESPAÑA

Boletín Oficial del Estado
Trafalgar, 27
28010 Madrid
Tel. (91) 44 82 135

Mundi-Prensa Libros, S.A.
Castelló, 37
28001 Madrid
Tel. (91) 431 33 99 (Libros)
431 32 22 (Suscripciones)
435 36 37 (Dirección)
Télex 49370-MPLI-E
Fax (91) 575 39 98

Sucursal:

Librería Internacional AEDOS
Consejo de Ciento, 391
08009 Barcelona
Tel. (93) 301 86 15
Fax (93) 317 01 41

Llibreria de la Generalitat de Catalunya
Rambla dels Estudis, 118 (Palau Moja)
08002 Barcelona
Tel. (93) 302 68 35
302 64 62
Fax (93) 302 12 99

FRANCE

Journal officiel
Service des publications des Communautés européennes
26, rue Desaix
75727 Paris Cedex 15
Tél. (1) 40 58 75 00
Fax (1) 40 58 75 74

IRELAND

Government Supplies Agency
4-5 Harcourt Road
Dublin 2
Tel. (1) 61 31 11
Fax (1) 78 06 45

ITALIA

Licosa Spa
Via Duca di Calabria, 1 1
Casella postale 552
50125 Firenze
Tel. (055) 64 54 15
Fax 64 12 57
Telex 570466 LICOSA I
CCP 343 509

GRAND-DUCHÉ DE LUXEMBOURG

Messageries Paul Kraus
11, rue Christophe Plantin
2339 Luxembourg
Tel. 499 88 88
Télex 2515
Fax 499 88 84 44
CCP 49242-63

NEDERLAND

SDU Overheidsinformatie
Externe Fondsen
Postbus 20014
2500 EA 's-Gravenhage
Tel. (070) 37 89 911
Fax (070) 34 75 778

PORTUGAL

Imprensa Nacional
Casa da Moeda, EP
Rua D. Francisco Manuel de Melo, 5
1092 Lisboa Codex
Tel. (01) 69 34 14

Distribuidora de Livros Bertrand, Ld.ª
Grupo Bertrand, SA
Rua das Terras dos Vales, 4-A
Apartado 37
2700 Amadora Codex
Tel. (01) 49 59 050
Telex 15798 BERDIS
Fax 49 60 255

UNITED KINGDOM

HMSO Books (PC 16)
HMSO Publications Centre
51 Nine Elms Lane
London SW8 5DR
Tel. (071) 873 2000
Fax GP3 873 8463
Telex 29 71 138

ÖSTERREICH

Manz'sche Verlags- und Universitätsbuchhandlung
Kohlmarkt 16
1014 Wien
Tel. (0222) 531 61-0
Telex 11 25 00 BOX A
Fax (0222) 531 61-39

SUOMI

Akateeminen Kirjakauppa
Keskuskatu 1
PO Box 128
00101 Helsinki
Tel. (0) 121 41
Fax (0) 121 44 41

NORGE

Narvesen information center
Bertrand Narvesens vei 2
PO Box 6125 Etterstad
0602 Oslo 6
Tel. (2) 57 33 00
Telex 79668 NIC N
Fax (2) 68 19 01

SVERIGE

BTJ
Box 200
22100 Lund
Tel. (046) 18 00 00
Fax (046) 18 01 25

SCHWEIZ / SUISSE / SVIZZERA

OSEC
Stampfenbachstraße 85
8035 Zurich
Tel. (01) 365 54 49
Fax (01) 365 54 11

CESKOSLOVENSKO

NIS
Havelkova 22
13000 Praha 3
Tel. (02) 235 84 46
Fax 42-2-264775

MAGYARORSZÁG

Euro-Info-Service
Budapest I. Kir.
Attila út 93
1012 Budapest
Tel. (1) 56 82 11
Telex (22) 4717 AGINF H-61
Fax (1) 17 59 031

POLSKA

Business Foundation
ul. Krucza 38/42
00-512 Warszawa
Tel. (22) 21 99 93, 628-28 82
International Fax&Phone
(0-39) 12-00-77

JUGOSLAVIJA

Privredni Vjesnik
Bulevar Lenjina 171 XIV
11070 Beograd
Tel. (11) 123 23 40

CYPRUS

Cyprus Chamber of Commerce and Industry
Chamber Building
38 Grivas Dhigenis Ave
3 Deligiorgis Street
PO Box 1455
Nicosia
Tel. (2) 449500/462312
Fax (2) 458630

TURKIYE

Pres Gazete Kitap Dergi Pazarlama Dağitim Ticaret ve sanayi AŞ
Narlibahçe Sokak N. 15
Istanbul-Cagaloğlu
Tel. (1) 520 92 96 - 528 55 66
Fax 520 64 57
Telex 23822 DSVO-TR

CANADA

Renouf Publishing Co. Ltd
Mail orders — Head Office:
1294 Algoma Road
Ottawa, Ontario K1B 3W8
Tel. (613) 741 43 33
Fax (613) 741 54 39
Telex 0534783

Ottawa Store:
61 Sparks Street
Tel. (613) 238 89 85

Toronto Store:
211 Yonge Street
Tel. (416) 363 31 71

UNITED STATES OF AMERICA

UNIPUB
4611 F Assembly Drive
Lanham, MD 20706-4391
Tel. Toll Free (800) 274 4888
Fax (301) 459 0056

AUSTRALIA

Hunter Publications
58A Gipps Street
Collingwood
Victoria 3066

JAPAN

Kinokuniya Company Ltd
17 7 Shinjuku 3-Chome
Shinjuku-ku
Tokyo 160-91
Tel. (03) 3439-0121

Journal Department
PO Box 55 Chitose
Tokyo 156
Tel. (03) 3439-0124

AUTRES PAYS
OTHER COUNTRIES
ANDERE LÄNDER

Office des publications officielles des Communautés européennes
2, rue Mercier
2985 Luxembourg
Tel. 49 92 81
Telex PUBOF LU 1324 b
Fax 48 85 73 48 68 17
CC bancaire BIL 8-109/6003/700

15

CD-NC-13647-EN-C

NOTICE TO THE READER

All scientific and technical reports published by the Commission of the European Communities are announced in the monthly periodical **'euro abstracts'**. For subscription (1 year: ECU 110) please write to the address below.

Price (excluding VAT) in Luxembourg: (Volume 3) ECU 48
(Volumes 1-3) ECU 90

OFFICE FOR OFFICIAL PUBLICATIONS
OF THE EUROPEAN COMMUNITIES

L-2985 Luxembourg

ISBN 92-826-3796-4